INSIGHTS IN GENITOURINARY ONCOLOGY: 2021

EDITED BY: Ronald M. Bukowski and Michael Kattan
PUBLISHED IN: Frontiers in Oncology

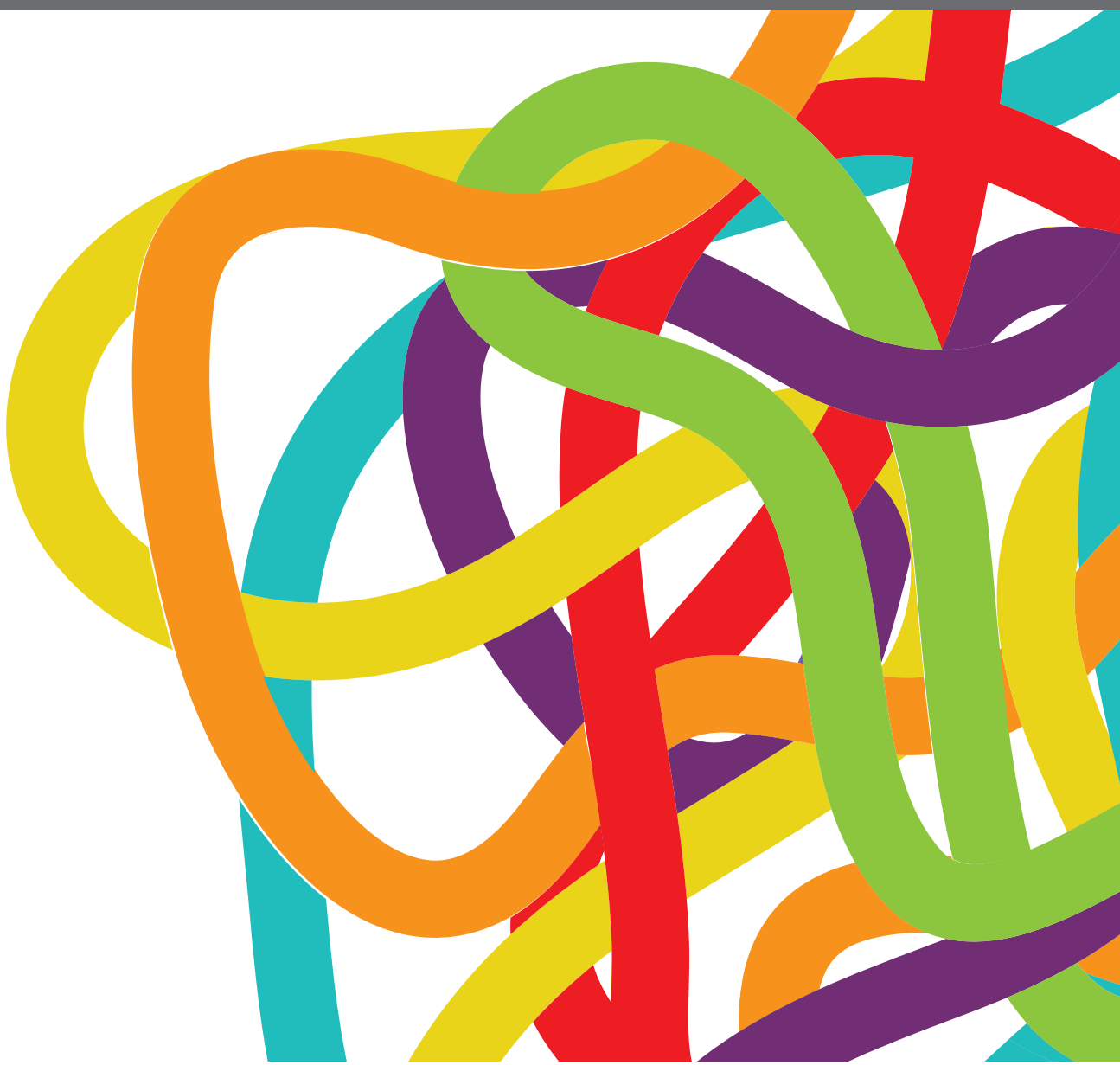

frontiers Research Topics

frontiers

ISSN 1664-8714
ISBN 978-2-83250-240-2
DOI 10.3389/978-2-83250-240-2

About Frontiers

Frontiers is more than just an open-access publisher of scholarly articles: it is a pioneering approach to the world of academia, radically improving the way scholarly research is managed. The grand vision of Frontiers is a world where all people have an equal opportunity to seek, share and generate knowledge. Frontiers provides immediate and permanent online open access to all its publications, but this alone is not enough to realize our grand goals.

Frontiers Journal Series

The Frontiers Journal Series is a multi-tier and interdisciplinary set of open-access, online journals, promising a paradigm shift from the current review, selection and dissemination processes in academic publishing. All Frontiers journals are driven by researchers for researchers; therefore, they constitute a service to the scholarly community. At the same time, the Frontiers Journal Series operates on a revolutionary invention, the tiered publishing system, initially addressing specific communities of scholars, and gradually climbing up to broader public understanding, thus serving the interests of the lay society, too.

Dedication to Quality

Each Frontiers article is a landmark of the highest quality, thanks to genuinely collaborative interactions between authors and review editors, who include some of the world's best academicians. Research must be certified by peers before entering a stream of knowledge that may eventually reach the public - and shape society; therefore, Frontiers only applies the most rigorous and unbiased reviews.
Frontiers revolutionizes research publishing by freely delivering the most outstanding research, evaluated with no bias from both the academic and social point of view. By applying the most advanced information technologies, Frontiers is catapulting scholarly publishing into a new generation.

What are Frontiers Research Topics?

Frontiers Research Topics are very popular trademarks of the Frontiers Journals Series: they are collections of at least ten articles, all centered on a particular subject. With their unique mix of varied contributions from Original Research to Review Articles, Frontiers Research Topics unify the most influential researchers, the latest key findings and historical advances in a hot research area! Find out more on how to host your own Frontiers Research Topic or contribute to one as an author by contacting the Frontiers Editorial Office: frontiersin.org/about/contact

INSIGHTS IN GENITOURINARY ONCOLOGY: 2021

Topic Editors:
Ronald M. Bukowski, Cleveland Clinic, United States
Michael Kattan, Case Western Reserve University, United States

Citation: Bukowski, R. M., Kattan, M., eds. (2022). Insights in Genitourinary Oncology: 2021. Lausanne: Frontiers Media SA. doi: 10.3389/978-2-83250-240-2

Table of Contents

frontiers in Oncology

CASE REPORT
published: 12 May 2021
doi: 10.3389/fonc.2021.691996

Genomic and Pathological Characterization of Multiple Renal Cell Carcinoma Regions in Patient With Tuberous Sclerosis Complex: A Case Report

Tetsuya Yamamoto[1], Taigo Kato[1], Koji Hatano[1], Atsunari Kawashima[1], Takeshi Ujike[1], Shinichiro Fukuhara[1], Hiroshi Kiuchi[1], Ryoichi Imamura[1], Naokazu Ibuki[2], Kazuma Kiyotani[3], Masako Kurashige[4], Eichi Morii[4], Kazutoshi Fujita[1], Norio Nonomura[1] and Motohide Uemura[1]*

[1] Department of Urology, Osaka University Graduate School of Medicine, Osaka, Japan, [2] Department of Urology, Osaka Medical College, Osaka, Japan, [3] Cancer Precision Medicine Center, Japanese Foundation for Cancer Research, Tokyo, Japan, [4] Department of Pathology, Osaka University Graduate School of Medicine, Osaka, Japan

OPEN ACCESS

Edited by:
Masaki Shiota,
Kyushu University, Japan

Reviewed by:
Tatsuo Yoneda,
Nara Medical University, Japan
Kenji Zennami,
Fujita Health University, Japan

***Correspondence:**
Taigo Kato
kato@uro.med.oaska-u.ac.jp

Specialty section:
This article was submitted to Genitourinary Oncology, a section of the journal Frontiers in Oncology

Received: *07 April 2021*
Accepted: *26 April 2021*
Published: *12 May 2021*

Citation:
Yamamoto T, Kato T, Hatano K, Kawashima A, Ujike T, Fukuhara S, Kiuchi H, Imamura R, Ibuki N, Kiyotani K, Kurashige M, Morii E, Fujita K, Nonomura N and Uemura M (2021) Genomic and Pathological Characterization of Multiple Renal Cell Carcinoma Regions in Patient With Tuberous Sclerosis Complex: A Case Report. Front. Oncol. 11:691996. doi: 10.3389/fonc.2021.691996

Tuberous sclerosis complex is a genetic disorder characterized by facial angiofibromas, intellectual disability, epilepsy, and tumor formation in multiple organs, including the kidney. Renal cell carcinoma occurs in 2%–4% of patients with tuberous sclerosis complex, often developing multiply and bilaterally. Renal cell carcinoma associated with this genetic disorder may include complex tumor heterogeneity caused by the spatially different mutational landscape. Herein, we report the case of a female patient with tuberous sclerosis complex who developed multiple renal tumors. A 44-year-old female patient with tuberous sclerosis complex developed three different histological types of tumor—angiomyolipoma, clear cell renal cell carcinoma, and papillary renal cell carcinoma—in the left kidney at first renal cell carcinoma recurrence. The papillary renal cell carcinoma was morphologically atypical, indicating that its occurrence was associated with the genetic disorder. Furthermore, whole-exome sequencing revealed distinct patterns of somatic mutation in the three tumor types, and the atypical papillary renal cell carcinoma possessed a different mutational landscape than that of typical papillary renal cell carcinomas. Our findings indicate that tumors associated with tuberous sclerosis complex may be diagnosed with careful pathological examination. Furthermore, somatic mutation profiles of these tumors revealed their unique features, providing important information for further

understanding the mechanism of multiple tumor development in patients with tuberous sclerosis complex.

Keywords: tuberous sclerosis complex, renal cell carcinoma, papillary renal cell carcinoma, whole-exome sequencing, cancer gene

INTRODUCTION

Tuberous sclerosis complex (TSC) is a rare autosomal dominant genetic disorder with manifestations such as facial angiofibromas, intellectual disability, and epilepsy occurring in 1 of every 6,000 births (1–3). This disorder is associated with mutations in *TSC1* or *TSC2*; these genes encode proteins (hamartin and tuberin) that act as a complex involved in tumor suppression and regulation of the rapamycin (mTOR) signaling pathway mammalian target.

Disorders affecting the mTOR pathway comprise clinical features indicating a predisposition to tumor development in multiple organs, including the kidney. Specifically, renal tumors are found in 70%–80% of patients with TSC (4). The three major types of renal manifestations occurring in these patients are angiomyolipoma (AML), renal cyst, and renal cell carcinoma (RCC). TSC-associated RCC occurs in 2%–4% of patients with TSC (5), an estimated incidence rate higher than that in the general population. Moreover, TSC-associated RCC often occurs in the younger individuals, requiring close monitoring for recurrent RCC throughout their lifetime (5, 6). TSC-associated RCC is also characterized by multiple occurrences in the same patient (7, 8). This renal tumor occurs bilaterally in approximately 30% of cases and often comprises several types of morphology, including clear cell, papillary, and chromophobe RCC, as well as benign AML (5, 7, 9).

Herein, we describe a case of a patient with TSC who presented with three types of tumors—clear cell RCC, papillary RCC, and AML—in the same kidney. In the present study, we demonstrated that immunohistochemical analysis is an important tool to identify the occurrence of RCC associated with TSC, especially when the patient was not previously diagnosed with this genetic disorder. Moreover, we examined the somatic mutation profiles of the tumors, highlighting their unique features and mutational landscapes, which may contribute to understanding the mechanism involved in multiple tumor formation in patients with TSC.

CASE PRESENTATION

A 44-year-old Japanese woman was referred to our hospital for treatment of a recurrent tumor in the left kidney. Five years prior to this referral, the patient underwent right-kidney nephrectomy for RCC and received a histopathological diagnosis of clear cell RCC (pT1aN0M0) at another institution. Two years after this, computed tomography (CT) imaging identified three tumors in her left kidney; the patient underwent left-kidney partial nephrectomy for these tumors (**Figures 1A–C**). Histopathological examination determined that the tumors were AML, clear cell RCC (pT1a), and papillary RCC (pT1a) (**Figures 1D–F**). A periodic CT examination 3.5 years later revealed the tumor recurrence in her left kidney.

Upon initial visit to the Osaka University Hospital, abdominal CT scan showed a renal mass (diameter: 22 mm) with early enhancement in the left kidney (**Figure 2A**). Additional screening tests revealed the presence of lung cysts and calcifications in the left ventricular wall of the brain (**Figures 2B, C**), leading to the suspicion of TSC. Moreover, physical examination revealed five major (ungual fibromas, shagreen patches, lymphangioleiomyomatosis, subependymal nodule, and angiomyolipoma) and one minor (dental enamel pits) TSC manifestations according to clinical and genetic diagnostic criteria (10). Combining these findings, we diagnosed the patient with recurrence of left-kidney RCC and TSC.

Considering the high recurrence rate of TSC-associated RCC, the patient received CT-guided percutaneous cryoablation for the left-kidney recurrent tumor to maintain maximal renal function. Tumor biopsy performed after cryoablation identified the tumor as clear cell RCC by immunohistochemical staining. To evaluate kidney function, we calculated the estimated glomerular filtration rate (eGFR) before and 3 mo after cryoablation. The rate of kidney functional deterioration was 3.5%. The patient remained recurrence-free for 3 years without renal function deterioration.

Histopathological Features of Renal Cell Carcinoma

Upon the diagnosis of a second RCC recurrence, we retrospectively examined the three tumors that were identified at first recurrence considering that TSC-associated RCC has several unique features. We observed prominent papillary architecture lined by clear cells with delicate eosinophilic cytoplasmic thread-like strands that occasionally appeared more prominent and aggregated to form eosinophilic globules in the papillary RCC sample (**Figures 3A, B**). Immunohistochemical analysis revealed that CK7 and CD10 were positive, whereas succinate dehydrogenase subunit B (SDHB) and α-methylacyl-CoA racemase (AMACR) were negative (**Figures 3C–F**). These findings demonstrated that the characteristics of the papillary RCC in our patient were consistent with those of TSC-associated papillary RCC, which

Abbreviations: AMACR, α-methylacyl-CoA racemase; AML, angiomyolipoma; CT, Computed tomography; FFPE, Formalin-fixed paraffin-embedded; RCC, Renal cell carcinoma; SDHB, Succinate dehydrogenase subunit B; TSC, Tuberous sclerosis complex.

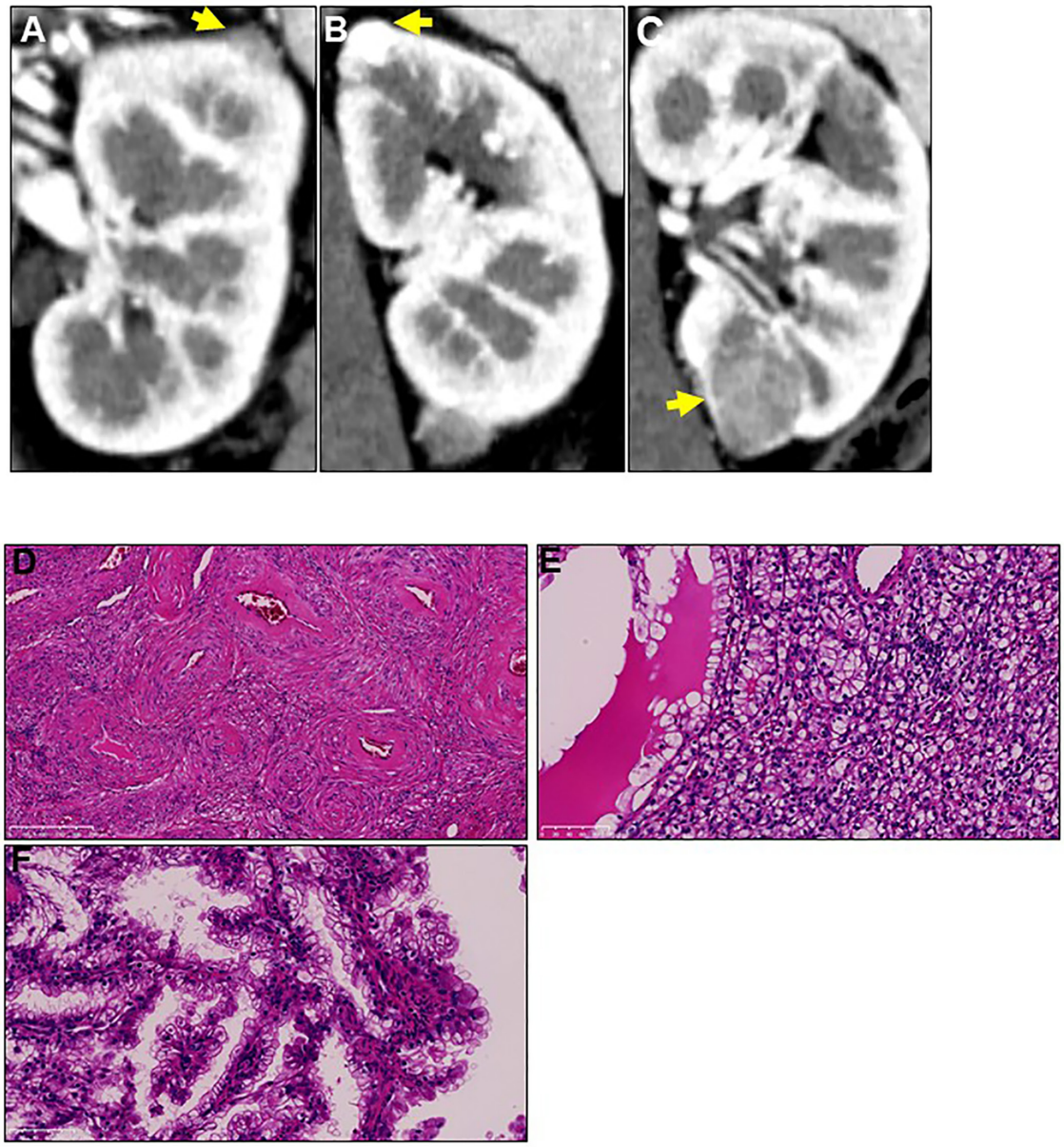

FIGURE 1 | Three different tumors located in the patient's left kidney at first recurrence. Two years after radical right-kidney nephrectomy, the patient was diagnosed with three different tumors **(A-C)** in her left kidney on computed tomography examination. Yellow arrows show the three tumors. The patient underwent left-kidney partial nephrectomy for all tumors, and immunohistochemical analysis showed that their histopathological types were **(D)** angiomyolipoma, **(E)** clear cell renal cell carcinoma, and **(F)** papillary renal cell carcinoma. Magnification: 200× for hematoxylin and eosin staining.

was recently reported as a new type of papillary tumor occurring in patients with TSC (11).

Somatic Mutations and Alterations in Cancer-Related Genes

To characterize the intra-tumoral genetic heterogeneity of this case, we performed whole-exome sequencing using genomic DNA extracted from the tumors surgically resected at first recurrence. We obtained an average sequencing depth of 82.3× per base and identified 221 non-silent mutations and insertions/deletions (indels) (124–154 non-silent mutations per tumor, **Additional Table 1**). We found that 36.7% of these somatic mutations—including cancer driver genes such as *PABPC1* and *DICER1*, which are common in parental clones of many cancer types—were shared among the three tumors (common mutations, **Figure 4**). Some mutations were uniquely observed in one or two tumors (unique mutations), which may have been

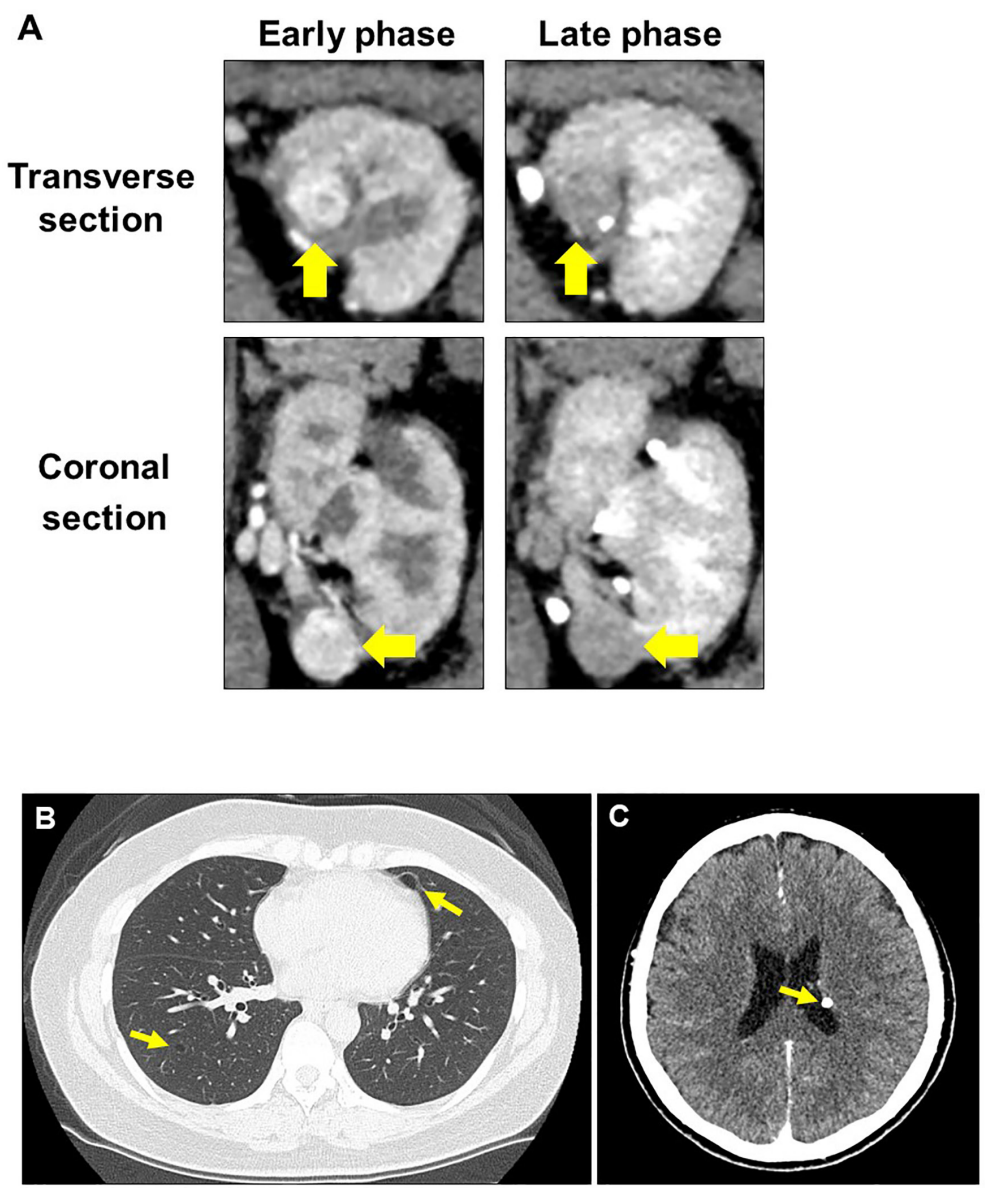

FIGURE 2 | Radiographic evaluation at second recurrence. **(A)** Computed tomography examination shows typical findings of clear cell renal cell carcinoma in the left kidney. **(B)** Lung lymphangioleiomyomatosis. **(C)** Subependymal nodule at the left lateral ventricular wall of the brain.

acquired during individual tumor formation, contributing to the high intra-tumoral genetic heterogeneity.

Interestingly, in our patient's papillary RCC sample, 37.1% of common mutations and 25.5% of unique mutations were not previously reported as non-silent mutations in the Cancer Genome Atlas database (**Additional Figure 1**). Regarding *TSC1* and *TSC2* mutations, TSC-associated papillary RCC harbored frameshift *TSC1* mutation (c.2142del, p.Asn715fs), a pathogenic variant for patients with TSC reported in the ClinVar database. Conversely, *TSC1* and *TSC2* germline mutations were not found in our patient, implying that she may possess the phenotype with mosaic forms of TSC.

DISCUSSION

The occurrence of RCC in patients with TSC has been recognized for several decades. Unlike typical RCC, TSC-associated RCC has several unique features, including early onset (around 40 years old), predominance in female patients, and multiple and bilateral tumors with distinct pathological characteristics (1, 2, 5, 8). Therefore, because chronic kidney disease is a common cause of death in patients with TSC, physicians need to carefully determine therapeutic strategies for TSC-associated RCC to avoid renal function impairment (4). Herein, we described a case of TSC-associated RCC and identified distinct patterns of

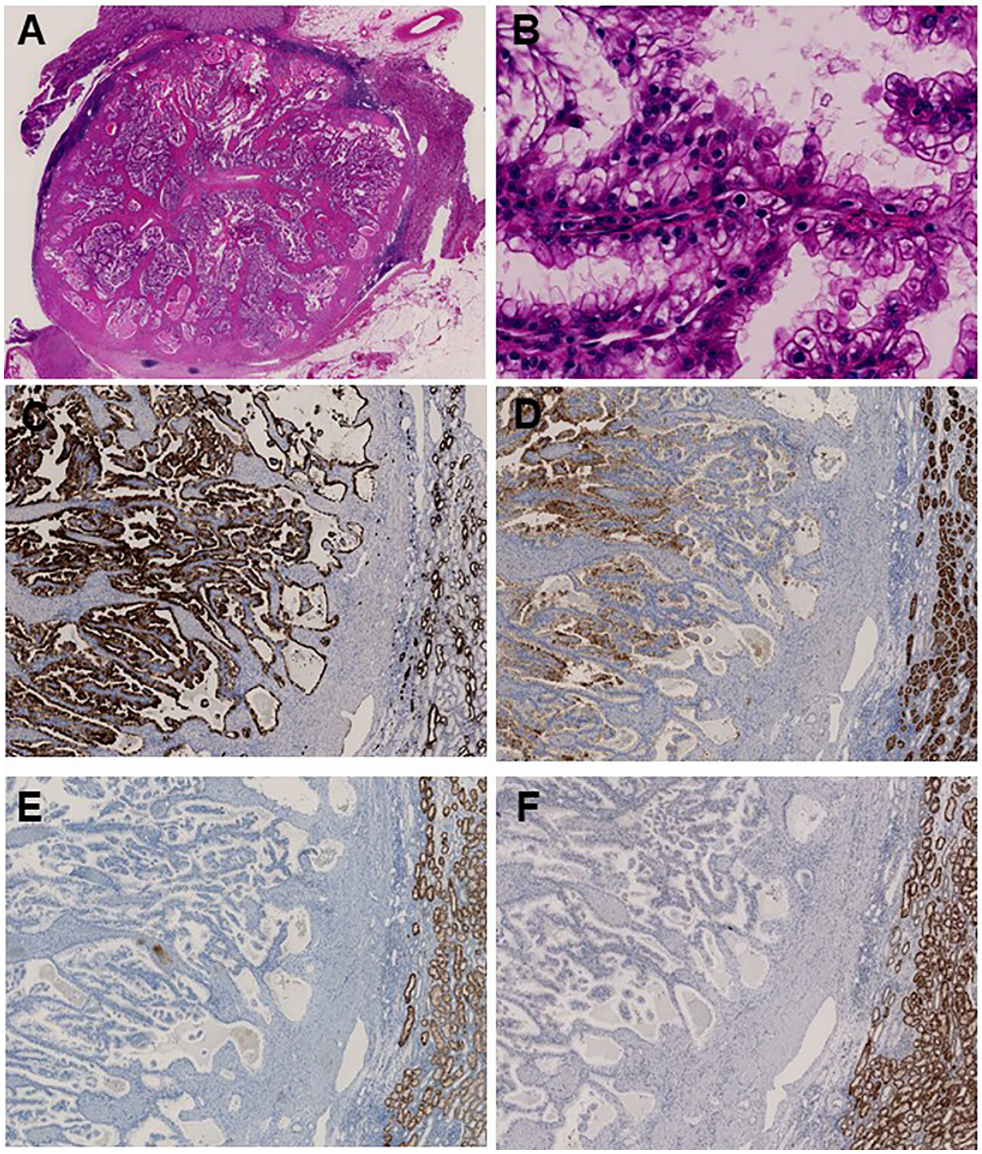

FIGURE 3 | Immunohistochemical analysis identifies papillary renal cell carcinoma associated with tuberous sclerosis complex. **(A)** Main tumor nodule surrounded by thick fibrous stroma on low power; **(B)** Prominent papillary architecture lined by large clear cells with delicate eosinophilic cytoplasmic thread-like strands, which occasionally appeared more outstanding and aggregated to form eosinophilic globules on high power. Immunohistochemical analysis revealed positive staining for **(C)** CK7 and **(D)** CD10, whereas **(E)** SDHB and **(F)** AMACR were negative.

pathological findings and mutational landscapes among clear cell RCC, papillary RCC, and AML occurring in the same kidney, leading to several important implications.

First, upon immunohistochemical analysis, we identified several TSC-associated papillary RCC characteristics that differed from typical papillary RCC, including prominent papillary architecture, abundant clear cell cytoplasm, uniformly deficient SDHB expression, and negative staining for AMACR (11). These findings strongly indicate the presence of TSC, especially in patients displaying fewer clinical features associated with this disorder. Considering that TSC-associated RCC may show multiple and bilateral recurrence, the timely recognition of this atypical form of RCC using immunohistochemical analysis may allow treatment with local therapy instead of radical nephrectomy, possibly avoiding the development of chronic kidney disease in these patients.

Second, we identified that each of the tumors occurring in the same kidney had unique somatic mutations, contributing to their different morphologies. So far, genomic characterization of multifocal renal tumors in TSC patients have not well been

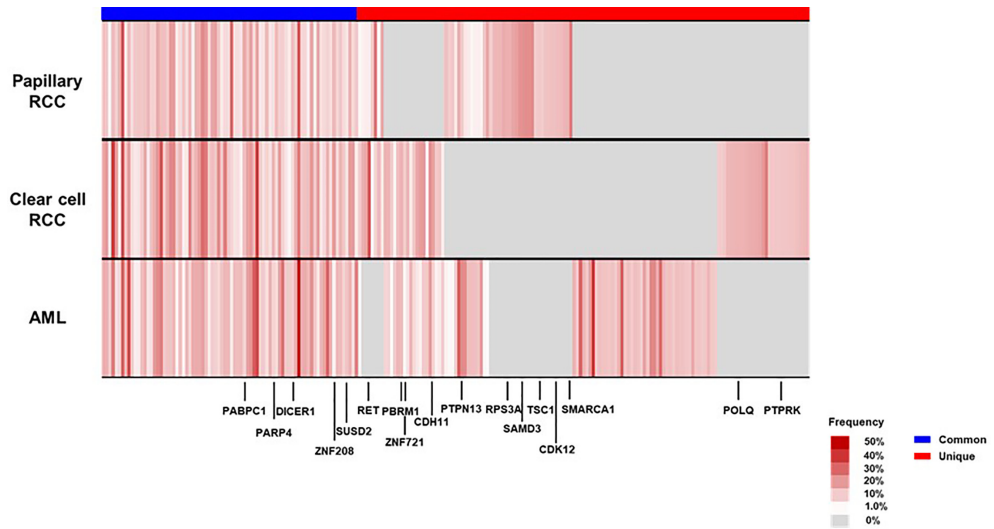

FIGURE 4 | Mutational landscape of the three renal tumors in the patient's left kidney at first recurrence. We visualized the somatic mutation profiles of each tumor—angiomyolipoma (AML), clear cell renal cell carcinoma (RCC), and papillary RCC—as heat maps (black-colored genes indicate driver gene mutations in many cancer types). *CDH11*, Cadherin 11; *CDK12*, Cyclin Dependent Kinase 12; *DICER1*, Dicer 1; *PABPC1*, Poly(A) Binding Protein Cytoplasmic 1; *PARP4*, Poly(ADP-Ribose) Polymerase Family Member 4; *PBRM1*, Polybromo 1; *POLQ*, DNA Polymerase Theta; *PTPN13*, Protein Tyrosine Phosphatase Non-Receptor Type 13; *PTPRK*, Protein Tyrosine Phosphatase Receptor Type K; *RET*, Ret Proto-Oncogene; *RPS3A*, Ribosomal Protein S3A; *SAMD3*, Sterile Alpha Motif Domain Containing 3; *SMARCA1*, SWI/SNF Related, Matrix Associated, Actin Dependent Regulator Of Chromatin, Subfamily A, Member 1; *SUSD2*, Sushi Domain Containing 2; *TSC1*, TSC Complex Subunit 1; *ZNF208*, Zinc Finger Protein 208; *ZNF721*, Zinc Finger Protein 721.

described. Tyburczy et al. reported that two patients with germline *TSC* mutation possessed distinct pathological features of multiple TSC-associated papillary RCCs and different second-hit mutations in *TSC1* or *TSC2* in the same patient, which may develop multifocal renal tumors. Interestingly, 35.2% of the somatic mutations identified in our papillary RCC sample were absent in typical papillary RCC, which might have led to the occurrence of TSC-associated papillary RCC in our patient. Moreover, driver mutations such as *PABPC1* and *DICER1* other than *TSC*1 or *TSC*2 may affect the TSC-associated tumor formation (**Figure 4**). Considering that 10%–15% of patients with TSC have no mutation in *TSC1* or *TSC2* as in our case, the acquisition of somatic mutations may also lead to the occurrence of multiple renal tumors with distinct phenotypes in these patients. These findings may contribute to further understanding the various aspects of TSC-associated RCC, although more cases are needed to fully elucidate this phenomenon.

In conclusion, our case report indicates that immunohistochemistry analysis is an important tool to diagnose TSC-associated papillary RCC. Moreover, our findings demonstrate that the accumulation of somatic mutation profiles is important to further understand the occurrence of TSC-associated RCC.

DATA AVAILABILITY STATEMENT

The original contributions presented in the study are included in the article/**Supplementary Material**. Further inquiries can be directed to the corresponding author.

ETHICS STATEMENT

The studies involving human participants were reviewed and approved by Institutional Review Board of Osaka University (approval number: 668-5). The patients/participants provided their written informed consent to participate in this study.

AUTHOR CONTRIBUTIONS

TY performed data analysis and drafted the article. TK planned the entire project, performed data analysis, and completed the article. MU planned, supervised the entire project and completed the article. NN provided the study design and the working hypothesis and completed the article. KK conducted experiments, performed data analysis, and completed the article. MK and EM conducted experiments and completed the article. KH, AK, TU, SF, HK, RI, NI, and KF conducted data analysis and provided scientific advice. All authors contributed to the article and approved the submitted version.

FUNDING

This work was supported by JSPS KAKENHI (Grant-in-Aid for Scientific Research (C), grant number 18K09133).

SUPPLEMENTARY MATERIAL

The Supplementary Material for this article can be found online at: https://www.frontiersin.org/articles/10.3389/fonc.2021.691996/full#supplementary-material

REFERENCES

1. Crino PB, Nathanson KL, Henske EP. The Tuberous Sclerosis Complex. *N Engl J Med* (2006) 355:1345–56. doi: 10.1056/NEJMra055323
2. Lam HC, Siroky BJ, Henske EP. Renal Disease in Tuberous Sclerosis Complex: Pathogenesis and Therapy. *Nat Rev Nephrol* (2018) 14:704–16. doi: 10.1038/s41581-018-0059-6
3. Rakowski SK, Winterkorn EB, Paul E, Steele DJ, Halpern EF, Thiele EA. Renal Manifestations of Tuberous Sclerosis Complex: Incidence, Prognosis, and Predictive Factors. *Kidney Int* (2006) 70:1777–82. doi: 10.1038/sj.ki.5001853
4. Shepherd CW, Gomez MR, Lie JT, Crowson CS. Causes of Death in Patients With Tuberous Sclerosis. *Mayo Clin Proc* (1991) 66:792–6. doi: 10.1016/s0025-6196(12)61196-3
5. Bjornsson J, Short MP, Kwiatkowski DJ, Henske EP. Tuberous Sclerosis-Associated Renal Cell Carcinoma. Clinical, Pathological, and Genetic Features. *Am J Pathol* (1996) 149:1201–8.
6. Washecka R, Hanna M. Malignant Renal Tumors in Tuberous Sclerosis. *Urology* (1991) 37:340–3. doi: 10.1016/0090-4295(91)80261-5
7. Tyburczy ME, Jozwiak S, Malinowska IA, Chekaluk Y, Pugh TJ, Wu CL, et al. A Shower of Second Hit Events as the Cause of Multifocal Renal Cell Carcinoma in Tuberous Sclerosis Complex. *Hum Mol Genet* (2015) 24:1836–42. doi: 10.1093/hmg/ddu597
8. Guo J, Tretiakova MS, Troxell ML, Osunkoya AO, Fadare O, Sangoi AR, et al. Tuberous Sclerosis-Associated Renal Cell Carcinoma: A Clinicopathologic Study of 57 Separate Carcinomas in 18 Patients. *Am J Surg Pathol* (2014) 38:1457–67. doi: 10.1097/PAS.0000000000000248
9. Kubo M, Iwashita K, Oyachi N, Oyama T, Yamamoto T. Two Different Types of Infantile Renal Cell Carcinomas Associated With Tuberous Sclerosis. *J Pediatr Surg* (2011) 46:E37–41. doi: 10.1016/j.jpedsurg.2011.06.035
10. Northrup H, Krueger DA. Tuberous Sclerosis Complex Diagnostic Criteria Update: Recommendations of the 2012 Iinternational Tuberous Sclerosis Complex Consensus Conference. *Pediatr Neurol* (2013) 49:243–54. doi: 10.1016/j.pediatrneurol.2013.08.001
11. Yang P, Cornejo KM, Sadow PM, Cheng L, Wang M, Xiao Y, et al. Renal Cell Carcinoma in Tuberous Sclerosis Complex. *Am J Surg Pathol* (2014) 38:895–909. doi: 10.1097/PAS.0000000000000237

Conflict of Interest: The authors declare that the research was conducted in the absence of any commercial or financial relationships that could be construed as a potential conflict of interest.

frontiers in Oncology

ORIGINAL RESEARCH
published: 20 May 2021
doi: 10.3389/fonc.2021.693684

PSA Density Help to Identify Patients With Elevated PSA Due to Prostate Cancer Rather Than Intraprostatic Inflammation: A Prospective Single Center Study

Salvatore M. Bruno[1], Ugo G. Falagario[1], Nicola d'Altilia[1], Marco Recchia[1], Vito Mancini[1], Oscar Selvaggio[1], Francesca Sanguedolce[2], Francesco Del Giudice[3], Martina Maggi[3], Matteo Ferro[4], Angelo Porreca[5], Alessandro Sciarra[3], Ettore De Berardinis[3], Carlo Bettocchi[1], Gian Maria Busetto[1], Luigi Cormio[1] and Giuseppe Carrieri[1]*

[1] Department of Urology and Renal Transplantation, University of Foggia, Foggia, Italy, [2] Department of Pathology, University of Foggia, Foggia, Italy, [3] Department of Urology, Sapienza Rome University, Rome, Italy, [4] Department of Urology, European Institute of Oncology (IEO) IRCCS, Milan, Italy, [5] Department of Urology, Veneto Institute of Oncology (IOV) IRCCS, Padua, Italy

OPEN ACCESS

Edited by:
Andrea Mari,
Careggi University Hospital, Italy

Reviewed by:
Riccardo Tellini,
Careggi University Hospital, Italy
Judith Stangl-Kremser,
Medical University of Vienna, Austria

***Correspondence:**
Gian Maria Busetto
gianmaria.busetto@unifg.it

Specialty section:
This article was submitted to Genitourinary Oncology, a section of the journal Frontiers in Oncology

Received: 11 April 2021
Accepted: 30 April 2021
Published: 20 May 2021

Citation:
Bruno SM, Falagario UG, d'Altilia N, Recchia M, Mancini V, Selvaggio O, Sanguedolce F, Del Giudice F, Maggi M, Ferro M, Porreca A, Sciarra A, De Berardinis E, Bettocchi C, Busetto GM, Cormio L and Carrieri G (2021) PSA Density Help to Identify Patients With Elevated PSA Due to Prostate Cancer Rather Than Intraprostatic Inflammation: A Prospective Single Center Study. Front. Oncol. 11:693684. doi: 10.3389/fonc.2021.693684

The association between PSA density, prostate cancer (PCa) and BPH is well established. The aim of the present study was to establish whether PSA density can be used as a reliable parameter to predict csPCa and to determine its optimal cutoff to exclude increased PSA levels due to intraprostatic inflammation. This is a large prospective single-center, observational study evaluating the role of PSA density in the discrimination between intraprostatic inflammation and clinically significant PCa (csPCa). Patients with PSA ≥ 4 ng/ml and/or positive digito-rectal examination (DRE) and scheduled for prostate biopsy were enrolled. Prostatic inflammation (PI) was assessed and graded using the Irani Scores. Multivariable binary logistic regression analysis was used to assess if PSA density was associated with clinically significant PCa (csPCa) rather than prostatic inflammation. A total of 1988 patients met the inclusion criteria. Any PCa and csPCa rates were 47% and 24% respectively. In the group without csPCa, patients with prostatic inflammation had a higher PSA (6.0 vs 5.0 ng/ml; p=0.0003), higher prostate volume (58 vs 52 cc; p<0.0001), were more likely to have a previous negative biopsy (29% vs 21%; p=0.0005) and a negative DRE (70% vs 65%; p=0.023) but no difference in PSA density (0.1 vs 0.11; p=0.2). Conversely in the group with csPCa, patients with prostatic inflammation had a higher prostate volume (43 vs 40 cc; p=0.007) but no difference in the other clinical parameters. At multivariable analysis adjusting for age, biopsy history, DRE and prostate volume, PSA density emerged as a strong predictor of csPCA but was not associated with prostatic inflammation. The optimal cutoffs of PSA density to diagnose csPCa and rule out the presence of prostatic inflammation in patients with an elevated PSA (>4 ng/ml) were 0.10 ng/ml^2 in biopsy naïve patients and 0.15 ng/ml^2 in patients with a previous negative biopsy. PSA density

rather than PSA, should be used to evaluate patients at risk of prostate cancer who may need additional testing or prostate biopsy. This readily available parameter can potentially identify men who do not have PCa but have an elevated PSA secondary to benign conditions.

Keywords: PSA density, PSA, prostate cancer, Irani score, prostate inflammation

INTRODUCTION

"There is moderate certainty that the benefits of prostate-specific antigen (PSA)-based screening for prostate cancer (PCa) do not outweigh the harms". In 2012, based on the results of two large-scale randomized clinical trials (RCT's), the United States Preventive Services Task Force (USPSTF) issued a grade D recommendation discouraging PSA-based screening (1). Since this strategy could lead to a substantial number of men with aggressive disease being missed, the USPSTF issued an updated statement in 2017. While the grade of recommendation remained unchanged for men over 70 years old, it has been changed from D to C in men aged 55-69 years old. PSA testing should be offered to selected man depending on individual circumstances and counseling patients about the potential benefits and harms of PSA-based screening, as this might be associated with a small survival benefit (2). Similarly, European association of urology (EAU) Guidelines suggest offering an individualized risk-adapted strategy for early detection to a well-informed man and a life-expectancy of at least 10 to 15 years (3).

The major limitations of screening using PSA have been underlined in a Cochrane review of five available RCT's. Screening is associated with an increased diagnosis of PCa, with detection of more localized disease and less advanced PCa with no benefit on PCa-specific and overall survival (4).

Still, screening for PCa is one of the most controversial topics in the urological literature. PSA is not specific for PCa. Several other benign conditions can cause a man's PSA level to rise such as inflammation and benign prostatic hyperplasia (BPH). To date there is no evidence that inflammation or BPH leads to prostate cancer, but it is possible for a man to have one or both conditions and to develop PCa as well.

In this scenario PSA density, expressed as the PSA value (in ng/ml) divided by prostate volume (in CC), can potentially identify men who do not have PCa but have an elevated PSA secondary to benign conditions.

The association between PSA density, PCa and BPH is well established (5, 6). The aim of the present study was to establish whether PSA density can be used as a reliable parameter to predict csPCa and to determine its optimal cutoff to exclude increased PSA levels due to intraprostatic inflammation.

MATERIALS AND METHODS

Study Population

This is a prospective single center, observational study evaluating the role of intraprostatic inflammation in prostate cancer screening and treatment. From March 2014 to December 2019, all patients referred to our institution to perform prostate biopsy (PBx) for a PSA ≥ 4 ng/ml and/or positive digital rectal examination (DRE) were enrolled, and data were prospectively entered into our database. Sample size was not computed *a priori* and according to the protocol we enrolled all eligible patients during the study period. Patients on active surveillance with a previous positive biopsy (n=87), men receiving 5 alfa-reductase inhibitors (5-ARIs) (n=65), or who had previously undergone invasive treatment for BPH (n=36), or with dwelling urethral catheters (n=22) and man with PSA > 20 ng/ml (n=96) were excluded. The study protocol was approved by the University of Foggia Ethics Committee and written informed consent to take part was given by all participants (Decision n. 152/CE/2014 of September 03, 2014; Ethical Committee at the University Hospital "Ospedali Riuniti", Foggia, Italy).

All patients underwent PSA measurement before DRE and transrectal ultrasound (TRUS). Uroflowmetry (UFM) was carried out with "Flowline II" before PBx, waiting for the patient to report a strong sensation to void. Peak flow rate (Qmax) and ultrasound post void residual volume (PVR) were annotated. Additionally, all patients filled the International Prostate Symptom Score (IPSS) survey (7). Following local non-infiltrative anesthesia (8), prostate biopsy was performed according to our 18 cores standard biopsy template (9) under TRUS guidance (BK Medical Flex Focus 500) and using an 18 gauge/25 cm biopsy needle (Bard Max-Core). As per our protocol, patients had a single shot of cefazolin right before the procedure or a course of quinolones or cotrimoxazole starting the night before the procedure.

Pathological Examination

A senior uropathologist (FS) prospectively evaluated all PBx specimens according to the International Society of Urological Pathology (ISUP) recommendations (10). Additionally, prostatic inflammation (PI) was assessed and graded using the Irani Scores (5) subsequently validated by Sciarra et al. (11). Specifically, the inflammatory infiltration was graded as "G0" = no inflammatory cells, "G1" = scattered inflammatory cell infiltrate within the stroma without lymphoid nodules, "G2" = nonconfluent lymphoid nodules and "G3" = large inflammatory areas with confluence of infiltrate. Inflammatory aggressiveness was graded as "A0" = no contact between inflammatory cells and glandular epithelium (epithelium cells lining acini and ducts), "A1" = contact between inflammatory cell infiltrate and glandular epithelium, "A2" = interstitial inflammatory infiltrate associated with a clear but limited (less than 25% of the examined material) glandular epithelium disruption and "A3" = glandular epithelium disruption on more than 25% of the examined material. Irani total score was computed as the sum of the Irani G and Irani A scores. Grading did not

include the types of inflammatory cells (polymorphonuclear leukocytes, lymphocytes, monocytes or plasma cells).

Statistical Analysis

Outcomes of this study were clinically significant PCa (csPCa) defined as Gleason Grade Group (GGG) ≥ 2(≥3+4) and presence of prostatic inflammation defined as Irani total score ≥2. Variables of interest were available in all patients included in the study.

Descriptive statistics was performed for the overall population and according to biopsy results. Continuous variables were reported as median and interquartile range and compared by the Mann-Whitney U-test, whereas categorical variables were reported as rates and tested by the Fisher's exact test or the chi-square test, as appropriate.

Since inflammation and csPCa often coexists, we stratified patients in four groups (both present, both absent, prostatic inflammation without csPCa and csPCa without inflammation) and we compared clinical characteristics in patients with and without inflammation but no csPCa, and patients with and without inflammation but diagnosed with csPCa. Multivariable binary logistic regression analysis was then used to assess if PSA density was associated with csPCa rather than prostatic inflammation. Age, biopsy history, DRE and PSA density were included in the multivariable model. In order to provide clinicians with a readily available tool to evaluate risk of elevated PSA due to csPCa, rather than inflammation, we graphically presented the histological findings of patients with a PSA >4 ng/ml according to PSA density groups and biopsy history. Finally, the actual probability of biopsy-detected prostate cancer and prostatic inflammation for a given PSA density value were calculated using locally weighted scatterplot ("lowess") smoothing.

Statistical analyses were performed using Stata-SE 15 (StataCorp LP, College Station, TX, USA) using the following syntax: kwallis, chi2, logistic, graph bar. All tests were 2-sided with a significance level set at $p<0.05$.

RESULTS

Descriptive Characteristics of the Overall Population

A total of 1988 patients met the inclusion criteria. Clinical characteristics and histopathological results of the overall population and according to biopsy results are shown in **Table 1**. The majority of patients (78% n=1547) were biopsy naïve. Any PCa and csPCa rates were 47% and 24% respectively. High grade inflammation (Irani G 2-3) was present in 639 (32.1%) patients and 984 (49.5%) patients had highly aggressive inflammation (Irani A 1-2-3). Patients diagnosed with any PCa (GGG1) and csPCa (GGG≥2) were older, had greater PSA and PSA density suspicious DRE and Qmax, but lower prostate volume, PVR and IPSS than those without cancer. Interestingly, high- grade inflammation (Irani G 2-3) was significantly more common in patients with benign prostate than in those with any PCa and csPCa, and the same applied to highly aggressive inflammation (Irani A 1-2-3).

The distribution of mild (Irani total score 2-3) and high (Irani total score >3) prostatic inflammation according to GGG is graphed in **Figure 1** showing that these two conditions often coexist.

TABLE 1 | Clinical characteristics and histopathological results of the overall population and according to biopsy results.

Variable	Overall population N=1988	Negative Biopsy N=1045 (52.6%)	GGG 1 N=458 (23.0%)	GGG ≥2 N=485 (24.4%)	P Value
Age	67 (61, 72)	65 (60, 70)	67 (62, 72)	70 (65, 75)	<0.0001
PSA	6.0 (4.6, 8.7)	5.9 (4.6, 8.1)	5.6 (4.4, 8.5)	6.7 (5.0, 10.5)	<0.0001
Biopsy History, n (%)					
Biopsy Naive	1547 (77.8%)	745 (71.3%)	371 (81.0%)	431 (88.9%)	<0.0001
Prev. Negative	441 (22.2%)	300 (28.7%)	87 (19.0%)	54 (11.1%)	
DRE, n (%)					
Negative	1232 (62.0%)	724 (69.3%)	298 (65.1%)	210 (43.3%)	<0.0001
Suspicious	756 (38.0%)	321 (30.7%)	160 (34.9%)	275 (56.7%)	
Prostate volume	52 (38, 70)	60 (45, 80)	48 (35, 61)	41 (32, 57)	<0.0001
PSA density	0.12 (0.08, 0.18)	0.10 (0.07, 0.14)	0.13 (0.09, 0.18)	0.17 (0.11, 0.26)	<0.0001
Qmax, ml/s	14 (10, 20)	13 (10, 19)	14 (10, 20)	15 (10, 23)	0.001
PVR, ml	30 (1, 50)	30 (1, 50)	20 (1, 40)	20 (1, 40)	<0.0001
IPSS	9 (5, 16)	10 (6, 17)	8 (4, 13)	8 (4, 15)	<0.0001
Alpha blocker, n (%)					
No	1288 (64.8%)	636 (60.9%)	306 (66.8%)	346 (71.3%)	0.0002
Yes	700 (35.2%)	409 (39.1%)	152 (33.2%)	139 (28.7%)	
Irani G, n (%)					
0-1	1349 (67.9%)	644 (61.6%)	350 (76.4%)	355 (73.2%)	<0.0001
2-3	639 (32.1%)	401 (38.4%)	108 (23.6%)	130 (26.8%)	
Irani A, n (%)					
0	1004 (50.5%)	449 (43.0%)	277 (60.5%)	278 (57.3%)	<0.0001
1-2-3	984 (49.5%)	596 (57.0%)	181 (39.5%)	207 (42.7%)	
Irani Sum					
0-1	951 (47.8%)	421 (40.3%)	268 (58.5%)	262 (54.0%)	<0.0001
2-3	797 (40.1%)	465 (44.5%)	139 (30.3%)	193 (39.8%)	
>3	240 (12.1%)	159 (15.2%)	51 (11.1%)	30 (6.2%)	

Predictors of Prostatic Inflammation and csPCa

To evaluate specific predictors of prostatic inflammation (Irani score>1) we first divided the population in two groups based on the presence or absence of csPCa (**Table 2**). In the group without csPCa, patients with prostatic inflammation had a higher PSA (6.0 vs 5.0 ng/ml; p=0.0003), higher prostate volume (58 vs 52 cc; p<0.0001), were more likely to have a previous negative biopsy (29% vs 21%; p=0.0005) and a negative DRE (70% vs 65%; p=0.023) but no difference in PSA density (0.1 vs 0.11; p=0.2). Qmax, PVR and IPSS were slightly worse in patients with prostatic inflammation. Conversely in the group with csPCa, patients with prostatic inflammation had a higher prostate volume (43 vs 40 cc; p=0.007) but no difference in the other clinical parameters. At multivariable analysis adjusting for age, biopsy history and DRE, PSA density emerged as a strong predictor of csPCa (OR per 0.1 increase: 2.09; CI: 1.85, 2.35; p<0.001) but was not associated with prostatic inflammation (OR per 0.1 increase: 0.92; CI: 0.84, 1.01; p=0.073) (**Table 3**).

Histological Findings According to PSA Density

Figure 2 graphically present histological findings of man who underwent prostate biopsy for a PSA >4 ng/ml (n=1694) according to biopsy history. Biopsy naïve patients with a PSA density below 0.1, were more likely to be diagnosed with prostatic inflammation (Irani total score >1) rather than csPCa (51% vs 11%, p <0.001). Conversely the rate of patients with csPCa was much higher with a PSA density between 0.10 and 0.15 (22%) and above 0.15 (47%). Similar results were found in patients with a previous negative biopsy, however rates of patients with csPCa were lower at each PSA density cut-off and resulted 6%, 9% and 21% in patients with a PSA density below 0.10, between 0.10 and 0.15 and above 0.15 respectively (all p <0.01). According to these findings, the optimal cutoffs of PSA density to diagnose csPCa and rule out the presence of prostatic inflammation in patients with an elevated PSA (>4 ng/ml) were 0.10 ng/ml^2 in biopsy naïve patients and 0.15 ng/ml^2 in patients with a previous negative biopsy.

Using the locally weighted scatterplot smoothing method we further evaluated the association between PSA density, csPCa and prostatic inflammation. With increasing PSA density, the actual probability of csPCa increases while the likelihood of prostatic inflammation decreases (**Figure 3**).

DISCUSSION

A close correlation has been shown between prostate inflammation, BPH and csPCa.

The inflammatory process of the prostate through the release of cytokines and growth factors, promotes tissue injury, chronic immune response, and abnormal remodeling processes which can result in prostate enlargement and BPH as well as in malignant transformation of high proliferative cells (12).

In this scenario, several interesting findings emerged from our study. First of all, we found that prostatic inflammation and PCa are two conditions that often coexist. Although prostate tissue has been described in the past as an immunological desert, we

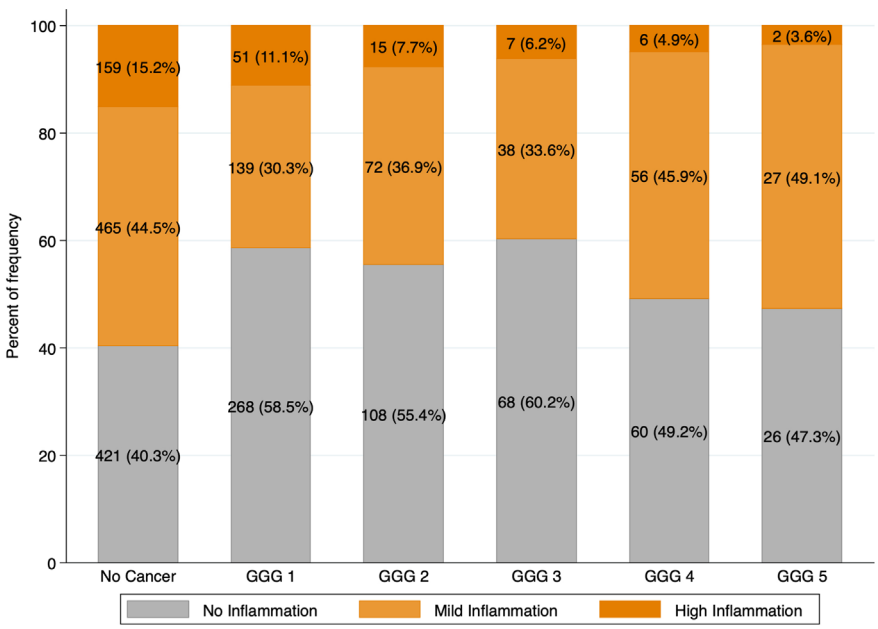

FIGURE 1 | Intraprostatic inflammation according to Prostate Cancer Gleason Grade Groups. Intraprostatic inflammation was graded using Irani total score and categorized in three groups: no inflammation (Irani Sum 0-1); mild inflammation (Irani Sum 2-3); high inflammation (Irani Sum >3).

TABLE 2 | Predictors of prostatic inflammation (Irani Score>1) in patients with and without csPCa.

	Negative Biopsy + GGG 1 PCa		P Value	csPCa (GGG≥2)		P Value
	IRANI Score 0-1 689 (34.7%)	IRANI Score >1 814 (40.9%)		IRANI Score 0-1 262 (13.2%)	IRANI Score >1 223 (11.2%)	
Age	66 (60, 70)	66 (60, 70)	0.5	70 (64, 75)	70 (65, 75)	0.3
PSA	5.5 (4.4, 7.8)	6.0 (4.6, 8.6)	**0.0003**	6.6 (4.7, 10.4)	7.0 (5.1, 10.8)	0.3
Biopsy History, n (%)						
Biopsy Naive	541 (78.5%)	575 (70.6%)	**0.0005**	237 (90.5%)	194 (87.0%)	0.2
Previous Neg.	148 (21.5%)	239 (29.4%)		25 (9.5%)	29 (13.0%)	
DRE, n (%)						
Negative	448 (65.0%)	574 (70.5%)	**0.023**	120 (45.8%)	90 (40.4%)	0.2
Suspicious	241 (35.0%)	240 (29.5%)		142 (54.2%)	133 (59.6%)	
Volume, cc	52 (40, 69)	58 (43, 80)	**<0.0001**	40 (30, 55)	43 (34, 60)	**0.007**
PSA density	0.11 (0.08, 0.16)	0.10 (0.07, 0.16)	0.2	0.18 (0.11, 0.26)	0.16 (0.11, 0.26)	0.3
Qmax, ml/s	14 (11, 21)	13 (10, 19)	**0.004**	16 (10, 25)	15 (10, 22)	0.3
PVR, ml	22 (1, 50)	30 (1, 50)	**0.005**	20 (1, 40)	20 (1, 40)	0.5
IPSS	9 (5, 16)	10 (5, 17)	**0.029**	8 (4, 15)	9 (5, 15)	0.2
α blocker, n (%)	242 (35.1%)	319 (39.2%)	0.10	70 (26.7%)	69 (30.9%)	0.3
Bx GGG, n (%)						
Negative	421 (61.1%)	624 (76.7%)	**<0.0001**	N/A	N/A	
GGG 1	268 (38.9%)	190 (23.3%)		N/A	N/A	

Bold means statistically significant.

TABLE 3 | Univariable and Multivariable analysis to evaluate predictors of intraprostatic inflammation and clinically significant prostate cancer in the overall population (N=1988).

Covariate	Multivariable analysis predicting Intraprostatic inflammation			Multivariable analysis predicting csPCa		
	OR	95% CI	P>|z|	OR	95% CI	P>|z|
Age, per y	1.01	0.99,1.02	0.328	1.08	1.06,1.10	**<0.001**
Biopsy History						
Biopsy Naive	Ref.			Ref.		
Previous Neg.	1.55	1.25,1.92	**<0.001**	0.32	0.23,0.44	**<0.001**
DRE						
Negative	Ref.			Ref.		
Suspicious	0.85	0.71,1.03	0.097	2.21	1.76,2.78	**<0.001**
PSA density, per 0.1	0.92	0.84,1.01	0.073	2.09	1.85,2.35	**<0.001**

Intraprostatic inflammation was defined as Irani total score >1.
Bold means statistically significant.

found that patients with csPCa have moderate and severe inflammation in 30-50% and 5-10%, respectively.

The inflammatory process of the prostate through the release of cytokines and growth factors, promotes tissue injury, chronic immune response, and abnormal remodeling processes (12).

Preclinical studies provide a biological rationale for the association between inflammation and the risk of PCa, however clinical investigations report conflicting results. A recent meta-analysis of 25 studies involving a total of 20585 patients of whom 6641 with PCa demonstrated an inverse relationship between prostate inflammation on biopsy needle and malignant disease (6).

Similarly, in our previous publications we demonstrated that prostatic inflammation is a common finding in prostate biopsy samples, it is associated with benign prostatic obstruction rather than PCa (13) and can be used as a risk stratification tool in patients with a diagnosis of low to intermediate risk of PCa. Indeed, high grade inflammation was associated with a lower risk of upgrading and upstaging in patients undergoing radical prostatectomy (14). Since high grade prostatic inflammation is also associated with higher PSA levels and higher prostate volume, one of the possible explanations to these findings might be the role of prostatic inflammation as a confounding factor in the diagnosis of PCa. On the other side, prostatic inflammation may result in worse LUTS due to prostate enlargement and bladder outlet obstruction resulting in patient's referral for urological evaluation. What we face here is the question of which comes first, the chicken or the egg. Either way prostatic inflammation and BHP parameters demonstrated an inverse correlation with PCa diagnosis (15–17) and with the present study we sought to determine the potential role of PSA density to rule out the presence of PI and benign disease in patients at risk of PCa. We found that PSA density is not affected by the presence of prostatic inflammation while, the actual probability of csPCa increases with increasing PSA density. Although this is, to the best of our knowledge, the first study focusing on PSA density and histologically confirmed prostatic inflammation, several studies corroborate our findings pointing out that PSA density outperform PSA alone in the prediction of

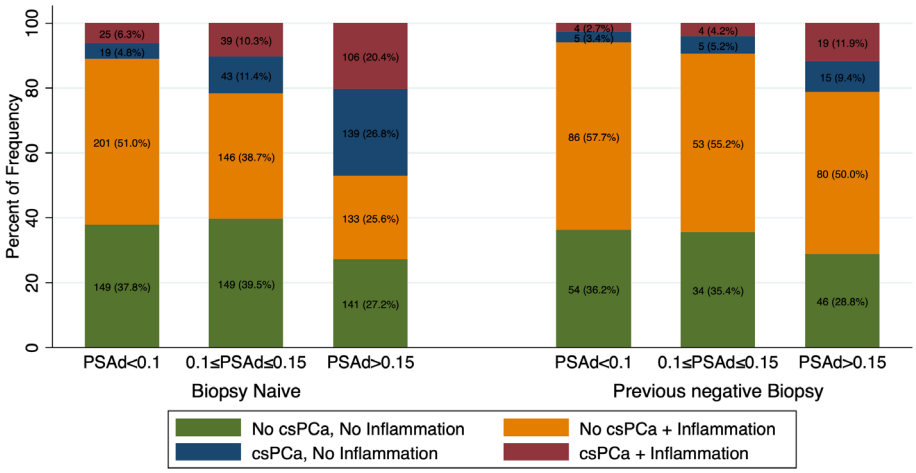

FIGURE 2 | Bar graph showing frequency and rates of csPCa and Inflammation according to PSA density (PSAd) and biopsy history in patients with a PSA>4ng/ml (n=1694). Patients were stratified in four groups according to presence or absence of inflammation and csPCa: both present, both absent, intraprostatic inflammation without csPCa and csPCa without inflammation.

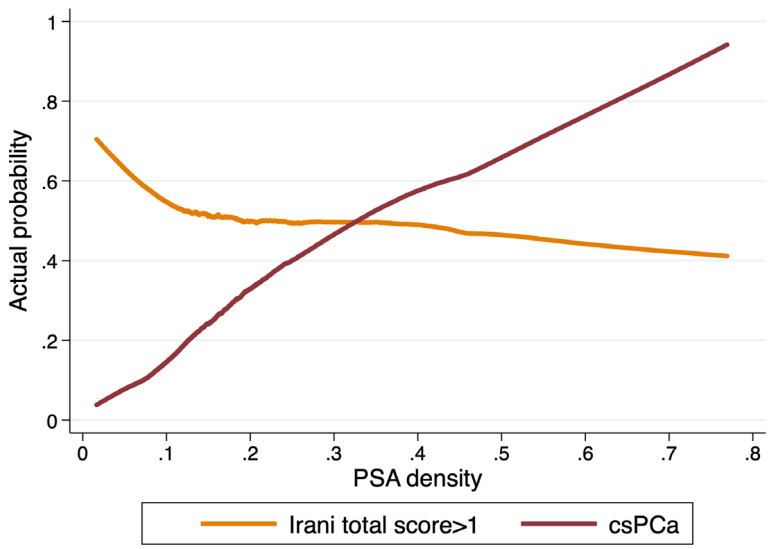

FIGURE 3 | Actual probability of csPCa and prostatic inflammation (Irani score>1) in prostate biopsy samples according to PSA density in patients with PSA>4ng/ml (n=1694).

csPCa. In a study including 1290 patients, Jue et al. showed that PSA density outperformed total PSA in the diagnosis of csPCa both in patients with a PSA in the "gray zone" (between 4 and 10 ng/ml) and in patients with PSA > 10 mg/ml. The difference in the predictive accuracy of PSA and PSA density was even higher in patients with a previous negative PBx (18).

What is the optimal cut-off of PSA density to suggest a prostate biopsy is still unclear. A PSA density cut-off of 0.15 ng/ml^2 was suggested in previous studies (3). However, Nordström et al. showed that a PSA density cutoff of 0.10 and 0.15 ng/ml^2 resulted in detection of only 77% and 49% of csPCa. Conversely, omitting prostate biopsy for men with PSA density ≤0.07 ng/ml^2 would save 19.7% of biopsy procedures, while missing 6.9% of csPCa (19). In the present study, stratifying the population according to biopsy history, we showed that the optimal cutoffs of PSA density to rule out the presence of prostatic inflammation in patients with an elevated PSA (>4 ng/ml) were 0.10 ng/ml^2 in biopsy naïve patients and 0.15 ng/ml^2 in patients with a previous negative biopsy.

Still, PSA density it has not been incorporated into the early detection guidelines as a baseline measure because of the lack of

precision of both PSA and prostate volume measurements using transrectal ultrasound.

MRI helped to overcome this limitation and recent studies pointed out that the combination of MRI parameters and PSA density could help to predict not only prostate biopsy results (20, 21), but also active surveillance outcomes (22), adverse pathologic features at RP (23) and biochemical recurrence after surgical treatment (24).

While several blood and urine biomarkers and imaging techniques have been developed to predict PCa (25, 26), as far as we know no biomarker is available for the diagnosis of prostate inflammation. At a time when immunotherapy is taking hold, the identification of cases with prostatic inflammation is of considerable interest for targeted immunological therapies (27).

The present study has few limitations. First, this is a single center study and histological evaluation was carried out by a single dedicated genitourinary pathologist. Even if the IRANI score is a validated score, a certain degree of interobserver variability may exist and limit the generalizability of our findings. Additionally, most patients underwent prostate biopsy without a prebiopsy MRI. The potential utility of MRI to rule out the presence of prostatic inflammation, as well as MRI diagnostic accuracy in patients with and without prostate inflammation should be further evaluated. Finally, we enrolled in the present study only patients in whom the clinical suspicion of PCa was deemed enough to perform PBx. While this may represent a potential source of inclusion bias, performing PBx in patients with low risk of PCa would be unethical.

Prostatic inflammation is a common cause of increased PSA. PSA density rather than PSA, should be used to evaluate patients at risk of prostate cancer who may need additional testing or prostate biopsy. This readily available parameter can potentially identify men who do not have PCa but have an elevated PSA secondary to benign conditions.

DATA AVAILABILITY STATEMENT

The raw data supporting the conclusions of this article will be made available by the authors, without undue reservation.

ETHICS STATEMENT

The study was approved by the local Ethical Committee (Ethical Committee at the University Hospital "Ospedali Riuniti", Foggia, Italy) and was carried out in agreement with the provisions of the Helsinki Declaration held in 1995. The patients/participants provided their written informed consent to participate in this study.

AUTHOR CONTRIBUTIONS

UF, SB, GB: study concept and design. Nd'A, FS, OS, VM: acquisition of data. VM, OS, UF, FG, MM: analysis and interpretation of data. UF: statistical analysis. SB, MR, GB: drafting and reviewing the paper. LC, GC, AS, EB, AP, MF, CB: supervision. All authors contributed to the article and approved the submitted version.

FUNDING

This paper has been published with the financial support of the Dept. of Medical and Surgical Sciences of the University of Foggia.

REFERENCES

1. Moyer VA, Force U.S.P.S.T. Screening for Prostate Cancer: U.S. Preventive Services Task Force Recommendation Statement. *Ann Intern Med* (2012) 157:120–34. doi: 10.7326/0003-4819-157-2-201207170-00459
2. Force U.S.P.S.T, Grossman DC, Curry SJ, Owens DK, Bibbins-Domingo K, Caughey AB, et al. Screening for Prostate Cancer: US Preventive Services Task Force Recommendation Statement. *JAMA* (2018) 319:1901–13. doi: 10.1001/jama.2018.3710
3. Mottet N, van den Bergh RCN, Briers E, Cornford P, De Santis M, Fanti S, et al. Eau - ESTRO - ESUR - SIOG Guidelines on Prostate Cancer 2020. In: . *European Association of Urology Guidelines. 2020 Edition*. Arnhem, The Netherlands: European Association of Urology Guidelines Office (2020). presented at the EAU Annual Congress Amsterdam 2020.
4. Ilic D, Neuberger MM, Djulbegovic M, Dahm P. Screening for Prostate Cancer. *Cochrane Database Syst Rev* (2013) (1):CD004720. doi: 10.1002/14651858.CD004720.pub3
5. Irani J, Levillain P, Goujon JM, Bon D, Dore B, Aubert J. Inflammation in Benign Prostatic Hyperplasia: Correlation With Prostate Specific Antigen Value. *J Urol* (1997) 157:1301–3. doi: 10.1016/S0022-5347(01)64957-7
6. Vasavada SR, Dobbs RW, Kajdacsy-Balla AA, Abern MR, Moreira DM. Inflammation on Prostate Needle Biopsy is Associated With Lower Prostate Cancer Risk: A Meta-Analysis. *J Urol* (2018) 199:1174–81. doi: 10.1016/j.juro.2017.11.120
7. Cicione A, Cormio L, Cantiello F, Palumbo IM, D.E.N C, Lima E, et al. Presence and Severity of Lower Urinary Tract Symptoms are Inversely Correlated With the Risk of Prostate Cancer on Prostate Biopsy. *Minerva Urol Nefrol* (2017) 69:486–92. doi: 10.23736/S0393-2249.17.02737-0
8. Cormio L, Pagliarulo V, Lorusso F, Selvaggio O, Perrone A, Sanguedolce F, et al. Combined Perianal-Intrarectal (PI) Lidocaine-Prilocaine (LP) Cream and Lidocaine-Ketorolac Gel Provide Better Pain Relief Than Combined PI LP Cream and Periprostatic Nerve Block During Transrectal Prostate Biopsy. *BJU Int* (2012) 109:1776–80. doi: 10.1111/j.1464-410X.2011.10622.x
9. Cormio L, Scattoni V, Lorusso F, Perrone A, Di Fino G, Selvaggio O, et al. Prostate Cancer Detection Rates in Different Biopsy Schemes. Which Cores for Which Patients? *World J Urol* (2014) 32:341–6. doi: 10.1007/s00345-012-0989-8
10. Epstein JI, Egevad L, Amin MB, Delahunt B, Srigley JR, Humphrey PA, et al. The 2014 International Society of Urological Pathology (Isup) Consensus Conference on Gleason Grading of Prostatic Carcinoma: Definition of Grading Patterns and Proposal for a New Grading System. *Am J Surg Pathol* (2016) 40:244–52. doi: 10.1097/PAS.0000000000000530
11. Sciarra A, Di Silverio F, Salciccia S, Autran Gomez AM, Gentilucci A, Gentile V. Inflammation and Chronic Prostatic Diseases: Evidence for a Link? *Eur Urol* (2007) 52:964–72. doi: 10.1016/j.eururo.2007.06.038
12. Gandaglia G, Zaffuto E, Fossati N, Cucchiara V, Mirone V, Montorsi F, et al. The Role of Prostatic Inflammation in the Development and Progression of Benign and Malignant Diseases. *Curr Opin Urol* (2017) 27:99–106. doi: 10.1097/MOU.0000000000000369
13. Falagario U, Selvaggio O, Carrieri G, Barret E, Sanguedolce F, Cormio L. Prostatic Inflammation is Associated With Benign Prostatic Hyperplasia Rather Than Prostate Cancer. *J Gerontol Geriatr* (2018) 2018:178–82.

14. Sanguedolce F, Falagario UG, Castellan P, Di Nauta M, Silecchia G, Bruno SM, et al. Bioptic Intraprostatic Chronic Inflammation Predicts Adverse Pathology At Radical Prostatectomy in Patients With Low-Grade Prostate Cancer. *Urol Oncol* (2020) 38(10):793.e19–e25. doi: 10.1016/j.urolonc.2020.02.025
15. Cormio L, Lucarelli G, Selvaggio O, Di Fino G, Mancini V, Massenio P, et al. Absence of Bladder Outlet Obstruction is an Independent Risk Factor for Prostate Cancer in Men Undergoing Prostate Biopsy. *Med (Baltimore)* (2016) 95:e2551. doi: 10.1097/MD.0000000000002551
16. Cormio L, Cindolo L, Troiano F, Marchioni M, Di Fino G, Mancini V, et al. Development and Internal Validation of Novel Nomograms Based on Benign Prostatic Obstruction-Related Parameters to Predict the Risk of Prostate Cancer At First Prostate Biopsy. *Front Oncol* (2018) 8:438. doi: 10.3389/fonc.2018.00438
17. Cormio L, Lucarelli G, Netti GS, Stallone G, Selvaggio O, Troiano F, et al. Post-Void Residual Urinary Volume is an Independent Predictor of Biopsy Results in Men At Risk for Prostate Cancer. *Anticancer Res* (2015) 35:2175–82.
18. Jue JS, Barboza MP, Prakash NS, Venkatramani V, Sinha VR, Pavan N, et al. Re-Examining Prostate-specific Antigen (Psa) Density: Defining the Optimal Psa Range and Patients for Using Psa Density to Predict Prostate Cancer Using Extended Template Biopsy. *Urology* (2017) 105:123–8. doi: 10.1016/j.urology.2017.04.015
19. Nordstrom T, Akre O, Aly M, Gronberg H, Eklund M. Prostate-Specific Antigen (PSA) Density in the Diagnostic Algorithm of Prostate Cancer. *Prostate Cancer Prostatic Dis* (2018) 21:57–63. doi: 10.1038/s41391-017-0024-7
20. Knaapila J, Jambor I, Perez IM, Ettala O, Taimen P, Verho J, et al. Prebiopsy IMPROD Biparametric Magnetic Resonance Imaging Combined With Prostate-Specific Antigen Density in the Diagnosis of Prostate Cancer: An External Validation Study. *Eur Urol Oncol* (2020) 3(5):648–56. doi: 10.1016/j.euo.2019.08.008
21. Distler FA, Radtke JP, Bonekamp D, Kesch C, Schlemmer HP, Wieczorek K, et al. The Value of PSA Density in Combination With PI-RADS for the Accuracy of Prostate Cancer Prediction. *J Urol* (2017) 198:575–82. doi: 10.1016/j.juro.2017.03.130
22. Tosoian JJ, Mamawala M, Epstein JI, Landis P, Macura KJ, Simopoulos DN, et al. Active Surveillance of Grade Group 1 Prostate Cancer: Long-term Outcomes From a Large Prospective Cohort. *Eur Urol* (2020) 77:675–82. doi: 10.1016/j.eururo.2019.12.017
23. Lantz A, Falagario UG, Ratnani P, Jambor I, Dovey Z, Martini A, et al. Expanding Active Surveillance Inclusion Criteria: A Novel Nomogram Including Preoperative Clinical Parameters and Magnetic Resonance Imaging Findings. *Eur Urol Oncol* (2020) S2588-9311(20):30125–5. doi: 10.1016/j.euo.2020.08.001
24. Jambor I, Falagario U, Ratnani P, Perez IM, Demir K, Merisaari H, et al. Prediction of Biochemical Recurrence in Prostate Cancer Patients Who Underwent Prostatectomy Using Routine Clinical Prostate Multiparametric MRI and Decipher Genomic Score. *J Magn Reson Imaging* (2019) 51(4):1075–85. doi: 10.1002/jmri.26928
25. Falagario UG, Busetto GM, Netti GS, Sanguedolce F, Selvaggio O, Infante B, et al. Prospective Validation of Pentraxin-3 as a Novel Serum Biomarker to Predict the Risk of Prostate Cancer in Patients Scheduled for Prostate Biopsy. *Cancers (Basel)* (2021) 13(7):1211. doi: 10.3390/cancers13071611
26. Falagario UG, Martini A, Wajswol E, Treacy PJ, Ratnani P, Jambor I, et al. Avoiding Unnecessary Magnetic Resonance Imaging (MRI) and Biopsies: Negative and Positive Predictive Value of MRI According to Prostate-specific Antigen Density, 4Kscore and Risk Calculators. *Eur Urol Oncol* (2019) 3(5):700–4. doi: 10.1016/j.euo.2019.08.015
27. Cai T, Santi R, Tamanini I, Galli IC, Perletti G, Bjerklund Johansen TE, et al. Current Knowledge of the Potential Links Between Inflammation and Prostate Cancer. *Int J Mol Sci* (2019) 20(15):3833. doi: 10.3390/ijms20153833

Conflict of Interest: The authors declare that the research was conducted in the absence of any commercial or financial relationships that could be construed as a potential conflict of interest.

frontiers in Oncology

ORIGINAL RESEARCH
published: 25 May 2021
doi: 10.3389/fonc.2021.697955

Differential Impact of *TGFB1* Variation by Metastatic Status in Androgen-Deprivation Therapy for Prostate Cancer

Masaki Shiota[1], Naohiro Fujimoto[2], Takashi Matsumoto[1], Shigehiro Tsukahara[1,3], Shohei Nagakawa[1], Shohei Ueda[1], Miho Ushijima[1], Eiji Kashiwagi[1], Ario Takeuchi[1], Junichi Inokuchi[1], Takeshi Uchiumi[3] and Masatoshi Eto[1]*

[1] Department of Urology, Kyushu University, Fukuoka, Japan, [2] Department of Urology, School of Medicine, University of Occupational and Environmental Health, Kitakyushu, Japan, [3] Department of Clinical Chemistry and Laboratory Medicine, Graduate School of Medical Sciences, Kyushu University, Fukuoka, Japan

OPEN ACCESS

Edited by:
Kouji Izumi,
Kanazawa University, Japan

Reviewed by:
Takeshi Sasaki,
Mie University, Japan
Daisuke Obinata,
Nihon University, Japan

***Correspondence:**
Masaki Shiota
shiota.masaki.101@m.kyushu-u.ac.jp

Specialty section:
This article was submitted to Genitourinary Oncology, a section of the journal Frontiers in Oncology

Received: *20 April 2021*
Accepted: *28 April 2021*
Published: *25 May 2021*

Citation:
Shiota M, Fujimoto N, Matsumoto T, Tsukahara S, Nagakawa S, Ueda S, Ushijima M, Kashiwagi E, Takeuchi A, Inokuchi J, Uchiumi T and Eto M (2021) Differential Impact of TGFB1 Variation by Metastatic Status in Androgen-Deprivation Therapy for Prostate Cancer. Front. Oncol. 11:697955. doi: 10.3389/fonc.2021.697955

Transforming growth factor-β1 (TGF-β1) plays a dual role in cancer, acting as a tumor suppressor in the early stage of cancer development and as a tumor promoter in the later stage of cancer progression in various cancers. In this study, we investigated the association between genetic polymorphisms in *TGFB1* and clinicopathological characteristics or oncological outcome in prostate cancer cases treated with androgen-deprivation therapy (ADT) according to metastasis status. Japanese male patients with hormone-sensitive prostate cancer treated with ADT from 1993 to 2005 were included in this study. Genomic DNA was obtained from whole blood samples, and genotyping of *TGFB1* (rs2241716 and rs4803455) was performed by PCR-based technique. No significant association between genetic polymorphisms in *TGFB1* (rs2241716 and rs4803455) and clinicopathological parameters or prognosis was observed in patients with non-metastatic disease. In patients with metastatic disease, Gleason score in CT/TT carriers (rs2241716) and CA/AA carriers (rs4803455) was unfavorable compared with CC carriers. In addition, the CT/TT alleles in rs2241716 (hazard ratio, 1.82; 95% confidence interval, 1.12–2.94; P = 0.015) and the CA/AA alleles in rs4803455 (hazard ratio, 1.75; 95% confidence interval, 1.03–2.98; P = 0.040) were associated with a higher risk of progression during ADT compared with the CC allele in patients with metastatic disease. *TGFB1* genetic variations were associated with adverse characteristics and progression risk in ADT among patients with metastatic disease, but not those with non-metastatic disease, supporting a distinct role of TGF-β signaling between non-metastatic and metastatic prostate cancer.

Keywords: androgen-deprivation therapy, metastasis, prostate cancer, SNP, TGFB1

INTRODUCTION

Although most prostate cancer cases primarily respond to androgen-deprivation therapy (ADT), most of them eventually progress to castration-resistant prostate cancer (CRPC) (1). The aberrant activation of androgen receptor (AR) signaling, despite low levels of serum androgen, has been revealed to be critical in the progression to CRPC (2). Recently, intensive up-front therapies using docetaxel or novel AR-pathway inhibitors for metastatic hormone-sensitive prostate cancer have been proven to prolong survival and become standard therapy (3–5). However, although several risk models have been developed to estimate patient prognosis, it has been difficult to precisely predict the survival (3, 4, 6, 7).

Metastasis is the critical step for cancer progression, and the major cause of cancer-related mortality (8). Epithelial-mesenchymal transition (EMT) of cancer cells, which involves morphological and functional changes, is required for cells to metastasize to distant regions (9). Transforming growth factor-β1 (TGF-β1) is a pleiotropic polypeptide that forms multimeric complexes with two type I and two type II receptors and regulates various cellular functions such as differentiation, cellular proliferation, survival, apoptosis, migration, adhesion, angiogenesis, and immune surveillance (10). TGF-β1 has been shown to play a dual role in cancer, acting as a tumor suppressor in the early stage of cancer development and as a tumor promoter in the later stage of various cancers including prostate cancer (11). TGF-β signaling also interacts with EMT as well as AR signaling in prostate cancer, which may affect the therapeutic effect of ADT (12–15). Several studies have reported an association of genetic polymorphisms in *TGFB1*, which encodes TGF-β1, with cancer phenotypes in prostate cancer (16–19). Together, these findings suggest that genetic polymorphisms in *TGFB1* may be associated with cancer phenotypes in the early and later stages.

In this study, we investigated the association between genetic polymorphisms in *TGFB1* and clinicopathological characteristics or oncological outcomes in patients with prostate cancer during ADT by cancer stage.

PATIENTS AND METHODS

Patients

This study included Japanese patients with non-metastatic prostate cancer treated with primary ADT or salvage ADT for prostate-specific antigen (PSA) recurrence after definitive therapy with radical prostatectomy or radiotherapy to prostate (non-metastatic disease) as well as patients with *de novo* metastatic prostate cancer to distant sites treated with primary ADT (metastatic disease) at the University of Occupational and Environmental Health (Kitakyushu, Japan) and Kyushu University Hospital (Fukuoka, Japan) from 1993 to 2005, as described previously (20–22).

Clinical TNM staging was determined in accordance with the unified TNM criteria based on the results of digital rectal examination, transrectal ultrasound, magnetic resonance imaging, computed tomography, and bone scan (23). ADT was performed with surgical castration or continuous medical castration using a gonadotropin-releasing hormone agonist (goserelin acetate or leuprorelin acetate) and/or an antiandrogen agent (bicalutamide, flutamide, or chlormadinone acetate). Progressive disease was defined as an increase in serum PSA levels >2 ng/mL and a 25% increase over the nadir, the appearance of a new lesion, or the progression of one or more known lesions classified according to the Response Evaluation Criteria in Solid Tumors (24).

Written informed consent was obtained from all patients. Patients who chose not to participate in this study were excluded. This study was performed in accordance with the principles described in the Declaration of Helsinki and the Ethical Guidelines for Epidemiological Research enacted by the Japanese Government and was approved by each institutional review board.

Genotyping

Genomic DNA was extracted from whole blood samples from patients as previously described (20–22). Rs2241716 and rs4803455 were selected as representative single nucleotide polymorphisms of the *TGFB1* gene as described previously (20). Minimum minor allele frequency was set as 0.05 according to the HapMap database (http://hapmap.ncbi.nlm.nih.gov/index.html). Linkage disequilibrium analysis was performed with HaploView and the minimum r^2 threshold was set as 0.8. Genotyping of *TGFB1* (rs2241716 and rs4803455) was performed on a CFX Connect Real-Time System (Bio-Rad, Hercules, CA, USA) with pre-designed TaqMan SNP Genotyping Assays (C_15873887_10 and C_30031638_10, respectively; Life Technologies, Carlsbad, CA, USA) and TaqMan Gene Expression Master Mix (Life Technologies), according to the manufacturers' protocols.

Statistical Analyses

All statistical analyses were performed using JMP14 software (SAS Institute, Cary, NC, USA). Categorical and continuous data were analyzed by Pearson's chi-square and Wilcoxon rank sum tests, respectively. Survival analyses were conducted using the Kaplan–Meier method and the log-rank test. Univariate and multivariate analyses were performed using the Cox hazard proportional model to estimate hazard ratios (HRs). The differential prognostic value of *TGFB1* genotype was investigated through interaction tests. All *P*-values were two-sided. *P*-values < 0.05 were considered significant.

RESULTS

The clinical and pathological characteristics of the 101 prostate cancer patients with non-metastatic disease and 93 prostate cancer patients with metastatic disease included in this study are listed in **Tables 1** and **2**. In patients with non-metastatic disease, during the median follow-up for patients alive at the date of censor of 78 months (interquartile range [IQR], 44–114 months), 27 patients (26.7%) and 18 patients (17.8%) experienced progression and any-cause mortality, respectively. In patients with metastatic disease, during the median follow-up for patients alive at the date of censor of 70 months (IQR, 33–112 months), 78 patients (93.9%) and 55 patients (59.1%) experienced progression and any-cause mortality, respectively.

TABLE 1 | Clinicopathological characteristics of patients with non-metastatic prostate cancer according to TGFB1 polymorphisms.

Variables	*TGFB1* (rs2241716)			*TGFB1* (rs4803455)		
	CC (n = 44)	CT/TT (n = 57)	P-value	CC (n = 13)	CA/AA (n = 88)	P-value
Median age, years (IQR)	73 (69–77)	71 (65–77)	0.19	70 (61–75)	72 (67–77)	0.31
Median PSA at diagnosis, ng/ml (IQR)	17.3 (8.3–56.1)	9.3 (6.1–31.6)	0.078	12.8 (6.4–91.5)	14.0 (6.6–37.7)	0.96
Biopsy Gleason score, n (%)						
<8	28 (68.3%)	31 (67.4%)		6 (60.0%)	53 (68.8%)	
≥8	13 (31.7%)	15 (32.6%)	0.93	4 (40.0%)	24 (31.2%)	0.58
NA	3	11		3	11	
Clinical T-stage, n (%)						
cT1/2	24 (55.8%)	34 (66.7%)		5 (41.7%)	53 (64.6%)	
cT3/4	19 (44.2%)	17 (33.3%)	0.28	7 (58.3%)	29 (35.4%)	0.13
NA	1	6		1	6	
Clinical N-stage, n (%)						
cN0	39 (88.6%)	50 (89.3%)		10 (76.9%)	79 (90.8%)	
cN1	5 (11.4%)	6 (10.7%)	0.92	3 (23.1%)	8 (9.2%)	0.14
NA	0	1		0	1	
Therapeutic setting, n (%)						
Primary	24 (54.5%)	35 (61.4%)		8 (61.5%)	51 (58.0%)	
Salvage	20 (45.5%)	22 (38.6%)	0.49	5 (38.5%)	37 (42.0%)	0.81
Hormonal therapy						
Combined androgen blockade	16 (36.4%)	21 (36.8%)		5 (38.5%)	32 (36.4%)	
Castration	17 (38.6%)	25 (43.9%)		7 (53.8%)	35 (39.8%)	
Antiandrogen agent	11 (25.0%)	11 (19.3%)	0.77	1 (7.7%)	21 (23.9%)	0.38

IQR, interquartile range; PSA, prostate-specific antigen; NA, not available.

TABLE 2 | Clinicopathological characteristics of patients with metastatic prostate cancer according to TGFB1 polymorphisms.

Variable	*TGFB1* (rs2241716)			*TGFB1* (rs4803455)		
	CC (n = 38)	CT/TT (n = 55)	P-value	CC (n = 27)	CA/AA (n = 66)	P-value
Median age, years (IQR)	72 (66–78)	72 (67–76)	0.92	73 (66–77)	72 (67–77)	0.90
Median PSA level at diagnosis, ng/ml (IQR)	144 (62.5–458)	320 (93.4–1400)	0.032*	141 (63.0–566)	294 (87.8–972)	0.21
Biopsy Gleason score, n (%)						
<8	17 (47.2%)	11 (21.6%)		13 (52.0%)	15 (24.2%)	
≥8	19 (52.8%)	40 (78.4%)	0.012*	12 (48.0%)	47 (75.8%)	0.012*
NA	2	4		2	4	
Clinical T-stage, n (%)						
cT1/2	7 (21.9%)	2 (4.3%)		5 (20.8%)	4 (7.3%)	
cT3/4	25 (78.1%)	45 (95.7%)	0.016*	19 (79.2%)	51 (92.7%)	0.081
NA	6	8		3	11	
Clinical N-stage, n (%)						
N0	20 (62.5%)	20 (41.7%)		14 (58.3%)	26 (46.4%)	
N1	12 (37.5%)	28 (58.3%)	0.068	10 (41.7%)	30 (53.6%)	0.33
NA	6	7		3	10	
Hormonal therapy						
Combined androgen blockade	32 (84.2%)	52 (94.5%)		25 (92.6%)	59 (89.4%)	
Castration	6 (15.8%)	3 (5.5%)	0.098	2 (7.4%)	7 (10.6%)	0.64

**Statistically significant. IQR, interquartile range; PSA, prostate-specific antigen; NA, not available.*

We analyzed the association of genetic polymorphisms in *TGFB1* with clinicopathological characteristics and prognosis in patients with non-metastatic disease. Patient backgrounds were comparable in the two subgroups of *TGFB1* genotypes (rs2241716 and rs4803455) in patients with non-metastatic prostate cancer (**Table 1**). No significant association between genetic polymorphisms in *TGFB1* (rs2241716 and rs4803455) and prognosis including progression-free survival (PFS) and overall survival (OS) in patients with non-metastatic disease was observed (**Table 3**, **Supplementary Table 1** and **Figures 1A, B**).

We next analyzed the significance of *TGFB1* genotype among patients with metastatic prostate cancer in the same manner. Analysis of patient backgrounds revealed that PSA value at diagnosis in CT/TT carriers (rs2241716) was higher than that of CC carriers in patients with metastatic disease (**Table 2**). In addition, Gleason score in CT/TT carriers (rs2241716) and CA/AA carriers (rs4803455) was unfavorable compared with that in CC carriers in patients with metastatic disease (**Table 2**). Moreover, clinical T-stage in CT/TT carriers (rs2241716) was more advanced than that of CC carriers in patients with

TABLE 3 | Progression-free survival according to TGFB1 polymorphisms.

Variable	Non-metastatic disease				Metastatic disease			
	n	HR	95% CI	P-value	n	HR	95% CI	P-value
TGFB1 (rs2241716)								
CC	44	ref			38	ref		
CT	48	0.78	0.35–1.76	0.56	45	1.85	1.13–3.05	0.015*
TT	9	0.98	0.28–3.51	0.98	10	1.64	0.76–3.56	0.21
Dominant model								
CC	44	ref			38	ref		
CT/TT	57	0.82	0.38–1.76	0.61	55	1.82	1.12–2.94	0.015*
Recessive model								
CC/CT	92	ref			83	ref		
TT	9	1.12	0.33–3.73	0.86	10	1.16	0.57–2.34	0.68
TGFB1 (rs4803455)								
CC	13	ref			27	ref		
CA	58	0.47	0.18–122	0.12	48	1.71	0.98–2.98	0.059
AA	30	0.54	0.18–1.63	0.28	18	1.87	0.95–3.68	0.069
Dominant model								
CC	13	ref			27	ref		
CA/AA	88	0.49	0.20–1.22	0.13	66	1.75	1.03–2.98	0.040*
Recessive model								
CC/CA	71	ref			75	ref		
AA	30	0.97	0.41–2.31	0.95	18	1.32	0.76–2.28	0.32

**Statistically significant. CI, confidence interval; HR, hazard ratio.*

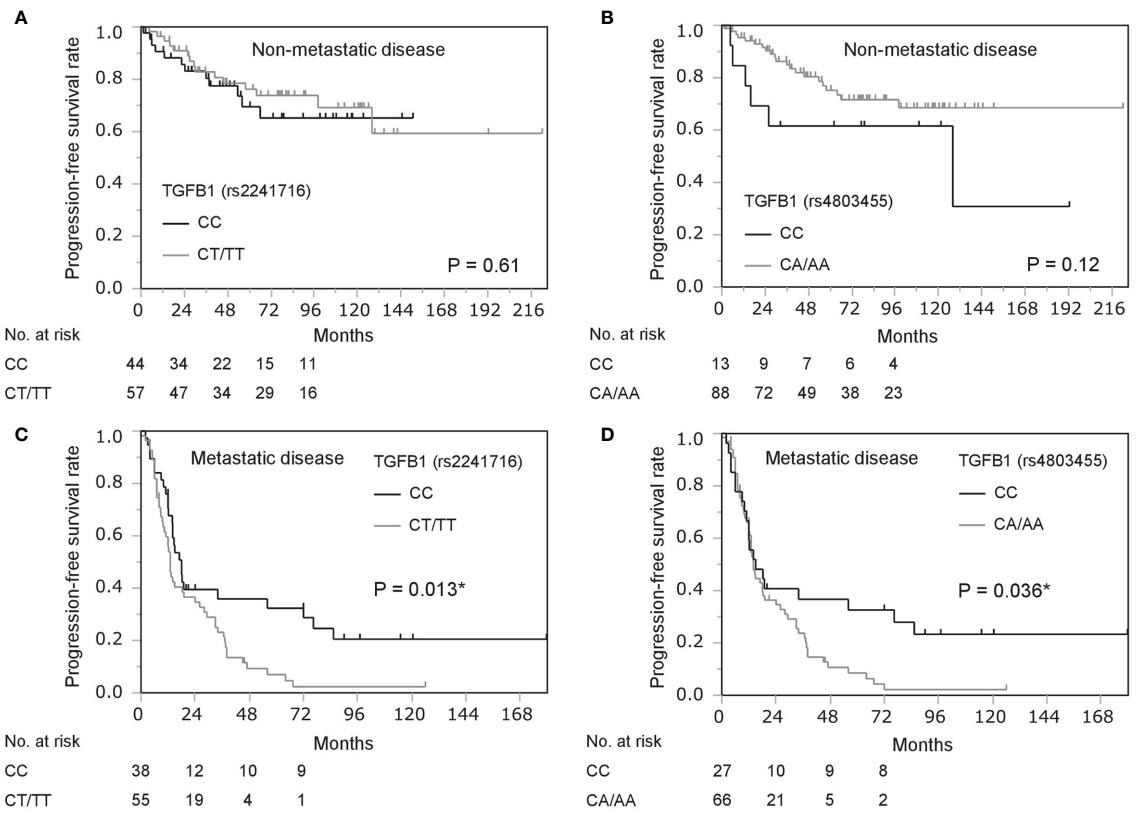

FIGURE 1 | Kaplan–Meier survival analysis of progression-free survival in prostate cancer patients stratified by gene polymorphisms in *TGFB1* (rs2241716 and rs4803455). **(A, B)** Progression-free survival in patients with non-metastatic disease by gene polymorphisms in *TGFB1* [rs2241716 **(A)** and rs4803455 **(B)**]. **(C, D)** Progression-free survival in patients with metastatic disease by gene polymorphisms in *TGFB1* [rs2241716 **(C)** and rs4803455 **(D)**]. *Statistically significant.

metastatic disease (**Table 2**). Consistent with these findings, the CT/TT alleles in rs2241716 (HR, 1.82; 95% confidence interval [CI], 1.12–2.94; $P = 0.015$) and the CA/AA alleles in rs4803455 (HR, 1.75; 95% CI, 1.03–2.98; $P = 0.040$) were associated with a higher risk of progression during ADT compared with that of the CC allele in patients with metastatic disease (**Table 3**). Similarly, Kaplan–Meier curve showed worse PFS among patients carrying the CT/TT alleles in rs2241716 and the CA/AA alleles in rs4803455 compared with patients carrying the CC allele (**Figures 1C, D**). However, when multivariate analyses incorporating PSA value, Gleason score, clinical T-stage for rs2241716, and Gleason score for rs4803455 were performed, the significance of the CT/TT alleles in rs2241716 (HR, 1.79; 95% CI, 0.98–3.27; $P = 0.057$) and the CA/AA alleles in rs2241716 (HR, 1.34; 95% CI, 0.76–2.35; $P = 0.31$) on PFS diminished. With regard to OS, there was no significant association between the genetic polymorphisms in *TGFB1* and mortality risk in patients with metastatic disease (**Supplementary Table 1**).

Finally, we analyzed the impact of *TGFB1* genotype on survival between patients with non-metastatic and metastatic diseases. Intriguingly, the dominant model of rs4803455 (CC vs. CA/AA; interaction test, P = 0.016) but not the dominant model of rs2241716 (CC vs. CT/TT; Interaction test, $P = 0.091$) was differentially associated with PFS between patients with non-metastatic and metastatic diseases. However, the significance of *TGFB1* genotypes (rs2241716 and rs4803455) on patient backgrounds and OS did not differ between patients with non-metastatic and metastatic diseases (data not shown).

DISCUSSION

This study showed that genetic polymorphisms in *TGFB1* were associated with unfavorable clinicopathological parameters including PSA value, Gleason score, and clinical T-stage patients with metastatic prostate cancer. Consistent with these associations between *TGFB1* variations and clinicopathological characteristics, the progression risk during ADT was associated with *TGFB1* genotypes, suggesting that *TGFB1* genotypes were associated with PFS through unfavorable tumor characteristics. In addition, *TGFB1* variations were not associated with clinicopathological characteristics and prognosis in patients with non-metastatic disease, and a differential impact of *TGFB1* variation (rs4803455) on PFS between non-metastatic and metastatic disease was observed. Since TGF-β1 has been suggested to play a dual role in the early and later stages of cancer development (11), the differential impact of *TGFB1* genotype on non-metastatic and metastatic diseases may be explained by the distinct biological role of TGF-β signaling according to tumor stage.

A previous study showed that genetic variation in *TGFB1* (509C>T, rs1800469) was associated with Gleason score and tumor stage in prostate cancer (17, 18). Similarly, another genetic polymorphism (*TGFB1*+869T>C, rs1982073) combined with a genetic polymorphism in epidermal growth factor was reported to be associated with time to CRPC (19). Similarly, it has been reported that genetic polymorphism in the promoter region of *TGFBR2* gene coding TGF-βRII was associated with Gleason score and risk of early relapse after ADT among patients with both non-metastatic and metastatic prostate cancer (25). In addition, this study showed that other polymorphisms in *TGFB1* (rs2241716 and rs4803455) were associated with adverse characteristics and progression risk during ADT. These results support the robustness of the association between *TGFB1* genotype and tumor aggressiveness in metastatic prostate cancer, which indicates altered progression risk according to *TGFB1* genotype.

The interactions of TGF-β signaling with EMT and AR signaling may be a possible molecular basis underlying the findings in this study. We previously showed that TGF-β induces AR expression including AR variants through the Twist1 transcription factor, which results in increased EMT phenotype and augmented castration resistance, which is reversed by TGF-β1 inhibitor (13, 14). Therefore, *TGFB1* genotyping may be helpful to identify promising candidates for therapeutics using TGF-β inhibitors, which are under clinical trials (26, 27). As well, TGFB1 genotype could predict durable responders to primary ADT as shown by Kaplan-Meier curve on PFS (**Figures 1C, D**). Although the reason why durable responders carried CC genotype in TGFB1 (rs2241716 and rs4803455), it was suggested that EMT regulated by TGF signaling may play an important role in long-lasting response to ADT.

This study had several limitations. First, this study had a retrospective design. In addition, the study population was limited to Japanese patients, and intensive up-front therapies using docetaxel and novel AR pathway inhibitors were not used at the time of the study. Thus, the significance of *TGFB1* variation in up-front therapies for metastatic hormone-sensitive prostate cancer should be investigated in the future. In addition, the functional effects of the genetic polymorphisms investigated in this study remain unclear. Finally, the correlation between *TGFB1* variation and genetic polymorphism in *TGFBR* or the expression of TGF-β receptor in prostate cancer has not been investigated. Comprehensive investigation on the relationship between TGF-β signaling and ADT would be required in the future.

In conclusion, this study showed that *TGFB1* genetic variations were associated with adverse characteristics and risk of progression during ADT among patients with metastatic disease, but not those with non-metastatic disease. This finding supports a distinct functional role of TGF-β signaling in non-metastatic and metastatic prostate cancer. In addition, *TGFB1* genotyping may be useful to identify candidates for TGF-β signaling–targeting therapies.

DATA AVAILABILITY STATEMENT

All data relevant to the study are included in the article or uploaded as supplemental information. Deidentified participant data are available upon request.

ETHICS STATEMENT

The studies involving human participants were reviewed and approved by Kyushu University Hospital and University of Occupational and Environmental Health review boards. The patients/participants provided their written informed consent to participate in this study.

AUTHOR CONTRIBUTIONS

Conception and design: MS. Acquisition of data: MS, NF, TM, ST, SN, SU, MU, EK, AT, JI, and TU. Analysis and interpretation of data (e.g., statistical analysis): MS and NF. Writing, review, and/or revision of the manuscript: MS and NF. Study supervision: ME. All authors contributed to the article and approved the submitted version.

FUNDING

This work was supported by a grant from Takeda Science Foundation.

ACKNOWLEDGMENTS

We would like to thank Ms. Noriko Hakoda and Ms. Eriko Gunshima for technical assistance. We thank Gabrielle White Wolf, PhD, from Edanz Group (https://en-author-services.edanzgroup.com/ac) for editing a draft of this manuscript.

SUPPLEMENTARY MATERIAL

The Supplementary Material for this article can be found online at: https://www.frontiersin.org/articles/10.3389/fonc.2021.697955/full#supplementary-material

REFERENCES

1. Shiota M, Eto M. Current Status of Primary Pharmacotherapy and Future Perspectives Toward Upfront Therapy for Metastatic Hormone-Sensitive Prostate Cancer. *Int J Urol* (2016) 23:360–9. doi: 10.1111/iju.13091
2. Shiota M, Yokomizo A, Naito S. Pro-Survival and Anti-Apoptotic Properties of Androgen Receptor Signaling by Oxidative Stress Promote Treatment Resistance in Prostate Cancer. *Endocr Relat Cancer* (2012) 19:R243–53. doi: 10.1530/ERC-12-0232
3. Sweeney CJ, Chen YH, Carducci M, Liu G, Jarrard DF, Eisenberger M, et al. Chemohormonal Therapy in Metastatic Hormone-Sensitive Prostate Cancer. *N Engl J Med* (2015) 373:737–46. doi: 10.1056/NEJMoa1503747
4. Fizazi K, Tran N, Fein L, Matsubara N, Rodriguez-Antolin A, Alekseev BY, et al. Abiraterone Plus Prednisone in Metastatic, Castration-Sensitive Prostate Cancer. *N Engl J Med* (2017) 377:352–60. doi: 10.1056/NEJMoa1704174
5. Sathianathen NJ, Koschel S, Thangasamy IA, Teh J, Alghazo O, Butcher G, et al. Indirect Comparisons of Efficacy Between Combination Approaches in Metastatic Hormone-Sensitive Prostate Cancer: A Systematic Review and Network Meta-Analysis. *Eur Urol* (2020) 77:365–72. doi: 10.1016/j.eururo.2019.09.004
6. Cooperberg MR, Hinotsu S, Namiki M, Ito K, Broering J, Carroll PR, et al. Risk Assessment Among Prostate Cancer Patients Receiving Primary Androgen Deprivation Therapy. *J Clin Oncol* (2009) 27:4306–13. doi: 10.1200/JCO.2008.21.5228
7. Akamatsu S, Kubota M, Uozumi R, Narita S, Takahashi M, Mitsuzuka K, et al. Development and Validation of a Novel Prognostic Model for Predicting Overall Survival in Treatment-Naïve Castration-Sensitive Metastatic Prostate Cancer. *Eur Urol Oncol* (2019) 2:320–8. doi: 10.1016/j.euo.2019.01.013
8. Dongre A, Weinberg RA. New Insights Into the Mechanisms of Epithelial-Mesenchymal Transition and Implications for Cancer. *Nat Rev Mol Cell Biol* (2019) 20:69–84. doi: 10.1038/s41580-018-0080-4
9. Thiery JP, Sleeman JP. Complex Networks Orchestrate Epithelial-Mesenchymal Transitions. *Nat Rev Mol Cell Biol* (2006) 7:131–42. doi: 10.1038/nrm1835
10. Elliott RL, Blobe GC. Role of Transforming Growth Factor Beta in Human Cancer. *J Clin Oncol* (2005) 23:2078–93. doi: 10.1200/JCO.2005.02.047
11. Morikawa M, Derynck R, Miyazono K. Tgf-β and the TGF-β Family: Context-Dependent Roles in Cell and Tissue Physiology. *Cold Spring Harb Perspect Biol* (2016) 8:a021873. doi: 10.1101/cshperspect.a021873
12. Fuzio P, Ditonno P, Rutigliano M, Battaglia M, Bettocchi C, Loverre A, et al. Regulation of TGF-β1 Expression by Androgen Deprivation Therapy of Prostate Cancer. *Cancer Lett* (2012) 318:135–44. doi: 10.1016/j.canlet.2011.08.034
13. Shiota M, Zardan A, Takeuchi A, Kumano M, Beraldi E, Naito S, et al. Clusterin Mediates TGF-β-Induced Epithelial-Mesenchymal Transition and Metastasis *Via* Twist1 in Prostate Cancer Cells. *Cancer Res* (2012) 72:5261–72. doi: 10.1158/0008-5472.CAN-12-0254
14. Shiota M, Itsumi M, Takeuchi A, Imada K, Yokomizo A, Kuruma H, et al. Crosstalk Between Epithelial-Mesenchymal Transition and Castration Resistance Mediated by Twist1/AR Signaling in Prostate Cancer. *Endocr Relat Cancer* (2015) 22:889–900. doi: 10.1530/ERC-15-0225
15. Pu H, Begemann DE, Kyprianou N. Aberrant TGF-β Signaling Drives Castration-Resistant Prostate Cancer in a Male Mouse Model of Prostate Tumorigenesis. *Endocrinology* (2017) 158:1612–22. doi: 10.1210/en.2017-00086
16. Li Z, Habuchi T, Tsuchiya N, Mitsumori K, Wang L, Ohyama C, et al. Increased Risk of Prostate Cancer and Benign Prostatic Hyperplasia Associated With Transforming Growth Factor-Beta 1 Gene Polymorphism At Codon10. *Carcinogenesis* (2004) 25:237–40. doi: 10.1093/carcin/bgg197
17. Ewart-Toland A, Chan JM, Yuan J, Balmain A, Ma J. A Gain of Function TGFB1 Polymorphism may be Associated With Late Stage Prostate Cancer. *Cancer Epidemiol Biomarkers Prev* (2004) 13:759–64.
18. Brand TC, Bermejo C, Canby-Hagino E, Troyer DA, Baillargeon J, Thompson IM, et al. Association of Polymorphisms in TGFB1 and Prostate Cancer Prognosis. *J Urol* (2008) 179:754–8. doi: 10.1016/j.juro.2007.09.020
19. Teixeira AL, Ribeiro R, Morais A, Lobo F, Fraga A, Pina F, et al. Combined Analysis of EGF+61G>A and TGFB1+869T>C Functional Polymorphisms in the Time to Androgen Independence and Prostate Cancer Susceptibility. *Pharmacogenom J* (2009) 9:341–6. doi: 10.1038/tpj.2009.20
20. Shiota M, Fujimoto N, Imada K, Yokomizo A, Itsumi M, Takeuchi A, et al. Potential Role for YB-1 in Castration-Resistant Prostate Cancer and Resistance to Enzalutamide Through the Androgen Receptor V7. *J Natl Cancer Inst* (2016) 108:djw005. doi: 10.1093/jnci/djw005
21. Shiota M, Fujimoto N, Itsumi M, Takeuchi A, Inokuchi J, Tatsugami K, et al. Gene Polymorphisms in Antioxidant Enzymes Correlate With the Efficacy of Androgen-Deprivation Therapy for Prostate Cancer With Implications of Oxidative Stress. *Ann Oncol* (2017) 28:569–75. doi: 10.1093/annonc/mdw646
22. Shiota M, Narita S, Akamatsu S, Fujimoto N, Sumiyoshi T, Fujiwara M, et al. Association of Missense Polymorphism in HSD3B1 With Outcomes Among Men With Prostate Cancer Treated With Androgen-Deprivation Therapy or Abiraterone. *JAMA Netw Open* (2019) 2:e190115. doi: 10.1001/jamanetworkopen.2019.0115
23. International Union Against Cancer: Urologic Tumors. In: Sobin LH, Wittekind CH, editors. *Prostate Tnm Classification of Malignant Tumors. 5th*. New York: John Wiley & Sons (1997) p. 170–3.
24. Scher HI, Halabi S, Tannock I, Morris M, Sternberg CN, Carducci MA, et al. Design and End Points of Clinical Trials for Patients With Progressive Prostate Cancer and Castrate Levels of Testosterone: Recommendations of the Prostate Cancer Clinical Trials Working Group. *J Clin Oncol* (2008) 26:1148–59. doi: 10.1200/JCO.2007.12.4487
25. Teixeira AL, Gomes M, Nogueira A, Azevedo AS, Assis J, Dias F, et al. Improvement of a Predictive Model of Castration-Resistant Prostate Cancer: Functional Genetic Variants in Tgfβ1 Signaling Pathway Modulation. *PLoS One* (2013) 8:e72419. doi: 10.1371/journal.pone.0072419
26. Teixeira AF, Ten Dijke P, Zhu HJ. On-Target Anti-TGF-β Therapies Are Not Succeeding in Clinical Cancer Treatments: What Are Remaining Challenges? *Front Cell Dev Biol* (2020) 8:605. doi: 10.3389/fcell.2020.00605
27. Ciardiello D, Elez E, Tabernero J, Seoane J. Clinical Development of Therapies Targeting Tgfβ: Current Knowledge and Future Perspectives. *Ann Oncol* (2020) 31:1336–49. doi: 10.1016/j.annonc.2020.07.009

Conflict of Interest: The authors declare that the research was conducted in the absence of any commercial or financial relationships that could be construed as a potential conflict of interest.

frontiers in Oncology

ORIGINAL RESEARCH
published: 10 June 2021
doi: 10.3389/fonc.2021.684144

Monoprophylaxis With Cephalosporins for Transrectal Prostate Biopsy After the Fluoroquinolone-Era: A Multi-Institutional Comparison of Severe Infectious Complications

Mike Wenzel[1,2,3], Jost von Hardenberg[3,4], Maria N. Welte[1,3], Samuel Doryumu[4], Benedikt Hoeh[1], Clarissa Wittler[1], Thomas Höfner[3,5], Maximilian C. Kriegmair[4], Maurice S. Michel[4], Felix KH. Chun[1], Jonas Herrmann[3,4], Philipp Mandel[1] and Niklas Westhoff[3,4]*

[1] Department of Urology, University Hospital Frankfurt, Goethe University Frankfurt am Main, Frankfurt, Germany, [2] Cancer Prognostics and Health Outcomes Unit, Division of Urology, University of Montreal Health Center, Montreal, QC, Canada, [3] GeSRU Academics Prostate Cancer Working Group, Planegg, Germany, [4] Department of Urology and Urosurgery, University Medical Center Mannheim, Medical Faculty Mannheim, Heidelberg University, Mannheim, Germany, [5] Department of Urology, University Hospital Mainz, Mainz, Germany

OPEN ACCESS

Edited by:
Riccardo Schiavina,
University of Bologna, Italy

Reviewed by:
Ugo Giovanni Falagario,
University of Foggia, Italy
Riccardo Bartoletti,
University of Pisa, Italy
Andrea Benedetto Galosi,
Marche Polytechnic University, Italy

***Correspondence:**
Mike Wenzel
Mike.Wenzel@kgu.de

Specialty section:
This article was submitted to Genitourinary Oncology, a section of the journal Frontiers in Oncology

Received: 22 March 2021
Accepted: 18 May 2021
Published: 10 June 2021

Citation:
Wenzel M, von Hardenberg J, Welte MN, Doryumu S, Hoeh B, Wittler C, Höfner T, Kriegmair MC, Michel MS, Chun FKH, Herrmann J, Mandel P and Westhoff N (2021) Monoprophylaxis With Cephalosporins for Transrectal Prostate Biopsy After the Fluoroquinolone-Era: A Multi-Institutional Comparison of Severe Infectious Complications. Front. Oncol. 11:684144. doi: 10.3389/fonc.2021.684144

Background: To compare severe infectious complication rates after transrectal prostate biopsies between cephalosporins and fluoroquinolones for antibiotic monoprophylaxis.

Material and Methods: In the multi-institutional cohort, between November 2014 and July 2020 patients received either cefotaxime (single dose intravenously), cefpodoxime (multiple doses orally) or fluoroquinolones (multiple-doses orally or single dose intravenously) for transrectal prostate biopsy prophylaxis. Data were prospectively acquired and retrospectively analyzed. Severe infectious complications were evaluated within 30 days after biopsy. Logistic regression models predicted biopsy-related infectious complications according to antibiotic prophylaxis, application type and patient- and procedure-related risk factors.

Results: Of 793 patients, 132 (16.6%) received a single dose of intravenous cefotaxime and were compared to 119 (15%) who received multiple doses of oral cefpodoxime and 542 (68.3%) who received fluoroquinolones as monoprophylaxis. The overall incidence of severe infectious complications was 1.0% (n=8). No significant differences were observed between the three compared groups (0.8% *vs.* 0.8% *vs.* 1.1%, p=0.9). The overall rate of urosepsis was 0.3% and did not significantly differ between the three compared groups as well.

Conclusion: Monoprophylaxis with third generation cephalosporins was efficient in preventing severe infectious complications after prostate biopsy. Single intravenous dose of cefotaxime and multiday regimen of oral cefpodoxime showed a low incidence of infectious complications <1%. No differences were observed in comparison to fluoroquinolones.

Keywords: cephalosporins, urosepsis, urinary tract infections, biopsy, prostatic neoplasms, fluoroquinolones

INTRODUCTION

Prostate cancer, the most common cancer in men worldwide, is diagnosed with prostate biopsies (1). Currently, two different applicable biopsy approaches are available, a transrectal and transperineal approach (2). Several studies reported that cancer detection rates by systematic biopsies are comparable between both approaches (3, 4). However, regarding infectious rates, some studies suggest that the transperineal approach is associated with lower rates of infectious complications, while other report comparable infectious rates (4–6). Nonetheless, sufficient prospective data is lacking. In consequence, the transrectal approach is still used worldwide and guidelines do not recommend one approach over the other, since the advantage of the transrectal approach is the quick and easy performance in an outpatient setting under local anesthesia, while a transperineal biopsy is widely performed under general anesthesia (2, 4).

The U.S. Food and Drug Administration in 2018 and the European Medicine Association (EMA) in 2019 suspended the indication for fluoroquinolones as antibiotic prophylaxis due to its toxicity profile (7). In addition, as a consequence of increasing resistance rates, there were more severe infections during the past years after administration of fluoroquinolones (8). Since fluoroquinolones have been the antibiotic prophylaxis of choice for transrectal prostate biopsies for decades, no current guideline recommendation exists for other antimicrobial agents in prophylaxis (2, 9, 10). Cephalosporins represent an alternative as a monotherapeutic antibiotic prophylaxis. The application type, either as a single intravenous dose or multiple oral doses, has different advantages. However, although several studies investigated appropriate complication rates of other antibiotic regimes after transrectal prostate biopsy, these studies mostly focused on augmented regimes (11, 12). In consequence, studies comparing a monotherapeutic prophylaxis with cephalosporins *vs*. fluoroquinolones in a homogenous cohort are still pending (13).

We addressed this void and relied on a multi-institutional prostate biopsy database of two tertiary care university hospitals. We hypothesized that differences according to severe complication rates after transrectal prostate biopsy may not exist in the comparison of cephalosporins vs. fluoroquinolones. Moreover, we hypothesized that application form and duration of the antibiotic prophylaxis does not affect complication rates.

MATERIALS AND METHODS

Study Population

The study was conducted in accordance with the Declaration of Helsinki. After ethic committee's approval, patients who underwent a transrectal systematic prostate biopsy or combined magnetic resonance imaging (MRI)-targeted and transrectal systematic biopsy at either the Department of Urology, University Hospital Frankfurt (UKF), Germany or the Department of Urology and Urosurgery, University Medical Center Mannheim (UMM), Germany, between November 2014 and July 2020 were prospectively acquired and retrospectively analyzed. Exclusion criteria for the subsequent analyses were other antibiotic prophylaxis for transrectal prostate biopsies than cephalosporins or fluoroquinolones or augmented (combination of at least two antibiotic agents) antibiotic regimes (n=62). Indications for prostate biopsies were a primary cancer suspicion or patients under active surveillance in accordance with current guidelines (2).

Transrectal Prostate Biopsy

According to the former institutional standards, at UMM, a urine culture was taken from every patient prior to prostate biopsies. During the study period, rectal swabs were not obtained by default. At UKF, urine cultures or rectal swabs were not performed on regular basis. Prior to transrectal prostate biopsy, a periprostatic local anesthesia was injected under ultrasound-guidance, as recommended (2). For systematic prostate biopsy, 12 cores (six cores from each prostate lobe) were taken according to current guidelines. For fusion biopsies, at least two cores were taken from each target, with high-end ultrasound machines (University Hospital Frankfurt: HiVison, Hitachi Medical Systems; University Medical Center Mannheim: Artemis^{TM}). In addition to targeted biopsy, systematic biopsy was performed in all patients.

Antibiotic Prophylaxis and Follow-Up

All prostate biopsies were taken under antibiotic prophylaxis with a monotherapy with either cephalosporins or fluoroquinolones. The choice of an antibiotic regimen was based on the institutional standard at the time of biopsy. Since bioavailability may differ between the application types of both third generation cephalosporins, tabulation was made for cefotaxime (single dose intravenous application of 2g 20-60 minutes prior to biopsy) vs. cefpodoxime (multiple doses of 200mg oral application twice daily, beginning at least 24 hours prior to biopsy for five days according to current recommendations (14)). Due to the comparable bioavailability between oral and intravenous application, this stratification was not made for fluoroquinolones (intravenous or oral five-day application according to the historical fluoroquinolone standard). Patients at risk for an infectious endocarditis received an agent active against enterococci and were not included in this analysis. Patient and tumor characteristics, as well as severe infectious complication rates, defined as an emergency hospital consultation due to an UTI (according to current guidelines (14)) with or without fever, were collected from the patients' hospital files within 30 days after prostate biopsy. Urosepsis was defined as previously described (15). During the pre-interventional briefing, patients were routinely instructed to inform a urologist in case of relevant complications.

Statistical Analysis

Descriptive statistics included frequencies and proportions for categorical variables. Medians and interquartile ranges (IQR) were reported for continuously coded variables. The Chi-square test was used for statistical significance in proportions'

differences. The t-test and Kruskal-Wallis test examined the statistical significance of means' and distributions' differences.

All tests were two sided with a level of significance set at $p<0.05$ and R software environment for statistical computing and graphics (version 3.4.3) was used for all analyses.

RESULTS

Patient and Procedure Characteristics

Overall, 793 patients were eligible for analyses. The median age was 66 years (IQR 61-72 years). Among all patients, 66.7% were biopsy naïve. A median number of 14 cores (IQR 13-15) per biopsy were obtained. In total, 36 patients (4.5%) had diabetes mellitus, 33 patients (4.2%) had at least three chronical diseases (defined as multimorbidity), 16 patients (2%) were immunosuppressed, nine patients (1.1%) had an indwelling catheter and six patients (0.8%) reported recurrent UTIs. In the group of patients who received multiple oral doses of cefpodoxime, significantly more patients had comorbidities ($p<0.001$). An UTI during the past twelve months was reported by nine patients (1.1%) and 50 patients received an antibiotic treatment for any cause within the last six months prior to biopsy (6.3%).

Significant differences between the subgroups of antibiotic regimens existed in the median number of cores per biopsy, a history of UTIs within the last 12 months and application of antibiotics within the last six months, as well as cancer detection rates (all $p<0.05$).

All patient characteristics and biopsy results are displayed in **Table 1**.

TABLE 1 | Patient characteristics stratified by antibiotic prophylaxis for transrectal prostate biopsy.

Variable		Overall N=793	Cefotaxime single dose (intravenous) N=132 (16.6%)	Cefpodoxime multiple doses(oral) N=119 (15.0%)	Fluoroquinolones N=542 (68.3%)	P value
Age, years	Median (IQR)	66 (61-72)	66 (60-73)	66 (60-72)	67 (61-72)	0.7
PSA, ng/ml	Median (IQR)	7.3 (5.3-11.9)	7.0 (5.2-9.6)	7.4 (5.0-12.2)	7.4 (5.3-12.2)	0.1
Prostate volume, ml	Median (IQR)	50 (38-70)	58 (43-73)	50 (36-72)	50 (38-70)	0.8
Biopsy positive, n (%)	Yes	516 (65.1)	95 (72.0)	84 (70.6)	337 (62.2)	0.04
Cores per biopsy	Median (IQR)	14 (13-15)	16 (14-16)	13 (12-14)	14 (12-15)	<0.001
Positive cores per biopsy	Median (IQR)	2 (0-6)	3 (0-6)	3 (0-5)	2 (0-6)	0.2
Core ratio in %	Median (IQR)	40 (20-50)	30 (20-40)	40 (20-50)	30 (20-60)	0.05
Hospital, n (%)	UKF	441 (55.6)	0 (0)	99 (83.2)	342 (63.1)	
	UMM	352 (44.4)	132 (100)	20 (16.8)	200 (36.9)	
DRE, n (%)	suspicious	214 (27)	33 (25)	32 (26.9)	149 (27.5)	0.9
Previous biopsies, n (%)	0	529 (66.7)	83 (62.9)	84 (70.6)	362 (66.8)	0.6
	1	182 (23)	30 (22.7)	27 (22.7)	125 (23.1)	
	2	56 (7.1)	13 (9.8)	5 (4.2)	38 (7.0)	
	≥3	26 (3.3)	6 (4.5)	3 (2.5)	17 (3.1)	
Comorbidities, n (%)	Diabetes	36 (4.5)	6 (4.5)	14 (11.8)	16 (3.0)	<0.001
	Immunosuppression	16 (2.0)	0 (0)	10 (8.4)	6 (1.1)	
	Catheter	9 (1.1)	0 (0)	2 (1.7)	7 (1.3)	
	Multimorbidity	33 (4.2)	11 (8.3)	2 (1.7)	20 (3.7)	
	Recurrent UTI	6 (0.8)	0 (0)	3 (2.5)	3 (0.6)	
Rectal swab prior to biopsy, n (%)	Yes	32 (4.0)	10 (7.6)	8 (6.7)	14 (2.6)	<0.001
Urine culture prior to biopsy, n (%)	Yes	368 (46.4)	132 (100)	31 (26.1)	205 (37.8)	<0.001
Urine culture positive prior to biopsy, n (%)	Yes	45 (5.7)	15 (11.4)	3 (2.5)	27 (5.0)	0.9
Histologically confirmed prostatitis, n (%)	Yes	266 (33.5)	74 (56.1)	42 (35.3)	150 (27.7)	0.6
UTI within last 12 months, n (%)	Yes	9 (1.1)	1 (0.8)	5 (4.2)	3 (0.6)	<0.001
Antibiotics within last 6 months, n (%)	Yes	50 (6.3)	16 (12.1)	10 (8.4)	24 (4.4)	<0.001

Descriptive characteristics of 793 patients who underwent transrectal prostate biopsy stratified according to prescribed antibiotic prophylaxis and single dose (intravenous) or multiple doses (oral) application. PSA, initial Prostate Specific Antigen; DRE, Digital rectal examination; UTI, Urinary tract infection; UKF, University Hospital Frankfurt; UMM, University Hospital Mannheim.

Incidence of Infectious Complications

A single dose of cefotaxime was administered intravenously to 132 patients (16.6%), whereas 119 patients (15%) received multiple oral doses of cefpodoxime. Both groups were compared to 542 patients (68.3%) who received fluoroquinolones either as an intravenous single dose (28.4%) or multiple oral doses (71.6%) prophylaxis. A multiple dose approach was applied for a median of five days (IQR 5-5) for oral cephalosporins and fluoroquinolones.

The total number of patients with severe infectious complications after biopsy was eight (1.0%). One patient per cephalosporine group (0.8% each) and six patients (1.1%) in the fluoroquinolone group reported a complication (p=0.9). The rate of urosepsis was 0.3% (n=2) including one patient in the cefotaxime group and one patient in the fluoroquinolone group. Two patients with an UTI (0.4%) and three patients with a prostatitis (0.6%) received a prophylaxis with fluoroquinolones, one patient with an epididymitis (0.8%) received cefpodoxime. However, there were no significant differences regarding the single infectious complications (p=0.3).

Moreover, according to fever after biopsy, no significant differences were detected between all groups (p=0.6). **Table 2** summarizes infectious complications and treatments.

DISCUSSION

Due to the increasing bacterial resistance rates of fluoroquinolones, reported to be up to 50% in Escherichia coli, and the suspended indication for prophylaxis due to rare, but potentially severe side effects (e.g., confusion, arterial aneurysms, tendinopathy), a paradigm shift in antibiotic prophylaxis for prostate biopsies is required (9, 16). We aimed to address this void and revealed several important observations:

First, the results of this large multicenter retrospective analysis of patients undergoing a transrectal prostate biopsy demonstrated a low rate of clinically relevant overall infectious complications (1.0%). Moreover, no significant differences between the usage of cephalosporins vs. fluoroquinolones as a monotherapeutic antibiotic prophylaxis were observed (0.8% *vs.* 1.1%, p=0.9). These observations are noteworthy, since in a recent meta-analysis among 1141 evaluating antibiotic prophylaxis vs. placebo, the rate of infectious complications was 5.6% (10). The lower rate in our cohort might be explained by the definition of infectious complications. We focused exclusively on complications leading to an emergency department visit. Since most studies did not distinguish between the severity of infectious complications, inclusion of e.g., a mild cystitis led to higher rates of overall complications. Importantly, the incidence of complications also depends on geographic regions which results in variation of complication rates from 0-6%, as reported in the systematic review of Roberts et al. (17).

Second, the pathophysiology of post-biopsy infectious complications is explained by two mechanisms: Firstly, flora of the large bowel is directly translocated into the prostate including Escherichia coli as the most frequent causative microorganism (70-90%) and secondly, a bacterial colonization of the prostate or urogenital mucosa before the procedure is considered to cause an UTI afterwards (18, 19). By now, there is an ongoing debate on the optimal alternative non-fluoroquinolone antibiotic regimens to avoid post-biopsy complications. The current European Urology Position Paper on the Prevention of Infectious Complications recommends performing a transperineal biopsy

TABLE 2 | Infectious complication related to the antibiotic prophylaxis regimen.

Variable		Overall N=793	Cefotaxime single dose (intravenous) N=132 (16.6%)	Cefpodoxime multiple doses (oral) N=119 (15%)	Fluoroquinolones N=542 (68.3%)	P value
Duration of antibiotic prophylaxis, days	Median (IQR)	5 (1-5)	1 (1-1)	5 (5-5)	5 (1-5)	
Application of prophylaxis, n (%)	intravenous	176 (22.2)	132 (100)	0 (0)	44 (8.1)	
	oral	577 (72.8)	0 (0)	119 (100)	458 (84.5)	
	Unknown	40 (5.0)	0 (0)	0 (0)	40 (7.4)	
Infectious complication after biopsy, n (%)	Yes	8 (1.0)	1 (0.8)	1 (0.8)	6 (1.1)	0.9
Infectious complication, n (%)	Epididymitis	1 (0.1)	0 (0)	1 (0.8)	0 (0)	0.3
	UTI	2 (0.3)	0 (0)	0 (0)	2 (0.4)	
	Prostatitis	3 (0.4)	0 (0)	0 (0)	3 (0.6)	
	Urosepsis	2 (0.3)	1 (0.8)	0 (0)	1 (0.2)	
Fever after biopsy, n (%)	Yes	5 (0.6)	1 (0.8)	0 (0)	4 (0.7)	0.6
Treatment of infectious complication, n (%)	Outpatient treatment	3 (0.4)	0 (0)	1 (0.8)	2 (0.4)	0.3
	Hospital	5 (0.6)	1 (0.8)	0 (0)	4 (0.7)	
Antibiotic treatment of infectious complication, n (%)	nonoral	4 (0.5)	1 (0.8)	0 (0)	3 (0.6)	0.4
	oral	4 (0.5)	0 (0)	1 (0.8)	3 (0.6)	
Duration of infect treatment, days	Median (IQR)	10 (6-13)	11 (11-11)	5 (5-5)	11 (7-16)	0.7

Antibiotic prophylaxis, infectious complication rates and infect treatment of 793 patients who underwent transrectal prostate biopsy stratified according to the prescribed antibiotic prophylaxis application form. UTI: Urinary tract infection.

whenever possible (20). If not feasible, three ways of antibiotic prophylaxis for transrectal biopsy are available: i) targeted prophylaxis based on a rectal swab or stool culture, ii) augmented prophylaxis with a combination of at least two different classes of antibiotics or iii) empirical monotherapeutic alternatives to fluoroquinolones (20). Since no superiority of an augmented prophylaxis has yet been demonstrated by ten previous published randomized controlled trials, a monoprophylaxis presents a safe strategy at present. Moreover, since rectal swabs are not available everywhere, an optimal empirical treatment has to be defined. In consequence, our data suggest that third generation cephalosporins, intravenously or orally administered, represent a safe empirical treatment strategy in accordance with the current European Urology Position Paper.

Third, cephalosporins of the third generation, a class of ß-lactam antibiotics, have a broad-spectrum antimicrobial activity against gram-positive, but more relevant gram-negative organisms and are therefore suitable candidates for prostate biopsy prophylaxis. Concerns against their usage have been made since resistancies against ß-lactams in gram-negative pathogens may lead to failure of prophylaxis (21). Nonetheless, the low incidence of severe infectious complications in our cohort strengthens the evidence for the appropriate use of cephalosporins, either orally or intravenously administered, in transrectal prostate biopsy. This observation is in an agreement with four RCTs, which investigated complication rates of cephalosporins (cefuroxime, cefixime or ceftriaxone) vs. fluoroquinolones or piperacillin/tazobactam (22–25). Moreover, in a pooled analysis of three of these studies, including 244 men receiving non-cephalosporins *vs.* 254 men receiving cephalosporins, no statistically significant differences were detected regarding infectious complication and hospitalization rates (RR 0.57, 95% CI 0.12-2.63). Additionally, the same meta-analysis compared 14 studies of non-fluoroquinolones vs fluoroquinolones, where significantly less infectious events were observed with non-fluoroquinolones prophylaxis (8). However, it is of note that consideration of the local resistance patterns increases the safety of cephalosporins since resistance varies widely depending on the geographical region. A rectal swab or stool culture prior to biopsy to detect resistances beforehand and perform a targeted therapy showed significantly lower infection rates compared to an empirical fluoroquinolone prophylaxis (RR 2.1, 95% CI 1.53-2.88) although data on non-fluoroquinolones-targeted prophylaxes is lacking (10). Due to the former institutional standards, only 32 patients had received a rectal swab. None of these patients had an infectious complication, independent of the antibiotic prophylaxis. Those study results and our observations may be indicative for a general performance of rectal swabs.

With respect to other monotherapeutic antibiotic prophylaxis options, the European Commission recommended 2020 a fosfomycin trometamol usage for prophylaxis in men undergoing prostate biopsy (26). Promising results were demonstrated in different meta-analyses, although one large case-control study revealed inferiority compared to ciprofloxacin (27, 28). Consequently, the definite effect of fosfomycin trometamol remains under debate and no recent trial compared cephalosporins vs. fosfomycin trometamol yet. Further trials or network meta-analyses are needed to directly compare the promising results of cephalosporins vs. fosfomycin for transrectal prostate biopsy.

Fourth, we also assessed whether the application type and duration of the cephalosporins affected the occurrence of severe infectious complications. Although urosepsis occurred in one patient in the single dose group and epididymitis in one patient in the multiple doses group, we observed no significant differences between the application types according to overall infections. This result is contradictory to the recent meta-analysis by Pilatz et al. The available studies on fluoroquinolones indicate that a 1-day prophylaxis beginning at least 24 hours prior to biopsy is comparable to a 3-day course, whereas a single-shot prophylaxis less than 24 hours prior to biopsy is inferior compared to a longer course (10). However, this recommendation was not corroborated in a Cochrane review and data mainly relied on fluoroquinolones (29). In consequence, with regard to duration and application type, a comparison to our results cannot be made.

The different antibiotic strategies of both tertiary care hospitals demonstrated comparable efficacy in prevention of severe infectious complications in this study. Whereas from an antibiotic stewardship point of view a single dose prophylaxis is especially beneficial to avoid antibiotic resistances, the advantage of the multiple oral doses' application might be extended drug levels. Despite pharmacokinetic differences, patients might prefer the oral application over an intravenous access or *vice versa*.

Limitations of this work are firstly the non-randomized retrospective cohort design, which nevertheless increases the knowledge on usage of cephalosporins as a monoprophylaxis due to its large multicenter population size. Second, infectious complications were not assessable from outpatient visits, meaning that mild complications might be underestimated. Moreover, small numbers of infectious complications precluded more complex analyses, such as logistic regression models. Third, definitions of UTI complications were not based on urine cultures but on self-reported symptoms and in-hospital examinations and reports. Finally, despite the large cohort size, it is likely that the low incidence of complication events limited the statistical power of some variables of interest and the majority of patients received fluoroquinolones. Thus, especially the evaluation of other risk factors or comorbidities associated with infectious complications was unfortunately not possible.

DATA AVAILABILITY STATEMENT

The raw data supporting the conclusions of this article will be made available by the authors, without undue reservation.

ETHICS STATEMENT

The studies involving human participants were reviewed and approved by the Department of Urology, University Hospital Frankfurt (UKF), Germany and the Department of Urology and Urosurgery, University Medical Center Mannheim (UMM).

AUTHOR CONTRIBUTIONS

Conceptualization: MW, JH, PM, and NW. Data curation: MW, JH, MNW, SD, BH, CW, PM, and NW. Formal analysis: MW, JH, PM, and NW. Funding acquisition: — Investigation: MW, JH, PM, and NW. Methodology: MW, PM, and NW. Supervision: TH, MK, MM, and FC. Validation: TH, MK, MM, FC, JH, PM, and NW. All authors contributed to the article and approved the submitted version.

REFERENCES

1. Siegel RL, Miller KD, Jemal A. Cancer Statistics, 2019. *CA Cancer J Clin* (2019) 69(1):7–34. doi: 10.3322/caac.21551
2. Mottet N, Cornford P, Van den Bergh RCN, Briers E, De Santis M, Fanti S, et al. *EAU Guidelines*. Edn. Presented at the EAU Annual Congress Amsterdam 2020 (2020).
3. Xue J, Qin Z, Cai H, Zhang C, Li X, Xu W, et al. Comparison Between Transrectal and Transperineal Prostate Biopsy for Detection of Prostate Cancer: A Meta-Analysis and Trial Sequential Analysis. *Oncotarget* (2017) 8(14):23322–36. doi: 10.18632/oncotarget.15056
4. Xiang J, Yan H, Li J, Wang X, Chen H, Zheng X. Transperineal Versus Transrectal Prostate Biopsy in the Diagnosis of Prostate Cancer: A Systematic Review and Meta-Analysis. *World J Surg Oncol* (2019) 17(1):31. doi: 10.1186/s12957-019-1573-0
5. Wajswol E, Winoker JS, Anastos H, Falagario U, Okhawere K, Martini A, et al. A Cohort of Transperineal Electromagnetically Tracked Magnetic Resonance Imaging/Ultrasonography Fusion-Guided Biopsy: Assessing the Impact of Inter-Reader Variability on Cancer Detection. *BJU Int* (2020) 125 (4):531–40. doi: 10.1111/bju.14957
6. Winoker JS, Wajswol E, Falagario U, Maritini A, Moshier E, Voutsinas N, et al. Transperineal Versus Transrectal Targeted Biopsy With Use of Electromagnetically-Tracked Mr/Us Fusion Guidance Platform for the Detection of Clinically Significant Prostate Cancer. *Urology* (2020) 146:278–86. doi: 10.1016/j.urology.2020.07.072
7. Bonkat G, Pilatz A, Wagenlehner F. Time to Adapt Our Practice? The European Commission Has Restricted the Use of Fluoroquinolones Since March 2019. *Eur Urol* (2019) 76(3):273–5. doi: 10.1016/j.eururo.2019.06.011
8. Liss MA, Ehdaie B, Loeb S, Meng MV, Raman JD, Spears V, et al. An Update of the American Urological Association White Paper on the Prevention and Treatment of the More Common Complications Related to Prostate Biopsy. *J Urol* (2017) 198(2):329–34. doi: 10.1016/j.juro.2017.01.103
9. European Medical Association. *Disabling and Potentially Permanentside Effects Lead to Suspension or Restrictionsof Quinolone and Fluoroquinolone Antibiotics* (2019). Available at: https://www.ema.europa.eu/en/documents/referral/quinolone-fluoroquinolone-article-31-referral-disabling-potentially-permanent-side-effects-lead_en.pdf.
10. Pilatz A, Dimitropoulos K, Veeratterapillay R, Yuan Y, Omar MI, MacLennan S, et al. Antibiotic Prophylaxis for the Prevention of Infectious Complications Following Prostate Biopsy: A Systematic Review and Meta-Analysis. *J Urol* (2020) 204(2):224–30. doi: 10.1097/JU.0000000000000814
11. Luong B, Danforth T, Visnjevac O, Suraf M, Duff M, Chevli KK. Reduction in Hospital Admissions With the Addition of Prophylactic Intramuscular Ceftriaxone Before Transrectal Ultrasonography-Guided Prostate Biopsies. *Urology* (2015) 85(3):511–6. doi: 10.1016/j.urology.2014.10.047
12. Adamczyk P, Juszczak K, Prondzinska M, Kędzierska A, Szwajkert-Sobiecka H, Drewa T. Fluoroquinolone-Resistant Escherichia Coli in Intestinal Flora of Patients Undergoing Transrectal Ultrasound-Guided Prostate Biopsy - Possible Shift in Biopsy Prophylaxis. *Cent Eur J Urol* (2017) 70(2):192–6. doi: 10.5173/ceju.2017.739
13. Wenzel M, Welte MN, Theissen LH, Wittler C, Hoeh B, Humke C, et al. Comparison of Complication Rates With Antibiotic Prophylaxis With Cefpodoxime Versus Fluoroquinolones After Transrectal Prostate Biopsy. *Eur Urol Focus* (2020). doi: 10.1016/j.euf.2020.11.006
14. *Interdisziplinä Epidemiologie, Diagnostik, Therapie Prävention Unkompliziert Ererworbener Harnwegsinfektionen Bei Erwachsenen* (2017). Available at: https://www.awmf.org/uploads/tx_szleitlinien/043044l_S3_Harnwegsinfektionen_2017-05.pdf.
15. Wagenlehner FME, Pilatz A, Weidner W. Urosepsis–From the View of the Urologist. *Int J Antimicrob Agents* (2011) 38(Suppl):51–7. doi: 10.1016/j.ijantimicag.2011.09.007
16. European Centre for Disease Prevention and Control. *Surveillance of Antimicrobial Resistance in Europe – Annual Report of the European Antimicrobial Resistance Surveillance Network (Eras-Net)*. Stockholm: ECD (2017). Available at: https://ecdc.europa.eu/sites/portal/files/documents/AMR-surveillance-EARS-Net-2017.pdf.
17. Roberts MJ, Bennett HY, Harris PN, Holmes M, Grummet J, Naber K, et al. Prostate Biopsy-related Infection: A Systematic Review of Risk Factors, Prevention Strategies, and Management Approaches. *Urology* (2017) 104:11–21. doi: 10.1016/j.urology.2016.12.011
18. Williamson DA, Barrett LK, Rogers BA, Freeman JT, Hadway P, Paterson DL. Infectious Complications Following Transrectal Ultrasound-Guided Prostate Biopsy: New Challenges in the Era of Multidrug-Resistant Escherichia Coli. *Clin Infect Dis Off Publ Infect Dis Soc Am* (2013) 57(2):267–74. doi: 10.1093/cid/cit193
19. Zowawi HM, Harris PNA, Roberts MJ, Tambyah PA, Schembri MA, Pezzani MD, et al. The Emerging Threat of Multidrug-Resistant Gram-negative Bacteria in Urology. *Nat Rev Urol* (2015) 12(10):570–84. doi: 10.1038/nrurol.2015.199
20. Pilatz A, Veeratterapillay R, Dimitropoulos K, Omar MI, Pradere B, Yuan Y, et al. European Association of Urology Position Paper on the Prevention of Infectious Complications Following Prostate Biopsy. *Eur Urol* (2021) 79 (1):11–5. doi: 10.1016/j.eururo.2020.10.019
21. Azap OK, Arslan H, Serefhanoğlu K, Colakoğlu S, Erdoğan H, Timurkaynak F, et al. Risk Factors for Extended-Spectrum Beta-Lactamase Positivity in Uropathogenic Escherichia Coli Isolated From Community-Acquired Urinary Tract Infections. *Clin Microbiol Infect Off Publ Eur Soc Clin Microbiol Infect Dis* (2010) 16(2):147–51. doi: 10.1111/j.1469-0691.2009.02941.x
22. Cam K, Kayikci A, Akman Y, Erol A. Prospective Assessment of the Efficacy of Single Dose Versus Traditional 3-Day Antimicrobial Prophylaxis in 12-Core Transrectal Prostate Biopsy. *Int J Urol Off J Jpn Urol Assoc* (2008) 15(11):997–1001. doi: 10.1111/j.1442-2042.2008.02147.x
23. Brewster SF, MacGowan AP, Gingell JC. Antimicrobial Prophylaxis for Transrectal Prostatic Biopsy: A Prospective Randomized Trial of Cefuroxime Versus Piperacillin/Tazobactam. *Br J Urol* (1995) 76(3):351–4. doi: 10.1111/j.1464-410x.1995.tb07713.x
24. Samarinas M, Skriapas K AK. Efficacy of Prophylactic Administration of Prurifloxacin vs. Cefixime in Patients Undergoing Ultrasound Guided Prostate Biopsy: A Prospective Randomized Study. *Eur Urol Suppl* (2019) 18:e118. doi: 10.1016/S1569-9056(19)30088-0
25. Pipitpanpipit T, Sntanirand P, Kongchareonsombat K. A Comparative Study of Oral Medication to Prevent Transient Bacteriemia and Adverse Events From Transrectal Prostatic Biopsy: Ciprofloxacin Versus Cefixime. *J Med Assoc Thailand* (2017) 100:528.
26. *Recommendations to Restrict Use of Fosfomycin Antibiotics*. Available at: https://www.ema.europa.eu/en/documents/referral/fosfomycin-article-31-referral-recommendations-restrict-use-fosfomycin-antibiotics_en.pdf.
27. Carignan A, Sabbagh R, Masse V, Gagnon N, Montpetit LP, Smith MA, et al. Effectiveness of Fosfomycin Tromethamine Prophylaxis in Preventing Infection Following Transrectal Ultrasound-Guided Prostate Needle Biopsy: Results From a Large Canadian Cohort. *J Glob Antimicrob Resist* (2019) 17:112–6. doi: 10.1016/j.jgar.2018.11.020
28. Noreikaite J, Jones P, Fitzpatrick J, Amitharaj R, Pietropaolo A, Vasdev N, et al. Fosfomycin vs. Quinolone-Based Antibiotic Prophylaxis for Transrectal Ultrasound-Guided Biopsy of the Prostate: A Systematic Review and Meta-Analysis. *Prostate Cancer Prostatic Dis* (2018) 21(2):153–60. doi: 10.1038/s41391-018-0032-2

29. Zani EL, Clark OAC, Rodrigues Netto N. Antibiotic Prophylaxis for Transrectal Prostate Biopsy. *Cochrane Database Syst Rev* (2011) (5): CD006576. doi: 10.1002/14651858.CD006576.pub2

Conflict of Interest: The authors declare that the research was conducted in the absence of any commercial or financial relationships that could be construed as a potential conflict of interest.

frontiers in Oncology

ORIGINAL RESEARCH
published: 16 June 2021
doi: 10.3389/fonc.2021.701345

Racial Differences in Clinical Outcomes for Metastatic Renal Cell Carcinoma Patients Treated With Immune-Checkpoint Blockade

T. Anders Olsen[1,2†], Dylan J. Martini[1,2†], Subir Goyal[3], Yuan Liu[3], Sean T. Evans[1,2], Benjamin Magod[1,2], Jacqueline T. Brown[1,2], Lauren Yantorni[2], Greta Anne Russler[2], Sarah Caulfield[1,4], Jamie M. Goldman[1,2], Wayne B. Harris[1,2], Omer Kucuk[1,2], Bradley C. Carthon[1,2], Viraj A. Master[5], Bassel Nazha[1,2‡] and Mehmet Asim Bilen[1,2‡]*

[1] Department of Hematology and Medical Oncology, Emory University School of Medicine, Atlanta, GA, United States, [2] Winship Cancer Institute of Emory University, Atlanta, GA, United States, [3] Departments of Biostatistics and Bioinformatics, Emory University, Atlanta, GA, United States, [4] Department of Pharmaceutical Services, Emory University School of Medicine, Atlanta, GA, United States, [5] Department of Urology, Emory University School of Medicine, Atlanta, GA, United States

Background: Immune-checkpoint-inhibitors (ICIs) have become the cornerstone of metastatic renal-cell-carcinoma (mRCC) therapy. However, data are limited regarding clinical outcomes by race. In this study, we compared the real-world outcomes between African American (AA) and Caucasian mRCC patients treated with ICIs.

Methods: We performed a retrospective study of 198 patients with mRCC who received ICI at the Emory Winship Cancer Institute from 2015-2020. Clinical outcomes were measured by overall survival (OS), progression-free survival (PFS), and overall response rate (ORR) defined as a complete or partial response maintained for at least 6 months per response evaluation criteria in solid tumors version 1.1. Univariate and multivariable analyses were carried out for OS and PFS by Cox proportional-hazard model and ORR by logistical-regression model. Descriptive statistics compared rates of immune-related adverse events (irAEs) and non-clear-cell-RCC (nccRCC) histology were assessed using Chi-square test.

Results: Our cohort was comprised of 38 AA and 160 Caucasian patients. Most were diagnosed with clear-cell-RCC (ccRCC) (78%) and more than half received (57%) PD-1/PD-L1 monotherapy. Most patients were intermediate or poor-risk groups (83%). Comparing to Caucasians, our AA cohort contained more females and nccRCC cases. Kaplan-Meier method showed AAs had no statistically different median OS (17 *vs* 25 months, p=0.368) and PFS (3.1 *vs* 4.4 months, p=0.068) relative to Caucasian patients. On multivariable analysis, AA patients had significantly shorter PFS (HR=1.52, 95% CI: 1.01-2.3, p=0.045), similar ORR (OR=1.04, 95% CI: 0.42-2.57, p=0.936) and comparable OS (HR=1.09, 95% CI: 0.61-1.95, p=0.778) relative to Caucasians.

Conclusions: Our real-world analysis of ICI-treated mRCC patients showed that AAs experienced shorter PFS but similar OS relative to Caucasians. This similarity in survival

OPEN ACCESS

Edited by:
Marijo Bilusic, National Cancer Institute, National Institutes of Health (NIH), United States

Reviewed by:
Paul Denis Leger, MedStar Georgetown University Hospital, United States
Jure Murgic, Sisters of Charity Hospital, Croatia
Peter Joseph DeMaria, National Cancer Institute, United States

***Correspondence:**
Mehmet Asim Bilen
mehmet.a.bilen@emory.edu

†These authors share first authorship

‡These authors share senior authorship

Specialty section:
This article was submitted to Genitourinary Oncology, a section of the journal Frontiers in Oncology

Received: *27 April 2021*
Accepted: *28 May 2021*
Published: *16 June 2021*

Citation:
Olsen TA, Martini DJ, Goyal S, Liu Y, Evans ST, Magod B, Brown JT, Yantorni L, Russler GA, Caulfield S, Goldman JM, Harris WB, Kucuk O, Carthon BC, Master VA, Nazha B and Bilen MA (2021) Racial Differences in Clinical Outcomes for Metastatic Renal Cell Carcinoma Patients Treated With Immune-Checkpoint Blockade. Front. Oncol. 11:701345. doi: 10.3389/fonc.2021.701345

outcomes is reassuring for the use of ICI amongst real-world patient populations, however, the difference in treatment response is poorly represented in early outcomes data from clinical trials. Thus, the literature requires larger prospective studies to validate these findings.

Keywords: renal cell carcinoma, immunotherapy, immune-checkpoint-inhibitors, racial disparities, real-world outcomes, anti-PD-1/PD-L1, disparities (health racial)

INTRODUCTION

Immune checkpoint inhibitors (ICIs) are now a major treatment option for metastatic renal cell carcinoma (mRCC). There have been numerous agents developed including Programmed Death Receptor-1 (PD-1: Nivolumab, Pembrolizumab), Programmed Death Receptor Ligand-1 (PDL-1: Atezolizumab) and Cytotoxic T-lymphocyte Protein-4 blockers (CTLA-4: Ipilimumab) (1, 2). In clinical trials, ICI monotherapy and combination therapies have displayed improved efficacy and favorable toxicity profiles for mRCC patients relative to the older regimens (3–5). However, patients of racial and ethnic minorities were underrepresented in the ICI clinical trials that led to the regulatory approval of these agents in several tumor types, including mRCC (6). For instance, only 5 AA patients were enrolled in the 821 patient CHECKMATE-025 trial comparing nivolumab to everolimus in mRCC patients receiving prior standard of care treatment (7). A study that compared the demographics of RCC clinical trials to the overall RCC patient population found that AAs made up less than 7% of the clinical trial samples despite comprising nearly 10% of the population with disease (PWD) (8). Researchers have identified numerous reasons for the poor participation of certain minority groups in clinical trials citing both structural and patient-specific factors such as age, socioeconomic status, financial barriers, culturally based mistrust of medical institutions and medical comorbidities (9).

The major classification schema for RCC exists between the predominating clear cell and non-clear cell histology. NccRCC makes up the minority of patients comprising 20-25% of all RCC diagnosis (10). The nccRCC pathophysiology does not show a clear correlation to the well-studied Von Hippel Lindau (VHL) pathway that develops ccRCC and, thus, nccRCC behaves through poorly understood cellular mechanisms (10). In general, nccRCC, especially in the papillary and chromophobe subtypes, have been correlated with a poorer prognosis (11). AAs are four times as likely to have papillary nccRCC and twice as likely to have chromophobe nccRCC relative to their Caucasian counterparts (11). Indeed, AA patients face a myriad of risk factors related to RCC disease epidemiology and social determinants of health that could contribute to their measurably worse outcomes.

Despite the wide adoption of ICIs in real-world settings, there is a paucity of data on differences or similarities experienced by AA and Caucasian mRCC patients with respect to treatment efficacy and safety (2). Durable responses to ICI are seen in only a subset of treated patients, creating a critical need to elucidate the balance of risks and benefits in different racial groups. In this manuscript, we studied ICI outcomes in a real-world patient cohort and analyzed the differences between AA and Caucasian patients with the hope of better informing the use of ICI in AA mRCC patient populations.

METHODS

Patients and Data Collection

We retrospectively reviewed the clinical outcomes of 198 patients with biopsy-proven diagnoses of mRCC who received at least one dose of ICIs for any line of therapy at the Emory University Winship Cancer Institute from Jan 2015- Jul 2020. A drug administration pharmacy database was used to identify patients. Our cutoff for collecting data was July 12th, 2020. Exclusion criteria included incomplete medical records, initiation of ICI at another institution and non-AA or Caucasian racial status, which included 3 patients of Asian descent. Demographic information such as age, gender, disease histology, self-reported race and treatment initiation/termination dates were collected. Additional metrics regarding direct and surrogate measures of clinical efficacy, immune-related adverse events (irAEs) and laboratory data were also collected through the electronic medical records. Responses to therapy were recorded by radiologic evaluation collected at treatment baseline and follow-up appointments. Using computed-tomography scans and magnetic resonance imaging, radiologists at Winship would measure the size of the primary and secondary lesions to gauge the treatment responses after baseline. These findings were later confirmed by study staff using the response evaluation criteria in solid tumors (RECIST) version 1.1.

Statistical Analysis

Clinical outcomes were measured by overall survival (OS), progression-free survival (PFS), and overall response rate (ORR). OS and PFS were calculated from ICI-initiation to date of death and radiographic or clinical progression, respectively. ORR was defined as the summation of patients who experienced the best radiographic evidence of complete response (CR) or partial response (PR) maintained for at least 6 months per RECIST version 1.1 (12). Statistical analysis was conducted using SAS Version 9.4, and SAS macros developed by Biostatistics Shared Resource at the Winship Cancer Institute (13). The association with OS and PFS was modeled by Cox proportional hazards model and the multivariable models were

built by a backward variable selection procedure with an Alpha > 0.2 removal criteria. Univariate associations between each variable and self-identified race was assessed using Chi-square or Fisher's exact tests for categorical covariates and the ANOVA test for numerical covariates. Univariable and multivariable logistic regression models with the same variable selection strategy were used to estimate odds ratios for ORR.

RESULTS

Patients and Tumor Characteristics

Demographic information and baseline disease characteristics for all patients in this cohort are presented in **Table 1**. Our cohort was comprised of 38 AA (19%) and 160 Caucasian (81%) patients (**Table 1**). The median age was 64 years old and the majority of our patients (71%) identified as male. Most of the patients were diagnosed with ccRCC (78%) and more than half received PD-1 monotherapy (57%) with nivolumab. While most patients received ICI monotherapy using a single agent acting through the PD-1/PD-L1 pathway, many of the patients (85) received combination regimens. These consisted of either dual-ICI therapy (n=70) or, amongst a minority of patients in our cohort (n=15), ICI plus a vascular endothelial growth factor (VEGF) inhibitor (**Table 1**). The median number of therapy lines prior to ICI initiation was 1 with 39% of patients having no prior line of therapy. Most patients were international mRCC database consortium (IMDC) intermediate (57%) or poor-risk (25%) groups. The Eastern Cooperative Oncology Groups performance status (ECOG-PS) breakdown for our cohort showed most patients had a score of 1 (46%) or 0 (37%) at ICI initiation. AA patients were significantly more likely to have nccRCC compared to Caucasian patients (41.7% *vs* 17.5% nccRCC, p-0.002). Of note, females constituted 23.8% of the Caucasian group and 50% of the AA group (p=0.002) (**Table 1**).

Univariate Analysis of Clinical Efficacy of ICI by Race

The results of Kaplan-Meier analysis demonstrated no statistically significant difference for AA patients in median OS (17 *vs* 25 months, p=0.368) compared to Caucasians (**Figure 1**). Similarly, there was no statistically significant difference in median PFS for AA patients compared to Caucasians (3.1 *vs* 4.4 months, p=0.068) (**Figure 2**). Total events and number of

TABLE 1 | Baseline Demographic and Clinical Characteristics of Patients with metastatic RCC by Race.

Covariate	Statistics	Level	Total N=198	Race		P-value*
				Black N=38	White N=160	
Age	Mean		64	61.6	63.2	0.395
	Median		11	62.5	64	
	Std Dev			13.3	10.4	
Gender	N (%)	Female	57 (28.8)	19 (50)	38 (23.8)	**0.001**
	N (%)	Male	141 (71.2)	19 (50)	122 (76.3)	
Non-Clear	N (%)	No	148 (77.9)	21 (58.3)	127 (82.5)	**0.002**
Cell RCC	N (%)	Yes	42 (22.1)	15 (41.7)	27 (17.5)	
Prior Lines (#)	N (%)	0	34 (17.4)	13 (34.2)	64 (40)	0.527
	N (%)	1	83 (41.9)	19 (50)	64 (40)	
	N (%)	2+	38 (19.2)	6 (15.8)	32 (20)	
PD-1 Monotherapy	N (%)	Yes	113 (57)	25 (65.8)	88 (55)	0.472
	N (%)	No (Dual-ICI)	70 (35.4)	11 (28.9)	59 (36.9)	
	N (%)	No (ICI-VEGF)	15 (7.6)	2 (5.3)	13 (8.1)	–
irAEs	N (%)	No	131 (66.2)	29 (76.3)	102 (64.2)	0.153
	N (%)	Yes	66 (33.3)	9 (23.7)	57 (35.8)	
IMDC Risk Group	N (%)	0=Poor	34 (17.4)	4 (10.5)	30 (19.1)	0.354
	N (%)	1=Intermediate	112 (57.4)	22 (57.9)	90 (57.3)	
	N (%)	2=Favorable	49 (25.1)	12 (31.6)	37 (23.6)	
ECOG-PS	N (%)	0	72 (37.3)	7 (19)	64 (41)	–
	N (%)	1	89 (46.1)	19 (51)	70 (45)	
	N (%)	2,3	32 (16.6)	11 (30)	21 (14)	
Best Response	N (%)	CR	9 (4.9)	3 (8.8)	6 (4)	0.06
	N (%)	PR	34 (18.4)	5 (14.7)	29 (19.2)	
	N (%)	SD	57 (30.8)	5 (14.7)	52 (34.4)	
	N (%)	PD	85 (45.9)	21 (61.8)	64 (42.4)	

**The p-value is calculated by ANOVA for numerical covariates; and chi-square test or Fisher's exact for categorical covariates, where appropriate.*

IO, Immunotherapy; PD-L1, Programmed death-ligand 1; RCC, renal cell carcinoma; CC, clear cell; NCC, non-clear cell; IMDC, International Metastatic RCC Database Consortium; ECOG PS, Eastern Cooperative Oncology Groups Performance Status.

***Bold** denotes statistical significance.*

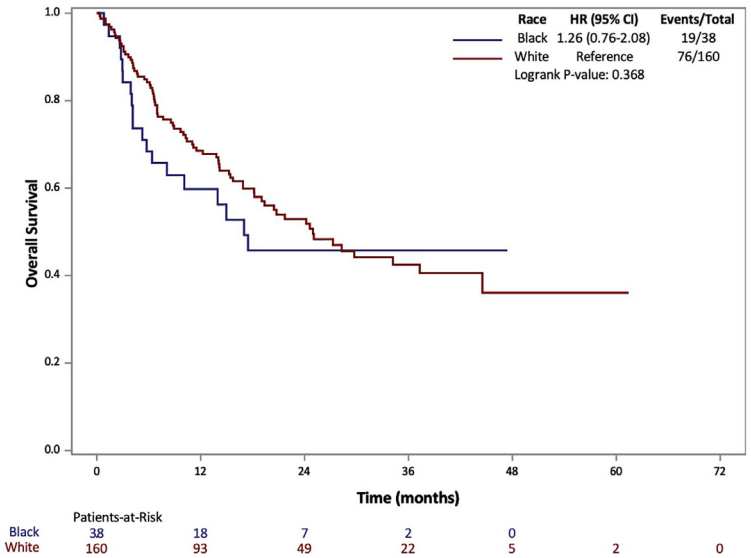

FIGURE 1 | Overall Survival (OS) of patients with metastatic RCC by race: African-American (black) and Caucasian (white).

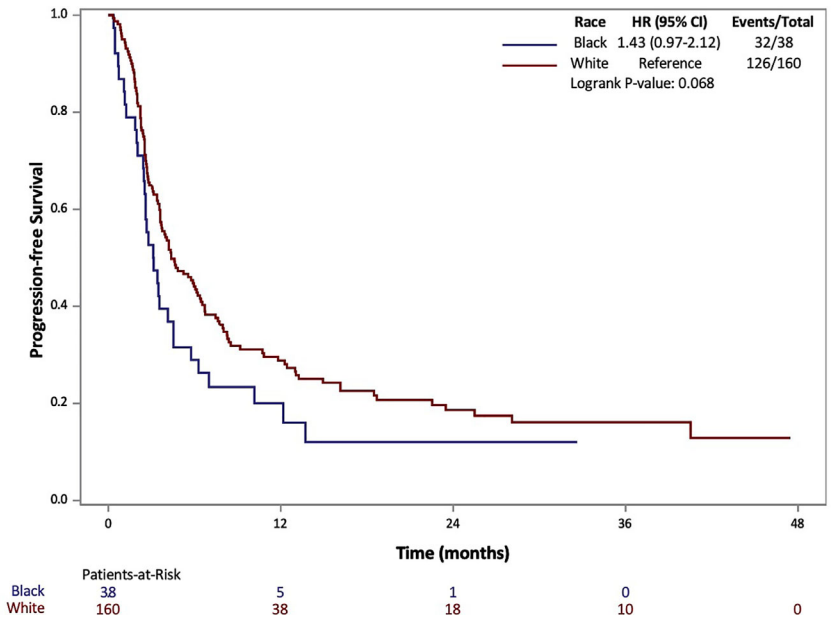

FIGURE 2 | Progression Free Survival (PFS) of patients with metastatic RCC by race: African-American (black) and Caucasian (white).

patients at risk of events for PFS and OS during the study period are also included in **Figures 1** and **2**. For OS and PFS events, AAs experienced 19/38 and 32/38 respectively. Compared to 76/160 and 126/160 events amongst our Caucasian cohort for OS and PFS respectively.

Both PFS and OS were numerically shorter in AA patients at the 12-month and 24-month marks. In fact, AA patients had a 12-month PFS rate of 20.1% (95% CI: 8.9-34.3%) [*vs.* 28.9% (95% CI: 21.8-36.2%) for Caucasians] and 24-month PFS rate of 12.0% (95% CI: 3.5-26.2%) [*vs.* 18.6% (95% CI: 12.5-25.7%) for Caucasians]. Similarly, AA patients had a 12-month OS rate of 59.8% (95% CI: 42.3-73.5%) [*vs.* 68.5 (95% CI: 60.5-75.3%) for Caucasians] and 24-month OS rate of 45.7% (95% CI: 28.3-61.5%) [*vs.* 52.9 (95% CI: 44.0-61.1%) for Caucasians. Response

rates based on radiographic disease surveillance were recorded for the cohort and compared based on self-identified race in UVA (p=0.006). The responses were divided into CR, PR, stable disease (SD) and progressive disease (PD) per RECIST version 1.1. AAs displayed a greater proportion of patients with CR and PD, yet lower rates of PR and SD compared to Caucasian patients. Further details on the rates of treatment responses by race can be found in **Table 1**. AAs also had a numerically lower incidence of irAEs compared to Caucasian patients (23.7% *vs* 64.2%, p=0.153), yet, these findings were not statistically significant. The rates of irAEs predominately consisted of gastro-intestinal (10.7%), endocrine (13.2%) and dermatologic (10.2%) side effects. These rates differed most with irAEs of the endocrine system (2 of 38 AA *vs*. 24 of 160 Caucasian p=0.108) on univariate analysis. More details on irAEs in our cohort can be found in **Supplemental Table 2**.

Multivariable Analysis of Clinical Efficacy of ICI by Race

AA race was associated with a shorter PFS (HR=1.52, 95% CI: 1.01-2.3, p=0.045) on multivariable analysis (**Table 2**). Higher IMDC risk score and a greater number of prior therapies also predicted worse PFS on multivariable analysis. Interestingly, race was not associated with differences in OS under univariate and multivariate analysis of clinical characteristics. As with the PFS analysis, higher IMDC risk group and prior lines of therapy were associated with worse OS (**Table 3**). AA race was associated with a similar ORR (OR=1.04, 95% CI: 0.42-2.57, p=0.936) after controlling for age, race, gender, IMDC risk group, number of prior lines of therapy, PD-1 monotherapy and ccRCC in MVA (**Supplemental Table 1**).

DISCUSSION

In our study of clinical outcomes for patients with mRCC, we found similar efficacy (median OS and PFS) and safety (incidence of irAEs) profiles for ICI therapy when comparing self-identified racial groups. AA race was associated with shorter PFS with no difference in OS compared to Caucasian patients after controlling for confounders such as age, RCC histology and gender. These observations are most plausibly due to a multifactorial cause, and, in this discussion, we will highlight some potential contributors to these differences. Nonetheless, our study displays reassuring outcomes data for the use of ICI therapy in real-world patient populations.

AAs comprised 10% of total RCC diagnosis from 2001-2010 (14). Our study cohort, composed of nearly 20% AAs, offers an analysis of clinical outcomes that can better represent the efficacy and safety of ICIs with AA patients. To our best knowledge, the outcomes analysis in this study contains the largest percentage of AA mRCC patients treated with ICI therapy to date. Our results better represent the patient outcomes for AAs in the real-world setting when compared to other available studies of mRCC and ICI. Most notably, we included all patients at our center with RCC who received at least one dose of ICI. This provided a more generalizable sample relative to the real-world patient population we hoped to emulate. This representative cohort included

TABLE 2 | Univariate and Multivariate Association between PFS and Clinical Characteristics in Patients with Metastatic RCC.

Covariate	Level	N	Progression Free Survival					
			Univariate Analysis			Multivariate Analysis		
			Hazard Ratio (95% CI)	HR P-value	P-value	Hazard Ratio (95% CI)	HR P-value	P-value
Race	Black	38	1.43 (0.97-2.12)	0.07	0.068	1.50 (1.01-2.32)	**0.048**	**0.048**
	White	160	–	-		–	–	
Gender	Female	57	0.87 (0.61-1.22)	0.412	0.41	0.75 (0.52-1.08)	0.123	0.123
	Male	141	–	-		–	–	
Non-Clear Cell RCC	Yes	42	1.12 (0.76-1.64)	0.581	0.58	–	–	–
	No	148	–	-		–	–	
PD-1 Monotherapy	Yes	113	1.38 (1.00-1.91)	0.051	**0.049**	–	–	–
	No	85	–	-		–	–	
IMDC Risk Group	0=Poor	34	–	-	**0.002**	–	-	0.008
	1=Intermediate	112	2.05 (1.28-3.31)	**0.003**		1.87 (1.16-3.02)	**0.01**	
	2=Favorable	49	2.47 (1.45-4.19)	**<.001**		2.33 (1.35-4.01)	**0.002**	
Prior Lines (#)	0	77	–	-	**<.001**	–	-	**0.001**
	1	83	1.17 (0.81-1.67)	0.397		1.20 (0.83-1.74)	0.325	
	2+	38	2.32 (1.52-3.54)	**<.001**		2.22 (1.43-3.43)	**<.001**	
Age		198	0.99 (0.98-1.01)	0.299	0.299	–	–	–

**The p-value is calculated by ANOVA for numerical covariates; and chi-square test or Fisher's exact for categorical covariates, where appropriate.*

IO, Immunotherapy; PD-L1, Programmed death-ligand 1; RCC, renal cell carcinoma; CC, clear cell; NCC, non-clear cell; IMDC, International Metastatic RCC Database Consortium; ECOG PS, Eastern Cooperative Oncology Groups Performance Status.

***Bold** denotes statistical significance.*

TABLE 3 | Univariate and Multivariate Association between OS and Clinical Characteristics in Patients with Metastatic RCC.

Covariate	Level	N	Overall Survival					
			Univariate Analysis			Multivariate Analysis		
			Hazard Ratio (95% CI)	HR P-value	P-value	Hazard Ratio (95% CI)	HR P-value	P-value
Race	Black	38	1.26 (0.76-2.08)	0.369	0.368	1.02 (0.57-1.84)	0.947	
	White	160	–	-		–	–	0.947
Gender	Female	57	0.77 (0.49-1.21)	0.255	0.253	0.60 (0.35-1.02)	0.061	
	Male	141	–	-		–	–	0.061
Non-Clear Cell RCC	Yes	42	1.68 (1.05-2.69)	**0.031**	**0.029**	1.56 (0.95-2.55)	0.078	
	No	148	–	-		–	–	0.078
PD-1 Monotherapy	Yes	113	1.43 (0.93-2.21)	0.107	0.105	–	–	**-**
	No	85	–	-		–	–	
IMDC Risk Group	0=Poor	34	–	-	**<.001**	–	–	**0.001**
	1=Intermediate	112	2.14 (1.05-4.36)	**0.037**		1.80 (0.88-3.69)	0.11	
	2=Favorable	49	4.93 (2.36-10.33)	**<.001**		4.38 (2.03-9.44)	**<.001**	
Prior Lines (#)	0	77	–	-	**0.001**	–	–	0.011
	1	83	1.18 (0.72-1.94)	0.51		1.21 (0.71-2.05)	0.486	
	2+	38	2.43 (1.43-4.13)	**0.001**		2.10 (1.19-3.71)	**0.011**	
Age		198	198	1.00 (0.98-1.02)	0.743	–	–	–

**The p-value is calculated by ANOVA for numerical covariates; and chi-square test or Fisher's exact for categorical covariates, where appropriate.*

IO, Immunotherapy; PD-L1, Programmed death-ligand 1; RCC, renal cell carcinoma; CC, clear cell; NCC, non-clear cell; IMDC, International Metastatic RCC Database Consortium; ECOG PS, Eastern Cooperative Oncology Groups Performance Status.

Bold *denotes statistical significance.*

patients who were often less healthy and more diverse than the samples used in clinical trials (15). Of note, patients with an ECOG-PS of 2 or more made up only 8% of the study cohorts in phase III clinical trials (16). Meanwhile, our cohort included nearly twice as many as a percentage of total with more than 16% of our patients having an ECOG greater than 2.

The epidemiology of renal malignancies have a long history of racial disparities and researchers have begun to better quantify these disparate outcomes in the past decades (17). One factor often cited in RCC disparity research is the epidemiology of histologic phenotypes that are crucial for cancer diagnostics and prognostication. NccRCC specifically has shown limited efficacy with newer treatment modalities such as ICIs, and this diagnosis has a much greater prevalence in AA patient populations compared to Caucasian patients. Additionally, clinical trials studying RCC patients predominately study outcomes in ccRCC patients (10). Taken together, nccRCC's ill-defined histology, aggressive phenotype and limited therapy options makes it carry a poor prognosis compared to ccRCC. This is especially relevant in the age of targeted and pathway specific therapy, as these cellular diagnostics are becoming integral to the management of disease. In our cohort, AA patients displayed significantly higher rates of nccRCC. This is notable to mention because including a disproportionately large number of AA patients with nccRCC could skew the AA cohort towards worse outcomes on univariable analysis. However, even after controlling for cancer histology, we still found that AA race was associated with significantly shorter PFS compared to Caucasians. Additionally, while shorter PFS for AA patients was the only statistically significant difference on MVA, our AA cohort also displayed measurably shorter median OS, median PFS and ORR. We will attempt to highlight potential contributors for these disparities in the remainder of our discussion. However, put simply, we believe the difference noted in our analysis and from the RCC racial disparities literature can be largely attributed to a multifactorial etiology of socio-economic forces that impact the outcomes and access to care experienced by AA patients with oncologic disease. Nevertheless, these numeric differences did not translate into a significant difference for OS, which is noteworthy as an encouraging finding for ICI usage in the real-world setting.

Within the field of immuno-oncology, non-trivial differences are found amongst different racial groups in the way the immune system manages cancer (18). Researchers postulate that alterations in the stress response from the hypothalamic-pituitary-adrenal (HPA) axis, leading to systemic hormonal changes, can impair immune-related functions and cause decreased tumor clearance amongst certain groups of patients (19). *Neighborhood physical disorder* is a condition often cited in bio-psychosocial models that links societal and systemic stressors to chronic inflammation which can drive immune dysregulation and poor health outcomes amongst disadvantaged communities (20). Additionally, researchers have also considered the disproportionate rates of vitamin D deficiency amongst African Americans as another potential contributor to healthcare disparities and sub-optimal immune function in this population (21). Put simply, we feel it is important to identify the potential differences in cancer biology amongst racial groups because it could be useful in the application of IO therapy in minority populations with oncologic disease. That being said,

while these biologic differences were historically cited in the oncology literature to explain racially-based disparities, we agree with a growing body of evidence that highlights the considerable impact that social, economic and healthcare-access issues play in the racial disparities of cancer patients (22, 23). It is imperative that oncologists appreciate how historical and sociopolitical forces intertwine with race because of the insidious impacts they can have on patients managing complicated disease such as mRCC (24). The findings from our cohort are supported by the current stance within the racial disparities research of RCC and add specificity, primarily in PFS, to how clinical outcomes could differ with the use of immune acting therapies in AAs and Caucasian patients. These differences are likely due to a multifactorial etiology that stem from a combination of biological and societal factors.

The literature's stance on race and immune-related adverse events (irAE) is still developing; however, some studies have found minority groups, specifically AAs, experience lower rates of irAEs relative to Caucasian patients (25). Taking these immune toxicity rates into account, there is a possibility that these racial differences in the immune system could impact the function of immunotherapy in minority patients. Within our cohort, we found no statistically significant difference in the safety profile of ICI, yet a much lower incidence of irAE in AA patients (23.7%) compared to Caucasians (64.2%). This difference could become more (or less) pronounced upon studying a larger cohort.

Given the explosive rise of ICI therapy in the treatment of mRCC, it is important to appreciate the interplay of biologic and systemic contributors in the efficacy and safety of ICI utilization with AA patients. Overall, our study provides evidence that clinical outcomes are mostly comparable between AA and Caucasian patients managed on ICI. We found no differences on the Kaplan-Meir level, but did note an association of AA race with worse PFS on multivariable analysis. We hypothesize that the latter could be due to factors such as unmeasured comorbidities and complex social determinants of health. Despite this difference in PFS, our findings support an imperative notion within disparities research that equal treatment provided to equal patients, regardless of race, should result in similar outcomes. However, the presence of racial disparities within the literature displays the need for further research in this field to delineate the medical and socioeconomic factors that cause these population-level outcome inequities.

The limitations of this study include the smaller overall size of our cohort and the binary racial categories used. This is relevant since the racial disparities research within RCC has also attributed poorer outcomes to Hispanic and Native/Alaskan American populations (26). Another limitation is our lack of sociodemographic data on our cohort such as the income level of patients. While all patients included in this study had health insurance, they were not differentiated on the basis of private or public provision. We also used a retrospective study from a single cancer institute, which is subject to selection bias. However, we attempted to mitigate this concern by including all patients who received one dose of ICI regardless of histology or other disease-specific characteristics. While our inclusion criteria allowed us to collect a larger number of patients, there was some degree of heterogeneity for the different ICI therapy options patients could receive. This included IO-monotherapy, IO-dual therapy and IO-TKI combination therapy. The rates of dual *vs* mono-IO therapy can be seen in **Table 1**. Our findings in **Table 1** also show that AAs were more likely to receive monotherapy instead of combination therapy (65% *vs* 55%), and to be of a higher ECOG-PS 2-3 (30% *vs* 14%). Additionally, many patients did not receive these IO regimens as first-line therapy and our data displayed worsening prognosis as patients had more lines of prior therapy. This degree of variance between treatment approaches is commonplace in this type of real-world analysis and allows the results of our study to better emulate the expected effect of immunotherapy in practice. Since not every patient in our cohort was able to receive cancer genetic testing or mutation profiles, we chose not to include biomarkers of ICI response such as PD-L1 expression. Further, our secondary clinical outcome, overall response rate or ORR, is not standard in clinical trials. Larger datasets are needed to investigate the statistically significant findings in the current study, namely the association of shorter PFS and AA race on MVA.

Despite its limitations, we believe our current study has numerous strengths. Our patient sample was drawn from a single cancer institute and, therefore, represents a homogenous population in terms of geographic residence and access to cancer care in the United States. In our multivariable analysis, many demographic and clinical factors specific to our patients were controlled for.

The treatment landscape of RCC continues to evolve as more therapy options become available to patients, specifically ICI-VEGF TKI combinations. During our study period from 2015-2020, less than half of our patients (n=85) (**Table 1**) in the cohort received combination ICI-TKI or dual-ICI therapy. This is a lower proportion of patients than would have received combination therapy today in light of the FDA approvals for combination regimens in mRCC: nivolumab + ipilmumab (April 2018), pembrolizumab + axitinib (April 2019), avelumab + axitinib (May 2019) nivolumab + cabozantinib (January 2021) and lenvatinib + pembrolizumab (April 2021) (27, 28). We note that two contemporary analyses of mRCC patients treated with TKI showed that race (AA *vs* Caucasian) was not independently associated with differing survival outcomes (29, 30). Similar to our study, the comparable OS between AA and Caucasians are encouraging findings for the use of mono and combination immunotherapy in AA mRCC patient populations.

CONCLUSION

In our cohort, we analyzed clinical outcomes amongst mRCC patients treated on ICI therapy. Overall, our study suggested a favorable benefit-to-risk ratio of ICI for the treatment of mRCC in AA patients. We found comparable outcomes for AA and Caucasian patients for OS, median PFS, ORR and immune-related adverse events. Our multivariable analysis of outcomes showed an association of AA race with shorter PFS that warrants additional investigation. Larger prospective studies from multiple institutions are needed to validate these findings, especially

amongst other non-AA US minority populations. We hope our real-world data may help oncologic physicians appreciate a degree of nuance when treating increasingly diverse mRCC patients and emphasize the need for improved inclusion criteria for racial minority groups in future IO clinical trials.

DATA AVAILABILITY STATEMENT

The raw data supporting the conclusions of this article will be made available by the authors, without undue reservation.

ETHICS STATEMENT

The study was approved by the Emory University Institutional Review Board and was conducted in accordance with Good Clinical Practice Guidelines and the Declaration of Helsinki. The patients/participants provided their written informed consent to participate in this study.

AUTHOR CONTRIBUTIONS

TO was involved in collecting references as well as writing and editing the manuscript. DM was involved in the data acquisition and administrative support. BN and MAB provided advisory on the manuscript and final revisions prior to submission. YL and SG provided assistance with statistical analysis. All remaining authors were involved in the care of the patients in this study, interpretation and analysis of study results, and editing of the manuscript. All authors contributed to the article and approved the submitted version.

FUNDING

Research reported in this publication was supported in part by the Breen Foundation and the Biostatistics Shared Resource of Winship Cancer Institute of Emory University and NIH/NCI under award number P30CA138292. The content is solely the responsibility of the authors and does not necessarily represent the official views of the National Institutes of Health.

SUPPLEMENTARY MATERIAL

The Supplementary Material for this article can be found online at: https://www.frontiersin.org/articles/10.3389/fonc.2021.701345/full#supplementary-material

REFERENCES

1. Motzer RJ, Tannir NM, McDermott DF, Arén Frontera O, Melichar B, Choueiri TK, et al. Nivolumab Plus Ipilimumab Versus Sunitinib in Advanced Renal-Cell Carcinoma. *New Engl J Med* (2018) 378:1277–90. doi: 10.1056/NEJMoa1712126
2. Rijnders M, de Wit R, Boormans JL, Lolkema MPJ, van der Veldt AAM. Systematic Review of Immune Checkpoint Inhibition in Urological Cancers. *Eur Urol* (2017) 72:411–23. doi: 10.1016/j.eururo.2017.06.012
3. Garje R, An J, Greco A, Vaddepally RK, Zakharia Y. The Future of Immunotherapy-Based Combination Therapy in Metastatic Renal Cell Carcinoma. *Cancers* (2020) 12:143. doi: 10.3390/cancers12010143
4. Motzer RJ, Rini BI, McDermott DF, Redman BG, Kuzel TM, Harrison MR, et al. Nivolumab for Metastatic Renal Cell Carcinoma: Results of a Randomized Phase II Trial. *J Clin Oncol* (2015) 33:1430–7. doi: 10.1200/JCO.2014.59.0703
5. Rini BI, Plimack ER, Stus V, Gafanov R, Hawkins R, Nosov D, et al. Pembrolizumab Plus Axitinib Versus Sunitinib for Advanced Renal-Cell Carcinoma. *New Engl J Med* (2019) 380:1116–27. doi: 10.1056/NEJMoa1816714
6. Nazha B, Mishra M, Pentz R, Owonikoko TK. Enrollment of Racial Minorities in Clinical Trials: Old Problem Assumes New Urgency in the Age of Immunotherapy. *Am Soc Clin Oncol Educ Book* (2019) 39:3–10. doi: 10.1200/EDBK_100021
7. Escudier B, Motzer RJ, Sharma P, Wagstaff J, Plimack ER, Hammers HJ, et al. Treatment Beyond Progression in Patients With Advanced Renal Cell Carcinoma Treated With Nivolumab in CheckMate 025. *Eur Urol* (2017) 72:368–76. doi: 10.1016/j.eururo.2017.03.037
8. Kaldany A, Blum KA, Paulucci DJ, Beksac AT, Jayaratna I, Sfakianos JP, et al. An Evaluation of Race, Ethnicity, Age, and Sex-Based Representation in Phase I to II Renal Cell Carcinoma Clinical Trials in the United States. *Urol Oncol: Semin Orig Invest* (2018) 36:363.e1–6.
9. Shavers VL, Brown ML. Racial and Ethnic Disparities in the Receipt of Cancer Treatment. *JNCI: J Natl Cancer Inst* (2002) 94:334–57. doi: 10.1093/jnci/94.5.334
10. Linehan WM, Srinivasan R, Garcia JA. Non-Clear Cell Renal Cancer: Disease-Based Management and Opportunities for Targeted Therapeutic Approaches. *Semin Oncol* (2013) 40:511–20. doi: 10.1053/j.seminoncol.2013.05.009
11. Olshan AF, Kuo TM, Meyer AM, Nielsen ME, Purdue MP, Rathmell WK. Racial Difference in Histologic Subtype of Renal Cell Carcinoma. *Cancer Med* (2013) 2:744–9. doi: 10.1002/cam4.110
12. Nishino M, Jagannathan JP, Ramaiya NH, Van den Abbeele AD. Revised RECIST Guideline Version 1.1: What Oncologists Want to Know and What Radiologists Need to Know. *AJR Am J Roentgenol* (2010) 195:281–9. doi: 10.2214/AJR.09.4110
13. Liu Y, Nickleach DC, Zhang C, Switchenko JM, Kowalski J. Carrying Out Streamlined Routine Data Analyses With Reports for Observational Studies: Introduction to a Series of Generic SAS (®) Macros. *F1000Res* (2018) 7:1955. doi: 10.12688/f1000research.16866.1
14. King SC, Pollack LA, Li J, King JB, Master VA. Continued Increase in Incidence of Renal Cell Carcinoma, Especially in Young Patients and High Grade Disease: United States 2001 to 2010. *J Urol* (2014) 191:1665–70. doi: 10.1016/j.juro.2013.12.046
15. Unger JM, Barlow WE, Martin DP, Ramsey SD, LeBlanc M, Etzioni R, et al. Comparison of Survival Outcomes Among Cancer Patients Treated In and Out of Clinical Trials. *JNCI: J Natl Cancer Inst* (2014) 106. doi: 10.1093/jnci/dju002
16. Kouzy R, Jaoude JA, Mainwaring W, Lin T, Miller AB, Jethanandani A, et al. Performance Status Restriction in Phase III Cancer Clinical Trials. *J Clin Oncol* (2020) 38:2059–9. doi: 10.1200/JCO.2020.38.15_suppl.2059
17. Chow WH, Shuch B, Linehan WM, Devesa SS. Racial Disparity in Renal Cell Carcinoma Patient Survival According to Demographic and Clinical Characteristics. *Cancer* (2013) 119:388–94. doi: 10.1002/cncr.27690
18. King Thomas J, Mir H, Kapur N, Singh S. Racial Differences in Immunological Landscape Modifiers Contributing to Disparity in Prostate Cancer. *Cancers* (2019) 11:20–100. doi: 10.3390/cancers11121857
19. Dhabhar FS. Enhancing Versus Suppressive Effects of Stress on Immune Function: Implications for Immunoprotection and Immunopathology. *Neuroimmunomodulation* (2009) 16:300–17. doi: 10.1159/000216188

20. Lei M-K, Simons RL. The Association Between Neighborhood Disorder and Health: Exploring the Moderating Role of Genotype and Marriage. *Int J Environ Res Public Health* (2021) 18:898. doi: 10.3390/ijerph18030898
21. Ames BN, Grant WB, Willett WC. Does the High Prevalence of Vitamin D Deficiency in African Americans Contribute to Health Disparities? *Nutrients* (2021) 13:300–16. doi: 10.3390/nu13020499
22. Dess RT, Hartman HE, Mahal BA, Soni PD, Jackson WC, Cooperberg MR, et al. Association of Black Race With Prostate Cancer–Specific and Other-Cause Mortality. *JAMA Oncol* (2019) 5:975–83.
23. Siegel RL, Miller KD, Jemal A. Cancer Statistics, 2020. *CA Cancer J Clin* (2020) 70:7–30. doi: 10.3322/caac.21590
24. Zavala VA, Bracci PM, Carethers JM, Carvajal-Carmona L, Coggins NB, Cruz-Correa MR, et al. Cancer Health Disparities in Racial/Ethnic Minorities in the United States. *Br J Cancer* (2021) 124:315–32.
25. Ternyila D. Survival Advantage Associated With Immune-Related Toxicity Reveals Racial Disparities in Solid Tumors. *Target Oncol* (2020) 12:7025–7025. doi: 10.1200/JCO.2020.38.15_suppl.7025
26. Padala SA, Barsouk A, Thandra KC, Saginala K, Mohammed A, Vakiti A, et al. Epidemiology of Renal Cell Carcinoma. *World J Oncol* (2020) 11:79–87. doi: 10.14740/wjon1279
27. Killock D. ICI Rechallenge in Mrcc. *Nat Rev Clin Oncol* (2020) 17:520–0. doi: 10.1038/s41571-020-0407-x
28. Rassy E, Flippot R, Albiges L. Tyrosine Kinase Inhibitors and Immunotherapy Combinations in Renal Cell Carcinoma. *Ther Adv Med Oncol* (2020) 12:1758835920907504. doi: 10.1177/1758835920907504
29. Bossé D, Xie W, Lin X, Simantov R, Lalani AA, Graham J, et al. Outcomes in Black and White Patients With Metastatic Renal Cell Carcinoma Treated With First-Line Tyrosine Kinase Inhibitors: Insights From Two Large Cohorts. *JCO Glob Oncol* (2020) 6:293–306. doi: 10.1200/JGO.19.00380
30. Dizman N, Salgia NJ, Bergerot PG, Hsu J, Ruel N, Pal SK. Race/Ethnicity and Survival in Metastatic Renal Cell Carcinoma: Outcomes for Patients Receiving First Line Targeted Therapies. *Kidney Cancer* (2020) 4:159–66. doi: 10.3233/KCA-200092

Conflict of Interest: MB has acted as a paid consultant for and/or as a member of the advisory boards of Exelixis, Bayer, BMS, Eisai, Pfizer, AstraZeneca, Janssen, Genomic Health, Nektar, and Sanofi and has received grants to his institution from Xencor, Bayer, Bristol-Myers Squibb, Genentech/Roche, Seattle Genetics, Incyte, Nektar, AstraZeneca, Tricon Pharmaceuticals, Peleton Therapeutics, and Pfizer for work performed as outside of the current study. BN has acted as a paid member of the advisory board of Exelixis.

The remaining authors declare that the research was conducted in the absence of any commercial or financial relationships that could be construed as a potential conflict of interest.

frontiers in Oncology

REVIEW
published: 15 July 2021
doi: 10.3389/fonc.2021.704039

Study Progress of Noninvasive Imaging and Radiomics for Decoding the Phenotypes and Recurrence Risk of Bladder Cancer

Xiaopan Xu[1], Huanjun Wang[2], Yan Guo[2], Xi Zhang[1], Baojuan Li[1], Peng Du[1], Yang Liu[1] and Hongbing Lu[1]**

[1] School of Biomedical Engineering, Air Force Medical University, Xi'an, China, [2] Department of Radiology, The First Affiliated Hospital, Sun Yat-Sen University, Guangzhou, China

OPEN ACCESS

Edited by:
Matteo Ferro, European Institute of Oncology (IEO), Italy

Reviewed by:
Ning Li, Fourth Affiliated Hospital of China Medical University, China
Vito Mancini, University of Foggia, Italy
Francesco Del Giudice, Sapienza University of Rome, Italy

***Correspondence:**
Hongbing Lu
luhb@fmmu.edu.cn
Yang Liu
yliu@fmmu.edu.cn

Specialty section:
This article was submitted to Genitourinary Oncology, a section of the journal Frontiers in Oncology

Received: *01 May 2021*
Accepted: *30 June 2021*
Published: *15 July 2021*

Citation:
Xu X, Wang H, Guo Y, Zhang X, Li B, Du P, Liu Y and Lu H (2021) Study Progress of Noninvasive Imaging and Radiomics for Decoding the Phenotypes and Recurrence Risk of Bladder Cancer. Front. Oncol. 11:704039. doi: 10.3389/fonc.2021.704039

Urinary bladder cancer (BCa) is a highly prevalent disease among aged males. Precise diagnosis of tumor phenotypes and recurrence risk is of vital importance in the clinical management of BCa. Although imaging modalities such as CT and multiparametric MRI have played an essential role in the noninvasive diagnosis and prognosis of BCa, radiomics has also shown great potential in the precise diagnosis of BCa and preoperative prediction of the recurrence risk. Radiomics-empowered image interpretation can amplify the differences in tumor heterogeneity between different phenotypes, i.e., high-grade *vs.* low-grade, early-stage vs. advanced-stage, and nonmuscle-invasive *vs.* muscle-invasive. With a multimodal radiomics strategy, the recurrence risk of BCa can be preoperatively predicted, providing critical information for the clinical decision making. We thus reviewed the rapid progress in the field of medical imaging empowered by the radiomics for decoding the phenotype and recurrence risk of BCa during the past 20 years, summarizing the entire pipeline of the radiomics strategy for the definition of BCa phenotype and recurrence risk including region of interest definition, radiomics feature extraction, tumor phenotype prediction and recurrence risk stratification. We particularly focus on current pitfalls, challenges and opportunities to promote massive clinical applications of radiomics pipeline in the near future.

Keywords: urinary bladder cancer, multimodal imaging, radiomics, histopathological phenotype, recurrence

INTRODUCTION

Urinary bladder cancer (BCa) is the sixth most common malignancy and the ninth most common cause of cancer death among males worldwide (1–3). An estimated 573,278 new cases and 212,536 new deaths were reported to occur in 2020 globally (3, 4). BCa is more common in men than in women, and the incidence increases with age (1, 4, 5). Meanwhile, it has a high recurrence rate (5–7). Early diagnosis with personalized treatment and follow-up of patients is critical to a favorable outcome.

BCa usually originates from the epithelium (5, 7). As carcinomas invade the detrusor muscle, they are categorized as muscle-invasive BCa (MIBC, stage ≥ T2) and more likely to metastasize to

lymph nodes or other organs (5, 6). Approximately 75% of the patients at initial diagnosis have nonmuscle-invasive BCa (NMIBC, stage ≤ T1), and the rest have MIBC (6, 8–10). Nearly 50% of newly diagnosed NMIBCs are low grade, while most MIBCs are high grade (7, 11). According to the European Association of Urology (EAU) guidelines (10, 12), pathological phenotypes such as grade, stage and muscle-invasive status (MIS) are important predictors of BCa recurrence, and have immense implications for treatment decisions and prognosis. Preoperatively determining the histopathological phenotype and recurrence risk of BCa is, therefore, of critical importance for BCa patients.

The clinical first-line reference for the preoperative diagnosis of the histopathological phenotype of BCa is cystoscopic resection of a suspicious lesion during a biopsy (6, 8–10, 13, 14). Considering that bladder tumors are heterogeneous, local biopsy results may not be typical representatives of the entire tumor mass, and diagnostic errors are inevitable (5, 7, 15–19). Many studies have shown that 9 to 49% of BCa patients have their tumor stage misdiagnosed (14, 20–23), which leads to inappropriate treatment decision and unfavorable prognosis. Repeated cystoscopic resections are considered a practical way to reduce the misdiagnostic rate, but are unwanted due to the invasive, uncomfortable, time-consuming and costly process (21, 24–27). Besides, they may easily cause infection or urethral bleeding (6, 8–10, 28–30). Developing a noninvasive approach for the precise prediction of the histopathological phenotype of BCa and further stratifying its recurrence risk preoperatively is, therefore, crucial for patient treatment and management (16, 31–35).

In current clinical practice, easily accessible and noninvasive imaging tools such as pelvic CT and multiparametric MRI (mpMRI) provide immense assistance to clinicians for the preoperative diagnosis of BCa phenotypes (24, 30, 36–43). CT is mainly performed for evaluating the upper urinary tract and predicting lymph node metastasis of BCa (40, 42, 43). When clinicians identify the MIS, CT has drawbacks due to its limited soft-tissue contrast (40, 42, 43). In addition, radiation exposure is another concern (40, 42–44). The mpMRI, including conventional sequences like T2-weighted imaging (T2WI) and functional sequences such as diffusion-weighted imaging (DWI) with corresponding apparent diffusion coefficient (ADC) maps and dynamic contrast-enhanced imaging (DCE), may well overcome these drawbacks and enhance the diagnostic performance (**Figure 1**) (30, 39, 40, 44).

T2WI has the capability to illustrate the detailed structural information of the lesion and bladder wall, thus can potentially reflect the invasion depth of BCa into bladder wall. However, it may result in overstaging since tumor-associated inflammation has the same appearance of low signal intensity as that of the muscularis propria (20, 37, 40, 44). DWI and ADC have the favorable capability to reflect the signal intensity differences among muscle, peritumoral inflammation and fibrosis (36, 38, 44–47). The finding of a thickened hypointense submucosa beneath the NMIBC (inchworm sign or stalk) on DWI is a milestone for MIS identification and prognosis (13, 30, 41, 48).

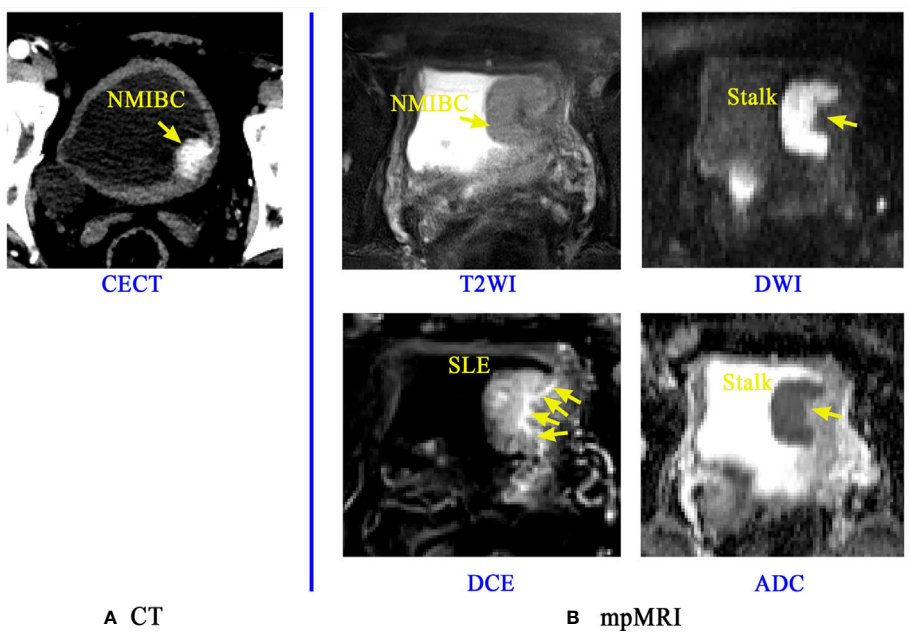

FIGURE 1 | Application of CT and mpMRI for the preoperative prediction of the muscle invasion status of BCa. A lesion of a patient confirmed with NMIBC is discernible on Contrast-enhanced CT (CECT) image **(A)**, but the boundaries and basal part of this lesion is rarely distinguishable. The mpMRI **(B)** including the T2WI, DCE, DWI and its corresponding ADC map can provide more important signs and information like the stalk at the tumor base and submucosal linear enhancement (SLE) for accurate diagnosis of muscle-invasive status (MIS) of BCa (38).

Submucosal linear enhancement (SLE) at the basal part of the tumor on DCE images has currently been recognized as another sign for precisely determining MIS (13, 30, 38, 39, 47), but its diagnostic performance is controversial (47, 49, 50).

Summarizing all these important clinical findings, Panebianco et al. proposed a Vesical Imaging-Reporting and Data System (VI-RADS), which uses tumor morphological signs, stalks and SLE on mpMRI to obtain a five-point rating score for the estimation of MIS (30, 39, 40, 51–53). However, it is a semiquantitative score which also relies most on experienced radiologists' visual perception, making it an expert-dependent tool for BCa diagnosis. In addition, the VI-RADS model, together with the existing noninvasive imaging tools, is still incapable of predicting BCa recurrence.

During the past 20 years, the field of computer-assisted medical image analysis has grown dramatically, resulting in many successful applications in the noninvasively accurate diagnosis and prognostication of cancers such as breast cancer, colorectal cancer and lung cancer (54–57). These advances have prompted the attempt of extracting high-throughput quantitative image features, namely, *radiomics*, to characterize different tissue properties and to accumulate certain strategies for BCa phenotypes diagnosis and recurrence risk prediction (24, 26, 58–61). However, most of these radiomics strategies only focus on the tumor region, regardless of the normal wall region and the basal part of tumor region that may also provide abundant information for this task (57, 59, 60, 62). Automated and accurate delineation of regions of interest (ROI) including the tumor, its basal part and the normal wall region is an essential step toward radiomics-based bladder cancer diagnosis and prognosis. With the increasing development of radiomics, systematic analyses of these multiple regions on noninvasive bladder images would allow for a better understanding of the disease and support more personalized treatment approaches. Therefore, this review aims to extensively discuss CT- and MRI-based imaging tools and radiomics in decoding BCa phenotypes and recurrence risk, inspiring methodological progression and broadening their clinical applications in the near future.

SEARCH CRITERIA

In this study, we systematically retrieved peer-reviewed papers published from 2000 to 2021 (last query 04-20-2020). If a study appears in multiple publications, only the latest version was analyzed. The querying terms we used with the PubMed database were as:

((((((((((((((bladder cancer[Title/Abstract]) OR (bladder tumor[Title/Abstract])) AND (CT[Title/Abstract])) OR (MRI [Title/Abstract])) OR (multiparametric MRI[Title/Abstract])) OR (radiomics[Title/Abstract])) OR (biomarker[Title/Abstract])) OR (exosome[Title/Abstract])) OR (VI-RADS[Title/Abstract])) OR (radiomics[Title/Abstract])) AND (grade[Title/Abstract])) OR (grading[Title/Abstract])) OR (stage[Title/Abstract])) OR (staging[Title/Abstract])) OR (muscle invasive bladder cancer [Title/Abstract])) OR (recurrence[Title/Abstract]).

We excluded the papers according to the following criteria: i) studies focused on nonhuman subjects; ii) studies intended to repeatedly validate the previous developed tools or important findings; iii) studies published in conference proceedings or paper responses. For each paper enrolled, the publication year, study aims, patient cohorts, methodologies, findings and limitations were specifically analyzed to extract the valuable information we need to outline the main topic of study progress on noninvasive imaging and radiomics for decoding the phenotype and recurrence risk of BCa.

OVERALL WORKFLOW

According to previous studies, the overall workflow of noninvasively decoding the BCa phenotypes and recurrence risk is illustrated in **Figure 2**. Currently, the widely used imaging tools for BCa diagnosis mainly include CT, contrast-enhanced CT (CECT) and mpMRI (42, 51, 52), from which important imaging signs, such as tumor intensity distribution inhomogeneity, stalk, and SLE, can be observed by radiologists for image interpretation. After that, two radiomics pipelines, namely *Path1* and *Path 2* in **Figure 2**, are widely used to extract the high-throughput features that well reflect tumor properties for BCa phenotype prediction and recurrence risk assessment (59, 60, 62).

Apparent differences between these two pipelines are the strategies for multiregion ROIs segmentation, including the tumor region, its basal part and the normal wall region. Manual segmentation of multiregion ROIs of BCa is the first choice to many researchers. However, it is a tedious process with a huge workload. Exploring the automatic segmentation methods based on specific mathematical theorems (model-driven methods), such as level sets and Markov random fields (MRFs), becomes a more practical way. Nevertheless, owing to the intrinsic mathematical limitations, most of these methods just focus on the accurate segmentation of inner border (IB) and outer border (OB) of the bladder, incapable of segmenting the bladder multiregion on images. Consequently, some people turn to adopt the data-driven strategies like the modified UNet frame with convolutional neural network (CNN) module in *Path 2* to deal with this issue.

After image segmentation, feature extraction is the next important step. Currently, three kinds of radiomics features are commonly used, including morphological features, intensity-based features and texture features (59, 63–72). In addition, other features, such as the invasion depth of the BCa, which quantitatively measures the relative invasive depth of the tumor into the bladder wall (73), have also been gradually developed. Given that redundancy among features might severely affect the predictive performance, feature selection is indispensable toward developing an optimal predictive mode. Statistical analyses in combination with other high-level selection strategies, such as support vector machine (SVM)-based recursive feature elimination (SVM-RFE), least absolute shrinkage and selection operator (LASSO), max-relevance and min-redundancy

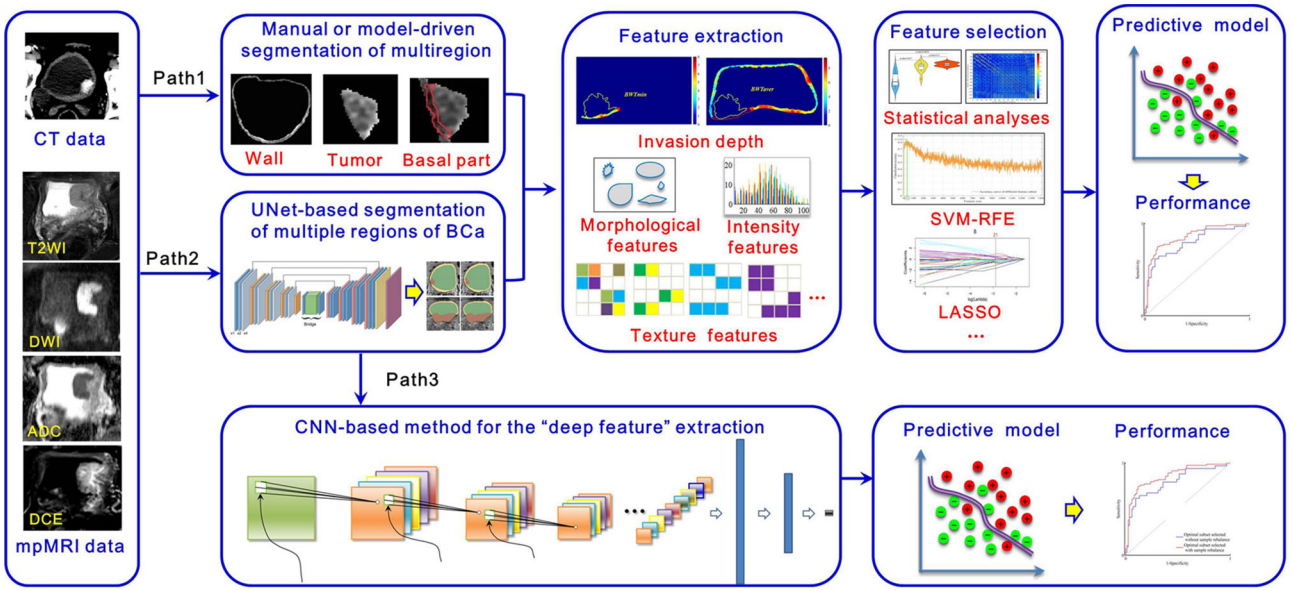

FIGURE 2 | Overall workflow of the radiomics strategy for decoding BCa phenotype and recurrence risk.

(mRMR), are widely used (26, 61, 74, 75). With the features selected, many machine learning classifiers, such as SVM, random forest (RF), and logistic regression, can be used for prediction model development (24, 58, 74–76). These steps in *Paths 1* and *2* constitute the traditional radiomics pipelines for noninvasive prediction of BCa phenotype and recurrence risk.

Considering the rapid development of deep learning (DL) methods in disease definition and identification, we also illustrate new radiomics pipeline in *Path 3* for this task. It includes two main steps, including *i)* a segmentation step that automatically segments multiregion ROIs of BCa from the original images by using a specific CNN module and *ii)* a diagnostic step that calculates deep features from these multiregion ROIs to develop a classifier for diagnosis by using another CNN module. Owing to the "black box" nature and complex procedures used in model building, this pipeline has yet to be comprehensively investigated. With the advent of explainable artificial intelligence (AI), we believe that *Path 3* will receive much more attention and investigation in the future.

MULTIREGION ROIS EXTRACTION

According to previous studies (77–82), the bladder wall and tumor regions contain plenty of information for BCa diagnosis and prognosis. A recent study (74) indicated that the basal part of bladder tumors on MRI has potential in determining MIS (**Figure 3**). Therefore, accurate delineation of the multiregion ROIs on bladder images other than using manual annotation is an essential step toward radiomics-based BCa diagnosis (83, 84).

Precise segmentation of bladder images is full of challenges, including partial volume effects, which usually occur where multiple tissues contribute to a single pixel in the image and cause blurry tissue boundaries, bladder shape variation, motion artifacts in the urine region and bladder wall, and complicated outer wall intensity distributions (83, 84). When further considering the precise segmentation of tumors in the bladder lumen, the problem becomes even more complicated (83). To address these challenges, many algorithms have been proposed since 2004 (83, 85, 86), as shown in **Table 1**. Li et al. (85, 86) first adopted the Markov random field to extract the IB of the bladder and to reduce the partial volume effects. Garnier et al. (87) adopted an active region growing strategy in a deformable model to realize the segmentation of both the IB and the OB. However, its performance for OB segmentation is far from satisfactory due to the complex tissue distribution surrounding the bladder (83).

Almost at the same time, level-set-based methods were introduced to extract both the IB and OB (77, 79, 80, 88, 89, 93). Duan et al. (80, 93) first proposed a coupled level-set framework with the modified Chan–Vese model to locate IB and OB from T1-weighted imaging (T1WI) in a 2-dimensional (2D) slice fashion. Based on the merits of this method for IB segmentation, Duan et al. (78, 79) further proposed an adaptive window-setting scheme with volume-based features to extract tumors on IB. Shortly afterward, Ma et al. (88) introduced the geodesic active contour (GAC) scheme into the Chan-Vese model to realize the shape-guided deformation of both IB and OB on the T2WI. A limitation of this approach is the intensity bias induced by the tumors inside the bladder lumen that easily leads to the leakage of IB segmentation. To overcome this limitation, Qin et al. (77) proposed an adaptive shape prior constrained level-set algorithm that evolves both IB and OB simultaneously from T2WI, greatly improving the accuracy for IB and OB segmentation. However, level-set-based methods are

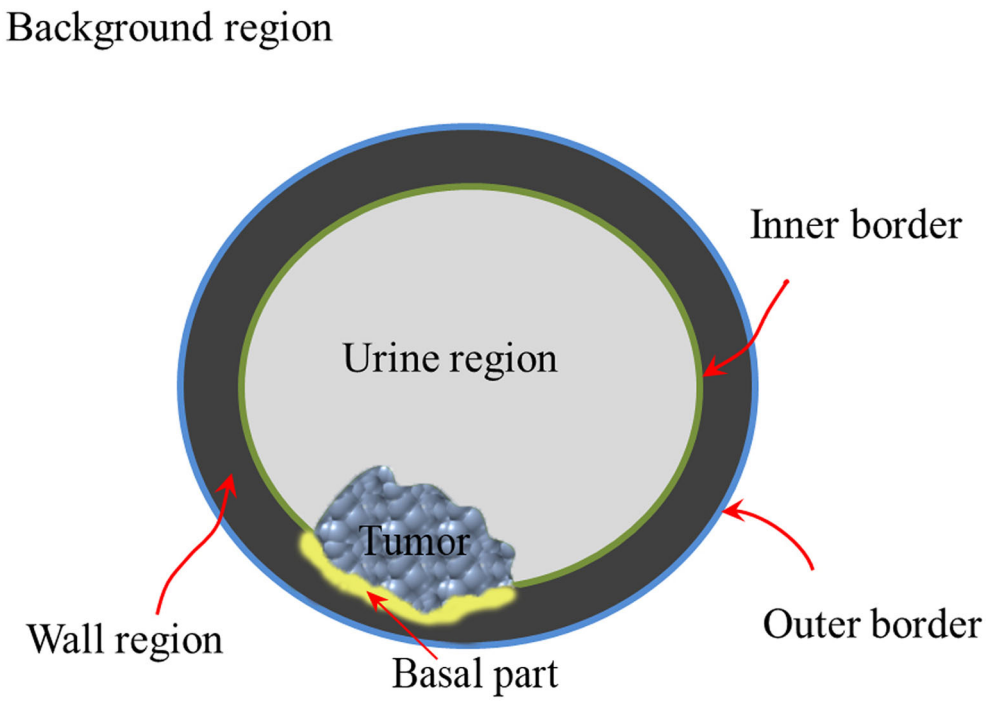

FIGURE 3 | Structure diagram of the multiregion of bladder on the noninvasive image.

TABLE 1 | Related studies and methodology of CT-/MRI-based bladder image segmentation during the past 20 years.

Study	Imaging	Approach or strategy	Region focused	Performance and Merits
Li et al., 2004 (86)	Multispectral MRI	Partial volume (PV) scheme	IB	More information extracted from the multispectral images, and feasible for the IB.
Li et al., 2008 (85)	Multispectral MRI	Markov random field (MRF)	IB	Realizing the inhomogeneity correction and overcoming the influence of partial volume and bias field.
Duan et al., 2010 (80)	T1WI	Coupled level-sets	*IB/OB	Realizing the simultaneous extraction of both IB and OB of the bladder.
Garnier et al., 2011 (87)	T2WI	3D deformable model based on active region growing strategy	IB/OB	Achieving good performance for the IB segmentation when tumors were not existed in the bladder lumen.
Duan et al., 2011 (78)	T1WI	Coupled level-sets + volume-based features	Tumor	Realizing the automatic detection of BCa.
Duan et al., 2012 (79)	T1WI	Coupled level-sets + volume-based features + Adaptive window-setting scheme	Tumor	Realizing the automatic detection and extraction of BCa.
Ma et al., 2011 (88)	T2WI	Geodesic active contour (GAC) + shape-guided Chan-Vese	IB/OB	Achieving good segmentation performance for both bladder borders without tumor regions using two datasets with 2D images.
Han et al., 2013 (89)	T1WI	Adaptive MRF with coupled level-set constraints	IB/OB	Fast convergence, robustness to initial estimates, and robustness against noise contaminations, as well as local shape variations of the bladder wall.
Qin et al., 2014 (77)	T2WI	Coupled directional level-sets with adaptive shape prior constraints	IB/OB	With the average DSC of 0.96 and 0.946, respectively, for the IB and OB segmentation using 11 datasets.
Cha et al., 2014 (90)	#CECT	Conjoint level set analysis and segmentation system (CLASS)	IB/OB	With the average DSC of 0.842 for the IB segmentation using 182 datasets.
Dolz et al., 2018 (83)	T2WI	Progressive dilated convolution-based U-NET model	IB/OB/ Tumor	With the average DSC of 0.9836, 0.8391 and 0.6856, respectively, for the IB, OB and tumor region segmentation using 60 datasets.
Gordon et al., *2018* (91)	CECT	Deep-learning convolutional neural network (DL-CNN)	IB/OB	With the average DSC of 0.9869 and 0.875, respectively, for the IB and OB segmentation using 172 datasets.
Ma et al., 2019 (92)	CECT	U-Net–based deep learning approach (U-DL)	IB	With the average DSC of 0.934 for the IB segmentation using 173 datasets.

**IB and OB represent the inner and outer borders of bladder, respectively.*
#CECT indicates contrast-enhanced CT.

modality-dependent and cannot be freely applied among different sequences or modalities. In addition, none of these methods can realize the simultaneous location and evolution of IB, OB and tumor regions.

Recently, CNN-based DL strategies have emerged as powerful tools for the semantic segmentation of bladder lumen CT images (90–92). During 2018, our group (83) proposed a modified UNet framework with a progressive dilated CNN module, realizing the simultaneous segmentation of IB, OB and BCa on T2WI for the first time. The average Dice's coefficient (DSC) of IB and OB were 0.9836 and 0.8391, respectively, but that of the tumor region was only 0.6856 (83).

Considering that different imaging sequences could provide complementary information for BCa diagnosis, how to realize the simultaneous segmentation of the multiple target regions on mpMRI bladder images becomes the ultimate goal in the workflow (**Figure 1**). To this end, we design an automatic bladder multiregion segmentation framework in **Figure 4**, which is based on the Mask-R-CNN (94) and mpMRI fusion strategy (95) with multiple labels to realize multiregion segmentation of mpMRI bladder images.

RADIOMICS-EMPOWERED DIAGNOSIS OF BCa PHENOTYPE

BCa Grading

The histological grade of BCa is a critical factor for the treatment decisions and prognosis (96). Cystoscopic resection and biopsy remains standard reference for BCa grading (76), but may easily cause diagnostic error due to the heterogeneity of tumor tissues (76).

With the development of noninvasive imaging, the imaging signs that reflect the BCa grade have been successively unearthed (96–102). For example, the peak time enhancement in the first minute ($E_{max/1}$) after contrast administration and the steepest slope of the DCE were first reported to be closely related to tumor angiogenesis (97). ADC values, including the mean ADC value and the normalized ADC value derived from DWI, have been demonstrated to be useful for BCa grading (98–103). In particular, Rosenkrantz et al. (37) adopted the quantitative metrics extracted from the tumor region on T2WI and DWI, including the tumor diameter, normalized T2 signal intensity and mean ADC value, for the assessment of tumor grade, as shown in **Table 2**. Although statistical analysis indicated that only the mean ADC value was a significant predictor, an area under the curve (AUC) of 0.804 was achieved for BCa grading (37), which could be recognized as the embryonic form of the mpMRI radiomics concept for BCa diagnosis.

In 2017, our group proposed a radiomics framework and investigated its feasibility for BCa grading (25). We adopted 102 radiomics features involving the histogram features and gray-level co-occurrence matrix-based (GLCM) features from the DWI and ADC maps to quantitatively describe the tumor properties. Then, the Mann–Whitney U-test and SVM-RFE were adopted for feature selection and diagnostic model development. The results based on 61 patients showed that the diagnostic model achieved a favorable performance for BCa grading, with an AUC of 0.861, which was significantly better than that of using the mean ADC values alone. Afterward, Wang et al. (76) investigated the performance of using the radiomics strategy with T2WI, DWI and ADC maps for BCa grading, achieving a more favorable diagnostic performance with an AUC of 0.9276 (76).

In addition, several studies have attempted to extract texture features from the tumor region on CT images for BCa grading. First-order texture features, such as the mean, standard deviation (SD), entropy, mean of positive pixels (MPP), skewness and kurtosis, and second-order features, such as GLCM features and

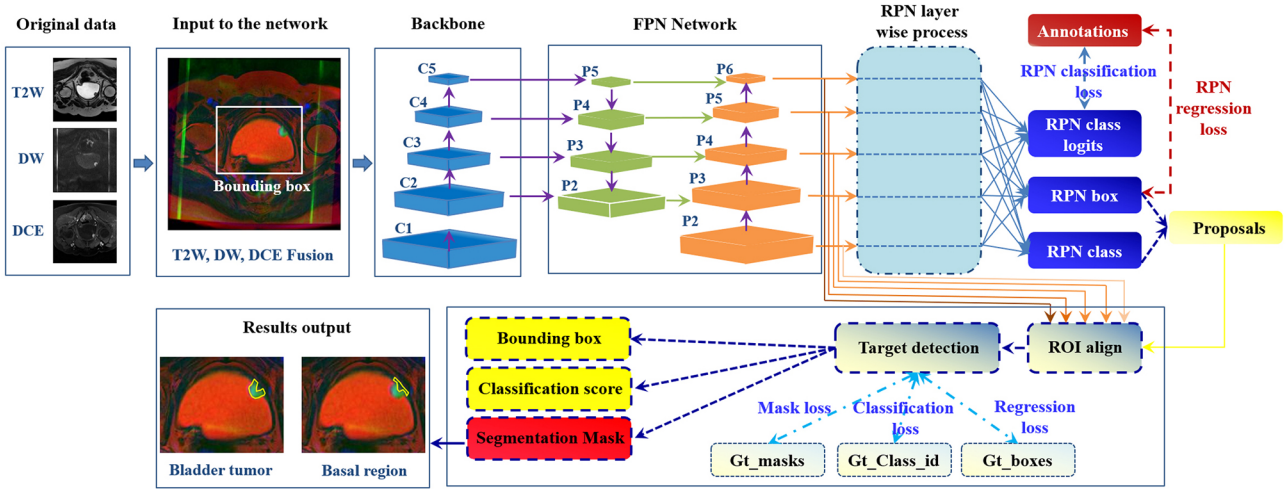

FIGURE 4 | Future framework of simultaneous segmentation of the multi-target regions from the bladder mpMRI. The Gt_class_id, Gt_boxes, and Gt_masks represent the ground truth of the multiregion anatation, position of the regions to be detected and focused, and segmentation mask (94).

TABLE 2 | Related studies and strategies of CT-/MRI-based BCa grading during the past 20 years.

Study	Patient	Imaging	Target	Approach or strategy	Results and findings
Tuncbilek et al., 2009 (97)	24 patients from single center	DCE	Tumor	Extracting *peak time enhancement in the first* ($E_{max/1}$), *second* ($E_{max/2}$), *third* ($E_{max/3}$), *fourth* ($E_{max/4}$) and *fifth* ($E_{max/5}$) minute after contrast administration, and the *steepest slope for* statistical analysis with tumor grade.	$E_{max/1}$and *steepest slope* had statistically significant correlation with tumor grade.
Avcu et al., 2011 (98)	63 patients from single center	DWI	Tumor	*Mean ADC values* were measured from the tumor mass.	The *mean ADC value* were significantly different between the high- and low-grade BCa.
Rosenkrantz et al., 2013 (37)	37 patients from double centers	T2WI, DWI	Tumor	*Tumor diameter, normalized T2 signal intensity* and *mean ADC value* were extracted.	*Mean ADC value* was statistically significant between the high- and low-grade BCa, with an AUC of 0.804 for the classification of this two groups.
Kobayashi et al., 2014 (104)	132 patients from single center	DWI	Tumor	*Mean ADC value* was calculated.	*Mean ADC value* was significantly lower in tumors with higher Ki-67 Lis and higher grade.
Sevcenco et al., 2014 (105)	43 patients from single center	DWI	Tumor	*Mean ADC value* was obtained.	*Mean ADC value* achieved favorable performance in predicting tumor grade, with an AUC of 0.906.
Sevcenco et al., 2014 (106)	41 patients from single center	DWI	Tumor	*Mean ADC value, p53 and p21* were obtained.	*Mean ADC value* and *p21* were the independent predictors for BCa grade, with an AUC of 0.981.
Wang et al., 2014 (102)	30 patients from single center	DWI	Tumor and referenced regions like urine	*Mean ADC value* and *normalized ADC (nADC)* values were calculated.	The performance of using the *nADC* with urine as reference was the best, with the AUC of 0.995.
Zhang et al., 2017 (107)	128 patients from single center	*CECT	Tumor	Six texture features, including *mean*, *SD*, *entropy*, *mean of positive pixels (MPP)*, *skewness* and *kurtosis*, were extracted.	*Mean*, *entropy* and *MPP* were significantly different between the high-grade BCa and low-grade on both unenhanced and enhanced images. *MPP* obtained from unenhanced images achieved the best performacne, with the AUC of 0.779.
Mammen et al., 2017 (108)	48 patients from single center	CT	Tumor	Texture features including *Kurtosis*, *skewness* and *entropy*, were extracted.	Only entropy showed significant inter-group differences, and it achieved an AUC of 0.83 in differentiation of low- and high-grade BCa.
Zhang et al., 2017 (25)	61 patients form single center	DWI ADC maps	Tumor	102 radiomics features, including the histogram and GLCM features	The model developed could achieve favorable performance for BCa grading, with the AUC of 0.861, significantly better than that of using the ADC value alone.
Wang et al., 2019 (76)	100 patients from single center	T2WI, DWI and ADC maps	Tumor	924 features were extracted, including morphological features and six categories of texture features like histogram features, GLCM features, *GLRLM features, *GLSZM features, *NGTDM features, and *GLDM features.	The multi-modal MRI-based radiomics approach has the potential in preoperative grading of BCa, with the AUC of 0.9276.
Wang et al., 2020 (15)	58 patients from single center	T2*-weighted imaging and DWI	Tumor	*Apparent transverse relaxation rate R2** and *mean ADC value* were calculated.	*R2** and *mean ADC value* were significantly different between low- and high-grade BCa, with the AUC of 0.714 and 0.779 in the classification process, respectively.
Zhang et al., 2020 (109)	145 patients	CT	Tumor	1316 radiomics features, involving the morphological features, histogram features, GLCM	The proposed radiomics model achieved a good performance, with AUC of 0.85 using the testing cohort.

(Continued)

TABLE 2 | Continued

Study	Patient	Imaging	Target	Approach or strategy	Results and findings
	from single center			features, GLRLM features, GLSZM features, GLDM features, were calculated.	

*CECT indicates the contrast enhanced CT.
*GLRLM indicates the gray-level run length matrix; GLSZM indicates the gray-level size zone matrix; NGTDM indicates the neighborhood gray tone difference matrix; GLDM indicates the gray-level dependence matrix.

gray-level run-length matrix (GLRLM) features, are commonly used and achieved the highest AUC of 0.83 (107–109).

MIS Prediction and Staging

Accurately predicting the stage and MIS of BCa is also crucial in making treatment decisions (37, 47, 105, 106). Pathological examination of transurethral resection of bladder tumor (TURBT) specimens is the first-line reference for preoperative BCa staging (38, 44, 47, 49, 51, 110). However, it may cause diagnostic errors such as understaging, misleading clinicians in making decisions (38, 44, 47, 51, 110, 111). A previous study reported that the error rate for preoperative BCa staging varies from 20 to 80% (20).

In current clinical practice, noninvasive imaging tools such as CT and MRI are also widely used for BCa staging and MIS prediction (15, 49, 51, 52, 112). However, the precision and robustness of using these imaging tools are unsatisfactory due to the challenges of discriminating between submucosal invasion and muscle invasion and between muscle invasion and perivesical fat proliferation by visual perception (15, 47, 50, 51, 112).

During 2000, Hayashi et al. (49) observed that the image sign of SLE often appears on NMIBC patients' DCE images (50). This finding is undoubtedly a milestone in imaging-based diagnosis of BCa stage and MIS. Afterward, Takeuchi et al. (44, 50) reported another important sign named the submucosal stalk or "inchworm" sign found among most NMIBCs on DWI, fortifying the precision and robustness of imaging-based diagnosis of BCa stage and MIS (49). Then, many studies found that the ADC values derived from high-stage (≥ T2) bladder tumors on DWI were significantly lower than those from low-stage (≤ T1) bladder tumors and thus could be used for the quantitative diagnosis of BCa stage and MIS with AUCs roughly between 0.65 and 0.96 (37, 38, 47, 49, 52, 104, 105, 110), as shown in **Table 3**.

By integrating all of these imaging signs, Panebianco et al. (114) proposed VI-RADS to quantify these signs on mpMRI and further standardize the image-based diagnostic procedures for MIS prediction (44, 45, 114). The performance was then evaluated by three groups, with the AUC varying between 0.873 and 0.94 (39, 40, 51, 111). Although VI-RADS has integrated all of the existing imaging signs, such as tumor intensity inhomogeneity, stalk and SLE, into the scoring system for MIS prediction, it is still a semiqualitative and expert-dependent process. Radiomics models based on high-throughput quantitative image features to implement automatic prediction of tumor phenotypes are considered a more practical method.

In fact, before VI-RADS was proposed, we reported the first radiomics strategy for the MIS prediction of BCa (24). This strategy utilized 63 radiomics features, including the histogram-based features and GLCM features extracted from the original T2WI and its high-order derivative maps for tumor characterization, achieving an AUC of 0.861 in MIS prediction (24). Shortly afterward, we extracted the GLCM and GLRLM features from the T2WI, DWI and ADC images and achieved a great performance improvement in MIS prediction, with an AUC of 0.9756 (26). Then, Zhang et al. (30) creatively included both the tumor region and the basal part with a radiomics nomogram that was proposed by Wu (29, 113), indicating that the basal part of bladder tumors is also critical for BCa MIS prediction.

All of these radiomics-based studies were based on single-center data. In 2020, we collected a double-centered mpMRI database involving 106 eligible patients, and adopted five categories of texture features and clinical factors to develop a new nomogram model for MIS prediction, achieving AUCs of 0.924 and 0.877 in both the training and validation cohorts, respectively (115).

RADIOMICS-EMPOWERED STRATIFICATION OF BCa RECURRENCE RISK

A high recurrence rate is a distinguishing epidemiological property of BCa. The recurrence rate of NMIBC patients who underwent TURBT at one year was as high as 70% (8, 10, 112). However, as many as 50% of MIBC patients who undergo radical cystectomy (RC) with bilateral lymph node dissection and ileal conduits develop local or metastatic recurrence during the next 24 months (61, 116, 117). Preoperatively predicting the recurrence risk of BCa patients is pivotal for facilitating appropriate adjuvant treatment strategies and the management of patients.

At present, the EAU has provided guidelines to stratify BCa patients into different groups to recommend more specific adjuvant therapy (8, 10, 15, 29, 112), as shown in **Figure 5**. The guidelines categorize NMIBC patients into low-, intermediate- and high-risk groups of recurrence using the European Organization for the Research and Treatment of Cancer (EORTC) risk table and recommend TURBT + intravesical chemotherapy (IVC), TURBT + one-year Bacillus Calmette-Guérin (BCG), and RC. Nevertheless, this risk table merely considers six predominant clinical and histopathological

TABLE 3 | Related studies and strategies of CT-/MRI-based BCa staging and MIS prediction during the past 20 years.

Study	Patient	Imaging	Target	Approach or strategy	Results and findings
Hayashi et al., 2000 (49)	71 patients from single center	DCE	Tumor	*Submucosal linear enhancement* (SLE)	*SLE* achieved an accuracy of 83% for BCa staging, and 87% for MIS prediction, respectively.
Takeuchi et al., 2009 (41)	40 patients with 52 bladder tumors from single center	T2WI, DWI, DCE	Tumor	*Submucosal stalk*	The overall accuracy of T stage diagnosis was 67% for T2WI alone, 88% for T2WI+ DWI, 79% for T2WI+DCE, and 92% for all three image types together.
Rosenkrantz et al., 2013 (37)	37 patients from double centers	T2WI, DWI	Tumor	*Tumor diameter, normalized T2 signal intensity* and *mean ADC value* were extracted.	High-stage (≥ T2) tumors showed greater tumor diameter and lower mean ADC value than the low-stage (≤ T1) tumors. The AUC for MIS prediction was 0.804 by jointly using the tumor diameter and mean ADC value.
Kobayashi et al., 2014 (104)	132 patients from single center	DWI	Tumor	*Mean ADC value* was calculated.	*Mean ADC value* was significantly lower with higher T stage bladder tumors.
Sevcenco et al., 2014 (105)	43 patients from single center	DWI	Tumor	*Mean ADC value* was obtained.	*Mean ADC value* achieved good performance in predicting MIS, with an AUC of 0.884.
Wang et al., 2016 (38)	59 patients from single center	T2WI, DWI, DCE	Tumor	*SLE, submucosal stalk*	The staging accuracy of DWI was 91.3%. When combining with DCE, the accuracy was improved to 94.6%.
Xu et al., 2017 (24)	68 patients from a single center	T2WI	Tumor	*A total of 63 three-dimensional radiomics features, including the histogram-based features and GLCM features, were extracted from the original images and their high-order derivative maps in association with the Student's *t*-test and SVM-RFE for feature selection and SVM classifier for the diagnostic model development.	13 features were finally selected, with an optimal AUC of 0.8610 for MIS diagnosis, which for the first time introduced the radiomics strategy into the preoperative MIS identification and demonstrated its feasibility.
Wu et al., 2017 (113)	118 patients from single center	CT	Tumor	# A radiomics signature was determined by the optimal features selected from the original 150 radiomics features uing the LASSO approach. In combination with the clinical factors, a radiomics nomogram was then developed.	The radiomics nomogram showed good discrimination in training and validation cohorts for the prediction of lymph node metastasis, with the AUC of 0.9262 and 0.8986, respectively.
Panebianco et al., 2018 (114)	/	T2WI, DWI, ADC, DCE	Tumor and submucosal layer	Quantitatively scoring the imaging signs like tumor shape, stalk and SLE on the multiparametric MRI.	The Vesical Imaging-Reporting and Data System (VI-RADS) could be a standard and useful tool to half quantify these imaging signs on the multiparametric MRI for BCa staging and MIS diagnosis.
Wu et al., 2018 (29)	103 patients from single center	T2WI	Tumor	A radiomics signature was determined by nine optimal features selected from the original 718 radiomics features uing the LASSO approach. In combination with the clinical factors, a radiomics nomogram was then developed.	The radiomics signature achieved the AUC of 0.8447 for the prediction of lymph node metastasis. And the nomogram consisted of the radiomics signature with the clinical factors achieved more favorable performance, with the AUC improved to 0.8902 in the validation cohort.
Xu et al.,2019 (26)	54 patients from single center	T2WI, DWI, ADC	Tumor	Radiomics features like histogram-based, GLCM and GLRLM features were extracted from the multimodal MRI data with the multi-grayscale normalization strategy.	The optimal 19 features derived from the three modalities finally achieved the best performance, with the AUC of 0.9756 for MIS diagnosis, indicating the great capacity of the multimodal MRI-based radiomics strategy for the preoperative MIS identification.
Zheng et al., 2019 (30)	199 patients	T2WI	Tumor and basal part	2602 radiomics features were extracted from both the tumorous region and basal part of the images. A radiomics	The radiomics signature showed good performance in MIS prediction. Integrating with

(Continued)

TABLE 3 | Continued

Study	Patient	Imaging	Target	Approach or strategy	Results and findings
	from single center			signature was determined uing the LASSO approach. In combination with the clinical factors, a radiomics nomogram was then developed.	the clinical factor, nomogram achieved much better diagnostic power, with the AUC improved to 0.876 in the validation cohort.
Barchetti et al., 2019 (51)	78 patients from single center	T2WI, DWI, ADC, DCE	Tumor and submucosal layer	VI-RADS	The VI-RADS achieved favorable performance for MIS diagnosis, with the AUC of 0.926 and 0.873 when conducted by reader 1 and 2, respectively.
Ueno et al., 2019 (39)	74 patients from single center	T2WI, DWI, ADC, DCE	Tumor and submucosal layer	VI-RADS	The VI-RADS achieved favorable performance for MIS diagnosis, with pooled AUC of 0.90 when conducted by five readers.
Wang et al., 2019 (40)	340 patients from single center	T2WI, DWI, ADC, DCE	Tumor and submucosal layer	VI-RADS	The VI-RADS achieved excellent performance for MIS diagnosis, with the AUC of 0.94 when conducted by two readers in consensus.
Wang et al., 2020 (115)	106 patients from double centers	T2WI, DWI, ADC	Tumor	1404 radiomics features were extracted. A radiomics signature was generated using the SVM-RFE and logistic regression. A nomogram was then developed using the signature and MRI-determined tumor stalk.	The signature alone achieved a good performance in MIS prediction. The nomogram integrating with the signature and tumor stalk achieved much better diagnostic performance, with the AUC improved to 0.877 in the validation cohort.

**SVM-RFE indicates the support vector-machine-based recursive feature elimination algorithm.*
#LASSO indicates the least absolute shrinkage and selection operator algorithm for feature selection.

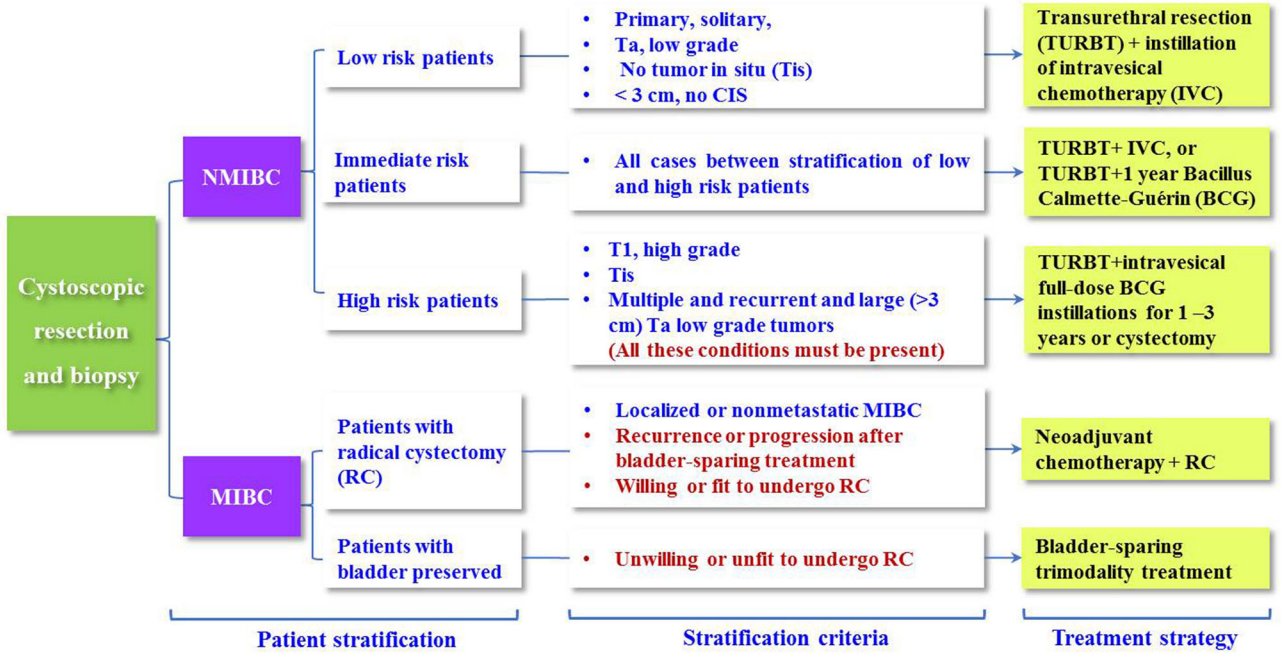

FIGURE 5 | Treatment recommendations for BCa patients based on the MIS, grade and recurrence risk stratification.

factors, including the number of tumors, tumor size, prior recurrence rate, T stage, grade, and presence of concurrent tumors *in situ* (Tis), to achieve a quantitative prediction of the recurrence risk (10, 29).

Then, the Club Urológico Español de Tratamiento Oncológico (CUETO) developed a new risk table to predict the short- and long-term recurrence risks for NMIBC patients with postoperative BCG treatment (15). Many studies subsequently

reported that the precision of the EORTC and CUETO risk tables was far less than satisfactory in the recurrence risk stratification of NMIBC, with Harrell's C-index ranging between 0.51 and 0.77 (8, 10, 35, 48, 118–122), as shown in **Table 4**. Other studies also reported that tumor sites in the bladder neck and/or trigone, grade and stage are independent risk factors for the prediction of BCa recurrence (48, 117, 123). In 2019, Yajima et al. (48) found that the tumor stalk (inchworm sign) on DWI is a significant sign for BCa prognosis.

Considering that the high-throughput radiomics features of the underlying tumor region have the potential to reflect tumor heterogeneity and the microenvironment, which are closely related to tumor recurrence, making full use of these features may achieve a more accurate prediction of the risk of BCa recurrence.

With this assumption, our group retrospectively collected the preoperative T2WI, DWI, ADC and DCE images of 71 patients who were confirmed with NMIBC or MIBC, treated with TURBT or RC accordingly, and followed for 2 years (61). Then, 1872 radiomics features were extracted from the tumor regions of their preoperative mpMRI, including histogram features, GLCM features, GLRLM features, neighborhood gray-tone difference matrix (NGTDM) features and gray-level size zone matrix (GLSZM) features. After that, these features in combination with important clinical risk factors, such as age, sex, grade, MIS, stalk, SLE, tumor size, number of lesions and surgery choice (TURBT or RC), were used for radiomics-clinical nomogram development. The performance of the nomogram model obtained AUCs of 0.915 and 0.838 for the training and validation cohorts, respectively. These results suggest that the radiomics strategy has excellent potential in the preoperative prediction of BCa recurrence.

DISCUSSION AND FUTURE PERSPECTIVES

Urinary bladder cancer is a highly prevalent disease among aged males (1–3). Accurate diagnosis of tumor phenotypes and recurrence risk serves as the "bedrock" of appropriate clinical therapeutic strategy and is of vital importance in the follow-up management of BCa patients. The standard reference for preoperatively diagnosing BCa phenotypes is cystoscopic biopsy, which is an invasive procedure that carries certain risks of bladder perforation (30). More importantly, a significant risk of misdiagnosis such as understaging or overstaging, may occur that induces incorrect estimation of the recurrence risk based on EORTC, and delays the proper radical treatment (8, 10, 13, 30).

In recent years, reading preoperative radiographic images produced by CT, CECT, PET, mpMRI, or US plays an essential role in the noninvasive diagnosis and recurrence prediction of BCa, in which radiomics strategies have also demonstrated their great power of identifying complex patterns precisely, effectively and stably (124). Integrating radiomics strategies with noninvasive imaging in the clinical setting is expected to provide more valuable supplementary information to the urologist for BCa diagnosis and prognosis, preoperatively.

However, the clinical application of noninvasive imaging-based radiomics strategies for preoperatively decoding BCa phenotypes and recurrence risk is still in its infancy. In this study, we reviewed the rapid progress in the field during the past 20 years, summarizing the entire pipeline of the radiomics strategy including region of interest definition, radiomics feature extraction, tumor phenotype prediction and recurrence risk stratification, sincerely hoping to further promote massive clinical applications of noninvasive radiomics tools for the preoperative BCa diagnosis and prognosis in the near future.

In this section, we particularly focused on the current pitfalls, challenges and opportunities of this field.

Public Imaging Datasets for BCa

Data collection is the first step to adopt radiomics strategies for the BCa phenotype and recurrence risk prediction. At present, there are several public databases for BCa research, including the *National Cancer Database* (NCDB), the *National Cancer Institute's Surveillance, Epidemiology, and End Results* cancer database (SEER) (125), and *The Cancer Imaging Archive* database (TCIA). Although the first two databases contain nearly 100 thousand BCa patients, most of them only contain the clinical diagnoses, treatments and end results, without the imaging datasets attached. TCIA aims to deidentify and host a large archive of medical images of cancer accessible for public research. However, it contains only 139 BCa patients' medical images. Therefore, the current public datasets are very limited for developing a radiomics model with sufficient training and testing for the prediction task.

Simultaneous Segmentation of Multiple Regions From Multimodal Bladder Images

Precise segmentation of multiple regions of the bladder on images, including tumor regions, basal parts, and bladder wall regions, is a critical step toward further extracting features for tumor phenotype prediction. Several previous studies adopted a two-step strategy to first segment the mixed region between IB and OB from the original image and then separate the tumor lesion from its adherent wall region (78, 79, 81). This strategy not only reduces the segmentation precision but also increases the complexity and time consumption.

So far, only one study implemented the simultaneous segmentation of the IB, OB and tumor regions from the bladder images (83), but its performance for tumor segmentation was unsatisfactory. As indicated in **Figure 4**, it is expected that the end-to-end framework based on the DL networks could facilitate better segmentation performance (126–129). In particular, with more domain priors, such as the bladder wall thickness distribution, shape variation and attention mechanism of the integrated target region (13, 30, 39, 53), more precise and robust DL-based models could be established to improve the accuracy and efficiency of multiregional bladder segmentation from multimodal images, such as mpMRI.

TABLE 4 | Related studies and strategies of BCa recurrence risk prediction during the past 20 years.

Study	Patient	Treatment	Follow-up/years	Predictionmodel	Findings	Conclusion
Sylvester et al., 2006 (118)	2596 NMIBC patients from 7 EORTC trials	TURBT + Intravesical treatment (78.4% of the patients)	Median follow-up of 3.9 years and maximum follow-up of 14.8 years	Univariate and multivariate analyses	The EORTC risk table was derived based on the number and size of tumors, prior recurrence rate, T category, carcinoma in situ, and grade.	EORTC risk table is a useful tool for the urologist to discuss the different options with the patient to determine the most appropriate treatment and frequency of follow-up.
Fernandez et al., 2009 (8)	1062 NMIBC patients from 4 CUETO trials	TURBT + BCG with 12 instillations	5 years	Univariate and multivariate analyses	The CUETO risk table was developed using gender, age, grade, tumor status, multiplicity and associated Tis.	The recurrence risks calculated by the CUETO table were lower than those obtained with EROTC table.
Seo et al., 2010 (122)	251 patients from single center	TURBT + full-doze maintenance BCG	5 years and 9 months	EORTC	C-index: 0.62	The recurrence rate and progression rate were almost similar to the EORTC risk tables. However, the recurrence rate was low in the intermediate-risk group.
Xylinas et al., 2013 (120)	4784 patients from 8 centers	TURBT +51% cohort of immediate single postoperative chemotherapy + 11% cohort of BCG	4 years and 9 months	EORTC, CUETO	C-index: 0.60, 0.52	Both models exhibited poor discrimination. Specific biomarkers should be exploited for improving the performance.
Xu et al., 2013 (48)	363 NMIBC patients from single center	TURBT +79% cohort of immediate single postoperative chemotherapy + 100% cohort of the entire course of intravesical chemotherapy	3 years	EORTC, CUETO	C-Index: 0.71, 0.66	The EORTC model showed more value in predicting recurrence and progression in patients with NMIBC.
Kohjimoto et al., 2014 (121)	366 NMIBC patients from single center	TURBT + BCG	5 years	EORTC, CUETO	C-index: 0.51, 0.58	Although both exhibited poorly for recurrence prediction, CUETO was a little better.
Vedder et al., 2014 (35)	1892 NMIBC patients from 18 centers	TURBT +13~22% cohort of the entire course of intravesical chemotherapy +17~30% cohort of BCG + 0.55~0.61% cohort of Re-TURBT	10 years	EORTC, CUETO	C-index: 0.56-0.59, 0.64-0.72	The discriminatory ability for BCa recurrence was unsatisfactory.
Cambier et al., 2016 (10)	1812 NMIBC patients from 2 EORTC trials	TURBT + 1~3 years of maintenance BCG	7 years 5 months	Updated EORTC	C-index: 0.59.	NMIBC patients treated with1~3 years of maintenance BCG had a heterogeneous prognosis among the high-risk patients, and early cystoscopy should be considered.
Dalkilic et al., 2018 (119)	400 NMIBC patients from single center	TURBT + BCG (45.3% of the patients)	5 years	EORTC, CUETO	C-index: 0.777, 0.703	EORTC risk table was better than the CUETO table for the recurrence prediction.
Kim et al., 2019 (35)	970 NMIBC patients from single center	TURBT + BCG	5 years	New model, EORTC	AUC: 0.65, 0.56	The new model developed by using gross hamartia, previous or concomitant upper urinary tract urothelial carcinoma, stage, grade, number of tumors, intravesical

(Continued)

TABLE 4 | Continued

Study	Patient	Treatment	Follow-up/years	Predictionmodel	Findings	Conclusion
						treatment performed better than the EORTC risk table.
Yajima et al., 2019 (48)	91 NMIBC patients from single center	TURBT	5 years	Inchworm sign (tumor stalk) on the DWI and ADC images	The progression rate of inchworm-sign-negative cases was significantly higher than that of inchworm-sign-positive cases, whereas there was no significant difference in the recurrence rate between two groups.	The absence of an inchworm sign and histological grade 3 were independent risk factors for progression.
Xu et al., 2019 (61)	71 patients including 36 NMIBC patients and 35 MIBC patients from single center	TURBT for the NMIBC patients and RC for the MIBC patients	2 years	Radiomics nomogram developed based on the radiomics features extracted from T2WI, DWI, ADC, and DCE MRI data, and the clinical risk factors	The proposed radiomics nomogram exhibited good performance both in the training cohort (AUC: 0.915) and the validation cohort (AUC: 0.838) for the prediction of the BCa recurrence during 2 years after operation.	The proposed radiomics-clinical nomogram has potential in the preoperative prediction

Quantitative Invasion Depth Definition for BCa Staging

Almost all of the previous studies were focused on the tumor region for feature extraction (24, 107, 109, 130, 131). Currently, only one study considered both the tumor region and the basal part for radiomics feature calculation and it reported the superiority of this new strategy for staging and MIS prediction (74). Considering that the bladder wall region also contains useful information such as bladder wall thickness (BWT) for BCa detection and diagnosis (81, 132), more features are expected to be designed for BCa staging and MIS prediction. For instance, using the tumor location and BWT distributed on the wall region, the invasive depth of BCa (D_{in}) might be defined by the entropy of minimum BWT (BWT_{min}) of the cancerous region and the average BWT (BWT_{aver}) other than the cancerous region, as shown in **Figure 6**.

Fully Using VI-RADS for BCa Phenotype Prediction and Recurrence Risk Stratification

During the past 20 years, mpMRI is increasingly introduced into pre-TURBT diagnosis, achieving favorable accuracy in BCa staging and differentiation of NMIBC and MIBC (30, 39, 40). Despite the undeniable advances in mpMRI for bladder imaging, a lack of standardization of imaging protocols and reporting basis becomes the main cause of performance variation. To this end, VI-RADS scoring system defines a standardized approach to imaging and reporting mpMRI for BCa (39). Nevertheless, most of the previous studies only focused the performance of using VI-RADS for the pre-TURBT discrimination between NMIBC and MIBC (13, 30, 51, 53), regardless of other valuable diagnostic information VI-RADS may contain for therapeutic strategy (133, 134).

Del Giudice et al. (135, 136), recently reported that *i)* VI-RADS could provide valuable information for the selection of patients who are candidate for repeated-TURBT among the high-risk NMIBC cases; *ii)* VI-RADS could be valid and reliable in discriminating between BCa patients with extravesical disease and those with muscle-confined BCa before TURBT, and VI-RADS score 5 could be used to predict significant delay in time-to-cystectomy independently from other clinico-pathological factors. Given that the muscle invasive status is significantly related to BCa recurrence, VI-RADS that well reflect the imaging difference between NMIBC and MIBC, may have potential in recurrence risk stratification of BCa patients.

In addition, concerning that many surgical subspecialties, including urology, have suspended elective services and delayed many time-sensitive surgeries during the midst of COVID-19 pandemic, BCa staging is considered a priority because of the potential aggressive behavior of this disease (137). VI-RADS at the present time period may help urologist to dramatically minimize elective procedures and realize an accurate evaluation of tumor staging from a single examination, providing a prognostic criterion for adjusting oncologic class priority among overwhelmed waiting lists (137).

Integrating the "Shallow" Features With the "Deep" Features for BCa Phenotype Diagnosis

Currently, the radiomics features adopted mainly involve the morphological features describing the geometric properties of the target region and texture features depicting the global, local and regional intensity distribution patterns of the target region (74, 115), which are designed based on certain physical or mathematical theories of the pixel intensity distribution characterized on the original images and thus can be regarded

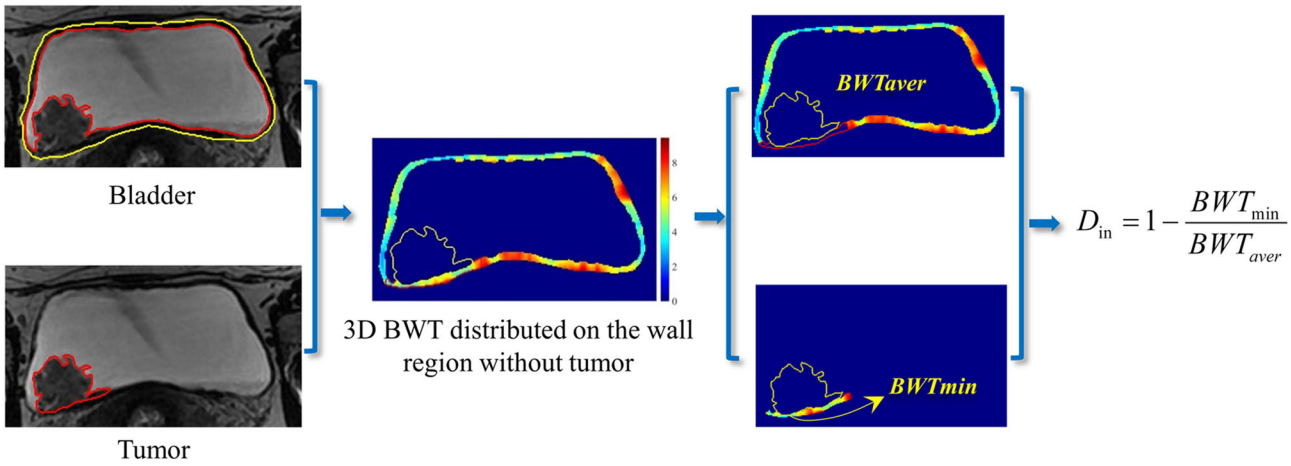

FIGURE 6 | A potential definition of the invasive depth of bladder tumor based on the BWT distribution on the bladder wall region.

as manual or "*shallow*" features. In recent years, the radiomics features extracted by using CNN-based deep learning networks have been increasingly used to characterize the deep properties of tumors for cancer diagnosis (126, 138, 139). Owing to the black-box nature of CNN networks, the "*deep*" feature selected and the model developed seem hard to explain, limiting their applications in clinics. With the improvements in the interpretability of deep features, it is expected that the integration of shallow and deep features would provide a more precise preoperative diagnosis of the BCa phenotype.

Macro-meso-micro Multiomics Information Fusion for More Precise, Explainable BCa Recurrence Prediction

Although both the EORTC and CUETO risk tables are extensively used as the clinical reference for NMIBC recurrence risk stratification (10), their predictive performance is far less than satisfactory (29, 120, 121, 140–142). Given that most of features in these two risk tables are macroscopic clinical factors, they may not well describe the hidden properties of BCa that are closely related to recurrence. Until now, only one study (61) has reproted the feasibility and performance of the radiomics strategy for BCa recurrence risk prediction, in which manually extracted or shallow features from a mesoscopic view were adopted in the framework.

It is now appreciated that bladder tumors are heterogeneous at the metabolomics and genomics levels (5). For example, the specific proteins and RNAs of exosomes in urine can be used as noninvasive biomarkers for BCa screening and phenotype prediction (143–149). Low-grade carcinomas can be characterized at the molecular level by loss of heterozygosity (LOH) of chromosome 9 and activating mutations of genes encoding fibroblast growth factor receptor 3 (FGFR3) and telomerase reverse transcriptase (TERT), while MIBC is thought to arise *via* flat dysplasia and Tis (5). The human epidermal growth factor receptor-2 (HER2) has been reported with overexpression among aggressive BCa for the past decade, suggesting that this biomarker might aid in patient risk stratification and treatent selection (150, 151). Ferro et al. reported that absolute basophil count is closely related to time to recurrence among patients with high-grade T1 BCa receiving BCG after TURBT (152). Whether these biomarkers can be used for BCa recurrence prediction, remains unknown. Therefore, in the future, it is believed that with macro-meso-micro information fusion of the multiomics features and multidisciplinary knowledge, the predictive performance of the recurrence risk will be greatly improved.

CONCLUSION

Noninvasive imaging technologies, such as CT, contrast-enhanced CT and multiparametric MRI, and radiomic strategies can promote the overall performance of the phenotype diagnosis and recurrence risk prediction for patients with bladder cancer.

AUTHOR CONTRIBUTIONS

XX and HW collected and reviewed the literature. XX and HW wrote the manuscript. XX, HL, and YL helped with the writing design and revised the manuscript. YG, XZ, BL, and PD provided insightful comments and suggestions on the manuscript. All authors contributed to the article and approved the submitted version.

FUNDING

This work was partially supported by the National Natural Science Foundation of China under grant (No. 81901698, 81871424, 61976248, and 82071989), Military Science and Technology Foundation under grant No. BLB19J0101, and Young Eagle Plan of High Ambition Project under grant No. 2020CYJHXXP.

REFERENCES

1. Bray F, Ferlay J, Soerjomataram I, Siegel RL, Torre LA, Jemal A. Global Cancer Statistics 2018: GLOBOCAN Estimates of Incidence and Mortality Worldwide for 36 Cancers in 185 Countries. *CA: A Cancer J Clin* (2018) 68 (6):349-424. doi: 10.3322/caac.21492
2. Siegel RL, Miller KD, Fuchs HE, Jemal A. Cancer Statistics, 2021. *CA Cancer J Clin* (2021) 71:7–33. doi: 10.3322/caac.21654
3. Sung H, Ferlay J, Siegel RL, Laversanne M, Soerjomataram I, Jemal A, et al. Global Cancer Statistics 2020: GLOBOCAN Estimates of Incidence and Mortality Worldwide for 36 Cancers in 185 Countries. *CA Cancer J Clin* (2021) 71(3):209–49. doi: 10.3322/caac.21660
4. Siegel RL, Miller KD, Jemal A. Cancer Statistics, 2020. *CA Cancer J Clin* (2020) 70(1):7–30. doi: 10.3322/caac.21590
5. Sanli O, Dobruch J, Knowles MA, Burger M, Alemozaffar M, Nielsen ME, et al. Bladder Cancer. *Nat Rev Dis Primers* (2017) 13(3):17022. doi: 10.1038/nrdp.2017.22
6. Burger M, Catto JW, Dalbagni G, Grossman HB, Herr H, Karakiewicz P, et al. Epidemiology and Risk Factors of Urothelial Bladder Cancer. *Eur Urol* (2016) 34(3):124–33. doi: 10.1016/j.eururo.2012.07.033
7. Kamat AM, Hahn NM, Efstathiou JA, Lerner SP, Malmström P-U, Choi W, et al. Bladder Cancer. *Lancet* (2016) 388(10061):2796–810. doi: 10.1016/S0140-6736(16)30512-8
8. Alfred Witjes J, Lebret T, Comperat EM, Cowan NC, De Santis M, Bruins HM, et al. Updated 2016 EAU Guidelines on Muscle-Invasive and Metastatic Bladder Cancer. *Eur Urol* (2017) 71(3):462–75. doi: 10.1016/j.eururo.2016.06.020
9. Antoni S, Ferlay J, Soerjomataram I, Znaor A, Jemal A, Bray F. Bladder Cancer Incidence and Mortality: A Global Overview and Recent Trends. *Eur Urol* (2017) 71(1):96–108. doi: 10.1016/j.eururo.2016.06.010
10. Babjuk M, Bohle A, Burger M, Capoun O, Cohen D, Comperat EM, et al. EAU Guidelines on Non-Muscle-Invasive Urothelial Carcinoma of the Bladder: Update 2016. *Eur Urol* (2017) 71(3):447–61. doi: 10.1016/j.eururo.2016.05.041
11. Moch H, Humphrey P, Ulbright T, Reuter V. Tumours of the Urinary Tract. In: *World Health Organization Classification of Tumours of the Urinary System and Male Genital Organs*, *4th edn.* IARC Press (2016). p. 77–133.
12. Witjes JA, Bruins HM, Cathomas R, Comperat EM, Cowan NC, Gakis G, et al. European Association of Urology Guidelines on Muscle-Invasive and Metastatic Bladder Cancer: Summary of the 2020 Guidelines. *Eur Urol* (2020). doi: 10.1016/j.eururo.2020.03.055
13. Ueno Y, Takeuchi M, Tamada T, Sofue K, Takahashi S, Kamishima Y, et al. Diagnostic Accuracy and Interobserver Agreement for the Vesical Imaging-Reporting and Data System for Muscle-Invasive Bladder Cancer: A Multireader Validation Study. *Eur Urol* (2019) S0302-2838(19):30198–8.
14. Soukup V, Capoun O, Cohen D, Hernandez V, Burger M, Comperat E, et al. Risk Stratification Tools and Prognostic Models in Non-Muscle-Invasive Bladder Cancer: A Critical Assessment From the European Association of Urology Non-Muscle-Invasive Bladder Cancer Guidelines Panel. *Eur Urol Focus* (2018).
15. Fernandez-Gomez J, Madero R, Solsona E, Unda M, Martinez–Pineiro L, Gonzalez M, et al. Predicting Nonmuscle Invasive Bladder Cancer Recurrence and Progression in Patients Treated With Bacillus Calmette-Guerin: The CUETO Scoring Model. *J Urol* (2009) 182(5):2195–203. doi: 10.1016/j.juro.2009.07.016
16. Kaffenberger SD, Miller DC, Nielsen ME. Editorial: Simplifying Treatment and Reducing Recurrence for Patients With Early-Stage Bladder Cancer. *JAMA* (2018) 319(18):1864–5. doi: 10.1001/jama.2018.4656.(18):1864-5
17. Vukomanovic I, Colovic V, Soldatovic I, Hadzi-Djokic J. Prognostic Significance of Tumor Location in High-Grade Non-Muscle-Invasive Bladder Cancer. *Med Oncol* (2012) 29(3):1916–20. doi: 10.1007/s12032-011-9999-4
18. Aerts HJ, Velazquez ER, Leijenaar RT, Parmar C, Grossmann P, Carvalho S, et al. Decoding Tumour Phenotype by Noninvasive Imaging Using a Quantitative Radiomics Approach. *Nat Commun* (2014) 5:4006. doi: 10.1038/ncomms5644
19. Verma S, Rajesh A, Prasad SR, Gaitonde K, Lall CG, Mouraviev V, et al. Urinary Bladder Cancer: Role of MR Imaging. *Radiographics* (2012) 32 (2):371–87. doi: 10.1148/rg.322115125
20. Turker P, Bostrom PJ, Wroclawski ML, van Rhijn B, Kortekangas H, Kuk C, et al. Upstaging of Urothelial Cancer at the Time of Radical Cystectomy: Factors Associated With Upstaging and its Effect on Outcome. *BJU Int* (2012) 110(6):804–11. doi: 10.1111/j.1464-410X.2012.10939.x
21. Jakse G, Algaba F, Malmstrom P, Oosterlinck W. A Second-Look TUR in T1 Transitional Cell Carcinoma: Why? *Eur Urol* (2004) 45(5):539–46. doi: 10.1016/j.eururo.2003.12.016
22. van Rhijn BW, Burger M, Lotan Y, Solsona E, Stief CG, Sylvester RJ, et al. Recurrence and Progression of Disease in non-Muscle-Invasive Bladder Cancer: From Epidemiology to Treatment Strategy. *Eur Urol* (2009) 56 (3):430–42. doi: 10.1016/j.eururo.2009.06.028
23. Makram M, Michaël P, Marc Z, Djillali S, Bernard D. The Value of a Second Transurethral Resection in Evaluating Patients With Bladder Tumours. *Eur Urol* (2003) 43(3):241–5. doi: 10.1016/S0302-2838(03)00040-X
24. Xu X, Liu Y, Zhang X, Tian Q, Wu Y, Zhang G, et al. Preoperative Prediction of Muscular Invasiveness of Bladder Cancer With Radiomic Features on Conventional MRI and its High-Order Derivative Maps. *Abdominal Radiol* (2017) 42(7):1896–905. doi: 10.1007/s00261-017-1079-6
25. Zhang X, Xu X, Tian Q, Li B, Wu Y, Yang Z, et al. Radiomics Assessment of Bladder Cancer Grade Using Texture Features From Diffusion-Weighted Imaging. *J magnetic resonance imaging: JMRI* (2017) 46(5):1281–8. doi: 10.1002/jmri.25669
26. Xu X, Zhang X, Tian Q, Wang H, Cui LB, Li S, et al. Quantitative Identification of Nonmuscle-Invasive and Muscle-Invasive Bladder Carcinomas: A Multiparametric MRI Radiomics Analysis. *J Magn Reson imaging: JMRI* (2019) 49(5):1489–98. doi: 10.1002/jmri.26327
27. Svatek RS, Hollenbeck BK, Holmang S, Lee R, Kim SP, Stenzl A, et al. The Economics of Bladder Cancer: Costs and Considerations of Caring for This Disease. *Eur Urol* (2014) 66(2):253–62. doi: 10.1016/j.eururo.2014.01.006
28. Burger M, van der Aa MN, van Oers JM, Brinkmann A, van der Kwast TH, Steyerberg EC, et al. Prediction of Progression of Non-Muscle-Invasive Bladder Cancer by WHO 1973 and 2004 Grading and by FGFR3 Mutation Status: A Prospective Study. *Eur Urol* (2008) 54(4):835–43. doi: 10.1016/j.eururo.2007.12.026
29. Cambier S, Sylvester RJ, Collette L, Gontero P, Brausi MA, van Andel G, et al. EORTC Nomograms and Risk Groups for Predicting Recurrence, Progression, and Disease-Specific and Overall Survival in Non-Muscle-Invasive Stage Ta-T1 Urothelial Bladder Cancer Patients Treated With 1-3 Years of Maintenance Bacillus Calmette-Guerin. *Eur Urol* (2016) 69(1):60–9. doi: 10.1016/j.eururo.2016.01.055
30. Panebianco V, Narumi Y, Barchetti G, Montironi R, Catto JWF. Should We Perform Multiparametric Magnetic Resonance Imaging of the Bladder Before Transurethral Resection of Bladder? Time to Reconsider the Rules. *Eur Urol* (2019) 76(1):57–8. doi: 10.1016/j.eururo.2019.03.046
31. van der Pol CB, Chung A, Lim C, Gandhi N, Tu W, McInnes MDF, et al. Update on Multiparametric MRI of Urinary Bladder Cancer. *J Magn Reson imaging: JMRI* (2018) 48(4):882–96. doi: 10.1002/jmri.26294
32. McKiernan J, Asafu-Adjei D. Bridging the Gender Gap: Bladder Cancer Is More Deadly in Women Than in Men That Needs To Change. *Nature* (2017) S39:1–2. doi: 10.1038/551S39a
33. Fahmy O, Khairul-Asri MG, Schubert T, Renninger M, Malek R, Kubler H, et al. A Systematic Review and Meta-Analysis on the Oncological Long-Term Outcomes After Trimodality Therapy and Radical Cystectomy With or Without Neoadjuvant Chemotherapy for Muscle-Invasive Bladder Cancer. *Urologic Oncol* (2018) 36(2):43–53. doi: 10.1016/j.urolonc.2017.10.002
34. Rais-Bahrami S, Pietryga JA, Nix JW. Contemporary Role of Advanced Imaging for Bladder Cancer Staging. *Urologic Oncol* (2016) 34(3):124–33. doi: 10.1016/j.urolonc.2015.08.018
35. Kim HS, Jeong CW, Kwak C, Kim HH, Ku JH. Novel Nomograms to Predict Recurrence and Progression in Primary Non-Muscle-Invasive Bladder Cancer: Validation of Predictive Efficacy in Comparison With European Organization of Research and Treatment of Cancer Scoring System. *World J Urol* (2019) 37(9):1867–77. doi: 10.1007/s00345-018-2581-3
36. Wang H, Pui M, Guo Y, Yang D, Pan B, Zhou X. Diffusion-Weighted MRI in Bladder Carcinoma: The Differentiation Between Tumor Recurrence and Benign Changes After Resection. *Abdominal Imaging* (2014) 39(1):135–41. doi: 10.1007/s00261-013-0038-0

37. Rosenkrantz AB, Haghighi M, Horn J, Naik M, Hardie AD, Somberg MB, et al. Utility of Quantitative MRI Metrics for Assessment of Stage and Grade of Urothelial Carcinoma of the Bladder: Preliminary Results. *AJR Am J Roentgenol* (2013) 201(6):1254–9. doi: 10.2214/AJR.12.10348
38. Wang H, Pui MH, Guan J, Li S, Lin J, Pan B, et al. Comparison of Early Submucosal Enhancement and Tumor Stalk in Staging Bladder Urothelial Carcinoma. *AJR-Am J Roentgenol* (2016) 207(4):797–803. doi: 10.2214/AJR.16.16283
39. Panebianco V, Narumi Y, Altun E, Bochner BH, Efstathiou JA, Hafeez S, et al. Multiparametric Magnetic Resonance Imaging for Bladder Cancer: Development of VI-RADS (Vesical Imaging-Reporting And Data System). *Eur Urol* (2018) 74(3):294–306. doi: 10.1016/j.eururo.2018.04.029
40. Thoeny HC, Bellin MF, Comperat EM, Thalmann GN. Vesical Imaging-Reporting and Data System (VI-RADS): Added Value for Management of Bladder Cancer Patients? *Eur Urol* (2018) 74(3):307–8. doi: 10.1016/j.eururo.2018.06.017
41. Takeuchi M, Sasaki S, Ito M, Okada S, Takahashi S, Kawai T, et al. Urinary Bladder Cancer: Diffusionweighted MR Imaging—Accuracy for Diagnosing T Stage and Estimating Histologic Grade1. *Radiology* (2009) 251(1):112–21. doi: 10.1148/radiol.2511080873
42. Renard-Penna R, Rocher L, Roy C, et al. Imaging Protocols for CT Urography: Results of a Consensus Conference From the French Society of Genitourinary Imaging. *Eur Radiol* (2020) 30(3):1387–96. doi: 10.1007/s00330-019-06529-6
43. Molen AJVD, Cowan NC, Mueller-Lisse UG, Nolte-Ernsting CCA, Takahashi S, Cohan RH, et al. CT Urography: Definition, Indications and Techniques. *A Guideline for Clinical Practice Eur Radiol* (2008) 18:4–17. doi: 10.1007/s00330-007-0792-x
44. Gandhi N, Krishna S, Booth CM, Breau RH, Flood TA, Morgan SC, et al. Diagnostic Accuracy of Magnetic Resonance Imaging for Tumour Staging of Bladder Cancer: Systematic Review and Meta-Analysis. *BJU Int* (2018) 122(5):744–53. doi: 10.1111/bju.14366
45. Woo S, Suh CH, Kim SY, Cho JY, Kim SH. Diagnostic Performance of MRI for Prediction of Muscle-Invasiveness of Bladder Cancer: A Systematic Review and Meta-Analysis. *Eur J Radiol* (2017) 95:46–55. doi: 10.1016/j.ejrad.2017.07.021
46. Zhang N, Wang X, Wang C, Chen S, Wu J, Zhang G, et al. Diagnostic Accuracy of Multi-Parametric Magnetic Resonance Imaging for Tumor Staging of Bladder Cancer: Meta-Analysis. *Front Oncol* (2019) 9:981. doi: 10.3389/fonc.2019.00981
47. Bollineni VR, Kramer G, Liu Y, Melidis C, deSouza NM. A Literature Review of the Association Between Diffusion-Weighted MRI Derived Apparent Diffusion Coefficient and Tumour Aggressiveness in Pelvic Cancer. *Cancer Treat Rev* (2015) 41(6):496–502. doi: 10.1016/j.ctrv.2015.03.010
48. Yajima S, Yoshida S, Takahara T, Arita Y, Tanaka H, Waseda Y, et al. Usefulness of the Inchworm Sign on DWI for Predicting Pt1 Bladder Cancer Progression. *Eur Radiol* (2019) 29(7):3881–8. doi: 10.1007/s00330-019-06119-6
49. Hayashi N, Tochigi H, Shiraishi T, Takeda K, Kawamura J. A New Staging Criterion for Bladder Carcinoma Using Gadolinium-Enhanced Magnetic Resonance Imaging With an Endorectal Surface Coil: A Comparison With Ultrasonography. *BJU Int* (2000) 85(1):32–6. doi: 10.1046/j.1464-410x.2000.00358.x
50. Tekes A, Kamel I, Imam K, Szarf G, Schoenberg M, Nasir K, et al. Dynamic MRI of Bladder Cancer: Evaluation of Staging Accuracy. *AJR Am J Roentgenol* (2005) 184(1):121–7. doi: 10.2214/ajr.184.1.01840121
51. Barchetti G, Simone G, Ceravolo I, Salvo V, Campa R, Del Giudice F, et al. Multiparametric MRI of the Bladder: Inter-Observer Agreement and Accuracy With the Vesical Imaging-Reporting and Data System (VI-RADS) at a Single Reference Center. *Eur Radiol* (2019) 29(10):5498–506. doi: 10.1007/s00330-019-06117-8
52. Luo C, Huang B, Wu Y, Chen J, Chen L. Use of Vesical Imaging-Reporting and Data System (VI-RADS) for Detecting the Muscle Invasion of Bladder Cancer: A Diagnostic Meta-Analysis. *Eur Radiol* (2020) 30(8):4606–14. doi: 10.1007/s00330-020-06802-z
53. Wang H, Luo C, Zhang F, Guan J, Li S, Yao H, et al. Multiparametric MRI for Bladder Cancer: Validation of VI-RADS for the Detection of Detrusor Muscle Invasion. *Radiology* (2019) 291(3):668–74. doi: 10.1148/radiol.2019182506
54. Zhu X, Dong D, Chen Z, Fang M, Zhang L, Song J, et al. Radiomic Signature as a Diagnostic Factor for Histologic Subtype Classification of Non-Small Cell Lung Cancer. *Eur Radiol* (2018) 28(7):1–7. doi: 10.1007/s00330-017-5221-1
55. Bashir U, Kawa B, Siddique M, Mak SM, Nair A, Mclean E, et al. Non-Invasive Classifcation of Non-Small Cell Lung Cancer: A Comparison Between Random Forest Models Utilising Radiomic and Semantic Features. *Br J Radiol* (2019) 92(20190159):1–8. doi: 10.1259/bjr.20190159
56. Li H, Zhu Y, Burnside ES, Huang E, Drukker K, Hoadley KA, et al. Quantitative MRI Radiomics in the Prediction of Molecular Classifications of Breast Cancer Subtypes in the TCGA/TCIA Data Set. *NPJ Breast Cancer* (2016) 2:16012. doi: 10.1038/npjbcancer.2016.12
57. Huang YQ, Liang CH, He L, Tian J, Liang CS, Chen X, et al. Development and Validation of a Radiomics Nomogram for Preoperative Prediction of Lymph Node Metastasis in Colorectal Cancer. *J Clin Oncol: Off J Am Soc Clin Oncol* (2016) 34(18):2157–64. doi: 10.1200/JCO.2015.65.9128
58. Xu X, Zhang X, Tian Q, Zhang G, Liu Y, Cui G, et al. Three-Dimensional Texture Features From Intensity and High-Order Derivative Maps for the Discrimination Between Bladder Tumors and Wall Tissues *via* MRI. *Int J Comput assisted Radiol Surg* (2017) 12(4):645–56. doi: 10.1007/s11548-017-1522-8
59. Lambin P, Leijenaar RTH, Deist TM, Peerlings J, de Jong EEC, van Timmeren J, et al. Radiomics: The Bridge Between Medical Imaging and Personalized Medicine. *Nat Rev Clin Oncol* (2017) 14(12):749–62. doi: 10.1038/nrclinonc.2017.141
60. Gillies RJ, Kinahan PE, Hricak H. Radiomics: Images Are More Than Pictures, They Are Data. *Radiology* (2016) 278(2):563–77. doi: 10.1148/radiol.2015151169
61. Xu X, Wang H, Du P, Zhang F, Li S, Zhang Z, et al. A Predictive Nomogram for Individualized Recurrence Stratification of Bladder Cancer Using Multiparametric MRI and Clinical Risk Factors. *J Magn Reson Imaging* (2019) 50(6):1893–904. doi: 10.1002/jmri.26749
62. Lambin P, Rios-Velazquez E, Leijenaar R, Carvalho S, van Stiphout RGPM, Granton P, et al. Radiomics: Extracting More Information From Medical Images Using Advanced Feature Analysis. *Eur J Cancer (Oxfo Engl: 1990)* (2012) 48(4):441–6. doi: 10.1016/j.ejca.2011.11.036
63. Majtner T, Svoboda D. *2012 Second International Conference on 3D Imaging, Modeling, Processing, Visualization & Transmission*, IEEE (2012):301–7. doi: 10.1109/3DIMPVT.2012.61
64. Sun C, Wee WG. Neighboring Gray Level Dependence Matrix for Texture Classification. *Compute Vision Graphics Image Process* (1983) 23:341–52. doi: 10.1016/0734-189X(83)90032-4
65. Galloway MM. Texture Analysis Using Gray Level Run Lengths. *Comput Graphics Image Process* (1975) 4:172–9. doi: 10.1016/S0146-664X(75)80008-6
66. Wang X, Albregtsen F, Foyn B. Texture Features from Gray level Gap Length Matrix. *MVA'94 IAPR Workshop on Machine Vision Applications*. Kawasaki, Japan (1994).
67. Thibault G, Angulo J, Meyer F. Advanced Statistical Matrices for Texture Characterization: Application to DNA Chromatin and Microtubule Network Classification. In: *IEEE International Conference on Image Processing*. IEEE (2011). p. 53–6. doi: 10.1109/ICIP.2011.6116401
68. Thibault G, Angulo J, Meyer F. Advanced Statistical Matrices for Texture Characterization: Application to Cell Classification. In: *IEEE Transactions on Biomedical Engineering*. (2014) vol. 61(3). p. 630–7.
69. Amadasun M, King R. Texural Features Corresponding to Texural Properties. In: *IEEE Transactions on Systems, Man, and Cybernetics*. (1989) vol. 19(5). p. 1264–74.
70. Haralick RM, Shanmugam K, Dinstein IH. Textural Features for Image Classification. In: *IEEE Transactions on Systems, Man, and Cybernetics*. (1973) vol. SMC-3(6). p. 610–21.
71. Tamura H, Mori S, Yamawaki T. Textural Features Corresponding to Visual Perception. In: *IEEE Transactions on Systems, Man, and Cybernetics*. (1978) vol. SMC-8. (1978). p. 460–73.
72. Thibault G, Fertil B, Navarro C, Pereira S, Levy N, Sequeira J, et al. Texture Indexes and Gray Level Size Zone Matrix Application to Cell Nuclei Classification. In: *In Pattern Recognition and Information Processing (PRIP)*. Minsk, Belarus (2009). p. 140–5.
73. Liu Y, Zheng H, Xu X, Zhang X, Du P, Liang J, et al. The Invasion Depth Measurement of Bladder Cancer Usingt2-Weighted Magnetic Resonance Imaging. *Biomed Eng Online* (2020) 19(1):92. doi: 10.21203/rs.2.22984/v4

74. Zheng J, Kong J, Wu S, Li Y, Cai J, Yu H, et al. Development of a Noninvasive Tool to Preoperatively Evaluate the Muscular Invasiveness of Bladder Cancer Using a Radiomics Approach. *Cancer* (2019) 125(24):4388–4398.
75. Wu S, Zheng J, Li Y, Wu Z, Shi S, Huang M, et al. Development and Validation of an MRI-Based Radiomics Signature for the Preoperative Prediction of Lymph Node Metastasis in Bladder Cancer. *EBioMedicine* (2018) 34:76–84. doi: 10.1016/j.ebiom.2018.07.029
76. Wang H, Hu D, Yao H, Chen M, Li S, Chen H, et al. Radiomics Analysis of Multiparametric MRI for the Preoperative Evaluation of Pathological Grade in Bladder Cancer Tumors. *Eur Radiol* (2019) 29(11):6182–90. doi: 10.1007/s00330-019-06222-8
77. Qin X, Li X, Liu Y, Lu H, Yan P. Adaptive Shape Prior Constrained Level Sets for Bladder MR Image Segmentation. *IEEE J OF Biomed AND Health Informatics* (2014) 18(5):1707–16. doi: 10.1109/JBHI.2013.2288935
78. Duan C, Yuan K, Liu F, Xiao P, Lv G, Liang Z. Volume-Based Features for Detection of Bladder Wall Abnormal Regions *via* MR Cystography. *IEEE Trans Biomed Eng* (2011) 58(9):2506–12. doi: 10.1109/TBME.2011.2158541
79. Duan C, Yuan K, Liu F, Xiao P, Lv G, Liang Z. An Adaptive Window-Setting Scheme for Segmentation of Bladder Tumor Surface *via* MR Cystography. *IEEE Trans Inf Technol Biomed: Publ IEEE Eng Med Biol Soc* (2012) 16 (4):720–9. doi: 10.1109/TITB.2012.2200496
80. Duan C, Liang Z, Bao S, Zhu H, Wang S, Zhang G, et al. A Coupled Level Set Framework for Bladder Wall Segmentation With Application to MR Cystography. *IEEE Trans Med Imaging* (2010) 29(3):903–15. doi: 10.1109/TMI.2009.2039756
81. Xiao D, Zhang G, Liu Y, Yang Z, Zhang X, Li L, et al. 3D Detection and Extraction of Bladder Tumors *via* MR Virtual Cystoscopy. *Int J Comput Assisted Radiol Surg* (2016) 11(1):89–97. doi: 10.1007/s11548-015-1234-x
82. Qin X, Lu H, Tian Y, Yan P. Partial Sparse Shape Constrained Sector-Driven Bladder Wall Segmentation. *Mach Vision Appl* (2015) 26(5):593–606. doi: 10.1007/s00138-015-0684-z
83. Dolz J, Xu X, Jeo R, Yuan J, Liu Y, Granger E, et al. Multiregion Segmentation of Bladder Cancer Structures in MRI With Progressive Dilated Convolutional Networks. *Med Phys* (2018) 45(12):5482–93. doi: 10.1002/mp.13240
84. Xu X, Zhang X, Liu Y, Tian Q, Zhang G, Yang Z, et al. Simultaneous Segmentation of Multiple Regions in 3D Bladder MRI by Efficient Convex Optimization of Coupled Surfaces. *Image Graphics* (2017) 10667. doi: 10.1007/978-3-319-71589-6_46
85. Li L, Liang Z, Wang S, Lu H, Wei X, Wagshul M, et al. Segmentation of Multispectral Bladder MR Images With Inhomogeneity Correction for Virtual Cystoscopy. *Proc SPIE - Int Soc Optical Eng* (2008) 6916:69160U-U-5. doi: 10.1117/12.769914
86. Li L, Wang Z, Xiang L, Wei X, Adler HL, Wei H, et al. A New Partial Volume Segmentation Approach to Extract Bladder Wall for Computer Aided Detection in Virtual Cystoscopy. *Proc SPIE - Int Soc Optical Eng* (2004). doi: 10.1117/12.535913
87. Garnier C, Ke W, Dillenseger JL. Bladder Segmentation in MRI Images Using Active Region Growing Model. *Int Conf IEEE Eng Med Biol Soc* (2011), 5702–5. doi: 10.1109/IEMBS.2011.6091380
88. Ma Z, Jorge RN, Mascarenhas T, Tavares JMRS. Novel Approach to Segment the Inner and Outer Boundaries of the Bladder Wall in T2-Weighted Magnetic Resonance Images. *Ann Biomed Eng* (2011) 39(8):2287–97. doi: 10.1007/s10439-011-0324-3
89. Han H, Li L, Duan C, Zhang H, Zhao Y, Liang Z. A Unified EM Approach to Bladder Wall Segmentation With Coupled Level-Set Constraints. *Med Image Anal* (2013) 17(8):1192–205. doi: 10.1016/j.media.2013.08.002
90. Cha K, Hadjiiski L, Chan HP, Caoili EM, Cohan RH, Zhou C. CT Urography: Segmentation of Urinary Bladder Using CLASS With Local Contour Refinement. *Phys Med Biol* (2014) 59(11):2767. doi: 10.1088/0031-9155/59/11/2767
91. Gordon MN, Hadjiiski LM, Cha KH, Samala RK, Chan HP, Cohan RH, et al. Deep-Learning Convolutional Neural Network: Inner and Outer Bladder Wall Segmentation in CT Urography. *Med Phys* (2019) 46(2):634–48. doi: 10.1002/mp.13326
92. Ma X, Hadjiiski LM, Wei J, Chan HP, Cha KH, Cohan RH, et al. U-Net Based Deep Learning Bladder Segmentation in CT Urography. *Med Phys* (2019) 46(4):1752–65. doi: 10.1002/mp.13438
93. Chi JW, Brady M, Moore NR, Schnabel JA. Segmentation of the Bladder Wall Using Coupled Level Set Methods. *IEEE Int Symposium Biomed Imaging: Nano to Macro* (2011). doi: 10.1109/ISBI.2011.5872721
94. Zhao X, Xie P, Wang M, Li W, Pickhardt PJ, Xia W, et al. Deep Learning-Based Fully Automated Detection and Segmentation of Lymph Nodes on Multiparametric-Mri for Rectal Cancer: A Multicentre Study. *EBioMedicine* (2020) 56:102780. doi: 10.1016/j.ebiom.2020.102780
95. Trebeschi S, van Griethuysen JJM, Lambregts DMJ, Lahaye MJ, Parmar C, Bakers FCH, et al. Deep Learning for Fully-Automated Localization and Segmentation of Rectal Cancer on Multiparametric MR. *Sci Rep* (2017) 7 (1):5301. doi: 10.1038/s41598-017-05728-9
96. Kirkali Z, Chan T, Manoharan M, Algaba F, Busch C, Cheng L, et al. Bladder Cancer: Epidemiology, Staging and Grading, and Diagnosis. *Urology* (2005) 66(6 Suppl 1):4–34. doi: 10.1016/j.urology.2005.07.062
97. Tuncbilek N, Kaplan M, Altaner S, Atakan IH, Süt N, Inci O, et al. Value of Dynamic ContrastEnhanced MRI and Correlation With Tumor Angiogenesis in Bladder Cancer. *AJR Am J Roentgenol* (2009) 192(4):949–55. doi: 10.2214/AJR.08.1332
98. Avcu S, Koseoglu MN, Ceylan K, Dbulut M, Unal O. The Value of Diffusion-Weighted MRI in the Diagnosis of Malignant and Benign Urinary Bladder Lesions. *Br J Radiol* (2011) 84(2011):875–82. doi: 10.1259/bjr/30591350
99. Kobayashi S, Koga F, Yoshida S, Masuda H, Ishii C, Tanaka H, et al. Diagnostic Performance of Diffusion-Weighted Magnetic Resonance Imaging in Bladder Cancer: Potential Utility of Apparent Diffusion Coefficient Values as a Biomarker to Predict Clinical Aggressiveness. *Eur Radiol* (2011) 21(10):2178–86. doi: 10.1007/s00330-011-2174-7
100. Green DA, Durand M, Gumpeni N, Rink M, Cha EK, Karakiewicz PI, et al. Role of Magnetic Resonance Imaging in Bladder Cancer: Current Status and Emerging Techniques. *BJU Int* (2012) 110(10):1463–70. doi: 10.1111/j.1464-410X.2012.11129.x
101. Bihan DL. Apparent Diffusion Coefficient and Beyond: What Diffusion MR Imaging Can Tell Us About Tissue Structure. *Radiology* (2013) 268(2):318–22. doi: 10.1148/radiol.13130420
102. Wang HJ, Pui MH, Guo Y, Li SR, Liu MJ, Guan J, et al. Value of Normalized Apparent Diffusion Coefficient for Estimating Histological Grade of Vesical Urothelial Carcinoma. *Clin Radiol* (2014) 69(7):727–31. doi: 10.1016/j.crad.2014.03.001
103. Suo S, Chen X, Ji X, Zhuang Z, Wu L, Yao Q, et al. Investigation of the Non-Gaussian Water Diffusion Properties in Bladder Cancer Using Diffusion Kurtosis Imaging: A Preliminary Study. *J Comput Assisted Tomog* (2015) 39:281–5. doi: 10.1097/RCT.0000000000000197
104. Kobayashi S, Koga F, Kajino K, Yoshita S, Ishii C, Tanaka H, et al. Apparent Diffusion Coefficient Value Reflects Invasive and Proliferative Potential of Bladder Cancer. *J Magn Reson Imaging: JMRI* (2014) 39(1):172–8. doi: 10.1002/jmri.24148
105. Sevcenco S, Ponhold L, Heinz-Peer G, Fajkovic H, Haitel A, Susani M, et al. Prospective Evaluation of Diffusion-Weighted MRI of the Bladder as a Biomarker for Prediction of Bladder Cancer Aggressiveness. *Urologic Oncol* (2014) 32(8):1166–71. doi: 10.1016/j.urolonc.2014.04.019
106. Sevcenco S, Haitel A, Ponhold L, Susani M, Fajkovic H, Shariat SF, et al. Quantitative Apparent Diffusion Coefficient Measurements Obtained by 3-Tesla MRI Are Correlated With Biomarkers of Bladder Cancer Proliferative Activity. *PloS One* (2014) 9(9):1–6. doi: 10.1371/journal.pone.0106866
107. Zhang G-M-Y, Sun H, Shi B, Jin Z-Y, Xue H-D. Quantitative CT Texture Analysis for Evaluating Histologic Grade of Urothelial Carcinoma. *Abdominal Radiol* (2017) 42(2):561–8. doi: 10.1007/s00261-016-0897-2
108. Mammen S, Krishna S, Quon M, Shabana WM, Hakim SW, Flood TA, et al. Diagnostic Accuracy of Qualitative and Quantitative Computed Tomography Analysis for Diagnosis of Pathological Grade and Stage in Upper Tract Urothelial Cell Carcinoma. *J Comput Assisted Tomog* (2017) 42 (2):204–10. doi: 10.1097/RCT.0000000000000664
109. Zhang G, Xu L, Zhao L, Mao L, Li X, Jin Z, et al. CT-Based Radiomics to Predict the Pathological Grade of Bladder Cancer. *Eur Radiol* (2020) 30 (12):6749–56. doi: 10.1007/s00330-020-06893-8
110. Huang L, Kong Q, Liu Z, Wang J, Kang Z, Zhu Y. The Diagnostic Value of MR Imaging in Differentiating T Staging of Bladder Cancer: A Meta-Analysis. *Radiology* (2017) 286(2):171028. doi: 10.1148/radiol.2017171028

111. Hassanien OA, Abouelkheir RT, El-Ghar MIA, Badawy ME, Gamal S-h, El-Hamid MA. Dynamic Contrast-Enhanced Magnetic Resonance Imaging as a Diagnostic Tool in the Assessment of Tumour Angiogenesis in Urinary Bladder Cancer. *Can Assoc Radiol J* (2019) 70(3):254–63. doi: 10.1016/j.carj.2018.11.004
112. Sylvester R, Meijden A, Oosterlinck W, Witjes J, Bouffioux C, Denis L, et al. Predicting Recurrence and Progression in Individual Patients With Stage Ta T1 Bladder Cancer Using EORTC Risk Tables: A Combined Analysis of 2596 Patients From Seven EORTC Trials. *Eur Urol* (2006) 49(3):466–75. doi: 10.1016/j.eururo.2005.12.031
113. Wang Y, Shen Y, Hu X, Li Z, Feng C, Hu D, et al. Application of R2* and Apparent Diffusion Coefficient in Estimating Tumor Grade and T Category of Bladder Cancer. *AJR Am J Roentgenol* (2020) 214(2):383–9. doi: 10.2214/AJR.19.21668
114. Panebianco V, Berardinis ED, Barchetti G, Simone G, Leonardo C, Grompone MD, et al. An Evaluation of Morphological and Functional Multi-Parametric MRI Sequences in Classifying non-Muscle and Muscle Invasive Bladder Cancer. *Eur Radiol* (2017) 27(9):3759–66. doi: 10.1007/s00330-017-4758-3
115. Wang H, Xu X, Zhang X, Liu Y, Ouyang L, Du P, et al. Elaboration of a Multisequence MRI-Based Radiomics Signature for the Preoperative Prediction of the Muscle-Invasive Status of Bladder Cancer: A Double-Center Study. *Eur Radiol* (2020) 30(9):4816–27. doi: 10.1007/s00330-020-06796-8
116. Ha HK, Koo PJ, Kim SJ. Diagnostic Accuracy of F-18 FDG PET/CT for Preoperative Lymph Node Staging in Newly Diagnosed Bladder Cancer Patients: A Systematic Review and Meta-Analysis. *Oncology* (2018) 95(1):31–8. doi: 10.1159/000488200
117. Fujii Y, Fukui I, Kihara K, Tsujii T, Ishizaka K, Kageyama Y, et al. Significance of Bladder Neck Involvement on Progression in Superficial Bladder Cancer. *Eur Urol* (1998) 33:464–8. doi: 10.1159/000019636
118. Wang Y, Hu D, Yu H, Shen Y, Tang H, Kamel IR, et al. Comparison of the Diagnostic Value of Monoexponential, Biexponential, and Stretched Exponential Diffusionweighted MRI in Differentiating Tumor Stage and Histological Grade of Bladder Cancer. *Acad Radiol* (2018) 26(2):239–46. doi: 10.1016/j.acra.2018.04.016
119. Kohjimoto Y, Kusumoto H, Nishizawa S, Kikkawa K, Kodama Y, Ko M, et al. External Validation of European Organization for Research and Treatment of Cancer and Spanish Urological Club for Oncological Treatment Scoring Models to Predict Recurrence and Progression in Japanese Patients With non-Muscle Invasive Bladder Cancer Treated With Bacillus Calmette–Guérin. *Int J Urol* (2014) 21(12):1201–7. doi: 10.1111/iju.12572
120. Xu T, Zhu Z, Zhang X, Wang X, Zhong S, Zhang M, et al. Predicting Recurrence and Progression in Chinese Patients With Nonmuscle-Invasive Bladder Cancer Using EORTC and CUETO Scoring Models. *Urology* (2013) 82(2):387–93. doi: 10.1016/j.urology.2013.04.007
121. Xylinas E, Kent M, Kluth L, Pycha A, Comploj E, Svatek RS, et al. Accuracy of the EORTC Risk Tables and of the CUETO Scoring Model to Predict Outcomes in non-Muscle-Invasive Urothelial Carcinoma of the Bladder. *Br J Cancer* (2013) 109(6):1460–6. doi: 10.1038/bjc.2013.372
122. Seo KW, Kim BH, Park CH, Kim CI, Chang HS. The Efficacy of the EORTC Scoring System and Risk Tables for the Prediction of Recurrence and Progression of non-Muscle-Invasive Bladder Cancer After Intravesical Bacillus Calmette-Guerin Instillation. *Korean J Urol* (2010) 51(3):165–70. doi: 10.4111/kju.2010.51.3.165
123. Fujii Y, Fukui I, Kihara K, Tsujii T, Kageyama Y, Oshima H. Late Recurrence and Progression After a Long Tumor-Free Period in Primary Ta and T1 Bladder Cancer. *Eur Urol* (1999) 36:309–13. doi: 10.1159/000020010
124. Ge L, Chen Y, Yan C, Zhao P, Zhang P, Runa A, et al. Study Progress of Radiomics With Machine Learning for Precision Medicine in Bladder Cancer Management. *Front Oncol* (2019) 9:1296. doi: 10.3389/fonc.2019.01296
125. Wang J, Wu Y, He W, Yang B, Gou X. Nomogram for Predicting Overall Survival of Patients With Bladder Cancer: A Population-Based Study. *Int J Biol Markers* (2020) 35(2):172460082090760. doi: 10.1177/1724600820907605
126. Lee H, Yune S, Mansouri M, Kim M, Tajmir SH, Guerrier CE, et al. An Explainable Deep-Learning Algorithm for the Detection of Acute Intracranial Haemorrhage From Small Datasets. *Nat Biomed Eng* (2019) 3(3):173–82. doi: 10.1038/s41551-018-0324-9
127. Yamamoto Y, Tsuzuki T, Akatsuka J, Ueki M, Morikawa H, Numata Y, et al. Automated Acquisition of Explainable Knowledge From Unannotated Histopathology Images. *Nat Commun* (2019) 10(1):5642. doi: 10.1038/s41467-019-13647-8
128. Arrieta A, Rodriguez N, Del Ser J, Bennetot A, Tabik S, González A, et al. Explainable Artificial Intelligence (XAI): Concepts, Taxonomies, Opportunities and Challenges Toward Responsible AI. *Inf Fusion* (2020) 58:82–115. doi: 10.1016/j.inffus.2019.12.012
129. Agius R, Brieghel C, Andersen MA, Pearson AT, Ledergerber B, Cozzi–Lepri A, et al. Machine Learning can Identify Newly Diagnosed Patients With CLL at High Risk of Infection. *Nat Commun* (2020) 11(1):363. doi: 10.1038/s41467-019-14225-8
130. Li H, Liu L, Ding L, Zhang Z, Zhang M. Quantitative Assessment of Bladder Cancer Reflects Grade and Recurrence: Comparing of Three Methods of Positioning Region of Interest for ADC Measurements at Diffusion-Weighted MR Imaging. *Acad Radiol* (2019) 26:1148–53. doi: 10.1016/j.acra.2018.10.016
131. Wu S, Zheng J, Li Y, Yu H, Shi S, Xie W, et al. A Radiomics Nomogram for the Preoperative Prediction of Lymph Node Metastasis in Bladder Cancer. *Clin Cancer Res* (2017) 23(22):6904–11. doi: 10.1158/1078-0432.CCR-17-1510
132. Zhang X, Liu Y, Yang Z, Tian Q, Zhang G, Xiao D, et al. Quantitative Analysis of Bladder Wall Thickness for Magnetic Resonance Cystoscopy. *IEEE Trans ON Biomed Eng* (2015) 62(10):2402–9. doi: 10.1109/TBME.2015.2429612
133. Panebianco V, Pecoraro M, Del Giudice F, Takeuchi V, Muglia V, Messina V, et al. VI-RADS for Bladder Cancer: Current Applications and Future Developments. *J Magn Reson Imaging: JMRI* (2020). doi: 10.1002/jmri.27361
134. Wong BS, Duran C, Williams SB. Vesical Imaging Reporting and Data System (VI-RADS) and Impact on Identifying Depth of Invasion With Subsequent Management in Bladder Cancer Patients: Ready for Prime Time? *Transl Androl Urol* (2020) 9(6):2467–70. doi: 10.21037/tau-20-839
135. Del Giudice F, Leonardo C, Simone G, Pecoraro M, Berardinis E, Cipollari S, et al. Preoperative Detection of Vesical Imaging-Reporting and Data System (VI-RADS) Score 5 Reliably Identifies Extravesical Extension of Urothelial Carcinoma of the Urinary Bladder and Predicts Significant Delayed Time to Cystectomy: Time to Reconsider the Need for Primary Deep Transurethral Resection of Bladder Tumour in Cases of Locally Advanced Disease? *BJU Int* (2020) 126(5):610–9. doi: 10.1111/bju.15188
136. Del Giudice F, Barchetti G, De Berardinis E, Pecoraro M, Salvo V, Simone G, et al. Prospective Assessment of Vesical Imaging Reporting and Data System (VI-RADS) and Its Clinical Impact on the Management of High-Risk Non-Muscle-Invasive Bladder Cancer Patients Candidate for Repeated Transurethral Resection. *Eur Urol* (2020) 77(1):101–9. doi: 10.1016/j.eururo.2019.09.029
137. Panebianco V, Del Giudice F, Leonardo C, Sciarra A, Catalano C, Catto JWF. VI-RADS Scoring Criteria for Alternative Risk-Adapted Strategies in the Management of Bladder Cancer During the COVID-19 Pandemic. *Eur Urol* (2020) 78(1):e18–20. doi: 10.1016/j.eururo.2020.04.043
138. Fellous JM, Sapiro G, Rossi A, Mayberg H, Ferrante M. Explainable Artificial Intelligence for Neuroscience: Behavioral Neurostimulation. *Front Neurosci* (2019) 13:1346. doi: 10.3389/fnins.2019.01346
139. Patel-Murray NL, Adam M, Huynh N, Wassie BT, Milani P, Fraenkel E. A Multi-Omics Interpretable Machine Learning Model Reveals Modes of Action of Small Molecules. *Sci Rep* (2020) 10(1):954. doi: 10.1038/s41598-020-57691-7
140. Dalkilic A, Bayar G, Kilinc M. A Comparison of EORTC And CUETO Risk Tables in Terms of the Prediction of Recurrence and Progression in All Non-Muscle-Invasive Bladder Cancer Patients. *J Urol* (2019) 16(1):37–43. doi: 10.22037/uj.v0i0.4091
141. Kohjimoto Y, Kusumoto H, Nishizawa S, Kikkawa K, Kodama Y, Ko M, et al. External Validation of European Organization for Research and Treatment of Cancer and Spanish Urological Club for Oncological Treatment Scoring Models to Predict Recurrence and Progression in Japanese Patients With non-Muscle Invasive Bladder Cancer Treated With Bacillus Calmette-Guerin. *Int J Urol* (2014) 21(12):1201–7. doi: 10.1111/iju.12572
142. Vedder MM, Marquez M, de Bekker-Grob EW, Calle ML, Dyrskjot L, Kogevinas M, et al. Risk Prediction Scores for Recurrence and Progression of non-Muscle Invasive Bladder Cancer: An International Validation in

Primary Tumours. *PloS One* (2014) 9(6):e96849. doi: 10.1371/journal.pone.0096849
143. Valadi H, Ekstrom K, Bossios A, Sjostrand M, Lee JJ, Lotvall JO. Exosome-Mediated Transfer of mRNAs and microRNAs Is a Novel Mechanism of Genetic Exchange Between Cells. *Nat Cell Biol* (2007) 9(6):654–9. doi: 10.1038/ncb1596
144. Izumi K, Zheng Y, Hsu JW, Chang C, Miyamoto H. Androgen Receptor Signals Regulate UDP-Glucuronosyltransferases in the Urinary Bladder: A Potential Mechanism of Androgen-Induced Bladder Carcinogenesis. *Mol Carcinog* (2013) 52(2):94–102. doi: 10.1002/mc.21833
145. Beckham CJ, Olsen J, Yin PN, Wu CH, Ting HJ, Hagen FK, et al. Bladder Cancer Exosomes Contain EDIL-3/Del1 and Facilitate Cancer Progression. *J Urol* (2014) 192(2):583–92. doi: 10.1016/j.juro.2014.02.035
146. Armstrong DA, Green BB, Seigne JD, Schned AR, Marsit CJ. MicroRNA Molecular Profiling From Matched Tumor and Bio-Fluids in Bladder Cancer. *Mol Cancer* (2015) 14:194. doi: 10.1186/s12943-015-0466-2
147. Braicu C, Cojocneanu-Petric R, Chira S, et al. Clinical and Pathological Implications of miRNA in Bladder Cancer. *Int J Nanomedicine* (2015) 10:791–800. doi: 10.2147/IJN.S72904
148. Cimadamore A, Gasparrini S, Santoni M, Cheng L, Lopez–Beltran A, Battelli N, et al. Biomarkers of Aggressiveness in Genitourinary Tumors With Emphasis on Kidney, Bladder, and Prostate Cancer. *Expert Rev Mol Diagn* (2018) 18(7):645–55. doi: 10.1080/14737159.2018.1490179
149. Ringuette Goulet C, Bernard G, Tremblay S, Chabaud S, Bolduc S, Pouliot F. Exosomes Induce Fibroblast Differentiation Into Cancer-Associated Fibroblasts Through TGFbeta Signaling. *Mol Cancer Res* (2018) 16 (7):1196–204. doi: 10.1158/1541-7786.MCR-17-0784
150. Sanguedolce F, Russo D, Mancini V, Selvaggio O, Calo B, Carrieri G, et al. Prognostic and Therapeutic Role of HER2 Expression in Micropapillary Carcinoma of the Bladder. *Mol Clin Oncol* (2019) 10(2):205–13. doi: 10.3892/mco.2018.1786
151. Sanguedolce F, Russo D, Mancini V, Selvaggio O, Calo B, Carrieri G, et al. Human Epidermal Growth Factor Receptor 2 in Non-Muscle Invasive Bladder Cancer: Issues in Assessment Methods and Its Role as Prognostic/Predictive Marker and Putative Therapeutic Target: A Comprehensive Review. *Urologia Int* (2019) 102(3):249–61. doi: 10.1159/000494359
152. Ferro M, Di Lorenzo G, Vartolomei MD, Bruzzese D, Cantiello F, Lucarelli G, et al. Absolute Basophil Count Is Associated With Time to Recurrence in Patients With High-Grade T1 Bladder Cancer Receiving Bacillus Calmette-Guerin After Transurethral Resection of the Bladder Tumor. *World J Urol* (2020) 38(1):143–50. doi: 10.1007/s00345-019-02754-2

Conflict of Interest: The authors declare that the research was conducted in the absence of any commercial or financial relationships that could be construed as a potential conflict of interest.

frontiers in Oncology

ORIGINAL RESEARCH
published: 21 July 2021
doi: 10.3389/fonc.2021.700543

Abiraterone *In Vitro* Is Superior to Enzalutamide in Response to Ionizing Radiation

Timothy C. Wright[1], *Victoria L. Dunne*[1], *Ali H. D. Alshehri*[1,2], *Kelly M. Redmond*[1], *Aidan J. Cole*[1,2,3] *and Kevin M. Prise*[1]*

[1] Patrick G. Johnston Centre for Cancer Research, Queen's University Belfast, Belfast, United Kingdom, [2] Department of Radiological Science, College of Applied Medical Sciences, Najran University, Najran, Saudi Arabia, [3] Northern Ireland Cancer Centre, Belfast Health & Social Care Trust, Belfast, United Kingdom

Abiraterone acetate and Enzalutamide are novel anti-androgens that are key treatments to improve both progression-free survival and overall survival in patients with metastatic castration-resistant prostate cancer. In this study, we aimed to determine whether combinations of AR inhibitors with radiation are additive or synergistic, and investigated the underlying mechanisms governing this. This study also aimed to compare and investigate a biological rationale for the selection of Abiraterone versus Enzalutamide in combination with radiotherapy as currently selection is based on consideration of side effect profiles and clinical experience. We report that AR suppression with Enzalutamide produces a synergistic effect only in AR-sensitive prostate models. In contrast, Abiraterone displays synergistic effects in combination with radiation regardless of AR status, alluding to potential alternative mechanisms of action. The underlying mechanisms governing this AR-based synergy are based on the reduction of key AR linked DNA repair pathways such as NHEJ and HR, with changes in HR potentially the result of changes in cell cycle distribution, with these reductions ultimately resulting in increased cell death. These changes were also shown to be conserved in combination with radiation, with AR suppression 24 hours before radiation leading to the most significant differences. Comparison between Abiraterone and Enzalutamide highlighted Abiraterone from a mechanistic standpoint as being superior to Abiraterone for all endpoints measured. Therefore, this provides a potential rationale for the selection of Abiraterone over Enzalutamide.

Keywords: prostate cancer, radiotherapy, androgen receptor, DNA damage, abiraterone, enzalutamide

OPEN ACCESS

Edited by:
Alfonso Urbanucci,
Oslo University Hospital, Norway

Reviewed by:
Alwyn Dart,
University of London, United Kingdom
Luke Gaughan,
Newcastle University, United Kingdom

***Correspondence:**
Kevin M. Prise
k.prise@qub.ac.uk

Specialty section:
This article was submitted to Genitourinary Oncology, a section of the journal Frontiers in Oncology

Received: *26 April 2021*
Accepted: *02 July 2021*
Published: *21 July 2021*

Citation:
Wright TC, Dunne VL, Alshehri AHD, Redmond KM, Cole AJ and Prise KM (2021) Abiraterone In Vitro Is Superior to Enzalutamide in Response to Ionizing Radiation. Front. Oncol. 11:700543. doi: 10.3389/fonc.2021.700543

INTRODUCTION

Despite recent advances, prostate cancer continues to represent the most common form of cancer and the second most common cause of cancer-related death among men globally (1). Normal maintenance and development of the prostate is dependent on androgens and androgen receptor (AR) signaling, which also plays a key driving role in the development and progression of prostate

cancer (2). However, although chemical castration is initially effective, progression to a castration-resistant setting occurs in a significant number of cases (3).

Metastatic castration-resistant prostate cancer (MCRPC) represents the lethal form of the disease with a number of interventions leading to improved overall survival. Two such interventions are Abiraterone acetate (Abi) and Enzalutamide (Enz), second-generation ADT agents that have been shown to lead to increased overall and progression-free survival (4, 5). Abiraterone acts as an indirect AR inhibitor through inhibition of Cytochrome p450- α-hydroxylase/17,20-lyase (CYP17A1), a key enzyme in the androgen biosynthetic pathway (6), while Enzalutamide acts as a direct AR inhibitor with multiple mechanisms, such as acting as an AR antagonist, preventing translocation of the AR and inhibiting the binding of the AR to DNA (7).

As with ADT, radiation continues to represent a key treatment of locally advanced and metastatic prostate cancer. However, radioresistance continues to represent a major hurdle in a clinical setting (8), making combinations of radiotherapy with additional therapeutics such as ADT an attractive option to help enhance outcomes. While combinations of ADT and radiotherapy have been shown to enhance clinical outcome (9–11), it is not known whether these effects are additive or synergistic. Recent studies have suggested the AR regulates a network of key DNA repair genes, providing a potential mechanism by which androgen deprivation may synergise with radiotherapy for prostate cancer (12, 13). Due to COVID-19, clinicians may opt to use abiraterone or enzalutamide in the up-front *de novo* metastatic setting as an alternative to the more immunosuppressive docetaxel chemotherapy. As such, increasing numbers of patients will be treated with radiotherapy and concomitant novel hormonal agents.

Treatment with ionizing radiation leads to the induction of DNA double-strand breaks (DSBs), which are repaired *via* two main mechanisms, Non-homologous end joining (NHEJ) and Homologous recombination (HR). NHEJ can occur at any stage of the cell cycle but is more error-prone. It involves the recruitment of the Ku70/80 heterodimer which acts as a scaffolding for the recruitment of other NHEJ repair factors such as DNA-dependent protein kinase catalytic subunit (DNA-PKcs) (14). HR requires a homologous template and so is restricted to the S and G2 phases of the cell cycle. It utilizes a core set of proteins, most notably Rad51 to catalyse key reactions with several other key factors (15). The AR has been shown to upregulate these key factors of DNA repair, although whether this is direct is still yet to be fully understood (12, 13). Suggesting that AR inhibition could play an important role in enhancing response to radiation.

Despite the clinical success of both Abiraterone acetate and Enzalutamide and both drugs achieving similar cancer control, there currently exists no biological rationale for the selection of one over the other, leaving the choice of therapy, a consideration of side effect profiles and clinical experience. Here we provide a direct comparison of the radiosensitizing potential of Abiraterone and Enzalutamide resultant of direct and indirect impacts on key DNA repair pathways such as NHEJ and HR and the significant benefit of Abiraterone over Enzalutamide across all metrics in an *in vitro* setting.

MATERIALS AND METHODS

Cell Lines

Two human prostate cell lines were used: the hormone insensitive PC3 and the hormone-sensitive LNCaP. One osteoblastic cell model was used SJSA-1. All cell lines were obtained from ATCC (Manassas, Virginia, USA). PC3s, LNCaPs and SJSA-1s were grown in RPMI 1640 media [Thermo Fisher (Waltham, Massachusetts, USA)], supplemented with 10% Fetal bovine serum (FBS) (Thermo Fisher) and 50 μg/ml penicillin/streptomycin (Thermo Fisher).

Antibodies

Antibodies were used according to manufacturer instructions. PARP [#9542, Santa Cruz (Dallas, Texas, USA)], PSA/KLK3 [D6B1, Cell Signalling (Danvers, Massachusetts, USA)], Rad51 (sc-398587, Santa Cruz), DNA-PK [ab70250, Abcam (Cambridge, UK)] and β-Actin (C4: sc-47778) primary antibodies were used in conjunction with HRP conjugated mouse and rabbit secondary antibodies (Life Technologies, USA).

Irradiation

Cells were irradiated across various doses at 225kVp,13.3 mA in an X-Rad 225 Radiation cabinet (Precision X-RAY Inc, North Branford, CT, USA). A constant dose rate of 0.55 Gy/min was used.

MTT Assay

Cells were treated in 96 well plates with a dose range of 10 nM to 100 μM Abiraterone, Enzalutamide or DMSO control for 72 hours, after which 20 μl of 3-(4,5-Dimethylthiazol-2-yl)-2,5-Diphenyltetrazolium Bromide (MTT) dye was added and left for a period of up to two hours. The solution was then removed and 100 μl DMSO added to allow the formazan product to dissolve. The absorbance was measured at 570 nm immediately in a FLUOstar Omega plate reader. LD25 values were determined from MTT curves and indicate the drug concentration at which cell viability was reduced by 25% of that of the DMSO control cells.

Colony Formation Assay

Colony formation assays were carried out according to published methods (16). Cells were pre-treated with 10μM of Abiraterone, Enzalutamide or DMSO two hours before radiation and drug incubation continued until stained. Cells were irradiated over a dose range of 0-8 Gy. Plating efficiency (PE) and survival fraction (SF) were calculated with the following equations:

$$PE = (\text{number of colonies formed}/\text{number of cells seeded}) \times 100\,\%$$

$$SF = \text{number of colonies formed after irradiation}/(\text{number of cells seeded} \times PE/100)$$

Sensitising enhancement ratio (SER) was calculated as the radiation dose needed for radiation alone divided by the dose needed for DMSO, Abiraterone or Enzalutamide at a survival fraction of 10%. Radiosensitization was determined through normalizing to drug-treated controls.

Western Blotting

Cells were pre-treated with 10μM of Abiraterone, Enzalutamide or DMSO one or 24 hours before radiation. Following radiation, cells were harvested and extracted according to published methods at predetermined time-points (17). 40 μg samples were loaded onto Invitrogen NuPAGE 8% Bis-Tris Midi gels and after electrophoresis transferred onto Invitrogen IBlot2 regular stacks and transferred using an IBlot. The membranes were then blocked with 5% non-fat dairy milk in PBS-Tween (PBS-T; 10 mM sodium phosphate, 0.15M NaCl, 0.05% Tween-20, pH 7.5) and incubated overnight at 4°C with the corresponding primary antibodies. After washing with PBS-T membranes were incubated in their secondary antibodies at room temperature for two hours. The membranes were then washed, developed by ECL reagent (7.5ml Tris HCl, 16.5μl coumaric acid, 37.5μl luminol, 2.5μl H2O2) and visualized, before being probed again if required.

Immunofluorescence

Cells were pre-treated with 10μM of Abiraterone, Enzalutamide or DMSO 24 hours before irradiation. Following irradiation, cells were permeabilized (0.5% of Triton X-100 in PBS) and fixed at pre-determined time points before being blocked in blocking buffer (5% FBS in PBS) and stained with 53BP1 primary antibody (1:5000) [NB100-304, Novus Biologicals (Colorado, USA)] for one hour before being washed four times and stained with Alexa Fluor 568 goat anti-rabbit IgG secondary antibody (1:2000) [A21429, Invitrogen (Massachusetts, USA)] in the dark for one hour. Following staining, cells were washed four times and mounted onto microscope slides using Prolong Gold antifade reagent with DAPI [P36930, Invitrogen (Massachusetts, USA)].

Cell Cycle Analysis

Cells were pre-treated with 10μM of Abiraterone, Enzalutamide or DMSO one or 24 hours before radiation. Following radiation, cells were harvested at predetermined time-points before being suspended in 100% ice-cold ethanol. Samples were then centrifuged, resuspended in 1% FBS in PBS and excess ethanol removed before resuspending pellets in 360μl of PI/RNaseA. Samples were incubated at 37°C for 30 minutes before being analyzed by flow cytometry on a BD Acuri C6 Plus Flow Cytometer (San Jose, CA, USA).

Statistical Analysis

All experiments were performed in triplicate. Unpaired students t-test was used for comparisons between two groups. All statistics and graph plotting used GraphPad 8.0 (GraphPad, La Jolla, CA, USA).

RESULTS

Impact of Abiraterone and Enzalutamide on Cell Growth

The cytostatic/cytotoxic effect of Abiraterone and Enzalutamide was studied using androgen-sensitive (LNCaP), androgen-insensitive (PC3) prostate cancer models and an osteoblastic bone model (SJSA-1). Both Abiraterone and Enzalutamide were shown to reduce the viability of all cell lines compared to DMSO controls (**Figure 1** and **Table 1**). Direct comparison of all models to determine the effect of AR status (**Figure 2**) showed both PC3s and SJSA-1s displayed similar responses to both Abiraterone (LD25 = 12.6 μM and 16.2 μM) and Enzalutamide (LD25 = 23.4 μM and 34.7 μM) treatment across the dose range, while LNCaPs displayed increased sensitivity to Abiraterone and Enzalutamide compared to both PC3s and SJSA-1s and also showed increased sensitivity to Abiraterone (LD25 = 5.8 μM) over Enzalutamide (LD25 = 12 μM). Investigations into fold sensitivity increase over DMSO (**Supplementary Table 1**) showed PC3s and SJSA-1s displayed similar fold sensitivity increases over DMSO for both Abiraterone (both 6.6) and Enzalutamide (3.5 and 3.1), while the androgen sensitive LNCaPs were more sensitive to Abiraterone (15.8) and Enzalutamide (7.6) as expected.

Is the Addition of Radiotherapy to Abiraterone or Enzalutamide Synergistic or Additive?

With both Enzalutamide and Abiraterone being shown to improve survival in an MCRPC setting, there, therefore, exists a biological rationale that their combination with radiotherapy could exceed that of their use as a monotherapy, which was investigated through use of clonogenic survival assays. For clonogenic survival (**Figure 3**), while DMSO showed little to no additive impact on survival fraction, both Enzalutamide (PC3: ***P ≤ 0.001, ≤ 0.0001, SJSA-1: **P ≤ 0.01 and LNCaP: **P ≤ 0.01) and Abiraterone (PC3: ****P ≤ 0.0001, SJSA-1: **P ≤ 0.01 and LNCaP: **P ≤ 0.01) as single agents were shown to significantly affect the survival fraction of all models, irrespective of AR status. Comparison 2 Gy radiation to 2 Gy radiation in combination with Enzalutamide (PC3: *P ≤ 0.05, SJSA-1: **P ≤ 0.01 and LNCaP: *P ≤ 0.05) or Abiraterone (PC3: *P ≤ 0.05, SJSA-1: ***P ≤ 0.001 and LNCaP: **P ≤ 0.01) showed significant additive effects across all models regardless of AR status.

To determine synergistic effects (i.e. whether the combination of Abiraterone or Enzalutamide with radiation is greater than combined individual toxicity), clonogenic survival assays were normalized to account for the additive drug-mediated cytotoxicity that had been observed previously, therefore allowing examination of only radiation-induced effects on proliferation (**Figure 4** and **Table 2**). LNCaPs showed increased radiosensitivity when pre-treated 24 hours before radiation with both Abiraterone (SER=1.23) and Enzalutamide (SER=1.23), while no radiosensitizing effects were observed with Enzalutamide in both PC3s (SER=0.96) and SJSA-1s (SER=1.01). Abiraterone displayed synergy with radiation in AR resistant PC3s (SER=1.19) and SJSA-1s (SER=1.17).

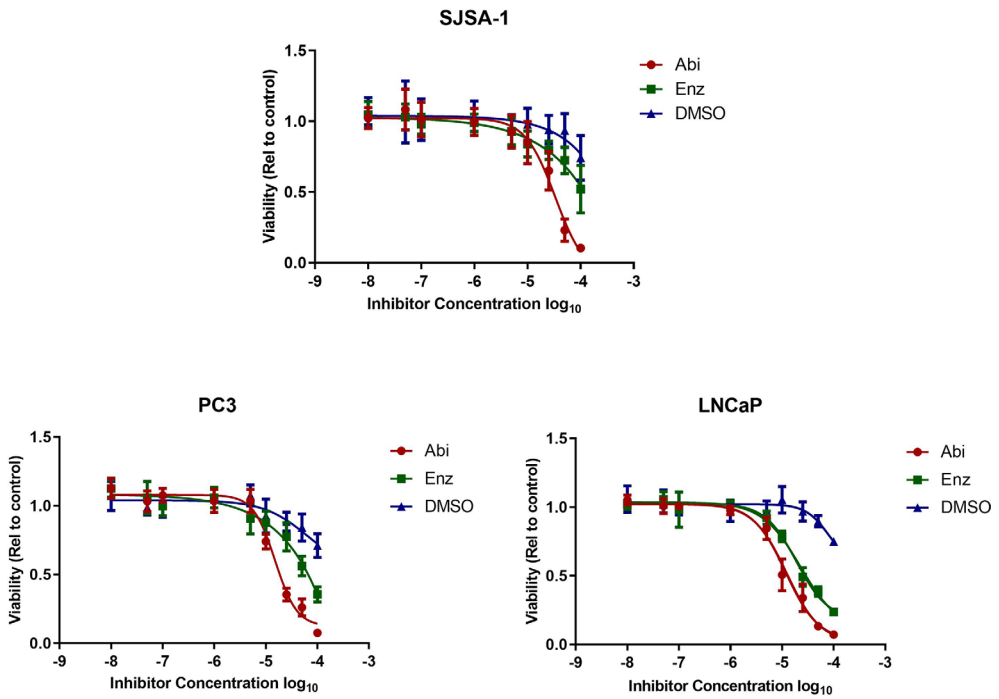

FIGURE 1 | Effect of Abiraterone and Enzalutamide treatment on cell viability of androgen-sensitive (LNCaP), androgen-insensitive (PC3) prostate cancer models and osteoblastic bone model (SJSA-1). LNCaP, PC3, and SJSA-1 cells were treated with a dose range of 10 nM to 100 μM of Abiraterone, Enzalutamide or DMSO. Cell viability was evaluated 72 hours post-treatment by MTT assay. Each value is the mean of three independent experiments performed in triplicate and error bars represent SEM.

TABLE 1 | LD25 values of MTT values across cell lines ± SEM. LD25 values were determined from MTT curves and indicate the drug concentration at which cell viability was reduced by 25%.

LD25 (μM)	Treatment	LNCaP	SJSA-1	PC3
	DMSO	91.2 ± 0.0052	107.15 ± 0.059	83.18 ± 0.072
	Enz	12.02 ± 0.051	34.67 ± 0.062	23.44 ± 0.061
	Abi	5.75 ± 0.053	16.22 ± 0.049	12.59 ± 0.043

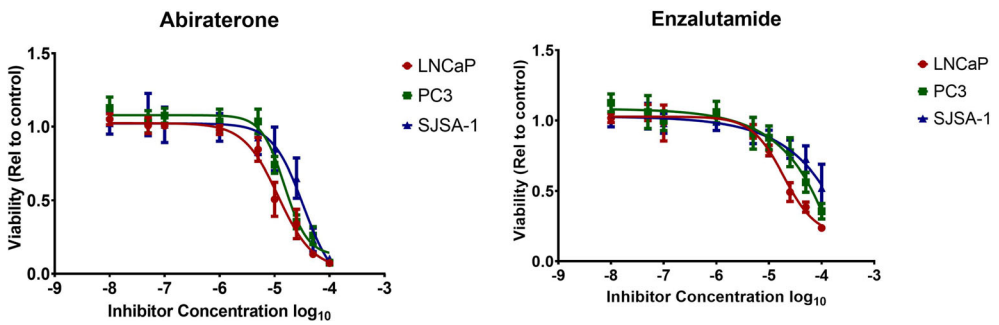

FIGURE 2 | Comparison of Abiraterone and Enzalutamide treatment on cell viability of androgen-sensitive (LNCaP), androgen-resistant (PC3) prostate cancer models and osteoblastic bone model (SJSA-1). LNCaP, PC3, SJSA-1 cells were treated with a dose range of 10 nM to 100 μM of Abiraterone and Enzalutamide or DMSO. Cell viability was evaluated 72 hours post-treatment by MTT assay. Each value is the mean of three independent experiments performed in triplicate (errors represent SEM).

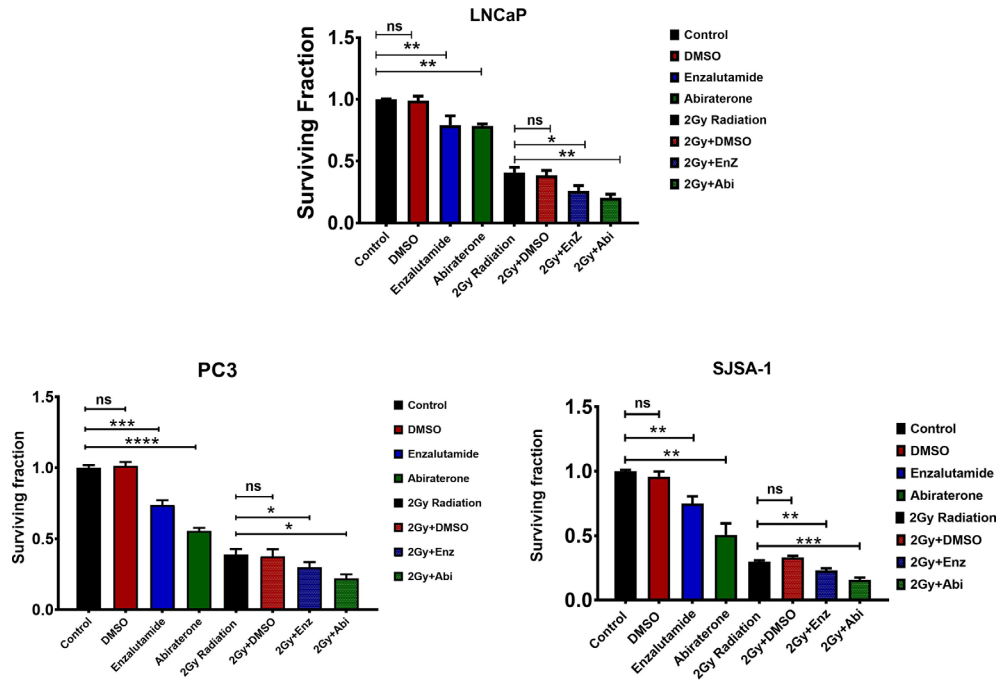

FIGURE 3 | Comparison of the combined effect of Abiraterone and Enzalutamide and DMSO as single agents or combined with 2 Gy radiation on survival fraction in androgen-sensitive LNCaPs and androgen insensitive PC3s prostate cancer models and osteoblastic bone model SJSA-1. PC3s and SJSA-1s were treated with 10 μM Abiraterone, Enzalutamide or DMSO 24 hours before radiation, while LNCaPs were treated with 200 nM due to their sensitivity. Cells were then left an appropriate amount of time to form sufficient colonies and any colonies of 50 cells or more counted. Each value is the mean of three independent experiments performed in triplicate (+/- SEM) and normalized to control. Unpaired students t-test was used for comparisons between two groups. *p ≤ 0.05, **p ≤ 0.01, ***p ≤ 0.001, ****p ≤ 0.0001, ns= non significant.

Impact of Abiraterone and Enzalutamide With or Without Radiotherapy on DNA Damage and Repair

The impact of Enzalutamide and Abiraterone on DNA damage was also assessed through quantifying changes in DSB levels by 53BP1 foci *via* immunofluorescence with and without 2Gy radiation (**Figure 5**). Treatment with either Abiraterone or Enzalutamide led to significant increases in DNA damage regardless of AR status 24 hours ((PC3 (*p ≤ 0.05 and *p ≤ 0.05), SJSA-1 (*p ≤ 0.05 and **p ≤ 0.01) and LNCaP (**p ≤ 0.01 and ***p ≤ 0.001)) and 48 hours post treatment ((PC3 (*p ≤ 0.05 and *p ≤ 0.05), SJSA-1 (*p ≤ 0.05 and **p ≤ 0.01) and LNCaP (***p ≤ 0.001 and ***p ≤ 0.001)).

The impact of Enzalutamide and Abiraterone mediated DNA damage with radiation damage was also assessed, with cells irradiated with 2 Gy X-rays 24-hour post treatment with Abiraterone or Enzalutamide (**Figure 6**). As expected, irradiation alone led to large increases in 53BP1 foci, one hour post radiation when DNA damage levels were at their highest, which decreased in a time dependent manner. The addition of Abiraterone and Enzalutamide was shown to significantly enhance DNA damage one hour ((PC3 (**p ≤ 0.01 and **p ≤ 0.01), SJSA-1 (**p ≤ 0.01 and **p ≤ 0.01) and LNCaP (***p ≤ 0.001 and ****p ≤ 0.0001)), 24 hours ((PC3 (*p ≤ 0.05 and *p ≤ 0.05), SJSA-1 (*p ≤ 0.05 and *p ≤ 0.05) and LNCaP (**p ≤ 0.01 and ***p ≤ 0.001)) and 48 hours ((PC3 (*p ≤ 0.05 and *p ≤ 0.05), SJSA-1 (*p ≤ 0.05 and *p ≤ 0.05) and LNCaP (***p ≤ 0.001 and ****p ≤ 0.0001)) post irradiation.

Impact of Abiraterone and Enzalutamide With or Without Radiotherapy on HR Repair

As previously described, the androgen receptor has been linked to the upregulation of key DNA repair genes. Therefore, the impact of AR suppression on HR was investigated through observations of RAD51 expression, a key component in mediating HR repair of DSBs. AR suppression with Abiraterone and Enzalutamide as single agents, as verified by showing a reduction in downstream PSA expression, directly correlated with a total visible reduction of RAD51 protein expression in LNCaPs (**Figure 7**). Supporting this is an AR-mediated effect, both PC3s and SJSA-1s showed no noticeable changes in RAD51 expression regardless of timepoint. PSA expression could not be measured in PC3, or SJSA-1 cells as they do no signal through their AR, resulting in no transcription of prostate-related proteins such as PSA (18). Comparisons between Abiraterone and Enzalutamide showed that while Abiraterone achieved a total reduction of RAD51 at an earlier timepoint than Enzalutamide, both achieved total reduction by 48 hours post-treatment.

Co-treatment of AR inhibitors with radiation was also investigated, to determine if these effects were conserved with

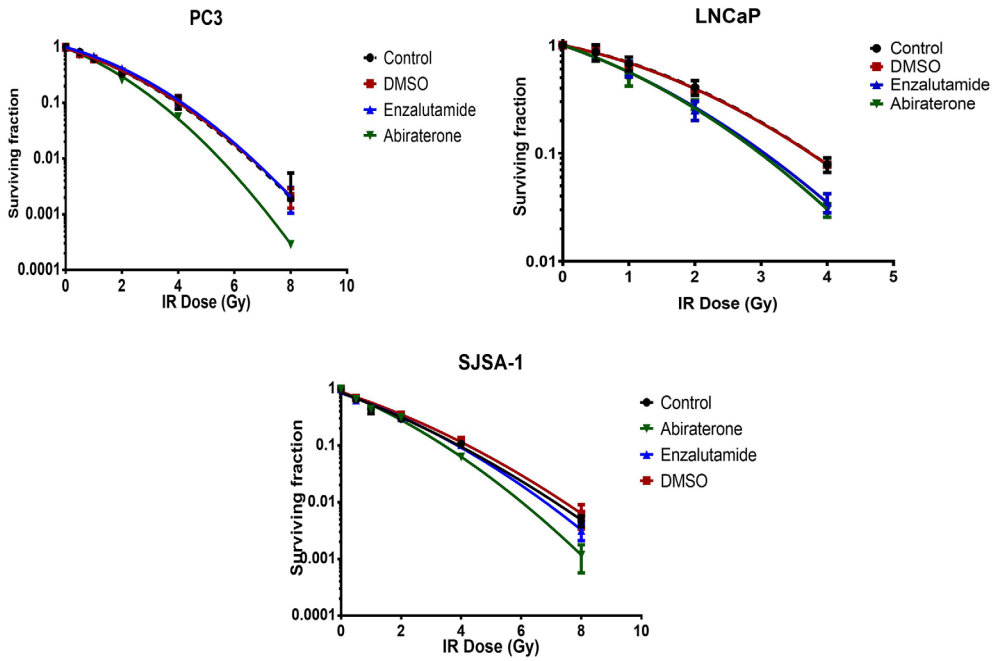

FIGURE 4 | Radiosensitization effects of Abiraterone, Enzalutamide and DMSO on radiation in androgen-insensitive PC3 prostate cancer model, androgen-sensitive LNCaP model and osteoblastic bone model SJSA-1 by colony formation assay. LNCaPs were treated with 200 nM, while PC3s and SJSA-1s were treated with 10 μM Abiraterone, Enzalutamide or DMSO 24 hours before X-Ray across a dose range of 0-8 Gy. Cells were then left to form appropriately sized colonies and survival fraction calculated using SF = (colonies counted) / (cells seeded x (PE/100) colonies counted). Error bars are standard error of the mean (+/- SEM) and for some points, the error bars are shorter than the height of the symbol (n=3).

TABLE 2 | SER values of inhibitors *vs* control at 10% with +/- SEM.

Cell line	DMSO	Enz	Abi
PC3	0.98 ± 0.042	0.96 ± 0.049	1.19 ± 0.045
LNCaP	1 ± 0.092	1.23 ± 0.069	1.23 ± 0.075
SJSA-1	0.94 ± 0.019	1.00 ± 0.022	1.16 ± 0.022

Sensitising enhancement ratio (SER) was calculated as the radiation dose needed for radiation alone divided by the dose needed for DMSO, Abiraterone or Enzalutamide at a survival fraction of 10%.

radiation (**Figure 8**), with both 1- and 24-hour pre-treatment with Abiraterone or Enzalutamide before irradiation investigated to evaluate whether any effects were time-dependent. As observed when used as a monotherapy, pre-treatment with Abiraterone or Enzalutamide in an AR-sensitive setting before irradiation with 2 Gy led to non-detectable RAD51 protein levels. Pre-treatment with Enzalutamide or Abiraterone 24 hours before radiation treatment was shown to cause large reductions in RAD51 levels even one-hour post-radiation, where DNA damage is at its maximum and levels of RAD51 at their highest. Abiraterone showed increased depletion of RAD51 levels one hour post-radiation with 24 hour pre-treatment compared to Enzalutamide.

Impact of Abiraterone and Enzalutamide With or Without RT on NHEJ Repair

DNA-PK expression was also investigated to determine if the observed impacts of Abiraterone and Enzalutamide on HR extended to other forms of DSB repair such as NHEJ (**Figure 9**). DNA-PK levels were shown to reduce in a time-dependent manner correlating with PSA levels following treatment with both Enzalutamide and Abiraterone in LNCaPs, however, only 48 hour treatment with Abiraterone was shown to be significant upon statistical testing (*$p \leq 0.05$). No significant changes in DNA-PK levels were observed in PC3s or SJSA-1s. Comparison of Abiraterone against Enzalutamide showed only Abiraterone caused significant reductions in DNA-PK levels (*$p \leq 0.05$). Combinations of Abiraterone or Enzalutamide with 2 Gy X-ray radiation (**Figure 10**) showed enhanced reductions of DNA-PK levels than with inhibitors alone. Pre-treatment with Abiraterone for 1 to 24 hours before radiation treatment was shown to induce significant reductions in DNA-PK levels both 24 and 48 hours post-radiation (*$p \leq 0.05$). Pre-treatment 24 hours prior to radiation showed larger observable reductions in DNA-PK levels then one hour pre-treatment.

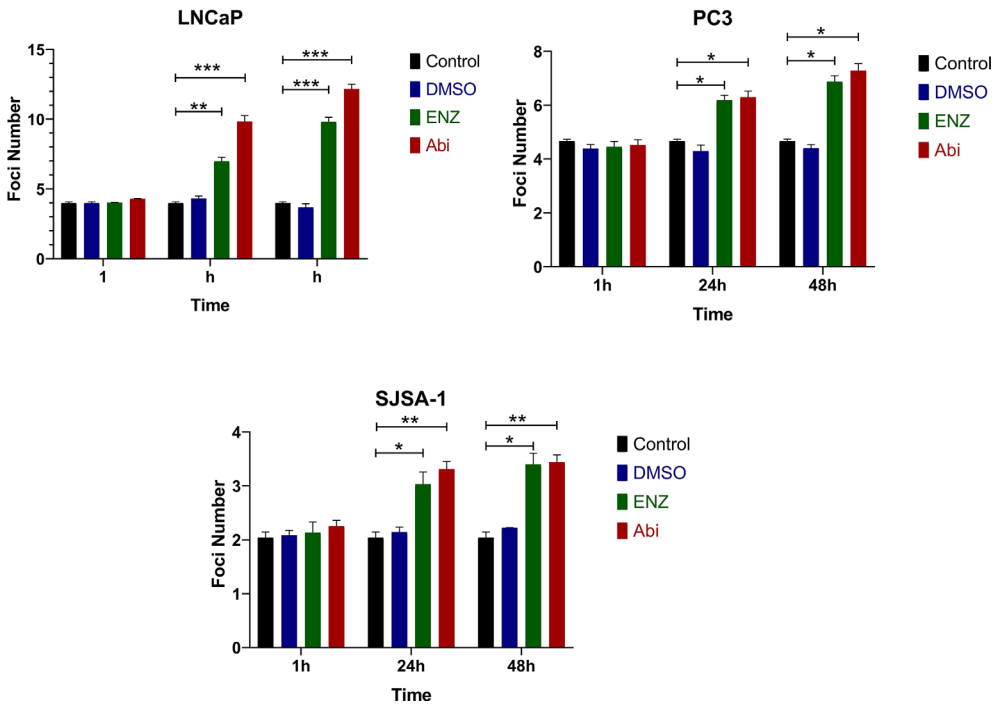

FIGURE 5 | Immunofluorescence of 53BP1 foci treated with Abiraterone and Enzalutamide on AR-insensitive PC3s and AR-sensitive LNCaP prostate models and osteoblastic bone model SJSA-1. All models were treated with 10 μM Abiraterone, Enzalutamide or DMSO and harvested 1-, 24 and 48-hours post-treatment before being fixed and stained with 53BP1 (n=3). Unpaired students t-test was used for comparisons between two groups *p ≤ 0.05, **p ≤ 0.01, ***p ≤ 0.001, and error bars represent SEM.

Impact of Abiraterone and Enzalutamide With or Without RT on Cell Cycle Distribution and Cell Death

The previous results have shown that AR suppression through Abiraterone and Enzalutamide has a significant impact on multiple DNA repair pathways involved in DSB repair. However, the choice of repair pathway is also dependent on which phase of the cell cycle the cell arrests in. Cell cycle distribution was therefore investigated to determine whether observed changes were due to the direct impact of these inhibitors on DNA repair genes, or indirectly through means of cell cycle distribution changes (**Figure 11**). Treatment with Enzalutamide and Abiraterone led to observed increases in sub-G1 levels in LNCaP cells, indicative of increased levels of apoptosis. With this effect shown to be more prominent with Abiraterone over Enzalutamide. Also evident were decreases in S and G2. These effects were not observed with PC3s and SJSA-1s.

Potential increases in apoptosis as indicated by the increases in the sub-G1 population of cells were investigated through looking at the expression of PARP cleavage (**Figure 12**), with PARP cleavage by activated caspases being a defined hallmark of apoptosis. There was a correlation between increases in sub-G1 levels and PARP cleavage in LNCaPs, with both Abiraterone and Enzalutamide showing increased levels of PARP cleavage in a time-dependent manner. Treatment with Abiraterone led to higher levels of PARP cleavage compared to treatment with Enzalutamide. Treatment with Abiraterone or Enzalutamide in PC3s and SJSA-1s showed little to no observable impact on PARP-cleavage levels.

Combinations of Enzalutamide or Abiraterone with 2 Gy radiation (**Figure 13**) showed both effects to be conserved, with increased sub-G1 levels and decreased S and G2 levels shown in LNCaPs and no observable changes in PC3s and SJSA-1s. Pre-treatment 24h before radiation resulted in reductions in the proportions of cells in S and G2 phases one-hour post-radiation. This highlights the importance of ensuring AR-deprivation is achieved before radiation treatment over treating concurrently with radiation.

As well as changes in the proportion of cells in S and G2, increased levels of PARP cleavage were also observed, with increased PARP cleavage following pre-treatment with Abiraterone or Enzalutamide one or 24 hours before 2 Gy radiation (**Figure 14**). Comparison of Abiraterone and Enzalutamide again showed increased levels of PARP cleavage following abiraterone treatment compared to Enzalutamide. Pre-treatment 24 hours before radiation was shown to be more effective at inducing apoptosis compared to one-hour pre-treatment, with increased PARP cleavage levels observed. Combination treatment of our AR-insensitive prostate model PC3 was again shown to have no impact on PARP-cleavage levels over radiation alone.

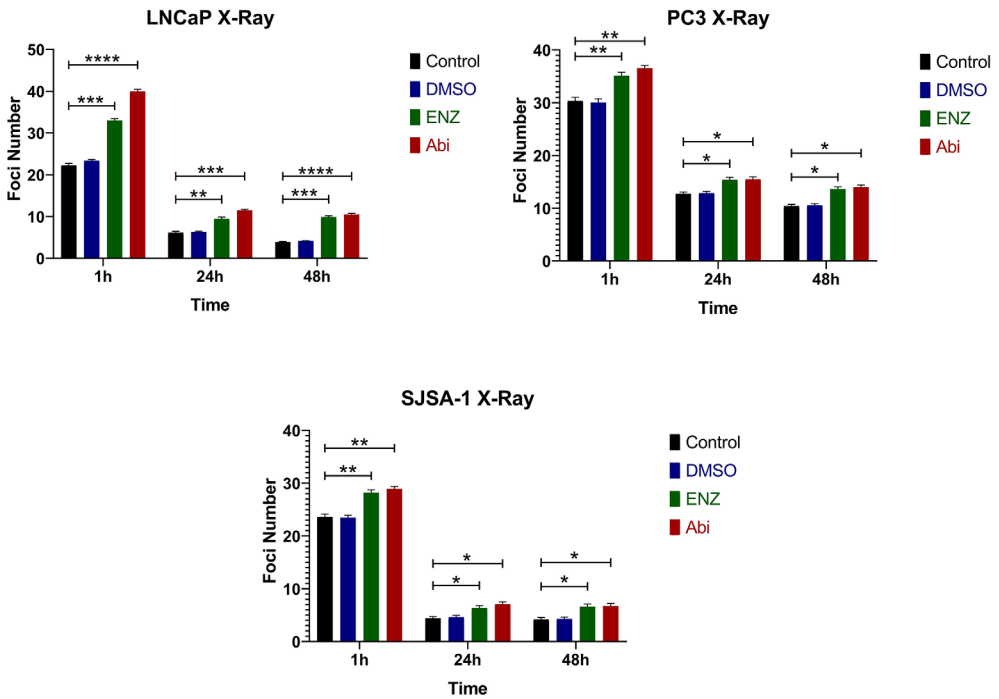

FIGURE 6 | Immunofluorescence of 53BP1 foci treated with Abiraterone and Enzalutamide in combination with 2 Gy X-ray in AR-insensitive PC3s and AR-sensitive LNCaP prostate models and osteoblastic bone model SJSA-1. All models were treated with 10 μM Abiraterone, Enzalutamide or DMSO 24 hours before being administered 2 Gy radiation. Samples were then harvested 1, 24- and 48-hours post-radiation before being fixed and stained with 53BP1 (n=3). Unpaired students t-test was used for comparisons between two groups *p ≤ 0.05, **p ≤ 0.01, ***p ≤ 0.001 ****p ≤ 0.0001, and error bars represent SEM.

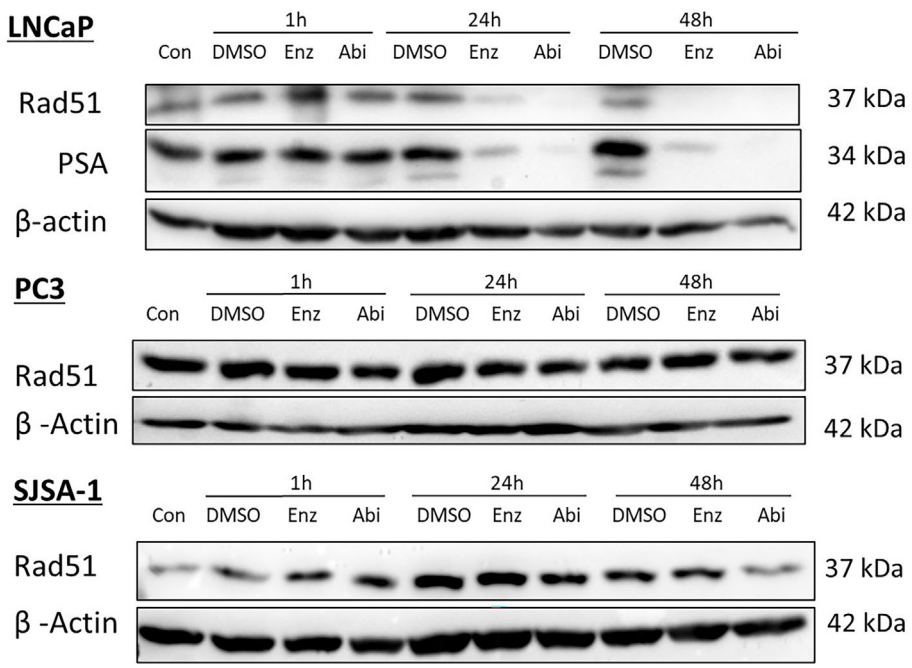

FIGURE 7 | Impact of Abiraterone and Enzalutamide on RAD51 and PSA protein expression in AR-sensitive LNCaP prostate model, AR-insensitive PC3 prostate model and osteoblastic bone model SJSA-1. All models were treated with 10 μM Abiraterone, Enzalutamide or DMSO. Samples were then harvested 1, 24- and 48-hours post-treatment and expression levels measured *via* Western blot. β-Actin was used as a loading control. (n=3).

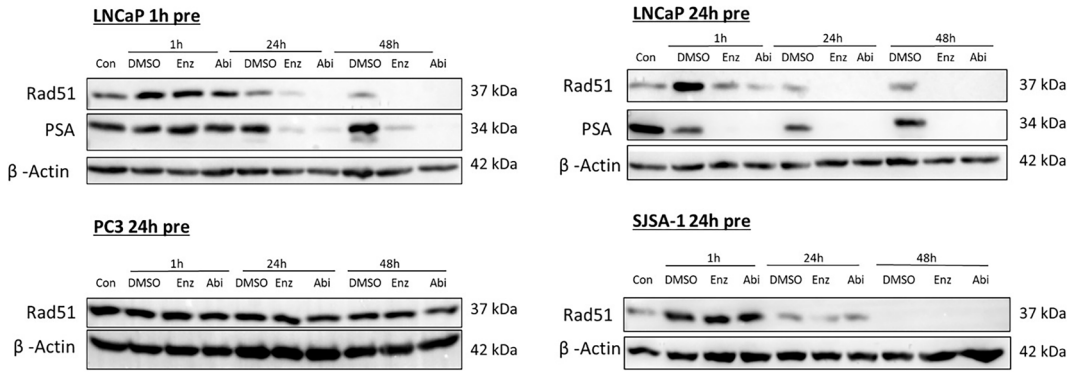

FIGURE 8 | Impact of Abiraterone and Enzalutamide in combination with 2 Gy X-ray on RAD51 and PSA expression in AR-insensitive PC3s and AR-sensitive LNCaP prostate models and osteoblastic bone model SJSA-1. All models were treated with 10 μM Abiraterone, Enzalutamide or DMSO 1 or 24 hours before radiation. Samples were then harvested 1, 24 and 48 hours post-radiation and expression levels measured *via* Western blot. β-Actin was used as a loading control. (n=3).

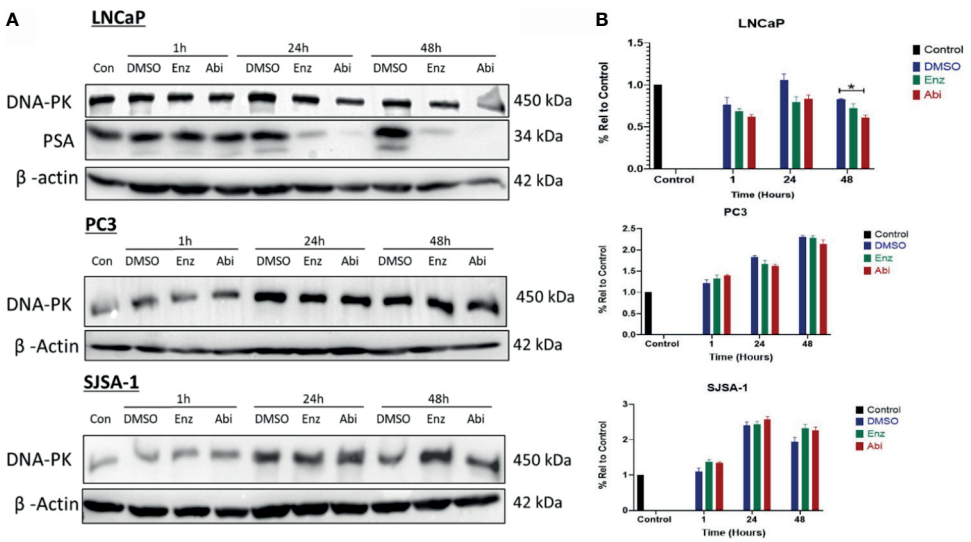

FIGURE 9 | Impact of Abiraterone and Enzalutamide on DNA-PK and PSA protein expression in AR-sensitive LNCaP and AR-insensitive PC3 prostate models and osteoblastic bone model SJSA-1. All models were treated with 10 μM Abiraterone, Enzalutamide or DMSO. Samples were then harvested 1, 24 and 48 hours post-treatment and expression levels measured *via* Western blot **(A)** and densitometric analysis **(B)**. β -Actin was used as a loading control. (n=3). Unpaired students t-test was used for comparisons between two groups *$p < 0.05$ and error bars represent SEM.

DISCUSSION

Abiraterone acetate and Enzalutamide have seen significant clinical success in an MCRPC setting (4, 5). However, a lack of comparative studies in a prospective, randomized, controlled trial has led to the selection of Abiraterone or Enzalutamide being primarily based on patient factors and side effect profiles.

Reports into the 'additive' or 'synergistic' nature of Abiraterone and Enzalutamide in combination with radiation in a castration-resistant setting have so far been inconclusive. Several reports have suggested an additive effect (defined as the interaction of Abiraterone or Enzalutamide with radiation being equal to the sum of the two added separately) (19, 20), while others suggest a synergistic effect (defined as the interaction of Abiraterone or Enzalutamide with radiation exceeding the sum of their separate effects) (13, 21–23). We have shown that irrespective of AR status, treatment with Abiraterone or Enzalutamide exerts a significant cytotoxic and additive effect. Which was further supported by observed increases in DNA damage. The reasons behind this effect in AR-insensitive models remains unclear, but may be a consequence of the potential effect of these inhibitors on other signaling mechanisms that can

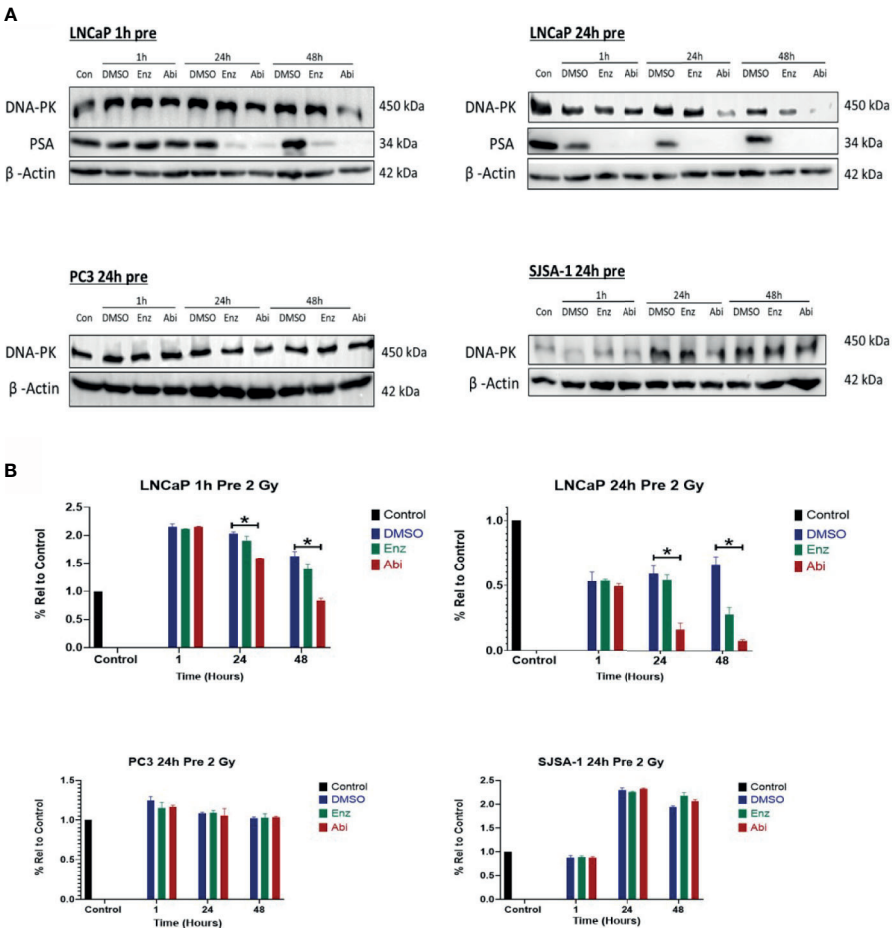

FIGURE 10 | Impact of Abiraterone and Enzalutamide in combination with 2 Gy X-ray on DNA-PK and PSA expression in AR-insensitive PC3s, AR-sensitive LNCaP prostate models and osteoblastic bone model SJSA-1. All models were treated with 10 μM Abiraterone, Enzalutamide or DMSO for 1 or 24 hours before being administered 2 Gy radiation. Samples were then harvested 1, 24 and 48 hours post-radiation and expression levels measured *via* Western blot **(A)** and densitometric analysis **(B)**. β -Actin was used as a loading control. (n=3). Unpaired students t-test was used for comparisons between two groups *$p < 0.05$ and error bars represent SEM.

bypass AR signaling such as the glucocorticoid receptor (23). Only in our AR-sensitive LNCaP model was there a synergistic radiosensitive effect with Enzalutamide.

However, Abiraterone was shown to confer a synergistic radiosensitivity effect in all our androgen-insensitive, androgen-sensitive and osteoblastic bone models regardless of AR status, suggesting, as has been previously eluded to (24) the presence of an alternative mechanism of action not dependent on AR inhibition. This potential alternative mechanism of Abiraterone has wider implications, being not only a promising drug for AR-insensitive prostate cancer but Abiraterone may also prove to be beneficial in other malignancies apart from PC.

The interplay between the AR and DNA repair remains a topic of much debate, with previous reports discovering the presence of an AR-mediated transcriptome, leading to the upregulation of various DNA repair genes (12, 13). This in theory suggests that AR-suppression should lead to down-regulation of these genes and thus the enhancement of radiation co-treatment. Our results support this theory, as we have shown in an AR-sensitive setting, that treatment with commonly clinically used AR inhibitors of different modalities i.e., directly (Enzalutamide) or indirectly (Abiraterone) leads to the suppression of key DSB DNA repair pathways such as NHEJ and HR and can be seen to correlate with levels of AR suppression as observed by decreased PSA expression levels. Reductions in HR repair can also be explained in part by shifts in the cell cycle, with Abiraterone and Enzalutamide treatment leading to decreased S and G2 phase, which has also previously been suggested by Zhang et al. (22). This suggests that AR suppression can potentially impact HR repair in both a direct and an indirect manner. Furthermore, suppression of these key repair pathways leads to increased levels of cell death *via* apoptosis as shown by increased levels of PARP-cleavage, supporting the use of these agents clinically as a monotherapy.

Importantly, we have also shown, that downregulation of these key DNA repair genes was conserved when AR suppression

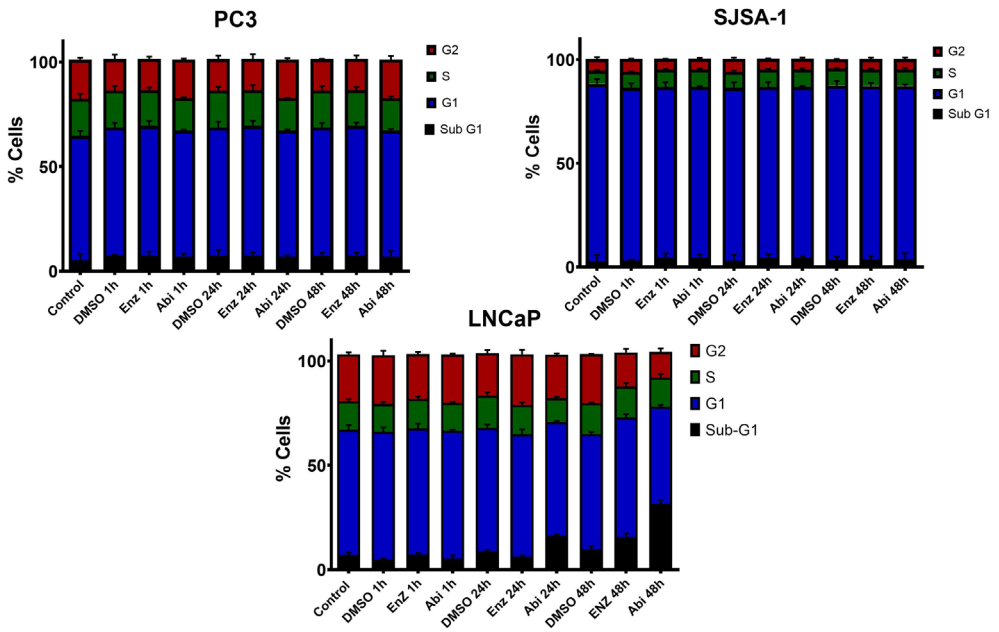

FIGURE 11 | Cell-cycle analysis of AR-sensitive LNCaP prostate model, AR- insensitive PC3 prostate model and osteoblastic bone model SJSA-1. Cells were treated with 10 μM Abiraterone, Enzalutamide or DMSO, fixed in ice cold ethanol 1h, 24h and 48h post-treatment and stained with PI/RNaseA for 30 minutes before the cell-cycle profile was determined by flow cytometry. Error bars are standard error of the mean (SEM) (n=3).

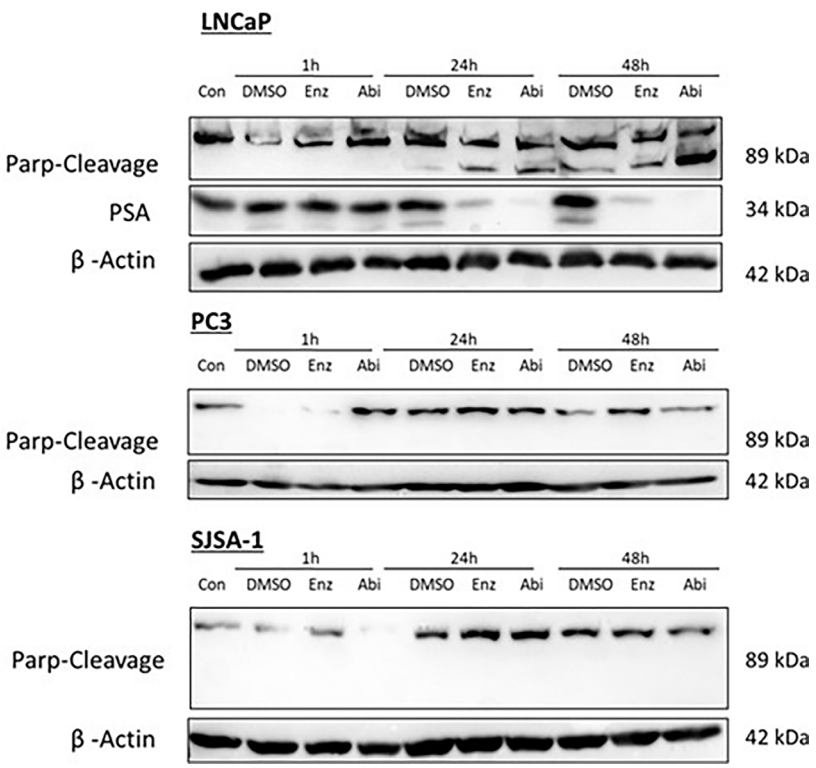

FIGURE 12 | Impact of Abiraterone and Enzalutamide on PARP cleavage in AR-insensitive PC3s, AR-sensitive LNCaP prostate models and osteoblastic bone model SJSA-1. Models were treated with 10 μM Abiraterone, Enzalutamide or DMSO. Samples were then harvested 1, 24 and 48 hours post-treatment and expression levels measured *via* Western blot. β-Actin was used as a loading control. (n=3).

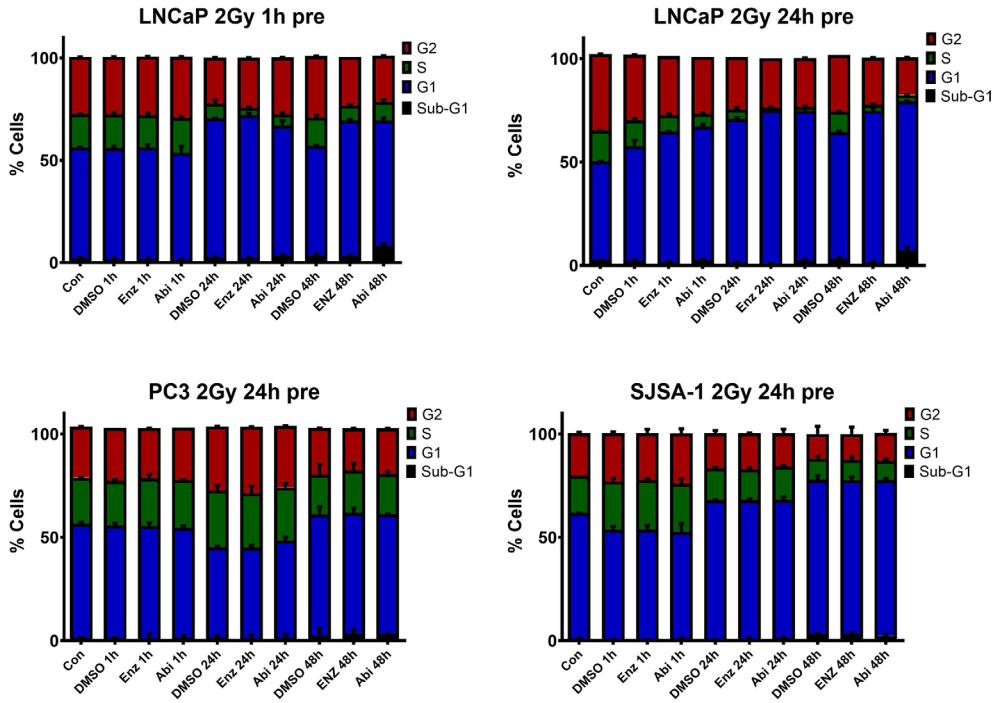

FIGURE 13 | Cell-cycle analysis of AR-sensitive LNCaP prostate model, AR- insensitive PC3 prostate model and osteoblastic bone model SJSA-1. Cells were treated with 10 μM Abiraterone, Enzalutamide or DMSO 1 or 24 hours before radiation with 2 Gy. Post radiation cells were fixed in ice cold ethanol 1h, 24h and stained with PI/RNaseA for 30 minutes before the cell-cycle profile was determined by flow cytometry. Error bars are standard error of the mean (SEM) (n=3).

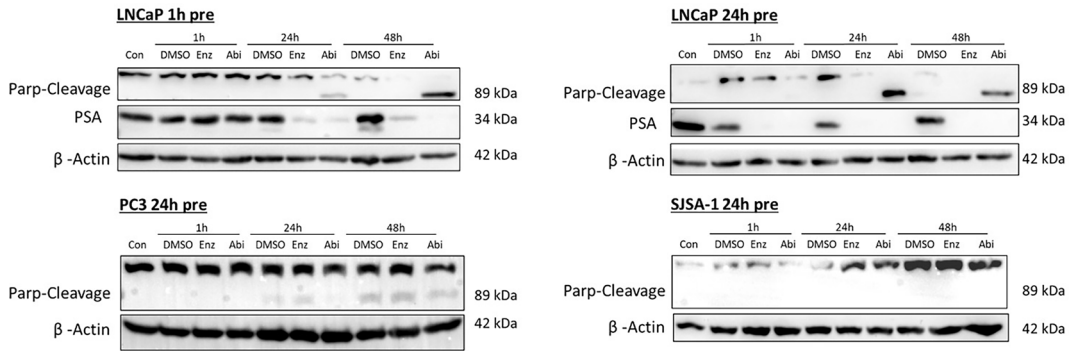

FIGURE 14 | Impact of Abiraterone and Enzalutamide and 2Gy radiation on PARP cleavage in AR-insensitive PC3s and AR-sensitive LNCaP prostate models and osteoblastic bone model SJSA-1. Models were treated with 10 μM Abiraterone, Enzalutamide or DMSO 1 or 24 hours before radiation with 2Gy. Samples were then harvested 1,24 and 48 hours post-radiation and expression levels measured *via* Western blot. β -Actin was used as a loading control. (n=3).

through Abiraterone or Enzalutamide is combined with 2Gy radiation (a standard clinical fractionated dose). Thus, supporting the suggestion (25) that it is this key downregulation of key DSB DNA repair pathways that is responsible for our observed radiosensitizing effects with radiation. Our comparisons between one-hour pre-treatment and 24-hour pre-treatment have also shown that for maximal impact, complete AR suppression should be achieved before radiation over concurrent treatment, as even one-hour post-radiation, where DNA damage should be at its maximum, we observed decreased levels of both key NHEJ and HR proteins.

This observed impact on key DSB repair genes raises interest in the potential enhancement of these effects through synthetic lethality approaches, with mounting evidence supporting the combination of inhibiting both the AR and the PARP pathway (26–29). The potential combination of AR suppression and DNA damage response (DDR) inhibitors to increase clinical efficacy is not only limited to PARP inhibition. Several papers have also

linked increased cellular toxicity to combinations with ATR inhibitors (30) and Chk1/2 inhibition (31). However, whether this can translate into a clinical setting requires further testing, as, although studies have demonstrated a manageable safety profile (32) there are conflicting reports regarding the clinical efficacy of PARP and AR inhibitor combinations (33, 34).

Regarding the question of selection of Abiraterone or Enzalutamide, our results to date have suggested from a purely biological perspective the increased cytotoxic benefit of Abiraterone over Enzalutamide. This was also shown to be the case mechanistically, with Abiraterone being significantly more impactful on the downregulation of key DNA repair pathway proteins examined (RAD51 and DNA-PK) over Enzalutamide, with this downregulation also occurring at earlier timepoints. Our results have also shown Abiraterone is more effective at inducing cell death than Enzalutamide as observed through increased PARP-cleavage. However, although our results support the preference of the selection of Abiraterone over Enzalutamide, it is important to consider that this is in a strictly *in vitro* setting and does not accurately represent the tumor microenvironment underpinning patients response, which could potentially affect the outcomes. Recent studies have also suggested a sequencing approach of Abiraterone followed by Enzalutamide may result in an increased clinical benefit (35), although many centres adopt an either/or approach with regards to the selection of these two agents. There has been an increase in the use of both agents in the frontline setting which in turn will lead to increased number of patients receiving high dose radiotherapy to the prostate in combination with these agents. This has been amplified to negate any immunosuppressive impact of the previous standard of care, docetaxel.

In conclusion, we have demonstrated that while Abiraterone and Enzalutamide have an additive cytotoxic effect regardless of AR status, radiosensitization in an AR-sensitive setting is due to downregulation of multiple key DNA repair pathways such as NHEJ and HR, which may also be mediated by cell cycle distribution changes. Furthermore, comparisons of Abiraterone versus Enzalutamide have shown Abiraterone to be significantly more effective in terms of inhibiting key DNA repair proteins and cell death than Enzalutamide, providing a rationale of its selection over Enzalutamide in a clinical setting should side effect profiles not be a consideration.

DATA AVAILABILITY STATEMENT

The raw data supporting the conclusions of this article will be made available by the authors, without undue reservation.

AUTHOR CONTRIBUTIONS

Conceptualization, AC and KP. Methodology, TW, VD, KR, AC, and KP. Investigation, TW, AA, and VD. Data curation, TW and VD. Writing—original draft preparation, TW, AC, and KP. Writing—review and editing, TW, VD, AC, and KP. Supervision, VD, AC, and KP. Funding acquisition, AC and KP. All authors contributed to the article and approved the submitted version.

FUNDING

This research was funded by the Belfast-Manchester Movember Centre of Excellence (CE013_2-004), funded in partnership with Prostate Cancer UK. TW was supported by a studentship from the Northern Ireland Department of the Economy. VD is supported by the LFT Charitable Trust.

SUPPLEMENTARY MATERIAL

The Supplementary Material for this article can be found online at: https://www.frontiersin.org/articles/10.3389/fonc.2021.700543/full#supplementary-material

REFERENCES

1. Siegel RL, Miller KD, Jemal A. Cancer Statistics, 2020. *CA Cancer J Clin* (2020) 70(1):7–30. doi: 10.3322/caac.21590
2. Heinlein CA, Chang C. Androgen Receptor in Prostate Cancer. *Endocrine Rev Endocr Rev;* (2004) 25:276–308. doi: 10.1210/er.2002-0032
3. Anderson J. The Role of Antiandrogen Monotherapy in the Treatment of Prostate Cancer. *BJU Int* (2003) 91p:455–61. John Wiley & Sons, Ltd. doi: 10.1046/j.1464-410X.2003.04026.x
4. Ryan CJ, Smith MR, Fizazi K, Saad F, Mulders PFA, Sternberg CN, et al. Abiraterone Acetate Plus Prednisone Versus Placebo Plus Prednisone in Chemotherapy-Naive Men With Metastatic Castration-Resistant Prostate Cancer (COU-AA-302): Final Overall Survival Analysis of a Randomised, Double-Blind, Placebo-Controlled Phase 3 Study. *Lancet Oncol* (2015) 16 (2):152–60. doi: 10.1016/S1470-2045(14)71205-7
5. Semenas J, Dizeyi N, Persson JL. Enzalutamide as a Second Generation Antiandrogen for Treatment of Advanced Prostate Cancer. *Drug Design Dev Ther* (2013) 7:875–81. doi: 10.2147/DDDT.S45703
6. Bedoya DJ, Mitsiades N. Abiraterone Acetate, a First-in-Class CYP17 Inhibitor, Establishes a New Treatment Paradigm in Castration-Resistant Prostate Cancer. *Expert Rev Anticancer Ther Expert Rev Anticancer Ther;* (2012) 12:1–3. doi: 10.1586/era.11.196
7. Tran C, Ouk S, Clegg NJ, Chen Y, Watson PA, Arora V, et al. Development of a Second-Generation Antiandrogen for Treatment of Advanced Prostate Cancer. *Sci (80-).* (2009) 324(5928):787–90. doi: 10.1126/science.1168175
8. Chang L, Graham PH, Hao J, Bucci J, Cozzi PJ, Kearsley JH, et al. Emerging Roles of Radioresistance in Prostate Cancer Metastasis and Radiation Therapy. *Cancer Metastasis Rev* (2014) 33p:469–96. Kluwer Academic Publishers. doi: 10.1007/s10555-014-9493-5
9. D'Amico AV, Manola J, Loffredo M, Renshaw AA, DellaCroce A, Kantoff PW. 6-Month Androgen Suppression Plus Radiation Therapy vs Radiation Therapy Alone for Patients With Clinically Localized Prostate Cancer: A Randomized Controlled Trial. *J Am Med Assoc* (2004) 292(7):821–7. doi: 10.1001/jama.292.7.821
10. Jones CU, Hunt D, McGowan DG, Amin MB, Chetner MP, Bruner DW, et al. Radiotherapy and Short-Term Androgen Deprivation for Localized Prostate Cancer. *N Engl J Med* (2011) 365(2):107–18. doi: 10.1056/NEJMoa1012348
11. Schmidt-Hansen M, Hoskin P, Kirkbride P, Hasler E, Bromham N. Hormone and Radiotherapy Versus Hormone or Radiotherapy Alone for Non-Metastatic Prostate Cancer: A Systematic Review With Meta-Analyses. *Clin Oncol* (2014) 26(10):e21–46. doi: 10.1016/j.clon.2014.06.016

12. Polkinghorn WR, Parker JS, Lee MX, Kass EM, Spratt DE, Iaquinta PJ, et al. Androgen Receptor Signaling Regulates DNA Repair in Prostate Cancers. *Cancer Discovery* (2013) 3(11):1245–53. doi: 10.1158/2159-8290.CD-13-0172
13. Goodwin JF, Schiewer MJ, Dean JL, Schrecengost RS, de Leeuw R, Han S, et al. A Hormone-DNA Repair Circuit Governs the Response to Genotoxic Insult. *Cancer Discovery* (2013) 3(11):1254–71. doi: 10.1158/2159-8290.CD-13-0108
14. Uematsu N, Weterings E, Yano KI, Morotomi-Yano K, Jakob B, Taucher-Scholz G, et al. Autophosphorylation of DNA-PKCS Regulates its Dynamics at DNA Double-Strand Breaks. *J Cell Biol* (2007) 177(2):219–29. doi: 10.1083/jcb.200608077
15. Li X, Heyer WD. Homologous Recombination in DNA Repair and DNA Damage Tolerance. *Cell Res* (2008) 18:99–113. NIH Public Access. doi: 10.1038/cr.2008.1
16. Franken NAP, Rodermond HM, Stap J, Haveman J, van Bree C. Clonogenic Assay of Cells *In Vitro*. *Nat Protoc* (2006) 1(5):2315–9. doi: 10.1038/nprot.2006.339
17. Schumann S, Eberlein U, Muhtadi R, Lassmann M, Scherthan H. DNA Damage in Leukocytes After Internal *Ex-Vivo* Irradiation of Blood With the α-Emitter Ra-223. *Sci Rep* (2018) 8(1):2286. doi: 10.1038/s41598-018-20364-7
18. Tai S, Sun Y, Squires JM, Zhang H, Oh WK, Liang CZ, et al. PC3 Is a Cell Line Characteristic of Prostatic Small Cell Carcinoma. *Prostate* (2011) 71 (15):1668–79. doi: 10.1002/pros.21383
19. Chou FJ, Chen Y, Chen D, Niu Y, Li G, Keng P, et al. Preclinical Study Using Androgen Receptor (AR) Degradation Enhancer to Increase Radiotherapy Efficacy *via* Targeting Radiation-Increased AR to Better Suppress Prostate Cancer Progression. *EBioMedicine* (2019) 40:504–16. doi: 10.1016/j.ebiom.2018.12.050
20. Ghashghaei M, Paliouras M, Heravi M, Bekerat H, Trifiro M, Niazi TM, et al. Enhanced Radiosensitization of Enzalutamide *via* Schedule Dependent Administration to Androgen-Sensitive Prostate Cancer Cells. *Prostate* (2018) 78(1):64–75. doi: 10.1002/pros.23445
21. Sekhar KR, Wang J, Freeman ML, Kirschner AN. Radiosensitization by Enzalutamide for Human Prostate Cancer Is Mediated Through the DNA Damage Repair Pathway. Budunova I, Editor. *PloS One* (2019) 14(4): e0214670. doi: 10.1371/journal.pone.0214670
22. Zhang W, Liao CY, Chtatou H, Incrocci L, Van Gent DC, Van Weerden WM, et al. Apalutamide Sensitizes Prostate Cancer to Ionizing Radiation via Inhibition of non-Homologous End-Joining DNA Repair. *Cancers (Basel)* (2019) 11(10):1593. doi: 10.3390/cancers11101593
23. Smith R, Liu M, Liby T, Bayani N, Bucher E, Chiotti K, et al. Enzalutamide Response in a Panel of Prostate Cancer Cell Lines Reveals a Role for Glucocorticoid Receptor in Enzalutamide Resistant Disease. *Sci Rep* (2020) 10(1):1–13. doi: 10.1038/s41598-020-78798-x
24. Grossebrummel H, Peter T, Mandelkow R, Weiss M, Muzzio D, Zimmermann U, et al. Cytochrome P450 17A1 Inhibitor Abiraterone Attenuates Cellular Growth of Prostate Cancer Cells Independently From Androgen Receptor Signaling by Modulation of Oncogenic and Apoptotic Pathways. *Int J Oncol* (2016) 48(2):793–800. doi: 10.3892/ijo.2015.3274
25. Elsesy ME, Oh-Hohenhorst SJ, Löser A, Oing C, Mutiara S, Köcher S, et al. Second-Generation Antiandrogen Therapy Radiosensitizes Prostate Cancer Regardless of Castration State Through Inhibition of DNA Double Strand Break Repair. *Cancers (Basel)* (2020) 12(9):1–21. doi: 10.3390/cancers12092467
26. Li L, Karanika S, Yang G, Wang J, Park S, Broom BM, et al. Androgen Receptor Inhibitor-Induced "BRCAness" and PARP Inhibition Are Synthetically Lethal for Castration-Resistant Prostate Cancer. *Sci Signal* (2017) 10(480):eaam7479. doi: 10.1126/scisignal.aam7479
27. Zhang M, Lai Y, Vasquez JL, James DI, Smith KM, Waddell ID, et al. Androgen Receptor and Poly(ADP-Ribose) Glycohydrolase Inhibition Increases Efficiency of Androgen Ablation in Prostate Cancer Cells. *Sci Rep* (2020) 10(1):1–12. doi: 10.1038/s41598-020-60849-y
28. Asim M, Tarish F, Zecchini HI, Sanjiv K, Gelali E, Massie CE, et al. Synthetic Lethality Between Androgen Receptor Signalling and the PARP Pathway in Prostate Cancer. *Nat Commun* (2017) 8(1):1–10. doi: 10.1038/s41467-017-00393-y
29. Min A, Jang H, Kim S, Lee KH, Kim DK, Suh KJ, et al. Androgen Receptor Inhibitor Enhances the Antitumor Effect of PARP Inhibitor in Breast Cancer Cells by Modulating DNA Damage Response. *Mol Cancer Ther* (2018) 17 (12):2507–18. doi: 10.1158/1535-7163.MCT-18-0234
30. Gui B, Gui F, Takai T, Feng C, Bai X, Fazli L, et al. Selective Targeting of PARP-2 Inhibits Androgen Receptor Signaling and Prostate Cancer Growth Through Disruption of FOXA1 Function. *Proc Natl Acad Sci USA* (2019) 116 (29):14573–82. doi: 10.1073/pnas.1908547116
31. Wengner AM, Siemeister G, Lucking U, Lefranc J, Wortmann L, Lienau P, et al. The Novel ATR Inhibitor BAY 1895344 is Efficacious as Monotherapy and Combined With DNA Damage–Inducing or Repair–Compromising Therapies in Preclinical Cancer Models. *Mol Cancer Ther* (2020) 19(1):26–38. doi: 10.1158/1535-7163.MCT-19-0019
32. Karanika S, Karantanos T, Li L, Wang J, Park S, Yang G, et al. Targeting DNA Damage Response in Prostate Cancer by Inhibiting Androgen Receptor-CDC6-ATR-Chk1 Signaling. *Cell Rep* (2017) 18(8):1970–81. doi: 10.1016/j.celrep.2017.01.072
33. Agarwal N, Shore ND, Dunshee C, Karsh LI, Sullivan B, Di Santo N, et al. Clinical and Safety Outcomes of TALAPRO-2: A Two-Part Phase III Study of Talazoparib (TALA) in Combination With Enzalutamide (ENZA) in Metastatic Castration-Resistant Prostate Cancer (mCRPC). *J Clin Oncol* (2019) 37(15_suppl):5076–6. doi: 10.1200/JCO.2019.37.15_suppl.5076
34. Hussain M, Daignault-Newton S, Twardowski PW, Albany C, Stein MN, Kunju LP, et al. Targeting Androgen Receptor and DNA Repair in Metastatic Castration-Resistant Prostate Ancer: Results From NCI 9012. *J Clin Oncol* (2018) 36(10):991–9. doi: 10.1200/JCO.2017.75.7310
35. Khalaf DJ, Annala M, Taavitsainen S, Finch DL, Oja C, Vergidis J, et al. Optimal Sequencing of Enzalutamide and Abiraterone Acetate Plus Prednisone in Metastatic Castration-Resistant Prostate Cancer: A Multicentre, Randomised, Open-Label, Phase 2, Crossover Trial. *Lancet Oncol* (2019) 20(12):1730–9. doi: 10.1016/S1470-2045(19)30688-6

Conflict of Interest: The authors declare that the research was conducted in the absence of any commercial or financial relationships that could be construed as a potential conflict of interest.

frontiers in Oncology

ORIGINAL RESEARCH
published: 28 July 2021
doi: 10.3389/fonc.2021.695251

Clinicopathological Analysis of the ISUP Grade Group And Other Parameters in Prostate Cancer: Elucidation of Mutual Impact of the Various Parameters

Yoichiro Okubo[1], Shinya Sato[2], Kimito Osaka[3], Yayoi Yamamoto[4], Takahisa Suzuki[3], Arika Ida[1], Emi Yoshioka[1], Masaki Suzuki[1,5], Kota Washimi[1], Tomoyuki Yokose[1], Takeshi Kishida[3] and Yohei Miyagi[2]*

[1] Department of Pathology, Kanagawa Cancer Center, Kanagawa, Japan, [2] Molecular Pathology and Genetics Division, Kanagawa Cancer Center Research Institute, Kanagawa, Japan, [3] Department of Urology, Kanagawa Cancer Center, Kanagawa, Japan, [4] Department of Radiology, Kanagawa Cancer Center, Kanagawa, Japan, [5] Department of Pathology, University of Tokyo Hospital, Tokyo, Japan

OPEN ACCESS

Edited by:
Alcides Chaux, Universidad del Norte, Paraguay

Reviewed by:
Ali Amin, The Warren Alpert Medical School of Brown University, United States
Hiroshi Miyamoto, University of Rochester Medical Center, United States

***Correspondence:**
Yoichiro Okubo
yoichiro0207@hotmail.com;
yoichiro0207@kcch.jp

Specialty section:
This article was submitted to Genitourinary Oncology, a section of the journal Frontiers in Oncology

Received: *14 April 2021*
Accepted: *13 July 2021*
Published: *28 July 2021*

Citation:
Okubo Y, Sato S, Osaka K, Yamamoto Y, Suzuki T, Ida A, Yoshioka E, Suzuki M, Washimi K, Yokose T, Kishida T and Miyagi Y (2021) Clinicopathological Analysis of the ISUP Grade Group And Other Parameters in Prostate Cancer: Elucidation of Mutual Impact of the Various Parameters. Front. Oncol. 11:695251. doi: 10.3389/fonc.2021.695251

Background: Prostate cancer has become increasingly common worldwide. Although Grade group (GG) is widely accepted as an indicator of prostate cancer grade, there are malignancies that cannot be defined by GG alone. Moreover, the relationship between GG and other parameters remains unclear. Herein, we aimed to explore the biological characteristics of prostate cancer.

Methods: This study included 299 radical prostatectomy cases. The Chi-square test and analysis of variance were used to analyze the association of GG with binary and continuous variables. We then conducted morphological analyses. Multivariate analyses were performed to extract the data on risk factors for biochemical recurrence (BCR) and lymph node metastasis.

Results: The lymphatic, venous, perineural, and seminal vesicle invasion rates were 37/299 (12.4%), 25/299 (8.4%), 280/299 (93.6%), and 23/299 (7.7%), respectively. The extraprostatic extension (EPE), positive surgical margin, tertiary Gleason pattern 5, intraductal carcinoma of the prostate gland, and lymph node metastasis rates were 89/299 (29.8%), 106/299 (35.5%), 33/260 (12.7%), 56/299 (18.7%), and 23/299 (7.7%), respectively. As GG increased, various parameters became easier to visualize; however, there were differences between the parameters. Postoperative BCR was observed in 31/242 (12.8%) cases without preoperative hormone therapy; GG2, GG3, GG4, and GG5 accounted for 4, 7, 7, and 13 cases, respectively. Multivariate analyses revealed that GG and tumor diameter were significant risk factors for early BCR, whereas lymphatic invasion, EPE, and seminal vesicle invasion were significant risk factors for lymph node metastasis. For BCR, the odds ratios (ORs) for GG and tumor diameter were 2.253 (95% confidence interval (CI]): 1.297–3.912; P=0.004) and 1.074 (95% CI: 1.011–1.142;

P=0.022), respectively. For lymph node metastasis, ORs for the presence of lymphatic invasion, EPE, and seminal vesicle invasion were 7.425 (95% CI: 1.688–22.583; P=0.004), 4.391 (95% CI: 1.037–18.589; P=0.044), and 5.755 (95% CI: 1.308–25.316; P=0.021), respectively.

Conclusions: We summarized various parameters correlating with each GG. Through multivariate analyses, we established the independent risk factors for early BCR and lymph node metastasis. In addition to GG, other important indices of malignancy were determined and weighted to provide a basis for future investigations.

Keywords: prostate, grade group, Gleason Score, metastasis, adenocarcinoma, lymphatic invasion, biochemical recurrence

INTRODUCTION

Prostate cancer has become increasingly prevalent worldwide (1–4). Although the incidence rate of this tumor is lower in Japan than that in Western countries (the incidence rates in Japan, the United States, and the United Kingdom are 27.0, 98.2, and 73.2 per 100,000 population, respectively) (5), its incidence is rapidly increasing with the westernization of lifestyles (6). Most malignant prostatic neoplasms (~90%) are adenocarcinomas (7–9). In patients who are required to undergo radical prostatectomy, various parameters can be evaluated through preoperative clinical investigations and histopathological analyses of surgical specimens. These parameters include age, preoperative serum prostate-specific antigen (PSA) concentration, body mass index (BMI), tumor diameter, Grade group (GG) and Gleason score (GS), lymphatic, venous, perineural, and seminal vesicle invasion, extraprostatic extension (EPE) of the tumor, positive surgical margins, and lymph node metastasis (10). In addition, postoperative follow-up surveys allow examination of the relationship between biochemical recurrence (BCR) and various parameters after radical prostatectomy.

Among these parameters, GG (2), lymphovascular invasion (11), EPE, seminal vesicle invasion, and lymph node metastasis (12) have been established as independent poor prognostic factors. More recently, tertiary Gleason pattern 5 and intraductal carcinoma of the prostate gland (IDC-P) have also been reported as poor prognostic factors (3, 13). However, few studies have investigated lymphatic invasion and venous invasion separately (14, 15), and the relationship between GG and various clinicopathological evaluation parameters has not yet been fully elucidated. Furthermore, the extent to which each evaluation parameter affects lymph node metastasis, which is an important prognostic factor in patients with prostate cancer, remains unclear (15).

Recently, the use of robot-assisted radical prostatectomy (RARP) has gained popularity. Studies have found that RARP allows for both safe operation and efficient lymph node evaluation (16, 17). Nevertheless, one study (18) suggested that lymph node dissection using RARP does not directly contribute to the prognosis and may increase complications; however, this finding remains controversial. Therefore, in this study, instead of performing a literature search, we aimed to analyze the risk factors for lymph node metastasis using detailed morphological, immunohistochemical, and statistical analyses of surgical specimens of patients who had undergone RARP. Specifically, we initially investigated the relationship between GG and the evaluation parameters. Thereafter, we conducted a multivariate logistic regression analysis to determine the risk factors for lymph node metastasis, which has been strongly established as a poor prognostic factor postoperatively (12). We also confirmed the status of BCR after RARP, extracted risk factors using multivariate logistic regression analysis, and attempted to integrate the results with morphological analysis.

Abbreviations: PSA, prostate-specific antigen; BMI, body mass index; GG, Grade group; GS, Gleason Score; EPE, extraprostatic extension; BCR, biochemical recurrence; IDC-P, intraductal carcinoma of the prostate gland; RARP, robot-assisted radical prostatectomy; HE, hematoxylin and eosin.

MATERIALS AND METHODS

Identification of the Cases Used in the Analysis (Kanagawa Cancer Center, Japan)

RARP, using the da Vinci surgical system (Intuitive Surgical, Inc.; Sunnyvale, CA, United States), was introduced at our institution in August 2018. Considering the combined experience of the operators and co-medicals, prostate cancer cases treated using RARP between January 2019 and December 2020 were included in this study. In addition, for enabling the safe and most appropriate treatment using RARP, an author of this manuscript, KO, was assigned to our institution in April 2018. KO had more than four years of prior experience in operating da Vinci surgical system and had experienced approximately 400 cases before this assignment, of which he was the primary surgeon in approximately 100 cases.

Specifically, we recorded various parameters using hematoxylin and eosin (HE) staining and immunohistochemical analysis under a light microscope as our routine diagnostic procedures. In addition, a pathological diagnosis support software ("EXpath" Laboratory Information Systems for Pathology, INTEC Inc., Tokyo, Japan) was used to confirm the pathological diagnoses and clinical information. This study was performed in alignment with the tenets of the Declaration of Helsinki and approved by the Ethics Review Committee of the Kanagawa Cancer Center (Approval Number: 2019-36). Furthermore, written informed

consent was obtained from the patients for the future use of their materials for research.

Clinicopathological Parameters of the Prostate Adenocarcinoma Cases

We extracted the below mentioned clinicopathological parameters for analysis. Most of these parameters were recorded during the routine pathological diagnosis process in our institute. We also checked the medical records in May 2021 to confirm the presence of BCR. The specific tabulation method for each parameter was as follows:

GG

In this analysis, we adopted the 2014 International Society of Urological Pathology (ISUP) grading system for GG evaluation (19, 20). According to the invasive pattern of prostate cancer, the GG system was divided into the following five groups: GG1, 2, 3, 4, and 5 (GS: 3 + 3 = 6, 3 + 4 = 7, 4 + 3 = 7, 4 + 4 = 8, and 4 + 5 or more, respectively). We have adopted the highest GG for cases with multiple lesions. At least two pathologists evaluated the post-RARP specimens as per the 2014 ISUP system. After one of the two pathologists (YO or SS) described the primary pathology findings, the specimens were reviewed by the third pathologist (YM) using a multi-viewing biological microscope. In case of disagreement on various diagnostic findings, the three pathologists discussed; however, if they still could not agree, the opinion of the third pathologist with the longer experience as a prostate cancer diagnostician was prioritized.

Age

We recorded the patients' ages when the surgery was performed.

BMI

BMI was determined using the patient's body weight and height at the time of the surgery and was calculated as follows: body weight (kilograms)/height squared (meters^2).

PSA Value

Each patient's highest PSA value from the collection of the preoperative serum PSA values was recorded.

Tumor Diameter

After formalin fixation, we recorded the length of the prostate in three directions (vertical, transverse, and sagittal). After photography, both the prostate apex and base were examined using the cone method with sagittal sectioning (21). The remaining prostate was entirely cut at approximately 5-mm intervals from the apex to the base, perpendicular to the long axis. All sections were embedded into paraffin and examined. The pathologist examined the specimen and measured the tumor diameter. Appropriate mapping was conducted, and even the lesions in the different sections were included in the tumor diameter if they were determined to be a series of lesions based on their location. In the case of multiple lesions, the tumor diameter with the highest GG was included in this study.

Lymphatic and Venous Invasion

To confirm the presence of lymphatic or venous invasion separately, HE-stained specimens were first evaluated. Then, we prepared sections from the paraffin-blocks corresponding to the respective HE-stained specimen, and D2-40 and CD31 immunostaining together with HE staining was conducted for each case (**Figures 1** and **2**). If there was obvious lymphatic or venous invasion in the HE-stained specimen, then that was recorded accordingly. If there were cancer cells in the lumen lined with endothelial cells positive for the expression of D2-40 or CD31, the decision was based on the concordance of the results of immunohistochemistry with the results of the re-sliced HE-stained specimen. Since D2-40 can stain non-specifically, especially cells other than those of the lymphatic endothelium, including the basal cells (22), we emphasized the comparison with the re-sliced HE-stained specimen. As CD31 immunostaining also faintly stains lymphatic endothelial cells,

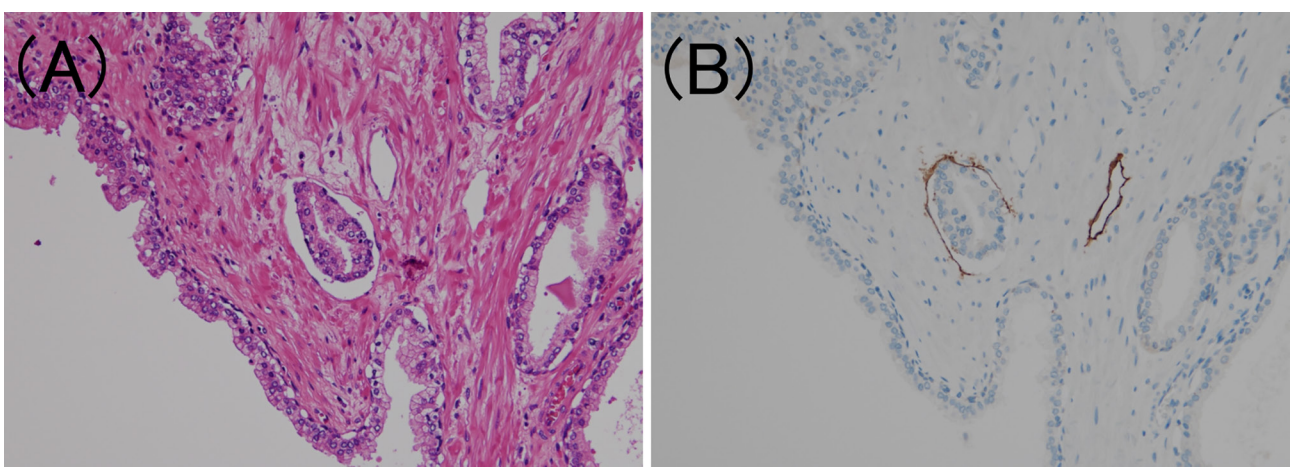

FIGURE 1 | Lymphatic invasion in prostate cancer. **(A)** Small clusters of carcinoma cells are present in the lumen (hematoxylin and eosin staining, ×200). **(B)** The luminal surface of the duct is lined with D2-40 positive lymphatic endothelium (D2-40 immunohistochemistry, ×200).

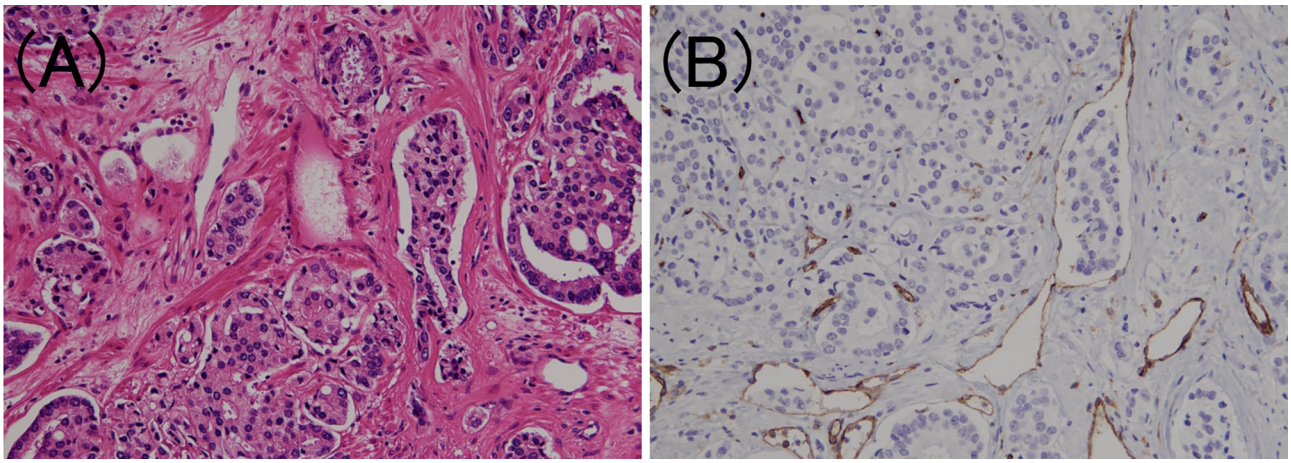

FIGURE 2 | Venous invasion in prostate cancer. **(A)** Small clusters of carcinoma cells are present in the lumen (hematoxylin and eosin staining, ×200). **(B)** The luminal surface of the duct is lined with CD31 positive venous endothelium (CD31 immunohistochemistry, ×200).

for cases in which both the expressions of D2-40 and CD31 were positive, we considered the staining intensity of obvious venous endothelial cells on the same section in our decision (**Figure 3**).

Perineural Invasion

The presence of perineural invasion was confirmed using the HE-stained specimen, which was routinely prepared for pathological diagnosis. Perineural invasion was defined as complete circumferential or direct invasion of peripheral nerve structures by the adenocarcinoma (23).

EPE

EPE is defined as an extension of a tumor into the periprostatic soft tissue (24). This definition has been adopted by the tumor, lymph node, and metastasis staging system for prostate cancer and the ISUP (25). Although EPE in the posterolateral area can be diagnosed when the presence of carcinoma cells is confirmed in the loose connective tissue or perineural spaces of the neurovascular bundles (25), there were no such cases in this study, and cases with firm invasion into the adipose tissue were included as EPE.

Surgical Margins

As mentioned above, both the prostate apex and base were examined using the cone method with sagittal sectioning (21). The remaining prostate was entirely cut at approximately 5-mm intervals from the apex to the base, perpendicular to the long axis. All sections were embedded into paraffin and examined.

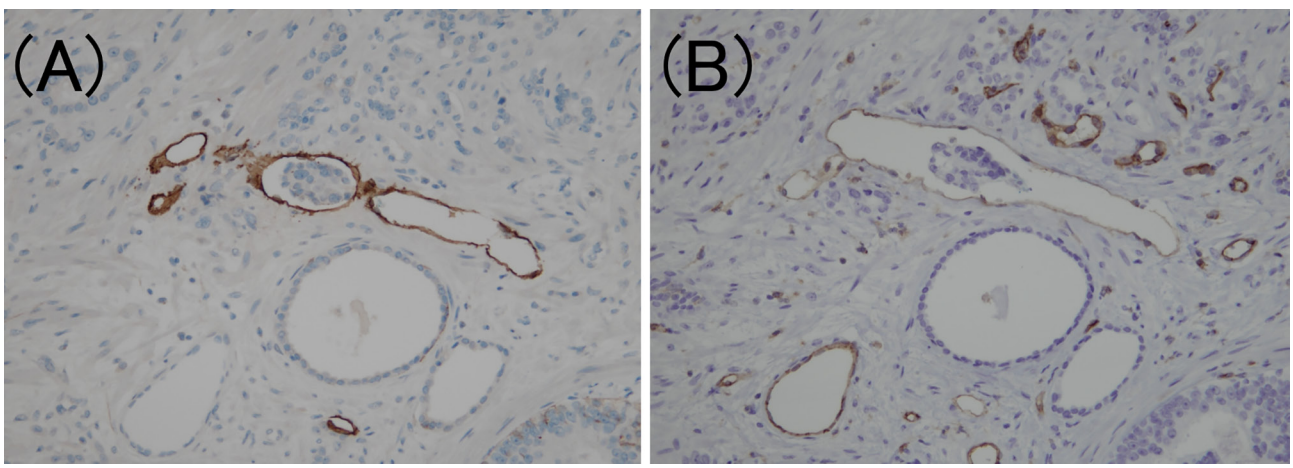

FIGURE 3 | Criteria for determining lymphovascular invasion using D2-40 and CD31 immunostaining. **(A)** The lymphatic vessel is clearly stained using D2-40 immunostaining (D2-40 immunohistochemistry, ×200). **(B)** The same location as **(A)**; however, the CD31 immunostaining also faintly stains the lymphatic vessels (CD31 immunohistochemistry, ×200).

Positive or negative surgical margins were confirmed using the HE-stained specimen, which is prepared routinely for diagnosis. At our institution, blue ink is applied to the prostate's surface when it is cut. If the cancer cells extend to the ink line at the edge of the prostate tissue, the margin is considered positive.

Seminal Vesicle Invasion

Seminal vesicle invasion was detected using histopathological evaluation and defined as a firm invasion of cancer cells into the muscle wall of the seminal vesicle (26). Although EPE and seminal vesicle invasion are similar in that they involve the outside of the prostate, they are considered independent parameters (27) and were evaluated individually in this analysis.

IDC-P

According to the latest ISUP consensus (2), we defined IDC-P as an extension of adenocarcinoma cells into the preexisting prostatic ducts and acini, distending them, with some preservation of the basal cells. Since IDC-P typically arises adjacent to invasive cancer cells and rarely occurs without invasion, we also confirmed the presence of invasive cancer in the surrounding area. Previous studies have reported the following morphological features of IDC-P: expanded growth of carcinoma cells forming large dense cribriform and/or solid structures (28), which were also confirmed in this study. Furthermore, the basal cells are not always confirmed through HE-stained specimens alone (2); therefore, PIN4 immunostaining (combined AMACR (P504S)/34bE12/p63 immunostaining) was performed on one representative section of the specimen to confirm the presence of IDC-P (**Figure 4**). In addition, although controversial, it is commonly considered that IDC-P is not incorporated into GG (29); hence, we exclude it from the GG assessment for IDC-P areas.

Tertiary Gleason Pattern 5

Tertiary Gleason pattern 5 was defined as the percentage of cases with Gleason pattern 5 <5% (30). Cases with tertiary Gleason pattern 5 in GG4 or less were included (**Figure 5**).

Biochemical Recurrence After RARP

In line with the American Urological Association (31) and European Association of Urology Guidelines (32) (as well as the Japanese guidelines), BCR was defined by two consecutive rising PSA values >0.2 ng/mL after radical prostatectomy (in this case, the date of the first rise was defined as the date of the BCR). If the serum PSA level did not fall below 0.2 ng/mL after RARP and was 0.2 ng/mL or higher in two successive tests, the date of surgery was assigned as the day of BCR.

Lymph Node Metastasis

The presence or absence of lymph node metastasis was confirmed in cases in which lymph node dissection was performed. At our institution, patients who were at a high risk according to the D'Amico classification or those with 7% or higher predicted lymph node metastasis rates according to the Briganti 2012 nomogram (33) underwent lymph node resection.

Additional Morphological Analysis

Morphological analysis was conducted in cases where the carcinoma cells had metastasized (cases with EPE, seminal vesicle invasion, or lymph node metastasis were included in the analysis). Specifically, in each case, we identified the Gleason patterns 4 and 5 components of the lesions, which were recognized as high grade. We recorded the presence of the five subtypes each of Gleason patterns 4 and 5 (in this study, papillary/ductal adenocarcinomas were also included as subtypes). These 10 subtypes were based on the ISUP 2014

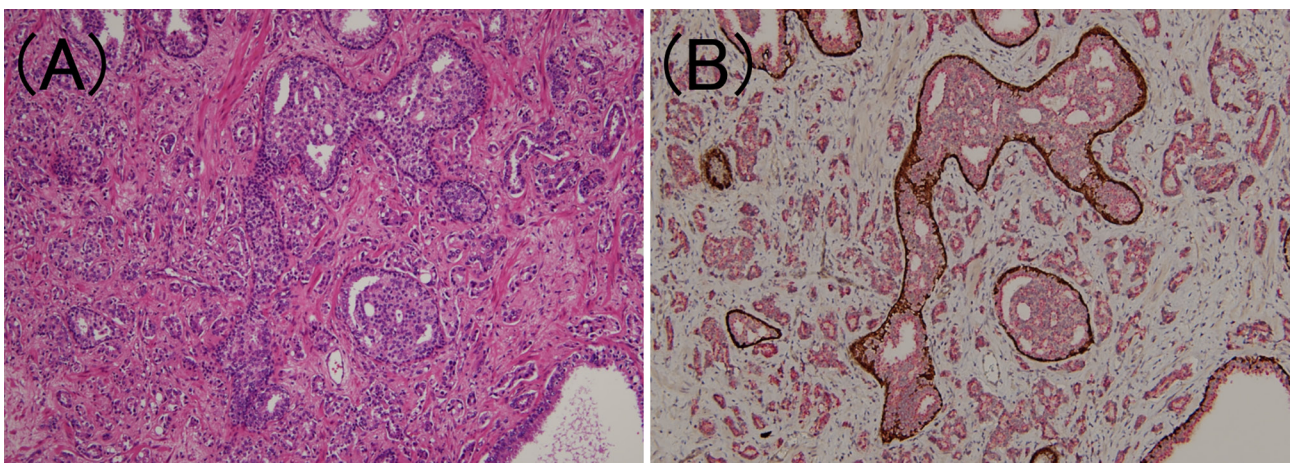

FIGURE 4 | Intraductal carcinoma of the prostate. **(A)** In the lumen of the prostate gland, carcinoma cells identical to those of the surrounding prostate adenocarcinoma components have developed (hematoxylin and eosin staining, ×100). **(B)** Tumor components are stained red owing to P504S immunoreactivity, while the periprostatic gland lumen is stained brown owing to p63 immunoreactivity (PIN4 immunohistochemistry, ×100).

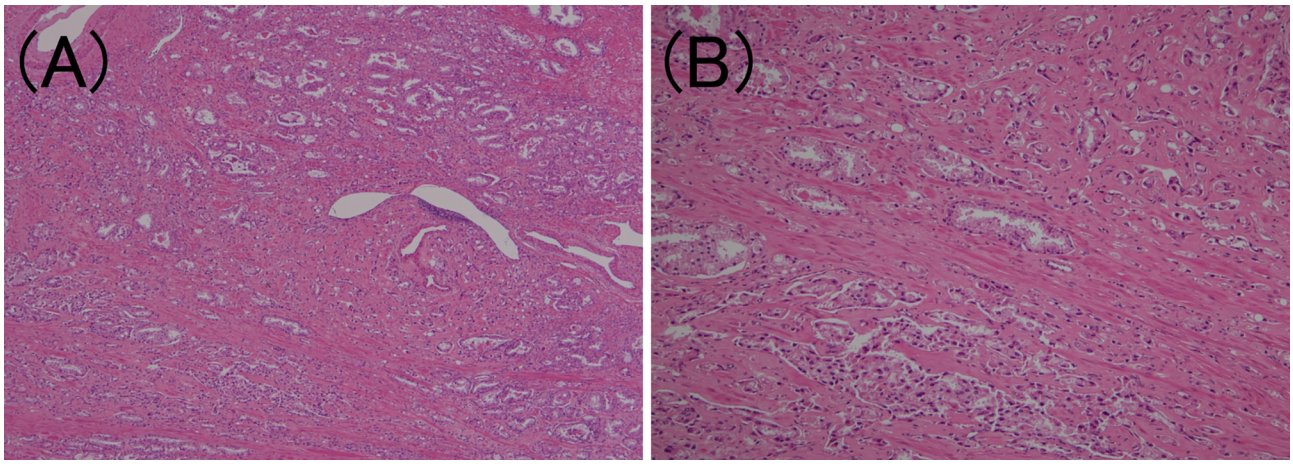

FIGURE 5 | Tertiary Gleason pattern 5 in prostatic adenocarcinoma. **(A)** Most cancer cells correspond to Gleason pattern 4 or 3. (hematoxylin and eosin (HE) staining, ×40). **(B)** The overall picture shows that <5% of the carcinoma cells are solitary or grow in a linear fashion. (HE staining, ×200).

grading system (20). We recorded subtypes that accounted for at least 10% of the intraprostatic, invasive, and metastatic lesions, respectively. We also recorded the most predominant subtypes. The primary subtype decision was made by YO or AI, who described the specimens. Then, together with the third pathologist (YM), the specimens were reviewed using a multi-viewing biological microscope. In case of disagreement on the subtype, the three pathologists discussed the findings, but if they still failed to agree, the opinion of YM, who had a longer experience of prostate cancer diagnosis, was prioritized.

Statistical Analyses

For binary variables that could take two values (lymphatic, venous, perineural, seminal vesicle invasion, EPE, positive surgical margins, tertiary Gleason pattern 5, and IDC-P), the Chi-square test was used for statistical analysis of GG and the various parameters. Statistical significance was set at $P<0.05$. We also measured the adjusted residuals to test for an association between GG and each of the parameters. A value of ±1.96 or higher was considered significant.

Analysis of variance was used to analyze GG and continuous variables (age, preoperative PSA, BMI, and tumor diameter). $P<0.05$ was considered significant for each group.

Multivariate logistic regression analysis was performed to extract risk factors for BCR and lymph node metastasis in prostate cancer. The dependent variable was the presence or absence of BCR or lymph node metastasis, and the explanatory variables included GG; lymphatic, venous, perineural, and seminal vesicle invasion; EPE; positive surgical margins; tertiary Gleason pattern 5, IDC-P, age, preoperative PSA, BMI, and tumor diameter. These parameters were recorded during the routine pathological diagnosis process. Differences were considered significant at $P<0.05$. In the present study, all currently available cases were subjected to statistical analyses, but cases involving preoperative hormonal therapy were excluded owing to the impossibility of GG evaluation. In addition, GG1 was also excluded owing to the presence of only two cases.

RESULTS

The rates of the parameters were as follows: lymphatic invasion, 37/299 (12.4%); venous invasion, 25/299 (8.4%); perineural invasion, 280/299 (93.6%); EPE, 89/299 (29.8%); positive surgical margins, 106/299 (35.5%); seminal vesicle invasion, 23/299 (7.7%); tertiary Gleason pattern 5, 33/260 (12.7%); ICD-P, 56/299 (18.7%); and lymph node metastasis, 23/299 (7.7%). These results are summarized in **Table 1** and **Figure 6**. In addition, there were no cases of GS 3 + 5 = 8 or GS 5 + 3 = 8 or cases with microscopic invasion of the bladder neck in this study.

For all parameters, detailed values, percentages, and adjusted residuals (Chi-square test) for each GG were as follows

TABLE 1 | The mean, standard deviation, or detection rates for the various study parameters.

Total cases	299
Lymphatic invasion rate	37/299 (12.4%)
Venous invasion rate	25/299 (8.4%)
Perineural invasion rate	280/299 (93.6%)
EPE rate	89/299 (29.8%)
Positive surgical margins rate	106/299 (35.5%)
Seminal vesicle invasion rate	23/299 (7.7%)
Tertiary Gleason pattern 5 rate	33/260 (12.7%)
Intraductal carcinoma of the prostate rate	56/299 (18.7%)
Lymph node metastasis rate	23/299 (7.7%)
Age (years, mean ± SD)	67.6 ± 6.4
BMI (mean ± SD)	24 ± 3.1
Preoperative PSA value (ng/ml, mean ± SD)	10.9 ± 13.2
Tumor diameter from surgical specimen (mm, mean ± SD)	24.3 ± 10.2

SD, standard deviation; BMI, body mass index; EPE, extraprostatic extension.
Results of the analysis of the various parameters for all 299 cases.

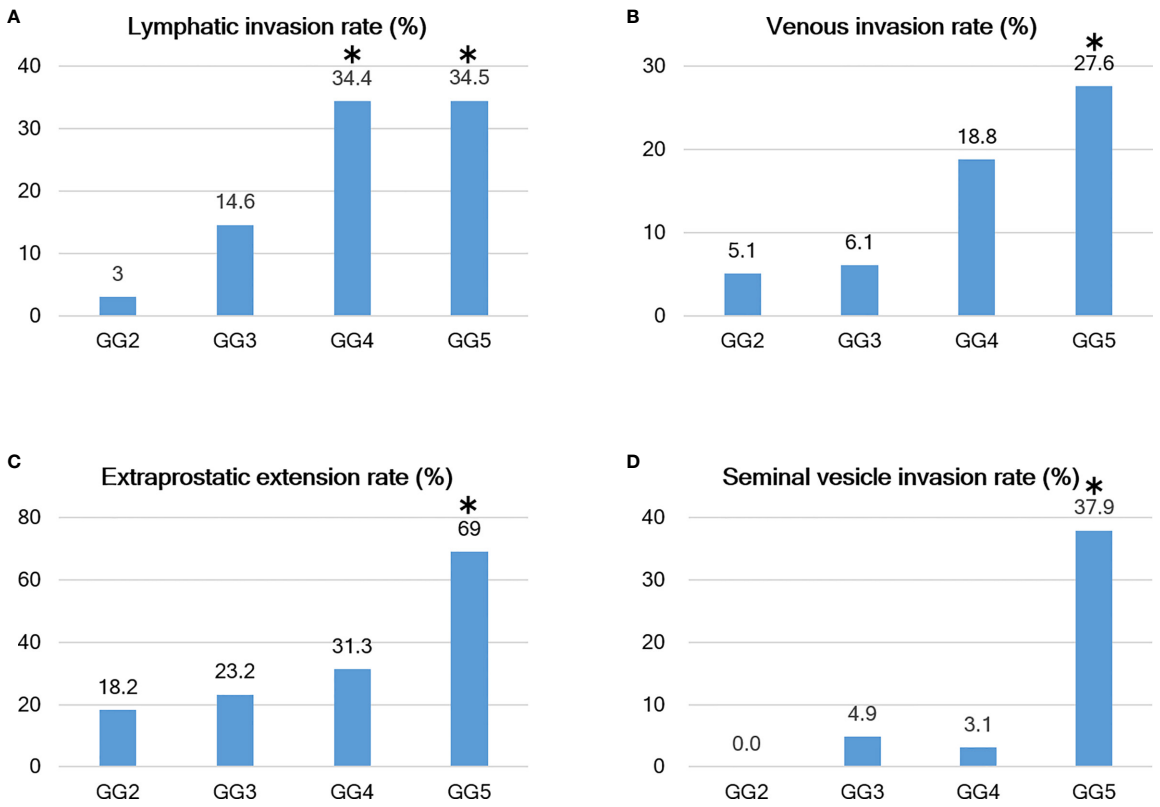

FIGURE 6 | Relationship between Grade group and positive rates of various parameters. **(A–D)** As the Grade group (GG) increases, various evaluation parameters become easier to visualize; however, there are differences between the parameters. For example, the lymphatic invasion rate increases from GG3 and reaches a plateau at GG4, while the venous invasion rate begins to increase at GG4 and is even higher at GG5. Extraprostatic extension (EPE) is detected at a constant frequency starting at GG2 (but becomes extremely high at GG5), and seminal vesicle invasion has a sharp increase in positivity at GG5. The bars with the asterisk symbol (*) in each graph mean that the adjusted residuals are greater than 1.96 in the Chi-square test, indicating that the corresponding values are significantly higher between the groups (e.g., 37.9% for GG5 in seminal vesicle invasion rate is statistically significant).

(**Tables 2** and **3**): Up to GG1 and GG2, there was rarely any lymphatic invasion; however, it was observed in >10% of GG3 cases. In particular, it was confirmed in approximately one-third of the cases for GG4 and GG5. The adjusted residuals for GG4 and GG5 were notably >1.96. GG4 and GG5 had a significant impact on the increased risk of lymphatic invasion. Venous invasion was rarely seen below GG3; contrarily, it was confirmed in approximately one-fifth and one-fourth of the GG4 and GG5 cases, respectively. However, only GG5 had an adjusted residual >1.96, and the overall positivity rate was low compared to that of lymphatic invasion.

Most of the cases were positive for perineural invasion. EPE occurred at a constant frequency of approximately one-fifth to one-fourth of the cases in GG2 to GG4, though its occurrence was significantly lower in GG2. By contrast, GG5 exhibited a significantly higher rate of positivity than the other groups (slightly more than two-thirds were confirmed in GG5).

Positive surgical margins were found at a constant rate but were significantly higher in GG5. The rates in 2019 and 2020 were different, at 49/120 (40.8%) and 39/124 (31.5%), respectively, but the difference was not significant (Chi-square test, P-value=0.152).

Seminal vesicle invasion was the most strongly affected parameter in GG5 and was significantly higher in GG5. The invasion was found in approximately one-third of the GG5 cases but less than 5% in GG4 or below cases.

The incidence of tertiary Gleason pattern 5 was significantly higher in GG3 than in GG2. In GG4, the rate was relatively lower than that in GG3.

The incidence of IDC-P represented approximately one-fifth of cases with GG3. The adjusted residuals for GG4 and GG5 were notably >1.96. GG4 and GG5 had a significant impact on the increased risk of IDC-P. In addition, there were no cases of comedonecrosis with IDC-P in this study.

Regarding the lymph node metastasis rate in patients who underwent lymph node dissection up to GG4, it was <10% (some difference was present; however, it was not significant). Contrastingly, GG5 exhibited lymph node metastasis in approximately one-third of cases, which was significantly higher than the findings from other GG groups.

The continuous variables PSA levels and tumor diameter were significantly higher in GG5 than in other groups. In contrast, there were no significant differences in any variables between GG2 and GG4.

TABLE 2 | Summary of the evaluation items for each Grade group.

	GG1	GG2	GG3	GG4	GG5
Cases	2	99	82	32	29
Age (years, mean ± SD)	68.5 ± 7.8	67.4 ± 6.2	68.5 ± 5.8	66.2 ± 7.2	68.2 ± 6.2
BMI (mean ± SD)	23.1 ± 0.2	23.8 ± 2.9	23.8 ± 2.9	24.2 ± 3.7	24.7 ± 4.1
Preoperative PSA value (ng/ml, mean ± SD)	12.8 ± 10.6	7.6 ± 4.7	8.4 ± 4.4	9.1 ± 4.8	16.1 ± 24.2
Tumor diameter from surgical specimen (mm, mean ± SD)	10 ± 7.1	23.8 ± 8.2	25.7 ± 9.3	23.2 ± 9.4	31.2 ± 12.8
Lymphatic invasion	0/2 (0%)	3/99 (3.0%)	12/82 (14.6%)	11/32 (34.4%)	10/29 (34.5%)
Venous invasion rate	0/2 (0%)	5/99 (5.1%)	5/82 (6.1%)	6/32 (18.8%)	8/29 (27.6%)
Perineural invasion rate	0/2 (0%)	93/99 (93.9%)	82/82 (100%)	32/32 (100%)	29/29 (100%)
EPE rate	0/2 (0%)	18/99 (18.2%)	19/82 (23.2%)	10/32 (31.3%)	20/29 (69%)
Positive surgical margins rate	0/2 (0%)	29/99 (29.3%)	29/82 (35.4%)	10/32 (31.3%)	20/29 (69%)
Seminal vesicle invasion rate	0/2 (0%)	0/99 (0%)	4/82 (4.9%)	1/32 (3.1%)	11/29 (37.9%)
Tertiary Gleason pattern 5 rate	0/2 (0%)	8/99 (8.1%)	21/82 (25.6%)	4/32 (12.5%)	none
IDC-P rate	0/2 (0%)	4/99 (4.0%)	15/82 (18.3%)	11/32 (34.4%)	17/29 (58.6%)
Lymph node metastasis rate (All patients except for those who underwent preoperative hormonal therapy)	0/2 (0%)	2/99 (2.0%)	4/82 (4.9%)	1/32 (3.1%)	9/29 (31.0%)
Lymph node metastasis rate (Only cases in which lymph node dissection was conducted)	None	2/31 (6.5%)	4/50 (8.0%)	1/26 (3.8%)	9/27 (33.3%)

GG, Grade group; SD, standard deviation; BMI, body mass index; EPE, extraprostatic extension; IDC-P, Intraductal carcinoma of the prostate.
Summary of the mean, standard deviation, or detection rate of the various parameters for each Grade group.

In this study, postoperative BCR was observed in 31/242 (12.8%) cases; cases with preoperative hormone therapy were excluded from this analysis. At our hospital, serum PSA levels are measured at least twice for each radical prostatectomy to decide the treatment and follow-up strategy. Therefore, patients who received additional treatment before being diagnosed as BCR were not included in this study. GG2, GG3, GG4, and GG5 accounted for four, seven, seven, and 13 cases, respectively. The average time to diagnosis of BCR was 111.8 days (range: 0 to 543 days); 19/31 (61.3%) cases never had PSA<0.2 ng/mL, postoperatively, and BCR for them was assigned to the day of surgery. We also examined the incidence of BCR in cases with EPE, seminal vesicle invasion, or lymph node metastasis, which were 17/67 (25.4%), 8/16 (50%), and 9/16 (56.3%), respectively. Our morphological analysis showed that in each of the analyses, the most prominent subtypes of intraprostatic lesions were small and large fused glands, but there were differences in their distribution (**Tables 4**–**6**). We conducted multivariate logistic regression analysis to extract independent risk factors for BCR in this study and found that GG and tumor diameter were significant risk factors for BCR. Lymph node metastasis was not a significant risk factor, though it tended toward significance. The odds ratios for BCR with respect to GG and tumor diameter were 2.253 (95% confidence interval: 1.297–3.912; P=0.004) and 1.074 (95% confidence interval: 1.011–1.142; P=0.022), respectively (**Table 7**).

TABLE 3 | Results from the adjusted residuals, in which various parameters based on the Chi-square test were detected, for each Grade group.

	GG2	GG3	GG4	GG5
Lymphatic invasion	-4.3	0	3.3	3.1
Venous invasion rate	-2.1	-1.4	1.8	3.4
Perineural invasion rate	-3.0	1.8	1	0.9
EPE	-2.8	-1.1	0.5	5.3
Positive surgical margin	-1.9	-0.2	-0.7	3.9
Seminal vesicle invasion	-3.5	-0.8	-0.9	7.2
Tertiary Gleason pattern 5	-2.8	-3.2	-0.5	None
IDC-P	-5.1	-0.3	2.3	5.8
Lymph node metastasis rate (Only cases in which lymph node dissection was conducted)	-1.1	-1.1	-1.4	3.8

GG, Grade group; EPE, extraprostatic extension; IDC-P, Intraductal carcinoma of the prostate.
Based on the Chi-square test, the adjusted residuals for the various parameters between the groups were evaluated; ± 1.96 was used as a criterion for the presence of a significant difference, and the detection rate was considered significantly high if it was >1.96 and significantly low if it was ≤1.96. GG1 was excluded from the analysis owing to the excessively limited number of cases.

TABLE 4 | Association between morphological characteristics of intraprostatic and invasive lesions in cases with EPE.

	Predominant morphological variant (intraprostatic lesion)	Cases with BCR (intraprostatic lesion)	Cases with BCR (invasion lesion)	Cases without BCR (intraprostatic lesion)	Cases without BCR (invasive lesion)
Ill formed	5/67 (7.5%)	9/17 (52.9%)	8/17 (47.1%)	28/50 (56%)	13/50 (26%)
Small and large fused	32/67 (47.8%)	11/17 (64.7%)	8/17 (47.1%)	40/50 (80%)	40/50 (80%)
Glomeruloid	4/67 (6%)	4/17 (23.5%)	0/17 (0%)	17/50 (34%)	8/50 (16%)
Cribriform	15/67 (22.4%)	10/17 (58.8%)	5/17 (29.4%)	26/50 52%)	9/50 (18%)
Papillary	8/67 (11.9%)	3/17 (17.6%)	1/17 (5.9%)	16/50 (32%)	0/50 (0%)
Single cell	0/67 (0%)	9/17 (52.9%)	3/17 (17.6%)	13/50 (26%)	2/50 (4%)
Single file	0/67 (0%)	8/17 (47.1%)	3/17 (17.6%)	12/50 (24%)	1/50 (2%)
Cribriform with comedonecrosis	0/67 (0%)	3/17 (17.6%)	0/17 (0%)	9/50 (18%)	1/50 (2%)
Pseudorosetting	0/67 (0%)	0/17 (0%)	0/17 (0%)	0/50 (0%)	0/50 (0%)
Solid	3/67 (4.5%)	6/17 (35.3%)	1/17 (5.9%)	2/50 (4%)	1/50 (2%)

EPE, extraprostatic extension; BCR, biochemical recurrence.

The subtypes of Gleason patterns 4 and 5 in cases with EPE were examined both in intraprostatic and invasive lesions, respectively. Overall, the "small and large fused glands" subtype was the predominant subtype in the intraprostatic lesions. In addition, the Gleason pattern 5 component was more likely to be observed in cases with BCR than in cases without BCR in both intraprostatic and invasive lesions.

TABLE 5 | Association between morphological characteristics of intraprostatic and invasive lesions in cases with SVI.

	Predominant morphological variant (intraprostatic lesion)	Cases with BCR (intraprostatic lesion)	Cases with BCR (invasion lesion)	Cases without BCR (intraprostatic lesion)	Cases without BCR (invasive lesion)
Ill formed	1/16 (6.3%)	4/8 (50%)	5/8 (62.5%)	7/8 (87.5%)	5/8 (62.5%)
Small and large fused	7/16 (43.8%)	6/8 (75%)	0/8 (0%)	5/8 (62.5%)	5/8 (62.5%)
Glomeruloid	1/16 (6.3%)	0/8 (0%)	1/8 (12.5%)	4/8 (50%)	2/8 (25%)
Cribriform	4/16 (25%)	4/8 (50%)	0/8 (0%)	6/8 (75.0%)	1/8 (12.5%)
Papillary	0/16 (0%)	0/8 (0%)	5/8 (62.5%)	1/8 (12.5%)	0/8 (0%)
Single cell	0/16 (0%)	6/8 (75%)	4/8 (50%)	6/8 (75%)	2/8 (25.0%)
Single file	1/16 (6.3%)	6/8 (75%)	0/8 (0%)	6/8 (75%)	3/8 (37.5%)
Cribriform with comedonecrosis	0/16 (0%)	1/8 (12.5%)	0/8 (0%)	1/8 (12.5%)	0/8 (0%)
Pseudorosetting	0/16 (0%)	0/8 (0%)	2/8 (12.5%)	0/8 (0%)	0/8 (0%)
Solid	2/16 (12.5%)	3/8 (37.5%)	1/8 (12.5%)	2/8 (25%)	1/8 (12.5%)

SVI, seminal vesicle invasion; BCR, biochemical recurrence.

I In cases with seminal vesicle invasion, the subtypes of Gleason pattern 4 and 5 were examined in both intraprostatic and invasive lesions, respectively. Overall, the "small and large fused glands" subtype was the predominant subtype in the intraprostatic lesions. In addition, the Gleason pattern 5 component was more likely to be observed in both intraprostatic and invasive lesions, regardless of the presence of BCR.

TABLE 6 | Association between morphological characteristics of intraprostatic and metastatic lesions in cases with lymph node metastasis.

	Predominant morphological variant (intraprostatic lesion)	Cases with BCR (intraprostatic lesion)	Cases with BCR (metastatic lesion)	Cases without BCR (intraprostatic lesion)	Cases without BCR (metastatic lesion)
Ill formed	2/16 (12.5%)	5/9 (55.6%)	2/9 (22.2%)	5/7 (71.4%)	4/7 (57.1%)
Small and large fused	5/16 (31.3%)	6/9 (66.7%)	1/9 (11.1%)	5/7 (71.4%)	0/7 (0%)
Glomeruloid	0/16 (0%)	1/9 (11.1%)	7/9 (77.8%)	1/7 (14.3%)	4/7 (42.9%)
Cribriform	3/16 (18.8%)	4/9 (44.4%)	2/9 (22.2%)	6/7 (85.7%)	0/7 (0%)
Papillary	3/16 (18.8%)	2/9 (22.2%)	0/9 (0%)	3/7 (42.9%)	0/7 (0%)
Single cell	0/16 (0%)	5/9 (55.6%)	0/9 (0%)	3/7 (42.9%)	0/7 (0%)
Single file	1/16 (6.3%)	5/9 (55.6%)	1/9 (11.1%)	2/7 (28.6%)	3/7 (42.9%)
Cribriform with comedonecrosis	0/16 (0%)	2/9 (22.2%)	1/9 (11.1%)	1/7 (14.3%)	3/7 (28.6%)
Pseudorosetting	0/16 (0%)	0/9 (0%)	3/9 (33.3%)	0/7 (0%)	2/7 (28.6%)
Solid	2/16 (12.5%)	3/9 (33.3%)	1/9 (11.1%)	2/7 (28.6%)	1/7 (14.3%)

BCR, biochemical recurrence.

In cases with lymph node metastasis, the subtypes of Gleason pattern 4 and 5 were examined in both intraprostatic and metastatic lesions, respectively. Though the "small and large fused glands" subtype was slightly predominant, various subtypes tended to be identified in the intraprostatic lesions. In addition, lymph node metastatic lesions tended to congregate to some extent rather than being solitary, while the "Pseudorosetting" formation was observed at a certain frequency.

TABLE 7 | Multivariate logistic regression analysis of biochemical recurrence.

Variable	OR (95% CI)	*P*-value
GG	2.253 (1.297–3.912)	0.004
Tumor diameter	1.074 (1.011–1.142)	0.022
Lymph node metastasis	4.074 (0.857–19.358)	0.077

CI, confidence interval; OR, odds ratio; GG, Grade group.
In this multivariate analysis, the GG and tumor diameter were significant independent risk factors for biochemical recurrence. Though it tended to be significant, lymph node metastasis was not a significant factor. This statistical analysis only included cases in which lymph node dissection was conducted.

To explore the risk factors for lymph node metastasis, we performed a multivariate logistic regression analysis. The results established that the presence of lymphatic invasion, EPE, and seminal vesicle invasion were independent risk factors for lymph node metastasis. The odds ratios for the presence of lymphatic invasion, EPE, and seminal vesicle invasion were 7.425 (95% confidence interval: 1.688–22.583; P=0.004), 4.391 (95% confidence interval: 1.037–18.589; P=0.044), and 5.755 (95% confidence interval: 1.308–25.316; P=0.021), respectively (**Table 8**).

As the analysis found three independent risk factors for lymph node metastasis (lymphatic invasion, EPE, and seminal vesicle invasion), we investigated the relationship between the presence of EPE, seminal vesicle invasion, and lymphatic invasion rate using the Chi-square test. The results verified that there was no significant difference between the lymphatic invasion rate and EPE in patients with EPE when compared with those without EPE. In contrast, more than half of the patients with seminal vesicle invasion had lymphatic invasion, while the lymphatic invasion rate was significantly lower in patients who did not have seminal vesicle invasion (Chi-square test, P< 0.001, **Table 9**).

DISCUSSION

In this study, we analyzed the risk factors for BCR and lymph node metastasis in patients who underwent RARP using detailed morphological, immunohistochemical, and statistical analyses of surgical specimens. Furthermore, we clarified the relationship between GG and the assessment of parameters. Though GG is the best known indicator for identifying malignant potential (30), few studies have investigated the relationship between GG and the various clinicopathological parameters that were precisely evaluated through immunohistochemistry for lymphatic invasion, venous invasion, and IDC-P identification. In addition, all risk factors for lymph node metastasis in patients who have undergone RARP have not yet been elucidated (17). Thus, herein, we discuss BCR and lymph node metastasis as prognostic factors in prostate cancer.

TABLE 8 | Multivariate logistic regression analysis of lymph node metastasis.

Variable	OR (95% CI)	*P*-value
Lymphatic invasion	7.425 (1.688–22.583)	0.004
EPE	4.391 (1.037–18.589)	0.044
Seminal vesicle invasion	5.755 (1.308–25.316)	0.021

CI, confidence interval; OR, odds ratio; EPE, extraprostatic extension.
In this multivariate analysis, lymphatic invasion, EPE, and seminal vesicle invasion were significant independent risk factors for lymph node metastasis. This statistical analysis only included cases in which lymph node dissection was conducted.

TABLE 9 | Relationship between lymphatic invasion, extraprostatic extension, and seminal vesicle invasion.

Variable	Lymphatic invasion rate	*P*-value (Chi-square test)
Cases with extraprostatic extension	19.4% (13/67)	0.208
Cases without extraprostatic extension	13% (23/177)	
Cases with seminal vesicle invasion	56.3% (9/16)	<0.001
Cases without seminal vesicle invasion	11.8% (27/228)	

The presence of extraprostatic extension did not differ significantly from the lymphatic invasion rate. In contrast, patients with seminal vesicle invasion had a significantly higher lymphatic invasion rate.

Approximately 10% of the cases in the present study were diagnosed as BCR, but for more than half of them, the event was assigned to the day of surgery. This can be partly explained by the short observation period of this study. According to the multivariate analysis, GG and tumor diameter were independent significant factors for BCR, while lymph node metastasis was not a significant factor in this study, even though its P-value tended toward significance. Many previous studies demonstrated lymph node metastasis as a risk factor for BCR instead of GG and tumor diameter (34–37). Detectable serum PSA values after prostatectomy should be closely associated with the presence of residual tumor (38) and intraprostatic incision into benign glands (39). In this study, the BCR was assessed for a short period of time, and hence, further follow-up studies are required to clarify the factors that influence each other.

Considering the overall short follow-up period of this study, we would like to raise a possibility that GG and tumor diameter may have implications as risk factors for very early BCR. In addition, extraprostatic involvement including EPE, seminal vesicle invasion, and lymph node metastasis was not a significant factor for BCR in the multivariate analysis in this study.

We also added the morphological analysis referring to the ISUP 2014 grading system (19, 20). Specifically, in each case, we identified the Gleason patterns 4 and 5 components of the lesions, which are recognized as high grade (3, 40). Our morphological analysis showed that among the cases with EPE, those with BCR tended to have a component of GG5 in both intraprostatic and invasive lesions. Furthermore, GG5 was more likely to be identified in cases with seminal vesicle invasion regardless of BCR occurrence (in both intraprostatic and invasive lesions). In comparison, various subtypes of histology were found in the main lesions of the prostate in cases with lymph node metastasis. It was also found that isolated carcinoma cells were not evident in the metastatic foci in the lymph nodes; thus,

showing some degree of aggregation. Expression of paxillin, reported in prostate cancer (41) and involved in cancer cell aggregation (42), could be implicated to this observation; further studies are needed to clarify this relationship. The glomeruloid pattern was relatively rare in the present study. We also examined the most predominant GG4 and GG5 histological subtypes in prostatic lesions using cases with EPE, seminal vesicle invasion, or lymph node metastasis. In all analyses, the cribriform pattern, which has been reported (43–45) to be a poor prognostic factor, was the second common subtype after the small and large fused glands subtype. Thus, a re-evaluation of BCR with a longer observation period is required.

Meanwhile, in this study, 23 (12.8%) of the 179 patients who underwent lymph node dissection had lymph node metastasis. The Chi-square test demonstrated no significant difference between GG2 and GG4; however, lymph node metastasis was found in about one-third of the GG5 cases and this finding was significantly higher than that for the other groups. This result shows that compared with other groups, GG5 exhibited a significantly higher risk of lymph node involvement. Interestingly, GG was not an independent risk factor for lymph node metastasis in the multivariate analysis in this study. Though GG is considered a risk factor for lymph node metastasis (11), the results from our multivariate analysis were inconsistent with those of previous reports (8, 30, 46). One reason for this could be that there were few lymph nodes. In particular, only one GG4 case had lymph node metastasis, which may have affected the results. To mitigate this problem, additional case detail collection is required. In this article, we would like to further discuss the results of the multivariate analysis using cases in which lymph node dissection was conducted. In the statistical analysis, lymphatic invasion, EPE, and seminal vesicle invasion were independent risk factors for lymph node metastasis. At our institution, to avoid prolonged operative times, damage to blood vessels and nerves, and postoperative lymphatic circulation disturbance, lymph node dissection is conducted if the patient is at high risk according to the D'Amico classification or if the predicted Briganti 2012 lymph node metastasis rate is >7%. Because the criteria for lymph node dissection included factors other than GG (PSA, preoperative staging by radiologists, and core-positive rates on preoperative biopsy), the influence of other factors may have been stronger in patients with relatively low GG. Consequently, we propose that GG may not have been an independent risk factor for patients who underwent lymph node dissection at our institution. From another perspective, the three independent risk factors for lymph node metastasis identified in the present multivariate analysis were assumed to have a strong influence on lymph node metastasis in addition to GG. Therefore, we would like to discuss these risk factors further.

Lymphatic vessels are the pathways to lymph nodes, and lymphatic invasion is a risk factor for lymph node metastasis (11, 47). It should be noted that venous invasion was not a risk factor for lymph node metastasis in our study. Considering that only lymphatic invasion is an independent risk factor for lymph node metastasis (15), lymphatic and venous invasion should be assessed separately rather than combined into the category of lymphovascular invasion. However, venous invasion is generally considered a risk factor for distant metastasis, and previous studies that evaluated lymphatic and venous invasion separately (but not in the prostate) reported that venous invasion is a risk factor for distant metastasis (48, 49). Unfortunately, studies analyzing only venous invasion in prostate cancer are scarce, and further long-term studies are required to elucidate its significance.

It is worth mentioning that seminal vesicle invasion was also an independent risk factor for lymph node metastasis. This could be owing to the anatomy of the seminal vesicle or its proximity to the prostate. The area surrounding the seminal vesicle is rich with lymphatic vessels (4.1 mm^2) (50). In contrast, the lymphatic vessel density in a normal prostate is approximately 1.58 mm^2 (51). In fact, the lymphatic invasion rate is significantly higher in patients with seminal vesicle invasion than in those without seminal vesicle invasion. In this study, it was approximately five times greater (**Table 5**). It is possible that cancer cells that invade the seminal vesicles may be more directly related to the lymphatic pathway owing to the high density of lymphatic vessels in the area.

EPE was also an independent risk factor for lymph node metastasis. However, we did not observe a significant relationship between EPE and lymphatic invasion in this study. Though we precisely evaluated lymphatic invasion with HE staining, supported by D2-40 immunohistochemistry, there could have been lymphatic invasion that was not detectable microscopically (52). In addition, cases with EPE had approximately two times the total incidence of BCR even in the short period of time in this study. However, multivariate analysis of this study showed that EPE was not an independent significant factor for BCR. To better understand these observations, further analysis, preferably molecular analysis, is required.

Further discussion is warranted regarding the relationship between GG and other parameters. Our analysis established that, in general, as the GG increased, the positive rates of various pathological evaluation parameters increased. However, a detailed examination of the mean values and detection rates of the various evaluation parameters for each GG confirmed the differences between the parameters. Thus, we would like to discuss the various parameters in terms of the statistical analysis results. At first, in addition to the routine examination of HE-stained specimens, we conducted an additional re-evaluation of HE staining and immunohistochemistry with D2-40 or CD31 for representative sections and precisely evaluated the vessel invasions. D2-40 is reported to also stain cells other than those of the lymphatic endothelium (22) and CD31 also faintly stains lymphatic vessels; therefore, it is essential to ensure that both D2-40 and CD31 immunohistochemistry are conducted with HE staining. Our precise differential evaluation of lymphatic and venous invasions confirmed that lymphatic invasion was positively associated with lymph node metastasis and extraprostatic extension. Perineural invasion was positive in most cases, but its value for evaluation is questionable. Semi-

quantitative methods of evaluation, such as infiltration severity could improve the value, but further verification is required. From GG2 to GG4, positive surgical margins were observed in about one-third of cases, and in GG5, positive surgical margins were observed in more than two-thirds of cases. Thus, the positive surgical margins in GG5 were significantly higher than in cases up to GG4. As a matter of concern, the rate of positive surgical margins was lower in 2020 than in 2019, although not significantly different. Therefore, we must follow the progress carefully, including the rate of positive surgical margins in the future. Seminal vesicle invasion was rarely observed in GG4 and below, but similar to the findings for EPE, the frequency was significantly elevated in GG5 cases. Cases of GG5 seemed to be an apparently malignant disease compared with cases of GG4. The incidence of tertiary Gleason pattern 5 was significantly higher in GG3 than in GG2, while the incidence in GG4 was relatively lower than that in GG3. When the amount of pattern 5 exceeds 5%, the pattern 5 was not considered as the tertiary component but included in the grade. The higher grade tumors tend to have larger amounts of pattern 5 >5%, which might be the reason for the relatively low incidence of tertiary Gleason pattern 5 in GG4 cases in this study. IDC-P is a poor prognostic factor in prostate cancer (8), and it was observed at a frequency of about one-fifth even in GG3 cases. Therefore, in cases of GG3 and above, immunohistochemical analysis using PIN4 or other methods should actively be performed when there is a suspicious site in the routine diagnosis using HE staining. The continuous variables, PSA and tumor diameter, were significantly higher in GG5 than in other groups. In contrast, there were no significant differences in any variables up to GG4. This might be because the present statistical analysis was limited to patients who were judged as operable. Nevertheless, we once more wish to state the limitations of this study. The study includes cases of radical prostatectomy, which were performed after January 2019. Therefore, the maximum follow-up period is approximately 2.5 years. The short follow-up duration is a limitation of this study. Further follow-up is required for analysis of biochemical and clinical recurrence, metastasis, and prognosis. Furthermore, accumulation of morphological analysis is also necessary.

In conclusion, this study elucidated the risk factors for BCR and lymph node metastasis in patients who underwent RARP using detailed morphological and immunohistochemical analyses, and found that the independent risk factors for BCR were GG and tumor diameter, while the independent risk factors for lymph node metastasis were lymphatic and seminal vesicle invasion and the presence of EPE. Additionally, the study successfully characterized the status of various parameters for each GG in prostate cancer. As GG increased, various parameters could be easily visualized. Compared with other groups, the GG5 group exhibited higher frequencies of various parameters for disease progression. Furthermore, these results have identified the assessment parameters for each GG as well as the differences in the biological malignancy of GG5. Further investigation of the differences between GG5 and other groups regarding various aspects (including morphological analyses) may provide the basis for delineating some of the malignant features of prostate cancer.

DATA AVAILABILITY STATEMENT

The raw data supporting the conclusions of this article will be made available by the authors, without undue reservation.

ETHICS STATEMENT

The studies involving human participants were reviewed and approved by Ethics Review Committee of the Kanagawa Cancer Center (Approval Number: 2019-36). The patients/participants provided their written informed consent to participate in this study.

AUTHOR CONTRIBUTIONS

YO diagnosed RARP specimens, collected the parameters, performed the statistical analysis, and wrote the manuscript. SS diagnosed RARP specimens and discussed the GG with YO and YM. KO was the primary operator of the RARP procedure, mentored other urologists, and provided YO with the clinical information in this study. YY provided information on preoperative imaging findings to YO. TS actively performed the RARP surgery together with KO and provided YO with clinical information in this study. AI confirmed the presence of BCR, date of diagnosis of the BCR, and serum PSA level from the medical records during the manuscript revision. AI also reviewed the specimens with YO and participated in the morphological examinations. EY, MS, KW, and TY diagnosed some of the preoperative biopsies and provided that information to YO. In addition, they revise this article from the perspective of a pathologist. TK, as head of the urologist department, provided clinical information to YO and revise parts of the manuscript. YM reviewed and reassessed the specimens and revised the manuscript as the senior pathologist. All authors contributed to the article and approved the submitted version.

FUNDING

This work was supported by JSPS KAKENHI (grant number: JP17K08713 to YO, 20K09422 to SS, 20K16210 to KW, 18K15111 to MS, 20K09093 to YM) from the Ministry of Education, Culture, Sports, Science, and Technology of Japan and by Kanagawa Cancer Center and Research Institute/ Kanagawa Prefectural Hospital Organization (grant number: 2020-4/2021-1 to YO).

ACKNOWLEDGMENTS

We would like to thank Sachie Osanai and Mitsuyo Yoshihara for their excellent technical support. We also wish to thank Editage (www.editage.jp) for English language editing.

REFERENCES

1. Bou-Dargham MJ, Sha L, Sang QA, Zhang J. Immune Landscape of Human Prostate Cancer: Immune Evasion Mechanisms and Biomarkers for Personalized Immunotherapy. *BMC Cancer* (2020) 20(1):572. doi: 10.1186/s12885-020-07058-y
2. van Leenders G, van der Kwast TH, Grignon DJ, Evans AJ, Kristiansen G, Kweldam CF, et al. The 2019 International Society of Urological Pathology (ISUP) Consensus Conference on Grading of Prostatic Carcinoma. *Am J Surg Pathol* (2020) 44(8):e87–99. doi: 10.1097/PAS.0000000000001497
3. Taguchi S, Uemura Y, Fujimura T, Morikawa T, Naito A, Kawai T, et al. Quantification of the Individual Risk of Each Gleason Pattern, Including Tertiary Gleason Pattern 5, After Radical Prostatectomy: Development of the Modified Gleason Grade Grouping (mGGG) Model. *BMC Cancer* (2020) 20(1):371. doi: 10.1186/s12885-020-06880-8
4. Okubo Y, Nukada S, Shibata Y, Osaka K, Yoshioka E, Suzuki M, et al. Primary Solitary Fibrous Tumour of the Prostate: A Case Report and Literature Review. *Malays J Pathol* (2020) 42(3):449–53.
5. Han HH, Park JW, Na JC, Chung BH, Kim CS, Ko WJ. Epidemiology of Prostate Cancer in South Korea. *Prostate Int* (2015) 3(3):99–102. doi: 10.1016/j.prnil.2015.06.003
6. Sawada N. Risk and Preventive Factors for Prostate Cancer in Japan: The Japan Public Health Center-Based Prospective (JPHC) Study. *J Epidemiol* (2017) 27(1):2–7. doi: 10.1016/j.je.2016.09.001
7. H Moch, P Humphrey, TM Ulbright, VE Reuter eds. *WHO Classification of Tumours of Urinary System & Male Genital Organs. 4th Edition*. Lyon, France: World Health Organization (2016).
8. Gillessen S, Attard G, Beer TM, Beltran H, Bjartell A, Bossi A, et al. Management of Patients With Advanced Prostate Cancer: Report of the Advanced Prostate Cancer Consensus Conference 2019. *Eur Urol* (2020) 77(4):508–47. doi: 10.1016/j.eururo.2020.01.012
9. Zhao F, Yu X, Xu M, Ye S, Zang S, Zhong W, et al. Mucinous Prostate Cancer Shows Similar Prognosis to Typical Prostate Acinar Carcinoma: A Large Population-Based and Propensity Score-Matched Study. *Front Oncol* (2019) 9:1467. doi: 10.3389/fonc.2019.01467
10. Grignon DJ. Prostate Cancer Reporting and Staging: Needle Biopsy and Radical Prostatectomy Specimens. *Mod Pathol* (2018) 31(S1):S96–109. doi: 10.1038/modpathol.2017.167
11. Xu N, Ke ZB, Chen YH, Wu YP, Chen SH, Wei Y, et al. Risk Factors for Pathologically Confirmed Lymph Nodes Metastasis in Patients With Clinical T2N0M0 Stage Prostate Cancer. *Front Oncol* (2020) 10:1547. doi: 10.3389/fonc.2020.01547
12. Shieh AC, Guler E, Ojili V, Paspulati RM, Elliott R, Ramaiya NH, et al. Extraprostatic Extension in Prostate Cancer: Primer for Radiologists. *Abdom Radiol (NY)* (2020) 45(12):4040–51. doi: 10.1007/s00261-020-02555-x
13. Divatia MK, Ro JY. Intraductal Carcinoma of the Prostate Gland: Recent Advances. *Yonsei Med J* (2016) 57(5):1054–62. doi: 10.3349/ymj.2016.57.5.1054
14. Hashimoto T, Nakashima J, Inoue R, Komori O, Yamaguchi Y, Kashima T, et al. The Significance of Micro-Lymphatic Invasion and Pathological Gleason Score in Prostate Cancer Patients With Pathologically Organ-Confined Disease and Negative Surgical Margins After Robot-Assisted Radical Prostatectomy. *Int J Clin Oncol* (2020) 25(2):377–83. doi: 10.1007/s10147-019-01561-4
15. Wilczak W, Wittmer C, Clauditz T, Minner S, Steurer S, Buscheck F, et al. Marked Prognostic Impact of Minimal Lymphatic Tumor Spread in Prostate Cancer. *Eur Urol* (2018) 74(3):376–86. doi: 10.1016/j.eururo.2018.05.034
16. Ploussard G, Briganti A, de la Taille A, Haese A, Heidenreich A, Menon M, et al. Pelvic Lymph Node Dissection During Robot-Assisted Radical Prostatectomy: Efficacy, Limitations, and Complications-a Systematic Review of the Literature. *Eur Urol* (2014) 65(1):7–16. doi: 10.1016/j.eururo.2013.03.057
17. Saika T, Miura N, Fukumoto T, Yanagihara Y, Miyauchi Y, Kikugawa T. Role of Robot-Assisted Radical Prostatectomy in Locally Advanced Prostate Cancer. *Int J Urol* (2018) 25(1):30–5. doi: 10.1111/iju.13441
18. Fossati N, Willemse PM, Van den Broeck T, van den Bergh RCN, Yuan CY, Briers E, et al. The Benefits and Harms of Different Extents of Lymph Node Dissection During Radical Prostatectomy for Prostate Cancer: A Systematic Review. *Eur Urol* (2017) 72(1):84–109. doi: 10.1016/j.eururo.2016.12.003
19. Epstein JI, Egevad L, Amin MB, Delahunt B, Srigley JR, Humphrey PA, et al. The 2014 International Society of Urological Pathology (ISUP) Consensus Conference on Gleason Grading of Prostatic Carcinoma: Definition of Grading Patterns and Proposal for a New Grading System. *Am J Surg Pathol* (2016) 40(2):244–52. doi: 10.1097/PAS.0000000000000530
20. Kweldam CF, van Leenders GJ, van der Kwast T. Grading of Prostate Cancer: A Work in Progress. *Histopathology* (2019) 74(1):146–60. doi: 10.1111/his.13767
21. Samaratunga H, Montironi R, True L, Epstein JI, Griffiths DF, Humphrey PA, et al. International Society of Urological Pathology (ISUP) Consensus Conference on Handling and Staging of Radical Prostatectomy Specimens. Working Group 1: Specimen Handling. *Mod Pathol* (2011) 24(1):6–15. doi: 10.1038/modpathol.2010.178
22. Kanner WA, Galgano MT, Atkins KA. Podoplanin Expression in Basal and Myoepithelial Cells: Utility and Potential Pitfalls. *Appl Immunohistochem Mol Morphol* (2010) 18(3):226–30. doi: 10.1097/PAI.0b013e3181c65141
23. Zareba P, Flavin R, Isikbay M, Rider JR, Gerke TA, Finn S, et al. Perineural Invasion and Risk of Lethal Prostate Cancer. *Cancer Epidemiol Biomarkers Prev* (2017) 26(5):719–26. doi: 10.1158/1055-9965.EPI-16-0237
24. Srigley JR. Key Issues in Handling and Reporting Radical Prostatectomy Specimens. *Arch Pathol Lab Med* (2006) 130(3):303–17. doi: 10.5858/2006-130-303-KIIHAR
25. Magi-Galluzzi C, Evans AJ, Delahunt B, Epstein JI, Griffiths DF, van der Kwast TH, et al. International Society of Urological Pathology (ISUP) Consensus Conference on Handling and Staging of Radical Prostatectomy Specimens. Working Group 3: Extraprostatic Extension, Lymphovascular Invasion and Locally Advanced Disease. *Mod Pathol* (2011) 24(1):26–38. doi: 10.1038/modpathol.2010.158
26. Epstein JI, Partin AW, Potter SR, Walsh PC. Adenocarcinoma of the Prostate Invading the Seminal Vesicle: Prognostic Stratification Based on Pathologic Parameters. *Urology* (2000) 56(2):283–8. doi: 10.1016/s0090-4295(00)00640-3
27. Rehman A, El-Zaatari ZM, Han SH, Shen SS, Ayala AG, Miles B, et al. Seminal Vesicle Invasion Combined With Extraprostatic Extension is Associated With Higher Frequency of Biochemical Recurrence and Lymph Node Metastasis Than Seminal Vesicle Invasion Alone: Proposal for Further Pt3 Prostate Cancer Subclassification. *Ann Diagn Pathol* (2020) 49:151611. doi: 10.1016/j.anndiagpath.2020.151611
28. Zhou M. High-Grade Prostatic Intraepithelial Neoplasia, PIN-Like Carcinoma, Ductal Carcinoma, and Intraductal Carcinoma of the Prostate. *Mod Pathol* (2018) 31(S1):S71–9. doi: 10.1038/modpathol.2017.138
29. Varma M, Delahunt B, Egevad L, Samaratunga H, Kristiansen G. Intraductal Carcinoma of the Prostate: A Critical Re-Appraisal. *Virchows Arch* (2019) 474(5):525–34. doi: 10.1007/s00428-019-02544-6
30. Taguchi S, Morikawa T, Shibahara J, Fukuhara H. Prognostic Significance of Tertiary Gleason Pattern in the Contemporary Era of Gleason Grade Grouping: A Narrative Review. *Int J Urol* (2021) 26(6):614–21. doi: 10.1111/iju.14524
31. Cookson MS, Aus G, Burnett AL, Canby-Hagino ED, D'Amico AV, Dmochowski RR, et al. Variation in the Definition of Biochemical Recurrence in Patients Treated for Localized Prostate Cancer: The American Urological Association Prostate Guidelines for Localized Prostate Cancer Update Panel Report and Recommendations for a Standard in the Reporting of Surgical Outcomes. *J Urol* (2007) 177(2):540–5. doi: 10.1016/j.juro.2006.10.097
32. Cornford P, Bellmunt J, Bolla M, Briers E, De Santis M, Gross T, et al. EAU-ESTRO-SIOG Guidelines on Prostate Cancer. Part II: Treatment of Relapsing, Metastatic, and Castration-Resistant Prostate Cancer. *Eur Urol* (2017) 71(4):630–42. doi: 10.1016/j.eururo.2016.08.002
33. Soeterik TFW, Hueting TA, Israel B, van Melick HHE, Dijksman LM, Stomps S, et al. External Validation of the MSKCC and Briganti Nomograms For Prediction of Lymph Node Involvement of Prostate Cancer Using Clinical Stage Assessed by Magnetic Resonance Imaging. *BJU Int* (2021). doi: 10.1111/bju.15376
34. Salomon L, Anastasiadis AG, Johnson CW, McKiernan JM, Goluboff ET, Abbou CC, et al. Seminal Vesicle Involvement After Radical Prostatectomy: Predicting Risk Factors for Progression. *Urology* (2003) 62(2):304–9. doi: 10.1016/s0090-4295(03)00373-x
35. Carlsson SV, Tafe LJ, Chade DC, Sjoberg DD, Passoni N, Shariat SF, et al. Pathological Features of Lymph Node Metastasis for Predicting Biochemical Recurrence After Radical Prostatectomy for Prostate Cancer. *J Urol* (2013) 189(4):1314–8. doi: 10.1016/j.juro.2012.10.027

36. Fajkovic H, Mathieu R, Lucca I, Hiess M, Hubner N, Al Hussein Al Awamlh B, et al. Validation of Lymphovascular Invasion Is an Independent Prognostic Factor for Biochemical Recurrence After Radical Prostatectomy. *Urol Oncol* (2016) 34(5):233 e1–6. doi: 10.1016/j.urolonc.2015.10.013
37. Swanson GP, Chen W, Trevathan S, Hermans M. Long-Term Follow-Up After Prostatectomy for Prostate Cancer and the Need for Active Monitoring. *Prostate Cancer* (2020) 2020:7196189. doi: 10.1155/2020/7196189
38. Zhang L, Wu B, Zha Z, Zhao H, Jiang Y, Yuan J. Positive Surgical Margin is Associated With Biochemical Recurrence Risk Following Radical Prostatectomy: A Meta-Analysis From High-Quality Retrospective Cohort Studies. *World J Surg Oncol* (2018) 16(1):124. doi: 10.1186/s12957-018-1433-3
39. Park SW, Readal N, Jeong BC, Humphreys EB, Epstein JI, Partin AW, et al. Risk Factors for Intraprostatic Incision Into Malignant Glands at Radical Prostatectomy. *Eur Urol* (2015) 68(2):311–6. doi: 10.1016/j.eururo.2014.07.012
40. Hassan O, Matoso A. Clinical Significance of Subtypes of Gleason Pattern 4 Prostate Cancer. *Transl Androl Urol* (2018) 7(Suppl 4):S477–83. doi: 10.21037/tau.2018.02.06
41. Zheng QS, Chen SH, Wu YP, Chen HJ, Chen H, Wei Y, et al. Increased Paxillin Expression in Prostate Cancer Is Associated With Advanced Pathological Features, Lymph Node Metastases and Biochemical Recurrence. *J Cancer* (2018) 9(6):959–67. doi: 10.7150/jca.22787
42. Lopez-Colome AM, Lee-Rivera I, Benavides-Hidalgo R, Lopez E. Paxillin: A Crossroad in Pathological Cell Migration. *J Hematol Oncol* (2017) 10(1):50. doi: 10.1186/s13045-017-0418-y
43. Kweldam CF, van der Kwast T, van Leenders GJ. On Cribriform Prostate Cancer. *Transl Androl Urol* (2018) 7(1):145–54. doi: 10.21037/tau.2017.12.33
44. Hollemans E, Verhoef EI, Bangma CH, Rietbergen J, Osanto S, Pelger RCM, et al. Cribriform Architecture in Radical Prostatectomies Predicts Oncological Outcome in Gleason Score 8 Prostate Cancer Patients. *Mod Pathol* (2021) 34 (1):184–93. doi: 10.1038/s41379-020-0625-x
45. Iczkowski KA, van Leenders G, Tarima S, Wu R, van der Kwast T, Berney DM, et al. Cribriform Prostate Cancer: Morphologic Criteria Enabling a Diagnosis, Based on Survey of Experts. *Ann Diagn Pathol* (2021) 52:151733. doi: 10.1016/j.anndiagpath.2021.151733
46. Culp MB, Soerjomataram I, Efstathiou JA, Bray F, Jemal A. Recent Global Patterns in Prostate Cancer Incidence and Mortality Rates. *Eur Urol* (2020) 77 (1):38–52. doi: 10.1016/j.eururo.2019.08.005
47. Nukada S, Okubo Y, Shiozawa M, Yoshioka E, Suzuki M, Washimi K, et al. Signet-Ring Cell Carcinoma Component as an Indicator of Anaplastic Lymphoma Kinase Mutations in Colorectal Cancer. *J Anus Rectum Colon* (2021) 5(2):167–72. doi: 10.23922/jarc.2020-068
48. Okubo Y, Sakai M, Yamazaki H, Sugawara Y, Samejima J, Yoshioka E, et al. Histopathological Study of Carcinoma Showing Thymus-Like Differentiation (CASTLE). *Malays J Pathol* (2020) 42(2):259–65.
49. Fujii T, Sutoh T, Morita H, Yajima R, Yamaguchi S, Tsutsumi S, et al. Vascular Invasion, But Not Lymphatic Invasion, of the Primary Tumor is a Strong Prognostic Factor in Patients With Colorectal Cancer. *Anticancer Res* (2014) 34(6):3147–51.
50. Yudai O, Nobuyuki H, Gen M, Yukari B, Kei K, Ahmed A, et al. Aspects of Lymphatic Vessel Configuration of the Human Male Urinary Bladder and Adjacent Organs: A Histological Basis for Understanding the Spread of Cancer Metastases. *Transl Res Anat* (2018) 11:10–7. doi: 10.1016/j.tria.2018.05.001
51. Roma AA, Magi-Galluzzi C, Kral MA, Jin TT, Klein EA, Zhou M. Peritumoral Lymphatic Invasion is Associated With Regional Lymph Node Metastases in Prostate Adenocarcinoma. *Mod Pathol* (2006) 19(3):392–8. doi: 10.1038/modpathol.3800546
52. Aleskandarany MA, Sonbul SN, Mukherjee A, Rakha EA. Molecular Mechanisms Underlying Lymphovascular Invasion in Invasive Breast Cancer. *Pathobiology* (2015) 82(3-4):113–23. doi: 10.1159/000433583

Conflict of Interest: The authors declare that the research was conducted in the absence of any commercial or financial relationships that could be construed as a potential conflict of interest.

frontiers in Oncology

ORIGINAL RESEARCH
published: 23 August 2021
doi: 10.3389/fonc.2021.718644

N6-Methyladenosine Writer Gene ZC3H13 Predicts Immune Phenotype and Therapeutic Opportunities in Kidney Renal Clear Cell Carcinoma

Tao Guo[1], Hongxiang Duan[2], Jinbo Chen[1], Jinhui Liu[1], Belaydi Othmane[1], Jiao Hu[1], Huihuang Li[1] and Xiongbing Zu[1]**

[1] Department of Urology, Xiangya Hospital, Central South University, Changsha, China, [2] School of Computer Science and Engineering, Central South University, Changsha, China

OPEN ACCESS

Edited by:
Benyi Li,
University of Kansas Medical Center, United States

Reviewed by:
Shuheng Bai,
The First Affiliated Hospital of Xi'an Jiaotong University, China
Hailin Tang,
Sun Yat-sen University Cancer Center (SYSUCC), China

****Correspondence:***
Xiongbing Zu
zuxbxyyy@126.com
Huihuang Li
lhhuang1994@163.com

Specialty section:
This article was submitted to Genitourinary Oncology, a section of the journal Frontiers in Oncology

Received: *01 June 2021*
Accepted: *05 August 2021*
Published: *23 August 2021*

Citation:
Guo T, Duan H, Chen J, Liu J, Othmane B, Hu J, Li H and Zu X (2021) N6-Methyladenosine Writer Gene ZC3H13 Predicts Immune Phenotype and Therapeutic Opportunities in Kidney Renal Clear Cell Carcinoma. Front. Oncol. 11:718644. doi: 10.3389/fonc.2021.718644

Background: Although the RNA modification N6-methyladenosine ZC3H13 has been found to play vital regulatory roles in many types of cancers, its role in predicting the tumor immune microenvironment (TME) and response to immune checkpoint blockade (ICB) in kidney renal clear cell carcinoma (KIRC) remains unclear.

Methods: We comprehensively analyzed the expression, prognostic significance and immunological role of ZC3H13 in pan-cancers and systematically correlated ZC3H13 with TME cell-infiltration, ICB response and targeted therapy in KIRC. The data were collected from The Cancer Genome Atlas (TCGA), Gene Expression Omnibus (GEO), Genotype-Tissue Expression (GTEx), Broad Institute Cancer Cell Line Encyclopedia (CCLE) and DrugBank database. Also, we performed RNA sequencing (RNA-seq) of 46 renal cell carcinoma tissues and 11 adjacent normal tissues to validate our result. All analyses were implemented using R software, version 3.6.3.

Results: ZC3H13 was significantly differentially expressed in most tumors. However, its expression profiles and prognostic significance were consistent only in KIRC, regardless of overall survival, progression-free survival and cancer-specific survival. Additionally, ZC3H13 expression was correlated with clinicopathological factors in KIRC. Furthermore, we found that ZC3H13 might shape a noninflamed phenotype and could predict a lower response to ICB in KIRC. These results could be validated in our own RNA-seq data. Tumor mutation burden (TMB) was significantly higher in the low ZC3H13 group. Finally, we found that ZC3H13 could predict the sensitivity of targeted therapy for KIRC.

Conclusions: ZC3H13 might shape a noninflamed phenotype in KIRC. Moreover, ZC3H13 could predict the prognosis and clinical response of ICB and the sensitivity to targeted therapies in KIRC.

Keywords: ZC3H13, RNA modification N6-methyladenosine, kidney renal clear cell carcinoma, tumor immune microenvironment, immunotherapy

BACKGROUND

Kidney renal clear cell carcinoma (KIRC) is one of the most common cancers of the urinary system (1). The prognosis of early-stage KIRC is favorable, while advanced KIRC is associated with an extremely poor prognosis. Targeted therapy is the most important treatment option for advanced KIRC, but improvements in its efficacy has encountered bottlenecks in recent years (1). With the development of anticancer immune checkpoint blockade (ICB), an increasing number of clinical trials have suggested that KIRC is sensitive to ICB (2–4). ICB can significantly improve the overall survival of patients who are resistant to targeted therapy. Therefore, ICB has also become an important treatment option for advanced KIRC. However, similar to other treatment options, only a portion of patients are sensitive to ICB treatment (5). It is vital to find reliable predictors of ICB efficacy considering the economic burden and fatal side effects.

RNA modification of N6-methyladenosine (m6A) is the most prominent and abundant RNA modification pattern in eukaryotic cells (6). An increasing number of studies have shown that m6A has an important regulatory role in tumor immune regulation and ICB resistance (7). ZC3H13 (zinc finger CCCH domain-containing protein 13) is an m6A writer gene. ZC3H13 is a potential regulator of nuclear RNA m6A methylation and mouse embryonic stem cell self-renewal (8). The role of ZC3H13 in carcinomas is still not clear. It has been reported that ZC3H13 could serve as a tumor suppressor gene that inhibits the proliferation of colon cancer cells by inhibiting the RAS-ERK pathway (9). However, some studies have shown that ZC3H13 could act as an oncogene to activate the NF-kB signaling pathway to promote tumor proliferation and invasion (10, 11). Currently, there are no studies elaborating the role of ZC3H13 in KIRC, especially its relationship with tumor immune characteristics.

In this study, we first explored the expression pattern and prognostic value of ZC3H13 in pan-cancers and its relationship with immune characteristics through pan-cancer analysis. Next, we performed synthetic analysis and then focused on KIRC. Finally, we further explored the predictive value of ZC3H13 for immune phenotypes and therapeutic sensitivities in KIRC.

Abbreviations: TME, tumor immune microenvironment; ICB, immune checkpoint blockade; KIRC, kidney renal clear cell carcinoma; TMB, tumor mutation burden; m6A, RNA modification of N6-methyladenosine; ZC3H13, zinc finger CCCH domain-containing protein 13; TPM, transcripts per kilobase million; MSI, microsatellite instability; DEG, differentially expressed genes; GO, Gene Ontology; KEGG, Kyoto Encyclopedia of Genes and Genomes; TIIC, tumor-infiltrating immune cell; EMT, epithelial-mesenchymal transition; BLCA, bladder urothelial carcinoma; BRCA, breast invasive carcinoma; CESC, cervical squamous cell carcinoma and endocervical adenocarcinoma; CHOL, cholangiocarcinoma; ESCA, esophageal carcinoma; SKCM, skin cutaneous melanoma; KIRP, kidney renal papillary cell carcinoma; PRAD, prostate adenocarcinoma; THYM, thymoma; OS, overall survival; PFS, progression-free survival; CSS, cancer-specific survival; ICI, immune checkpoint inhibitor; MDSC, myeloid-derived suppressor cell; NK, natural killer cell; Th, helper T cell; Treg, regulatory T cell; EMT, epithelial–mesenchymal transition; Pan-F-TBRS, panfibroblast TGF-b response signature; MANTIS, microsatellite analysis for normal-tumor instability.

METHODS

Data Retrieval and Preprocessing

The R package "TCGAbiolinks" was used to download the RNA sequencing data (FPKM values) and clinical data of TCGA-KIRC from the Genomic Data Commons (GDC, https://portal.gdc.cancer.gov/) (12). Then, we transformed the FPKM values into transcripts per kilobase million (TPM) values. The pan-cancer RNA sequencing data (FPKM values), somatic mutation data, and survival information were downloaded from the UCSC Xena data portal (https://xenabrowser.net) (13). The TMB data was calculated by using VarScan2. The microsatellite instability (MSI) data were collected from the supplementary files of Bonneville's study (14). In addition, we also downloaded the RNA sequencing data of normal tissues in the GTEx (https://www.gtexportal.org/home/) database and the RNA sequencing data of cancer cells in the CCLE (https://portals.broadinstitute.org/ccle) database. To compare the drug sensitivities between different ZC3H13-expression groups, we collected common anticancer drugs and their target genes from the DrugBank database (www.drugbank.ca). The expression matrix of GSE53757 (15) was downloaded using the "GEOquery" package and then transformed gene symbols using GPL570. Single-cell RNA-seq (scRNA-seq) data of six adjacent normal tissues was downloaded from the supplementary file of GSE159115 (16). Main clinical information of the included cohorts was summarized in **Supplementary Table 1**. Also, we summarized the clinicopathological characteristics of TCGA-KIRC patients according to the expression of ZC3H13 in **Supplementary Table 2**.

Analysis Procedures of scRNA-seq

Following the guide reported by Luecken et al. (17), we used the "Seurat" v4.0.1 package to analyze and visualize scRNA-seq data. For quality control, we filtered out the data with unique molecular identifiers (UMIs) fewer than 500, or fewer than 250 genes, or mitochondrial ratio more than 0.20. Then, we normalized and checked the cell cycle phase based on the filtered data. We chose the top 2000 variable genes to create anchors using the "FindIntegrationAnchors" function and integrated the six data into a new matrix using the "IntegrateData" function. After integration, we run principal component analysis (PCA) and chose the top 40 PCs to run UMAP. Finally, we visualized the clusters with the resolution set as 0.8 and annotated the clusters using HumanPrimaryCellAtlasData() based on the "SingleR" package.

Functional Analysis of the High and Low ZC3H13 Groups

First, the empirical Bayesian algorithm in the R package "limma" was used to identify the differentially expressed genes (DEGs) between the high and low ZC3H13 groups. Adjusted P value < 0.05 and $|\log FC| > 1$ were set as the significance criteria for significant DEGs. Then, Gene Ontology (GO) and Kyoto Encyclopedia of Genes and Genomes (KEGG) analyses were performed by using the "ClusterProfiler" R package based on the DEGs. In addition, we collected 50 hallmark pathways that could represent most of the biological functional pathways from the

MSigDB database (18). Finally, we calculated the enrichment scores of these pathways in each sample by using the ssGSEA algorithm.

Depicting the Tumor Immune Microenvironment of KIRC

The tumor microenvironment includes tumor cells, tumor-infiltrating immune cells (TIICs), stromal cells and a series of tumor-related regulatory factors. Here, we conducted a comprehensive analysis of immune-related factors in the tumor microenvironment. First, we described the seven main steps of the antitumor immune response in the KIRC tumor microenvironment, including the release and presentation of cancer cell antigens (Steps 1 and 2), priming and activation of the immune system (Step 3), trafficking and infiltration of immune cells into tumors (Steps 4 and 5), and recognition and killing of cancer cells by T cells (Steps 6 and 7) (19). These seven steps were called cancer-immunity cycle. The vitality of these steps, which determines the direction of the antitumor immune response process in the tumor microenvironment and affects the level of infiltration of TIICs, was downloaded from the TIP (Tracking Tumor Immunophenotype) (http://biocc.hrbmu.edu.cn/TIP/) (20). The TIP is a meta-server using the ssGSEA and CIBERSORT algorithm based on specific marker gene sets (**Supplementary Table 3**), which can analyze the level of anti-cancer immunity (20). Furthermore, we calculated the infiltration level of these 22 immune cells using the ssGSEA algorithm based on the specific marker gene sets (**Supplementary Table 4**) (21).

Calculating the Enrichment Scores of Immunotherapy Response Signatures and Stroma Signatures

Mariathsan et al. identified 19 ICB response-related gene signatures, including 18 positive signatures (such as DNA replication, Fanconi_anemia_pathway, Homologous_recombination, MicroRNAs_in_cancer, Mismatch_repair, Nucleotide_excision_repair, Oocyte_meiosis, p53_signaling_pathway, Progesterone_mediated_oocyte_maturation) and 1 negative signature (Cytokine_cytokine_receptor_interaction) (**Supplementary Table 5**) (22). In addition, we identified four stromal pathways with immunosuppressive effects from previous literature, including epithelial-mesenchymal transition (EMT) markers and the pan-fibroblast TGF-b response signature (Pan-FTBRS) (22). The ssGSEA algorithm was used to calculate the enrichment score of these signatures in individuals.

RNA Sequencing of Renal Cell Carcinoma Samples

Forty-seven renal cell carcinoma tissues and thirteen adjacent normal tissues stored in liquid nitrogen were collected from our hospital. We called it Xiangya cohort. All the clinicopathological data of the patients were included and summarized in **Supplementary Table 6**. Total RNA was extracted from the samples using Trizol (Invitrogen, Carlsbad, CA, USA) according to the manufacturer's instructions. Then, the quality of RNA was evaluated using NanoDrop and Agilent 2100 bioanalyzer (Thermo Fisher Scientific, MA, USA). We next constructed the mRNA library. The RNA was purified using Oligo(dT)-attached magnetic beads and then fragmented into small pieces. Random hexamer-primed reverse transcription was used to generate the first and second-strand cDNA. After adding A-Tailing Mix and RNA Index Adapters by incubating to end repair, the obtained cDNA was amplified by PCR and purified by Ampure XP Beads. The double-stranded PCR products were heated, denatured and circularized by the splint oligo sequence to get the final library. There were 46 qualified renal cell carcinoma tissues among the 47 samples and 11 qualified adjacent normal tissues among the 13 samples. Finally, the qualified samples were sequenced on a BGISEQ-500 platform (BGI-Shenzhen, China). The gene expression levels were calculated using RSEM (v1.2.12).

Statistical Analysis

For the continuous variables, Pearson or Spearman coefficients were used to explore pairwise correlations. The median ZC3H13 expression (30.25) was applied as a cutoff value. Then, the cohort was classified into high and low ZC3H13 groups. The t-test was applied to analyze the difference between groups for variables with a normal distribution. Otherwise, the Mann-Whitney U test was applied. The Kaplan-Meier method was used to plot the survival curves for prognostic analyses, and the log-rank test was applied to estimate the statistical significance. $P < 0.05$ indicated a significant difference. All statistical tests were two-sided. Finally, all statistical data analyses were implemented using R software, version 3.6.3 (http://www.r-project.org).

RESULTS

Expression Profiles of ZC3H13 in Pan-Cancers

We found that ZC3H13 was significantly differentially expressed in most tumors by comprehensively analyzing the expression data from the TCGA and GTEx databases (**Supplementary Figures 1A, B**). This indicated that ZC3H13 may be closely related to the occurrence and development of tumors. However, it is worth noting that ZC3H13 had significantly different expression in different tumors, and its expression might depend on the different types of tumors and the heterogeneity of the tumors. For example, the expression of ZC3H13 was significantly lower in tumor tissues than in adjacent normal tissues in KIRC, bladder urothelial carcinoma (BLCA), breast invasive carcinoma (BRCA), cervical squamous cell carcinoma and endocervical adenocarcinoma (CESC) etc. In contrast, the expression of ZC3H13 was significantly higher in the tumor tissues in cholangiocarcinoma (CHOL), esophageal carcinoma (ESCA), skin cutaneous melanoma (SKCM) etc. For KIRC, TCGA combined with GTEx also indicated that ZC3H13 was significantly lower in tumor tissues (**Supplementary Figure 1B**). In addition, **Supplementary Figure 1C** shows the expression level of ZC3H13 in various normal tissues in the GTEx database. We found that ZC3H13 had the lowest expression level in blood, which indicated that as a target for drug therapy, ZC3H13 might

have low blood system toxicity and side effects. Finally, we also explored the expression of ZC3H13 in each tumor cell line in the CCLE database as shown in **Supplementary Figure 1D**.

Prognostic Significance and Immunological Role of ZC3H13 in Pan-Cancers

The differential expression patterns of ZC3H13 in pan-cancers prompted us to explore its prognostic value. Therefore, we performed survival analyses in pan-cancers in terms of overall survival (OS), progression-free survival (PFS) and cancer-specific survival (CSS) by using the Cox regression model, Kaplan-Meier analysis and log-rank test. For OS, high expression of ZC3H13 was associated with favorable prognosis in KIRC and poor prognosis in CESC (**Supplementary Figure 2**). For PFS, high expression of ZC3H13 was also associated with favorable prognosis in KIRC, kidney renal papillary cell carcinoma (KIRP) and prostate adenocarcinoma (PRAD) and poor prognosis in CESC (**Supplementary Figure 3**). Similarly, for CSS, high expression of ZC3H13 was still associated with favorable prognosis in KIRC, KIRP, and thymoma (THYM) and poor prognosis in CESC (**Supplementary Figure 4**). There is clear heterogeneity in the prognostic value of ZC3H13 in different tumors. In CESC, high expression of ZC3H13 was associated with poor prognosis regardless of OS, PFS or CSS, which suggested that ZC3H13 might be a carcinogenic factor in CESC. It is worth noting that the expression analysis from TCGA-CESC data indicated that ZC3H13 was significantly expressed at lower levels in CESC tumor tissues (**Supplementary Figure 1A**). This result suggested that ZC3H13 was more likely to be a tumor suppressor in CESC. More importantly, there was no significant difference in the expression of ZC3H13 between cancer and adjacent tissues when combining the TCGA-CESC and GTEx databases (**Supplementary Figure 1B**). However, high expression of ZC3H13 was associated with favorable prognosis regardless of OS, PFS or CSS. In line with this result, ZC3H13 was also significantly expressed at low levels in KIRC tumor tissues. Therefore, we choose KIRC for further research.

To explore whether ZC3H13 could be a predictor for immunotherapy, we analyzed the relationship between ZC3H13 and multiple immune checkpoint inhibitors (ICIs) and TIICs. As shown in **Supplementary Figure 5A**, ZC3H13 was significantly related to the expression level of immune checkpoint molecules in most tumors. Additionally, ZC3H13 was significantly related to TIICs in most tumor microenvironments (**Supplementary Figure 5B**). TMB and MSI are the most accurate markers for predicting the efficacy of ICB so far. The higher the TMB and MSI scores are, the more sensitive the tumor is to the efficacy of ICB. Here, we found that ZC3H13 was significantly related to the TMB and MSI of many types of tumors. For example, ZC3H13 was negatively correlated with the MSI scores of BRCA, THCA, PRAD, HNSC, and DLBC, but it was positively correlated with the MSI scores of READ, OV and LUSC (**Supplementary Figure 5C**). ZC3H13 was significantly negatively correlated with TMB in KIRC, BRCA, THCA, STAD, PRAD, LUSC, and LIHC. However, ZC3H13 was significantly positively correlated with TMB in SKCM (**Supplementary Figure 5D**). All of these results suggested that ZC3H13 might have the potential to be a predictor of ICB efficacy.

The Relationship Between ZC3H13 and Clinicopathological and Prognostic Characteristics in KIRC

Based on the previous results, we further analyzed the correlation between ZC3H13 and some important clinicopathological characteristics here. In line with the previous results, we found that the expression of ZC3H13 in tumor tissues, higher grade and higher stage was significantly lower (**Figures 1A–C**). In our own RNA-seq cohort, though without significant difference, there was a trend that the expression was higher in the normal tissues (**Figure 1D**). And this no significant difference may be caused by the small sample size. To eliminate the influence of sample size, we chose a large GEO database (GSE53757), which contains 72 KIRC tumor tissues and matched adjacent normal tissues, and successfully validated this result (**Figure 1E**). As we found that ZC3H13 was significantly higher expressed in the normal tissues, we further explored which cell types ZC3H13 expressed in adjacent normal tissues using scRNA-seq. To our surprise, ZC3H13 was almost not expressed in T and NK cells and expressed abundantly in endothelial cells, macrophage, neurons and tissue stem cells (**Figures 1F, G**). The expression of ZC3H13 of these cells might inhibit T and NK cells from infiltrating into the tumor microenvironment as ZC3H13 was negatively correlated with the infiltration of TIICs in KIRC (**Supplementary Figure 5B**). Finally, we conducted a single factor Cox analysis on sex, age, ZC3H13 expression, grade and stage. The results suggested that older age, higher grade and stage, and lower expression of ZC3H13 were all unfavorable prognostic factors (**Figure 1H**).

Identifying DEGs Between the High and Low ZC3H13 Groups and Functional Analyses of DEGs

A heatmap and volcano plot (**Figures 2A, B**) were used to display the screened DEGs. Eventually, we identified 271 significant DEGs (**Supplementary Table 7**). The results of GO analysis suggested that these DEGs were enriched in several biological processes, including organic anion transport, apical part of cell, receptor ligand activity, apical plasma membrane, collagen-containing extracellular matrix, and anion transmembrane transporter activity (**Supplementary Figures 6A–C** and **Supplementary Table 8**). The results of KEGG analysis indicated that these DEGs were enriched in pathways such as neuroactive ligand-receptor interaction and cholesterol metabolism (**Supplementary Figure 6D** and **Supplementary Table 9**). Additionally, the enrichment scores of several hallmark signatures were significantly different between the high and low ZC3H13 groups. Mitotic spindle, UV response down, protein secretion, TGF-β signaling, Hedgehog signaling, androgen response, Wnt-β-Catenin signaling, G2M checkpoint, heme metabolism, PI3K-AKT-MTOR signaling and Notch signaling were enriched in the high ZC3H13 group. In contrast,

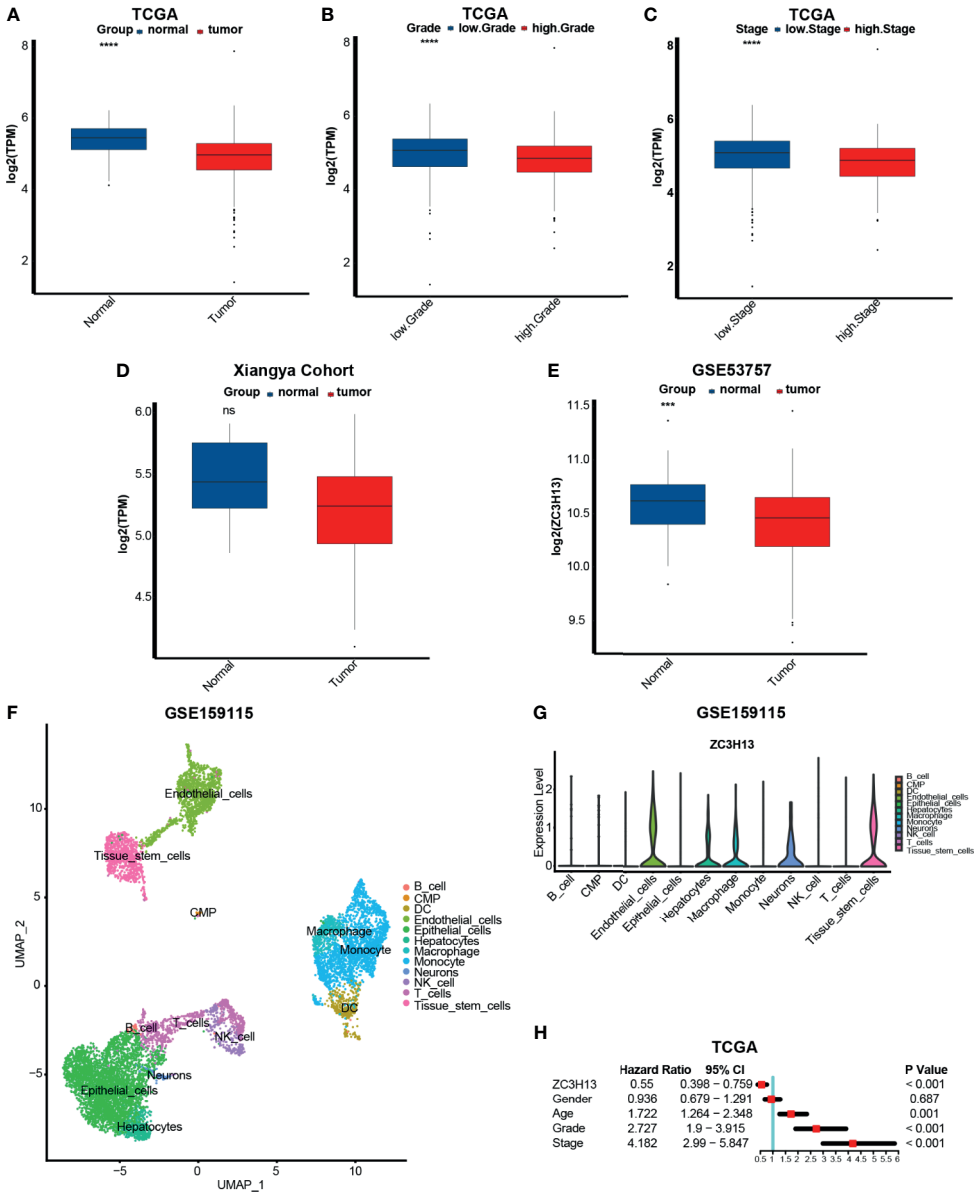

FIGURE 1 | The relationship between ZC3H13 and clinicopathological and prognostic characteristics in KIRC. **(A)** The histogram of log2(TPM) of ZC3H13 between normal and cancer tissues based on TCGA database. Normal tissue, blue; Cancer tissue, red. (T test, ****P < 0.0001). **(B)** The histogram of log2(TPM) of ZC3H13 between low and high grade based on TCGA database. Low grade, blue; High grade, red. (T test, ****P < 0.0001).. **(C)** The histogram of log2(TPM) of ZC3H13 between low and high stages based on TCGA database. Low stage, blue; High stage, red. (T test, ****P < 0.0001). **(D)** The histogram of log2(TPM) of ZC3H13 between normal and cancer tissues in Xiangya cohort. Normal tissue, blue; Cancer tissue, red. (T test, ns, not statistically significant). **(E)** The histogram of log2(ZC3H13) between normal and cancer tissues based on GSE53757. Normal tissue, blue; Cancer tissue, red. (T test, ****P < 0.0001). **(F)** Single-cell atlas of KIRC adjacent normal tissues. UMAP plot of 6046 cells obtained from GSE159115, which was visualized and annotated using "Seurat" and "Single" R package respectively. CMP, common myeloid progenitor; DC, dendritic cell. **(G)** Violin plot of ZC3H13 expression pattern between different cell types in KIRC adjacent normal tissues. **(H)** Forest figure of single factor Cox analysis on sex, age, ZC3H13 expression, grade and stage. Calculated using Cox proportional hazard model and visualized using "forestplot" R package.

spermatogenesis, p53 pathway, myogenesis, DNA repair, UV response up, xenobiotic metabolism, coagulation, estrogen response late, glycolysis, allograft rejection, Kras signaling down, and reactive oxygen species pathway were enriched in the low ZC3H13 group (**Figure 2C** and **Supplementary Table 10**).

ZC3H13 Shaped a Noninflamed Phenotype and Predicted a Lower Response to ICB in KIRC

The previous results indicated that ZC3H13 is closely related to the immune characteristics of a variety of tumors. We further

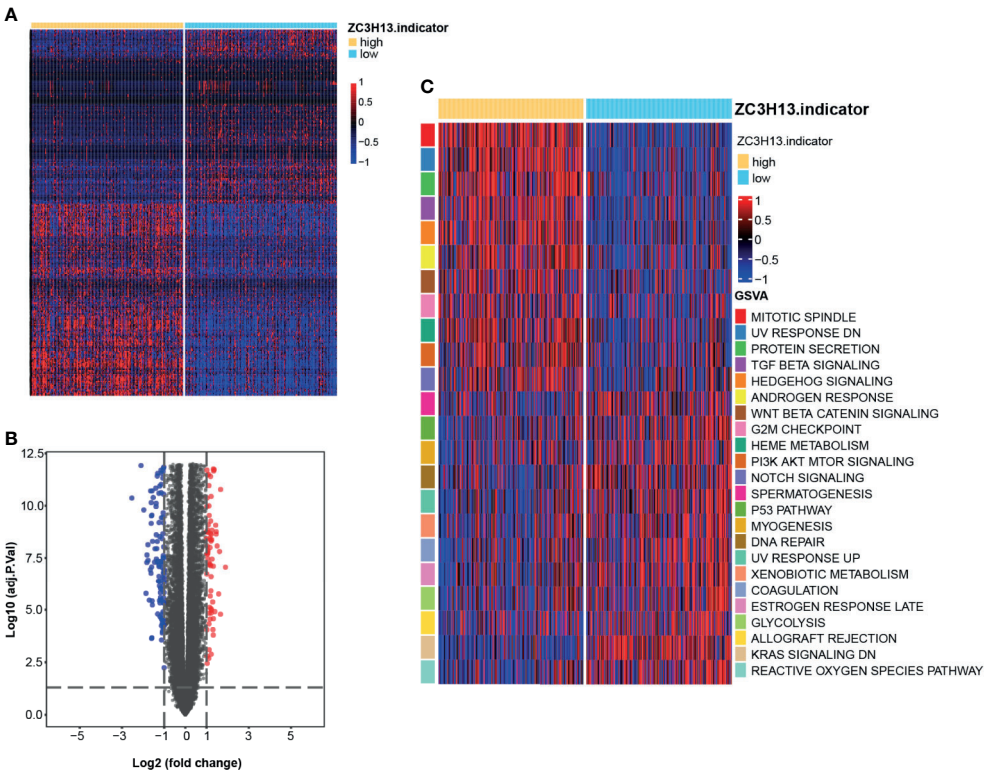

FIGURE 2 | DEGs between the high and low ZC3H13 groups and functional analyses of DEGs. **(A)** Heatmap drawn based on the 271 DEGs between the high and low ZC3H13 groups. Lowly expressed DEGs, blue; Highly expressed DEGs, red. ("limma" R package, adjusted P value < 0.05 and |logFC| > 1 were set as the significance criteria for significant DEGs). **(B)** Volcano plot drawn based on the DEGs between the high and low ZC3H13 groups. Log2(FC) < -1, blue; Log2(FC) > 1, red; ("limma" R package, adjusted P value < 0.05 and |logFC| > 1 were set as the significance criteria for significant DEGs). **(C)** Heatmap drawn based on the GSVA analysis of biological pathways between the high and low ZC3H13 groups. Inhibition pathways, blue; Activation pathways, red.

compared the different activities of the immune response between the ZC3H13 high and low groups. As shown in **Figure 3A**, the activities of the majority of immune cycles were downregulated in the high ZC3H13 group, including the activities of priming, activation and trafficking of immune cells to tumors (macrophage recruitment, NK cell recruitment, DC recruitment, and TH17 recruitment). In addition, the activities of infiltration of immune cells into tumors and recognition of cancer cells by T cells were also significantly lower in the high ZC3H13 group. The recruiting ability of CD8 T cells was also lower in the high ZC3H13 group, although there was no significant difference. To further verify these results, we applied the ssGSEA algorithm to calculate the infiltration levels of various immune cells in the TME. In line with previous results, the infiltration level of anticancer immune cells, including activated CD4 T cells, activated CD8 T cells, activated dendritic cells, CD56 bright natural killer cells, central memory CD4 T cells, macrophages, type 1 T helper cells, and type 17 T helper cells, was significantly lower in the high ZC3H13 group. Additionally, the infiltration level of protumor immune cells, such as regulatory T cells, plasmacytoid dendritic cells, neutrophils, and type 2 T helper cells, was significantly higher in the high ZC3H13 group. These results suggested that high ZC3H13 promoted the formation of a noninflamed phenotype (**Figure 3B**). It is well known that significant activation of the stromal pathway can inhibit tumor immunity and promote the formation of a noninflamed phenotype. We further found that the enrichment score of stromal pathways, including EMT1 and EMT3, was significantly higher in the high ZC3H13 group. Although there was no significant difference, the enrichment score of Pan-F-TBRS was also higher in the high ZC3H13 group (**Figure 3C**).

An inflamed tumor microenvironment (TME) in conjunction with pre-existing anticancer immunity is necessary for ICB (23–26). Therefore, we further analyzed the difference in enrichment scores of ICB efficacy prediction pathways between the high and low ZC3H13 groups. As expected, the enrichment scores of pathways that were positively related to the response to ICB were significantly lower in the high ZC3H13 group, such as nucleotide excision repair, oocyte meiosis, DNA replication, mismatch repair, systemic lupus erythematosus, alcohol, microRNAs in cancer, and the cell cycle (**Figure 3D** and **Supplementary Figure 6F**). Additionally, the enrichment scores of the cytokine-cytokine receptor pathway, which was

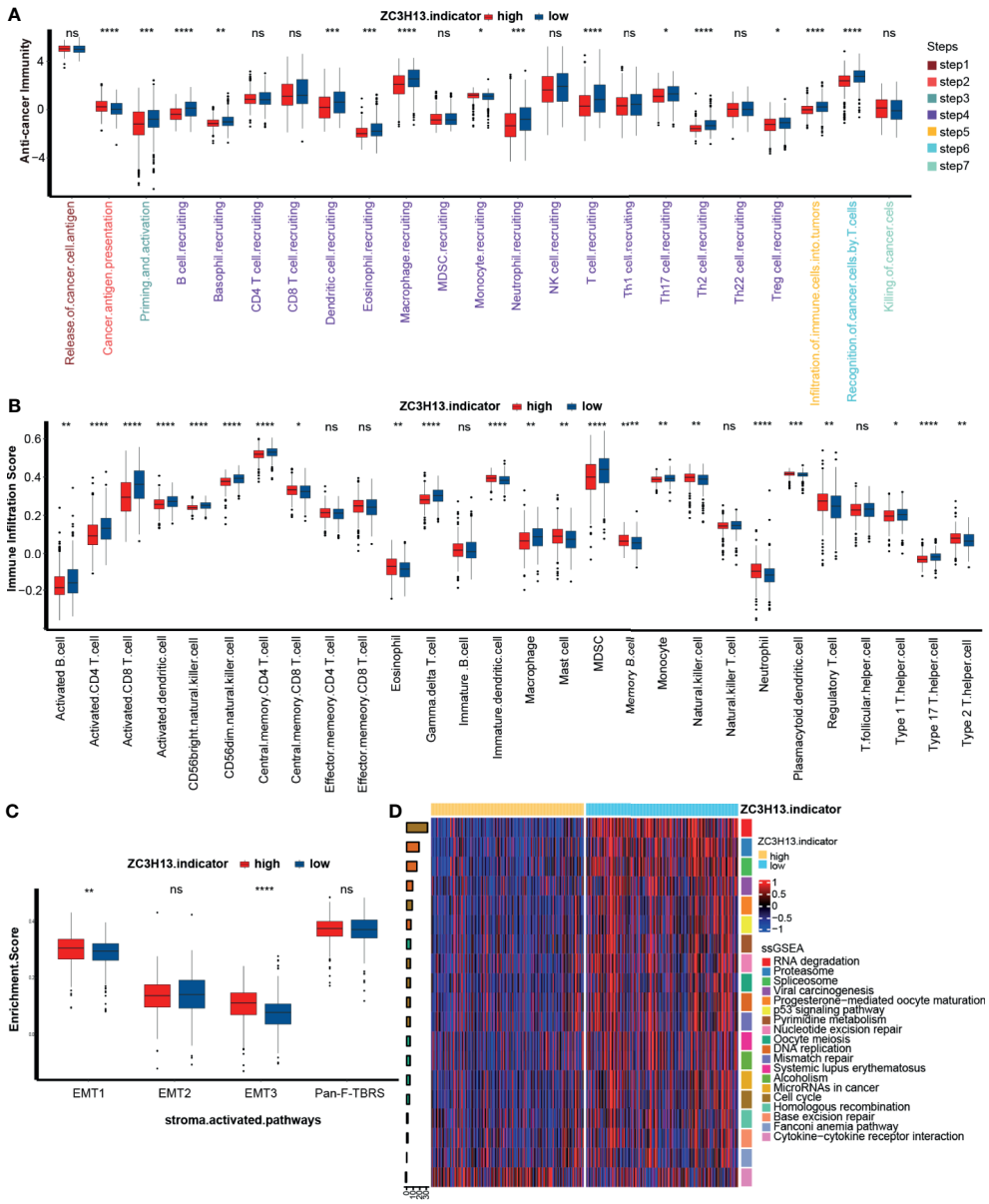

FIGURE 3 | Different immunological characteristics between the high and low ZC3H13 groups **(A)** Activation of cancer immunity cycles between the high and low ZC3H13 groups; Low ZC3H13 group, blue; High ZC3H13 group, red. MDSC, myeloid-derived suppressor cell; NK, natural killer cell; Th, helper T cell; Treg, regulatory T cell. (T test, *P < 0.05; **P < 0.01; ***P < 0.001; ****P < 0.0001; ns, not statistically significant). **(B)** The scores of immune cell infiltration in the TME between the high and low ZC3H13 groups; Low ZC3H13 group, blue; High ZC3H13 group, red; MDSC, myeloid-derived suppressor cell. (T test, *P < 0.05; **P < 0.01; ***P < 0.001; ****P < 0.0001; ns, not statistically significant). **(C)** Activation of stroma-activated pathways between the high and low ZC3H13 groups; Low ZC3H13 group, blue; High ZC3H13 group, red; EMT, epithelial–mesenchymal transition; Pan-F-TBRS, panfibroblast TGF-b response signature. (GSVA analysis and T test, *P < 0.05; **P < 0.01; ***P < 0.001; ****P < 0.0001; ns, not statistically significant). **(D)** Heatmap based on different immunotherapy predicted pathways between the high and low ZC3H13 groups. The bar plots on the left represent log10 p-values; positive values, activation; negative values, inhibition; the bar plots on the right represent different pathways.

negatively related to the response to ICB, were significantly higher in the high ZC3H13 group (**Figure 3D** and **Supplementary Figure 6F**). Furthermore, we analyzed the linear relationship between the expression of ZC3H13 and the enrichment scores of these immune cycles and ICB efficacy prediction pathways. ZC3H13 was still significantly negatively correlated with the enrichment scores of the antitumor immune signatures (**Figure 4A** left, **Supplementary Figure 7** and **Supplementary Table 11**) and ICB efficacy prediction pathways (**Figure 4A** right, **Supplementary Figure 8** and

Supplementary Table 12). The expression of several critical immune checkpoints, including CTLA-4, PD-1, LAG-3, LAALS3 and TIGIT, was significantly higher in the low ZC3H13 group (**Figure 4B**). Then, we validated these results in our RNA-seq cohort. ZC3H13 was significantly negatively correlated with the ICB efficacy prediction pathways (**Figure 4C** right, **Supplementary Figure 9** and **Supplementary Table 13**) and most of the enrichment scores of the antitumor immune signatures (**Figure 4C** left, **Supplementary Figure 10** and **Supplementary Table 14**). Finally, we also validated that LAALS3 was significantly higher in the low ZC3H13 group (**Figure 4D**).

In summary, ZC3H13 may be a novel biomarker to predict the immune phenotypes and clinical response of ICB in KIRC.

The Relationship Between ZC3H13 and Tumor Mutation Spectrum, TMB, and MSI in KIRC

Here, we compared the distribution differences of the top 20 somatic mutations between ZC3H13 groups. Notably, VHL, PBRM1 and TNN were the most frequent mutations in KIRC (**Figure 5A**). The overall mutational profiles between the ZC3H13 groups were comparable (94.5% *vs* 95.7%). Despite this, TMB in the low ZC3H13 group was significantly higher than that in the high ZC3H13 group (**Figure 5B**). However, there was no significant difference in the MSI scores between the two groups (**Figure 5C**).

Role of ZC3H13 in Predicting the Sensitivity of Targeted Therapy for KIRC

Targeted therapy is the most important treatment option for KIRC. We selected 183 drugs for the treatment of solid tumors and the corresponding target genes from the DrugBank database. Then, we compared the sensitivity of these antitumor drugs between the high and low ZC3H13 groups. As shown in **Figure 6A** and **Supplementary Table 15**, the sensitivity of most drugs was significantly different between the two groups. Furthermore, we focused on several targeted therapies and genes that were most commonly used in advanced KIRC patients: sorafenib with its targeted genes, including BRAF, FLT1, FLT3, FLT4, KDR, KIT, and RAF1; sunitinib with its targeted genes, including CSF1R, FLT1, FLT3, FLT4, KDR, and RET; pazopanib with its targeted gene SH2B3; and bevacizumab with its targeted gene VEGFA. We found that the sensitivity of these drugs was significantly higher in the high ZC3H13 group (**Figure 6B**). This finding indicated that targeted therapy could be a treatment option for the high ZC3H13 group, though this group was less sensitive to ICB therapy.

DISCUSSION

This study comprehensively analyzed the different expression profiles, prognostic values and immunoregulatory effects of ZC3H13 in pan-cancers. We found that ZC3H13 was closely related to the occurrence of a variety of tumors, especially KIRC. Then, we focused the analyses of ZC3H13 on KIRC. ZC3H13 might be a tumor suppressor gene in KIRC. Interestingly, the high expression of KIRC represented a noninflamed phenotype and this result could be roughly validated in our own RNA-seq cohort. Patients with high ZC3H13 expression were less sensitive to ICB but were more sensitive to targeted therapy. These results suggested that ZC3H13 was a potential predictive marker for ICB and targeted therapy in KIRC.

Given the substantial economic burden and toxic side effects, it is vital to find more reliable and simpler ICB efficacy prediction markers. To date, some ICB efficacy prediction markers have been identified, including PD-L1, TMB, MSI and some other efficacy prediction models, such as the TIDE model (27). However, it is worth noting that all these predictive markers have encountered many obstacles in clinical practice. The most serious obstacle is that the prediction accuracy is not sufficient. For example, as a marker for predicting the efficacy of ICB, the accuracy of PD-L1 can be affected by many other factors, such as immunohistochemical test methods, detection antibodies, and the choice of positive threshold (28, 29). TMB and MSI have relatively higher accuracy in predicting the efficacy of ICB than PD-L1. However, the clinical detection of these two markers relies on expensive and complex molecular methods. The tumor microenvironment (TME) plays an important role in tumor immunotherapy. An inflamed TME in conjunction with pre-existing anticancer immunity is necessary for ICB (23–26). Therefore, finding a biomarker that can fully predict the immune phenotype opens a new road for predicting the efficacy of ICB. In this study, we found that ZC3H13 could predict the immune phenotype from multiple angles.

First, we indicated that ZC3H13 was significantly correlated with the activity of the antitumor immune response steps in the TME of KIRC (19). The activities of the major cycles were downregulated in the high ZC3H13 group, including the activities of priming and activation, trafficking of immune cells to tumors (macrophage recruitment, NK cell recruitment, DC recruitment, and TH17 recruitment), infiltration of immune cells into tumors, and recognition of cancer cells by T cells. This indicated that ZC3H13 could inhibit the body's immune monitoring of tumor cells from the origin and further promote the immune evasion of tumor cells. The types of immune cells in the tumor microenvironment are complex, and their infiltration varies greatly. In KIRC, high expression of ZC3H13 could significantly inhibit the infiltration of most tumor suppressor TIICs, including activated CD4 T cells, activated CD8 T cells, activated dendritic cells, CD56 bright natural killer cells, central memory CD4 T cells, type 1 T helper cells, and type 17 T helper cells. Additionally, the infiltration of cancer-promoting TIICs, including regulatory T cell, plasmacytoid dendritic cells, neutrophils, and type 2 T helper cells, was significantly increased in the high ZC3H13 group. In addition, the activation of stromal pathways could also affect antitumor immunity in the TME. We found that the stromal pathways (including EMT1 and EMT3) in the high ZC3H13 group were significantly activated. In summary, we have proven from

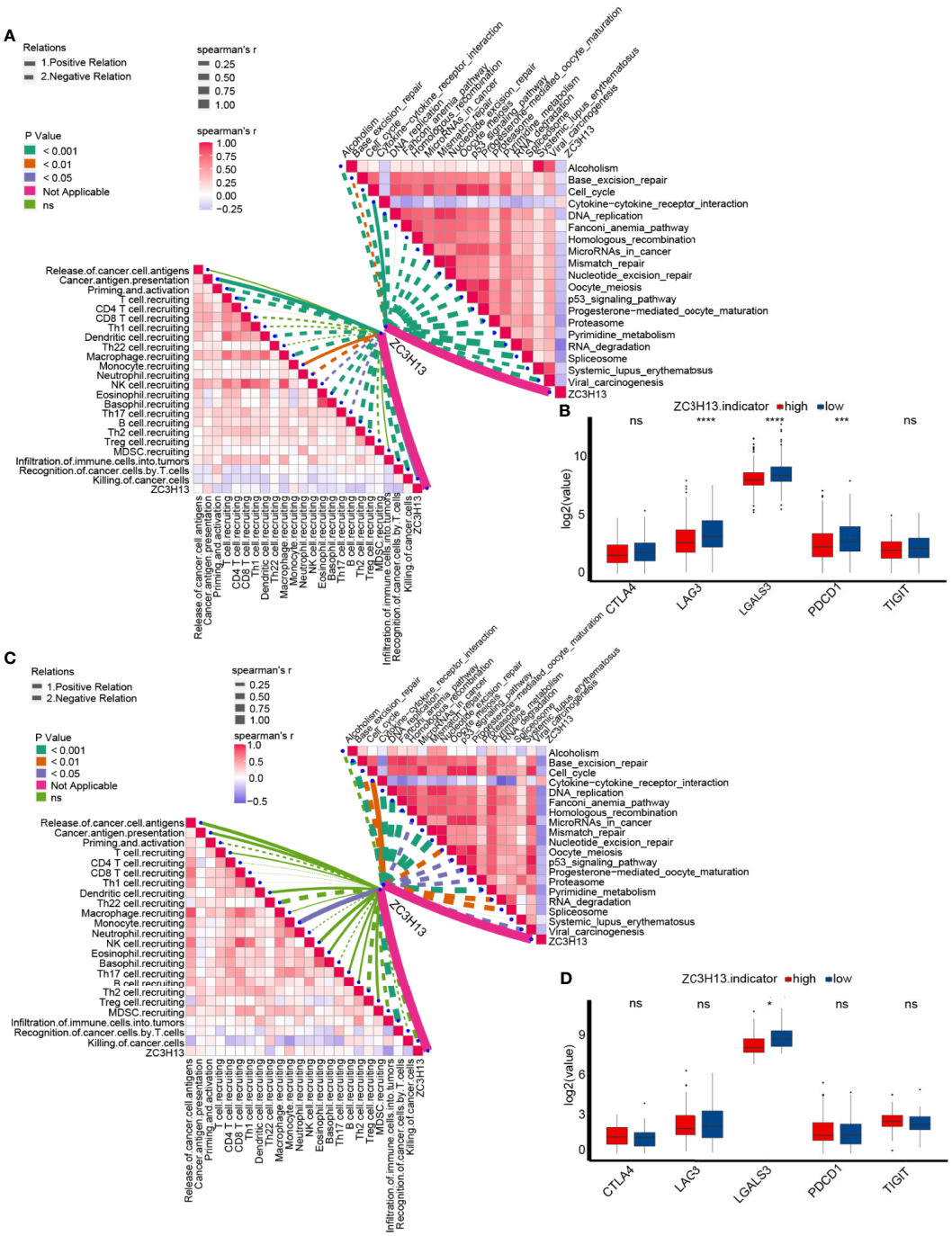

FIGURE 4 | The linear relationship between the expression of ZC3H13 and the enrichment scores of immune cycles and ICB efficacy prediction pathways. **(A)** Spearman correlation of ZC3H13 expression with cancer immunity and immune related pathways, presented on the left and right respectively. The different types of lines represent positive or negative correlations; the thickness of the lines and the color of the bar plots represent the strength of correlation; and the different colors of the lines represent p-values. MDSC, myeloid-derived suppressor cell; NK, natural killer cell; Th, helper T cell; Treg, regulatory T cell. **(B)** The histogram of log2(TPM) values of immune checkpoint genes between different ZC3H13 groups. Low ZC3H13 group, blue; High ZC3H13 group, red. (T test, ***P < 0.001; ****P < 0.0001; ns, not statistically significant). **(C)** Spearman correlation of ZC3H13 expression with cancer immunity and immune related pathways in our own RNA-seq cohort, presented on the left and right respectively. The different types of lines represent positive or negative correlations; the thickness of the lines and the color of the bar plots represent the strength of correlation; and the different colors of the lines represent p-values. MDSC, myeloid-derived suppressor cell; NK, natural killer cell; Th, helper T cell; Treg, regulatory T cell. **(D)** The histogram of log2(TPM) values of immune checkpoint genes between different ZC3H13 groups in our own RNA-seq cohort. Low ZC3H13 group, blue; High ZC3H13 group, red. (T test, *P < 0.05; ns, not statistically significant).

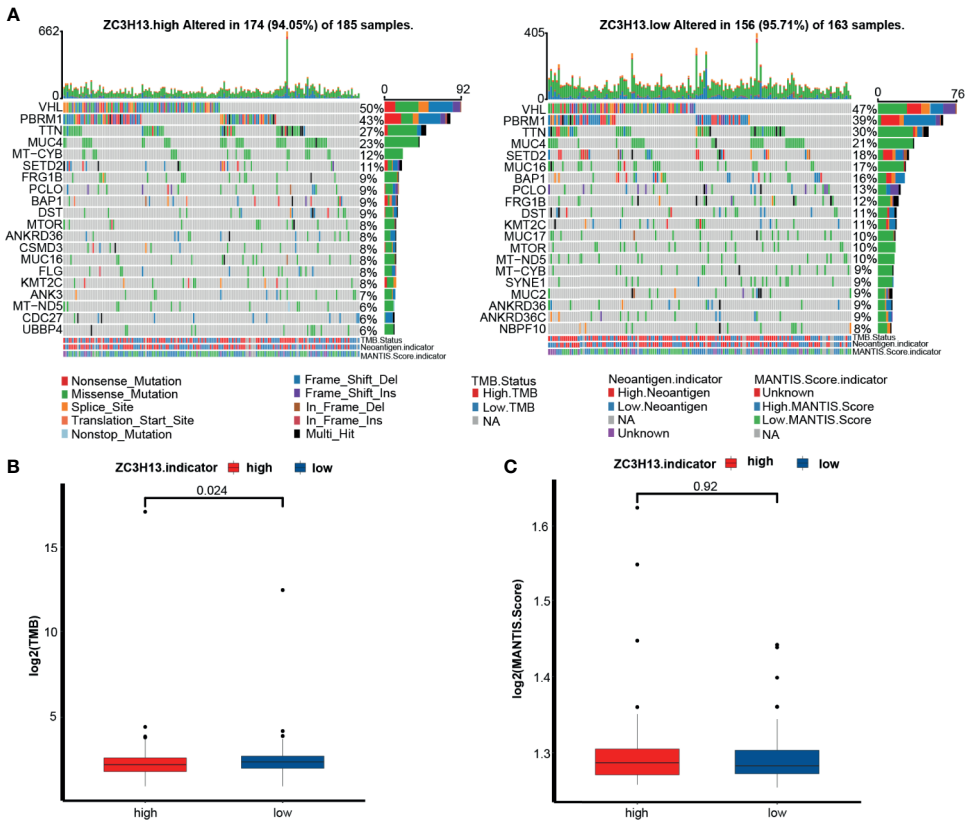

FIGURE 5 | The relationship between ZC3H13 and the tumor mutation spectrum, TMB and MSI in KIRC. **(A)** Mutation spectrum of the high (left) and low (right) ZC3H13 groups in KIRC. Different colors represented different mutation types annotated at the bottom; The barplot on the top represented mutation burden. The numbers on the right represented mutation frequency. TMB, tumor mutation burden. MANTIS, microsatellite analysis for normal-tumor instability. **(B)** The histogram of log2(value) of TMB between the different ZC3H13 groups. Low ZC3H13 group, blue; High ZC3H13 group, red. (T test). **(C)** The histogram of log2(value) of MANTIS score between the different ZC3H13 groups. Low ZC3H13 group, blue; High ZC3H13 group, red. (T test).

multiple angles that high expression of ZC3H13 represents a noninflamed phenotype.

Since high expression of ZC3H13 can predict a noninflamed phenotype, patients with high ZC3H13 expression may not be sensitive to ICB treatment. Unfortunately, we lacked a database containing patients treated with ICB to directly analyze the relationship between ZC3H13 and ICB efficacy. Therefore, we analyzed the relationship between ZC3H13 and the predictive pathways that were closely related to the efficacy of ICB (22). As expected, the enrichment scores of pathways that were positively related to the response to ICB, such as nucleotide excision repair, oocyte meiosis, DNA replication, mismatch repair, systemic lupus erythematosus, alcohol, microRNAs in cancer, and the cell cycle, were significantly lower in the high ZC3H13 group. In contrast, the enrichment score of the cytokine-cytokine receptor interaction, which was negatively related to the response to ICB, was significantly higher in the high ZC3H13 group. At the same time, we found that ZC3H13 and several critical immune checkpoints, such as CTLA-4, PD-1, LAG-3, LAALS3, and TIGIT, were also significantly negatively correlated. Most importantly, we found that ZC3H13 was also significantly negatively correlated with TMB in KIRC. The above results indicated that high expression of ZC3H13 could not only predict a noninflamed phenotype but also indicate a lower sensitivity to ICB. Nevertheless, patients with high expression of ZC3H13 were more sensitive to targeted therapy.

There are some limitations in the study. First, this study was based on an analysis of public databases and our small sample size RNA-seq cohort. Therefore, the conclusions need further verification in larger cohort, especially the cohort receiving ICB treatment. Second, this study chose the median expression of ZC3H13 as the cutoff value. This cutoff value may not be suitable for use in further external datasets. Third, further mechanistic experiments are still needed to clarify the immunoregulatory effects of ZC3H13 on the tumor microenvironment of KIRC.

CONCLUSION

This study demonstrated that ZC3H13 might shape a noninflamed phenotype in KIRC. Moreover, ZC3H13 could predict the prognosis and clinical response of ICB and the sensitivity to targeted therapies in KIRC.

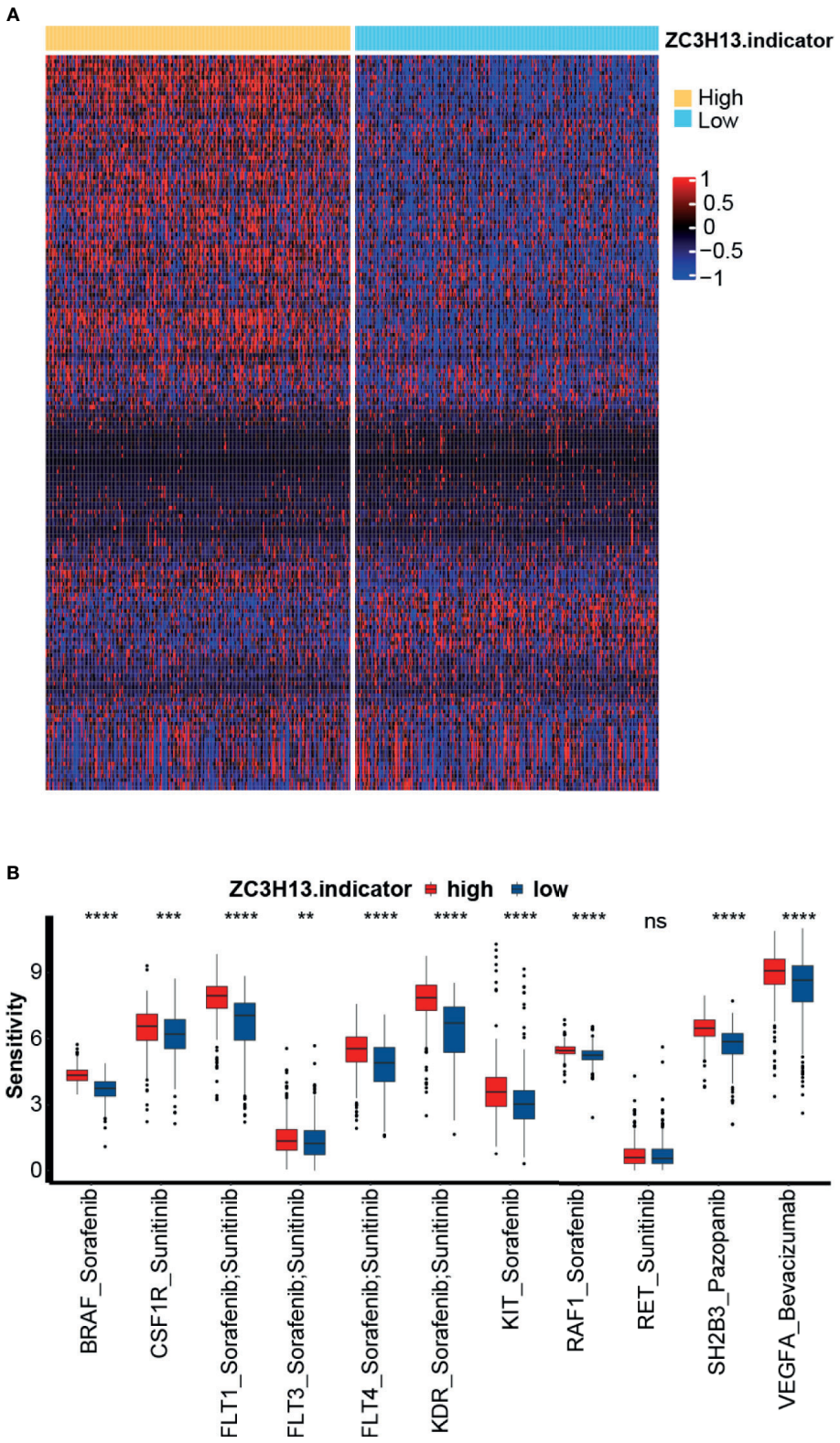

FIGURE 6 | The relationship between ZC3H13 and the sensitivity to targeted therapy of KIRC. **(A)** Heatmap drawn based on the different sensitivities to the 183 drugs selected from the DrugBank database. **(B)** The histogram of sensitivities to the selected targeted therapy between the different ZC3H13 groups. Low ZC3H13 group, blue; High ZC3H13 group, red. (T test, **P < 0.01; ***P < 0.001; ****P < 0.0001; ns, not statistically significant).

DATA AVAILABILITY STATEMENT

The datasets presented in this study can be found in online repositories. The names of the repository/repositories and accession number(s) can be found in the article/**Supplementary Material**.

ETHICS STATEMENT

The studies involving human participants were reviewed and approved by the Ethics Committee of the Xiangya Hospital of Central South University. The patients/participants provided their written informed consent to participate in this study.

AUTHOR CONTRIBUTIONS

(I) Conception and design: TG, HL, JH, and XZ. Administrative support: TG and XZ. Provision of study materials or patients: TG, JC, and JL. Collection and assembly of data: JL, BO, and HL. Data analysis and interpretation: HD, TG, HL, and JH. All authors contributed to the article and approved the submitted version.

FUNDING

This work was supported by the Hunan Province Science and Technology Program (2018SK51714).

ACKNOWLEDGMENTS

We sincerely thank all participants in the study.

SUPPLEMENTARY MATERIAL

The Supplementary Material for this article can be found online at: https://www.frontiersin.org/articles/10.3389/fonc.2021.718644/full#supplementary-material

Supplementary Figure 1 | Expression pattern of ZC3H13 in pan-cancers. **(A, B)** The expression pattern of ZC3H13 of pan-cancers in TCGA and TCGA combined with GTEx. The asterisks indicate a significant statistical p value calculated with the T test (*P < 0.05; **P < 0.01; ***P < 0.001). **(C)** The expression of ZC3H13 in normal tissues from the GTEx database. **(D)** The expression of ZC3H13 in cancer cell lines in CCLE.

Supplementary Figure 2 | Prognostic analysis of ZC3H13 for overall survival in pan-cancers. **(A)** The prognostic analyses of ZC3H13 in pan-cancers using a univariate Cox regression model. A hazard ratio >1 indicated a risk factor, and a hazard ratio <1 represented a protective factor. **(B, C)** The prognostic analyses of ZC3H13 in pan-cancers using the Kaplan-Meier method and log-rank test. Only cancers in which ZC3H13 was a significant prognostic biomarker are shown.

Supplementary Figure 3 | Prognostic analysis of ZC3H13 for progression-free survival in pan-cancers. **(A)** The prognostic analyses of ZC3H13 in pan-cancers using a univariate Cox regression model. A hazard ratio >1 indicats a risk factor, and a hazard ratio <1 represents a protective factor. **(B–E)** The prognostic analyses of ZC3H13 across cancers using the Kaplan-Meier method and log-rank test. Only cancers in which ZC3H13 was a significant prognostic biomarker are shown.

Supplementary Figure 4 | Prognostic analysis of ZC3H13 for disease-specific survival in pan-cancers. **(A)** The prognostic analyses of ZC3H13 in pan-cancers using a univariate Cox regression model. A hazard ratio >1 indicates a risk factor, and a hazard ratio <1 represents a protective factor. **(B–E)** The prognostic analyses of ZC3H13 in pan-cancers using the Kaplan-Meier method and log-rank test. Only cancers in which ZC3H13 was a significant prognostic biomarker are shown.

Supplementary Figure 5 | Correlations between ZC3H13 and immune checkpoints, tumor infiltrating immune cells, TMB, and MSI in pan-cancers. **(A)** Correlation between ZC3H13 and immune checkpoints in pan-cancers. **(B)** Correlation between ZC3H13 and MSI in pan-cancers. **(C)** Correlation between ZC3H13 and tumor infiltrating immune cells in pan-cancers. **(D)** Correlation between ZC3H13 and MSI in pan-cancers. The asterisks indicate a significant statistical p value calculated with Spearman correlation analysis (*P < 0.05; **P < 0.01; ***P < 0.001).

Supplementary Figure 6 | Functional annotation for different expression genes between the high and low ZC3H13 groups. **(A)** Biological Processes (BP) **(B)** Cellular Components (CC); **(C)** Molecular Functions (MF); **(D)** Kyoto Encyclopedia of Genes and Genomes (KEGG). **(F)** The histogram of immunotherapy predicted pathways between the high and low ZC3H13 groups. Low ZC3H13 group, blue; High ZC3H13 group, red. (T test, *P < 0.05; **P < 0.01; ***P < 0.001; ****P < 0.0001; ns, not statistically significant).

Supplementary Figure 7 | Spearman correlation of ZC3H13 expression with cancer immunity in TCGA cohort.

Supplementary Figure 8 | Spearman correlation of ZC3H13 expression with immune related pathways in TCGA cohort.

Supplementary Figure 9 | Spearman correlation of ZC3H13 expression with immune related pathways in our own cohort.

Supplementary Figure 10 | Spearman correlation of ZC3H13 expression with cancer immunity in our own cohort.

REFERENCES

1. Ljungberg B, Albiges L, Abu-Ghanem Y, Bensalah K, Dabestani S, Fernández-Pello S, et al. European Association of Urology Guidelines on Renal Cell Carcinoma: The 2019 Update. *Eur Urol* (2019) 75(5):799–810. doi: 10.1016/j.eururo.2019.02.011
2. McGregor BA, McKay RR, Braun DA, Werner L, Gray K, Flaifel A, et al. Results of a Multicenter Phase II Study of Atezolizumab and Bevacizumab for Patients With Metastatic Renal Cell Carcinoma With Variant Histology and/or Sarcomatoid Features. *J Clin Oncol* (2020) 38(1):63–70. doi: 10.1200/jco.19.01882
3. Diab A, Tannir NM, Bentebibel SE, Hwu P, Papadimitrakopoulou V, Haymaker C, et al. Bempegaldesleukin (NKTR-214) Plus Nivolumab in Patients With Advanced Solid Tumors: Phase I Dose-Escalation Study of Safety, Efficacy, and Immune Activation (PIVOT-02). *Cancer Discov* (2020) 10(8):1158–73. doi: 10.1158/2159-8290.Cd-19-1510
4. Ravi P, Mantia C, Su C, Sorenson K, Elhag D, Rathi N, et al. Evaluation of the Safety and Efficacy of Immunotherapy Rechallenge in Patients With Renal Cell Carcinoma. *JAMA Oncol* (2020) 6(10):1606–10. doi: 10.1001/jamaoncol.2020.2169
5. Kandoth C, McLellan MD, Vandin F, Ye K, Niu B, Lu C, et al. Mutational Landscape and Significance Across 12 Major Cancer Types. *Nature* (2013) 502(7471):333–9. doi: 10.1038/nature12634
6. Zaccara S, Ries RJ, Jaffrey SR. Reading, Writing and Erasing mRNA Methylation. *Nat Rev Mol Cell Biol* (2019) 20(10):608–24. doi: 10.1038/s41580-019-0168-5

7. Shulman Z, Stern-Ginossar N. The RNA Modification N(6)-Methyladenosine as a Novel Regulator of the Immune System. *Nat Immunol* (2020) 21(5):501–12. doi: 10.1038/s41590-020-0650-4
8. Wen J, Lv R, Ma H, Shen H, He C, Wang J, et al. Zc3h13 Regulates Nuclear RNA M(6)A Methylation and Mouse Embryonic Stem Cell Self-Renewal. *Mol Cell* (2018) 69(6):1028–38.e6. doi: 10.1016/j.molcel.2018.02.015
9. Zhu D, Zhou J, Zhao J, Jiang G, Zhang X, Zhang Y, et al. ZC3H13 Suppresses Colorectal Cancer Proliferation and Invasion *via* Inactivating Ras-ERK Signaling. *J Cell Physiol* (2019) 234(6):8899–907. doi: 10.1002/jcp.27551
10. Park MH, Hong JT. Roles of NF-κB in Cancer and Inflammatory Diseases and Their Therapeutic Approaches. *Cells* (2016) 5(2):15. doi: 10.3390/cells5020015
11. Panahi Y, Darvishi B, Ghanei M, Jowzi N, Beiraghdar F, Varnamkhasti BS. Molecular Mechanisms of Curcumins Suppressing Effects on Tumorigenesis, Angiogenesis and Metastasis, Focusing on NF-κB Pathway. *Cytokine Growth Factor Rev* (2016) 28:21–9. doi: 10.1016/j.cytogfr.2015.12.004
12. Colaprico A, Silva TC, Olsen C, Garofano L, Cava C, Garolini D, et al. TCGAbiolinks: An R/Bioconductor Package for Integrative Analysis of TCGA Data. *Nucleic Acids Res* (2016) 44(8):e71. doi: 10.1093/nar/gkv1507
13. Goldman MJ, Craft B, Hastie M, Repečka K, McDade F, Kamath A, et al. Visualizing and Interpreting Cancer Genomics Data *via* the Xena Platform. *Nat Biotechnol* (2020) 38(6):675–8. doi: 10.1038/s41587-020-0546-8
14. Bonneville R, Krook MA, Kautto EA, Miya J, Wing MR, Chen HZ, et al. Landscape of Microsatellite Instability Across 39 Cancer Types. *JCO Precis Oncol* (2017) 2017:PO.17.00073. doi: 10.1200/po.17.00073
15. von Roemeling CA, Radisky DC, Marlow LA, Cooper SJ, Grebe SK, Anastasiadis PZ, et al. Neuronal Pentraxin 2 Supports Clear Cell Renal Cell Carcinoma by Activating the AMPA-Selective Glutamate Receptor-4. *Cancer Res* (2014) 74(17):4796–810. doi: 10.1158/0008-5472.Can-14-0210
16. Zhang Y, Narayanan SP, Mannan R, Raskind G, Wang X, Vats P, et al. Single-Cell Analyses of Renal Cell Cancers Reveal Insights Into Tumor Microenvironment, Cell of Origin, and Therapy Response. *Proc Natl Acad Sci USA* (2021) 118(24):e2103240118. doi: 10.1073/pnas.2103240118
17. Luecken MD, Theis FJ. Current Best Practices in Single-Cell RNA-Seq Analysis: A Tutorial. *Mol Syst Biol* (2019) 15(6):e8746. doi: 10.15252/msb.20188746
18. Liberzon A, Birger C, Thorvaldsdóttir H, Ghandi M, Mesirov JP, Tamayo P. The Molecular Signatures Database (MSigDB) Hallmark Gene Set Collection. *Cell Syst* (2015) 1(6):417–25. doi: 10.1016/j.cels.2015.12.004
19. Chen DS, Mellman I. Oncology Meets Immunology: The Cancer-Immunity Cycle. *Immunity* (2013) 39(1):1–10. doi: 10.1016/j.immuni.2013.07.012
20. Xu L, Deng C, Pang B, Zhang X, Liu W, Liao G, et al. TIP: A Web Server for Resolving Tumor Immunophenotype Profiling. *Cancer Res* (2018) 78 (23):6575–80. doi: 10.1158/0008-5472.Can-18-0689
21. Charoentong P, Finotello F, Angelova M, Mayer C, Efremova M, Rieder D, et al. Pan-Cancer Immunogenomic Analyses Reveal Genotype-Immunophenotype Relationships and Predictors of Response to Checkpoint Blockade. *Cell Rep* (2017) 18(1):248–62. doi: 10.1016/j.celrep.2016.12.019
22. Mariathasan S, Turley SJ, Nickles D, Castiglioni A, Yuen K, Wang Y, et al. TGFβ Attenuates Tumour Response to PD-L1 Blockade by Contributing to Exclusion of T Cells. *Nature* (2018) 554(7693):544–8. doi: 10.1038/nature25501
23. Chen DS, Mellman I. Elements of Cancer Immunity and the Cancer-Immune Set Point. *Nature* (2017) 541(7637):321–30. doi: 10.1038/nature21349
24. Gajewski TF, Corrales L, Williams J, Horton B, Sivan A, Spranger S. Cancer Immunotherapy Targets Based on Understanding the T Cell-Inflamed *Versus* Non-T Cell-Inflamed Tumor Microenvironment. *Adv Exp Med Biol* (2017) 1036:19–31. doi: 10.1007/978-3-319-67577-0_2
25. Ji RR, Chasalow SD, Wang L, Hamid O, Schmidt H, Cogswell J, et al. An Immune-Active Tumor Microenvironment Favors Clinical Response to Ipilimumab. *Cancer Immunol Immunother* (2012) 61(7):1019–31. doi: 10.1007/s00262-011-1172-6
26. Tumeh PC, Harview CL, Yearley JH, Shintaku IP, Taylor EJ, Robert L, et al. PD-1 Blockade Induces Responses by Inhibiting Adaptive Immune Resistance. *Nature* (2014) 515(7528):568–71. doi: 10.1038/nature13954
27. Jiang P, Gu S, Pan D, Fu J, Sahu A, Hu X, et al. Signatures of T Cell Dysfunction and Exclusion Predict Cancer Immunotherapy Response. *Nat Med* (2018) 24(10):1550–8. doi: 10.1038/s41591-018-0136-1
28. McLaughlin J, Han G, Schalper KA, Carvajal-Hausdorf D, Pelekanou V, Rehman J, et al. Quantitative Assessment of the Heterogeneity of PD-L1 Expression in Non-Small-Cell Lung Cancer. *JAMA Oncol* (2016) 2(1):46–54. doi: 10.1001/jamaoncol.2015.3638
29. Nishino M, Ramaiya NH, Hatabu H, Hodi FS. Monitoring Immune-Checkpoint Blockade: Response Evaluation and Biomarker Development. *Nat Rev Clin Oncol* (2017) 14(11):655–68. doi: 10.1038/nrclinonc.2017.88

Conflict of Interest: The authors declare that the research was conducted in the absence of any commercial or financial relationships that could be construed as a potential conflict of interest.

frontiers in Oncology

ORIGINAL RESEARCH
published: 15 September 2021
doi: 10.3389/fonc.2021.739134

Treatment Outcome of Different Chemotherapy in Patients With Relapsed or Metastatic Malignant Urachal Tumor

Meiting Chen[1†], Cong Xue[1†], Ri-qing Huang[1], Meng-qian Ni[1], Lu Li[1], Hai-feng Li[1], Wei Yang[1], An-qi Hu[1], Zhou-san Zheng[2], Xin An[1] and Yanxia Shi[1*]*

[1] Department of Medical Oncology, Sun Yat-sen University Cancer Center, State Key Laboratory of Oncology in South China, Collaborative Innovation Center for Cancer Medicine, Guangzhou, China, [2] Department of Oncology, The First Affiliated Hospital of Sun Yat-sen University, Guangzhou, China

OPEN ACCESS

Edited by:
Alcides Chaux,
Universidad del Norte, Paraguay

Reviewed by:
Hiroshi Yaegashi,
Kanazawa University, Japan
Wojciech Krajewski,
Wroclaw Medical University, Poland

***Correspondence:**
Xin An
anxin@sysucc.org.cn
Yanxia Shi
shiyx@sysucc.org.cn

[†]These authors have contributed equally to this work

Specialty section:
This article was submitted to Genitourinary Oncology, a section of the journal Frontiers in Oncology

Received: 10 July 2021
Accepted: 20 August 2021
Published: 15 September 2021

Citation:
Chen M, Xue C, Huang R-q, Ni M-q, Li L, Li H-f, Yang W, Hu A-q, Zheng Z-s, An X and Shi Y (2021) Treatment Outcome of Different Chemotherapy in Patients With Relapsed or Metastatic Malignant Urachal Tumor. Front. Oncol. 11:739134. doi: 10.3389/fonc.2021.739134

Background: Malignant urachal tumor is a rare subtype of genitourinary cancer. Our aim was to explore the optimal chemotherapy regimens for relapsed or metastatic urachal carcinoma.

Materials and Methods: We retrospectively enrolled 24 adult patients with relapsed or metastatic urachal carcinoma from January 2014 to September 2020 at Sun Yat-sen University Cancer Center. We summarized the chemotherapy regimens and classified them as fluorouracil based, platinum based, and paclitaxel based. Nine patients received XELOX (capecitabine and oxaliplatin) regimens, seven patients received TX (paclitaxel and capecitabine) regimens, and eight of them received chemotherapy including GP (gemcitabine and cisplatin), TP (paclitaxel and cisplatin), TN (paclitaxel and nedaplatin), and tislelizumab.

Results: The disease control rate was 75%. Among all patients, one patient treated with XELOX achieved partial remission (PR), while 17 patients showed stable disease. The median progression-free survival (PFS) and overall survival (OS) in all treated patients was 7.43 and 29.7 months, respectively. The patients receiving first-line platinum-based chemotherapy presented better PFS than those without platinum (median PFS 8.23 *vs*. 3.80 months, $p = 0.032$), but not significant for OS between two groups. There is no significant difference in PFS and OS for fluorouracil-based and paclitaxel-based groups as first-line regimen. Next-generation gene sequencing revealed TP53 mutation and low tumor mutational burden in five out of seven cases.

Conclusion: The platinum-based chemotherapy regimen is effective for relapsed or metastatic urachal carcinoma.

Keywords: urachal carcinoma, metastatic, chemotherapy, efficacy, survival

INTRODUCTION

Malignant urachal tumor (MUT) is a rare genitourinary tumor derived from the urachus at the dome of the bladder, accounting for 0.1%–0.7% of all malignant bladder cancers (1). Patients with MUTs are usually diagnosed at an advanced stage with extravesical extension and lymph node metastasis, and the prognosis is generally poor (2). Literatures about MUT are mainly based on some of case reports and few retrospective studies (3–6). MUT mostly affects male patients at 50 to 60 years (3, 7). The common clinical manifestation is hematuria (8, 9). Abdominal pain and dysuria are less commonly seen. The diagnosis for MUT is difficult due to the rarity of tumor and similarity to adenocarcinoma of other origins (4, 10, 11). Several retrospective studies reported the clinicopathological features of MUT, resulting in the 5-year overall survival (OS) rate of 12%–50% (3, 12). Although surgery is a standard of care for localized MUT, the most appropriate care for metastatic or relapsed cases has not been established. MUT resembles enteric adenocarcinoma histologically and may respond to chemotherapy used to treat colorectal cancer (13). Most of MUT cases expressed CDX2 and CK20 (9, 13, 14), which was also positive in adenocarcinoma of colorectal cancer. Several genomic analyses showed that MUT presented a similar molecular profile with colorectal carcinoma, with a RAS mutation rate of 32%–57% and BRAF mutation rate of 18% (13, 15, 16). But the standard treatment modalities for MUT are lacking. Although the backbone therapy for localized disease remains surgical resection, the systemic therapy for recurrence and metastasis cases is not well known (17). The chemotherapy regimens are also similar to those for colorectal cancer, but the efficacy varies in different reports (4, 18–20). Here, we present the results of a retrospective study of treatment outcome in different chemotherapy regimens in patients with advanced or relapsed MUT in Sun Yat-sen Cancer Center (SYSUCC).

MATERIALS AND METHODS

Patient Selection and Treatment

From January 2014 to September 2020, we enrolled 24 patients with relapsed or advanced MUT at SYSUCC. The study protocol was approved by the ethical committee of Sun Yat-sen University Cancer Center. Eligible patients had histologically confirmed MUT and had adequate organ function apart from organ function affected by disease. Evaluation included. The data reviewed included the patients' demographics, tumor characteristics, standard laboratory tests, CT scans of the whole body, and the treatment regimens applied. The staging information was based on the 7th UICC TNM Classification (21). Besides, MUT was also staged according to the Sheldon staging system (22), which defines four stages, including I, no invasion beyond urachal mucosa; II, invasion confined to the urachus; III, local extension into bladder (IIIA), abdominal wall (IIIB), peritoneum (IIIC), or viscera other than the bladder (IIID); and IV, metastasis to regional lymph nodes (IVA) or distant sites (IVB).The chemotherapy regimens applied for each patient were decided by experienced oncologists in SYSUCC. The common chemotherapy regimens included gemcitabine (1 g/m2, i.v., d1, d8, q21d), oxaliplatin (130 mg/m^2, i.v., d1, q21d), capecitabine (1 g/m^2, po, d1–14, q21d), nanoparticle paclitaxel (260 mg/m^2, i.v., d1, q21d), and cisplatin (25 mg/m^2, i.v., d1–3, q21d). All cycles were repeated at 21-day intervals. Treatment was administered until death, progressive disease (PD), unacceptable toxicity, lost to follow-up, or patient or investigator decision.

Toxicity Evaluation

Adverse events (AEs) were graded according to the Common Terminology Criteria for Adverse Events version 4.0. The relative frequency of each AE considered possibly, probably, or likely related to chemotherapy was estimated as the proportion of all toxicity-evaluable cycles in which toxicity was observed.

Response Assessment

The objective response was sustained for a minimum of two consecutive imaging evaluations at least 4 weeks apart. Disease was also evaluated using RECIST version 1.1 for response assessment. CT was used to assess treatment response at baseline and after every two cycles of chemotherapy. Follow-up CT scans were performed every 6 months for 2 years or until PD.

Statistical Analysis

The study population for all analyses included patients enrolled in the study who had an adequate baseline tumor assessment. Descriptive statistics were used to summarize patient characteristics, treatment administration, antitumor activity, and safety. Survival was measured from initiation of therapy until death. The disease control rate (DCR), objective response rate (ORR), progression-free survival (PFS), OS, and AEs were also analyzed. A cutoff date of April 20, 2021, was established for analyzing data for this report. OS and PFS rates were assessed using Kaplan–Meier analyses with SPSS 25.0 software (SPSS Inc., Chicago, IL, USA) and R version 4.0.2.

RESULTS

Twenty-four eligible patients were enrolled and treated (**Table 1**). Patients were aged from 28 to 69 years, with three patients (12.5%) were aged more than 60 years. Most patients were male (83.3%). All patients received primary surgery. Nineteen patients received urachal excision or transurethral bladder tumor resection, and five patients received partial cystectomy (**Table 1**). Six patients also received pelvic lymph node dissection. Three patients received second surgery after local relapse. No patients received neo-adjuvant chemotherapy.

Abbreviations: PFS, progression-free survival; OS, overall survival; MUT, malignant urachal tumor; SYSUCC, Sun Yat-sen Cancer Center; PD, progressive disease; AE, adverse event; DCR, disease control rate; ORR, objective response rate; PR, partial remission; CR, complete remission; SD, stable disease; NGS, next-genome sequencing; TMB, tumor mutational burden; PD-L1, programmed death ligand-1.

TABLE 1 | Characteristics of patients.

Characteristics	*n* (%)
Male sex	20 (83.3%)
Age (years)	
Median (range)	45 (28~69)
TNM stage at diagnosis	
I	1 (4.2%)
II	4 (16.7%)
III	13 (54.2%)
IV	4 (16.7%)
Not applicable	2 (8.3%)
Sheldon tumor stage	
I	1 (4.2%)
II	4 (16.7%)
III	14 (58.3%)
IV	5 (20.8%)
Initial treatment	
Surgery with/without radiotherapy or chemotherapy	24 (100%)
Urachal excision or transurethral bladder tumor resection	19 (79.2%)
Partial cystectomy	5 (20.8%)
Radical cystectomy	0
Radiotherapy with/without chemotherapy	0
Chemotherapy	0
Metastasis site	
Local relapse	15 (62.5%)
Peritoneal or omental implantation	15 (62.5%)
Lymph node metastasis	11 (45.8%)
Lung	11 (45.8%)
Bone	4 (16.7%)
Liver	3 (12.5%)

Seven patients received adjuvant chemotherapy after surgery. Fourteen (58.3%) patients were diagnosed at staged III after surgery.

The most common metastasis was peritoneal or omental implantation (62.5%) and local relapse of the bladder (62.5%), lung (45.8%), and lymph nodes (45.8%). For first-line systematic chemotherapy, nine patients received XELOX (capecitabine and oxaliplatin), seven patients received TX (paclitaxel and capecitabine), and eight of them received other chemotherapy including GP (gemcitabine and cisplatin), TP (paclitaxel and cisplatin), TN (paclitaxel and nedaplatin), and tislelizumab (**Supplementary Table 1**). Since the regimens were heterogeneous and decided case by case, we compared the survival outcome in the following methods: 1) platinum-based (patients administered cisplatin, oxaliplatin, carboplatin, or nedaplatin) *vs.* non-platinum based; 2) taxol-based (patients received nanoparticle paclitaxel, paclitaxel liposome, or docetaxel) *vs.* non-taxol based; and 3) fluorouracil based (5-fluorouracil or capecitabine) *vs.* non-fluorouracil based. Sixteen patients received platinum-based regimens, 11 patients received taxol-based regimens, and 15 received fluorouracil-based regimens. The remaining one received tislelizumab monotherapy.

Overall, only one patient treated with XELOX achieved partial remission (PR), and no patient achieved complete remission (CR); the ORR among all treated patients was 4.2% (1/24). Seventeen patients presented stable disease (SD) after treatment. The DCR for all patients was 75% (18/24). The median PFS and OS were 7.43 and 29.7 months, respectively. The 6-month and 1-year PFS rates were 56.5% and 13.6%, respectively. The 2-year and 3-year OS rates were 57.3% and 19.1%, respectively (**Figures 1A, B**).

The DCR for patients treated with XELOX and TX as first-line chemotherapy was 100% (9/9) and 83.3% (5/6), respectively. The ORR for patients treated with XELOX was 11.1% (1/9). The median PFS in patients treated with and without platinum-based chemotherapy was 8.23 and 3.80 months (p = 0.032), respectively (**Figure 2A**). The 6-month PFS rates in patients with and without platinum-based chemotherapy were 56.5% and 19.0%, respectively. The median OS in in patients treated with and without platinum-based chemotherapy was 29.7 and 16.2 months (p = 0.63), respectively (**Figure 2B**). No significant difference was shown for both PFS and OS in patients treated with and without fluorouracil-based chemotherapy (**Figures 2C, D**). The patients treated with non-fluorouracil-based chemotherapy seemed to achieve longer OS

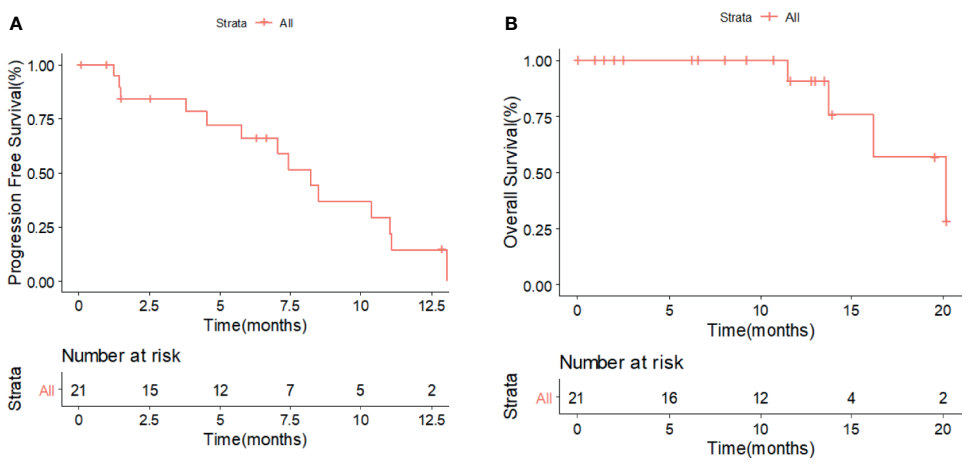

FIGURE 1 | Kaplan–Meier survival analysis for PFS **(A)** and OS **(B)** in all patients with advanced or metastatic MUT. PFS, progression-free survival; OS, overall survival; MUT, malignant urachal tumor.

(median OS: 34.6 *vs.* 16.2 months, $p = 0.094$). The patients treated with and without taxol-based chemotherapy presented similar median PFS (7.07 *vs.* 7.43 months) and median OS (29.7 *vs.* 20.2 months) (**Figures 2E, F**). The PFS and OS for patients with XELOX, TX, and other regimens revealed no significant difference (**Figures 3A, B**).

Among patients who achieved SD or PR, four patients received capecitabine maintenance therapy after combination chemotherapy of XELOX or TX. Two patients remained stable and still received capecitabine till now. Two patients progressed during maintenance at 8.2 and 18.4 months. Twelve patients received second-line chemotherapy after disease progression. The second-line chemotherapy was decided case by case. Two patients received XELOX, two patients received GP, two patients tried a combination of chemotherapy and immunotherapy, two patients received everolimus, and two patients were treated with bevacizumab combined with gemcitabine and nanoparticle paclitaxel. The remaining two patients were treated with irinotecan and capecitabine, and irinotecan and 5-FU (FOLFIRI). A total of five patients received immunotherapy, among which two received tislelizumab, one kind of immune checkpoint inhibitors, as a first-line treatment. A total of three patients received everolimus as second-line or third-line therapy. The median PFS for second-line regimens was 2.85 months (**Figure 4**). One patient achieved PFS for 13.7 months, taking on everolimus monotherapy. The patients were followed up in the outpatient clinic *via* telephone. The median follow-up for all patients was 13.0 months.

The incidences of any AEs and grade III to IV AEs in all patients are summarized in **Table 2**. The AEs for platinum and non-platinum-based regimens are also listed in **Table 2**. The principal AEs were hematological and gastrointestinal events, including leukopenia (70.8%), anemia (70.8%), elevated transaminase levels (33.3%), nausea (25.0%), hand and foot syndrome (16.7%), elevated serum creatinine levels (12.5%), and intestinal obstruction (12.5%). The major grade 3–4 AEs included thrombocytopenia (8.3%) and elevated transaminase levels (4.2%). One patient received changes in treatment of TX instead of TP due to severe intolerant creatinine elevation without progression. No treatment-related death occurred in all groups.

Seven patients received next-genome sequencing (NGS) test for potential targets (**Figure 5**). TP53 mutation was detected in five patients. One patient reported high tumor mutational burden (TMB), while the others presented low TMB. Patient 1 in **Figure 5** with high TMB presented the best response of SD and PFS of 5.2 months for second-line therapy of TX combined with tislelizumab after progression from tislelizumab monotherapy. Fibroblast growth factor receptor (FGFR) amplification, Myc amplification, ERBB4 amplification, and programmed death ligand-1 (PD-L1) expression of less than

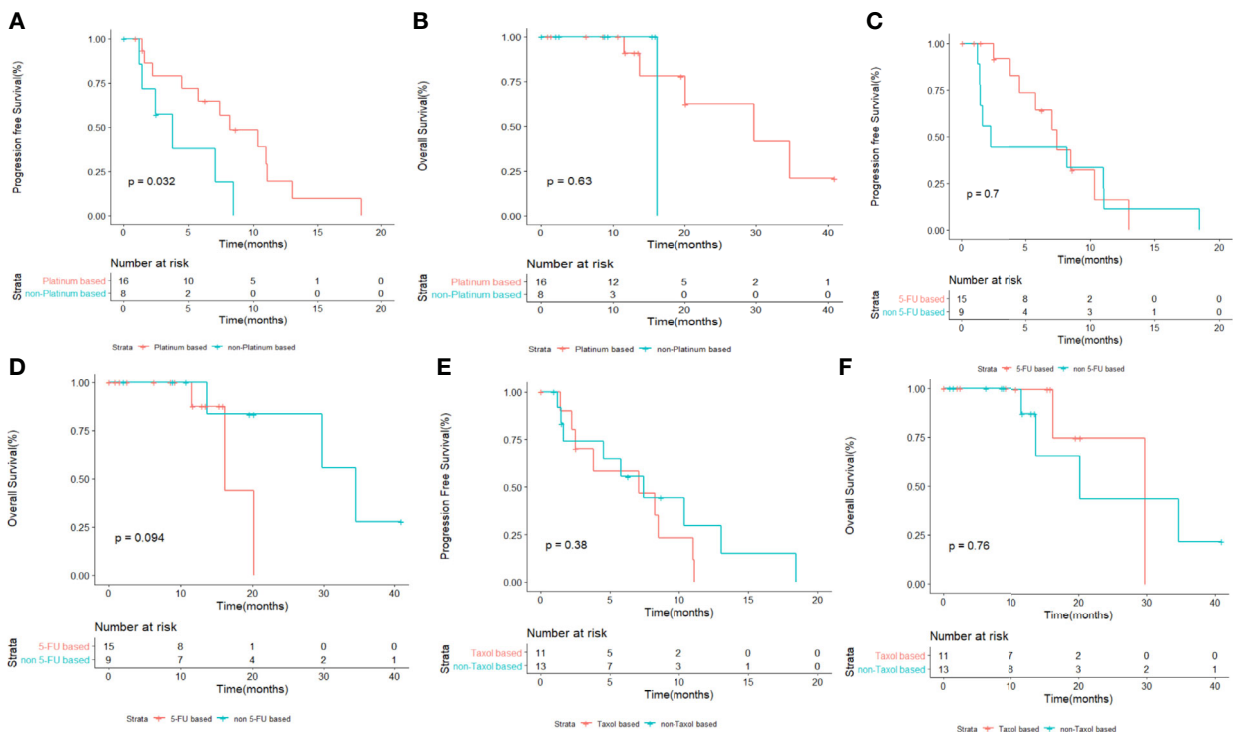

FIGURE 2 | Kaplan–Meier survival analysis for PFS **(A)** and OS **(B)** in patients with or without platinum-based therapy. Kaplan–Meier survival analysis for PFS **(C)** and OS **(D)** in patients with or without platinum-based therapy. Kaplan–Meier survival analysis for PFS **(E)** and OS **(F)** in patients with or without taxol-based therapy. PFS, progression-free survival; OS, overall survival.

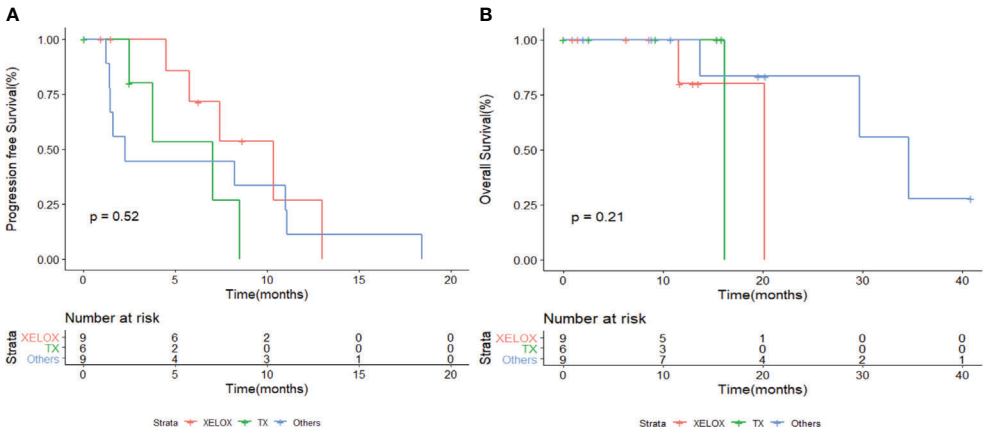

FIGURE 3 | Kaplan–Meier survival analysis for PFS **(A)** and OS **(B)** in patients with different chemotherapy regimens. PFS, progression-free survival; OS, overall survival.

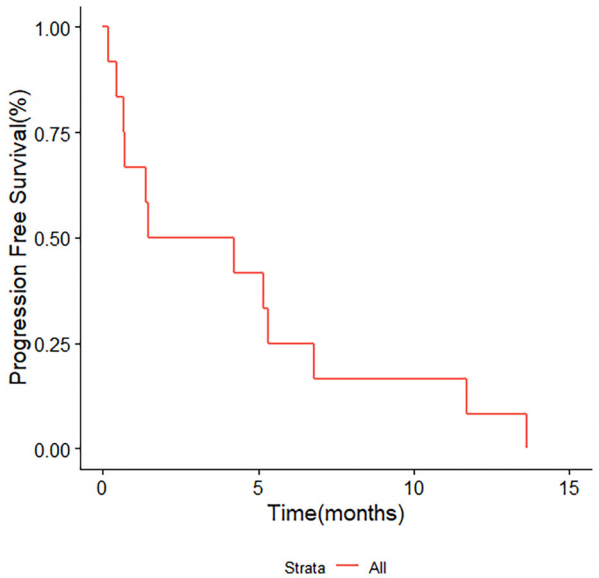

FIGURE 4 | Kaplan–Meier survival analysis for PFS in 12 patients treated with second-line chemotherapy. PFS, progression-free survival.

1% was detected in patient 4, with a PFS of 6.53 months for third-line therapy of XELOX and toripalimab after progression from TX and FOLFIRI regimens. Epidermal growth factor receptor (EGFR) amplification was detected in patient 5, with PR after XELOX treatment and undergoing capecitabine maintenance treatment until now.

DISCUSSION

The carcinoma of the urachus is a rare and aggressive malignant tumor with consequent few data about treatment outcome. We reported the experience in chemotherapy treatment for 24 patients of advanced or metastatic MUT. In our study, patients treated with platinum-based chemotherapy indicated prolonged PFS as compared with non-platinum-based regimens, providing promising options for systemic treatment. Second-line therapy varied in 12 patients, among which everolimus seemed to be effective for the longest PFS. NGS in seven cases revealed a prevalence of TP53 mutation.

Some population-based cohort reported the clinical outcome and prognostic factors in MUT (3, 7, 12). Hager et al. reported 154 and 152 cases of MUT in Germany and SEER database from 2011 to 2015, respectively; the relative 5 year-survival rates were 54.8% in Germany and 64.4% in the United States (7). Another population-based study, which summarized 152 cases of MUT in Netherlands, reported that only 13 out of 45 patients in stage IV received chemotherapy, with poor survival (3). Nagumo et al. reported the clinicopathological features of 456 patients with MUT in Japan (12). In this large retrospective study, it was showed that the most common modality for MUT was surgery alone. However, the chemotherapy regimens for metastatic cases in the article were not available (12). Thus, the proper treatment for metastatic MUT was still unknown. Histologically similar to colorectal adenocarcinoma, a few case reports showed the efficacy for 5-fluorouracil- and cisplatin-based chemotherapy, such as GP and FOLFOX (18, 19, 23). Yanagihara et al. reported modified FOLFOX chemotherapy in five patients with metastatic MUT, resulting in an ORR of 40% and a median OS of 42 months (19). Our study analyzed the first-line chemotherapy of 24 patients, demonstrating that platinum-based regimens were beneficial for patients. The DCR for patients who received platinum-based regimens was 75% (12/16). Most of the patients received oxaliplatin. Both platinum-based and non-platinum-based chemotherapy regimens were well tolerant, with anemia and leukopenia as the most common AEs. In **Figure 3**, it seemed that XELOX presented better PFS but was not statistically significant. Prospective studies are warranted to explore optimal chemotherapy regimens.

Some reports demonstrated that MUT had remarkable molecular similarities to colorectal cancer (24). Colorectal

TABLE 2 | Summary of adverse events.

	Patients (*n* = 24)		Platinum based (*n* = 16)		Non-platinum based (*n* = 8)	
Events, *n* (%)	Any grade	Grade 3~4	Any grade	Grade 3~4	Any grade	Grade 3~4
Any AE	24 (100%)	3 (12.5%)	16 (100%)	2 (12.5%)	8 (100%)	1 (12.5%)
Hematological toxic effects						
Anemia	17 (70.8%)	0	11 (68.7%)	0	6 (75.0%)	0
Leukopenia	17 (70.8%)	0	7 (62.5%)	0	7 (87.5%)	0
Thrombocytopenia	2 (8.3%)	2 (8.3%)	2 (12.5%)	2 (12.5%)	0	0
Fatigue	2 (8.3%)	0	2 (12.5%)	0	0	0
Diarrhea	1 (4.2%)	0	1 (6.2%)	0	0	0
Dyspepsia	2 (8.3%)	0	2 (12.5%)	0	0	0
Nausea	6 (25.0%)	0	5 (31.2%)	0	1 (12.5%)	0
Elevated transaminases	8 (33.3%)	1 (4.2%)	5 (31.2%)	0	2 (25.0%)	1 (12.5%)
Hand and foot syndrome	4 (16.7%)	0	1 (6.2%)	0	3 (37.5%)	0
Intestinal obstruction	3 (12.5%)	0	1 (6.2%)	0	2 (25.0%)	0
Serum creatinine increased	3 (12.5%)	0	2 (12.5%)	0	1 (12.5%)	0

AE, adverse event.

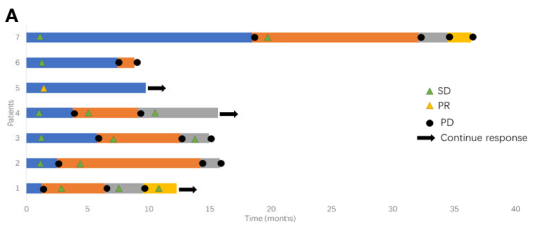

FIGURE 5 | **(A)** The swimmer's plot for patients with NGS detection and **(B)** summary for the NGS results. NGS, next-genome sequencing.

cancers are typified by alterations in several pathways, including adenomatous polyposis coli (APC) loss, the activation of the RAS/MAPK signaling pathway, and TGFβ (by SMAD4 inactivation) pathways (25). Nagy et al. analyzed 40 MUT cases and revealed the prevalence of APC and *PTEN* gene alternation (26). Henning Reis et al. presented 66% of TP53 mutation, 21% of KRAS mutation, 5% of EGFR amplification, and 16% of PD-L1 expression in 70 MUT patients (13). In our study, TP53 mutation was detected in five patients out of seven. We also detected FGFR amplification, EGFR amplification, APC mutation, and KRAS mutation among them. But none of them received anti-EGFR antibody. However, the efficacy of targeted therapy and immune therapy was still not clear. Collazo-Lorduy et al. found that one patient with EGFR amplification and wild-type KRAS achieved 8 months' response when treated with cetuximab (27). Microsatellite instability (MSI), detected in approximately 15% of all colorectal cancers, is a hypermutable phenotype leading to the loss of DNA MMR activity. MSI-high leads to the accumulation of mutation loads in cancer-related genes and the generation of neoantigens, which stimulate the antitumor immune response of the host, represents a better prognosis and significant association with long-term immunotherapy-related responses (28). In a study of Kardos et al., 25% of urachal tumors harbor inactivating mutations of MMR, MSH6, and MSH2, which might be predictive markers for immune checkpoint blockade (24). One patient with MSH6 mutation resulted in SD after treatment with atezolizumab (24). In our study, most patients were microsatellite stable (MSS). One patient with TMB-high presented more than 5-month PFS when treated with second-line TX and tislelizumab. One patient became SD for 13.7 months when treated with everolimus. Five patients tried different types of PD-1 antibodies, including tislelizumab and toripalimab. However, patients treated with immune checkpoint inhibitors did not present longer PFS and OS than those without immune checkpoint inhibitors. The application of immune checkpoint inhibitors and the biomarkers for prognosis in MUT needs more exploration. It is indicated that a combination of platinum-based chemotherapy with everolimus or anti-EGFR antibody might be promising in the future.

The limitation of this study lies in its retrospective nature and its heterogeneity in baseline risk and treatment factors, which may have led to potential bias. Nonetheless, only seven out of 24 patients underwent NGS, and more genome information is needed in the future. The main strength of the present study was that it analyzed chemotherapy in advanced MUT and showed optimal regimens among the Chinese population. Therefore, prospective clinical trials for this rare disease are warranted for confirmation.

DATA AVAILABILITY STATEMENT

The raw data supporting the conclusions of this article will be made available by the authors, without undue reservation.

ETHICS STATEMENT

The studies involving human participants were reviewed and approved by Sun Yat-Sen University Cancer Center. The ethics committee waived the requirement of written informed consent for participation.

AUTHOR CONTRIBUTIONS

YS and XA designed the study. M-TC, R-QH, M-QN, LL, H-FL, WY, A-QH, and Z-SZ collected the data. CX and M-TC analyzed and interpreted the data. M-TC and CX drafted the manuscript. YS and XA supervised and gave critical revision of the manuscript for important intellectual content. YS and XA provided administrative, technical, and material support. All authors contributed to the article and approved the submitted version.

ACKNOWLEDGMENTS

The authors thank all the patients, their families, and the institutions for supporting this study. They acknowledge all medical staff, staff nurses, and research nurses, all of whom strongly contributed to the success of the study.

SUPPLEMENTARY MATERIAL

The Supplementary Material for this article can be found online at: https://www.frontiersin.org/articles/10.3389/fonc.2021.739134/full#supplementary-material

REFERENCES

1. Claps M, Stellato M, Zattarin E, Mennitto A, Sepe P, Guadalupi V, et al. Current Understanding of Urachal Adenocarcinoma and Management Strategy. *Curr Oncol Rep* (2020) 22(1):9. doi: 10.1007/s11912-020-0878-z
2. Mylonas K, O Malley P, Ziogas I, El-Kabab L, Nasioudis D. Malignant Urachal Neoplasms: A Population-Based Study and Systematic Review of Literature. *Urol Oncol* (2017) 35(1):33.e11–9. doi: 10.1016/j.urolonc.2016.07.021
3. Bruins H, Visser O, Ploeg M, Hulsbergen-van de Kaa C, Kiemeney L, Witjes J. The Clinical Epidemiology of Urachal Carcinoma: Results of a Large, Population Based Study. *J Urol* (2012) 188(4):1102–7. doi: 10.1016/j.juro.2012.06.020
4. Szarvas T, Módos O, Niedworok C, Reis H, Szendröi A, Szász MA, et al. Clinical, Prognostic, and Therapeutic Aspects of Urachal Carcinoma-A Comprehensive Review With Meta-Analysis of 1,010 Cases. *Urol Oncol* (2016) 34(9):388–98. doi: 10.1016/j.urolonc.2016.04.012
5. Chen D, Li Y, Yu Z, Su Z, Ni L, Gui Y, et al. Investigating Urachal Carcinoma for More Than 15 Years. *Oncol Lett* (2014) 8(5):2279–83. doi: 10.3892/ol.2014.2502
6. Bi X, Wu Z, Han H, Zhou F. Clinical Comparison of Patients With Benign Urachal Masses *Versus* Urachal Carcinomas. *Chin J Cancer* (2017) 36(1):2. doi: 10.1186/s40880-016-0173-4
7. Hager T, Kraywinkel K, Szarvas T, Hadaschik B, Schmid K, Reis H. Urachal Cancer in Germany and the USA: An RKI/SEER Population-Based Comparison Study. *Urol Int* (2020) 104:803–9. doi: 10.1159/000509481
8. Dhillon J, Liang Y, Kamat A, Siefker-Radtke A, Dinney CP, Czerniak B, et al. Urachal Carcinoma: A Pathologic and Clinical Study of 46 Cases. *Hum Pathol* (2015) 46(12):1808–14. doi: 10.1016/j.humpath.2015.07.021
9. Niedworok C, Panitz M, Szarvas T, Reis H, Reis AC, Szendröi A, et al. Urachal Carcinoma of the Bladder: Impact of Clinical and Immunohistochemical Parameters on Prognosis. *J Urol* (2016) 195(6):1690–6. doi: 10.1016/j.juro.2015.11.067
10. Paner G, Lopez-Beltran A, Sirohi D, Amin M. Updates in the Pathologic Diagnosis and Classification of Epithelial Neoplasms of Urachal Origin. *Adv Anat Pathol* (2016) 23(2):71–83. doi: 10.1097/PAP.0000000000000110
11. Nambiyar K, Mitra S, Das A, Bal A. Adenocarcinoma of the Colon and Urinary Bladder: A Fortuitous or an Embryological Phenomenon? *Indian J Pathol Microbiol* (2021) 64(1):132–5. doi: 10.4103/IJPM.IJPM_825_19
12. Nagumo Y, Kojima T, Shiga M, Kojo K, Tanaka K, Kandori S, et al. Clinicopathological Features of Malignant Urachal Tumor: A Hospital-Based Cancer Registry Data in Japan. *Int J Urol* (2020) 27(2):157–62. doi: 10.1111/iju.14154
13. Reis H, van der Vos K, Niedworok C, Herold T, Módos O, Szendrői A, et al. Pathogenic and Targetable Genetic Alterations in 70 Urachal Adenocarcinomas. *Int J Cancer* (2018) 143(7):1764–73. doi: 10.1002/ijc.31547
14. Behrendt M, van Rhijn B. Genetics and Biological Markers in Urachal Cancer. *Transl Androl Urol* (2016) 5(5):655–61. doi: 10.21037/tau.2016.04.01
15. Riva G, Mian C, Luchini C, Girolami I, Ghimenton C, Cima L, et al. Urachal Carcinoma: From Gross Specimen to Morphologic, Immunohistochemical, and Molecular Analysis. *Virchows Arch* (2019) 474(1):13–20. doi: 10.1007/s00428-018-2467-1
16. Lee S, Lee J, Sim S, Lee Y, Moon KC, Lee C, et al. Comprehensive Somatic Genome Alterations of Urachal Carcinoma. *J Med Genet* (2017) 54(8):572–8. doi: 10.1136/jmedgenet-2016-104390
17. Gopalan A, Sharp D, Fine S, Tickoo SK, Herr HW, Reuter VE, et al. Urachal Carcinoma: A Clinicopathologic Analysis of 24 Cases With Outcome Correlation. *Am J Surg Pathol* (2009) 33(5):659–68. doi: 10.1097/PAS.0b013e31819aa4ae
18. Yaegashi H, Kadomoto S, Naito R, Makino T, Iwamoto H, Nohara T, et al. Metastatic Urachal Cancer Treated Effectively With Gemcitabine/Cisplatin Combination Chemotherapy and Radiotherapy: A Case Report. *Mol Clin Oncol* (2019) 11(2):139–42. doi: 10.3892/mco.2019.1865
19. Yanagihara Y, Tanji N, Miura N, Shirato A, Nishimura K, Fukumoto T, et al. Modified FOLFOX6 Chemotherapy in Patients With Metastatic Urachal Cancer. *Chemotherapy* (2013) 59(6):402–6. doi: 10.1159/000362400
20. Kume H, Tomita K, Takahashi S, Fukutani K. Irinotecan as a New Agent for Urachal Cancer. *Urol Int* (2006) 76(3):281–2. doi: 10.1159/000091635
21. Edge S, Compton C. The American Joint Committee on Cancer: The 7th Edition of the AJCC Cancer Staging Manual and the Future of TNM. *Ann Surg Oncol* (2010) 17(6):1471–4. doi: 10.1245/s10434-010-0985-4
22. Sheldon C, Clayman R, Gonzalez R, Williams R, Fraley E. Malignant Urachal Lesions. *J Urol* (1984) 131(1):1–8. doi: 10.1016/S0022-5347(17)50167-6
23. Tran B, McKendrick J. Metastatic Urachal Cancer Responding to FOLFOX Chemotherapy. *Can J Urol* (2010) 17(2):5120–3.
24. Kardos J, Wobker S, Woods M, Nielsen ME, Smith AB, Wallen EM, et al. Comprehensive Molecular Characterization of Urachal Adenocarcinoma Reveals Commonalities With Colorectal Cancer, Including a Hypermutable Phenotype. *JCO Precis Oncol* (2017) 1. doi: 10.1200/PO.17.00027
25. Schell M, Yang M, Teer J, Lo FY, Madan A, Coppola D, et al. A Multigene Mutation Classification of 468 Colorectal Cancers Reveals a Prognostic Role for APC. *Nat Commun* (2016) 7:11743. doi: 10.1038/ncomms11743

26. Nagy N, Reis H, Hadaschik B, Niedworok C, Módos O, Szendrői A, et al. Prevalence of APC and PTEN Alterations in Urachal Cancer. *Pathol Oncol Res POR* (2020) 26(4):2773–81. doi: 10.1007/s12253-020-00872-6
27. Collazo-Lorduy A, Castillo-Martin M, Wang L, Patel V, Iyer G, Jordan E, et al. Urachal Carcinoma Shares Genomic Alterations With Colorectal Carcinoma and May Respond to Epidermal Growth Factor Inhibition. *Eur Urol* (2016) 70 (5):771–5. doi: 10.1016/j.eururo.2016.04.037
28. Zhao P, Li L, Jiang X, Li Q. Mismatch Repair Deficiency/Microsatellite Instability-High as a Predictor for Anti-PD-1/PD-L1 Immunotherapy Efficacy. *J Hematol Oncol* (2019) 12(1):54. doi: 10.1186/s13045-019-0738-1

Conflict of Interest: The authors declare that the research was conducted in the absence of any commercial or financial relationships that could be construed as a potential conflict of interest.

Publisher's Note: All claims expressed in this article are solely those of the authors and do not necessarily represent those of their affiliated organizations, or those of the publisher, the editors and the reviewers. Any product that may be evaluated in this article, or claim that may be made by its manufacturer, is not guaranteed or endorsed by the publisher.

frontiers in Oncology

ORIGINAL RESEARCH
published: 24 September 2021
doi: 10.3389/fonc.2021.712553

Lymph Node Dissections for T3T4 Stage Penile Cancer Patients Without Preoperatively Detectable Lymph Node Metastasis Bring More Survival Benefits: A Propensity Matching Analysis

Han Li[1,2†], Yucheng Ma[1†], Zhongyu Jian[1†], Xi Jin[1], Liyuan Xiang[1], Hong Li[1] and Kunjie Wang[1]*

[1] Department of Urology, Institute of Urology (Laboratory of Reconstructive Urology), West China Hospital, Sichuan University, Chengdu, China, [2] Department of Urology, Chengdu No. 5 People's Hospital, Chengdu, China

Background and Aims: The current guidelines for the treatment of penile cancer patients with clinically non-invasive normal inguinal lymph nodes are still broad, so the purpose of this study is to determine which patients are suitable for lymph node dissection (LND).

Methods: Histologically confirmed penile cancer patients (primary site labeled as C60.9-Penis) from 2004 to 2016 in the Surveillance, Epidemiology, and Results database were included in this analysis. Univariate and multivariate Cox regression analyses were applied to determine an overall estimate of LND on overall survival and cancer-specific survival. A 1:1 propensity matching analysis (PSM) was applied to enroll balanced baseline cohort, and further Kaplan–Meier (KM) survival analysis was used to get more reliable results.

Results: Out of 4,458 histologically confirmed penile cancer patients with complete follow-up information, 1,052 patients were finally enrolled in this analysis. Age, pathological grade, T stage, and LND were identified as significant predictors for overall survival (OS) in the univariate Cox analysis. In the multivariate Cox regression, age, pathological grade, T stage, and LND were found significant. The same results were also found in the univariate and multivariate Cox regression analyses for cancer-specific survival (CSS). After the successful PSM, further KM analysis revealed that LND could bring significant OS and CSS benefits for T3T4 patients without lymph node metastasis.

Conclusion: Lymph node dissection may bring survival benefits for penile cancer patients without preoperatively detectable lymph node metastasis, especially for T3T4 stage patients. Further randomized control trial is needed.

Keywords: penile cancer, lymph node metastasis, lymph node dissections, propensity matching analysis, SEER

OPEN ACCESS

Edited by:
Francesca Sanguedolce, University of Foggia, Italy

Reviewed by:
Ugo Giovanni Falagario, University of Foggia, Italy
Oliver Walther Hakenberg, University Hospital Rostock, Germany
Ning Zhang, Peking University Cancer Hospital, China
Zheng Liu, National Cancer Center of China, China

****Correspondence:***
Kunjie Wang
wangkj@scu.edu.cn

†These authors have contributed equally to this work and share first authorship

Specialty section:
This article was submitted to Genitourinary Oncology, a section of the journal Frontiers in Oncology

Received: *20 May 2021*
Accepted: *06 September 2021*
Published: *24 September 2021*

Citation:
Li H, Ma Y, Jian Z, Jin X, Xiang L, Li H and Wang K (2021) Lymph Node Dissections for T3T4 Stage Penile Cancer Patients Without Preoperatively Detectable Lymph Node Metastasis Bring More Survival Benefits: A Propensity Matching Analysis. Front. Oncol. 11:712553. doi: 10.3389/fonc.2021.712553

INTRODUCTION

Penile cancer is a malignant disease with a high mortality rate. According to reported data, about one-third of patients with radical treatment still fail to achieve 5-year survival (1). Regional lymph node (LN) metastasis is a crucial prognostic factor for penile cancer (2). For pN0 penile cancer patients, 5-year cancer-specific survival (CSS) is about 85%–100%, but for lymph node metastasis patients, 5-year CSS is about 79%–89% for pN1, 17%–60% for pN2, and 0%–17% for pN3 (3, 4). Some previously published studies indicated that for patients with low-graded penile cancer (≤T1a), lymph node metastasis could be 0%–30%. For patients with higher graded penile cancer (≥T1b), lymph node metastasis could approach nearly 50% (5). Due to the high incidence of lymph node metastasis in penile cancer, a study has suggested that prophylactic lymph node dissection may provide survival benefits for patients with penile cancer regardless of their stage or grade (6). In the EAU guidelines of penile cancer, for patients with clinically normal inguinal lymph nodes (cN0), surveillance, invasive nodal staging, and prophylactic lymph node dissection (LND) are three main strategies; however, surveillance is only recommended in patients with pTis/pTa tumor. Invasive nodal staging is recommended because there is still no effective imaging technique that can be applied to detect micrometastasis (3).

However, previous studies have tended to include a small number of cases. Given the low incidence of penile cancer, therefore, a larger case-size study is needed to discuss the effect of preoperative prophylactic lymph node dissection for penile cancer on survival (6–10). The purpose of this study it is to figure out the effect of preoperative prophylactic LND on patient survival with the large number of penile cancer patients in the Surveillance, Epidemiology, and Results (SEER) database.

MATERIAL AND METHODS

Study Population

Histologically confirmed penile cancer patients (primary site labeled as C60.9-Penis) from 2004 to 2016 with complete follow-up information in the SEER database were included in this analysis. The exclusion criteria were as follows: 1) patients with any other cancer before penile cancer diagnosis, 2) patients with unclear age information or unclear tumor grade information, 3) patients with any identified positive N stage or M stage before surgery, 4) patients with any unclear TNM stage information, 5) patients with unclear lymph node dissection information, 6) patients with unclear follow-up information, and 7) patients who did not receive surgery.

Overall survival (OS) and penile CSS were the two main outcome events in this study, and the SEER follow-up project offered related information. In this study, LND was defined as four or more lymph nodes that were removed.

Statistical Analysis

Based on the LND definition mentioned above, patients were classified as LND and non-LND groups. Baseline characteristic comparisons were performed as follows: *t*-test and the Mann–Whitney test were used to test for continuous variables that were normally distributed and non-normally distributed, respectively. Categorical variables were presented with the number (percentage) and tested by the chi-square test or the Fisher's exact test. Univariate and multivariate Cox regression analyses were carried out to find significant risk factors for OS and CSS in penile cancer patients. To more objectively evaluate the effect of LND on the survival of penile cancer patients without lymphatic or distant organ metastasis, a 1:1 propensity score matching (PSM) was applied to generate a baseline balanced cohort. Standardized mean difference (SMD, $|d|$) was calculated to evaluate baseline balance (11). After PSM, Kaplan–Meier (KM) analysis was conducted between LND and non-LND groups for OS and CSS. Since there can be randomness in the PSM cohort, further 100 times PSM and consequent KM analysis were performed to obtain a complete result. Log-rank tests were used for KM analysis.

Since we do not know if patients have positive nodes before we take it out, so it is reasonable to recheck our results obtained from lymphatic metastasis-free cohort in the primary SEER penile cancer cohort in which patients with positive N stage or M stage were retained.

All statistical analyses above were achieved through R v.4.0.3 (www.r-project.org), and *rms*, *survival*, *caret*, *broom*, *survminer*, *Matching*, and *tableone* were the main R packages used in this study. All the reported *P*-values were two-sided, and significance was indicated as $P < 0.05$.

RESULTS

Characteristics of the Patients

Out of 4,458 patients identified in the SEER database between 2004 and 2019, 1,052 patients were finally enrolled in this analysis based on inclusion and exclusion criteria.

Table 1 demonstrates the characteristics of included patients. One hundred forty-six (13.9%) patients received LND, and LND patients were significantly younger than non-LND patients ($P < 0.001$). Compared with non-LND patients, more high-grade patients ($P < 0.001$) and T3T4 patients ($P < 0.001$) received LND treatment. Since all the positive N and M stage patients were excluded, only a few patients receive chemotherapy (30, 2.9%) and radiation therapy (28, 2.7%). In all patients with LND, no positive lymph nodes were reported.

Univariate and Multivariate Cox Regression

Table 2 demonstrates the univariate and multivariate for OS in penile cancer patients. In the univariate analysis stage, age (<0.001), pathological grade (grade I as the reference, grade II $P < 0.001$, grade III $P < 0.001$), and LND were significant ($P < 0.001$), but T stage (T1T2 as the reference, T3T4 $P = 0.54$) was not significant. However, T stage was identified as a significant factor (HR: 1.47, $P = 0.007$) for OS in the multivariate analysis.

TABLE 1 | Baseline characteristics of included patients.

Variables	Non-LND (*n* = 906)	LND (*n* = 146)	*P*
Age (years, mean ± SD)	63.4 ± 12.57	57.81 ± 13.16	<0.001
Race (*n*)			0.421
White	749 (82.7)	123 (84.2)	
Black	104 (11.5)	13 (8.9)	
Asian or Pacific Islander	40 (4.4)	7 (4.8)	
American Indian/Alaska Native	10 (1.1)	1 (0.7)	
Unknown	3 (0.3)	2 (1.3)	
Grade (*n*)			<0.001
Well differentiated, grade I	352 (38.9)	28 (19.2)	
Moderately differentiated, grade II	423 (46.7)	94 (64.4)	
Poorly differentiated, grade III	127 (14.0)	24 (16.4)	
Undifferentiated, grade IV	4 (0.4)	9 (6.2)	
T stage			<0.001
TaTx	4 (0.4)	0 (0.0)	
T1T2	794 (87.6)	109 (74.7)	
T3T4	108 (11.9)	37 (25.3)	
Pathological type			0.691
Squamous cell carcinoma	902 (99.6)	145 (99.3)	
Other type	4 (0.4)	1 (0.7)	
Chemotherapy (*n*)	27 (3.0)	3 (2.1)	0.533
Radiation therapy (*n*)	23 (2.5)	5 (3.4)	0.537
Regional nodes positive	/	0 (0)	/

TABLE 2 | Univariate and multivariate Cox regression for overall survival.

	Univariate analysis			Multivariate analysis		
	HR	95% CI	*P*	Adjusted HR	95% CI	*P*
Age (per year old)	1.05	(1.04, 1.06)	<0.001	1.05	(1.04, 1.06)	<0.001
Grade						
Well differentiated, grade I	Ref.			Ref.		
Moderately differentiated, grade II	1.59	(1.25, 2.01)	<0.001	1.64	(1.29, 2.09)	<0.001
Poorly differentiated, grade III	1.90	(1.39, 2.59)	<0.001	1.77	(1.29, 2.43	<0.001
Undifferentiated, grade IV[a]	/	/	/	/	/	/
T stage						
T1T2	Ref.			Ref.		
T3T4	1.31	(0.99, 1.73)	0.54	1.47	(1.11, 1.94)	0.007
Pathological type			0.36			0.39
Squamous cell carcinoma	2.50	(0.35, 17.83)		2.38	(0.33, 17.07)	
Other type	Ref.			Ref.		
Lymph node dissection (yes)	0.41	(0.27, 0.61)	<0.001	0.42	(0.28, 0.63)	<0.001
Chemotherapy (yes)	0.60	(0.35, 1.02)	0.58	0.64	(0.34, 1.14)	0.131
Radiation therapy (yes)	1.23	(0.71, 2.15)	0.457	1.14	(0.63, 2.08)	0.664

[a]*Insufficient endpoint event for univariate or multivariate analysis.*

Similar results could be found in the Cox regression for CSS (**Table 3**). LND was a significant predictive factor for penile cancer CSS (HR = 0.42, $P = 0.005$) in the univariate analysis, and it also could be identified as a predictive factor for CSS (HR: 0.32, $P < 0.001$) after the adjustment (**Table 3**).

Propensity Score Matching and Further KM Analysis

After the PSM, out of 86 LND patients, 139 patients were matched to 139 non-LND patients, and a total of 278 patients were enrolled into consequent KM analysis. Before the PSM, there were potential baseline differences found in age ($|d| = 0.436$), race ($|d| = 0.148$), grade ($|d| = 0.463$), and T stage ($|d| = 0.414$) between LND and non-LND patients according to $|d|$ values. After the PSM, most potential baseline differences were well balanced (**Table 4**). In the KM analysis conducted within the PSM cohort ($n = 162$), LND could offer better OS ($P = 0.00025$) and CSS ($P = 0.0043$) (**Figure 1**). The main PSM cohort was generated with random seed 202104. To avoid selection bias caused by the randomness of the PSM, further 100 times PSM without random seed and consequent KM analysis were performed, and the results indicated that the main PSM results were robust for OS ($P = 0.0025$, 95% CI: 0.0014–0.0036, **Figure S3A**) and CSS ($P = 0.024$, 95% CI: 0.018–0.030, **Figure S3B**).

To clarify which T stage and tumor pathological grade patients could benefit from LND treatment, subgroup KM analysis was conducted. In the T stage subgroup analysis, it

TABLE 3 | Univariate and multivariate Cox regression for cancer-specific survival.

	Univariate analysis			Multivariate analysis		
	HR	**95% CI**	***P***	**Adjusted HR**	**95% CI**	***P***
Age (per year old)	1.02	(1.00, 1.03)	0.01	1.01	(1.00, 1.03)	0.049
Grade						
Well differentiated, grade I	Ref.			Ref.		
Moderately differentiated, grade II	3.34	(2.16, 5.18)	<0.001	3.51	(2.26, 5.44)	<0.001
Poorly differentiated, grade III	3.38	(1.97, 5.79)	<0.001	3.24	(1.88, 5.59)	<0.001
Undifferentiated, grade IV	4.11	(0.56, 30.31)	0.166	4.56	(0.62, 33.75)	0.137
T stage						
T1T2	Ref.			Ref.		
T3T4	1.81	(1.23, 2.66)	0.002	1.84	(1.25, 2.73)	0.002
Pathological type						
Squamous cell carcinoma[a]	/	/	/	/	/	/
Other type	Ref.			Ref.		
Lymph node dissection (yes)	0.42	(0.23, 0.77)	0.005	0.32	(0.17, 0.60)	<0.001
Chemotherapy (yes)	2.05	(1.01, 4.19)	0.048	1.63	(0.76, 3.51)	0.211
Radiation therapy (yes)	1.66	(0.78, 3.55)	0.188	1.38	(0.61, 3.11)	0.434

[a]*Insufficient endpoint event for univariate or multivariate analysis.*

TABLE 4 | Comparison of clinical patient characteristics between LND and non-LND groups before and after propensity score matching.

Parameters	**Before propensity matching (*n* = 1,051)**				**After propensity matching (*n* = 1,278)**			
	Non-LND (*n* = 906)	**LND patients (*n* = 146)**	***P***	**|*d*|**	**LND patients (*n* = 139)**	**Non-LND patients (*n* = 139)**	***P***	**|d|**
Age (mean ± SD)	63.4 ± 12.57	57.81 ± 13.16	<0.001	0.436	58.48 ± 12.86	59.02 ± 12.27	0.721	0.043
Race (*n*, %)			0.421	0.148			0.800	0.154
White	749 (82.7)	123 (84.2)			122 (87.8)	117 (84.2)		
Black	104 (11.5)	13 (8.9)			10 (7.2)	13 (9.4)		
Asian or Pacific Islander	40 (4.4)	7 (4.8)			4 (2.9)	7 (5.0)		
American Indian/Alaska Native	10 (1.1)	1 (0.7)			2 (1.4)	1 (0.7)		
Unknown	3 (0.3)	2 (1.3)			1 (0.7)	1 (0.7)		
Grade (*n*, %)			<0.001	0.463			0.947	0.040
Well differentiated, grade I	352 (38.9)	28 (19.2)			28 (20.1)	28 (20.1)		
Moderately differentiated, grade II	423 (46.7)	94 (64.4)			89 (64.0)	87 (62.6)		
Poorly differentiated, grade III	127 (14.0)	24 (16.4)			22 (15.8)	24 (17.3)		
Undifferentiated, grade IV	4 (0.4)	9 (6.2)			0 (0.0)	0 (0.0)		
T stage (*n*, %)			<0.001	0.414			0.778	0.034
TaTx	4 (0.4)	0 (0.0)			0 (0.0)	0 (0.0)		
T1T2	794 (87.6)	109 (74.7)			107 (77.0)	105 (75.5)		
T3T4	108 (11.9)	37 (25.3)			32 (23.0)	34 (24.5)		
Pathological type			0.691	0.032			1.000	0.120
Squamous cell carcinoma	902 (99.6)	145 (99.3)			139 (100.0)	138 (99.3)		
Other type	4 (0.4)	1 (0.7)			0 (0.0)	0 (0.7)		
Chemotherapy (*n*, %)	27 (3.0)	3 (2.1)	0.533	0.059	1 (0.7)	3 (2.2)	0.615	0.121
Radiation therapy (*n*, %)	23 (2.5)	5 (3.4)	0.537	0.052	2 (1.4)	5 (3.6)	0.444	0.138

was found that no OS benefit could be obtained from LND for T1T2 patients, but CSS benefit could not be achieved (**Figures 2A–D**). T3T4 patients could benefit from LND for both OS and CSS (**Figures 2E–H**). In the pathological tumor grade subgroup analysis, it was found that grade 1/2 patients might obtain OS and CSS benefit from LND treatment according to the PSM results (**Figures 3A–D**), and grade 3/4 patients could not obtain OS or CSS benefit from LND (**Figures 3E–H**). However, there were only 40 T3T4 penile cancer patients analyzed in this study, the sample size was small, and related results should be treated with caution.

Subgroup Analysis Based on the Combination of T Stage and G Stage

We further divided patients with penile cancer into Ta, T1a (G1, G2) *vs.* T1b (G3) and T2 *vs.* T3 (any G) *vs.* T4 groups to evaluate the benefit of LND in each subgroup. Considering the small number of patients in each subgroup, we did not conduct multivariate analysis and further PSM analysis. In the KM analysis, we found that in the Ta, T1a (G1, G2) group, LND could not offer OS (**Figure 4A**) or CSS (**Figure 4B**) benefits for penile cancer. This may be due to the small number of LND patients in this group, and the results were not robust. In the T1b

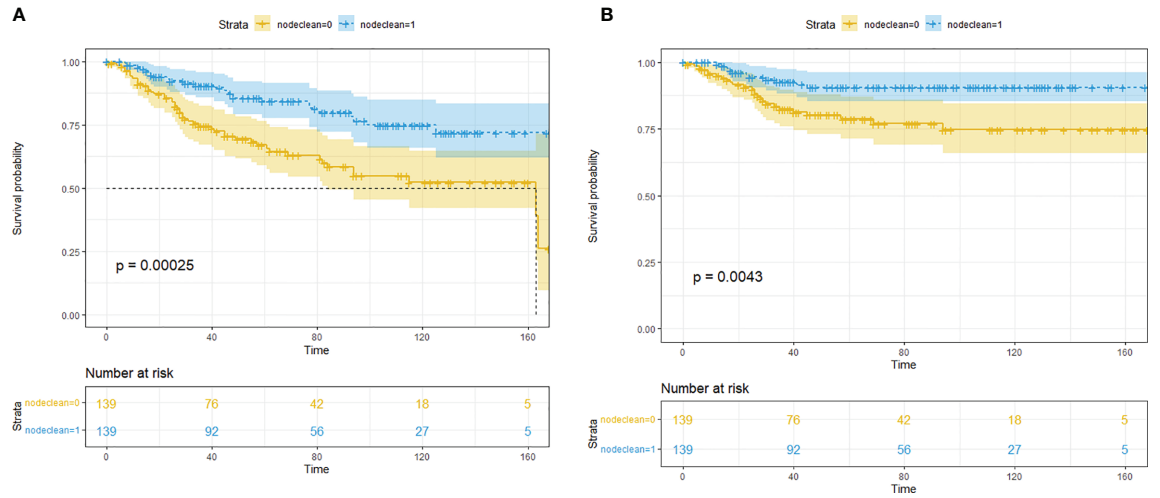

FIGURE 1 | Kaplan–Meier survival analysis for lymph node dissection (LND) in the propensity score matching (PSM) cohort. **(A)** Overall survival. **(B)** Cancer-specific survival.

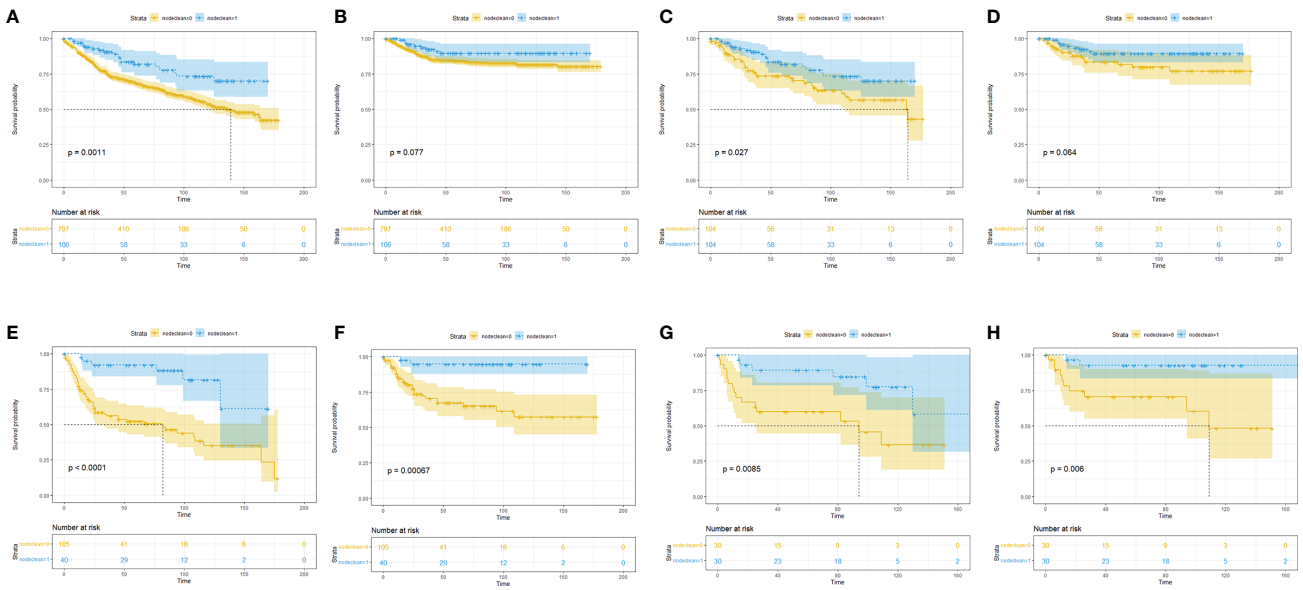

FIGURE 2 | Subgroup Kaplan–Meier survival analysis for LND. **(A)** Overall survival in the T1T2 subgroup based on the full cohort. **(B)** Cancer-specific survival in the T1T2 subgroup based on the full cohort. **(C)** Overall survival in the T1T2 subgroup based on the PSM cohort. **(D)** Cancer-specific survival in the T1T2 subgroup based on the PSM cohort. **(E)** Overall survival in the T3T4 subgroup based on the full cohort. **(F)** Cancer-specific survival in the T3T4 subgroup based on the full cohort. **(G)** Overall survival in the T3T4 subgroup based on the PSM cohort. **(H)** Cancer-specific survival in the T3T4 subgroup based on the PSM cohort.

(G3) and T2 group, LND could offer both significant OS (**Figure 4C**) and CSS (**Figure 4D**) benefits, and the same results could be also detected in the T3 (any G) group (**Figures 4E, F**). This phenomenon may indicate that the lower the degree of differentiation, the higher the possibility of metastasis for penile cancer cells. However, since there were only 12 patients in the T4 subgroup, KM analysis was omitted.

Validation in the Primary SEER Penile Cancer Cohort

The above analysis was based on a cohort of patients with non-lymph node metastatic penile cancer confirmed by preoperative physical examination, imaging examination, and postoperative pathology (although micrometastases are still possible). However, in clinical practice, it is difficult to confirm the status

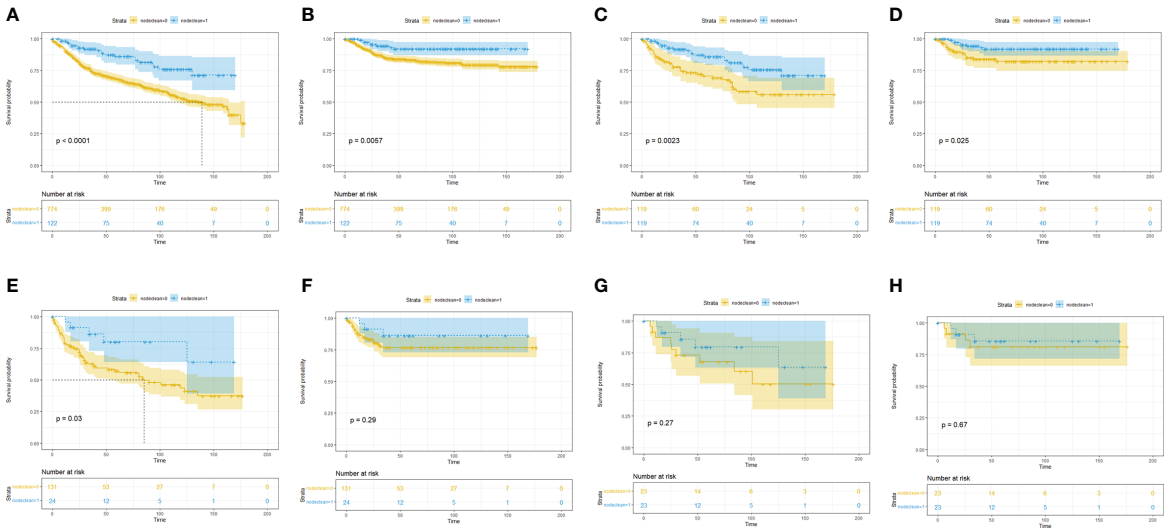

FIGURE 3 | Subgroup Kaplan–Meier survival analysis for LND. **(A)** Overall survival in the grade 1/2 subgroup based on the full cohort. **(B)** Cancer-specific survival in the grade 1/2 subgroup based on the full cohort. **(C)** Overall survival in the grade 1/2 subgroup based on the PSM cohort. **(D)** Cancer-specific survival in the grade 1/2 subgroup based on the PSM cohort. **(E)** Overall survival in the grade 3/4 subgroup based on the full cohort. **(F)** Cancer-specific survival in the grade 3/4 subgroup based on the full cohort. **(G)** Overall survival in the grade 3/4 subgroup based on the PSM cohort. **(H)** Cancer-specific survival in the grade 3/4 subgroup based on the PSM cohort.

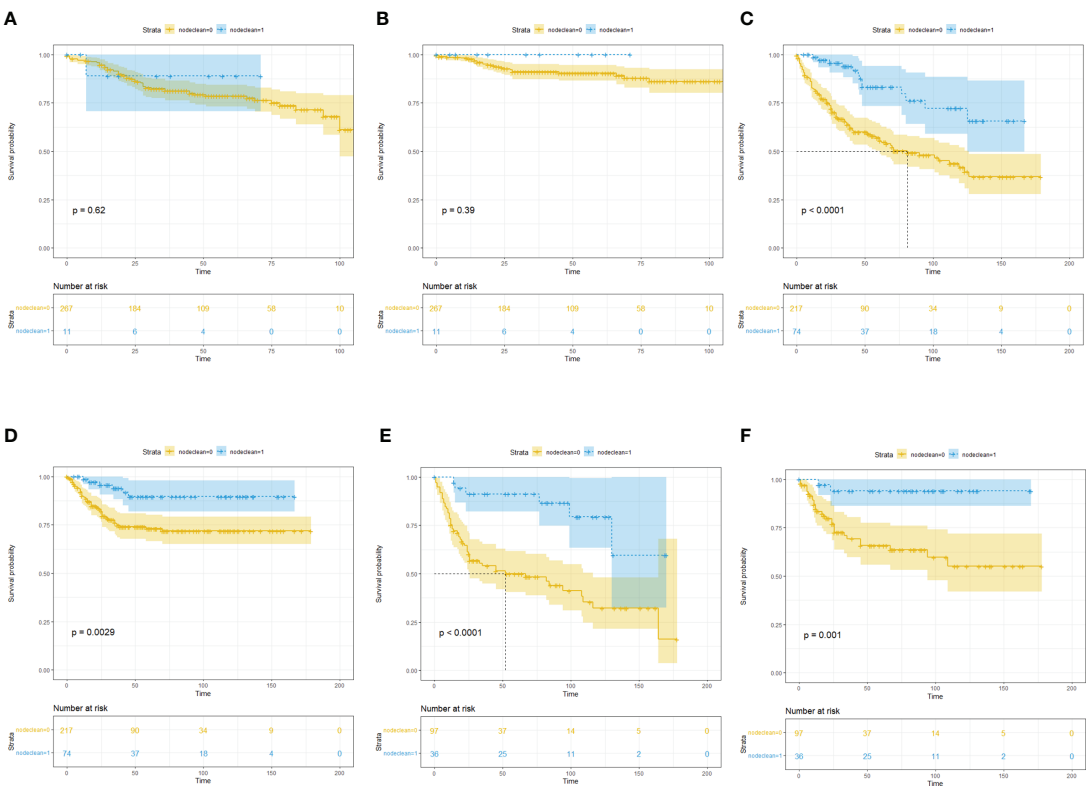

FIGURE 4 | Subgroup Kaplan–Meier survival analysis for LND. **(A)** Overall survival in the Ta, T1a (G1, G2) subgroup. **(B)** Cancer-specific survival in the Ta, T1a (G1, G2) subgroup. **(C)** Overall survival in the T1b (G3) and T2 subgroup. **(D)** Cancer-specific survival in the T1b (G3) and T2 subgroup. **(E)** Overall survival in the T3 (any G) subgroup. **(F)** Cancer-specific survival in the T3 (any G) subgroup.

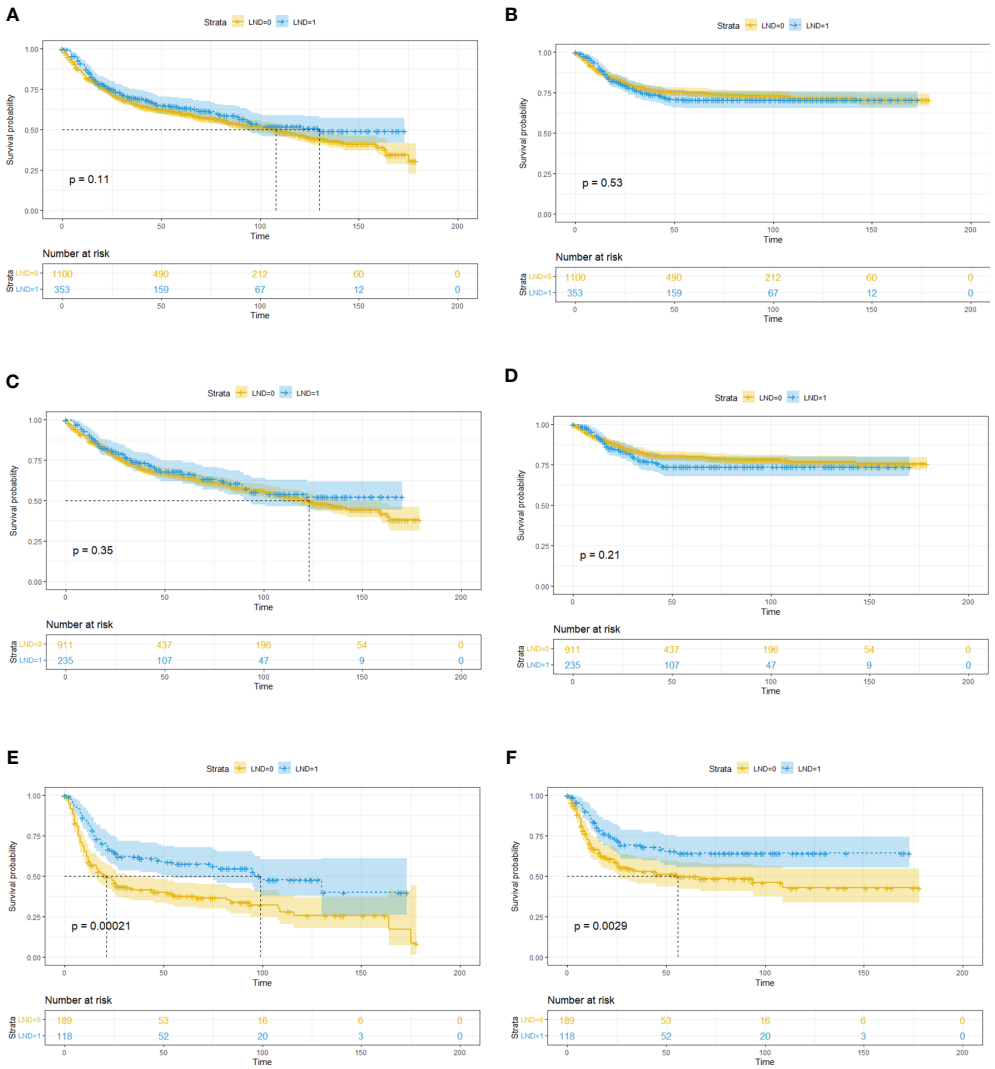

FIGURE 5 | Subgroup Kaplan–Meier survival analysis for LND in the primary SEER penile cancer cohort (patients with positive N stage or M stage were retained). **(A)** Overall survival for the whole cohort. **(B)** Cancer-specific survival for the whole cohort. **(C)** Overall survival in the T1T2 subgroup. **(D)** Cancer-specific survival in the T1T2 subgroup. **(E)** Overall survival in the T3T4 subgroup. **(F)** Cancer-specific survival in the T3T4 subgroup.

TABLE 5 | Multivariate Cox regression analysis for LND in the T3T4 subgroup penile cancer patients.

Clinical variable	Multivariate Cox regression		
	Adjusted HR*	95% CI	*P*
LND	0.51 (for OS)	(0.37, 0.72)	<0.001
	0.48 (for CSS)	(0.32, 0.72)	<0.001

**HR was adjusted by age, tumor grades, T stages, pathological type, chemotherapy history and radiation therapy history.*

of lymphatic metastases prior to lymph node biopsy or LND. Therefore, it is necessary to validate the above results in the original SEER database cohort without excluding the positive N stage patients.

Baseline comparisons for the primary SEER penile cancer cohort are shown in **Table S1**. In the KM analysis for the full cohort, T1T2 subgroup, and T3T4 group, LND could only bring OS and CSS benefits in the T3T4 subgroup, which was consistent with previous conclusions (**Figure 5**). In the further multivariate Cox regression analysis, LND was still a significant predictive factor for T3T4 penile cancer patients (**Table 5**), which was also robust.

DISCUSSION

In this study, we found that, parallel to many previous studies, T stage and pathological grading of penile cancer are important prognostic

factors (12, 13). In the univariate and multivariate analyses for OS, LND was a significant risk factor (HR: 1.81, $P < 0.001$). In the univariate and multivariate analyses for CSS, LND was a significant predictive factor (HR: 0.42, $P = 0.034$). To avoid potential selection bias and baseline imbalance bias, analysis after postrandomization procedures found that LND could offer both OS ($P = 0.0073$) and CSS ($P = 0.0063$) benefits in the PSM cohort. Further subgroup analysis indicated that LND could offer OS or CSS benefits for T3T4 patients but not for T1T2 patients. In the pathological grade subgroup analysis, grade 1/2 patients could obtain OS and CSS benefits from LND, but grade 3/4 patients could not.

Nowadays, penile cancer is a rare urinary cancer but with significant mortality (7). The primary pathological type of penile cancer is squamous cell carcinoma, and other pathological types only account for a tiny proportion of the total (14). In this study, more than 90% are squamous cell penile carcinoma (and its subtype). In developed countries, the incidence of penile cancer is very low, and this phenomenon may be related to penile cancer risk factors (15). Although no comprehensive meta-analysis of penile cancer risk factors has been published, some studies have indicated that HPV infection, circumcision, and hygiene may play a significant role (16, 17). The current surgical treatment for penile cancer includes organ-sparing therapy and radical treatment (3, 18). For non-invasive penile cancer involving only the glans, partial glansectomy and total glansectomy are the main surgical options (3). The most critical procedure of organ-sparing surgery is to ensure a negative margin (19). For invasive penile cancer, the surgical plan should be determined according to the different sites and extent of tumor invasion (20–22).

Lymph node metastases of penile carcinoma are usually carried out in anatomic order, starting with superficial or deep inguinal lymph nodes followed by pelvic lymph nodes (23, 24). Radical inguinal lymph node dissection or pelvic lymph node dissection should be recommended for patients with detectable preoperative lymph node metastasis (3, 25). For patients whose lymph node metastases cannot be detected preoperatively, the current main guidelines recommend that monitoring, lymph node biopsy, and radical lymphatic dissection are all acceptable (3, 26). However, considering the high probability of lymph node micrometastases in penile cancer patients, some studies suggest that active lymph node dissection can still benefit patients with negative lymph nodes examined preoperatively (27, 28). With the existing imaging methods, it is challenging to detect metastases in a small number of tumor cells before they form detectable tissue masses effectively. When the biopsy is used to detect lymph nodes, it is also challenging to avoid insufficient sampling. However, radical LND for penile cancer is highly associated with postoperative complications. Based on previously published studies, overall postoperative complication after the radical LND for penile cancer was about 80% including hematoma, lymphocele, skin necrosis, infection, and chronic scrotal pain, and the major complication was about 20% (29, 30). Therefore, if it is not clear that LND can indeed bring significant survival benefits, urologists always have many worries when taking LND for penile cancer.

According to the results of this study, a more aggressive lymph node dissection strategy for penile cancer patients with the higher stage (T3T4) may provide survival benefits. However, since the SEER database does not provide data about the intraoperative and postoperative complications of the patients, it is difficult to assess the impact of an aggressive lymph node dissection strategy on patients. Therefore, we suggest that when considering lymph node dissection strategies for patients with higher stages, the primary conditions of patients should also be considered to avoid complications as far as possible. At present, many valuable studies have been published on whether LND should be performed (31–33). We should make full use of existing tools to evaluate whether LND is needed.

There are still some limitations in this study. SEER is a population registry including a high percentage of patients diagnosed with penile cancer but not all of them. Second, no information on the template used for LND nor the technique are available (availability of frozen section, unilateral *vs.* bilateral, superficial *vs.* extended LND). Third, it does not include information on the performance status of the patients. This is clearly associated with the decision to perform LND or not.

CONCLUSION

Lymph node dissection may bring survival benefits for penile cancer patients without preoperatively detectable lymph node metastasis, especially for T3T4 stage patients. Further randomized control trial is needed.

DATA AVAILABILITY STATEMENT

The original contributions presented in the study are included in the article/**Supplementary Material**. Further inquiries can be directed to the corresponding author.

AUTHOR CONTRIBUTIONS

KW had full access to all the data in the study and takes responsibility for the integrity of the data and the accuracy of the data analysis. Study concept and design: HaL, YM, and KW. Acquisition of data: YM, ZJ, HaL, and KW. Analysis and interpretation of data: HaL, YM, ZJ, XJ, and LX. Drafting of the manuscript: YM, HL, KW, and HaL. Critical revision of the manuscript for important intellectual content: YM, ZJ, HaL, and KW. Statistical analysis: YM and ZJ. Obtaining funding: KW and HaL. Administrative, technical, or material support: KW. Supervision: HoL and KW. All authors contributed to the article and approved the submitted version.

FUNDING

This study was supported by the 1.3.5 Project for Disciplines of Excellence, West China Hospital, Sichuan University (ZY2016104, ZYGD18011).

SUPPLEMENTARY MATERIAL

The Supplementary Material for this article can be found online at: https://www.frontiersin.org/articles/10.3389/fonc.2021.712553/full#supplementary-material

Supplementary Table 1 | Baseline characteristic of included patients.

Supplementary Figure 1 | Schoenfeld residual test for variables included in the over-all survival Cox regression.

Supplementary Figure 2 | Schoenfeld residual test for variables included in the cancer-specific survival Cox regression.

Supplementary Figure 3 | P value distributions of KM analysis for over-all survival **(A)** and cancer-specific survival **(B)** in 100 PSM cohorts.

REFERENCES

1. Ghahhari J, Marchioni M, Spiess PE, Chipollini JJ, Nyirády P, Varga J, et al. Radical Penectomy, a Compromise for Life: Results From the PECAD Study. *Transl Androl Urol* (2020) 9(3):1306–13. doi: 10.21037/tau.2020.04.04
2. Jakobsen JK, Krarup KP, Sommer P, Nerstrøm H, Bakholdt V, Sørensen JA, et al. DaPeCa-1: Diagnostic Accuracy of Sentinel Lymph Node Biopsy in 222 Patients With Penile Cancer at Four Tertiary Referral Centres - A National Study From Denmark. *BJU Int* (2016) 117(2):235–43. doi: 10.1111/bju.13127
3. EAU Guidelines for Penile Cancer, Hakenberg OW, Compérat E, Minhas S, Necchi A, Protzel C, Watkin N. *EAU Annual Congress Amsterdam*. Arnhem, The Netherlands: EAU Guidelines Office (2020), ChairVice-chair. ISBN 978-94-92671-07-3.
4. Ficarra V, Akduman B, Bouchot O, Palou J, Tobias-Machado M. Prognostic Factors in Penile Cancer. *Urology* (2010) 76(2 Suppl 1):S66–73. doi: 10.1016/j.urology.2010.04.008
5. Protzel C, Alcaraz A, Horenblas S, Pizzocaro G, Zlotta A, Hakenberg OW, et al. Lymphadenectomy in the Surgical Management of Penile Cancer. *Eur Urol* (2009) 55(5):1075–88. doi: 10.1016/j.eururo.2009.02.021
6. Kulkarni JN, Kamat MR. Prophylactic Bilateral Groin Node Dissection Versus Prophylactic Radiotherapy and Surveillance in Patients With N0 and N1-2A Carcinoma of the Penis. *Eur Urol* (1994) 26(2):123–8. doi: 10.1159/000475360
7. Kieffer JM, Djajadiningrat RS, van Muilekom EA, Graafland NM, Horenblas S, Aaronson NK. Quality of Life for Patients Treated for Penile Cancer. *J Urol* (2014) 192(4):1105–10. doi: 10.1016/j.juro.2014.04.014
8. Serrano B, Brotons M, Bosch FX, Bruni L. Epidemiology and Burden of HPV-Related Disease. *Best Pract Res Clin Obstet Gynaecol* (2018) 47:14–26. doi: 10.1016/j.bpobgyn.2017.08.006
9. Yao K, Chen Y, Yen Y, Wu Z, Chen D, Han H, et al. Lymph Node Mapping in Patients With Penile Cancer Undergoing Pelvic Lymph Node Dissection. *J Urol* (2021) 205(1):145–51. doi: 10.1097/JU.0000000000001322
10. Wen S, Ren W, Xue B, Fan Y, Jiang Y, Zeng C, et al. Prognostic Factors in Patients With Penile Cancer After Surgical Management. *World J Urol* (2018) 36(3):435–40. doi: 10.1007/s00345-017-2167-5
11. Austin PC. An Introduction to Propensity Score Methods for Reducing the Effects of Confounding in Observational Studies. *Multivariate Behav Res* (2011) 46(3):399–424. doi: 10.1080/00273171.2011.568786
12. Chen X, Li X, Garcia MM, Gong K, Song Y, He Z, et al. Prognostic Factors in Chinese Patients With Penile Invasive Squamous Cell Carcinoma. *J Androl* (2012) 33(6):1276–81. doi: 10.2164/jandrol.112.016378
13. da Costa WH, Rosa de Oliveira RA, Santana TB, Benigno BS, da Cunha IW, de Cássio Zequi S, et al. Prognostic Factors in Patients With Penile Carcinoma and Inguinal Lymph Node Metastasis. *Int J Urol* (2015) 22(7):669–73. doi: 10.1111/iju.12759
14. Downes MR. Review of in Situ and Invasive Penile Squamous Cell Carcinoma and Associated non-Neoplastic Dermatological Conditions. *J Clin Pathol* (2015) 68(5):333–40. doi: 10.1136/jclinpath-2015-202911
15. Douglawi A, Masterson TA. Penile Cancer Epidemiology and Risk Factors: A Contemporary Review. *Curr Opin Urol* (2019) 29(2):145–9. doi: 10.1097/MOU.0000000000000581
16. Larke NL, Thomas SL, dos Santos Silva I, Weiss HA. Male Circumcision and Penile Cancer: A Systematic Review and Meta-Analysis. *Cancer Causes Control* (2011) 22(8):1097–110. doi: 10.1007/s10552-011-9785-9
17. Yu YB, Wang YH, Yang XC, Zhao Y, Wang ML, Liang Y, et al. The Relationship Between Human Papillomavirus and Penile Cancer Over the Past Decade: A Systematic Review and Meta-Analysis. *Asian J Androl* (2019) 21(4):375–80. doi: 10.4103/aja.aja_39_19
18. Yao HH, Sengupta S, Chee J. Penile Sparing Therapy for Penile Cancer. *Transl Androl Urol* (2020) 9(6):3195–209. doi: 10.21037/tau.2019.08.07
19. Djajadiningrat RS, van Werkhoven E, Meinhardt W, van Rhijn BW, Bex A, van der Poel HG, et al. Penile Sparing Surgery for Penile Cancer-Does it Affect Survival? *J Urol* (2014) 192(1):120–5. doi: 10.1016/j.juro.2013.12.038
20. Smith Y, Hadway P, Biedrzycki O, Perry MJ, Corbishley C, Watkin NA, et al. Reconstructive Surgery for Invasive Squamous Carcinoma of the Glans Penis. *Eur Urol* (2007) 52(4):1179–85. doi: 10.1016/j.eururo.2007.02.038
21. Philippou P, Shabbir M, Malone P, Nigam R, Muneer A, Ralph DJ, et al. Conservative Surgery for Squamous Cell Carcinoma of the Penis: Resection Margins and Long-Term Oncological Control. *J Urol* (2012) 188(3):803–8. doi: 10.1016/j.juro.2012.05.012
22. Ornellas AA, Kinchin EW, Nóbrega BL, Wisnescky A, Koifman N, Quirino R. Surgical Treatment of Invasive Squamous Cell Carcinoma of the Penis: Brazilian National Cancer Institute Long-Term Experience. *J Surg Oncol* (2008) 97(6):487–95. doi: 10.1002/jso.20980
23. Leijte JA, Kirrander P, Antonini N, Windahl T, Horenblas S. Recurrence Patterns of Squamous Cell Carcinoma of the Penis: Recommendations for Follow-Up Based on a Two-Centre Analysis of 700 Patients. *Eur Urol* (2008) 54(1):161–8. doi: 10.1016/j.eururo.2008.04.016
24. Shabbir M, Muneer A, Kalsi J, Shukla CJ, Zacharakis E, Garaffa G, et al. Glans Resurfacing for the Treatment of Carcinoma in Situ of the Penis: Surgical Technique and Outcomes. *Eur Urol* (2011) 59(1):142–7. doi: 10.1016/j.eururo.2010.09.039
25. Stuiver MM, Djajadiningrat RS, Graafland NM, Vincent AD, Lucas C, Horenblas S. Early Wound Complications After Inguinal Lymphadenectomy in Penile Cancer: A Historical Cohort Study and Risk-Factor Analysis. *Eur Urol* (2013) 64(3):486–92. doi: 10.1016/j.eururo.2013.02.037
26. Leone A, Diorio GJ, Pettaway C, Master V, Spiess PE. Contemporary Management of Patients With Penile Cancer and Lymph Node Metastasis. *Nat Rev Urol* (2017) 14(6):335–47. doi: 10.1038/nrurol.2017.47
27. Maciel CVM, Machado RD, Morini MA, Mattos PAL, Dos Reis R, Dos Reis RB, et al. External Validation of Nomogram to Predict Inguinal Lymph Node Metastasis in Patients With Penile Cancer and Clinically Negative Lymph Nodes. *Int Braz J Urol* (2019) 45(4):671–8. doi: 10.1590/s1677-5538.ibju.2018.0756
28. Niyogi D, Noronha J, Pal M, Bakshi G, Prakash G. Management of Clinically Node-Negative Groin in Patients With Penile Cancer. *Indian J Urol* (2020) 36(1):8–15. doi: 10.4103/iju.IJU_221_19
29. Sharma P, Zargar H, Spiess PE. Surgical Advances in Inguinal Lymph Node Dissection: Optimizing Treatment Outcomes. *Urol Clin North Am* (2016) 43(4):457–68. doi: 10.1016/j.ucl.2016.06.007
30. Sharma P, Zargar-Shoshtari K, Caracciolo JT, Richard GJ, Poch MA, Pow-Sang J, et al. Sarcopenia as a Predictor of Complications in Penile Cancer Patients Undergoing Inguinal Lymph Node Dissection. *World J Urol* (2015) 33(10):1585–92. doi: 10.1007/s00345-014-1471-6
31. Winters BR, Mossanen M, Holt SK, Lin DW, Wright JL. Predictors of Nodal Upstaging in Clinical Node Negative Patients With Penile Carcinoma: A National Cancer Database Analysis. *Urology* (2016) 96:29–34. doi: 10.1016/j.urology.2016.06.033
32. Zekan DS, Dahman A, Hajiran AJ, Luchey AM, Chahoud J, Spiess PE. Prognostic Predictors of Lymph Node Metastasis in Penile Cancer: A Systematic Review. *Int Braz J Urol* (2021) 47(5):943–56. doi: 10.1590/s1677-5538.ibju.2020.0959

33. Bandini M, Spiess PE, Pederzoli F, Marandino L, Brouwer OR, Albersen M, et al. A Risk Calculator Predicting Recurrence in Lymph Node Metastatic Penile Cancer. *BJU Int* (2020) 126(5):577–85. doi: 10.1111/bju.15177

Conflict of Interest: The authors declare that the research was conducted in the absence of any commercial or financial relationships that could be construed as a potential conflict of interest.

Publisher's Note: All claims expressed in this article are solely those of the authors and do not necessarily represent those of their affiliated organizations, or those of the publisher, the editors and the reviewers. Any product that may be evaluated in this article, or claim that may be made by its manufacturer, is not guaranteed or endorsed by the publisher.

frontiers in Oncology

ORIGINAL RESEARCH
published: 06 October 2021
doi: 10.3389/fonc.2021.754996

The Effect of 10 Most Common Nonurological Primary Cancers on Survival in Men With Secondary Prostate Cancer

Mike Wenzel[1,2], Luigi Nocera[2,3], Christoph Würnschimmel[2,4], Claudia Collà Ruvolo[2,5], Zhe Tian[2], Fred Saad[2], Alberto Briganti[3], Derya Tilki[4,6], Markus Graefen[4], Andreas Becker[1], Frederik C. Roos[1], Felix K. H. Chun[1] and Pierre I. Karakiewicz[2]*

[1] Department of Urology, University Hospital Frankfurt, Frankfurt am Main, Germany, [2] Cancer Prognostics and Health Outcomes Unit, Division of Urology, University of Montréal Health Center, Montréal, QC, Canada, [3] Department of Urology and Division of Experimental Oncology, Urological Research Institute (URI), Istituto di Ricovero e Cura a Carattere Scientifico (IRCCS) San Raffaele Scientific Institute, Milan, Italy, [4] Martini-Klinik Prostate Cancer Center, University Hospital Hamburg-Eppendorf, Hamburg, Germany, [5] Department of Neurosciences, University of Naples Federico II Reproductive Sciences and Odontostomatology, Naples, Italy, [6] Department of Urology, University Hospital Hamburg-Eppendorf, Hamburg, Germany

OPEN ACCESS

Edited by:
Srilakshmi Srinivasan, Queensland University of Technology, Australia

Reviewed by:
Sumit Isharwal, University of Virginia, United States
Piotr Bryniarski, Medical University of Silesia, Poland

***Correspondence:**
Mike Wenzel
Mike.Wenzel@kgu.de

Specialty section:
This article was submitted to Genitourinary Oncology, a section of the journal Frontiers in Oncology

Received: *07 August 2021*
Accepted: *20 September 2021*
Published: *06 October 2021*

Citation:
Wenzel M, Nocera L, Würnschimmel C, Collà Ruvolo C, Tian Z, Saad F, Briganti A, Tilki D, Graefen M, Becker A, Roos FC, Chun FKH and Karakiewicz PI (2021) The Effect of 10 Most Common Nonurological Primary Cancers on Survival in Men With Secondary Prostate Cancer. Front. Oncol. 11:754996. doi: 10.3389/fonc.2021.754996

Background: This study aims to test the effect of the 10 most common nonurological primary cancers (skin, rectal, colon, lymphoma, leukemia, pancreas, stomach, esophagus, liver, lung) on overall mortality (OM) after secondary prostate cancer (PCa).

Material and Methods: Within the Surveillance, Epidemiology, and End Results (SEER) database, patients with 10 most common primary cancers and concomitant secondary PCa (diagnosed 2004–2016) were identified and were matched in 1:4 fashion (age, year at diagnosis, race/ethnicity, treatment type, TNM stage) with primary PCa controls. OM was compared between secondary and primary PCa patients and was stratified according to primary cancer type, as well as according to time interval between primary cancer *vs.* secondary PCa diagnoses.

Results: We identified 24,848 secondary PCa patients (skin, n = 3,871; rectal, n = 798; colon, n = 3,665; lymphoma, n = 2,583; leukemia, n = 1,102; pancreatic, n = 118; stomach, n = 361; esophagus, n = 219; liver, n = 160; lung, n = 1,328) *vs.* 531,732 primary PCa patients. Secondary PCa characteristics were less favorable than those of primary PCa patients (PSA and grade), and smaller proportions of secondary PCa patients received active treatment. After 1:4 matching, all secondary PCa exhibited worse OM than primary PCa patients. Finally, subgroup analyses showed that the survival disadvantage of secondary PCa patients decreased with longer time interval since primary cancer diagnosis and subsequent secondary PCa.

Conclusion: Patients with secondary PCa are diagnosed with less favorable PSA and grade. Even after matching for PCa characteristics, secondary PCa patients still exhibit worse survival. However, the survival disadvantage is attenuated, when secondary PCa diagnosis is made after longer time interval, since primary cancer diagnosis.

Keywords: mortality, primary prostate cancer, lung cancer, colon cancer, secondary cancer

INTRODUCTION

The most recent US cancer statistics (2018) indicate over 17 million new cancer diagnoses annually. Of these, almost 9 million were made in men (1–3). In men, prostate cancer (PCa) ranks as first or second most frequently diagnosed cancer. Virtually, all contemporary epidemiological studies addressing PCa survival exclusively focused on primary PCa and excluded patients with prior cancers (4–9). It is particularly of note that an increased risk exists for secondary cancers and especially secondary PCa after prior primary cancers (10–16). However, only three epidemiological SEER-based studies (n = 18,225; n = 5,987; n = 1,457) and one European institutional study (n = 1,552) addressed mortality in patients with secondary PCa, after initial diagnosis of another malignancy (17–20). All three studies showed worse survival in secondary PCa patients, relative to primary PCa patients. However, none stratified their analyses according to the most common cancer types. However, primary skin cancer may have a different effect than lung cancer. Moreover, it may also be postulated that the time interval between primary cancer and secondary PCa diagnosis may also affect survival in secondary PCa patients but has not been examined to date.

We addressed these two important unaddressed points within the Surveillance, Epidemiology, and End Results (SEER) registry database and hypothesized that they may impact important survival differences.

MATERIAL AND METHODS

Study Population

Within the SEER database, we identified all patients ≥18 years old with secondary PCa diagnosed between 2004 and 2016, after prior diagnosis of one of 10 commonest nonurological malignancies (skin, rectal, colon, lymphoma, leukemia, pancreas, stomach, esophagus, liver, and lung). Moreover, we also identified all ≥18-year-old patients with biopsy-proven primary adenocarcinoma of the prostate diagnosed between 2004 and 2016 (International Classification of Disease for Oncology (ICD-O-3) code 8140, site code C61.9). Cases that were identified at autopsy or death certificate or with unknown histology were excluded. Patients with unavailable PSA values were excluded in both cohorts. We excluded concomitantly diagnosed primary cancer and secondary PCa (≤6 months apart), according to previously reported methodology (21, 22). Descriptive statistics addressed all included 24,848 secondary PCa patients and all 531,732 primary PCa patients (**Figure 1**; **Table 1**). Subsequently, survival analyses focused on overall mortality (OM). Here, we relied on a propensity score matched (age at diagnosis, year of diagnosis, race/ethnicity, PCa treatment, cT-stage, cN-stage, and M-stage) cohort of all 24,848 secondary PCa patients that were matched with four primary PCa controls (n = 99,392).

Statistical Analysis

Descriptive statistics included frequencies and proportions for categorical variables. Medians and interquartile ranges (IQR) were reported for continuously coded variables. The Chi-square tested the statistical significance in proportion differences. The t-test and Kruskal-Wallis test examined the statistical significance of mean and distribution differences.

The first part of the analyses compared patient and PCa characteristics between all identified secondary (n = 24,848) and primary PCa patients (n = 531,732). In the second part of the analyses, we focused on overall mortality (OM), after 1:4 propensity score matching. Kaplan-Meier illustrated OM in the overall comparisons, as well as in all subsequent subgroup analyses. Additionally, multivariable Cox regression quantified hazard ratios (HR) that compared secondary *vs.* primary PCa patients, after further adjusting for covariates of the 1:4 matched cohort: PSA, socioeconomic status, Gleason grade group, and D'Amico risk group (all not previously matched). All tests were two sided with a level of significance set at $p < 0.05$ and R software environment for statistical computing and graphics (version 3.4.3) was used for all analyses (23).

RESULTS

Descriptive Characteristics of the Study Population Prior to Matching

Prior to matching, 24,848 secondary PCa and 531,732 primary PCa were available for analyses (**Table 1**). Patients with secondary PCa more frequently harbored Gleason grade group IV (10.3% *vs.* 8.8%) and V (9.3% *vs.* 7.7%, $p < 0.001$). Median PSA at diagnosis showed marginal differences between secondary and primary PCa patients (6.9 [IQR 4.9–11.5] *vs.* 6.6 ng/ml [IQR 4.8–10.6], p <0.001). In secondary PCa patients, median PSA values at diagnosis of secondary PCa ranged from 6.5 (skin cancer) to 7.8 ng/ml (pancreatic and liver cancer). However, median age at secondary PCa diagnosis was more advanced than in primary PCa (69 *vs.* 65 years, $p < 0.001$). In secondary PCa patients (**Table 2**), median age at secondary PCa diagnoses ranged from respectively 66 (liver cancer) to 72 years (colon cancer). The average time interval between primary

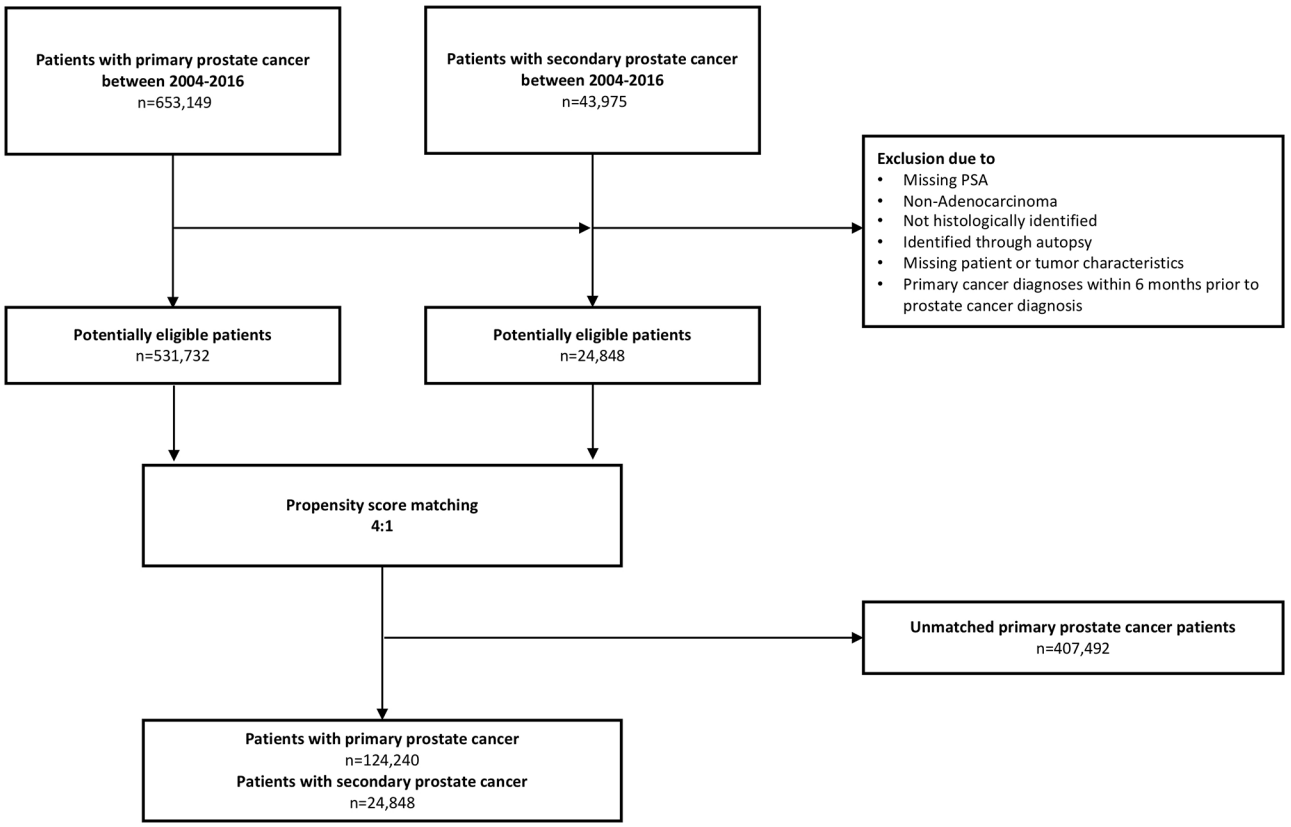

FIGURE 1 | Flow chart depicting included patients with primary and secondary prostate cancer in analyses.

cancer diagnosis and secondary PCa diagnosis ranged from 5 (pancreatic, esophagus, liver cancer) to 8 years (skin and rectum cancer). No clinically meaningful differences were recorded in cT-stage, cN-stage, and M-stages between secondary and primary PCa patients. Important differences existed according to use of local therapy [external beam radiation therapy (EBRT) and radical prostatectomy (RP)]. Specifically, in secondary PCa patients, the rate of EBRT was higher (25.7% *vs*. 22.7%) and the rate of RP was lower (23.8% *vs*. 33.5%), relative to primary PCa patients (all $p < 0.001$). In secondary PCa patients, rates of RP ranged from 11.3% (liver cancer) to 29.7% (skin cancer) and rates of EBRT ranged from 19.5% (rectal cancer) to 34.4% (liver cancer).

Survival Analyses After 1:4 Propensity Score Matching

After matching, OM at 10 years was 46.0% in secondary PCa *vs*. 35.7% in primary PCa (**Figure 2A**). The median survival of all 24,848 secondary PCa patients was 131 months and not reached for 99,392 primary PCa patients. This survival disadvantage translated into a 1.49-fold higher risk of OM in secondary PCa patients, relative to their primary PCa counterparts. After further multivariable adjustment, a 1.51-fold higher OM was observed (**Table 3**).

Survival Analyses After 1:4 Propensity Score Matching According to Local Treatment Type: RP *vs*. EBRT *vs*. No Local Treatment

Subsequently, we repeated Kaplan-Meier and Cox regression analyses, after stratification according to local PCa treatment type in patients treated with RP or EBRT or no local treatment (NLT) across all primary cancer types. Here, presence of secondary PCa resulted in worse OM, relative to primary PCa patients. Specifically, 10-year OM rates were respectively 22.1% *vs*. 11.7%, 47.4% *vs*. 36.5%, and 75.3% *vs*. 51.7% after RP, EBRT, or NLT in secondary *vs*. primary PCa patients (**Figures 2B–D**). In multivariable Cox regression models, the respective HRs were 2.3 after RP, 1.6 after EBRT, and 1.5 after NLT in secondary PCa patients, relative to primary PCa patients (**Table 3**, all <0.01).

Survival Analyses After 1:4 Propensity Score Matching According to Primary Cancer Type

Kaplan-Meier plots showed in secondary PCa patients with skin, rectal, pancreas, colon, lymphoma, leukemia, stomach, liver, esophagus, and lung cancer *vs*. for primary PCa patients respectively 10-year OM rates of 33.6% *vs*. 32.1%, 43.7% *vs*. 39.3%, 45.7% *vs*. 32.2%, 46.4% *vs*. 41.7%, 49.3% *vs*. 34.8%, 52.9%

TABLE 1 | Descriptive characteristics prior to matching and after matching for age at prostate cancer diagnosis, year of prostate cancer diagnoses, race/ethnicity, treatment type, and TNM stage for primary and secondary prostate cancer patients.

Variable		Prior to matching		After matching		
		Primary PCa *N* = 531,732	Secondary PCa *N* = 24,848	Overall *N* = 124,240	Primary PCa *N* = 99,392 (80%)	Secondary PCa *N* = 24,848 (20%)
Age at PCa diagnosis	Median (IQR)	65 (59–72)	69 (64–76)	69 (64–76)	69 (64–76)	69 (64–76)
Year of PCa diagnosis	Median (IQR)	2010 (2007–2013)	2013 (2007–2013)	2013 (2007–2013)	2013 (2007–2013)	2013 (2007–2013)
Age of primary cancer diagnosis	Median (IQR)	–	63 (56–69)	–	–	63 (56–69)
Year of primary cancer diagnosis	Median (IQR)	–	2004 (2000–2008)	–	–	2004 (2000–2008)
PSA (ng/ml)	Median (IQR)	6.6 (4.8–10.6)	6.9 (4.9–11.5)	6.9 (4.9–11.4)	6.9 (4.9–11.3)	6.9 (4.9–11.5)
Follow-up (months)	Median (IQR)	68 (32–104)	53 (23–88)	58 (25–93)	59 (26–94)	53 (23–88)
cT	cT1	324,967 (61.1)	14,719 (59.2)	74,330 (59.8)	59,611 (60.0)	14,719 (59.2)
	cT2	164,054 (30.9)	7,919 (31.9)	40,322 (32.5)	32,403 (32.6)	7,919 (31.9)
	cT3	14,084 (2.6)	635 (2.6)	2,853 (2.3)	2,218 (2.2)	635 (2.6)
	cT4	4,701 (0.9)	248 (1.0)	926 (0.7)	678 (0.7)	248 (1.0)
	cTx	23,926 (4.5)	1,327 (5.3)	5,809 (4.7)	4,482 (4.5)	1,327 (5.3)
cN stage	cN0	493,330 (92.8)	23,026 (92.7)	116,645 (93.9)	93,619 (94.2)	23,026 (92.7)
	cN1	15,055 (2.8)	573 (2.3)	2,295 (1.8)	1,722 (1.7)	573 (2.3)
	cNx	23,347 (4.4)	1,249 (5.0)	5,300 (4.3)	4,051 (4.1)	1,249 (5)
M stage	M0	495,768 (93.2)	23,021 (92.6)	116,431 (93.7)	93,410 (94.0)	23,021 (92.6)
	M1	22,396 (4.2)	1,131 (4.6)	4,834 (3.9)	3,703 (3.7)	1,131 (4.6)
	Mx	13,568 (2.6)	696 (2.8)	2,975 (2.4)	2,279 (2.3)	696 (2.8)
Gleason grade group at diagnosis	I	209,565 (39.4)	8,951 (36.0)	46,422 (37.4)	37,471 (37.7)	8,951 (36.0)
	II	137,937 (25.9)	6,117 (24.6)	30,986 (24.9)	24,869 (25.0)	6,117 (24.6)
	III	60,193 (11.3)	2,968 (11.9)	14,813 (11.9)	11,845 (11.9)	2,968 (11.9)
	IV	46,788 (8.8)	2,548 (10.3)	12,368 (10.0)	9,820 (9.9)	2,548 (10.3)
	V	40,687 (7.7)	2,299 (9.3)	10,795 (8.7)	8,496 (8.5)	2,299 (9.3)
	Unknown	36,562 (6.9)	1,965 (7.9)	8,856 (7.1)	6,891 (6.9)	1,965 (7.9)
D'Amico risk group	low	135,502 (25.5)	5,538 (22.3)	29,178 (23.5)	23,640 (23.8)	5,538 (22.3)
	intermediate	210,982 (39.7)	9,892 (39.8)	49,444 (39.8)	39,552 (39.8)	9,892 (39.8)
	high	144,985 (27.3)	7,319 (29.5)	36,118 (29.1)	28,799 (29.0)	7,319 (29.5)
	Unknown	40,263 (7.6)	2,099 (8.4)	9,500 (7.6)	7,401 (7.4)	2,099 (8.4)
Treatment	RP	178,084 (33.5)	5,909 (23.8)	29,099 (23.4)	23,190 (23.3)	5,909 (23.8)
	EBRT	120,891 (22.7)	6,377 (25.7)	32,032 (25.8)	25,655 (25.8)	6,377 (25.7)
	BT	39,655 (7.5)	1,718 (6.9)	9,023 (7.3)	7,305 (7.3)	1,718 (6.9)
	BT+EBRT	21,696 (4.1)	952 (3.8)	4,755 (3.8)	3,803 (3.8)	952 (3.8)
	RP+EBRT	15,121 (2.8)	554 (2.2)	2,684 (2.2)	2,130 (2.1)	554 (2.2)
	RT+RP	156 (0)	8 (0)	33 (0)	25 (0)	8 (0)
	NLT	140,081 (26.3)	8,430 (33.9)	42,278 (34.0)	33,848 (34.1)	8,430 (33.9)
	Unknown	16,048 (3.0)	900 (3.6)	4,336 (3.5)	3,436 (3.5)	900 (3.6)
Chemotherapy	No/Unknown	527,509 (99.2)	24,663 (99.3)	123,432 (99.3)	98,769 (99.4)	24,663 (99.3)
	Yes	4,223 (0.8)	185 (0.7)	808 (0.7)	623 (0.6)	185 (0.7)
Race/ethnicity	Caucasian	363,223 (68.3)	19,536 (78.6)	97,760 (78.7)	78,224 (78.7)	19,536 (78.6)
	African American	81,905 (15.4)	2,758 (11.1)	13,890 (11.2)	11,132 (11.2)	2,758 (11.1)
	Hispanic	48,835 (9.2)	1,494 (6.0)	7,468 (6.0)	5,974 (6.0)	1,494 (6.0)
	Native	1,861 (0.3)	80 (0.3)	340 (0.3)	260 (0.3)	80 (0.3)
	Asian	26,007 (4.9)	948 (3.8)	4,613 (3.7)	3,665 (3.7)	948 (3.8)
	Unknown	9,901 (1.9)	32 (0.1)	169 (0.1)	137 (0.1)	32 (0.1)
Marital status	Married	354,363 (66.6)	17,024 (68.5)	82,781 (66.6)	65,757 (66.2)	17,024 (68.5)
	Unmarried	116,788 (22.0)	5,049 (20.3)	26,519 (21.3)	21,470 (21.6)	5,049 (20.3)
	Unknown	60,581 (11.4)	2,775 (11.2)	14,940 (12)	12,165 (12.2)	2,775 (11.2)
Socioeconomic status	1st quartile	133,678 (25.1)	6,170 (24.8)	32,867 (26.5)	26,697 (26.9)	6,170 (24.8)
	2nd–4th quartile	397,946 (74.8)	18,678 (75.2)	91,373 (73.5)	72,695 (73.1)	18,678 (75.2)
Region	West	270,363 (50.8)	12,440 (50.1)	62,122 (50)	49,682 (50)	12,440 (50.1)
	Midwest	51,705 (9.7)	3,417 (13.8)	13,753 (11.1)	10,336 (10.4)	3,417 (13.8)
	North-East	89,653 (16.9)	4,363 (17.6)	21,531 (17.3)	17,168 (17.3)	4,363 (17.6)
	South	120,011 (22.6)	4,628 (18.6)	26,834 (21.6)	22,206 (22.3)	4,628 (18.6)

vs. 35.2%, 55.6% *vs.* 40.1%, 57.1% *vs.* 29.5%, 63.7% *vs.* 42.5%, and 67.0% *vs.* 37.9% (**Figures 3** and **4**). All secondary PCa patients harbored a significant OM disadvantage relative to primary PCa patients. The specific multivariable HRs were 1.2, 1.3, 1.8, 1.2, 1,8, 1.8, 1.9, 3.0, 1.8, and 2.5 for respectively secondary PCa patients with primary skin, rectal, pancreas, colon, lymphoma, leukemia, stomach, liver, esophagus, and lung cancer (all $p < 0.01$; **Table 3**).

The proportions of patients that died of secondary PCa (**Table 2**) ranged from 9.8% (in primary lung cancer patients) to 25.7% (in primary rectal cancer patients). Similarly, the proportions of patients that died of primary cancers ranged from 16.4% (skin

TABLE 2 | Baseline and prostate cancer characteristics of the 10 most common nonurological cancers prior to secondary prostate cancer.

	Median age at primary cancer diagnosis (IQR)	Median age at secondary prostate cancer diagnosis (IQR)	Median PSA at diagnosis in ng/ml (IQR)	RP vs. EBRT treatment (%)	Overall deaths	Died from secondary prostate cancer (%)	Died from primary cancer (%)
Skin cancer (*n* = 3,871)	61 (54–69)	69 (63–75)	6.5 (4.8–10.2)	29.7 *vs.* 22.6	749	164 (21.9)	123 (16.4)
Rectal cancer (*n* = 798)	62 (55–68)	70 (64–76)	7.6 (5.2–12.7)	20.4 *vs.* 19.5	214	55 (25.7)	40 (18.7)
Colon cancer (*n* = 3,665)	65 (58–71)	72 (66–78)	7.7 (5.2–14.0)	17.3 *vs.* 29.1	1,146	215 (18.8)	213 (18.6)
Lymphoma (*n* = 2,583)	62 (55–69)	69 (63–75)	6.9 (4.9–11.4)	22.5 *vs.* 27.5	766	123 (16.1)	274 (35.8)
Leukemia (*n* = 1,102)	63 (56–70)	69 (64–75)	6.8 (4.9–11.1)	22.2 *vs.* 23.6	340	45 (13.2)	135 (31.4)
Pancreatic cancer (*n* = 118)	65 (60–70)	70 (65–74)	7.8 (5.1–13.5)	14.4 *vs.* 26.3	34	6 (17.6)	11 (32.4)
Stomach cancer (*n* = 361)	64 (58–71)	71 (65–77)	7.1 (5.0–12.9)	20.2 *vs.* 28.0	118	29 (24.6)	26 (22.0)
Esophagus cancer (*n* = 219)	65 (59–69)	70 (65–75)	7.4 (5.1–11.2)	18.7 *vs.* 29.7	74	11 (14.9)	26 (35.1)
Liver cancer (*n* = 160)	61 (56–67)	66 (61–71)	7.8 (5.8–12.8)	11.3 *vs.* 34,4	52	11 (21.2)	26 (50.0)
Lung cancer (*N* = 1,328)	65 (59–71)	71 (66–76)	7.6 (5.0–12.8)	14.0 *vs.* 31.4	599	59 (9.8)	255 (42.6)
Overall (*n*=24,848)	63 (56–69)	69 (64–76)	6.9 (4.9–11.5)	23.8 *vs.* 25.7	4,069	715 (17.6)	1,122 (27.6)

PSA, prostate-specific antigen; RP, radical prostatectomy; EBRT, external beam radiation therapy.

cancer) to 50.0% (liver cancer). Unfortunately, these cancer-specific rates could not be translated into Kaplan-Meier-derived actuarial estimates due to unavailable time to death.

Survival Analyses After 1:4 Propensity Score Matching According to Time Interval Length Since Initial Cancer Diagnosis and Secondary PCa Diagnoses

Time interval length since initial cancer and secondary PCa diagnoses was stratified into four groups between 7 and 36 (n = 6,659) *vs.* 37 and 60 (n = 4,759) *vs.* 61 and 120 (n = 7,289) *vs.* ≥121 months (n = 6,141). In Kaplan-Meier plots (**Figure 5**) that addressed the comparison between secondary PCa diagnosed between 7 and 36 months after primary cancer diagnosis, relative to primary PCa, the respective 10-year OM rates were 47.4% *vs.* 30.4%. These OM rates translated into a multivariable HR of 1.95. The subsequent stratifications (37–60 *vs.* 61–120 *vs.* ≥121 months) resulted in 10-year OM rates in secondary PCa patients of 47.4% *vs.* 31.8%, 45.1% *vs.* 32.3%, and 44.0%% *vs.* 35.2% months in primary PCa patients. The respective multivariable HR for 7–36 *vs.* 37–60 *vs.* 61–120 *vs.* ≥121 months were 1.7, 1.6, and 1.3.

DISCUSSION

We hypothesized that secondary PCa patients will harbor less favorable disease characteristics in addition to exhibiting less favorable prognosis, relative to primary PCa patients. To test this hypothesis, we identified 24,848 secondary PCa patients and 531,732 primary PCa patients, for the purpose of comparisons. Here, secondary PCa patients were older than their primary PCa counterparts. On average, secondary PCa diagnosis (69 years) was made 6 years after primary cancer diagnosis (63 years). Moreover, age at diagnosis variability was also recorded according to primary cancer type in secondary PCa patients. The latter ranged from 66 (liver cancer) to 72 years (colon cancer). These observations are different from the more historical reports about secondary PCa. For example, in the study by Dinh et al., median age in patients with secondary PCa diagnosis was 73, which is significantly older than in the current study (17). It may be postulated that a selection bias is operational regarding the age at secondary PCa diagnosis. The latter may be directly related to aggressiveness and mortality probability of the primary cancer diagnosis. Although such simplified explanation is attractive, several confounding variables may be operational. For example, patients with most aggressive cancers may be expected to be never be diagnosed with secondary PCa. Conversely, long-term survivors of highly aggressive primary cancer variants may still be diagnosed with secondary PCa. The latter may render generalizations about the effect of aggressive primary cancer on rates and ages at secondary PCa diagnosis virtually uninterpretable.

Less pronounced differences were recorded in PSA distributions of secondary and primary PCa patients,

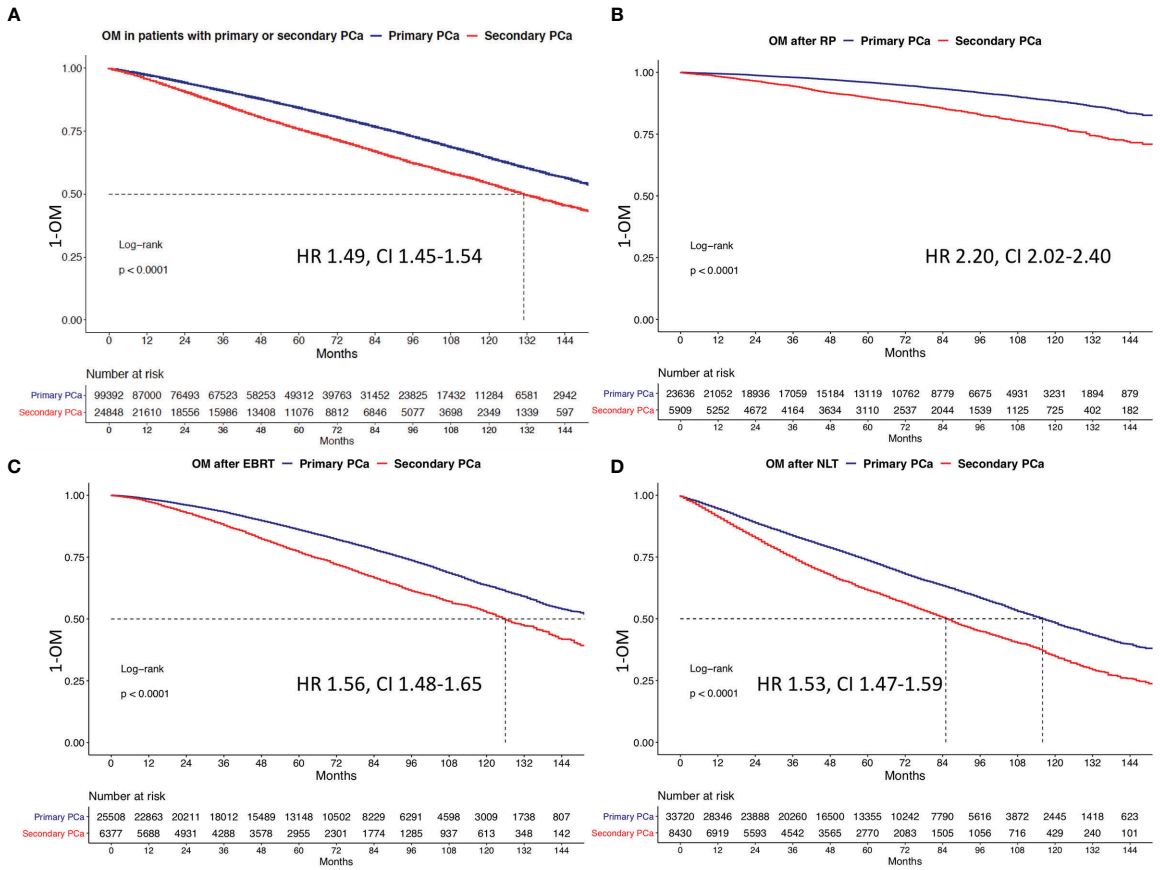

FIGURE 2 | Kaplan-Meier plots depicting overall mortality (OM) for primary and secondary prostate cancer for **(A)** the overall cohort, **(B)** patients treated with radical prostatectomy (RP), **(C)** patients treated with external beam radiation therapy (EBRT), and **(D)** no local treatment (NLT). HR, hazard ratio; CI, confidence interval.

evidenced by respectively 6.9 (IQR 4.9–11.5) *vs.* 6.6 ng/ml (IQR 4.8–10.6) PSA values at diagnoses. Additionally, small differences in PSA at diagnoses were recorded in secondary PCa patients, according to primary cancer type and ranged from 6.5 (skin cancer) to 7.8 ng/ml (pancreatic and liver cancers). Similarly, we also observed small differences in Gleason grade groups IV and V. Here, secondary PCa patients exhibited less favorable grade. This observation is in an agreement with previous publications, where secondary PCa patients also harbored higher rates of Gleason grade group IV/V (18, 19). Finally, no clinically meaningful differences were identified according to stage. Taken together, these data indicate that despite more advanced age and small disadvantage in PSA at diagnosis and PCa grade, secondary PCa patients do not exhibit crucial PCa characteristic differences at initial diagnosis. However, this interpretation may be biased and warrants methodologically more stringent analyses. This suspicion prompted the use of propensity score matching, according to age as well as patient and PCa characteristics. Moreover, we also applied additional multivariable adjustment in all subsequent survival analyses. The intent was to most thoroughly test for prognostic differences with strictest reduction of bias and/or confounding.

In part 1 of the OM analyses, the propensity-matched comparisons addressed the entire cohort of secondary PCa patients, relative to all primary PCa controls. In part 2 of OM analyses, we examined the effect of primary and secondary PCa in respectively RP-, EBRT-, and NLT-treated patients. In the third part of the analyses, we sequentially compared secondary PCa patients, relative to their primary PCa counterparts, according to the type of primary malignancy diagnosed prior to secondary PCa. In the fourth part of analyses, we stratified the comparisons according to the length of the time interval between primary cancer and secondary PCa diagnoses.

In 1:4 matched survival analyses that addressed the entire secondary PCa population, relative to their primary PCa controls, we identified pronounced survival disadvantage in secondary PCa patients (10-year OM 46% *vs.* 35.7%). A similar absolute and relative magnitude of the survival disadvantage in secondary PCa patients was also recorded in subgroup analyses of RP-, EBRT-, and NLT-treated patients. In the third part of the analyses, we invariably recorded a survival disadvantage in all secondary PCa patients diagnosed with the 10 most common

TABLE 3 | Univariable und multivariable Cox regression models after adjustment for PSA, socioeconomic status, Gleason grade group, and D'Amico risk stratification.

	Univariable		Multivariable	
	HR (CI)	***p*-value**	**HR (CI)**	***p*-value**
Cancers				
Primary prostate cancer	Ref	–	–	–
All secondary prostate cancer	1.49 (1.45–1.54)	<0.01	1.51 (1.47–1.55)	<0.01
Skin cancer	1.10 (1.02–1.20)	0.02	1.16 (1.07–1.26)	<0.001
Colon cancer	1.22 (1.15–1.31)	<0.001	1.15 (1.08–1.23)	<0.001
Rectal cancer	1.27 (1.09–1.47)	<0.01	1.30 (1.11–1.51)	<0.001
Lymphoma	1.70 (1.57–1.85)	<0.001	1.75 (1.61–1.91)	<0.001
Pancreatic cancer	1.72 (1.56–2.55)	<0.01	1.80 (1.20–2.70)	<0.01
Stomach cancer	1.73 (1.40–2.14)	<0.001	1.92 (1.54–2.38)	<0.001
Leukemia	1.81 (1.59–2.05)	<0.001	1.84 (1.62–2.09)	<0.001
Esophagus cancer	1.82 (1.39–2.38)	<0.001	1.81 (1.38–2.38)	<0.001
Lung cancer	2.43 (2.21–2.68)	<0.001	2.51 (2.28–2.77)	<0.001
Liver cancer	2.78 (1.98–3.91)	<0.001	2.95 (2.08–4.17)	<0.001
Treatments				
Primary prostate cancer and RP	Ref	–	–	–
Secondary RP	2.20 (2.02–2.40)	<0.001	2.25 (2.06–2.45)	<0.001
Primary prostate cancer and EBRT	Ref	–	–	–
Secondary EBRT	1.56 (1.48–1.65)	<0.001	1.59 (1.51–1.68)	<0.001
Primary prostate cancer and no local treatment	Ref	–	–	–
Secondary no local treatment	1.53 (1.47–1.59)	<0.001	1.53 (1.47–1.59)	<0.001
Time intervals				
Primary prostate cancer	Ref	–	–	–
Secondary cancer 7–36 months prior to prostate cancer	1.92 (1.83–2.02)	<0.001	1.95 (1.85–2.05)	<0.001
Secondary cancer 37–60 months prior to prostate cancer	1.77 (1.67–1.88)	<0.001	1.74 (1.64–1.85)	<0.001
Secondary cancer 61–120 months prior to prostate cancer	1.58 (1.50–1.67)	<0.001	1.61 (1.53–1.70)	<0.001
Secondary cancer >120 months prior to prostate cancer	1.34 (1.27–1.42)	<0.001	1.32 (1.24–1.40)	<0.001

HR, hazard ratio; CI, confidence interval.

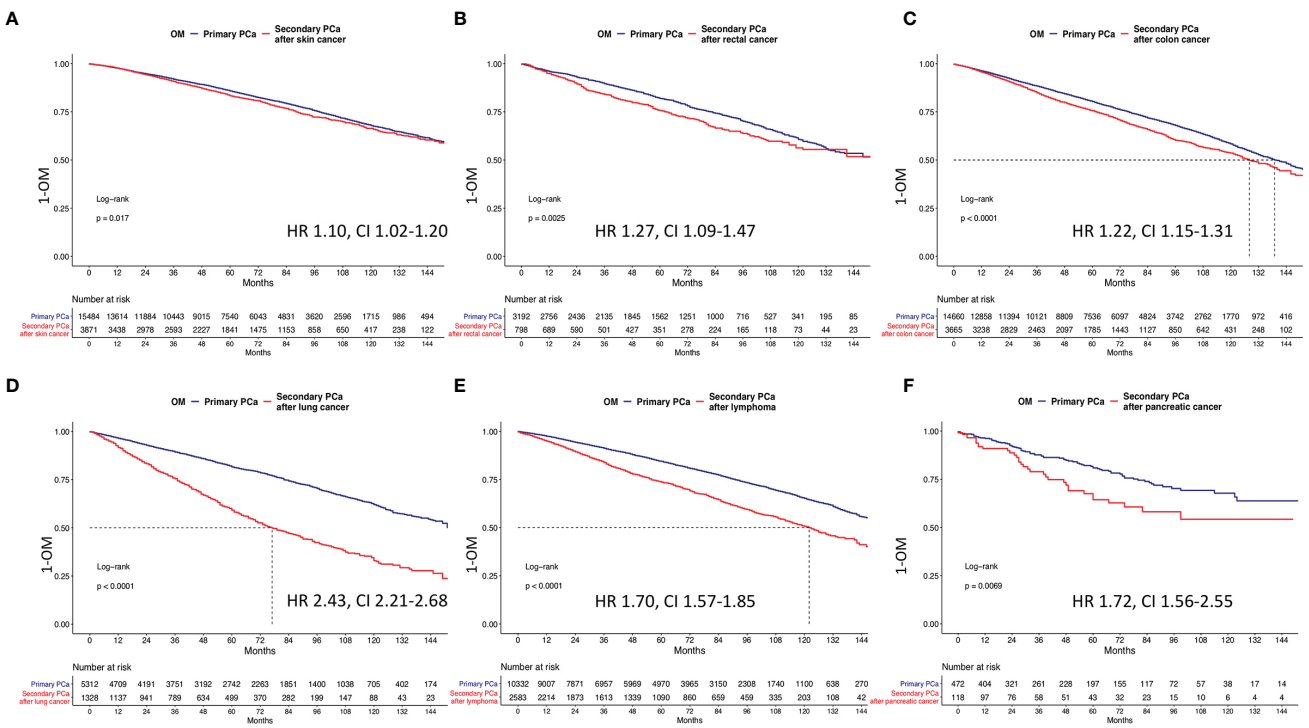

FIGURE 3 | Kaplan-Meier plots depicting overall mortality (OM) for primary and secondary prostate cancer after **(A)** primary skin cancer, **(B)** primary rectum cancer, **(C)** primary colon cancer, **(D)** primary lung cancer, **(E)** primary lymphoma, and **(F)** primary pancreatic cancer. HR, hazard ratio; CI, confidence interval.

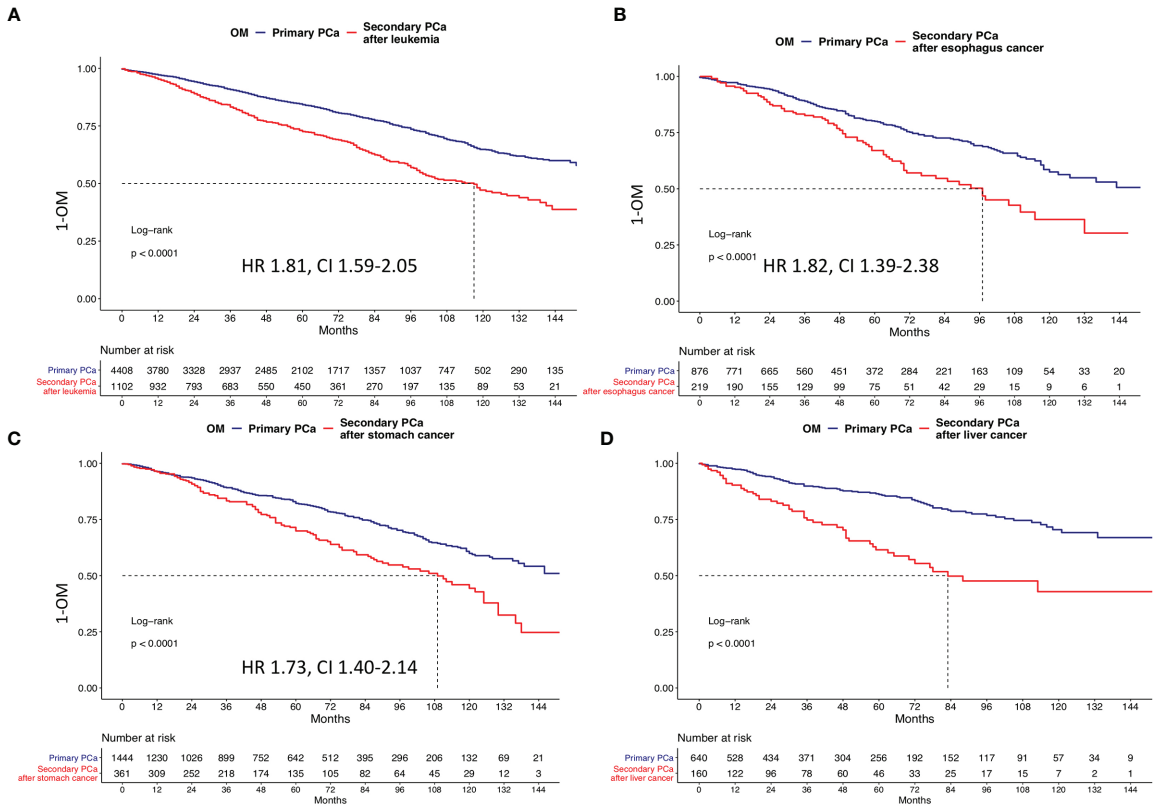

FIGURE 4 | Kaplan-Meier plots depicting overall mortality (OM) for primary and secondary prostate cancer after **(A)** primary leukemia, **(B)** primary liver cancer, **(C)** primary stomach cancer, and **(D)** primary esophagus cancer. HR, hazard ratio; CI, confidence interval.

nonurological initial cancers (HRs: 1.1–2.8). These observations are consistent with previous findings. For example, Klippstein et al. also investigated a survival disadvantage (overall and cancer-specific survival) of 1,552 secondary PCa patients, relative to primary PCa patients (19). However, due to sample size limitations, no primary cancer-specific analyses could be conducted in these analyses and should be ideally performed in further multi-institutional analyses.

Taken together, the above findings indicate that despite apparently small to no differences in patient and/or PCa characteristics at baseline between secondary and primary PCa patients, very important survival disadvantages were applied to secondary PCa patients. This observation was made despite most stringent and methodologically strict statistical matching and multivariable adjustment. In consequence, the persistence of this disadvantage across therapy types suggest that secondary PCa patient harbor a prognostic disadvantage, relative to primary PCa patients, despite exhibiting almost the same baseline characteristics. The observed disadvantage applies across all primary cancer types and persists regardless of primary treatment type (RP and EBRT) and also after further multivariable adjustment for Gleason grade group and PSA. In consequence, the detrimental effect of secondary PCa appears robust and generalizable. The observation of Zhu et al. validates our hypothesis about the aggressiveness of primary cancer that may impact, as well as determine the natural history of treated secondary malignancies (24). The above findings, especially that with longer time interval between primary cancer and secondary PCa life expectancy approximates the life expectancy to primary PCa, should be considered treatment decision making, when secondary PCa patients are counseled.

Finally, in analyses according to length of time interval between primary cancer and secondary PCa diagnoses, we observed that the survival disadvantage decreases with increasing length of time. This observation may indicate that in individuals in whom the time between initial and secondary cancer diagnoses is lengthy, the secondary PCa phenotype may be more comparable with primary PCa. Conversely, when the length of interval between primary cancer and secondary PCa is short, the phenotype might be more aggressive, as evidenced by greater survival disadvantage. We are the first to report this observation, which should be validated in other large-scale databases.

Our observations imply that patients with secondary PCa should be given more careful consideration to eliminate the survival disadvantages that we recorded. Unfortunately, the nature of our data does not allow to identify whether the increase in OM in secondary PCa patients, relative to their primary PCa counterparts,

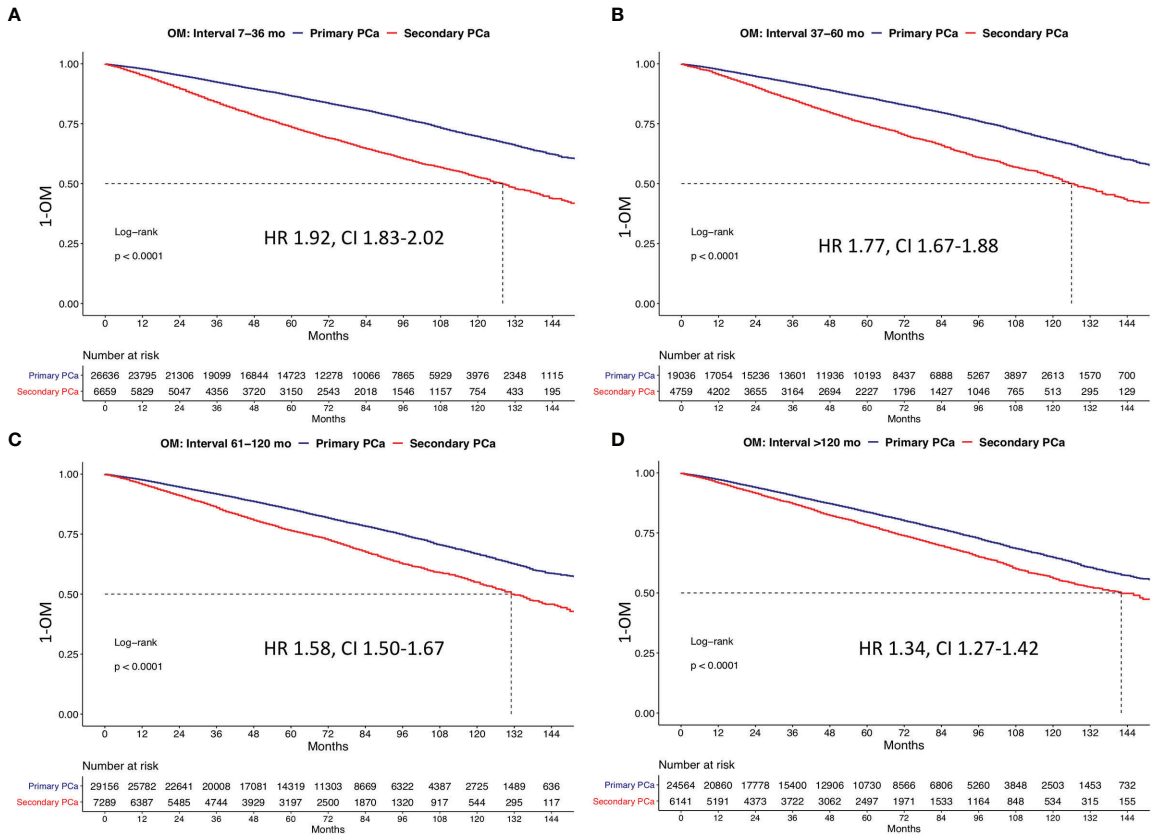

FIGURE 5 | Kaplan Meier plots depicting overall mortality (OM) for primary and secondary prostate cancer according to the time interval between primary cancer and secondary prostate cancer at **(A)** 7–46 months, **(B)** 37–60 months, **(C)** 61–120 months, and **(D)** >120 months. HR, hazard ratio; CI, confidence interval.

was related to the primary cancer or secondary PCa. In consequence, measures aimed at reducing this survival disadvantage of secondary PCa patients should not only focus on PCa treatments and follow-up but also on treatments and follow-up of their primary cancer. Finally, more detailed databases would allow to distinguish between mortality from primary or secondary cancer could help fine tuning further research and clinical management.

Our work has limitations and should be interpreted in the context of its retrospective and population-based design. Second, the nature of our data does not allow to define specific mortality time points to estimate Kaplan-Meier actuarial mortality rates. This limitation is shared with all previous publications focusing on secondary cancers, after specific primary cancers in large-scale databases (24–26). Limited stage and grade information was available for each of the 10 examined primary cancers and matching could not be performed for PSA and Gleason grade group without losing secondary PCa patients. Finally, important variables such as performance status and comorbidities are not available in the SEER database (27). These also contribute to OM rates but could neither be addressed in the current study or in previous analyses (24–26).

DATA AVAILABILITY STATEMENT

The raw data supporting the conclusions of this article will be made available by the authors, without undue reservation.

ETHICS STATEMENT

Ethical review and approval was not required for the study on human participants in accordance with the local legislation and institutional requirements. Written informed consent for participation was not required for this study in accordance with the national legislation and the institutional requirements.

AUTHOR CONTRIBUTIONS

Conceptualization: MW, LN, CR, FC, and PK. Methodology: MW and ZT. Formal analysis and investigation: MW, CW, and ZT. Writing (original draft preparation): MW, LN, FC, and PK. Writing (review and editing): FS, ABr, DT, MG, ABe, FR, and FC. Supervision: FS, ABr, FR, FC, and PK. All authors contributed to the article and approved the submitted version.

REFERENCES

1. Bray F, Ferlay J, Soerjomataram I, Siegel RL, Torre LA, Jemal A. Global Cancer Statistics 2018: GLOBOCAN Estimates of Incidence and Mortality Worldwide for 36 Cancers in 185 Countries. *CA Cancer J Clin* (2018) 68 (6):394–424. doi: 10.3322/caac.21492
2. Ferlay J, Colombet M, Soerjomataram I, Dyba T, Randi G, Bettio M, et al. Cancer Incidence and Mortality Patterns in Europe: Estimates for 40 Countries and 25 Major Cancers in 2018. *Eur J Cancer* (2018) 103:356–87. doi: 10.1016/j.ejca.2018.07.005
3. Siegel RL, Miller KD, Jemal A. Cancer Statistics, 2019. *CA Cancer J Clin* (2019) 69(1):7–34. doi: 10.3322/caac.21551
4. Wenzel M, Würnschimmel C, Chierigo F, Mori K, Tian Z, Terrone C, et al. Pattern of Biopsy Gleason Grade Group 5 (4 + 5 vs 5 + 4 vs 5 + 5) Predicts Survival After Radical Prostatectomy or External Beam Radiation Therapy. *Eur Urol Focus* (2021) 28:S2405–4569(21)00117-6. doi: 10.1016/j.euf.2021.04.011
5. Wenzel M, Würnschimmel C, Chierigo F, Tian Z, Shariat SF, Terrone C, et al. Assessment of the Optimal Number of Positive Biopsy Cores to Discriminate Between Cancer-Specific Mortality in High-Risk Versus Very High-Risk Prostate Cancer Patients. *Prostate* (2021) 81(14):1055–63. doi: 10.1002/pros.24202
6. Würnschimmel C, Wenzel M, Wang N, Tian Z, Karakiewicz PI, Graefen M, et al. Long-Term Overall Survival of Radical Prostatectomy Patients is Often Superior to the General Population: A Comparison Using Life-Table Data. *Prostate* (2021) 81(11):785–93. doi: 10.1002/pros.24176
7. Nocera L, Wenzel M, Collà Ruvolo C, Würnschimmel C, Tian Z, Gandaglia G, et al. The Effect of Race/Ethnicity on Active Treatment Rates Among Septuagenarian or Older Low Risk Prostate Cancer Patients. *Urol Oncol* (2021) 12:S1078–1439(21)00161-7. doi: 10.1016/j.urolonc.2021.04.004
8. Wenzel M, Würnschimmel C, Nocera L, Collà Ruvolo C, Tian Z, Shariat SF, et al. The Effect of Lymph Node Dissection on Cancer-Specific Survival in Salvage Radical Prostatectomy Patients. *Prostate* (2021) 81(6):339–46. doi: 10.1002/pros.24112
9. Würnschimmel C, Wenzel M, Collà Ruvolo C, Nocera L, Tian Z, Saad F, et al. Life Expectancy in Metastatic Prostate Cancer Patients According to Racial/Ethnic Groups. *Int J Urol* (2021) 28(8):862–9. doi: 10.1111/iju.14595
10. Soerjomataram I, Coebergh JW. Epidemiology of Multiple Primary Cancers. *Methods Mol Biol* (2009) 471:85–105. doi: 10.1007/978-1-59745-416-2_5
11. Donin N, Filson C, Drakaki A, Tan H-J, Castillo A, Kwan L, et al. Risk of Second Primary Malignancies Among Cancer Survivors in the United States, 1992 Through 2008. *Cancer* (2016) 122(19):3075–86. doi: 10.1002/cncr.30164
12. Ng AK, Travis LB. Subsequent Malignant Neoplasms in Cancer Survivors. *Cancer J* (2008) 14(6):429–34. doi: 10.1097/PPO.0b013e31818d8779
13. Van Hemelrijck M, Drevin L, Holmberg L, Garmo H, Adolfsson J, Stattin P. Primary Cancers Before and After Prostate Cancer Diagnosis. *Cancer* (2012) 118(24):6207–16. doi: 10.1002/cncr.27672
14. Kok DEG, van de Schans S a M, Liu L, Kampman E, Coebergh JWW, Kiemeney L a LM, et al. Risk of Prostate Cancer Among Cancer Survivors in the Netherlands. *Cancer Epidemiol* (2013) 37(2):140–5. doi: 10.1016/j.canep.2012.11.004
15. Moot AR, Polglase A, Giles GG, Garson OM, Thursfield V, Gunter D. Men With Colorectal Cancer Are Predisposed to Prostate Cancer. *ANZ J Surg* (2003) 73(5):289–93. doi: 10.1046/j.1445-2197.2003.t01-1-02621.x
16. Kawakami S, Fukui I, Yonese J, Ueda T, Ohno Y, Tsuzuki M, et al. Multiple Primary Malignant Neoplasms Associated With Prostate Cancer in 312 Consecutive Cases. *Urol Int* (1997) 59(4):243–7. doi: 10.1159/000283072
17. Dinh KT, Mahal BA, Ziehr DR, Muralidhar V, Chen Y-W, Viswanathan VB, et al. Risk of Prostate Cancer Mortality in Men With a History of Prior Cancer. *BJU Int* (2016) 117(6B):E20–8. doi: 10.1111/bju.13144
18. Mirabeau-Beale K, Chen M-H, D'Amico AV. Prior-Cancer Diagnosis in Men With Nonmetastatic Prostate Cancer and the Risk of Prostate-Cancer-Specific and All-Cause Mortality. *ISRN Oncol* (2014) 2014:736163. doi: 10.1155/2014/736163
19. Klippenstein P, Schlomm T, von Amsberg G, Beyer B, Pompe RS, Michl U, et al. Prostate Cancer Prognosis in Men With Other Malignancies Prior to Radical Prostatectomy. *Urol Oncol* (2019) 37(9):575.e1–7. doi: 10.1016/j.urolonc.2019.04.007
20. Wenzel M, Würnschimmel C, Nocera L, Ruvolo CC, Tian Z, Saad F, et al. The Effect of Primary Urological Cancers on Survival in Men With Secondary Prostate Cancer. *Prostate* (2021) 81(15):1149–58. doi: 10.1002/pros.24209
21. Kamath GR, Kim MK, Taioli E. Risk of Primary Neuroendocrine Pancreatic Tumor After a First Primary Cancer: A US Population-Based Study. *Pancreas* (2019) 48(2):161–8. doi: 10.1097/MPA.0000000000001232
22. Clift AK, Drymousis P, Al-Nahhas A, Wasan H, Martin J, Holm S, et al. Incidence of Second Primary Malignancies in Patients With Neuroendocrine Tumours. *Neuroendocrinology* (2015) 102(1–2):26–32. doi: 10.1159/000381716
23. *RCT. R: A Language and Environment for Statistical Computing* (2017). Available at: https://wwwr-projectorg2017.
24. Zhu K, Lin R, Zhang Z, Chen H, Rao X. Impact of Prior Cancer History on the Survival of Patients With Larynx Cancer. *BMC Cancer* (2020) 20(1):1137. doi: 10.1186/s12885-020-07634-2
25. Laccetti AL, Pruitt SL, Xuan L, Halm EA, Gerber DE. Prior Cancer Does Not Adversely Affect Survival in Locally Advanced Lung Cancer: A National SEER-Medicare Analysis. *Lung Cancer* (2016) 98:106–13. doi: 10.1016/j.lungcan.2016.05.029
26. He C, Zhang Y, Cai Z, Lin X. Effect of Prior Cancer on Survival Outcomes for Patients With Pancreatic Adenocarcinoma: A Propensity Score Analysis. *BMC Cancer* (2019) 19(1):509. doi: 10.1186/s12885-019-5744-8
27. Wenzel M, Würnschimmel C, Chierigo F, Tian Z, Shariat SF, Terrone C, et al. Non-Cancer Mortality in Elderly Prostate Cancer Patients Treated With Combination of Radical Prostatectomy and External Beam Radiation Therapy. *Prostate* (2021) 81(11):728–35. doi: 10.1002/pros.24169

Conflict of Interest: The authors declare that the research was conducted in the absence of any commercial or financial relationships that could be construed as a potential conflict of interest.

frontiers in Oncology

ORIGINAL RESEARCH
published: 21 October 2021
doi: 10.3389/fonc.2021.772348

Biological Predictors of *De Novo* Tumors in Solid Organ Transplanted Patients During Oncological Surveillance: Potential Role of Circulating *TERT* mRNA

Michela Cangemi[1†], Stefania Zanussi[2†], Enrica Rampazzo[3], Ettore Bidoli[4], Silvia Giunco[3,5], Rosamaria Tedeschi[6], Chiara Pratesi[7], Debora Martorelli[2], Mariateresa Casarotto[2], Ferdinando Martellotta[8], Ornella Schioppa[8], Diego Serraino[4], Agostino Steffan[2], Anita De Rossi[3,5‡], Riccardo Dolcetti[9,10,11,12‡] and Emanuela Vaccher[8‡]*

[1] Department of Biomedical Sciences, University of Sassari, Sassari, Italy, [2] Immunopathology and Cancer Biomarkers, CRO Aviano, National Cancer Institute, IRCCS, Aviano, Italy, [3] Department of Surgery, Oncology and Gastroenterology, Section of Oncology and Immunology, University of Padova, Padova, Italy, [4] Cancer Epidemiology Unit, CRO Aviano, National Cancer Institute, IRCCS, Aviano, Italy, [5] Immunology and Diagnostic Molecular Oncology Unit, Veneto Institute of Oncology (IOV) – IRCCS, Padova, Italy, [6] Microbiology and Virology Unit, "S. Maria degli Angeli" Hospital, Pordenone, Italy, [7] Clinical Pathology, "S. Maria degli Angeli" Hospital, Pordenone, Italy, [8] Division of Medical Oncology A, Centro di Riferimento Oncologico (CRO) Aviano, National Cancer Institute, Istituto di Ricovero e Cura a Carattere Scientifico (IRCCS), Aviano, Italy, [9] Centre for Cancer Immunotherapy, Peter MacCallum Cancer Centre, Melbourne, VIC, Australia, [10] Sir Peter MacCallum Department of Oncology, The University of Melbourne, Melbourne, VIC, Australia, [11] Department of Microbiology and Immunology, The University of Melbourne, Melbourne, VIC, Australia, [12] Faculty of Medicine, The University of Queensland Diamantina Institute, Brisbane, QLD, Australia

Background: *De novo* tumors are a major cause of morbidity and mortality after long-term solid organ transplantation. Chronic immunosuppression strongly affects solid organ transplanted (SOT) patients' immune system by promoting immune evasion strategies and reactivations of viruses with oncogenic potential, ultimately leading to cancer onset. In this scenario, an oncological Surveillance Protocol integrated with biobanking of peripheral blood samples and evaluation of immunovirological and molecular parameters was activated for SOT patients at CRO-IRCCS Aviano, with the aim of identifying suitable biomarkers of cancer development.

Methods: An exploratory longitudinal study was designed based on two serial peripheral blood samples collected at least three months apart. Forty nine SOT patients were selected and stratified by tumor onset during follow-up. Spontaneous T-cell responses to EBV, CMV and tumor associated antigens, EBV-DNA and CMV-DNA loads, and circulating *TERT* mRNA levels were investigated.

Results: Significantly higher levels of circulating *TERT* mRNA were observed 3.5-23.5 months before and close to the diagnosis of cancer as compared to tumor-free patients. Plasmatic *TERT* mRNA levels >97.73 copies/mL at baseline were significantly associated with the risk of developing *de novo* tumors (HR=4.0, 95%C.I. = 1.4-11.5, p=0.01).

OPEN ACCESS

Edited by:
Walter J. Storkus, University of Pittsburgh, United States

Reviewed by:
Diana Metes, University of Pittsburgh, United States
Gilda Alves Brown, Rio de Janeiro State University, Brazil

***Correspondence:**
Riccardo Dolcetti
Riccardo.Dolcetti@petermac.org

†These authors have contributed equally to this work and share first authorship

‡These authors have contributed equally to this work and share senior authorship

Specialty section:
This article was submitted to Genitourinary Oncology, a section of the journal Frontiers in Oncology

Received: *09 September 2021*
Accepted: *30 September 2021*
Published: *21 October 2021*

Citation:
Cangemi M, Zanussi S, Rampazzo E, Bidoli E, Giunco S, Tedeschi R, Pratesi C, Martorelli D, Casarotto M, Martellotta F, Schioppa O, Serraino D, Steffan A, De Rossi A, Dolcetti R and Vaccher E (2021) Biological Predictors of De Novo Tumors in Solid Organ Transplanted Patients During Oncological Surveillance: Potential Role of Circulating TERT mRNA. Front. Oncol. 11:772348. doi: 10.3389/fonc.2021.772348

In particular, the risk significantly increased by 4% with every ten-unit increment in *TERT* mRNA (HR=1.04, 95%C.I. = 1.01-1.07, p=0.01).

Conclusions: Although obtained in an exploratory study, our data support the importance of identifying early biomarkers of tumor onset in SOT patients useful to modulate the pace of surveillance visits.

Keywords: transplant, immunosuppression, oncological surveillance, cancer, circulating *TERT* mRNA, T cells

INTRODUCTION

Solid organ transplantation is currently recognized as the treatment of choice for patients with end-stage disease and the availability of potent anti-rejection drugs significantly reduced the occurrence of acute and chronic allograft rejections, even though long-term survival is still poor (1). Indeed, tumor development, viral infections/reactivations and cardiovascular complications are among the major causes of morbidity and mortality in solid organ transplanted (SOT) patients (2–4).

Combined with lifestyle habits, aging and concomitant comorbidities, chronic exposure to immunosuppressants plays a central role in the pathogenesis of these complications. The most common immunosuppressive drugs used after transplantation, calcineurin inhibitors (CNIs) and mTOR inhibitors (mTORi), while limiting the risk of allograft rejection, may have detrimental effects on antiviral and anti-tumor immunosurveillance. Indeed, CNIs, such as *Cyclosporine A* and *Tacrolimus*, exert their immunosuppressive action through the inhibition of the Calcineurin-NFAT signaling pathway, resulting in IL-2, TNFα, INF-γ downregulation and inhibition of T-cell activation and proliferation in response to foreign antigens (5–8). *Everolimus* and *Sirolimus* inhibit mTOR, a serine-threonine kinase involved in cell growth, proliferation, protein synthesis and apoptosis (9–11); they exert both immunosuppressant and anticancer activities. In particular, mTORi prevent dendritic cells maturation into antigen presenting cells, resulting in T-cell anergy and in the expansion of regulatory T-cells (12, 13).

In SOT patients under chronic immunosuppressive treatments, viral latent Epstein Barr virus (EBV) and/or Cytomegalovirus (CMV) reactivations can occur at any time after transplantation. In particular, CMV disease is the major cause of morbidity in this setting (14, 15). Chronic CMV infection is associated with functional alterations of the innate and adaptive arms of the immune system (16) with the expansion of terminally differentiated lymphocytes with reduced alloreactivity more evident with increasing age (17, 18). Hence, CMV reactivation and age potentially enhance pre-existing immunosuppression promoting immune escape in SOT patients. Moreover, the finding of CMV DNA and antigens in tumor cells from different types of cancer, such as colorectal cancer, malignant glioblastoma, EBV-negative Hodgkin lymphoma, prostatic carcinoma, and breast cancer, suggested an oncomodulatory role for this virus (19–22). EBV is involved in the pathogenesis of lymphoproliferative disorders and some epithelial tumors characterized by distinctive epidemiologic features and risk factors (23). Host immunity plays a crucial role in controlling EBV infection although the virus has evolved an elegant strategy to exploit B-cell differentiation and finally establish an asymptomatic latency in resting memory B lymphocytes (24). The iatrogenic impairment of host immunity against EBV may increase the risk to develop EBV-associated lymphoproliferative disorders, a heterogeneous group of diseases that may be a life-threatening complication after organ transplantation (25, 26).

The increased risk of developing tumors in SOT patients requires the activation of careful clinical and integrated laboratory follow-up protocols to detect cancer onset as early as possible. These strategies would greatly benefit from the availability of biomarkers that can reliably identify patients at high risk of developing tumors to be included in closer follow-up protocols. Monitoring EBV-DNA load coupled with the analysis of EBV-specific T-cell responses may be useful to identify patients at increased risk of EBV-driven lymphoproliferative disorders, while offering an indication for preemptive intervention (25). Under immunosuppressive conditions, latent CMV infection can reactivate and promote inflammatory responses that may contribute to cancer development (16–19). Nevertheless, the possible association between CMV reactivation and tumor onset in SOT recipients has been poorly investigated so far. Other candidate biomarkers have been identified that may be potentially useful to detect malignances early in SOT recipients. A polygenic risk score was recently associated with higher risk of non-melanoma skin cancers in patients receiving different solid organ transplants (27). The analysis of genome-wide DNA methylation of circulating T cells in kidney transplant recipients disclosed that a higher DNA methylation of SerpinB9, an intracellular inhibitor of granzyme B, was associated with the development of squamous cell carcinoma (28). Moreover, a significant reduction in Interleukin-27 expression and secretion by circulating immune cells was correlated with the risk of developing a malignancy in SOT recipients (29). Despite several efforts, however, the identification of reliable and clinically applicable biomarkers predictive of cancer risk in SOT recipients remains challenging due to the heterogeneity of cancers arising in this population and need of prospective series.

T-cell responses to tumor-associated antigens, particularly those specific for the so-called universal tumor associated antigens (TAAs) survivin and telomerase, may be detected in the blood of patients with various types of cancer, even in early phases of the disease (30–33). However, no information is

currently available on the frequency and extent of T-cell responses to universal TAAs in SOT patients, either at the time of tumor diagnosis or at earlier time points.

Besides providing epitopes for the detection of specific T-cell responses, telomerase may also be regarded as an attractive molecular biomarker. In fact, more than 90% of all cancers acquire the capability to replicate indefinitely through the re-activation of telomerase, a ribonucleoprotein complex containing an internal RNA template and the catalytic protein telomerase reverse transcriptase (TERT), with telomere specific reverse transcriptase activity (34). *TERT* is the major rate-limiting catalytic subunit, which has a low/absent expression in normal cells but considerably high expression in the vast majority of tumor cells, suggesting that *TERT* expression level could be a specific biomarker for tumor development (25).

Here we report the results of a prospective exploratory study on advanced immunovirological and molecular monitoring carried out in a pilot cohort of SOT patients enrolled in a long term institutional cancer prevention program. With the main goal of identifying immunologic and/or virologic biomarkers potentially predictive of tumor development, serial blood samples were collected and investigated for EBV and CMV viremia, and the presence of T cell-responses specific for EBV and CMV viral epitopes and for universal TAAs. In addition, stimulated by the recently reported predictive and prognostic relevance of blood *TERT* mRNA levels in various clinical settings (35), we also investigated the circulating *TERT* mRNA levels as early marker of tumor development in SOT recipients.

MATERIALS AND METHODS

Surveillance Protocol

Surveillance Protocol for SOT patients activated at the Centro di Riferimento Oncologico (CRO) in Aviano (PN), Italy, exploits a monitoring program focused on the most frequent and diagnosable *de novo* tumors with standardized screening (skin, lung, kidney, colorectum, cervix and pharynx carcinomas), and an integrated clinical follow-up. Moreover, the Surveillance Protocol includes a sub-protocol for translational research consisting in the biobanking of peripheral blood samples and in the evaluation of immunovirological and molecular parameters to identify candidate biomarkers predictive of *de novo* tumor development in SOT patients. The Surveillance Protocol was approved by the CRO Ethical Committee (ID number: CRO-2016-35). All study participants provided informed written consent at the enrolment. European and National ethical guidelines for research involving human subjects were respected. Criteria of inclusion in the Surveillance Protocol were: to have received a solid organ transplantation at least one year before the enrollment, age ≥18 years old, ECOG 0-2 performance status, life expectancy ≥6 months, and regular follow-up compliance. Subjects with pre-transplant tumors different from non-melanoma skin cancer, Tis cervix, and hepatocellular carcinoma (HCC) in liver transplant recipients were excluded, as well as subjects with complete remission <3 years or post-transplant and pre-enrolment active tumors. Moreover, patients have been considered not eligible for the study if showing the following severe co-morbidities at enrolment or in the previous year: heart failure, myocardial infarction, stroke, severe hepatic and/or renal failure, tuberculosis, psychiatric pathology. The appearance of these clinical conditions during surveillance was also considered as reason for withdrawal from the program along with organ rejection or return to dialysis, the development of advanced tumors requiring chemo and/or radiotherapy or treatment with major root surgery, and the occurrence of life-threatening chronic infections.

The pace of surveillance was established grounding on the classification of the patients by tumor risk. Patients were assigned to the high-risk group if they showed at least one of the following characteristics: duration of immunosuppression ≥10 years, age at transplant ≥50 years, metachronous transplants (i.e., multiple non-synchronous transplants), abuse of smoking/tobacco/alcohol within 15 years from enrolment in the surveillance program, presence of HIV infection. High-risk patients followed an intensive clinical surveillance focused on the diagnosis, by standardized screening protocols, of the more frequent *de novo* tumors, such as carcinoma of the skin, lung, kidney, liver, colorectal, cervix, and head-neck/esophagus. Low-risk patients followed the general population guidelines. Breast and prostate cancer screening complied the general population guidelines in both high and low-risk groups. Unless the patient did not access the visit for personal or health reasons, the clinical assessment was performed every six months for high-risk and annually for low-risk patients. Peripheral blood samples for the immunovirological and molecular surveillance were collected at each visit and close to the date of histological examination that defined the cancer diagnosis.

Sample Collection

Peripheral blood samples were processed within four hours from blood withdrawal. Two aliquots of fresh EDTA peripheral whole blood were immediately stored at -80°C. Thereafter, blood was centrifuged at 800 rpm for 10 minutes and the plasma fraction was further centrifuged at 2100 rpm for 15 minutes, aliquoted in two vials and frozen at -80°C. Peripheral blood mononuclear cells (PBMCs) to be used in functional assays were isolated by Ficoll-Hypaque gradient centrifugation, washed once in PBS, counted by ADAM Cell Counter (DigitalBio), resuspended in 1 mL of FCS containing 10% DMSO and, finally, stored at -120°C.

Biological Study Design

Among 109 SOT patients under surveillance from 2015 to 2018, 49 were selected for an exploratory longitudinal research design based on the availability of two serial peripheral blood samples collected for laboratory analyses at least three months apart and no evidence of tumor onset between enrolment in the Surveillance Protocol and the first sampling. The first and the second blood withdrawal will henceforth be referred to as baseline and follow-up, respectively. Patients' characteristics of this sub-cohort at the time of enrolment in the Surveillance Protocol were described in **Supplementary Table 1**. The biological parameters studied were: antigen-specific T-cell responses against two "universal" TAAs-derived peptide mixes (Survivin and TERT) and viral peptide pools (EBV, CMV), and

whole blood CMV and EBV viremia. Quantification of plasma *TERT* mRNA was also evaluated.

ELISpot Assay

Virus and tumor antigen-specific T cell responses were investigated by using an interferon (IFN)-γ enzyme-linked immunosorbent spot (ELISpot) commercial assay ("Human IFN-γ Single Color ELISPOT", ImmunoSpot®, Cellular Technology Limited (CTL), OH, USA), according to the manufacturer's instructions. Briefly, ninety-six-well plates were pre-coated by an overnight incubation at 4°C with 2μg/mL anti-human IFN-γ capture antibody. The next day, PBMCs were thawed and washed once in serum free RPMI 1640, counted and resuspended in CTL-test Medium at a concentration of 10.5x10^6/mL cells. CMV, EBV, Survivin, TERT peptide mixes (ProImmune, Oxford UK; 0.2ng/mL of each peptide mix) or unspecific stimuli (0.5mg/mL αCD3/αCD28) were resuspended in CTL-test Medium, plated in triplicate and incubated for 10-20 minutes. Triplicate wells without stimulus were used as negative control. Next, patient's PBMCs were placed in co-culture at a concentration of 500,000 PBMCs/well and incubated overnight. The next day, spots were detected with anti-human IFN-γ (biotin) streptavidin alkaline phosphatase, and Blue Developer Solution. Spots were counted and analyzed by using the Immunospot® plate scanning and analysis service (CTL-Europe GmbH, Bonn, Germany).

EBV and CMV Viral Load

For EBV viral load evaluation, cryo-preserved aliquots of 200 μl whole blood were processed for DNA extraction with the QIAamp Blood Mini kit (Qiagen, Gmbh, Hilden, Germany) within 15 days from collection, following the instructions from the manufacturer. A final elution volume of 50 μL was used and EBV-DNA was quantified by real time TaqMan PCR by using the ABI PRISM 7900 HT Sequence Detection System (Applied Biosystems), as previously described (36, 37). EBV viral load was expressed as copies of EBV-DNA genomes per milliliter of whole blood. For statistical analyses, a viral load of zero copies/mL was assigned to samples with undetectable EBV-DNA.

CMV viral load was assessed by the Abbott RealTime CMV assay and the automated m2000 RealTime system (Abbott Molecular Inc., IL, USA) according to manufacturer's instructions. For statistical analyses, a CMV viral load of 39 copies/mL was assigned to samples with detectable CMV-DNA, but below the threshold (40 copies/mL); a viral load of zero copies/mL was assigned to samples with undetectable CMV-DNA.

Quantification of Circulating *TERT* mRNA

RNA was extracted from plasma samples as previously described (38, 39), using 1 mL instead of 500 μL of plasma and reagents' quantities adjusted accordingly. RNA was reverse transcribed into cDNA using the SuperScript TM III RNase reverse transcriptase assay (Thermo Fisher Scientific) in a final volume of 80 μL, according to the manufacturer's instructions.

The expression of *TERT* transcripts in the plasma samples was quantified by real-time PCR, as previously described (38). Briefly, the primers AT1 (5′-CGGAAGAGTGTCTGGAGCAA-3′) and AT2b (5′-CGCAGCTGCACCCTCTTCA-3′), which bind to nucleotide sequences located upstream of the RT motif 1 on the *TERT* gene, thus allowing amplification of all *TERT* transcripts, and the fluorogenic probe AT (FAM 5′-TTGCAAAGCATTGGAATCAGACAGCAC-3′ TAMRA) recognizing the sequence located inside the product amplified by AT1/AT2b were employed (38). The PCR was performed using an ABI prism 7900 Sequence Detection System (PE Applied Biosystems, Foster City, CA, USA) in 50 μL of mixture containing 25 μL 2x TaqMan universal master mix (PE Applied Biosystems), 100 nM of fluorogenic probe, 600 nM of primer AT1, 900 nM of primer AT2b and 10 μl of cDNA sample. After 2 min at 50°C, to allow the uracil *N*-glycosylase to act, and a denaturation step lasting 10 min at 95°C, 50 cycles were run, each consisting of 30 s at 95°C, 30 s at 60°C and 30 s at 72°C. Each sample was run in triplicate and the mean Ct values were plotted against the standard *TERT* reference curve, which was generated with serial fivefold dilutions of the *TERT* amplicon, as previously described (40). *TERT* values were estimated per mL according to the X8 conversion factor and then expressed as *TERT* copies per mL.

Statistical Analysis

Comparisons of unmatched, and baseline-follow-up matched continuous variables were made using the non-parametric Mann-Whitney U test and the Wilcoxon signed rank test, respectively. Fisher's exact test was computed for discrete variables when appropriate. Successively, the impact of biological factors on tumor onset probability was assessed. Due to the exploratory nature of this study, Receiver Operating Characteristic (ROC) curves were calculated for continuous clinical and biological covariates at baseline to determine the best cut-off value that differentiated the risk of tumor onset with the highest specificity and sensitivity (41) (**Supplementary Table 2**). Time-to-tumor-onset was calculated from the date of baseline to the date of tumor diagnosis. Subjects who did not develop any tumor were censored at the date of follow-up. Time of immunosuppression was computed from the time of the first transplant to the date of baseline. Tumor onset probability was examined by means of the Kaplan-Meier method (42), and risk was quantified by means of univariate and multivariate Cox proportional hazard models. Hazard Ratio (HR) and corresponding 95%C.I.s were calculated by dichotomizing continuous clinical and biological variables by the cut-off assessed through the ROC curve. Age was categorized by the median value of the overall cohort and included for HR adjustment. Moreover, HR was computed for ten-unit increases in the level of *TERT* mRNA. Analyses were performed by means of SAS, version 9.4 (SAS Institute Inc., Cary, NC, 2002–2008). All statistical tests were considered statistically significant at a two-sided p-value <0.05.

RESULTS

Patients Characteristics

Table 1 shows the main patients' demographic and clinical characteristics of the 49 SOT patients at baseline: median age

TABLE 1 | Baseline demographic and clinical characteristics of the 49 SOT patients.

	Total N = 49	NT N = 33	T N = 16
Age			
Median years	60	58	64
(range)	(31-80)	(31-79)	(46-80)
p-value°			0.05
Gender			
M, n (%)	32 (65.3)	20 (60.6)	12 (76.5)
F, n (%)	17 (34.7)	13 (39.4)	4 (23.5)
p-value*			0.36
Transplanted Organ			
Kidney, n (%)	40 (81.6)	26 (78.8)	14 (87.5)
Liver, heart or heart+kidney, n (%)	9 (18.4)	7 (21.2)	2 (12.5)
p-value*			0.70
Type of Immunosuppressive therapy			
CNI, n (%)	38 (77.6)	26 (78.8)	12 (75.0)
mTOR/mTOR + CNI, n (%)	11 (22.4)	7 (21.2)	4 (25.0)
p-value*			1.00
Time of Immunosuppression			
Median years	10.5	10.2	11.8
(range)	(1.2-28.4)	(1.2-24.6)	(3.1-28.4)
p-value°			0.36
Pre-transplant immunosuppressive therapy			
No (%)	43 (87.8)	29 (87.9)	14 (87.5)
Yes (%)	6 (12.2)	4 (12.1)	2 (12.5)
p-value*			1.00

*NT, no tumor cohort; T, tumor cohort; M, males; F, females; °, Mann-Whitney U-test; *, Fisher exact test.*

was 60 (31–80) years, 32 (65.3%) were males and 17 (34.7%) were females; forty subjects (81.6%) were kidney transplanted and nine (18.4%) heart, liver or heart plus kidney transplanted. Thirty-eight (77.6%) were treated with CNI, four (8.2%) with mTORi and seven with CNI plus mTORi (14.3%). The median immunosuppression duration from first transplantation was 10.5 (1.2-28.4) years, while six patients received adjunctive pre-transplant immunosuppressive therapy.

During surveillance and after a median time of 10.4 (3.5-23.6) months from baseline, 16 patients were included in the tumor cohort (T) as the following *de novo* tumors were diagnosed: 13 BCC or SCC, one melanoma *in situ*, one indolent non-Hodgkin lymphoma and one renal carcinoma (**Supplementary Table 1**). The median time between baseline and follow-up sampling was 11.7 (6.0-24.2) months for patients who developed a tumor and 12.2 (5.8-28.8) months for those tumor-free (non-tumor cohort, NT) (p=0.13). Cancer was diagnosed before or after a maximum of 3.7 months from the second sample, which was therefore indicative of an underlying neoplastic condition. Patients of the T cohort were significantly older than subjects of the NT cohort (p=0.05). No statistically significant difference was observed in the distribution of the SOT patients for the other parameters analysed.

Immunovirological and Molecular Analyses

Table 2 summarizes the baseline and follow-up median values of the immunovirological and molecular parameters assessed in the SOT patients after stratification by tumor occurrence. No statistically significant difference was found in EBV- and CMV-specific T-cell responses between baseline and follow-up samples within both the NT and the T cohort. Patients in the T cohort showed significantly decreased levels of EBV-specific circulating T cells in the samples collected close to cancer diagnosis when compared with the follow-up samples from the NT cohort [median (range) T *vs.* NT: 45 (0–499) *vs.* 144 (1-1229) sfu/10^5 PBMCs, p=0.02] (**Figure 1A** and **Table 2**).

The percentage of SOT patients with detectable EBV-DNA did not change at baseline compared to follow-up within both the T and NT cohorts, with no statistically significant difference in viral load values throughout the time. No statistically significant difference was found between T and NT cohorts neither for EBV-DNA positivity rate nor for EBV-DNA levels neither at baseline [T *vs.* NT: 62.5% *vs.* 45.4%, p=0.36; median (range) 86 (0-3135) copies/mL *vs.* 0 (0-8845) copies/mL, p=0.38] nor at follow-up [T *vs.* NT: 62.5% *vs.* 45.4%, p=0.36; median (range) 38 (0-3485) copies/mL *vs.* 0 (0-4334) copies/mL, p=0.80].

The percentage of SOT patients with detectable CMV viremia and the CMV-DNA levels did not change from baseline to follow-up in the T and NT cohorts. There was no statistically significant difference in CMV-DNA positivity rate and CMV-DNA load between the T and NT cohorts at baseline [25.0% *vs.* 12.9%, p=0.42; median (range) 0 (0-81) *vs.* 0 (0-655), p=0.54] and at follow-up time [18.7% *vs.* 15.1%, p=0.71; median (range) 0 (0-79) *vs.* 0 (0-670), p=0.89].

The levels of Survivin and TERT-specific T-cells were similar in the NT and T cohorts at baseline [median (range) TAA reactivity in T *vs.* NT: 14 (1-538) *vs.* 9 (0-1329), p=0.73 for Survivin; 11 (1-1196) *vs.* 9 (0-1216), p=0.53 for TERT] or follow-up [median (range) TAA reactivity in T *vs.* NT: 10 (0-987) *vs.* 14 (0-1209), p= 0.53 for Survivin; 12 (0-378) *vs.* 10 (0-971), p=0.91 for TERT]. No significant changes in TAA-specific circulating T cell levels were observed over time (from baseline to follow-up) within each group.

Both T and NT cohorts of SOT patients showed no statistically significant differences in circulating cell-free *TERT* mRNA levels when comparing baseline to follow-up time. However, significantly higher levels of circulating *TERT* mRNA were detected at baseline in patients belonging to the T cohort [112 (0-576) copies/mL] as compared to those from the NT cohort [0 (0-120) copies/mL, p=0.03] (**Table 2** and **Figure 1B**). These findings suggest that a significant increase in the levels of plasmatic *TERT* mRNA can be detected in transplanted patients several months (range 3.5-23.5 months) before the diagnosis of cancer. Moreover, patients in the T cohort showed significantly higher levels of circulating *TERT* mRNA also in the samples obtained close to the date of cancer diagnosis [T *vs.* NT cohort: 115 (0-421) copies/mL *vs.* 0 (0-206) copies/mL, p<0.001] (**Table 2** and **Figure 1B**).

Potential Clinical and Biological Predictors of Tumor Occurrence

We evaluated the potential demographic, clinical and biological predictors of tumor occurrence for SOT patients at baseline. We found that patients ≥60 years had a higher likelihood to develop

TABLE 2 | Biological parameters in the 49 SOT patients after stratification by tumor occurrence.

	NT N = 33		T N = 16	
	Baseline	***Follow-up***	***Baseline***	***Follow-up***
T cell responses against EBV				
Median sfu/10^5 PBMCs (range)	139 (2-1019)	144 (1-1229)	72 (17-1084)	45 (0-499)
p-value (Mann-Whitney test)°			0.53	0.016
p-value (Wilcoxon test)‡		0.30		0.35
T cell responses against CMV				
Median sfu/10^5 PBMCs (range)	539 (1-5000)	614 (1-5000)	521 (13-1097)	501 (0-1726)
p-value (Mann-Whitney test)°			0.53	0.32
p-value (Wilcoxon test)‡		0.73		0.87
EBV-DNA				
Undetected, n (%)	18 (54.6)	18 (54.6)	6 (37.5)	6 (37.5)
Detected, n (%)	15 (45.4)	15 (45.4)	10 (62.5)	10 (62.5)
p-value (Fisher exact test)*			0.36	0.36
Median copies/mL (range)	0 (0-8845)	0 (0-4334)	86 (0-3135)	38 (0-3485)
p-value (Mann-Whitney test)°			0.38	0.80
p-value (Wilcoxon test)‡		0.44		0.38
CMV-DNA$				
Undetected, n (%)	27 (87.1)	28 (84.9)	12 (75.0)	13 (81.3)
Detected, n (%)	4 (12.9)	5 (15.1)	4 (25.0)	3 (18.7)
p-value (Fisher exact test)*			0.42	0.71
Median copies/mL (range)	0 (0-655)	0 (0-670)	0 (0-81)	0 (0-79)
p-value (Mann-Whitney test)°			0.54	0.89
p-value (Wilcoxon test)‡		N.E.		N.E.
T cell responses against SURVIVIN$				
Median sfu/10^5 PBMCs (range)	9 (0-1329)	14 (0-1209)	14 (1-538)	10 (0-987)
p-value (Mann-Whitney test)°			0.73	0.53
p-value (Wilcoxon test)‡		0.08		0.83
T cell responses against TERT$				
Median sfu/10^5 PBMCs (range)	9 (0-1216)	10 (0-971)	11 (1-1196)	12 (0-378)
p-value (Mann-Whitney test)°			0.53	0.91
p-value (Wilcoxon test)‡		0.13		0.94
***TERT* mRNA**				
Median copies/mL (range)	0 (0-120)	0 (0-206)	112 (0-576)	115 (0-421)
p-value (Mann-Whitney test)°			0.03	<0.001
p-value (Wilcoxon test)‡		0.90		0.60

*NT, no tumor cohort; T, tumor cohort; °, Mann-Whitney U test (no tumor vs. tumor cohort); ‡, Wilcoxon paired signed-rank test (baseline vs. follow-up values); *, Fisher exact test (no tumor vs. tumor cohort); N.E., not evaluable; $, the sum does not add up to the total because of missing values; sfu/10^5 PBMCs, spot forming units/10^5 Peripheral Blood Cells.*

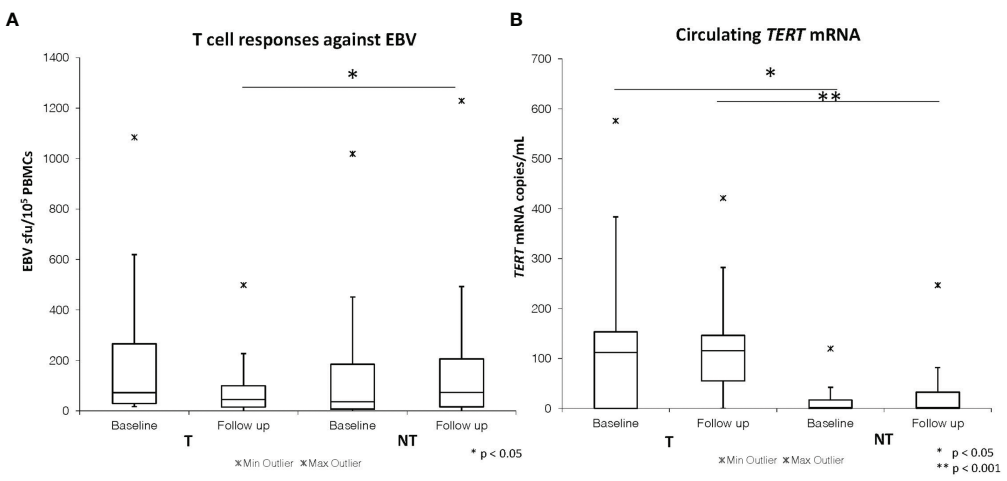

FIGURE 1 | Baseline and follow-up EBV ELISpot T cell responses **(A)** and plasma *TERT* mRNA levels **(B)** in SOT patients developing (T) and not developing tumors (NT).

tumors as compared to patients <60 years (Log-Rank test=9.58; p<0.01) (**Figure 2A**). More specifically, patients ≥60 years presented a higher risk of tumor onset than younger (HR=6.7 for patients ≥60 *vs.* <60 years, 95%C.I. = 1.7-22.6, p<0.01) (**Table 3**).

Kaplan-Meier's evaluation showed that patients with baseline circulating *TERT* mRNA levels above 97.73 copies/mL had a significant higher risk to develop tumors than patients with baseline *TERT* mRNA levels below this value (Log-Rank test=7.37; p<0.01) (**Figure 2B**). Accordingly, the risk of developing tumors was significantly higher in individuals with high baseline circulating *TERT* mRNA levels than patients with lower values (HR=4.0 for patients with >97.73 *vs.* ≤97.73 copies/mL, 95%C.I. = 1.4-11.5, p=0.01). The area under the ROC curve, sensibility, and specificity for this parameter were 0.70 (95% C.I. = 0.60-0.82), 0.53 (95%C.I. = 0.27-0.79), and 0.94 (95%C.I. = 0.80-0.99), respectively. Notably, every ten-unit increment of *TERT* mRNA was associated with a 4% increase in the risk of developing cancer (HR=1.04, 95%C.I. = 1.01-1.07, p=0.01) (**Table 3**). After adjustment for age, the association of *TERT* mRNA levels above the cut-off with the risk of tumor development was still high, but not significant (HR=2.5, 95% C.I. = 0.8-7.8, p=0.13). The risk of tumor development for patients over 60 years of age raised with increasing TERT mRNA levels [HR and 95%C.I. for patients over 60 years of age and *TERT* mRNA ≤97.73 or >97.73 copies/mL *vs.* patients under 60 and *TERT* mRNA ≤97.73 copies/mL=6.7 (1.1-40.4) or 12.3 (2.3-64.7)] (**Table 4**).

EBV-DNA higher than 29 copies/mL at baseline was associated to a higher, although not significant, risk to develop tumors (Log-rank test=3.51 for subjects with >29 *vs.* ≤29 copies/mL, p=0.06 (not shown); HR=2.6, 95%C.I. = 0.9-7.4, p=0.07, **Table 3**).

DISCUSSION

The identification of suitable biomarkers able to predict the risk of impending tumor development in SOT patients constitutes an important but still unmet clinical need. To address this relevant issue, we took advantage of the clinical and laboratory surveillance program for SOT patients recently activated at CRO-IRCCS Aviano. The routine clinical workup of these patients was implemented with the investigation of CD8 T-cell responses against EBV and CMV antigens and "universal" TAAs, the assessment of viral reactivations and quantification of circulating *TERT* mRNA in plasma as potential source of risk-predictive biomarkers for a broad spectrum of cancers, such as those occurring in SOT recipients. Here we report the results of the first prospective cohort of patients.

CMV and EBV infections are highly prevalent in the general population, and the immunosuppressive treatment of SOT recipients can occasionally trigger viral reactivations that directly or indirectly may enhance the risk of cancer development. In our series, CMV viremia was detected in a low fraction of cases (approximately 17%), consistent with a relatively infrequent CMV reactivation, which occurred at comparable frequency in patients of the T and NT cohorts. Similarly, the two groups of SOT recipients showed no significant difference in the extent of CMV-specific T cell responses, ruling out any possible pathogenic association between CMV reactivation and the occurrence of tumors. It should be considered, however, that the majority of tumors observed in our cohort were non-melanoma skin cancers, suggesting that these results warrant a confirmation in larger prospective series including higher numbers of non-skin tumors. By contrast, about half of the SOT recipients investigated had detectable EBV viremia, indicating a relatively more frequent reactivation of EBV. Comparative analysis of the T and NT cohorts did not disclose significant differences in the extent of EBV-specific T-cell responses, except for the significantly lower levels of circulating EBV-specific T-cells detected at the time of cancer diagnosis in the T cohort compared to the NT cohort samples at follow-up. This intriguing observation could be the result of additional immunosuppression imposed by cancer onset and/or the diversion of residual immune responses towards cancer-associated antigens different from Survivin or TERT and warrants further investigation in larger series. The fact that we did not observe significantly increased levels of T-cell responses to EBV is

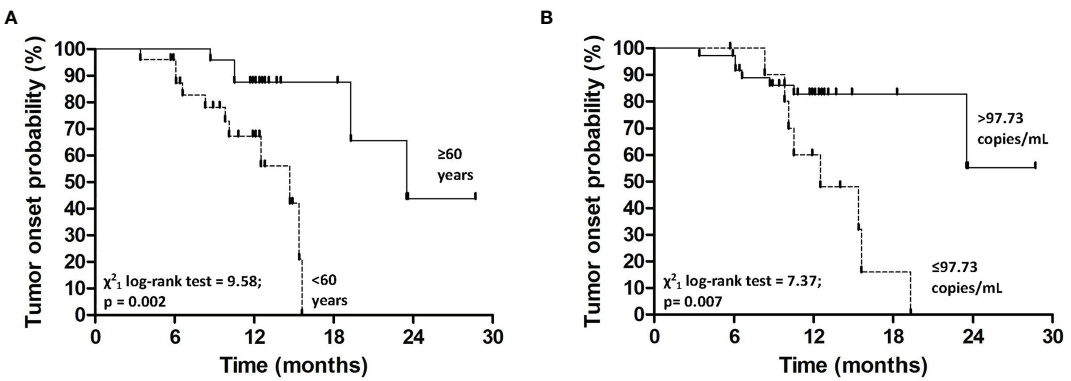

FIGURE 2 | Kaplan-Meier estimates for tumor onset probability according to age **(A)** and plasma *TERT* mRNA levels at baseline **(B)**.

TABLE 3 | Cox regression analysis evaluating the associations between baseline demographic, clinical or biological parameters and tumor onset.

	NT N = 33 n. (%)	T N = 16 n. (%)	HR (95%C.I.)	p-value	HR* (95%C.I.)	p-value
Age, years						
<60	14 (42.4)	11 (68.8)	1ł		–	
≥60	19 (57.6)	5 (31.3)	6.7 (1.7-22.6)	<0.01	–	–
Gender						
M	20 (60.6)	12 (76.5)	1ł		1ł	
F	13 (39.4)	4 (23.5)	0.7 (0.2-2.2)	0.52	0.6 (0.2-1.8)	0.31
Transplanted organ						
Kidney	26 (78.8)	14 (87.5)	1ł		1ł	
Liver/heart/heart + kidney	7 (21.2)	2 (12.5)	0.9 (0.2-4.2)	0.93	0.4 (0.1-2.1)	0.31
Type of immunosuppressive therapy						
CNI	26 (78.8)	12 (75.0)	1ł		1ł	
mTOR/mTOR + CNI	7 (21.2)	4 (25.0)	1.3 (0.4-4.2)	0.62	1.2 (0.4-3.7)	0.82
Time of Immunosuppression, years						
≤18.83	31 (93.9)	11 (68.8)	1ł		1ł	
>18.83	2 (6.1)	5 (31.3)	2.4 (0.8-7.1)	0.10	2.1 (0.7-6.2)	0.18
Pre-transplant immunosuppressive therapy						
No	29 (87.9)	14 (87.5)	1ł		1ł	
Yes	4 (12.1)	2 (12.5)	2.0 (0.4-9.4)	0.37	2.0 (0.4-9.4)	0.38
EBV-DNA, copies/mL						
≤29	19 (57.6)	6 (37.5)	1ł		1ł	
>29	14 (42.4)	10 (62.5)	2.6 (0.9-7.4)	0.07	2.0 (0.7-5.9)	0.19
CMV-DNA$, copies/mL						
Undetected	27 (87.1)	12 (75.0)	1ł		1ł	
Detected	4 (12.9)	4 (25.0)	1.6 (0.5-4.9)	0.45	1.7 (0.5-5.5)	0.36
T cell responses against EBV$, sfu/10^5 PBMCs						
>106	13 (39.4)	9 (64.3)	1ł		1ł	
≤106	20 (60.6)	5 (35.7)	2.3 (0.8-6.9)	0.14	2.0 (0.7-6.1)	0.23
T cell responses against CMV$, sfu/10^5 PBMCs						
>1097	7 (21.2)	1 (7.1)	1ł		1ł	
≤1097	26 (78.8)	13 (92.9)	0.6 (0.7-46.1)	0.10	3.9 (0.4-34.8)	0.22
***TERT* mRNA$, copies/mL**						
≤97.73	30 (90.9)	7 (46.7)	1ł		1ł	
>97.73	3 (9.1)	8 (53.3)	4.0 (1.4-11.5)	0.01	2.5 (0.8-7.8)	0.13
10-unit increases			1.04 (1.01-1.07)	0.01	1.02 (0.99-1.06)	0.22
T cell responses against TERT$, sfu/10^5 PBMCs						
≤8	16 (48.5)	4 (28.6)	1ł		1ł	
>8	17 (51.5)	10 (71.4)	1.4 (0.4-4.7)	0.58	1.7 (0.5-5.8)	0.37
T cell responses against SURVIVIN$, sfu/10^5 PBMCs						
≤13	20 (60.6)	7 (50.0)	1ł		1ł	
>13	13 (60.6)	7 (50.0)	1.2 (0.4-3.4)	0.78	1.4 (0.5-4.1)	0.59

*NT, no tumor cohort; T, tumor cohort; HR, Hazard Ratio; C.I., Confidence Interval; *, Adjusted for age; ł, reference category; $, the sum does not add up to the total because of missing values; sfu/10^5 PBMCs, spot forming units/10^5 Peripheral Blood Cells.*

TABLE 4 | HR and 95%C.I. according to the combined effect of age and circulating *TERT* mRNA levels among 49 SOT patients.

Age, years	*TERT* mRNA copies/mL					
	≤97.73			>97.73		
	N	HR	95% C.I.	N	HR	95% C.I.
<60	21	1ł	–	3	4.9	0.7-35.7
≥60	16	6.7	1.1-40.4	8	12.3	2.3-64.7

HR, Hazard Ratio; C.I., Confidence Interval; ł, reference category.

consistent with the observation that, in our series, no patient developed EBV-related lymphoproliferations, thus preventing the possibility to assess the predictive value of this analysis. Indeed, our results are in line with the observation that EBV-DNA load is generally high in the first year after transplantation in SOT patients with positive EBV-specific T cell responses, when the risk of EBV-driven lymphoproliferative disorders is high (43).

Despite T cell responses to "universal" TAAs can be detected also in patients with early stages of cancer (30, 31), no significantly higher levels of T-cells specific for TERT and Survivin were detected at baseline or at the time of diagnosis of cancer in the blood of T and NT patients. Globally, IFN-γ T cell responses against TERT and Survivin were not significantly different in T and NT cohorts also when values over time (i.e., baseline *vs.* follow-up) were considered. This could be due to the degree of variability of antigen-specific T cell responses among patients, as frequently observed in the cancer setting (44). The negative impact on tumor antigen priming potentially exerted by immunosuppressive drugs could also at least in part explain these findings, in particular considering that CNIs, the most frequently used drugs administered to our cohort of

SOT patients, were shown to markedly inhibit antigen presentation through both MHC class I and II (45).

Expression of TERT, which is usually repressed in normal somatic cells, is essential to sustain the unlimited replicative potential of cancer cells (34) showing a critical role in tumor formation and progression. Consistently with this critical pathogenic role, circulating cell-free *TERT* mRNA can be detected in plasma from cancer patients at levels that significantly correlate with those in tumor specimens (46), conversely, cell-free *TERT* mRNA is not detectable in plasma samples of healthy volunteers (46, 47). Importantly, several studies have been demonstrated that circulating *TERT* mRNA is an independent prognostic marker in different types of tumors (35), including gastric (48), prostatic (49), lung (50), and colorectal cancers (38, 46, 51). In addition, *TERT* mRNA levels in plasma samples of patients with rectal cancer were identified as a predictive marker of response to therapy (38, 39, 51). In the present study, we found that patients of the T cohort showed significantly higher levels of circulating *TERT* mRNA than those of the NT cohort both at baseline and follow-up. These findings are consistent with the evidence that *TERT* expression is a hallmark of cancer (34). Our observation that the levels of circulating *TERT* mRNA were significantly higher even before the diagnosis of cancer in the T cohort is intriguing and strongly suggests the potential clinical relevance of the inclusion of circulating *TERT* mRNA among the biomarkers to be investigated for monitoring of SOT recipients. Indeed, the univariate analysis shows that the risk of developing tumors was significantly higher in SOT recipients with high baseline circulating *TERT* mRNA levels than those with low values. The risk of tumor development in these patients remained high after adjusting for age even not at significant level as a probable consequence of the relatively limited sample size.

Considering that the majority of tumors occurred in our series of SOT recipients included non-melanoma skin cancers, our results suggest that monitoring the circulating *TERT* mRNA levels could identify SOT patients requiring a more frequent clinical and dermatologic follow-up. The need of non-invasive biomarkers for the management of BCC and SCC in SOT recipients is remarkably important given the high incidence of these malignancies in the post-transplant setting (52–55). It is noteworthy that non-melanoma skin cancers in SOT recipients tend to be more aggressive, with higher morbidity and mortality compared to the general population (56–59). Moreover, careful monitoring of circulating *TERT* mRNA could be helpful in pre-transplantation to define the minimum non-melanoma skin cancer remission times before the graft, due to the high rate of post-transplant relapse in the patients with pre-transplant skin malignancies (60, 61).

Because of the exploratory nature of this report, all types of cancer developed during surveillance were described instead of focusing on non-melanoma skin cancers only. Further studies in independent prospective cohorts will be however necessary to clinically validate the possible role of circulating *TERT* mRNA levels as predictor of non-melanoma skin cancers. Moreover, analysis of larger cohorts of SOT recipients developing tumors different from non-melanoma skin cancers is warranted to establish whether circulating *TERT* mRNA levels can serve as a global early marker of tumor development in this setting. Finally, it should be kept in mind that, despite the fact that in most of the tumors replicative immortality is sustained by the inappropriate re-activation of TERT, a small percentage of neoplasms (approximately 10-15%), mainly those of mesenchymal and neuroepithelial origin, grow independently from TERT/telomerase. In these tumors, telomere shortening that accompanies cell proliferation is compensated by the alternative lengthening of telomeres (ALT) mechanism, a homologous recombination-based process (62, 63). For the ALT-dependent neoplasms occurring in SOT patients, circulating TERT mRNA detection would not be informative, therefore other blood-based biomarkers of tumor development need to be investigated.

Our results, even if preliminary and on a relatively small cohort, emphasize the relevance of the implementation of a specific program of oncological monitoring for SOT patients, which considers the different variables present in such complex patients. Monitoring programs should be integrated with various investigative strategies that can identify and prospectively validate markers predictive of *de novo* tumors, to be combined with already established approaches that help identify high-risk patients. To the best of our knowledge, this is the first comprehensive immunovirological and molecular monitoring study in a prospective cohort of SOT patients aimed at identifying such biomarkers. The results obtained in this pilot series, although not conclusive, are consistent with the hypothesis that the detection of early tumor markers, such as increased levels of circulating *TERT* mRNA, may be of help to assess the risk of cancer in SOT patients.

DATA AVAILABILITY STATEMENT

The raw data supporting the conclusions of this article will be made available by the authors, without undue reservation.

ETHICS STATEMENT

The studies involving human participants were reviewed and approved by Ethical Committee of the Centro di Riferimento Oncologico, Aviano, Italy. The patients/participants provided their written informed consent to participate in this study.

AUTHOR CONTRIBUTIONS

MC participated in performing the experiments, data curation and analysis, drafting and editing the work, and final approval. SZ participated in performance of the research, data acquisition, curation, analysis and presentation, drafting, revising and editing the work, and final approval. ER participated in performing the experiments, revising the work, and final approval. EB Participated in data analysis and presentation, revising the work, and final approval. SG participated in performing the experiments, revising the work, and final approval. RT participated in performing the experiments, revising the work, and final approval.

CP participated in performing the experiments, data analysis, revising the work, and final approval. DM participated in performing the experiments, revising the work, and final approval. MTC participated in data curation, revising the work, and final approval. FM participated in performance of the research, and final approval. OS participated in performance of the research, and final approval. DS participated in funding acquisition and final approval. AS participated in supervision, resources acquisition, and final approval. AR participated in conception of the work, funding and resources acquisition, drafting, revising and editing the work, supervision and final approval. RD participated in conception of the work, funding acquisition, drafting, revising and editing the work, supervision and final approval. EV participated in project administration, data acquisition and curation, revising and editing the work, supervision and final approval.

FUNDING

This work was partly supported by grants from the Italian Ministry of Health (Ricerca Corrente), Associazione Italiana per la Ricerca sul Cancro (AIRC) [Grant no. IG-19112, PI DS], Department of Surgery, Oncology and Gastroenterology (DiSCOG), University of Padova, Italy [Grant no. BIRD181981/18, PI AR], Cancer Council Queensland [APP1145758, APP1165063, PI RD].

SUPPLEMENTARY MATERIAL

The Supplementary Material for this article can be found online at: https://www.frontiersin.org/articles/10.3389/fonc.2021.772348/full#supplementary-material

REFERENCES

1. Watson CJE, Dark JH. Organ Transplantation: Historical Perspective and Current Practice. *Br J Anaesth* (2012) 108(Suppl 1):i29–42. doi: 10.1093/bja/aer384
2. Schrem H, Kurok M, Kaltenborn A, Vogel A, Walter U, Zachau L, et al. Incidence and Long-Term Risk of *De Novo* Malignancies After Liver Transplantation With Implications for Prevention and Detection. *Liver Transplant* (2013) 19:1252–61. doi: 10.1002/lt.23722
3. Hall EC, Pfeiffer RM, Segev DL, Engels EA. Cumulative Incidence of Cancer After Solid Organ Transplantation. *Cancer* (2013) 119:2300–8. doi: 10.1002/cncr.28043
4. Chapman JR, Webster AC, Wong G. Cancer in the Transplant Recipient. *Cold Spring Harb Perspect Med* (2013) 3:a015677. doi: 10.1101/cshperspect.a015677
5. Liu J, Farmer JD Jr, Lane WS, Friedman J, Weissman I, Schreiber SL. Calcineurin Is a Common Target of Cyclophilin-Cyclosporin A and FKBP-FK506 Complexes. *Cell* (1991) 66:807–15. doi: 10.1016/0092-8674(91)90124-h
6. Borel JF, Feurer C, Gubler HU, Stähelin H. Biological Effects of Cyclosporin A: A New Antilymphocytic Agent. *Agents Actions* (1976) 6:468–75. doi: 10.1007/BF01973261
7. Kapturczak MH, Meier-Kriesche HU, Kaplan B. Pharmacology of Calcineurin Antagonists. *Transplant Proc* (2004) 36:25S–32S. doi: 10.1016/j.transproceed.2004.01.018
8. Reichenspurner H. Overview of Tacrolimus-Based Immunosuppression After Heart or Lung Transplantation. *J Heart Lung Transplant* (2005) 24:119–30. doi: 10.1016/j.healun.2004.02.022
9. Jacinto E, Hall MN. Tor Signalling in Bugs, Brain and Brawn. *Nat Rev Mol Cell Biol* (2003) 4:117–26. doi: 10.1038/nrm1018
10. Granata S, Dalla Gassa A, Carraro A, Brunelli M, Stallone G, Lupo A, et al. Sirolimus and Everolimus Pathway: Reviewing Candidate Genes Influencing Their Intracellular Effects. *Int J Mol Sci* (2016) 17:735. doi: 10.3390/ijms17050735
11. Thomson AW, Turnquist HR, Raimondi G. Immunoregulatory Functions of mTOR Inhibition. *Nat Rev Immunol* (2009) 9:324–37. doi: 10.1038/nri2546
12. Haidinger M, Poglitsch M, Geyeregger R, Kasturi S, Zeyda M, Zlabinger GJ, et al. A Versatile Role of Mammalian Target of Rapamycin in Human Dendritic Cell Function and Differentiation. *J Immunol* (2010) 185:3919–31. doi: 10.4049/jimmunol.1000296
13. Stallone G, Infante B, Di Lorenzo A, Rascio F, Zaza G, Grandaliano G. mTOR Inhibitors Effects on Regulatory T Cells and on Dendritic Cells. *J Transl Med* (2016) 14:152. doi: 10.1186/s12967-016-0916-7
14. Sagedal S, Hartmann A, Nordal KP, Osnes K, Leivestad T, Foss A, et al. Impact of Early Cytomegalovirus Infection and Disease on Long-Term Recipient and Kidney Graft Survival. *Kidney Int* (2004) 66:329–37. doi: 10.1111/j.1523-1755.2004.00735.x
15. Fica A, Cervera C, Pérez N, Marcos MA, Ramírez J, Linares L, et al. Immunohistochemically Proven Cytomegalovirus End-Organ Disease in Solid Organ Transplant Patients: Clinical Features and Usefulness of Conventional Diagnostic Tests. *Transpl Infect Dis* (2007) 9:203–10. doi: 10.1111/j.1399-3062.2007.00220.x
16. Varani S, Frascaroli G, Landini MP, Söderberg-Nauclér C. Human Cytomegalovirus Targets Different Subsets of Antigen-Presenting Cells With Pathological Consequences for Host Immunity: Implications for Immunosuppression, Chronic Inflammation and Autoimmunity. *Rev Med Virol* (2009) 19:131–45. doi: 10.1002/rmv.609
17. Chou JP, Effros RB. T Cell Replicative Senescence in Human Aging. *Curr Pharm Des* (2013) 19:1680–98. doi: 10.2174/138161213805219711
18. Weltevrede M, Eilers R, de Melker HE, van Baarle D. Cytomegalovirus Persistence and T-Cell Immunosenescence in People Aged Fifty and Older: A Systematic Review. *Exp Gerontol* (2016) 77:87–95. doi: 10.1016/j.exger.2016.02.005
19. Söderberg-Nauclér C. HCMV Microinfections in Inflammatory Diseases and Cancer. *J Clin Virol* (2008) 41:218–23. doi: 10.1016/j.jcv.2007.11.009
20. Bai B, Wang X, Chen E, Zhu H. Human Cytomegalovirus Infection and Colorectal Cancer Risk: A Meta-Analysis. *Oncotarget* (2016) 7:76735–42. doi: 10.18632/oncotarget.12523
21. Richardson AK, Walker LC, Cox B, Rollag H, Robinson BA, Morrin H, et al. Breast Cancer and Cytomegalovirus. *Clin Transl Oncol* (2020) 22:585–602. doi: 10.1007/s12094-019-02164-1
22. Cinatl J, Vogel JU, Kotchetkov R, Wilhelm Doerr H. Oncomodulatory Signals by Regulatory Proteins Encoded by Human Cytomegalovirus: A Novel Role for Viral Infection in Tumor Progression. *FEMS Microbiol Rev* (2004) 28:59–77. doi: 10.1016/j.femsre.2003.07.005
23. Ali AS, Al-Shraim M, Al-Hakami AM, Jones IM. Epstein- Barr Virus: Clinical and Epidemiological Revisits and Genetic Basis of Oncogenesis. *Open Virol J* (2015) 9:7–28. doi: 10.2174/1874357901509010007
24. Ohshima K, Suzumiya J, Kanda M, Kato A, Kikuchi M. Integrated and Episomal Forms of Epstein-Barr Virus (EBV) in EBV Associated Disease. *Cancer Lett* (1998) 122:43–50. doi: 10.1016/s0304-3835(97)00368-6
25. Petrara MR, Giunco S, Serraino D, Dolcetti R, De Rossi A. Post-Transplant Lymphoproliferative Disorders: From Epidemiology to Pathogenesis-Driven Treatment. *Cancer Lett* (2015) 369:37–44. doi: 10.1016/j.canlet.2015.08.007
26. Petrara MR, Serraino D, Di Bella C, Neri F, Del Bianco P, Brutti M, et al. Immune Activation, Immune Senescence and Levels of Epstein Barr Virus in Kidney Transplant Patients: Impact of mTOR Inhibitors. *Cancer Lett* (2020) 469:323–31. doi: 10.1016/j.canlet.2019.10.045
27. Stapleton CP, Chang BL, Keating BJ, Conlon PJ, Cavalleri GL. Polygenic Risk Score of Non-Melanoma Skin Cancer Predicts Post-Transplant Skin Cancer Across Multiple Organ Types. *Clin Transplant* (2020) 34:e13904. doi: 10.1111/ctr.13904
28. Peters FS, Peeters AMA, van den Bosch TPP, Mooyaart AL, van de Wetering J, Betjes MGH, et al. Disrupted Regulation of Serpinb9 in Circulating T Cells Is Associated With an Increased Risk for Post-Transplant Skin Cancer. *Clin Exp Immunol* (2019) 197:341–51. doi: 10.1111/cei.13309

29. Pontrelli P, Rascio F, Zaza G, Accetturo M, Simone S, Infante B, et al. Interleukin-27 Is a Potential Marker for the Onset of Post-Transplant Malignancies. *Nephrol Dial Transplant* (2019) 34:157–66. doi: 10.1093/ndt/gfy206
30. Coughlin CM, Fleming MD, Carroll RG, Pawel BR, Hogarty MD, Shan X, et al. Immunosurveillance and Survivin-Specific T-Cell Immunity in Children With High-Risk Neuroblastoma. *J Clin Oncol* (2006) 24:5725–34. doi: 10.1200/JCO.2005.05.3314
31. Negrini S, De Palma R, Filaci G. Anti-Cancer Immunotherapies Targeting Telomerase. *Cancers* (2020) 12:2260. doi: 10.3390/cancers12082260
32. Mizukoshi E, Nakamoto Y, Marukawa Y, Arai K, Yamashita T, Tsuji H, et al. Cytotoxic T Cell Responses to Human Telomerase Reverse Transcriptase in Patients With Hepatocellular Carcinoma. *Hepatology* (2006) 43:1284–94. doi: 10.1002/hep.21203
33. Yi JS, Ready N, Healy P, Dumbauld C, Osborne R, Berry M, et al. Immune Activation in Early-Stage Non-Small Cell Lung Cancer Patients Receiving Neoadjuvant Chemotherapy Plus Ipilimumab. *Clin Cancer Res* (2017) 23:7474–82. doi: 10.1158/1078-0432.CCR-17-2005
34. Hanahan D, Weinberg RA. Hallmarks of Cancer: The Next Generation. *Cell* (2011) 144:646–74. doi: 10.1016/j.cell.2011.02.013
35. Giunco S, Rampazzo E, Celeghin A, Petrara MR, De Rossi A. Telomere and Telomerase in Carcinogenesis: Their Role as Prognostic Biomarkers. *Curr Pathobiol Rep* (2015) 3:315–28. doi: 10.1007/s40139-015-0087-x
36. Bortolin MT, Pratesi C, Dolcetti R, Bidoli E, Vaccher E, Zanussi S, et al. Clinical Value of Epstein–Barr Virus DNA Levels in Peripheral Blood Samples of Italian Patients With Undifferentiated Carcinoma of Nasopharyngeal Type. *Cancer Lett* (2006) 233:247–54. doi: 10.1016/j.canlet.2005.03.015
37. Pratesi C, Zanussi S, Tedeschi R, Bortolin MT, Talamini R, Rupolo M, et al. γ-Herpesvirus Load as Surrogate Marker of Early Death in HIV-1 Lymphoma Patients Submitted to High Dose Chemotherapy and Autologous Peripheral Blood Stem Cell Transplantation. *PloS One* (2015) 10:e0116887. doi: 10.1371/journal.pone.0116887
38. Rampazzo E, Del Bianco P, Bertorelle R, Boso C, Perin A, Spiro G, et al. The Predictive and Prognostic Potential of Plasma Telomerase Reverse Transcriptase (TERT) RNA in Rectal Cancer Patients. *Br J Cancer* (2018) 118:878–86. doi: 10.1038/bjc.2017.492
39. Rampazzo E, Cecchin E, Del Bianco P, Menin C, Spolverato G, Giunco S, et al. Genetic Variants of the TERT Gene, Telomere Length, and Circulating TERT as Prognostic Markers in Rectal Cancer Patients. *Cancers (Basel)* (2020) 12:3115. doi: 10.3390/cancers12113115
40. Terrin L, Trentin L, Degan M, Corradini I, Bertorelle R, Carli P, et al. Telomerase Expression in B-Cell Chronic Lymphocytic Leukemia Predicts Survival and Delineates Subgroups of Patients With the Same igVH Mutation Status and Different Outcome. *Leukemia* (2007) 21:965–72. doi: 10.1038/sj.leu.2404607
41. DeLong ER, DeLong DM, Clarke-Pearson DL. Comparing the Areas Under Two or More Correlated Receiver Operating Characteristic Curves: A Nonparametric Approach. *Biometrics* (1988) 44:837–45. doi: 10.2307/2531595
42. Kaplan EL, Meier P. Nonparametric Estimation From Incomplete Observations. *J Am Stat Assoc* (1958) 53:457–81. doi: 10.1080/01621459.1958.10501452
43. Rittà M, Costa C, Sinesi F, Sidoti F, Di Nauta A, Mantovani S, et al. Evaluation of Epstein-Barr Virus–Specific Immunologic Response in Solid Organ Transplant Recipients With an Enzyme-Linked ImmunoSpot Assay. *Transplant Proc* (2013) 45:2754–7. doi: 10.1016/j.transproceed.2013.07.033
44. Muraro E, Merlo A, Martorelli D, Cangemi M, Dalla Santa S, Dolcetti R, et al. Fighting Viral Infections and Virus-Driven Tumors With Cytotoxic CD4+ T Cells. *Front Immunol* (2017) 8:197. doi: 10.3389/fimmu.2017.00197
45. Lee YH, Lee YR, Im SA, Park SI, Kim KH, Gerelchuluun T, et al. Calcineurin Inhibitors Block MHC-Restricted Antigen Presentation *In Vivo*. *J Immunol* (2007) 179:5711–6. doi: 10.4049/jimmunol.179.9.5711
46. Terrin L, Rampazzo E, Pucciarelli S, Agostini M, Bertorelle R, Esposito G, et al. Relationship Between Tumor and Plasma Levels of hTERT mRNA in Patients With Colorectal Cancer: Implications for Monitoring of Neoplastic Disease. *Clin Cancer Res* (2008) 14:7444–51. doi: 10.1158/1078-0432.CCR-08-0478
47. Tani N, Ichikawa D, Ikoma D, Tomita H, Sai S, Ikoma H, et al. Circulating Cell-Free mRNA in Plasma as a Tumor Marker for Patients With Primary and Recurrent Gastric Cancer. *Anticancer Res* (2007) 27:1207–12.
48. Kang Y, Zhang J, Sun P, Shang J. Circulating Cell-Free Human Telomerase Reverse Transcriptase mRNA in Plasma and Its Potential Diagnostic and Prognostic Value for Gastric Cancer. *Int J Clin Oncol* (2013) 18:478–86. doi: 10.1007/s10147-012-0405-9
49. March-Villalba JA, Martínez-Jabaloyas JM, Herrero MJ, Santamaria J, Aliño SF, Dasí F. Cell-Free Circulating Plasma hTERT mRNA Is a Useful Marker for Prostate Cancer Diagnosis and Is Associated With Poor Prognosis Tumor Characteristics. *PloS One* (2012) 7:e43470. doi: 10.1371/journal.pone.0043470
50. Miura N, Nakamura H, Sato R, Tsukamoto T, Harada T, Takahashi S, et al. Clinical Usefulness of Serum Telomerase Reverse Transcriptase (hTERT) mRNA and Epidermal Growth Factor Receptor (EGFR) mRNA as a Novel Tumor Marker for Lung Cancer. *Cancer Sci* (2006) 97:1366–73. doi: 10.1111/j.1349-7006.2006.00342.x
51. Pucciarelli S, Rampazzo E, Briarava M, Maretto I, Agostini M, Digito M, et al. Telomere-Specific Reverse Transcriptase (hTERT) and Cell-Free RNA in Plasma as Predictors of Pathologic Tumor Response in Rectal Cancer Patients Receiving Neoadjuvant Chemoradiotherapy. *Ann Surg Oncol* (2012) 19:3089–96. doi: 10.1245/s10434-012-2272-z
52. Huo Z, Li C, Xu X, Ge F, Wang R, Wen Y, et al. Cancer Risks in Solid Organ Transplant Recipients: Results From a Comprehensive Analysis of 72 Cohort Studies. *Oncoimmunology* (2020) 9:1848068. doi: 10.1080/2162402X.2020.1848068
53. Tessari G, Girolomoni G. Nonmelanoma Skin Cancer in Solid Organ Transplant Recipients: Update on Epidemiology, Risk Factors, and Management. *Dermatol Surg* (2012) 38:1622–30. doi: 10.1111/j.1524-4725.2012.02520.x
54. Garrett GL, Blanc PD, Boscardin J, Abramson Lloyd A, Ahmed RL, Anthony T, et al. Incidence of and Risk Factors for Skin Cancer in Organ Transplant Recipients in the United States. *JAMA Dermatol* (2017) 153:296–303. doi: 10.1001/jamadermatol.2016.4920
55. Krynitz B, Olsson H, Lundh Rozell B, Lindelöf B, Edgren G, Smedby KE. Risk of Basal Cell Carcinoma in Swedish Organ Transplant Recipients: A Population-Based Study. *Br J Dermatol* (2016) 174:95–103. doi: 10.1111/bjd.14153
56. Tessari G, Naldi L, Boschiero L, Nacchia F, Fior F, Forni A, et al. Incidence and Clinical Predictors of a Subsequent Nonmelanoma Skin Cancer in Solid Organ Transplant Recipients With a First Nonmelanoma Skin Cancer: A Multicenter Cohort Study. *Arch Dermatol* (2010) 146:294–9. doi: 10.1001/archdermatol.2009.377
57. Specchio F, Saraceno R, Chimenti S, Nisticò S. Management of Non-Melanoma Skin Cancer in Solid Organ Transplant Recipients. *Int J Immunopathol Pharmacol* (2014) 27:21–4. doi: 10.1177/039463201402700104
58. Acuna SA, Fernandes KA, Daly C, Hicks LK, Sutradhar R, Kim SJ, et al. Cancer Mortality Among Recipients of Solid-Organ Transplantation in Ontario, Canada. *JAMA Oncol* (2016) 2:463–9. doi: 10.1001/jamaoncol.2015.5137
59. Howard MD, Su JC, Chong AH. Skin Cancer Following Solid Organ Transplantation: A Review of Risk Factors and Models of Care. *Am J Clin Dermatol* (2018) 19:585–97. doi: 10.1007/s40257-018-0355-8
60. Acuna SA, Huang JW, Daly C, Shah PS, Kim SJ, Baxter NN. Outcomes of Solid Organ Transplant Recipients With Preexisting Malignancies in Remission: A Systematic Review and Meta-Analysis. *Transplantation* (2017) 101:471–81. doi: 10.1097/TP.0000000000001192
61. Acuna SA, Huang JW, Dossa F, Shah PS, Kim SJ, Baxter NN. Cancer Recurrence After Solid Organ Transplantation: A Systematic Review and Meta-Analysis. *Transplant Rev (Orlando)* (2017) 31(4):240–8. doi: 10.1016/j.trre.2017.08.003
62. Cesare AJ, Reddel RR. Alternative Lengthening of Telomeres: Models, Mechanisms and Implications. *Nat Rev Genet* (2010) 11:319–30. doi: 10.1038/nrg2763
63. Pickett HA, Reddel RR. Molecular Mechanisms of Activity and Derepression of Alternative Lengthening of Telomeres. *Nat Struct Mol Biol* (2015) 22:875–80. doi: 10.1038/nsmb.3106

Conflict of Interest: The authors declare that the research was conducted in the absence of any commercial or financial relationships that could be construed as a potential conflict of interest.

the publisher, the editors and the reviewers. Any product that may be evaluated in this article, or claim that may be made by its manufacturer, is not guaranteed or endorsed by the publisher.

frontiers in Oncology

ORIGINAL RESEARCH
published: 19 November 2021
doi: 10.3389/fonc.2021.754845

ACSL4 Expression Is Associated With CD8+ T Cell Infiltration and Immune Response in Bladder Cancer

Wenjie Luo[1,2†], *Jin Wang*[3†], *Xiaoyan Dai*[1,2†], *Hailiang Zhang*[1,2], *Yuanyuan Qu*[1,2], *Wenjun Xiao*[1,2*], *Dingwei Ye*[1,2*] *and Yiping Zhu*[1,2*]

[1] Department of Urology, Fudan University Shanghai Cancer Center, Shanghai, China, [2] Department of Oncology, Shanghai Medical College, Fudan University, Shanghai, China, [3] Department of Urology, The First Affiliated Hospital of Shandong First Medical University, Shandong, China

OPEN ACCESS

Edited by:
Ja Hyeon Ku,
Seoul National University, South Korea

Reviewed by:
Maria Carmen Mir,
Instituto Valenciano de Oncologia, Spain
Yanjie Zhao,
Qingdao University, China

***Correspondence:**
Yiping Zhu
qdzhuyiping@aliyun.com
Dingwei Ye
dwyelie@163.com
Wenjun Xiao
liebelove@aliyun.com

[†]These authors have contributed equally to this work

Specialty section:
This article was submitted to Genitourinary Oncology, a section of the journal Frontiers in Oncology

Received: 07 August 2021
Accepted: 29 October 2021
Published: 19 November 2021

Citation:
Luo W, Wang J, Dai X, Zhang H, Qu Y, Xiao W, Ye D and Zhu Y (2021) ACSL4 Expression Is Associated With CD8+ T Cell Infiltration and Immune Response in Bladder Cancer. Front. Oncol. 11:754845. doi: 10.3389/fonc.2021.754845

Objective: This study aimed to explore the role of *ACSL4* in CD8+ T cell tumor infiltration and outcomes of bladder cancer (BLCA) patients after immunotherapy.

Methods: The correlation between *ACSL4* expression and tumor infiltration of immune cells was analyzed using the Tumor Immune Estimation Resource database. The prognostic significance of *ACSL4* in BLCA was analyzed using Kaplan–Meier curves. Immunohistochemistry was used to detect CD8+ T cell infiltration in tumors with high and low *ACSL4* expression obtained from patients at the Fudan University Shanghai Cancer Center. The relationships between immune checkpoint genes and immune response were analyzed using The Cancer Genome Atlas and IMvigor 210 cohorts. The molecular functions, cellular components, and biological processes involving *ACSL4* were explored using Kyoto Encyclopedia of Genes and Genomes and Gene Ontology enrichment pathway analyses.

Results: The expression level of *ACSL4* was significantly correlated with the infiltration of CD8+ T cells in BLCA tumors (r = 0.192, P = 2.22e-04). Elevated *ACSL4* was associated with suppressed tumor progression and better outcomes for BLCA patients. The higher expression level of *ACSL4* predicted better immunotherapeutic responses and was associated with higher expression levels of core immune checkpoint genes, including *CD274*, *CTLA4*, *PDCD1*, and *LAG3*, compared with the low *ACSL4* expression group.

Conclusion: This study demonstrated for the first time that elevated *ACSL4* correlated significantly with CD8+ T cell infiltration and contributed to better immunotherapeutic responses in BLCA patients. Furthermore, *ACSL4* serves as a novel biomarker for predicting patient outcomes after immunotherapeutic treatments, which may improve the development of individualized immunotherapy for BLCA.

Keywords: bladder cancer, immune checkpoint, *ACSL4*, CD8+ T cell, immunotherapy

INTRODUCTION

Bladder cancer (BLCA) is the ninth most common malignant tumor worldwide, with approximately 81,400 new cases and 17,980 deaths reported in the United States in the year 2020 (1). Routine treatments for BLCA, such as platinum-based chemotherapy and intravesical bacillus Calmette-Guerin, frequently fail because of the biological behavior of malignant progression and high recurrence rate after treatment (2). According to the latest reports, the median overall survival of patients with relapsed or refractory BLCA after cisplatin treatment was only 14–15 months (3). In recent years, immune checkpoint inhibitor (ICI) therapies, especially anti-programmed cell death protein 1 (PD-1), anti-PD-ligand 1 (PD-L1), and anti-cytotoxic T lymphocyte-associated antigen 4 (CTLA4) antibodies, have achieved significant success in BLCA treatment. The United States Food and Drug Administration has approved five PD-1/PD-L1 inhibitors as first- or second-line treatments for patients with advanced BLCA (4). However, among patients with advanced BLCA, the overall response rates for ICI treatments are 13–24% (5, 6). Because the majority of advanced BLCA patients do not benefit from these immunotherapeutic agents, it is important to identify new biomarkers for predicting treatment response.

Acyl-CoA synthetase long-chain family member 4 (*ACSL4*) has been recognized as an important molecule in metabolism-associated diseases (7). Furthermore, *ACSL4* was reported to promote the esterification of arachidonoyl and adrenoyl into phosphatidylethanolamine, which is a process closely related to ferroptosis (8, 9). Intriguingly, recent evidence showed that ferroptosis-inducing therapy was potentiated by anti-PD-L1 antibodies. Specifically, anti-PD-L1 antibodies stimulated CD8+ T cells to secrete interferon γ, which suppressed the glutamate–cystine antiporter system in target cancer cells and sensitized them to ferroptosis (10). Therefore, immunotherapy in combination with ferroptosis induction represents a promising treatment because the two therapeutic modalities may mutually potentiate each other and lead to a synergistic anticancer effect.

As the main effector immune cells, CD8+ T cells play a critical role in preventing tumor occurrence and development (11). It has been reported that the populations of intratumoral CD8+ T cells are highly heterogeneous (12). Preclinical models have indicated that infiltration of CD8+ T-cells in tumors is strongly associated with anti-PD-1/PD-L1 treatment (12, 13). In the current study, we demonstrated that the expression level of *ACSL4* was positively correlated with the infiltration of CD8+ T-cells in BLCA. Furthermore, *ACSL4* was associated with the expression of immune checkpoint genes and may represent a predictive biomarker for anti-PD-1/PD-L1 treatment. This study is the first exploration of the comprehensive clinical value and immunological implication of *ACSL4* in BLCA.

Abbreviations: BLCA, bladder cancer; ICI, immune checkpoint inhibitor; PD-1, programmed cell death protein 1; PD-L1, programmed cell death protein-ligand 1; CTLA4, cytotoxic T lymphocyte-associated antigen 4; *ACSL4*, Acyl-CoA synthetase long-chain family member 4; TCGA, The Cancer Genome Atlas; HR, hazard ratios; TIMER, Tumor Immune Estimation Resource; KEGG, Kyoto Encyclopedia of Genes and Genomes; IHC, Immunohistochemistry; HPF, high-power field; TIS, tumor *in situ* bladder cancer; NMIBC, non-muscle-invasive bladder cancer; MIBC, muscle-invasive bladder cancer.

MATERIALS AND METHODS

Data Collection

We downloaded the BLCA gene expression profile of the Cancer Genome Atlas (TCGA) database from UCSC Xena (https://tcga.xenahubs.net, version of data: 2019-12-06). For validation, we enrolled a total of 30 BLCA patients at the Fudan University Shanghai Cancer Center (FUSCC, Shanghai, China) from August 2019 to May 2021. Our study was approved by the Ethics Committee of FUSCC. Informed consent was obtained from all patients who participated in this study. To discover the role of *ACSL4* in BLCA immunotherapy, we obtained the genetic profiles of 195 BLCA patients from the IMvigor 210 cohort (http://research-pub.gene.com/IMvigor210CoreBiologies/, accession number: EGAS00001002556), who underwent treatment with the PD-L1 inhibitor atezolizumab with documented ICI responsiveness (14).

Kaplan–Meier Survival Curve Analysis

Based on the analysis of hazard ratios (HR) and log-rank P-values, Kaplan–Meier plots (http://kmplot.com/analysis/) were used to analyze the relationship between *ACSL4* gene expression and survival rates in the TCGA BLCA cohort in combination with restricted analysis of cellular content (enriched or depleted CD8+ T cells) (15).

TIMER Analysis

To analyze the tumor-infiltrating immune cells in pan-cancers, we used the Tumor Immune Estimation Resource (TIMER) database (https://cistrome.shinyapps.io/timer/, version: 2.0) and >10,000 samples from the TCGA database (16). TIMER analysis was performed to obtain the abundance of tumor-infiltrating immune cells based on the statistical analysis of gene expression profiles (17). The correlations between the expression level of *ACSL4* and infiltrating immune cells, including CD4+, CD8+, regulatory T cells, B cells, neutrophils, dendritic cells, and M1 and M2 macrophages, were analyzed based on the expression of specific immune cell-related marker genes in BLCA. The marker genes of tumor-infiltrating immune cells were based on data from previous studies (18, 19). The associations between mRNA expression levels of *CD274* (*PD-L1*), *CTLA4*, *LAG3*, and *PDCD1* (*PD-1*) and the expression levels of *ACSL4* and CD8 cell markers, including *CD8A* and *CD8B* from the TCGA BLCA cohort, were determined using the TIMER database. The expression levels of *ACSL4*, *CD8A*, and *CD8B* genes were represented on the x-axes, and related marker genes were placed on the y-axes.

Immunohistochemistry Staining and Evaluation

IHC was performed on formalin-fixed, paraffin-embedded tissues obtained from patients with BLCA. The primary antibodies used for the detection of the targeted proteins were

anti-*ACSL4* (Clone OTI6B7, NOVUS, Dilution: 1:500) and anti-CD8 (Clone 66868, Proteintech, Dilution: 1:2,000). The positive cells were enumerated from the representative views in high-power field [high-power field (HPF), 40×, objective], and the mean value was adopted. For quantification of protein, positive and negative images of the IHC specimens were acquired and analyzed using the IHC Profiler in Image J software (NIH, Bethesda, MD, USA). All samples were evaluated by two independent, experienced pathologists.

Functional Analysis of *ACSL4*

Protein–protein interactions for *ACSL4* were predicted using the STRING database (https://string-db.org, version:11.5) (20). Kyoto Encyclopedia of Genes and Genomes (KEGG) and Gene Ontology enrichment pathway analyses were performed to evaluate molecular functions, cellular components, and biological processes involving *ACSL4*. To illustrate biological functions of prognostic genes in high-risk and low-risk patient groups, Gene Set Enrichment Analysis was explored to identify pathways and was based on TCGA data (21).

Statistics

The figures were partially drawn by GraphPad Prism 8.0 software (GraphPad Software Inc.). Two-tailed Student's t-test or One-way ANOVA was used to measure differences between groups. $P < 0.05$ was considered statistically significant.

RESULTS

The Level of *ACSL4* Expression Is Positively Correlated With the Infiltration Level of CD8+ T Cell in BLCA

As shown in **Figure 1A**, the level of *ACSL4* expression positively correlated with immune purity (R = 0.194, P = 1.76e-04) and the infiltration levels of specific subsets of immune cells, including B cells (R = 0.071, P = 1.78e-01), CD8+ T cells (R = 0.192, P = 2.22e-04), CD4+ T cells (R = 0.086, P = 1.00e-01), macrophages (R = 0.13, P = 1.27e-02), neutrophils (R = 0.3, P = 5.30e-09), and dendritic cells (R = 0.2140, P = 3.87e-05) in BLCA. The correlation between *ACSL4* expression level and immune cells in pan-cancers is presented in **Supplementary Figure 1**. The expression level of *ACSL4* was positively correlated with the expression of *CD8A* (R = 0.174, P = 4.1e-04) and *CD8B* (R = 0.267, P = 4.84e-08) marker genes, further confirming a role for *ACSL4* in CD8+ T cell infiltration (**Figure 1B**). And the correlation analysis between *ACSL4* and other immune cell–

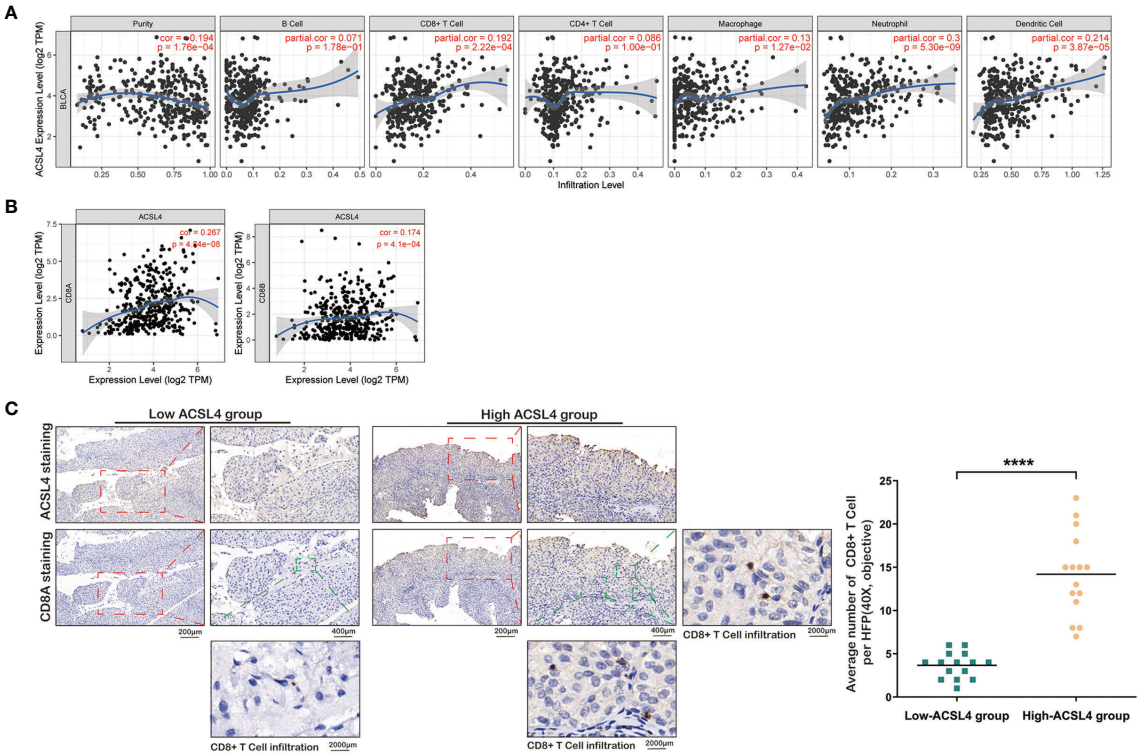

FIGURE 1 | Elevated *ACSL4* is associated with CD8+ T Cell infiltration. **(A)** The correlations between six kinds of immune cell, immune purity, and expression level of *ACSL4* were identified from TIMER analysis. **(B)** The expression level of *ACSL4* was proportional to the expression level of *ACSL4*. **(C)** IHC of *ACSL4* and CD8A staining detected the CD8+ T Cell infiltration in low-*ACSL4* group and high-*ACSL4* group. The red box stands for a representative image of *ACSL4* or CD8A staining. The green box stands for the observed CD8+ T Cells. Results are presented as mean ± SD. ****$P < 0.0001$. Data were obtained from three independent experiments.

related markers is presented in **Table 1**. The 30 patients from our Cancer Center were divided into high- and low-*ACSL4*-expression groups (15 samples each) for IHC analysis. As shown in **Figure 1C**, the average number of CD8+ T cells (HFP, 40×, objective) in the high-*ACSL4*-expression group was significantly greater than that in the low-*ACSL4*-expression group.

Dysregulated Expression of *ACSL4* in Patients With Tumor *In Situ* and Non-Muscle-Invasive or Muscle-Invasive BLCA

Immune cell infiltration is tightly associated with the invasive ability of tumors. Therefore, we applied IHC analysis to detect *ACSL4* expression in tumors from patients diagnosed with different types of BLCA (**Figure 2A**). The results showed that *ACSL4* expression was significantly higher in tumor *in situ* (TIS) and non-muscle-invasive BLCA (NMIBC) compared with muscle-invasive BLCA (MIBC), which suggested that *ACSL4* may play a role in preventing BLCA invasion by facilitating immune cell infiltration (**Figure 2B**).

The Prognostic Significance of *ACSL4* Expression in BLCA Patients With Enriched or Depleted CD8+ T Cells

Next, we explored the prognostic value of *ACSL4* for BLCA patients because there is a strong association between immune infiltration, tumor invasion, and patient survival. Kaplan–Meier analysis showed that patients with high *ACSL4* expression had a significantly better overall survival compared with patients with low *ACSL4* expression (P = 6.6e-04) (**Figure 3A**). Furthermore, we combined survival analysis with CD8+ T cell enrichment. In the CD8+ T cell-enriched cohort, the overall survival of patients with high *ACSL4* expression was greater compared with patients with low *ACSL4* expression (P = 0.012), while no significant differences were detected in the CD8− T cell-enriched cohort (P = 0.1) (**Figures 3B, C**). These results suggested that high expression of *ACSL4* may cooperate synergistically with infiltration of CD8+ T cells. The clinicopathological characteristics of enrolled cohorts are presented in **Supplementary Table 2**.

The Role of *ACSL4* and CD8+ T Cell Infiltration in the Expression of Immune Checkpoint-Related Genes and Immunotherapy Response

To further investigate the clinical significance of *ACSL4* and CD8+ T cell infiltration, we explored the associations between *ACSL4* and *CD8A* expression and expression of immune checkpoint genes, which are important markers for BLCA immunotherapy responses. As shown in **Figures 4A, B**, the expression of the immune checkpoint-related genes *CD274*, *CTLA4*, *LAG3*, and *PDCD1* positively correlated with *ACSL4* expression. Subsequently, to validate the role of *ACSL4* in response to immunotherapy, we applied the correlation analysis to the IMvigor 210 cohort. The results confirmed that the level of *CD8A* mRNA was significantly greater in the high-*ACSL4*-expression group compared with the low-*ACSL4*-expression group (**Figure 4C**). Both *ACSL4* and *CD8A* mRNA levels were significantly higher in the immunotherapy responsive group compared with the non-responsive group (**Figures 4D, E**). Together, these findings indicated that the upregulation of *ACSL4* was associated with increased infiltration of CD8+ T cells and, subsequently, facilitated the expression of

TABLE 1 | Correlation analysis between *ACSL4* and immune cell–related markers in TCGA BLCA cohort.

Description	Markers	None		Tumor purity		Age	
		Correlation	P-value	Correlation	P-value	Correlation	P-value
CD8+ T cell	CD8A	0.267	**4.84E-08**	0.188	**2.94E-04**	0.268	**4.19E-08**
	CD8B	0.174	**4.10E-04**	0.108	**3.83E-02**	0.174	**4.17E-04**
T cell (general)	CD3E	0.264	**9.50E-09**	0.165	**1.53E-03**	0.265	**6.15E-08**
	CD3D	0.201	**4.41E-05**	0.092	7.68E-02	0.202	**4.09E-05**
	CD2	0.257	**1.64E-07**	0.159	**2.26E-03**	0.258	**1.40E-07**
B cell	CD19	0.086	8.12E-02	–0.054	3.01E-01	0.085	8.89E-02
	CD79A	0.149	**2.57E-03**	0.017	7.44E-01	0.148	**2.85E-03**
M1 Macrophage	iNOS	–0.193	**9.01E-05**	–0.161	**1.96E-02**	–0.193	**8.73E-05**
	IRF5	–0.032	5.13E-01	–0.055	2.88E-01	–0.033	5.13E-01
	COX2	0.249	**3.76E-07**	0.237	**4.44E-06**	0.251	**3.16E-07**
M2 Macrophage	CD163	0.326	**1.92E-11**	0.256	**6.64E-07**	0.326	**1.55E-11**
	VSIG4	0.323	**2.94E-11**	0.254	**8.11E-07**	0.323	**2.56E-11**
Neutrophils	CD66b	0.054	2.78E-01	0.05	3.36E-01	0.054	2.78E-01
	CD11b	0.295	**1.57E-09**	0.179	**5.41E-04**	0.294	**1.52E-09**
	CCR7	0.073	1.43E-01	0.014	7.85E-01	0.071	1.52E-01
	MS4A4A	0.318	**6.29E-11**	0.231	**7.52E-06**	0.318	**5.57E-11**
Dendritic cell	HLA-DPB1	0.287	**4.21E-09**	0.202	**9.56E-05**	0.286	**4.20E-09**
	HLA-DQB1	0.277	**1.26E-08**	0.276	**3.94E-04**	0.184	**1.48E-08**
	HLA-DRA	0.333	**7.02E-12**	0.272	**1.17E-07**	0.333	**5.95E-12**
	HLA-DPA1	0.313	**9.67E-11**	0.249	**1.38E-06**	0.313	**1.08E-10**
Treg	FOXP3	0.344	**1.29E-12**	0.283	**3.36E-08**	0.346	**7.80E-13**
	CCR8	0.415	**2.14E-18**	0.372	**1.60E-13**	0.416	**1.85E-18**
	TGFβ	0.166	**7.63E-04**	0.14	**7.13E-03**	0.167	**7.35E-04**

P-value < 0.05 is highlighted using bold font.

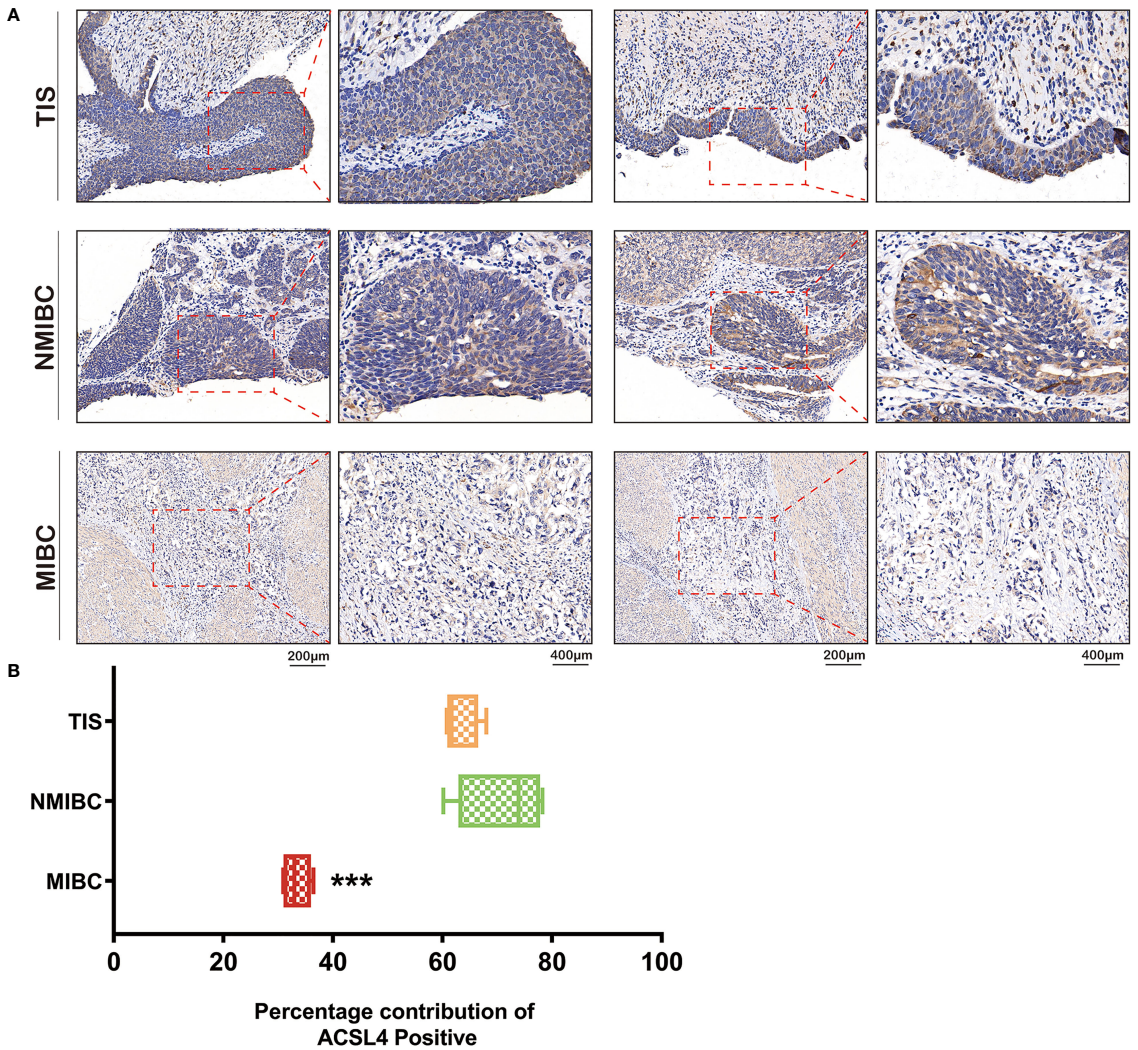

FIGURE 2 | Different expression of *ACSL4* in TIS, NMIBC, and MIBC. **(A)** IHC of *ACSL4* staining evaluated the expression level of *ACSL4* in TIS, NMIBC, and MIBC. **(B)** Analysis of Image J IHC Profiler indicated expression level of *ACSL4* in MIBC was significantly lower compared with that in TIS or NMIBC. ($P < 0.001$). The red box stands for a representative image of *ACSL4* staining. Results are presented as mean ± SD. ***$P < 0.001$. Data were obtained from three independent experiments.

immune checkpoint-related genes, which improved response to immunotherapy in BLCA.

Mechanistic Analysis of *ACSL4* in BLCA

We applied Gene Set Enrichment Analysis to predict functional changes between the high- and low-*ACSL4*-expression groups (**Figure 5A**). This biological analysis for *ACSL4* indicated that the top four enriched pathways were interferon γ production ($P < 0.0001$, normalized enrichment score [NES] = 2.0953), adaptive immune response ($P < 0.0001$, NES = 2.0925), leukocyte cell-cell adhesion ($P < 0.0001$, NES = 2.0729), and T cell activation ($P < 0.0001$, NES = 2.0193), which were consistent with results from the TIMER analysis (**Figure 5B**). Furthermore, we performed protein-protein interaction analysis to acquire targeted proteins of *ACSL4*, which included ACSL1, ACACA, FASN, PPARG, and PPARA (**Figure 6A**). As shown in **Figure 6B**, KEGG analysis indicated that *ACSL4*-correlated genes were mainly located in metabolic pathways, including the PPAR signaling pathway (false discovery rate [FDR] = 7.02e-33), fatty acid metabolism (FDR = 1.70e-24), fatty acid degradation (FDR = 1.56e-12), and cholesterol metabolism (FDR = 2.33e-12). Gene Ontology analysis of *ACSL4* including Cellular Component, Molecular Function, and Biological Process is shown in **Supplementary Table 1**, which confirmed the tight association between *ACSL4* expression and immune cell infiltration.

DISCUSSION

The traditional treatments for bladder cancer have not significantly improved the survival rates of patients. Recent studies have shown

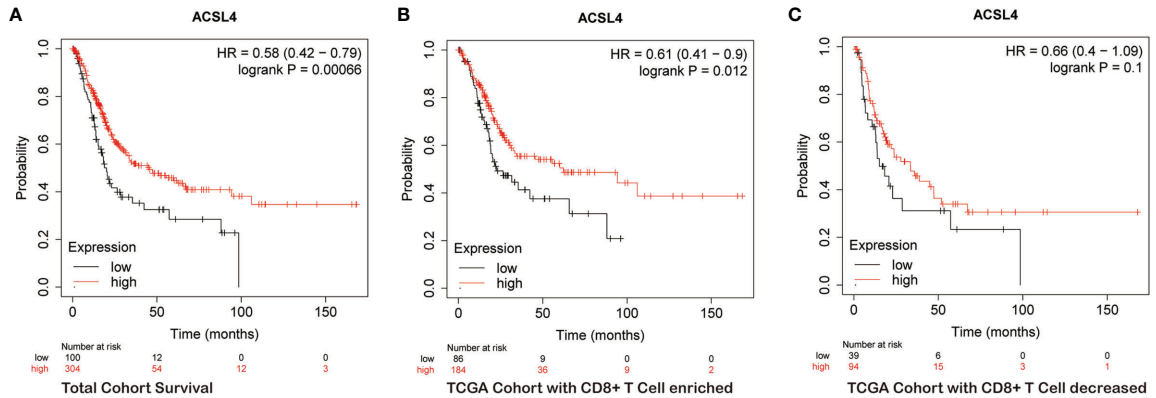

FIGURE 3 | *ACSL4* is significantly associated with prognosis of BLCA patients. **(A–C)** Kaplan-Meier plots evaluated the overall survival of patients in total TCGA BLCA cohort and cohorts with CD8+ T Cell enriched or decreased.

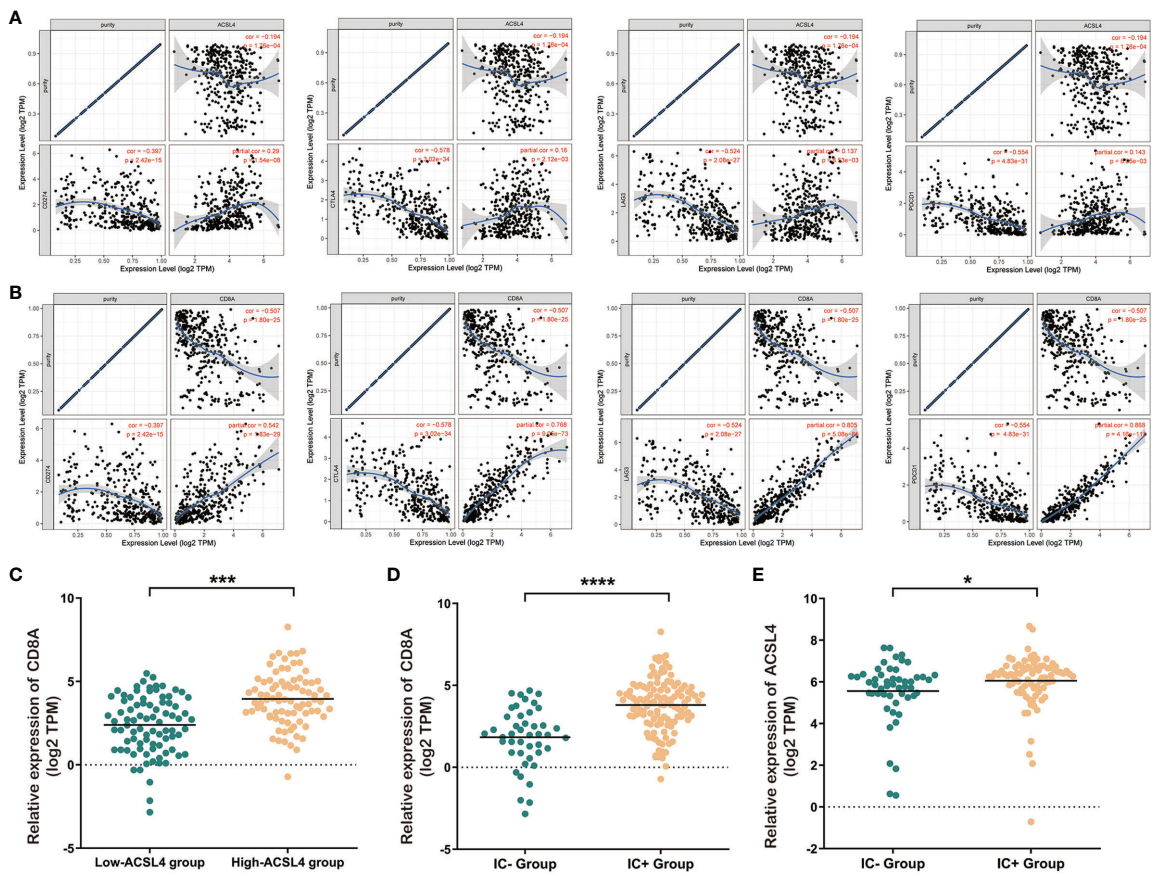

FIGURE 4 | Elevated expression level of *ACSL4* is associated with better immunotherapeutic response. **(A)** TIMER analysis showed the positive expression correlations between *ACSL4* and immune checkpoint genes including CD274 (PD-L1), CTLA-4, LAG-3, and PDCD1 (PD-1). **(B)** TIMER analysis showed the positive expression correlations between CD8A and immune checkpoint genes including CD274 (PD-L1), CTLA-4, LAG-3, and PDCD1 (PD-1). **(C)** Dysregulated expression of CD8A in low-*ACSL4* group and high-*ACSL4* group from IMvigor 210 cohort. **(D, E)** The immune cell response-positive (IC+) group showed significantly higher expression level of CD8A ($P < 0.0001$) and *ACSL4* ($P<0.05$). Results are presented as mean ± SD. *$P < 0.05$; ***$P < 0.001$, ****$P < 0.0001$. Data were obtained from three independent experiments.

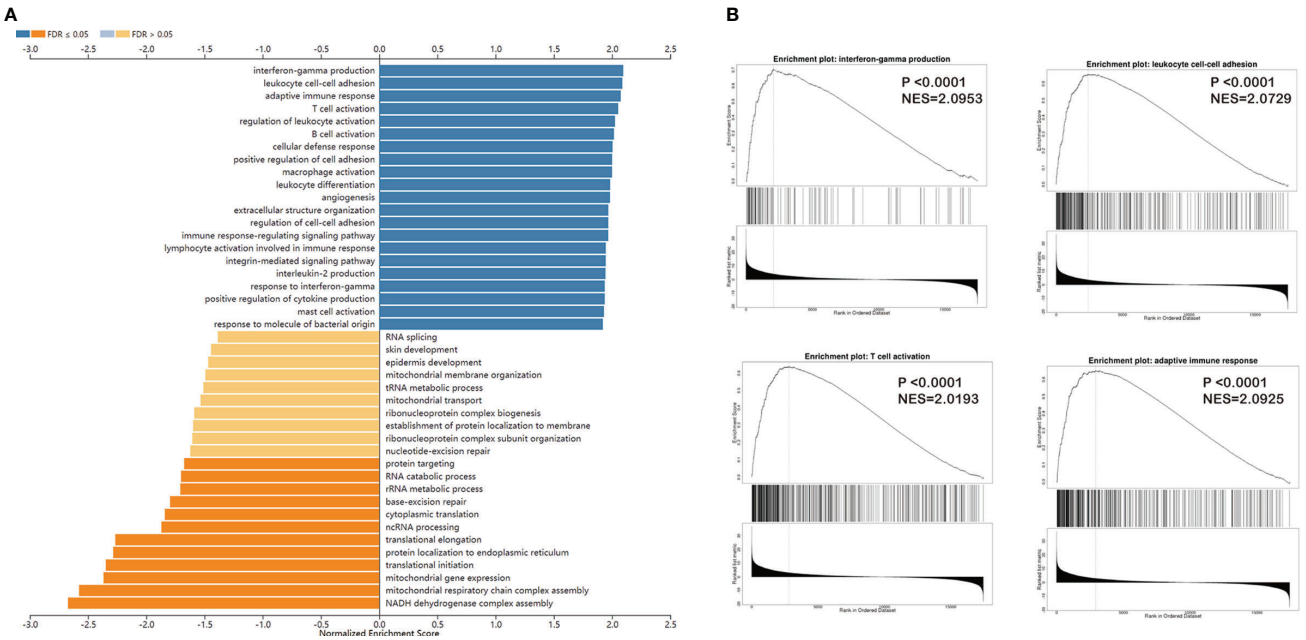

FIGURE 5 | Immune checkpoints genes are expressed differently in BCa groups. **(A)** GSEA analysis showed the related biological processes of *ACSL4* in TCGA cohort. **(B)** The top four of related processes were interferon-gamma production (P <0.0001, NES=2.0953), adaptive immune response (P <0.0001, NES=2.0925), leukocyte cell-cell adhesion (P <0.0001, NES=2.0729), and T cell activation (P <0.0001, NES=2.0193).

that immunotherapies based on immune checkpoint blockage, such as anti-PD-1/PD-L1 and anti-CTLA-4 antibodies, have prominent efficacy against bladder cancer (22, 23). However, immunotherapy lacks sufficient biomarkers because the majority of BLCA patients develop a negative antitumor immune response. Recent studies have discovered more and more immune-related genes in regulating important phenotypes through controlling different pathways in multiple cancers (24, 25). For example, BRCA1-associated protein was shown to regulate liver hepatocellular patients' prognosis *via* immune cell infiltration (26). In the current study, we found that the expression level of *ACSL4* in BLCA was positively correlated with tumor infiltration of CD8+ T cells, which may affect the efficacy of immunotherapy in BLCA patients.

Recently, there has been renewed interest in the regulation of *ACSL4* in oncology research because this protein plays a vital role as a hub gene in metabolism and ferroptosis of tumor cells (8, 27). For

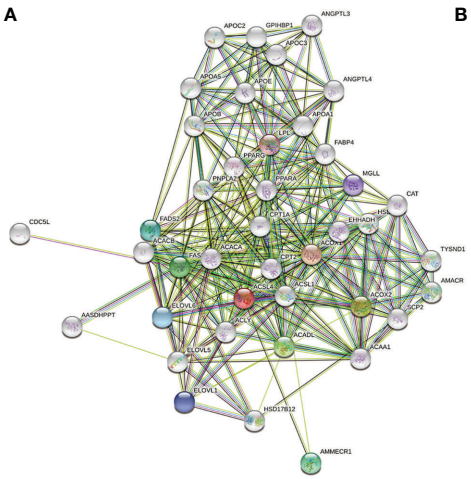

ID	Description	Observed gene count	Background gene count	Relative Strength	False discovery rate
hsa03320	PPAR signaling pathway	19	72	2.1	7.02E-33
hsa01212	Fatty acid metabolism	14	48	2.14	1.70E-24
hsa04146	Peroxisome	10	81	1.77	4.63E-14
hsa00071	Fatty acid degradation	8	44	1.94	1.56E-12
hsa04979	Cholesterol metabolism	8	48	1.9	2.33E-12
hsa01040	Biosynthesis of unsaturated fatty acids	6	23	2.1	2.18E-10
hsa00061	Fatty acid biosynthesis	5	12	2.3	1.32E-09
hsa01100	Metabolic pathways	17	1250	0.81	1.32E-09
hsa00120	Primary bile acid biosynthesis	4	17	2.05	5.33E-07
hsa00062	Fatty acid elongation	4	25	1.88	1.88E-06
hsa04920	Adipocytokine signaling pathway	5	69	1.54	2.05E-06
hsa04714	Thermogenesis	7	228	1.17	2.15E-06
hsa04152	AMPK signaling pathway	5	120	1.3	2.33E-05
hsa00592	alpha-Linolenic acid metabolism	3	25	1.76	9.58E-05
hsa00640	Propanoate metabolism	3	32	1.65	0.00018
hsa04922	Glucagon signaling pathway	4	100	1.28	0.0002
hsa04923	Regulation of lipolysis in adipocytes	3	53	1.43	0.00064
hsa00561	Glycerolipid metabolism	3	59	1.38	0.00082
hsa04977	Vitamin digestion and absorption	2	24	1.6	0.0035
hsa04931	Insulin resistance	3	107	1.13	0.0039
hsa04910	Insulin signaling pathway	3	134	1.03	0.007
hsa00380	Tryptophan metabolism	2	40	1.38	0.0076
hsa00620	Pyruvate metabolism	2	39	1.39	0.0076
hsa04216	Ferroptosis	2	40	1.38	0.0076
hsa04975	Fat digestion and absorption	2	39	1.39	0.0076

FIGURE 6 | Targeted genes and molecular pathways of *ACSL4*. **(A)** PPI network presented the targeted genes of *ACSL4*. **(B)** KEGG analysis showed the top 25 molecular pathways correlated with *ACSL4*.

example, *ACSL4* was shown to facilitate hepatocellular carcinoma (HCC) development and modulate aberrant lipid metabolism *via* the c-MYC/SREBP1 pathway (28). Our study found a tight association between *ACSL4* and tumor-related lymphocytes, including CD8+ T cells. Our results reflect those of Liu et al. (29), who confirmed the correlation between metabolism and the immune response. Furthermore, these authors found that the metabolic regulator fat mass- and obesity-associated protein was utilized by tumors to escape immune surveillance, which suppressed the checkpoint blockade and immunotherapeutic responsiveness (29).

We discovered that *ACSL4*, which meditated CD8+ T cell infiltration, was associated with tumor invasiveness. This observation is consistent with that of Li et al., who found that tumor metastasis was facilitated by elevated miR-301a levels, the latter of which correlated with subsequent antitumor-immunity and suppression of CD8+ T cell recruitment (30). Several studies have reported that tumor invasion and immune environment play significant roles in survival outcome and immunotherapy response in cancer patients (31–33). We propose that determining the expression levels of *ACSL4* and status of CD8+ T cell infiltration may be useful for clinicians to better predict the prognosis of patients who undergo BLCA immunotherapy.

Multiple studies have confirmed that the infiltration and effector function of CD8+ T cells in the tumor microenvironment can be enhanced by effective cancer immunotherapy (34–36). Philip and Schietinger recognized that predicting which patients will respond to immunotherapy is an important challenge and understanding CD8 T cell differentiation and dysfunction will be key to mediating a clinical response (37). From the analysis of the IMvigor 210 cohort in our study, we validated that the tight correlation between CD8+ T cell infiltration and expression level of *ACSL4* contributed to the immune response in BLCA patients who underwent immunotherapy.

We explored the mechanisms related to the immunological role of *ACSL4* in BLCA. The Gene Set Enrichment Analysis of tumors from BLCA patients confirmed that the immune cell recruitment and response mediated by *ACSL4* was consistent with the TIMER database analysis. Protein-protein interaction, KEGG, and Gene Ontology analyses indicated that metabolic regulation of tumors by *ACLS4* contributed to immunological responsiveness and the immunotherapeutic outcome of BLCA patients. This finding broadly supports the work of Vantaku et al., who linked tumor metabolism with progression of BLCA (38), and the review by Afonso et al. that focused on the role of metabolism in immunotherapeutic efficacy of ICIs used for treating BLCA patients. Afonso et al. found that molecular hallmarks of cancer cell metabolism suppressed malignant cells, facilitated immunotherapeutic responses, and represented potential therapeutic targets (39). Recently, the role of *ACSL4* in other types of tumors has been reported, especially in HCC (40–42). *ACSL4* modulated aberrant lipid metabolism (28) and survival outcome of HCC patients and was validated as a predictive biomarker of sorafenib-induced ferroptosis in HCC (43).

In conclusion, for the first time, we revealed a potential immunotherapeutic function for *ACSL4* in BLCA that may play a role in ICI interventions. This study demonstrated that *ACSL4* correlated significantly with the recruitment of immune cells, including critical CD8+ T cells, in the BLCA microenvironment, which may have prevented tumor invasion and improved survival outcomes for BLCA patients. However, more evidence and validation from multiple cohorts remains to be further investigated. The current study indicated that *ACSL4* as a biomarker may be useful for predicting outcomes of patients after immunotherapeutic treatments and may have important translational impacts in the development of precise therapy for BLCA.

DATA AVAILABILITY STATEMENT

The datasets presented in this study can be found in online repositories. The names of the repository/repositories and accession number(s) can be found below: https://www.ncbi.nlm.nih.gov/, 10.1038/nature25501.

ETHICS STATEMENT

The studies involving human participants were reviewed and approved by Fudan University Shanghai Cancer Center Ethics Committee. The patients/participants provided their written informed consent to participate in this study.

AUTHOR CONTRIBUTIONS

The work presented here was carried out in collaboration among all authors. YZ, DY, and WL defined the theme of the study and discussed analysis, interpretation, and presentation. WL and YQ drafted the manuscript, analyzed the data, developed the algorithm, and explained the results. WX and WL participated in the collection of relevant data and helped draft the manuscript. JW and XD helped to perform the statistical analysis. DY and HZ helped revise the manuscript and provided guiding suggestions. All authors contributed to the article and approved the submitted version.

FUNDING

This work is supported by grants from the National Natural Science Foundation of China (No. 81772706 and No. 81802525).

ACKNOWLEDGMENTS

We thank the TCGA databases and IMvigor 210 cohort for providing BLCA gene expression profiles. We thank Susan Zunino, PhD, from Liwen Bianji (Edanz) (www.liwenbianji.cn/), for editing the English text of a draft of this manuscript.

SUPPLEMENTARY MATERIAL

The Supplementary Material for this article can be found online at: https://www.frontiersin.org/articles/10.3389/fonc.2021.754845/full#supplementary-material

Supplementary Figure 1 | Landscape of *ACSL4* in correlation with immune cell infiltration in pan-cancers

REFERENCES

1. Siegel RL, Miller KD, Jemal A. Cancer Statistics, 2020. *CA: Cancer J Clin* (2020) 70:7–30. doi: 10.3322/caac.21590
2. Kamat AM, Hahn NM, Efstathiou JA, Lerner SP, Malmström PU, Choi W, et al. Bladder Cancer. *Lancet (London England)* (2016) 388:2796–810. doi: 10.1016/S0140-6736(16)30512-8
3. Rosenberg JE, Hoffman-Censits J, Powles T, van der Heijden MS, Balar AV, Necchi A, et al. Atezolizumab in Patients With Locally Advanced and Metastatic Urothelial Carcinoma Who Have Progressed Following Treatment With Platinum-Based Chemotherapy: A Single-Arm, Multicentre, Phase 2 Trial. *Lancet (London England)* (2016) 387:1909–20. doi: 10.1016/S0140-6736(16)00561-4
4. Cheng W, Fu D, Xu F, Zhang Z. Unwrapping the Genomic Characteristics of Urothelial Bladder Cancer and Successes With Immune Checkpoint Blockade Therapy. *Oncogenesis* (2018) 7:2. doi: 10.1038/s41389-017-0013-7
5. Sharma P, Callahan MK, Bono P, Kim J, Spiliopoulou P, Calvo E, et al. Nivolumab Monotherapy in Recurrent Metastatic Urothelial Carcinoma (CheckMate 032): A Multicentre, Open-Label, Two-Stage, Multi-Arm, Phase 1/2 Trial. *Lancet Oncol* (2016) 17:1590–8. doi: 10.1016/S1470-2045(16)30496-X
6. Balar AV, Galsky MD, Rosenberg JE, Powles T, Petrylak DP, Bellmunt J, et al. Atezolizumab as First-Line Treatment in Cisplatin-Ineligible Patients With Locally Advanced and Metastatic Urothelial Carcinoma: A Single-Arm, Multicentre, Phase 2 Trial. *Lancet (London England)* (2017) 389:67–76. doi: 10.1016/S0140-6736(16)32455-2
7. Killion EA, Reeves AR, El Azzouny MA, Yan QW, Surujon D, Griffin JD, et al. A Role for Long-Chain Acyl-CoA Synthetase-4 (ACSL4) in Diet-Induced Phospholipid Remodeling and Obesity-Associated Adipocyte Dysfunction. *Mol Metab* (2018) 9:43–56. doi: 10.1016/j.molmet.2018.01.012
8. Doll S, Proneth B, Tyurina YY, Panzilius E, Kobayashi S, Ingold I, et al. ACSL4 Dictates Ferroptosis Sensitivity by Shaping Cellular Lipid Composition. *Nat Chem Biol* (2017) 13:91–8. doi: 10.1038/nchembio.2239
9. Kagan VE, Mao G, Qu F, Angeli JP, Doll S, Croix CS, et al. Oxidized Arachidonic and Adrenic PEs Navigate Cells to Ferroptosis. *Nat Chem Biol* (2017) 13:81–90. doi: 10.1038/nchembio.2238
10. Wang W, Green M, Choi JE, Gijón M, Kennedy PD, Johnson JK, et al. CD8(+) T Cells Regulate Tumour Ferroptosis During Cancer Immunotherapy. *Nature* (2019) 569:270–4. doi: 10.1038/s41586-019-1170-y
11. Vesely MD, Kershaw MH, Schreiber RD, Smyth MJ. Natural Innate and Adaptive Immunity to Cancer. *Annu Rev Immunol* (2011) 29:235–71. doi: 10.1146/annurev-immunol-031210-101324
12. Simoni Y, Becht E, Fehlings M, Loh CY, Koo SL, Teng KWW, et al. Bystander CD8(+) T Cells are Abundant and Phenotypically Distinct in Human Tumour Infiltrates. *Nature* (2018) 557:575–9. doi: 10.1038/s41586-018-0130-2
13. Solomon BL, Garrido-Laguna I. TIGIT: A Novel Immunotherapy Target Moving From Bench to Bedside. *Cancer Immunol Immunother CII* (2018) 67:1659–67. doi: 10.1007/s00262-018-2246-5
14. Mariathasan S, Turley SJ, Nickles D, Castiglioni A, Yuen K, Wang Y, et al. Tgfβ Attenuates Tumour Response to PD-L1 Blockade by Contributing to Exclusion of T Cells. *Nature* (2018) 554:544–8. doi: 10.1038/nature25501
15. Lánczky A, Nagy Á, Bottai G, Munkácsy G, Szabó A, Santarpia L, et al. Mirpower: A Web-Tool to Validate Survival-Associated miRNAs Utilizing Expression Data From 2178 Breast Cancer Patients. *Breast Cancer Res Treat* (2016) 160:439–46. doi: 10.1007/s10549-016-4013-7
16. Li T, Fan J, Wang B, Traugh N, Chen Q, Liu JS, et al. TIMER: A Web Server for Comprehensive Analysis of Tumor-Infiltrating Immune Cells. *Cancer Res* (2017) 77:e108–10. doi: 10.1158/0008-5472.CAN-17-0307
17. Li B, Severson E, Pignon JC, Zhao H, Li T, Novak J, et al. Comprehensive Analyses of Tumor Immunity: Implications for Cancer Immunotherapy. *Genome Biol* (2016) 17:174. doi: 10.1186/s13059-016-1028-7
18. Danaher P, Warren S, Dennis L, D'Amico L, White A, Disis ML, et al. Gene Expression Markers of Tumor Infiltrating Leukocytes. *J Immunother Cancer* (2017) 5:18. doi: 10.1186/s40425-017-0215-8
19. Sousa S, Määttä J. The Role of Tumour-Associated Macrophages in Bone Metastasis. *J Bone Oncol* (2016) 5:135–8. doi: 10.1016/j.jbo.2016.03.004
20. Szklarczyk D, Franceschini A, Wyder S, Forslund K, Heller D, Huerta-Cepas J, et al. STRING V10: Protein-Protein Interaction Networks, Integrated Over the Tree of Life. *Nucleic Acids Res* (2015) 43:D447–452. doi: 10.1093/nar/gku1003
21. Vasaikar SV, Straub P, Wang J, Zhang B. LinkedOmics: Analyzing Multi-Omics Data Within and Across 32 Cancer Types. *Nucleic Acids Res* (2018) 46:D956–d963. doi: 10.1093/nar/gkx1090
22. Carosella E, Ploussard G, LeMaoult J, Desgrandchamps F. A Systematic Review of Immunotherapy in Urologic Cancer: Evolving Roles for Targeting of CTLA-4, PD-1/PD-L1, and HLA-G. *J E U* (2015) 68:267–79. doi: 10.1016/j.eururo.2015.02.032
23. Sharma A, Subudhi S, Blando J, Scutti J, Vence L, Wargo J, et al. Anti-CTLA-4 Immunotherapy Does Not Deplete FOXP3 Regulatory T Cells (Tregs) in Human Cancers. *Clinical Cancer Research : An Official Journal of the 352 American Association for Cancer Research* (2019) 25:1233–8. doi: 10.1158/1078-0432.Ccr-18-0762
24. Ju Q, Li X, Zhang H, Yan S, Li Y, Zhao Y, et al. NFE2L2 Is a Potential Prognostic Biomarker and Is Correlated With Immune Infiltration in Brain Lower Grade Glioma: A Pan-Cancer Analysis. *Oxid Med Cell Longev* (2020) 2020:3580719. doi: 10.1155/2020/3580719
25. Luo W, Tian X, Xu W, Qu Y, Zhu W, Wu J, et al. Construction of an Immune-Related LncRNA Signature With Prognostic Significance for Bladder Cancer. *J Cell Mol Med* (2021) 25:4326–39. doi: 10.1111/jcmm.16494
26. Ju Q, Li X-M, Zhang H, Zhao Y-J. BRCA1-Associated Protein Is a Potential Prognostic Biomarker and Is Correlated With Immune Infiltration in Liver Hepatocellular Carcinoma: A Pan-Cancer Analysis. *Front Molecular Biosci* (2020) 7:573619. doi: 10.3389/fmolb.2020.573619
27. Li Y, Feng D, Wang Z, Zhao Y, Sun R, Tian D, et al. Ischemia-Induced ACSL4 Activation Contributes to Ferroptosis-Mediated Tissue Injury in Intestinal Ischemia/Reperfusion. *Cell Death Differ* (2019) 26:2284–99. doi: 10.1038/s41418-019-0299-4
28. Chen J, Ding C, Chen Y, Hu W, Yu C, Peng C, et al. ACSL4 Reprograms Fatty Acid Metabolism in Hepatocellular Carcinoma *via* C-Myc/SREBP1 Pathway. *Cancer Lett* (2021) 502:154–65. doi: 10.1016/j.canlet.2020.12.019
29. Liu Y, Liang G, Xu H, Dong W, Dong Z, Qiu Z, et al. Tumors Exploit FTO-Mediated Regulation of Glycolytic Metabolism to Evade Immune Surveillance. *Cell Metabolism* (2021) 33:1221–33.e1211. doi: 10.1016/j.cmet.2021.04.001
30. Li X, Zhong M, Wang J, Wang L, Lin Z, Cao Z, et al. miR-301a Promotes Lung Tumorigenesis by Suppressing Runx3. *Mol Cancer* (2019) 18:99. doi: 10.1186/s12943-019-1024-0
31. Schulz-Heddergott R, Stark N, Edmunds S, Li J, Conradi L, Bohnenberger H, et al. Therapeutic Ablation of Gain-Of-Function Mutant P53 in Colorectal Cancer Inhibits Stat3-Mediated Tumor Growth and Invasion. *375 Cancer Cell* (2018) 34:298–314.e297. doi: 10.1016/j.ccell.2018.07.004
32. Cheng Y, Gunasegaran B, Singh H, Dutertre C, Loh C, Lim J, et al. Non-Terminally Exhausted Tumor-Resident Memory HBV-Specific T Cell Responses Correlate With Relapse-Free Survival in Hepatocellular Carcinoma. *Immunity* (2021) 54(8):1825–40.e7. doi: 10.1016/j.immuni.2021.06.013
33. Eschweiler S, Clarke J, Ramírez-Suástegui C, Panwar B, Madrigal A, Chee S, et al. Intratumoral Follicular Regulatory T Cells Curtail Anti-PD-1 Treatment Efficacy. *Nat Immunol* (2021) 22(8):1052–63. doi: 10.1038/s41590-021-00958-6
34. Zou W, Wolchok JD, Chen L. PD-L1 (B7-H1) and PD-1 Pathway Blockade for Cancer Therapy: Mechanisms, Response Biomarkers, and Combinations. *Sci Trans Med* (2016) 8:328rv324. doi: 10.1126/scitranslmed.aad7118
35. Khalil DN, Smith EL, Brentjens RJ, Wolchok JD. The Future of Cancer Treatment: Immunomodulation, CARs and Combination Immunotherapy. *Nat Rev Clin Oncol* (2016) 13:394. doi: 10.1038/nrclinonc.2016.65
36. Barry M, Bleackley RC. Cytotoxic T Lymphocytes: All Roads Lead to Death. *Nat Rev Immunol* (2002) 2:401–9. doi: 10.1038/nri819
37. Philip M, Schietinger ,A. CD8 T Cell Differentiation and Dysfunction in Cancer. *Nat Rev Immunol* (2021). doi: 10.1038/s41577-021-00574-3
38. Vantaku V, Dong J, Ambati C, Perera D, Donepudi S, Amara C, et al. Multi-Omics Integration Analysis Robustly Predicts High-Grade Patient Survival and Identifies CPT1B Effect on Fatty Acid Metabolism in Bladder Cancer. *Clinical Cancer Research : An Official Journal of the American Association for Cancer Research* (2019) 25:3689–701. doi: 10.1158/1078-0432.CCR-18-1515
39. Afonso J, Santos L, Longatto-Filho A, Baltazar F. Competitive Glucose Metabolism as a Target to Boost Bladder Cancer Immunotherapy. *Nat Rev Urol* (2020) 17:77–106. doi: 10.1038/s41585-019-0263-6
40. Belkaid A, Ouellette R, Surette MJC. 17β-Estradiol-Induced ACSL4 Protein Expression Promotes an Invasive Phenotype in Estrogen Receptor Positive Mammary Carcinoma Cells. *Carcinogenesis* (2017) 38:402–10. doi: 10.1093/carcin/bgx020

41. Cheng J, Fan Y, Liu B, Zhou H, Wang J, Chen QJOR. ACSL4 Suppresses Glioma Cells Proliferation via Activating Ferroptosis. *Oncol Rep* (2020) 43:147–58. doi: 10.3892/or.2019.7419
42. Chen J, Ding C, Chen Y, Hu W, Lu Y, Wu W, et al. ACSL4 Promotes Hepatocellular Carcinoma Progression *via* C-Myc Stability Mediated by ERK/FBW7/c-Myc Axis. *Oncogenesis* (2020) 9:42. doi: 10.1038/s41389-020-405
43. Feng J, Lu P, Zhu G, Hooi S, Wu Y, Huang X, et al. ACSL4 is a Predictive Biomarker of Sorafenib Sensitivity in Hepatocellular Carcinoma. *Acta Pharmacologica Sinica* (2021) 42:160–70. doi: 10.1038/s41401-020-408

Conflict of Interest: The authors declare that the research was conducted in the absence of any commercial or financial relationships that could be construed as a potential conflict of interest.

frontiers in Oncology

ORIGINAL RESEARCH
published: 23 November 2021
doi: 10.3389/fonc.2021.778858

Effect of Chemotherapy on Overall Survival in Contemporary Metastatic Prostate Cancer Patients

Benedikt Hoeh[1,2], Christoph Würnschimmel[2,3], Rocco S. Flammia[2,4], Benedikt Horlemann[2], Gabriele Sorce[2,5], Francesco Chierigo[2,6], Zhe Tian[2], Fred Saad[2], Markus Graefen[3], Michele Gallucci[4], Alberto Briganti[5], Carlo Terrone[6], Shahrokh F. Shariat[7,8,9,10,11,12], Derya Tilki[3,13], Luis A. Kluth[1], Philipp Mandel[1], Felix K. H. Chun[1] and Pierre I. Karakiewicz[2]*

[1] Department of Urology, University Hospital Frankfurt, Goethe University Frankfurt am Main, Frankfurt am Main, Germany, [2] Cancer Prognostics and Health Outcomes Unit, Division of Urology, University of Montréal Health Center, Montréal, QC, Canada, [3] Martini-Klinik Prostate Cancer Center, University Hospital Hamburg-Eppendorf, Hamburg, Germany, [4] Department of Maternal-Child and Urological Sciences, Sapienza Rome University, Policlinico Umberto I Hospital, Rome, Italy, [5] Division of Experimental Oncology/Unit of Urology, Urological Research Institute, San Raffaele Scientific Institute, Milan, Italy, [6] Department of Surgical and Diagnostic Integrated Sciences (DISC), University of Genova, Genova, Italy, [7] Department of Urology, Comprehensive Cancer Center, Medical University of Vienna, Vienna, Austria, [8] Department of Urology, Weill Cornell Medical College, New York, NY, United States, [9] Department of Urology, University of Texas Southwestern, Dallas, TX, United States, [10] Department of Urology, Second Faculty of Medicine, Charles University, Prague, Czechia, [11] Institute for Urology and Reproductive Health, Sechenov First Moscow State Medical University, Moscow, Russia, [12] Division of Urology, Department of Special Surgery, Jordan University Hospital, The University of Jordan, Amman, Jordan, [13] Department of Urology, University Hospital Hamburg-Eppendorf, Hamburg, Germany*

OPEN ACCESS

Edited by:
Izak Faiena, Columbia University, United States

Reviewed by:
Carlo Messina, Santa Chiara Hospital, Italy
Lorenzo Bianchi, University of Bologna, Italy

***Correspondence:**
Benedikt Hoeh
benedikt.hoeh@kgu.de

Specialty section:
This article was submitted to Genitourinary Oncology, a section of the journal Frontiers in Oncology

Received: *17 September 2021*
Accepted: *08 November 2021*
Published: *23 November 2021*

Citation:
Hoeh B, Würnschimmel C, Flammia RS, Horlemann B, Sorce G, Chierigo F, Tian Z, Saad F, Graefen M, Gallucci M, Briganti A, Terrone C, Shariat SF, Tilki D, Kluth LA, Mandel P, Chun FKH and Karakiewicz PI (2021) Effect of Chemotherapy on Overall Survival in Contemporary Metastatic Prostate Cancer Patients. Front. Oncol. 11:778858. doi: 10.3389/fonc.2021.778858

Introduction: Randomized clinical trials demonstrated improved overall survival in chemotherapy exposed metastatic prostate cancer patients. However, real-world data validating this effect with large scale epidemiological data sets are scarce and might not agree with trials. We tested this hypothesis.

Materials and Methods: We identified *de novo* metastatic prostate cancer patients within the Surveillance, Epidemiology, and End Results (SEER) database (2014-2015). Kaplan-Meier plots and Cox regression models tested for overall survival differences between chemotherapy-exposed patients *vs* chemotherapy-naïve patients. All analyses were repeated in propensity-score matched cohorts. Additionally, landmark analyses were applied to account for potential immortal time bias.

Results: Overall, 4295 *de novo* metastatic prostate cancer patients were identified. Of those, 905 (21.1%) patients received chemotherapy *vs* 3390 (78.9%) did not. Median overall survival was not reached at 30 months follow-up. Chemotherapy-exposed patients exhibited significantly better overall survival (61.6 *vs* 54.3%, multivariable HR:0.82, CI: 0.72-0.96, p=0.01) at 30 months compared to their chemotherapy-naïve counterparts. These findings were confirmed in propensity score matched analyses (multivariable HR: 0.77, CI:0.66-0.90, p<0.001). Results remained unchanged after landmark analyses were applied in propensity score matched population.

Conclusions: In this contemporary real-world population-based cohort, chemotherapy for metastatic prostate cancer patients was associated with better overall survival. However, the magnitude of overall survival benefit was not comparable to phase 3 trials.

Keywords: chemotherapy, overall survival, metastatic prostate cancer, SEER, contemporary

INTRODUCTION

Systemic treatments for metastatic prostate cancer have grown exponentially over the last two decades and exhibited significant survival benefits in randomized phase 3 trials (1–8). However, trial findings may be difficult to replicate in real-world conditions. Indeed, only one report demonstrated a modest benefit in overall survival after chemotherapy in contemporary, *de novo* metastatic prostate cancer patients (Weiner et al., National Cancer Database 2014-2015) (9). We addressed the same endpoint within the same study period. Within a different, large-scale database (SEER), we focused on the most contemporary patients (2014-2015) diagnosed with *de novo* metastatic prostate cancer. We hypothesized that chemotherapy use may result in a survival benefit for *de novo* metastatic prostate cancer patients (9). Unlike Weiner et al., we relied on propensity score matching to maximally reduce potential differences between chemotherapy-exposed and chemotherapy-naïve patients.

MATERIAL AND METHODS

Study Population

The current SEER database samples 34.6% of the United States population and approximates it in demographic composition and cancer incidence (10). Within the SEER database (2014-2015), we identified patients ≥18 years old with *de novo* metastatic, histologically confirmed adenocarcinoma of the prostate, diagnosed at biopsy (International Classification of Disease for Oncology [ICD-O-3] code 8140 site code C61.9) between 2014 and 2015. Patients with unknown M-stage, cases identified at autopsy or through death certificates, with unknown histology or non-primary prostate cancers were excluded. These selection criteria resulted in a cohort of 4295 *de novo* metastatic prostate cancer patients. This subgroup represented the study population.

Statistical Analyses

The statistical analyses consisted of four steps. First, we addressed overall survival prior to propensity score matching. We relied on Kaplan-Meier plots and Cox regression models to test for overall mortality differences according to chemotherapy exposure. Covariates consisted of age at diagnosis, PSA groups (<20, 20-90, >90 in ng/ml), Gleason Group Grade (GGG) at biopsy (≤III, IV/V, unknown), clinical T-stage (≤cT2, cT3/4, cTx), clinical N-stage (cN0, cN1, cNx), clinical M-stage (cM1a/b, cM1c, cM1x) and type of local treatment (no local treatment, local treatment, unknown).

Second, we relied on propensity score matching to address potential differences between chemotherapy-exposed *vs* chemotherapy-naïve patients using the 'nearest neighbor' and a caliper of 0.05. Matching variables consisted of age (per year interval), PSA (<20, 20-90, >90 in ng/ml), GGG (I, II, III, IV, V, unknown), T-stage (cT1, cT2, cT3, cT4, cTx), N-stage (cN0, cN1, cNx), M-stage (cM1a, cM1b, cM1c, cM1unspecific) socioeconomic status (1^{st}, $2^{nd}/3^{rd}/4^{th}$ quartile) and type of local treatment (RP, RT, RP+RT, none). Each chemotherapy exposed patient was matched to two chemotherapy naïve patient. Third, we relied on the propensity score matched cohorts of chemotherapy-exposed and chemotherapy-naïve patients and refitted Kaplan-Meier plots, as well as multivariable Cox regression models. The same covariates were used as above. Finally, survival analyses were repeated in propensity score matched cohorts after landmark analyses (3 months) was applied to account for confounding effects due to potential immortal time bias.

All tests were two sided with a level of significance set at $p<0.05$ and R software environment for statistical computing and graphics (version 3.4.3) was used for all analyses (11).

RESULTS

Descriptive Characteristics of Study Population

Between 2014 and 2015 we identified 4295 *de novo* metastatic prostate cancer patients. Of those, 905 patients (21.1%) received chemotherapy. Chemotherapy-exposed patients differed from their chemotherapy naïve counterparts with respect to age (64 *vs* 70 years, $p<0.001$), higher proportions of PSA >90 ng/ml (57.3 *vs* 51.8%, $p=0.01$), higher proportions of GGG V (52.3 *vs* 43.6%, $p=0.01$), higher proportions of cN1-stages (44.5 *vs* 31.6%, $p<0.001$) and higher proportions of cM1c-stages (19.8 *vs* 14.6%, $p<0.001$). No significant differences were recorded for type of local treatment.

Survival Analyses Without Propensity Score Matching

Based on the overall cohort, that included 905 chemotherapy-exposed *vs* 3390 chemotherapy-naïve patients, overall survival rates at 18 and 30 months were 76.3 *vs* 69.3% and 61.6 *vs* 54.3%, favoring chemotherapy-exposed patients (**Figure 1A**). In multivariable Cox regression models, chemotherapy exposed patients exhibited lower overall mortality (HR:0.82, CI: 0.72-0.96, $p=0.01$) compared to chemotherapy naïve patients (**Table 2**).

Propensity Score Matching

Propensity score matching focused on the overall study cohort, of who 905 chemotherapy-exposed *vs* 3390 chemotherapy-naïve patients. Of 905 chemotherapy-exposed patients, 879 could be

matched with up two chemotherapy-naïve patients, which resulted in two subgroups, respectively with 879 chemotherapy-exposed *vs* 1611 chemotherapy-naïve patients. No statistically significant differences in age at diagnosis, PSA groups, GGG, cT-stage, cN-stage, cM-stage, SES and approach of local treatment remained between these two cohorts (all p≥0.1; **Table 1**).

Survival Analyses After Propensity Score Matching

Based on the propensity matched cohorts of 879 chemotherapy-exposed *vs* 1611 chemotherapy-naïve patients, overall survival rates at 18 and 30 months were 76.3 *vs* 70.5% and 61.6 *vs* 56.0%, favoring chemotherapy-exposed patients (**Figure 1B**).

In multivariable Cox regression models, chemotherapy exposed patients exhibited lower overall mortality (HR:0.77, CI: 0.66-0.90, p<0.001) compared to chemotherapy naïve patients (**Table 2**). The effect of better survival in chemotherapy-exposed remained unchanged after landmark analyses was applied in the propensity score matched cohort (multivariable HR: 0.85; CI: 0.72-0.99; p=0.04).

DISCUSSION

We hypothesized that, in line with trial-derived findings and smaller population-based studies, chemotherapy exposed *de novo* metastatic prostate cancer patients exhibit better survival rates compared to their chemotherapy naïve counterparts. We tested this hypothesis within a large population-based cohort *de novo* metastatic prostate cancer patients diagnosed between 2014 and 2015.

First, we observed significantly worse cancer characteristics in chemotherapy-exposed patients compared to their chemotherapy naïve counterparts. Specifically, they exhibited higher proportions of high PSA, higher proportions of GGG V, higher proportions of cN1-stage and higher proportions of cM1c-stage. It is of note that

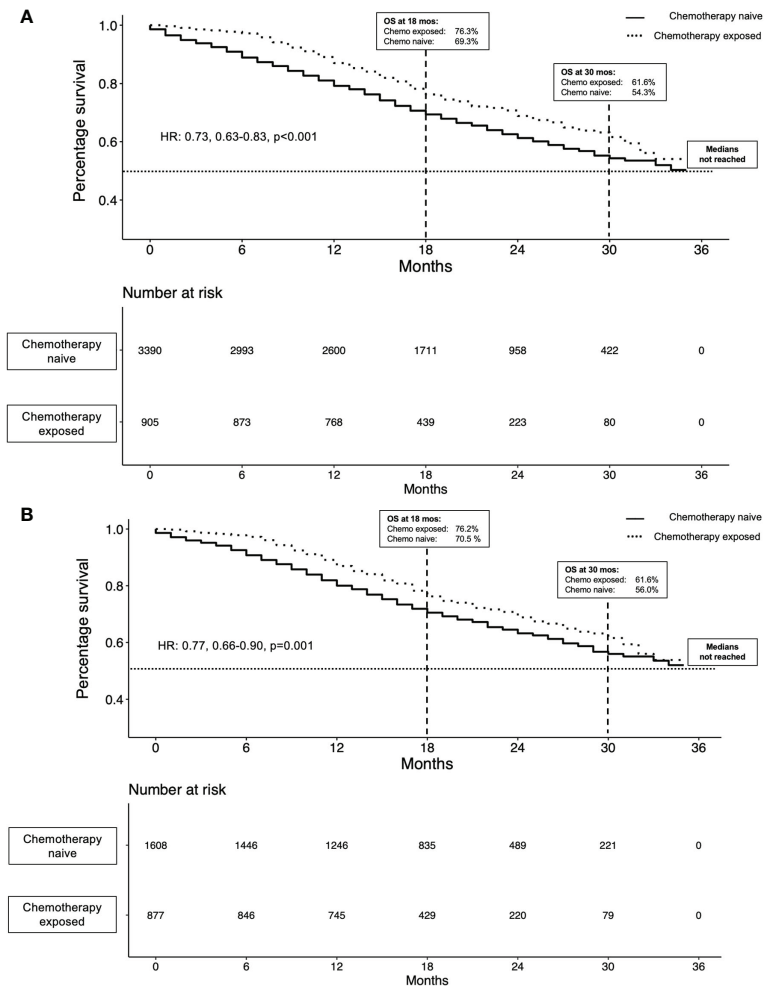

FIGURE 1 | Kaplan-Meier plots illustrating overall survival in metastatic prostate cancer (mPCa) patients (n=2495) prior to propensity score matching **(A)** and in 2490 mPCa patients after propensity score matching **(B)**, stratified by chemotherapy status.

TABLE 1 | Descriptive characteristics of *de novo* metastatic prostate cancer patients between 2014 and 2015, stratified by chemotherapy exposure.

	Unmatched data				Propensity score matched data			
	Overall, (n = 4295)	**Chemotherapy naïve, (n = 3390)**	**Chemotherapy exposed, (n = 905)**	**p-Value**	**Overall (n = 2490)**	**Chemotherapy naïve, (n = 1611)**	**Chemotherapy exposed, (n = 879)**	**p-Value**
Age in yrs	69	70	64	<0.001	64	64	64	0.1
median (IQR)	(61-77)	(63-79)	(58-70)		(59-71)	(59-71)	(58-71)	
PSA-groups in ng/ml				0.01				0.5
n (%)								
low (<20)	899 (20.9)	732 (21.6)	167 (18.5)		479 (19.3)	315 (19.6)	164 (18.7)	
intermediate (21-90)	1120 (26.1)	901 (26.6)	219 (24.2)		628 (25.3)	415 (25.8)	213 (24.3)	
high (>90)	2276 (53)	1757 (51.8)	519 (57.3)		1378 (55.5)	878 (54.6)	500 (57)	
GGG Biopsy				<0.001				1.0
n (%)								
I	59 (1.4)	51 (1.5)	8 (0.9)		26 (1)	18 (1.1)	8 (0.9)	
II	162 (3.8)	146 (4.3)	16 (1.8)		43 (1.7)	27 (1.7)	16 (1.8)	
III	312 (7.3)	261 (7.7)	51 (5.6)		151 (6.1)	100 (6.2)	51 (5.8)	
IV	799 (18.6)	646 (19.1)	153 (16.9)		436 (17.5)	284 (17.7)	152 (17.3)	
V	1951 (45.4)	1478 (43.6)	473 (52.3)		1284 (51.7)	831 (51.7)	453 (51.7)	
Unknown	1012 (23.6)	808 (23.8)	204 (22.5)		545 (21.9)	348 (21.6)	197 (22.5)	
cT-stage				0.3				0.9
n (%)								
cT1	1212 (28.2)	960 (28.3)	252 (27.8)		697 (28)	455 (28.3)	242 (27.6)	
cT2	1212 (28.2)	952 (28.1)	260 (28.7)		720 (29)	466 (29)	254 (29)	
cT3	466 (10.8)	366 (10.8)	100 (11)		289 (11.6)	190 (11.8)	99 (11.3)	
cT4	561 (13.1)	428 (12.6)	133 (14.7)		337 (13.6)	210 (13.1)	127 (14.5)	
cTx	844 (19.7)	684 (20.2)	160 (17.7)		442 (17.8)	287 (17.8)	155 (17.7)	
cN-stage				<0.001				0.6
n (%)								
cN0	2208 (51.4)	1805 (53.2)	403 (44.5)		1142 (46)	743 (46.2)	399 (45.5)	
cN1	1473 (34.3)	1070 (31.6)	403 (44.5)		1047 (42.1)	667 (41.5)	380 (43.3)	
cNX	614 (14.3)	515 (15.2)	99 (10.9)		296 (11.9)	198 (12.3)	98 (11.2)	
M-stage				<0.001				0.9
n (%)								
M1a	324 (7.5)	273 (8.1)	51 (5.6)		154 (6.2)	148 (6)	97 (6)	
M1b	3200 (74.5)	2539 (74.9)	661 (73)		1847 (74.2)	1849 (74.4)	1201 (74.7)	
M1c	674 (15.7)	495 (14.6)	179 (19.8)		451 (18.1)	445 (17.9)	281 (17.5)	
M1x	97 (2.3)	83 (2.4)	14 (1.5)		51 (1.7)	148 (6)	97 (6)	
Socioeconomic status				0.04				0.6
n (%)								
1st quartile	1082 (25.2)	830 (24.5)	252 (27.8)		668 (26.9)	426 (26.5)	242 (27.6)	
2nd-4th quartile	3213 (74.8)	2560 (75.5)	653 (72.2)		1817 (73.1)	1182 (73.5)	635 (72.4)	
Local treatment				0.2				1.0
n (%)								
None	3079 (71.7)	2419 (71.4)	660 (72.9)		1797 (72.3)	1157 (72)	640 (73)	
RP	99 (2.3)	88 (2.6)	11 (1.2)		36 (1.4)	25 (1.6)	11 (1.3)	
RT	843 (19.6)	664 (19.6)	179 (19.8)		489 (19.7)	318 (19.8)	171 (19.5)	
RP+RT	182 (4.2)	144 (4.2)	38 (4.2)		111 (4.5)	73 (4.5)	38 (4.3)	
Unknown	92 (2.1)	75 (2.2)	17 (1.9)		52 (2.1)	35 (2.2)	17 (1.9)	

All values are median (IQR) or frequencies (%).
RP, Radical prostatectomy; RT, Radiotherapy.

despite an obvious prostate cancer phenotype disadvantage in chemotherapy-exposed prostate cancer patients, their overall survival was better, as will be outlined below. These observations are similar to NCDB patient characteristics. In consequence, it may be postulated that both databases (NCDB and SEER) indicate that chemotherapy is offered to patients with more aggressive prostate cancer phenotype than average (9). The same observations regarding prostate cancer characteristics were made in smaller scale, retrospective studies (9, 12).

Second, within the current study cohort the rate of chemotherapy was 21.1% (n=905) *de novo* metastatic prostate cancer patients. This proportion is disappointingly low, however it is very comparable to NCDB, where chemotherapy was also given to a minority of patients (27.6%). Similarly low rates were recorded in other, smaller scale population-based studies (12, 13). These observations indicate a relatively low confidence level in systemic therapy. Additionally, risk of chemotherapy-related adverse events, which vary in regard to

TABLE 2 | Multivariable Cox regression models predicting overall mortality in *de novo* metastatic prostate cancer patients according to chemotherapy status prior to and after propensity score matching.

	Variable of interest	Univariable			Multivariable		
		Hazard Ratio	95%-CI	p-value	Hazard Ratio	95%-CI	p-value
Unmatched data	chemotherapy-exposed *vs*. naïve	0.73	0.63-0.83	<0.001	0.82	0.72-0.96	0.01
After propensity score matching	chemotherapy-exposed *vs*. naïve	0.77	0.66-0.90	0.001	0.77	0.66-0.90	<0.001

Cox regression models were adjusted for age, PSA, Gleason Group Grade, cT-stage, cN-stage, cM-stage and local treatment.

the dose and type of chemotherapeutical agent administered, may result in tendencies towards more restrictive chemotherapy administration policies. Even though that recent studies have recorded an increase of chemotherapy rates in more contemporary years (14, 15), efforts are further required to encourage referrals from within the urological community for systemic therapy, when metastatic prostate cancer is diagnosed (1).

Third, we recorded more favorable survival in chemotherapy-exposed *vs* chemotherapy-naïve patients (76.3 *vs* 69.3% and 61.6 *vs* 54.3% at 18 and 30 months). These rates resulted in a highly protective multivariable hazard ratio of 0.82 (CI:0.72-0.96, p=0.01). Finally, even after detailed propensity score matching for differences in patient and prostate cancer characteristics, a protective hazard ratio of 0.77 (CI:0.66-0.90, p<0.001) was recorded. Additionally, to propensity score matching, we furthermore repeated the survival analyses after landmark analyses was applied to maximally reduce potential biases that might have occurred due to immortal time biases. Irrespectively of these two strict methodological approaches to maximally reduce any biases which may arise from differences between chemotherapy exposed *vs* naïve *de novo* mPCa patients, survival trends remained in its quantity and quality unchanged.

These observations are highly consistent with NCDB-derived findings on the same topic (Weiner et al.) (9). Conversely, to the best of our knowledge, no other reports identified a survival benefit in contemporary, metastatic prostate cancer patients exposed to chemotherapy compared to their chemotherapy naïve counterparts. In consequence, it may be postulated that the survival benefit only became apparent in the most contemporary population-based metastatic prostate cancer patients, in both the SEER and the NCDB. To the best of our knowledge, prior to Weiner et al. and to the current study, a formal comparison between chemotherapy-exposed *vs* chemotherapy-naïve patients was not reported. Instead, previous population-based analyses examined survival trends regardless of chemotherapy exposure status. These trends exhibited only marginal improvement over time (14). For example, Cattrini et al. reported only a modest improvement of median overall survival (30 *vs* 26 months) in contemporary (2011-2014) metastatic prostate cancer patients in comparison to historical (2000-2003) metastatic prostate cancer patients exposed to chemotherapy. Since Cattrini et al. did not furthermore account for any treatment approach and primarily focused on the cohort of metastatic prostate cancer patients from an epidemiological aspect, results cannot directly be compared to the current study (16). In consequence, the current study, as well as the study by Weiner et al., cannot be directly compared to previous population-based studies with different designs and endpoints. Similarly, our findings cannot be directly compared to phase 3 trials, that focused on specific molecules and treatment regimens in randomized designs. In the current and Weiner et al. studies chemotherapy-exposed patients may have received one or multiple chemotherapy lines. Unfortunately, their specific time and duration of exposure is unknown in the current study, as well as in the Weiner et al. study. Consequently, some chemotherapy-exposed patients may have received a single line of chemotherapy with no overall survival benefit. Conversely, others may have received multiple lines with an important overall survival benefit. It is of note that combination therapies, including chemotherapeutic agents, are likely to play an important role in the near future. Recently, results derived from the PEACE-1 trial demonstrated for example that addition of abiraterone to androgen deprivation therapy (ADT) and docetaxel significantly improved radiographic progression-free survival in *de novo* metastatic castration sensitive prostate cancer patients (17). Last, but not least, the current study differed from Weiner et al. in its design. We relied on propensity score matching to maximally attenuate differences between chemotherapy-exposed and chemotherapy-naïve metastatic prostate cancer patients. Despite propensity score matching use in the current study, the previously recorded overall survival benefit observed in chemotherapy-exposed patients remained in the current analyses. Similarly, its magnitude remained virtually unchanged. It is noteworthy, that the magnitude of the benefit in the current study, as well as in the study of Weiner et al., cannot be directly compared to the magnitude of survival benefit recorded in phase 3 trials for specific systemic approaches for metastatic prostate cancer (18, 19). It is of note, that the magnitude of the survival benefit in most of phase 3 studies addressing overall survival in metastatic prostate cancer was greater than the magnitude recorded in our study, as well as that recorded in the study of Weiner et al. and other small scale institutional studies (20–22).

Regardless of the very important beneficial survival rates in chemotherapy exposed metastatic prostate cancer patients in respect to chemotherapy naïve patients, several limitations need to be acknowledged. First, the rate of chemotherapy exposure is low in the current study. It is nonetheless very similar to the rate observed in the study of Weiner et al. Moreover, the nature of administered chemotherapy is unknown with respect to the number of lines, their duration, as well as their individual efficacy. Furthermore, treatment approaches such as palliative care or observational approaches, are not available in the SEER database. Therefore, potential biases which may have occurred due to different supportive care measurements cannot be ruled

out and should be taken into account when data is interpreted. Similar to Weiner et al., we could not adjust or circumvent these limitations.

Second, the retrospective nature of the study introduces a number of selection biases, that distinguish chemotherapy exposed patients from others. As reported, chemotherapy-exposed patients tended to harbor more aggressive prostate cancer phenotypes. The same limitation applied to the study cohort focusing on NCDB. In the Weiner et al. study, these differences were addressed in multivariable analyses. Conversely, in the current study, multivariable analyses were complemented by propensity score matching to more completely and strictly address these differences.

Third, certain additional unmeasured variables could not be addressed. These variables, including performance status and comorbidities, were unavailable in the current study. Some of these variables, including comorbidities, were available in the Weiner et al. study (9). Despite their availability, overall survival rates virtually perfectly agreed with rates recorded in the current study. In consequence, lack of comorbidities does not appear to represent a rate limiting factor. Fourth, strict stratification according to low- and high-volume tumor burden, as performed in previously reported phase-3 trials is limited by the nature of SEER data collection (18). Finally, a number of established predictors of survival (Lactate dehydrogenase, hemoglobin) for metastatic prostate cancer patients were unavailable in both the current and NCDB analyses (23).

CONCLUSIONS

In the largest contemporary, North-American population-based study, chemotherapy exposure for metastatic prostate cancer patients was associated with a prolonged overall survival, however the magnitude of previous trial-based survival benefits could not be reassured in real-life population-based data.

DATA AVAILABILITY STATEMENT

The original contributions presented in the study are included in the article/supplementary material. Further inquiries can be directed to the corresponding author.

ETHICS STATEMENT

Ethical review and approval were not required for the study on human participants in accordance with the local legislation and institutional requirements. The patients/participants provided their written informed consent to participate in this study.

AUTHOR CONTRIBUTIONS

BHoe - conceptualization, methodology, formal analysis, writing original draft, writing review and editing, and visualization. FrC – writing review and editing and visualization. CW: writing review and editing and visualization. RF: writing review and editing and visualization. BHor: writing review and editing and visualization. GS: writing review and editing and visualization. ZT: methodology, software, validation, formal analysis, and resources. FS: writing review and editing and supervision. MaG - writing review and editing and supervision. MiG: writing review and editing and supervision. LK: writing review and editing and visualization. PM -writing review and editing and supervision. AB - writing review and editing and supervision. DT - writing review and editing and supervision. FeC: writing review and editing and supervision. SS: writing review and editing and supervision. CT: writing review and editing and supervision. PK: writing review and editing, supervision, project administration, and conceptualization. All authors contributed to the article and approved the submitted version.

ACKNOWLEDGMENTS

BH was awarded a scholarship by the GIERSCH STIFTUNG.

REFERENCES

1. Cornford P, Bellmunt J, Bolla M, Briers E, De Santis M, Gross T, et al. EAU-ESTRO-SIOG Guidelines on Prostate Cancer. Part II: Treatment of Relapsing, Metastatic, and Castration-Resistant Prostate Cancer. *Eur Urol* (2017) 71 (4):630–42. doi: 10.1016/j.eururo.2016.08.002
2. Miyake H, Sakai I, Harada K, Muramaki M, Fujisawa M. Significance of Docetaxel-Based Chemotherapy as Treatment for Metastatic Castration-Resistant Prostate Cancer in Japanese Men Over 75 Years Old. *Int Urol Nephrol* (2012) 44(6):1697–703. doi: 10.1007/s11255-012-0223-z
3. Aparicio J, Maroto P, García Del Muro X, Sánchez-Muñoz A, Gumà J, Margelí M, et al. Prognostic Factors for Relapse in Stage I Seminoma: A New Nomogram Derived From Three Consecutive, Risk-Adapted Studies From the Spanish Germ Cell Cancer Group (SGCCG). *Ann Oncol* (2014) 25 (11):2173–8. doi: 10.1093/annonc/mdu437
4. Tannock IF, de Wit R, Berry WR, Horti J, Pluzanska A, Chi KN, et al. Docetaxel Plus Prednisone or Mitoxantrone Plus Prednisone for Advanced Prostate Cancer. *N Engl J Med* (2004) 351(15):1502–12. doi: 10.1056/NEJMoa040720
5. Petrylak DP, Tangen CM, Hussain MHA, Lara PN, Jones JA, Taplin ME, et al. Docetaxel and Estramustine Compared With Mitoxantrone and Prednisone for Advanced Refractory Prostate Cancer. *N Engl J Med* (2004) 351(15):1513–20. doi: 10.1056/NEJMoa041318
6. Scher HI, Fizazi K, Saad F, Taplin M-E, Sternberg CN, Miller K, et al. Increased Survival With Enzalutamide in Prostate Cancer After Chemotherapy. *N Engl J Med* (2012) 367(13):1187–97. doi: 10.1056/NEJMoa1207506
7. Fizazi K, Pagliaro L, Laplanche A, Fléchon A, Mardiak J, Geoffrois L, et al. Personalised Chemotherapy Based on Tumour Marker Decline in Poor Prognosis Germ-Cell Tumours (GETUG 13): A Phase 3, Multicentre, Randomised Trial. *Lancet Oncol* (2014) 15(13):1442–50. doi: 10.1016/S1470-2045(14)70490-5
8. Shiota M, Yokomizo A, Eto M. Taxane Chemotherapy for Hormone-Naïve Prostate Cancer With Its Expanding Role as Breakthrough Strategy. *Front Oncol* (2016) 5:304/abstract. doi: 10.3389/fonc.2015.00304/abstract
9. Weiner AB, Ko OS, Li EV, Vo AX, Desai AS, Breen KJ, et al. Survival Following Upfront Chemotherapy for Treatment-Naïve Metastatic Prostate Cancer: A Real-World Retrospective Cohort Study. *Prostate Cancer Prostatic Dis* (2021) 24(1):261–7. doi: 10.1038/s41391-020-00278-0
10. *About the SEER Program*. SEER. Available at: https://seer.cancer.gov/about/overview.html. (last accessed: 15.09.2021).
11. RCT. *R: A Language and Environment for Statistical Computing* (2017). Available at: https://wwwr-projectorg2017.

12. Lissbrant IF, Garmo H, Widmark A, Stattin P. Population-Based Study on Use of Chemotherapy in Men With Castration Resistant Prostate Cancer. *Acta Oncol* (2013) 52(8):1593–601. doi: 10.3109/0284186X.2013.770164
13. Harris V, Lloyd K, Forsey S, Rogers P, Roche M, Parker C. A Population-Based Study of Prostate Cancer Chemotherapy. *Clin Oncol* (2011) 23(10):706–8. doi: 10.1016/j.clon.2011.04.014
14. Bandini M, Pompe RS, Marchioni M, Zaffuto E, Gandaglia G, Fossati N, et al. Improved Cancer-Specific Free Survival and Overall Free Survival in Contemporary Metastatic Prostate Cancer Patients: A Population-Based Study. *Int Urol Nephrol* (2018) 50(1):71–8. doi: 10.1007/s11255-017-1744-2
15. Hoeh B, Würnschimmel C, Flammia RS, Horlemann B, Sorce G, Chierigo F, et al. Improvement in Overall and Cancer-Specific Survival in Contemporary, Metastatic Prostate Cancer Chemotherapy Exposed Patients. *Prostate* (2021) 81(16):1374–81. doi: 10.1002/pros.24235.
16. Cattrini C, Soldato D, Rubagotti A, Zinoli L, Zanardi E, Barboro P, et al. Epidemiological Characteristics and Survival in Patients With *De Novo* Metastatic Prostate Cancer. *Cancers* (2020) 12(10):2855. doi: 10.3390/cancers12102855
17. Fizazi K, Maldonado X, Foulon S, Roubaud G, McDermott RS, Flechon A, et al. A Phase 3 Trial With a 2x2 Factorial Design of Abiraterone Acetate Plus Prednisone and/or Local Radiotherapy in Men With De Novo Metastatic Castration-Sensitive Prostate Cancer (mCSPC): First Results of PEACE-1. *J Clin Oncol* (2021) 39:15_suppl:5000–0. doi: 10.1200/JCO.2021.39.15_suppl.5000
18. Kyriakopoulos CE, Chen Y-H, Carducci MA, Liu G, Jarrard DF, Hahn NM, et al. Chemohormonal Therapy in Metastatic Hormone-Sensitive Prostate Cancer: Long-Term Survival Analysis of the Randomized Phase III E3805 CHAARTED Trial. *J Clin Oncol* (2018) 36(11):1080–7. doi: 10.1200/JCO.2017.75.3657
19. James ND, Sydes MR, Clarke NW, Mason MD, Dearnaley DP, Spears MR, et al. Addition of Docetaxel, Zoledronic Acid, or Both to First-Line Long-Term Hormone Therapy in Prostate Cancer (STAMPEDE): Survival Results From an Adaptive, Multiarm, Multistage, Platform Randomised Controlled Trial. *Lancet* (2016) 387(10024):1163–77. doi: 10.1016/S0140-6736(15)01037-5
20. Sartor O, Armstrong AJ, Ahaghotu C, McLeod DG, Cooperberg MR, Penson DF, et al. Survival of African-American and Caucasian Men After Sipuleucel-T Immunotherapy: Outcomes From the PROCEED Registry. *Prostate Cancer Prostatic Dis* (2020) 23(3):517–26. doi: 10.1038/s41391-020-0213-7
21. Raju R, Sahu A, Klevansky M, Torres J. Real-World Data on Outcomes in Metastatic Castrate-Resistant Prostate Cancer Patients Treated With Abiraterone or Enzalutamide: A Regional Experience. *Front Oncol* (2021) 11:656146. doi: 10.3389/fonc.2021.656146
22. Briones J, Khan M, Sidhu AK, Zhang L, Smoragiewicz M, Emmenegger U. Population-Based Study of Docetaxel or Abiraterone Effectiveness and Predictive Markers of Progression Free Survival in Metastatic Castration-Sensitive Prostate Cancer. *Front Oncol* (2021) 11:658331. doi: 10.3389/fonc.2021.658331
23. Smaletz O, Scher HI, Small EJ, Verbel DA, McMillan A, Regan K, et al. Nomogram for Overall Survival of Patients With Progressive Metastatic Prostate Cancer After Castration. *JCO* (2002) 20(19):3972–82. doi: 10.1200/JCO.2002.11.021

Conflict of Interest: The authors declare that the research was conducted in the absence of any commercial or financial relationships that could be construed as a potential conflict of interest.

Publisher's Note: All claims expressed in this article are solely those of the authors and do not necessarily represent those of their affiliated organizations, or those of the publisher, the editors and the reviewers. Any product that may be evaluated in this article, or claim that may be made by its manufacturer, is not guaranteed or endorsed by the publisher.

frontiers in Oncology

ORIGINAL RESEARCH
published: 13 January 2022
doi: 10.3389/fonc.2021.766576

Factors Predicting Oncological Outcomes of Radical Nephroureterectomy for Upper Tract Urothelial Carcinoma in Taiwan

I-Hsuan Alan Chen[1,2,3], Chao-Hsiang Chang[4,5], Chi-Ping Huang[4,5], Wen-Jeng Wu[6,7,8], Ching-Chia Li[6,7,8], Chung-Hsin Chen[9], Chao-Yuan Huang[9], Chi-Wen Lo[10], Chih-Chin Yu[10,11], Chung-You Tsai[12,13], Wei-Che Wu[12,14], Jen-Shu Tseng[15,16], Wun-Rong Lin[15,16], Yuan-Hong Jiang[17], Yu-Khun Lee[17], Yeong-Chin Jou[18,19], Ian-Seng Cheong[18], Thomas Y. Hsueh[20,21], Allen W. Chiu[22], Yung-Tai Chen[23], Jih-Sheng Chen[23], Bing-Juin Chiang[24,25,26], Yao-Chou Tsai[27,28], Wei Yu Lin[29,30,31], Chia-Chang Wu[27,32,33], Jen-Tai Lin[1†] and Chia-Cheng Yu[1*†]*

[1] Division of Urology, Department of Surgery, Kaohsiung Veterans General Hospital, Kaohsiung, Taiwan, [2] Institute of Clinical Medicine, School of Medicine, National Yang Ming Chiao Tung University, Taipei, Taiwan, [3] Division of Urology, Department of Surgery, Tri-Service General Hospital, National Defense Medical Center, Taipei, Taiwan, [4] Department of Urology, China Medical University and Hospital, Taichung, Taiwan, [5] School of Medicine, China Medical University, Taichung, Taiwan, [6] Department of Urology, Kaohsiung Medical University Hospital, Kaohsiung, Taiwan, [7] Department of Urology, School of Medicine, College of Medicine, Kaohsiung Medical University, Kaohsiung, Taiwan, [8] Graduate Institute of Clinical Medicine, College of Medicine, Kaohsiung Medical University, Kaohsiung, Taiwan, [9] Department of Urology, National Taiwan University Hospital, College of Medicine, National Taiwan University, Taipei, Taiwan, [10] Division of Urology, Department of Surgery, Taipei Tzu Chi Hospital, The Buddhist Tzu Chi Medical Foundation, New Taipei, Taiwan, [11] School of Medicine, Buddhist Tzu Chi University, Hualien, Taiwan, [12] Division of Urology, Department of Surgery, Far Eastern Memorial Hospital, New Taipei, Taiwan, [13] Department of Healthcare Information and Management, Ming Chuan University, Taipei, Taiwan, [14] Institute of Biomedical Engineering, National Taiwan University, Taipei, Taiwan, [15] Department of Urology, MacKay Memorial Hospital, Taipei, Taiwan, [16] Department of Medicine, Mackay Medical College, Taipei, Taiwan, [17] Department of Urology, Hualien Tzu Chi Hospital, Buddhist Tzu Chi Medical Foundation and Tzu Chi University, Hualien, Taiwan, [18] Department of Urology, Ditmanson Medical Foundation Chiayi Christian Hospital, Chiayi, Taiwan, [19] Department of Health and Nutrition Biotechnology, Asian University, Taichung, Taiwan, [20] Division of Urology, Department of Surgery, Taipei City Hospital Renai Branch, Taipei, Taiwan, [21] Department of Urology, School of Medicine, National Yang Ming Chiao Tung University, Taipei, Taiwan, [22] College of Medicine, National Yang Ming Chiao Tung University, Taipei, Taiwan, [23] Department of Urology, Taiwan Adventist Hospital, Taipei, Taiwan, [24] College of Medicine, Fu-Jen Catholic University, New Taipei City, Taiwan, [25] Department of Urology, Cardinal Tien Hospital, New Taipei City, Taiwan, [26] Department of Life Science, College of Science, National Taiwan Normal University, Taipei, Taiwan, [27] Department of Urology, School of Medicine, College of Medicine, Taipei Medical University, Taipei, Taiwan, [28] Department of Urology, Taipei Medical University Hospital, Taipei Medical University, Taipei, Taiwan, [29] Division of Urology, Department of Surgery, Chang Gung Memorial Hospital, Chia-Yi, Taiwan, [30] Chang Gung University of Science and Technology, Chia-Yi, Taiwan, [31] Department of Medicine, Chang Gung University, Taoyuan, Taiwan, [32] Department of Urology, Shuang Ho Hospital, Taipei Medical University, New Taipei, Taiwan, [33] TMU Research Center of Urology and Kidney, Taipei Medical University, Taipei, Taiwan

Background: Taiwan is one of the endemic regions where upper tract urothelial carcinoma (UTUC) accounts for approximately a third of all urothelial tumors. Owing to its high prevalence, extensive experience has been accumulated in minimally invasive radical nephroureterectomy (RNU). Although a variety of predictive factors have been explored in numerous studies, most of them were on a single-center or limited institutional basis and data from a domestic cohort are lacking.

OPEN ACCESS

Edited by:
Ke-hung Tsui,
Taipei Medical University, Taiwan

Reviewed by:
Xuesong Li,
Peking University, China
Chen Pang Hou,
Linkou Chang Gung Memorial Hospital, Taiwan
Horng-Heng Juang,
Chang Gung University, Taiwan

***Correspondence:**
Jen-Tai Lin
jtlin@vghks.gov.tw
Chia-Cheng Yu
mlee0857@gmail.com

[†]These authors have contributed equally to this work and share last authorship

Specialty section:
This article was submitted to Genitourinary Oncology, a section of the journal Frontiers in Oncology

Received: 17 September 2021
Accepted: 21 December 2021
Published: 13 January 2022

Citation:
Chen I-HA, Chang C-H, Huang C-P, Wu W-J, Li C-C, Chen C-H, Huang C-Y, Lo C-W, Yu C-C, Tsai C-Y, Wu W-C, Tseng J-S, Lin W-R, Jiang Y-H, Lee Y-K, Jou Y-C, Cheong I-S, Hsueh TY, Chiu AW, Chen Y-T, Chen J-S, Chiang B-J, Tsai Y-C, Lin WY, Wu C-C, Lin J-T and Yu C-C (2022) Factors Predicting Oncological Outcomes of Radical Nephroureterectomy for Upper Tract Urothelial Carcinoma in Taiwan. Front. Oncol. 11:766576. doi: 10.3389/fonc.2021.766576

Objective: This study aims to identify significant predicting factors of oncological outcomes, including overall survival (OS), cancer-specific survival (CSS), disease-free survival (DFS), and intravesical recurrence-free survival (IVRFS), following RNU for UTUC in Taiwan.

Methods: A multicenter registry database, Taiwan UTUC Collaboration Group, was utilized to analyze oncological outcomes of 3,333 patients undergoing RNU from 1988 to 2021 among various hospitals in Taiwan. Clinicopathological parameters were recorded according to the principles established by consensus meetings. The Kaplan-Meier estimator was utilized to estimate the survival rates, and the curves were compared using the stratified log-rank test. Univariate and multivariate analyses were performed with the Cox proportional hazard model to explore potential predicting factors.

Results: With a median follow-up of 41.8 months in 1,808 patients with complete information, the 5-year IVRFS, DFS, CSS, and OS probabilities were 66%, 72%, 81%, and 70%, respectively. In total, 482 patients experienced intravesical recurrence, 307 died of UTUC, and 583 died of any cause. Gender predominance was female (57%). A total of 1,531 patients (84.7%) had high-grade tumors; preoperative hydronephrosis presented in 1,094 patients (60.5%). Synchronous bladder UC was identified in 292 patients (16.2%). Minimally invasive procedures accounted for 78.8% of all surgeries, including 768 hand-assisted laparoscopic (42.5%) and 494 laparoscopic (27.3%) approaches. Synchronous bladder UC was the dominant adverse predicting factor for all survival outcomes. Other independent predicting factors for OS, CSS, and DFS included age ≧70, presence of preoperative hydronephrosis, positive surgical margin, LVI, pathological T and N staging, and laparoscopic RNU.

Conclusion: Synchronous UC of the urinary bladder is an independent adverse prognostic factor for survival in UTUC. The presence of preoperative hydronephrosis was also corroborated as a disadvantageous prognostic factor. Our multivariate analysis suggested that laparoscopic RNU might provide better oncological control.

Keywords: kidney pelvis, nephroureterectomy, risk factors, survival, ureter, urinary bladder, urinary tract, urothelial carcinoma

INTRODUCTION

Upper tract urothelial carcinoma (UTUC) comprises approximately 5% to 10% of all urothelial cancer (1). Taiwan is one of the endemic regions where UTUC accounts for 30% of all urothelial tumors (2). With the estimated annual incidence of up to 2 new cases per 100,000 person-years in the Western countries, the Taiwan Cancer Registry Annual Report depicted the age-standardized incidence rate of UTUC was 3.71 in men and 3.99 in women per 100,000 population in 2018. Radical nephroureterectomy (RNU) is the standard primary treatment for localized or even locally advanced UTUC. Owing to its high prevalence in Taiwan, apart from conventional open RNU, extensive experience was obtained in minimally invasive surgical approaches for managing UTUC.

On account of its relatively low incidence across the world, focused collaborative efforts are required to better understand the behavior of UTUC. Globally, a number of multi-institutional database have contributed to the prediction of prognosis and therapeutic responses following RNU (3), but the sample size was limited and interethnic variations and regional differences might exist in these cohorts. In order to obtain comprehensive information about the prognosis locally, a multicenter registry database, the Taiwan UTUC Collaboration Group, was established to record clinical data and treatment outcomes of patients who underwent RNU from 1988 to 2021 among various hospitals in Taiwan. In contrast with the National Health Insurance Research Database (NHIRD) of Taiwan, our dataset could provide detailed clinical information and mitigate the effects of unmeasured confounders. Additionally, diagnosis validity would be confirmed after serial consensus meetings. Robust results might be expected through collaborative work among medical centers and regional hospitals.

A variety of predictive factors have been explored in numerous studies, including patient, tumor, and pathological factors, to forecast outcomes of patients with UTUC (4). Gender (5),

preoperative blood-based biomarkers (6, 7), tumor stage (8), and location (9) had been identified as pivotal predictive factors for UTUC following RNU in a Taiwanese population. Nevertheless, most results were derived from single-center or limited institutional studies, and data from a domestic cohort are lacking. The aim of our study is to identify predicting factors of long-term oncological outcomes following radical nephroureterectomy in the largest multicenter Taiwanese database.

MATERIALS AND METHODS

Database Introduction

Ethics approvals were granted by the Internal Review Board of 15 participating hospitals, and data sharing agreements were required before commencing the multicenter cancer registry. In order to achieve consistent and accurate data registration, consensus meetings were undertaken to avoid any discrepancies. All patients in the database, Taiwan UTUC Collaboration Group, were waived from informed consent, and de-identified for privacy protection.

Data Extraction

A total of 3,333 patients with UTUC from August 1988 to April 2021 inclusive were enrolled. Those undergoing RNU and bladder cuff excision were included in the current study. A variety of surgical approaches, including open and minimally invasive techniques, either transperitoneal or retroperitoneal, were presented. The exclusion criteria entailed 448 patients receiving kidney-sparing treatment and 1,077 patients who lack complete information, including basic characteristics, perioperative parameters, pathological results, and follow-up outcomes. On account of the retrospective nature of our large multicenter database, missing data could be expected, which was also inevitable in prospective multicenter studies. In order to maintain the robustness and completeness of our results, stringent exclusion criteria were applied. Incomplete data were prevented, and no imputation was undertaken for statistical analysis (**Figure 1**). No missing data was managed in all the data extracted. Patient demographics were recorded and postoperative complications were reported and graded using the Clavien-Dindo classification.

Tumor location and size were defined by evaluation of the specimen following RNU. Synchronous presence of two or more

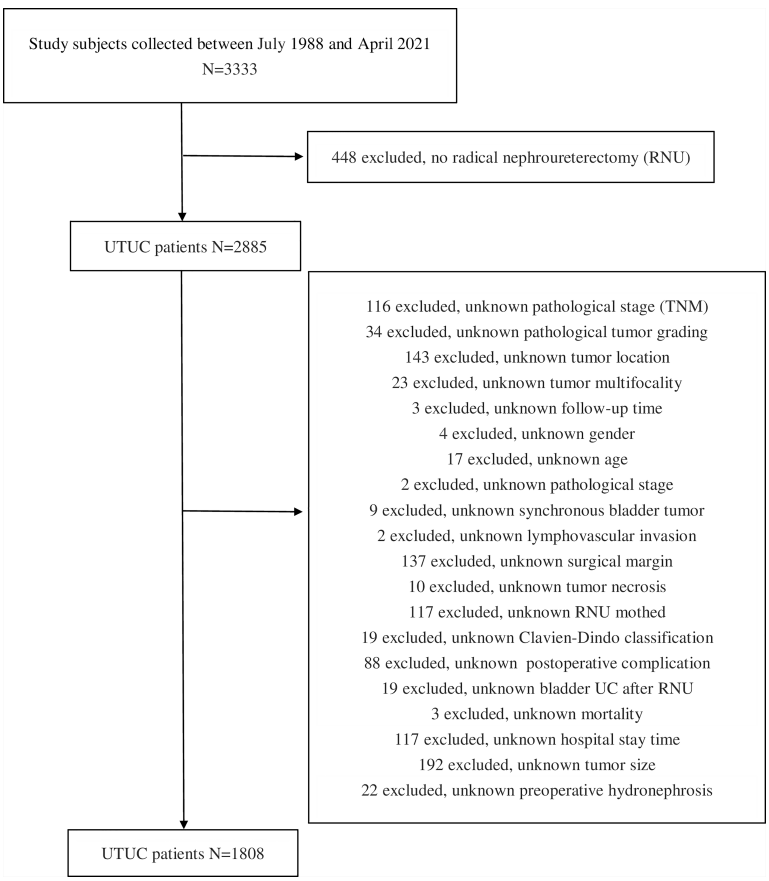

FIGURE 1 | Study flowchart.

pathologically confirmed lesions at different sites (renal pelvicalyceal system or ureter) was designated as multifocality. Tumor size was calculated by summing the longest diameters of all tumors. Preoperative hydronephrosis was assessed utilizing the computed tomography (CT) or magnetic resonance imaging (MRI). Various cell types, carcinoma *in situ*, lymphovascular invasion (LVI), tumor necrosis, and surgical margins were reviewed by the urological pathologists. Histological grading was determined according to the 2004 World Health Organization grading system. Pathological staging was referenced according to the 2017 TNM staging system of the American Joint Committee on Cancer (AJCC). In addition, the presence and chronology of bladder UC were recorded.

Survival Assessment

The primary endpoint of the study was to identify significant predicting factors of oncological outcomes, including overall survival (OS), cancer-specific survival (CSS), disease-free survival (DFS), and intravesical recurrence-free survival (IVRFS). The patients who died within 30 days after RNU or within the same hospital stay were censored at the time of mortality in the analysis of CSS. DFS was defined as time from RNU to either first local recurrence in the tumor bed, first lymph node or distant metastasis, or death from any cause. Recurrence and metastasis were assessed either radiologically or pathologically. Intravesical recurrence was coded with the presence of any subsequent histologically proven bladder UC during cystoscopy. All survival outcomes were evaluated with multivariate Cox proportional hazard models.

Statistical Analysis

Continuous variables were tested for normality using Kolmogorov-Smirnov test. Continuous data were stratified into categories, and categorical data were reported as number and percentage of all patients. The Kaplan-Meier estimator was utilized to estimate the rates of prognostic outcomes, and the survival curves were compared using the stratified log-rank test. The Cox proportional hazard model was selected to assess the effect of clinicopathological parameters on the prognostic outcomes, alone and after adjusting for potential confounders. All statistical assessments were two-tailed and considered statistically significant as $p < 0.05$. Statistical analyses were carried out with IBM SPSS statistical software version 26.

RESULTS

Patient, Tumors, and Surgical Approaches

The median follow-up for 1,808 patients undertaking RNU was 41.8 months; 482 (26.7%) patients experienced intravesical recurrence, 448 (24.8%) encountered disease recurrence outside of the bladder, 307 (17%) died of UTUC, and 583 (32.2%) died of any cause. The 5-year IVRFS, DFS, CSS, and OS probabilities were 66%, 72%, 81%, and 70%; the 10-year survival rates were 58%, 66%, 77%, and 51%, respectively. Patient demographics and pathological characteristics are shown in **Table 1**. The median age of diagnosis was 69 years, and 898 were equal to or more than 70 years old (49.7%). Gender predominance was female (57%); the most common sites of UTUC were renal pelvis (68%) and proximal ureter (22.7%). High-grade UTUC was diagnosed in 1,531 patients (84.7%); preoperative hydronephrosis presented in 1,094 patients (60.5%). Synchronous bladder UC was identified in 292 patients (16.2%). With regard to stage distribution, stage III predominated (29.4%) followed by stage I (24.9%) and stage II (18.6%). Interestingly, minimally invasive procedures accounted for 78.8% of all RNU surgeries, including 768 hand-assisted laparoscopic (42.5%), 494 laparoscopic (27.3%), 158 robot-assisted (8.7%), and 6 laparoendoscopic single site (LESS) (0.3%) approaches. The surgical margin was free in 1,732 patients (95.8%) but involved in 76 (4.2%) patients.

Identification of Predicting Factors for OS

In the univariate analysis of OS, the predictors demonstrating a p-value of <0.05 were taken into account in the subsequent multivariate analysis in which age, tumor size, preoperative hydronephrosis, distal ureteral or bladder cuff UC, multifocal UCs, previous or synchronous bladder UC, LVI, tumor necrosis, surgical margin, tumor grade, cell type, pathological T and N staging, and surgical approaches of RNU were included. Independent adverse predicting factors for OS were shown as follows: age ≧70, synchronous bladder UC, preoperative hydronephrosis, LVI, positive surgical margin, and pathological stages T2, T3, T4, N1, and N2. Adjusted Kaplan-Meier estimates of OS are demonstrated in **Figure 2**. Favorable predicting factors for OS were minimally invasive approaches, including laparoscopic (HR = 0.671), hand-assisted laparoscopic (HR 0.805), and robotic RNU (HR = 0.484).

Identification of Predicting Factors for CSS

By univariate analysis, worse CSS was associated with middle ureteral UC (HR = 1.372, $p = 0.032$); other statistically significant predictors for CSS included in the ensuing multivariate analysis were identical to those for OS. Independent adverse predicting factors for CSS were identified as follows: age ≧70, synchronous bladder UC, preoperative hydronephrosis, LVI, positive surgical margin, high-grade UC, and pathological stages T2, T3, T4, N1, and N2. Adjusted Kaplan-Meier estimates of CSS are shown in **Figure 3**. Merely one favorable predicting factor for CSS was laparoscopic RNU (HR = 0.551).

Identification of Predicting Factors for DFS

By univariate analysis, except for robotic RNU, all statistically significant predictors for DFS included in the successive multivariate analysis were equivalent to those for OS. Independent adverse predicting factors for DFS were identified as follows: age ≧70, multifocal UC, synchronous bladder UC, preoperative hydronephrosis, LVI, positive surgical margin, high-grade UC, and pathological stages T2, T3, T4, N1, and N2. Adjusted Kaplan-Meier estimates of DFS are displayed in **Figure 4**. Only one favorable predicting factor for DFS was laparoscopic RNU (HR = 0.726).

TABLE 1 | Baseline demographics and clinicopathological characteristics.

Parameters	*N* (%)
Gender	
Men	777 (43.0)
Women	1,031 (57.0)
Age	
<70	910 (50.3)
≥70	898 (49.7)
Tumor location	
Renal pelvis	1,229 (68.0)
Proximal ureter	410 (22.7)
Middle ureter	252 (13.9)
Distal ureter	360 (19.9)
Bladder cuff	49 (2.7)
Tumor size	
Nonvisible	34 (1.9)
<1 cm	128 (7.1)
≥1 and <2 cm	356 (19.7)
≥2 and <3 cm	396 (21.9)
≥3 cm	894 (49.4)
Multifocality	
No	1182 (65.4)
Yes	626 (34.6)
Cell type	
Urothelial carcinoma (UC)	1,633 (90.3)
UC with variants	128 (7.1)
Squamous	1 (0.1)
Small cell	2 (0.1)
Others	44 (2.4)
Carcinoma *in situ* (CIS)	
No	1,497 (82.8)
Yes	311 (17.2)
Bladder UC	
No	1,392 (77.0)
Previous	124 (6.9)
Synchronous	292 (16.2)
Tumor grading	
Low grade	277 (15.3)
High grade	1,531 (84.7)
Lymphovascular invasion	
No	1,391 (76.9)
Yes	417 (23.1)
Surgical margin	
Free	1,732 (95.8)
Positive	76 (4.2)
Preoperative hydronephrosis	
No	714 (39.5)
Yes	1,094 (60.5)
Tumor necrosis	
No	1,522 (84.2)
Yes	286 (15.8)
Pathological stage	
0a/0is	334 (18.5)
I	450 (24.9)
II	337 (18.6)
III	531 (29.4)
IV	156 (8.6)
Pathological T stage	
pTis	26 (1.4)
pTa	308 (17.0)
pT1	453 (25.1)
pT2	346 (19.1)
pT3	590 (32.6)
pT4	85 (4.7)
Pathological N stage	
pN0	408 (22.6)
pN1	33 (1.8)
pN2	56 (3.1)
pNx	1,311 (72.5)
RNU techniques	
Open	382 (21.1)
Laparoscopic hand-assisted	768 (42.5)
Robot-assisted	158 (8.7)
Laparoscopic	494 (27.3)
LESS	6 (0.3)
RNU approaches	
Transperitoneal	951 (52.6)
Retroperitoneal	857 (47.4)
Clavien-Dindo classification	
No	1,093 (60.5)
Grade I	236 (13.1)
Grade II	365 (20.2)
Grade III	50 (2.8)
Grade IV	45 (2.5)
Grade V	19 (1.1)
Postoperative complication	
No	1528 (84.5)
Yes	280 (15.5)
ESRD	218 (12.1)
Ileus	45 (2.5)
Ventral hernia	33 (1.8)
Bladder UC following RNU	
No	1,326 (73.3)
Yes	482 (26.7)
Disease free	
No	1,360 (75.2)
Yes	448 (24.8)
UTUC-specific mortality	
No	1,501 (83.0)
Yes	307 (17.0)
Overall mortality	
No	1,225 (67.8)
Yes	583 (32.2)

RNU, radical nephroureterectomy; UTUC, upper tract urothelial carcinoma.

Identification of Predicting Factors for IVRFS

In the univariate analysis of IVRFS, statistically significant predictors included gender, preoperative hydronephrosis, middle ureteral, distal ureteral or bladder cuff UC, multifocal UCs, previous or synchronous bladder UC, tumor grade, cell type, and pathological T staging. The following multivariate analysis highlighted that independent adverse predicting factors of BRFS were as below: distal ureteral UC, multifocal UCs, and previous and synchronous bladder UC. Adjusted Kaplan-Meier estimates of IVRFS are illustrated in **Figure 5**. Favorable predicting factors for BRFS were female gender (HR = 0.599) and pathological stage T4 (HR = 0.337).

All results of univariate and multivariate Cox regression analyses are depicted in **Tables 2**, **3**. Synchronous bladder UC was the dominant adverse predicting factor for all aspects of survival. Other independent predicting factors for OS, CSS, and

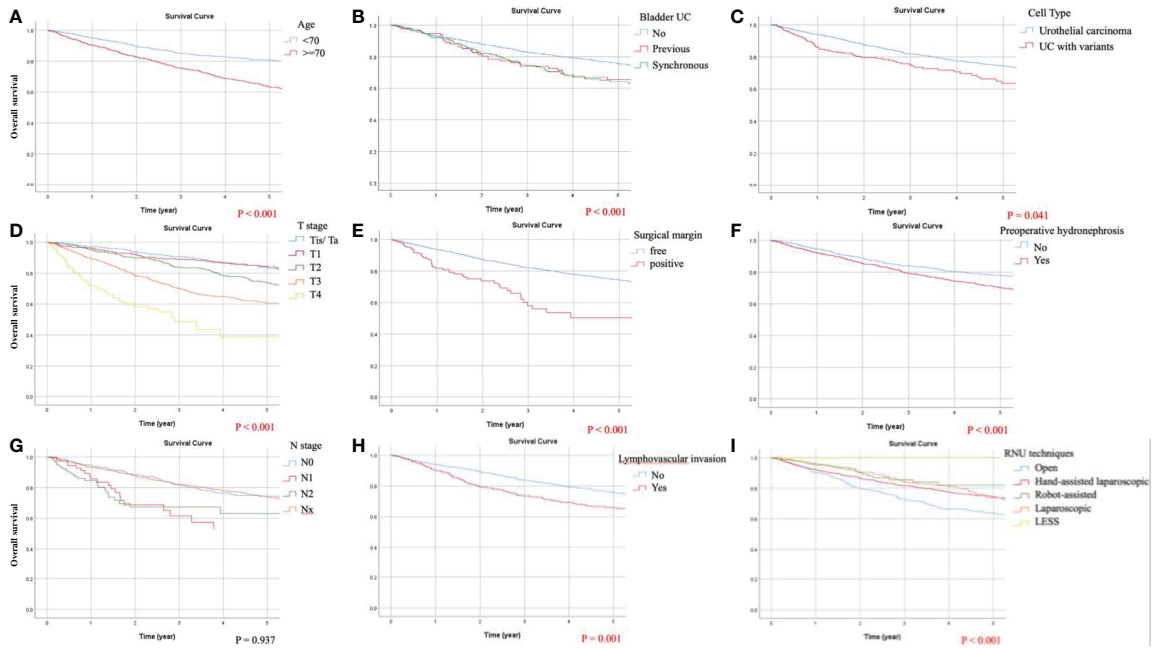

FIGURE 2 | Kaplan-Meier curves of overall survival (OS) following adjustment for age, tumor size, preoperative hydronephrosis, distal ureteral or bladder cuff urothelial carcinoma (UC), multifocal UCs, previous or synchronous bladder UC, lymphovascular invasion (LVI), tumor necrosis, surgical margin, tumor grading, cell type, pathological T and N staging, and surgical approaches of radical nephroureterectomy (RNU). Significant predicting factors for OS included: **(A)** age, **(B)** chronological history of bladder UC, **(C)** cell type, **(D)** T stage, **(E)** surgical margin, **(F)** preoperative hydronephrosis, **(H)** LVI, and **(I)** RNU techniques. **(G)** N staging did not demonstrate significant influence on OS because the proportion of lymphadenectomy was limited in the present study.

DFS included age ≧70, presence of preoperative hydronephrosis, positive surgical margin, LVI, pathological T and N staging, and laparoscopic RNU.

DISCUSSION

Despite the high prevalence of UTUC in Taiwan, patient demographics and perioperative data on a domestic basis are lacking. In order to better understand the behavior of UTUC in one of the endemic regions, a multicenter Taiwan UTUC Collaboration Group was established by 15 participating hospitals to collect detailed clinical information. In our large multicenter cohort of 1,808 patients receiving RNU, female predominance was observed, which was corresponding to previous hospital-based results (8, 10) as well as the crude incidence rate from the Taiwan Cancer Registry Annual Report. Different gender distributions were ascertained as compared with the reports from Western (11, 12) and other Asian countries (13, 14). Similar to previous studies (15, 16), no gender difference could be demonstrated in OS or CSS. Nevertheless, Huang et al. (10) highlighted that females had better OS and CSS in nonmuscle invasive UTUC; similarly, better IVRFS was exhibited in our female patients.

Approximately 8% to 13% of patients with UTUC present with synchronous bladder UC (17). In the French national UTUC database, 9.4% of the enrolled 662 patients showed synchronous bladder UC; 16.2% was reported in our study. It is noteworthy that synchronous bladder UC was an independently adverse predicting factor for OS, CSS, DFS, and IVRFS. Likewise, Mullerad et al. (18) maintained that a history of superficial or muscle-invasive bladder cancer was independently associated with CSS and IVRFS. Given that their survival analysis might be skewed by muscle-invasive bladder UC, Pignot et al. (17) focused on the influence of previous or synchronous superficial bladder UC unambiguously. As expected, the history of superficial bladder UC is a well-known predictor of intravesical recurrence (IVR), but they failed to reveal a prognostic effect on survival. Interestingly, as chronology was taken into consideration, the survival differences between previous and synchronous bladder UC were significantly manifested in the current study. Moreover, a previous bladder UC was again proven as a predicting factor for IVR.

In spite of a similar histologic appearance, distinct epidemiologic and clinicopathologic differences have been identified between UTUC and bladder UC (19, 20). Nevertheless, Doeveran et al. (21) conducted a systematic review to underline that UTUC and paired bladder UC (synchronous or metachronous) were likely clonally related. Later, they performed targeted genomic sequencing to support the hypothesis that metachronous bladder UCs following RNU were predominantly clonally derived recurrences (22). Furthermore, Petros et al. (23) indicated that, regardless of chronologic development or anatomic origin, most

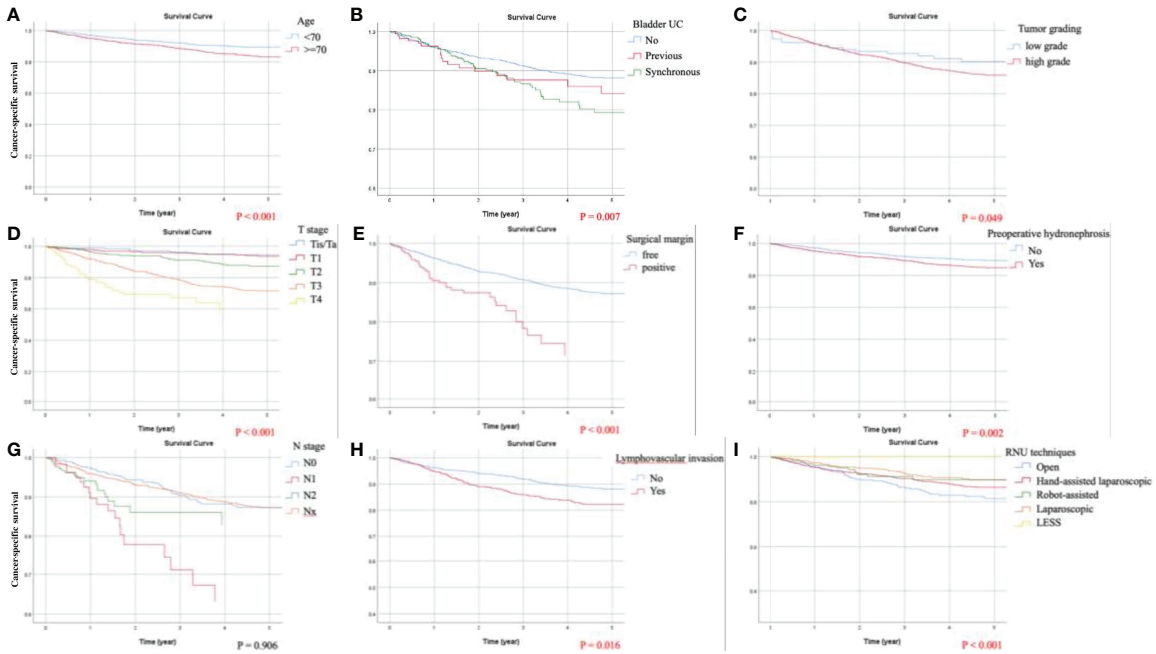

FIGURE 3 | Kaplan-Meier curves of cancer-specific survival (CSS) following adjustment for age, tumor size, preoperative hydronephrosis, middle ureteral, distal ureteral or bladder cuff urothelial carcinoma (UC), multifocal UCs, previous or synchronous bladder UC, lymphovascular invasion (LVI), tumor necrosis, surgical margin, tumor grading, cell type, pathological T and N staging, and surgical approaches of radical nephroureterectomy (RNU). Significant predicting factors for CSS included: **(A)** age, **(B)** chronological history of bladder UC, **(C)** tumor grading, **(D)** T stage, **(E)** surgical margin, **(F)** preoperative hydronephrosis, **(H)** LVI, and **(I)** RNU techniques. **(G)** N staging did not demonstrate significant influence on CSS because the proportion of lymphadenectomy was limited in the present study.

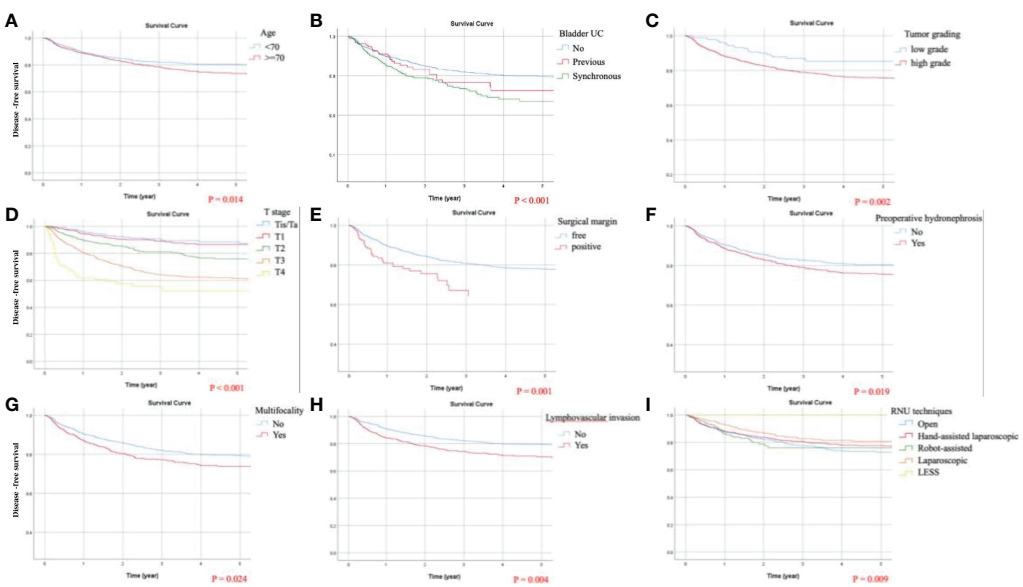

FIGURE 4 | Kaplan-Meier curves of disease-free survival (DFS) following adjustment for age, tumor size, preoperative hydronephrosis, distal ureteral or bladder cuff urothelial carcinoma (UC), multifocal UCs, previous or synchronous bladder UC, lymphovascular invasion (LVI), tumor necrosis, surgical margin, tumor grading, cell type, pathological T and N staging, and surgical approaches of radical nephroureterectomy (RNU). Significant predicting factors for DFS included: **(A)** age, **(B)** chronological history of bladder UC, **(C)** tumor grading, **(D)** T stage, **(E)** surgical margin, **(F)** preoperative hydronephrosis, **(G)** multifocality, **(H)** LVI, and **(I)** RNU techniques.

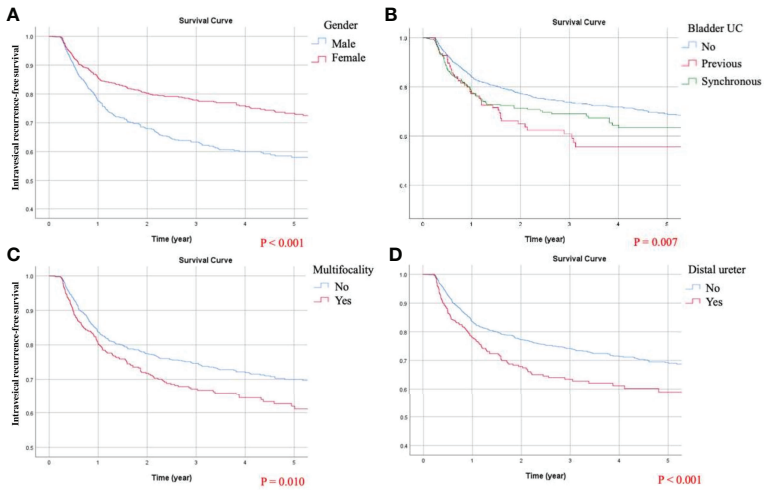

FIGURE 5 | Kaplan-Meier curves of intravesical recurrence-free survival (IVRFS) following adjustment for gender, preoperative hydronephrosis, middle ureteral, distal ureteral or bladder cuff urothelial carcinoma (UC), multifocal UCs, previous or synchronous bladder UC, tumor grading, cell type, and pathological T staging. Significant predicting factors for IVRFS included: **(A)** gender, **(B)** chronological history of bladder UC, **(C)** multifocality, and **(D)** tumor position at the distal ureter.

metachronous tumors maintained molecular subtype membership of the initial tumor. Most relevantly, the whole transcriptome RNA sequencing demonstrated luminal-like gene expression in same-patient samples of UTUC and synchronous bladder UC. When examining gene expression profiles of basal/luminal immunohistochemical markers, Sikic et al. (24) reported the luminal-like (CD20+/CK5−) subtype to be associated with worse cancer-specific survival. Given that most tumor cells of UTUC and paired bladder UC shared identical clonality, either UTUC metastasis to the bladder or bladder cancer metastasis to the upper tract, it is plausible to speculate that intraluminal cancer seeding may be a pivotal mechanism for drop or retrograde metastasis. Certainly, synchronous upper tract and bladder UCs express in a similar fashion and an aggressive clinical behavior of such disease entity may be expected.

Since preoperative hydronephrosis was regarded as a controversial risk factor, Tian et al. (25) conducted a thorough systematic review and meta-analysis to clarify its role in the prognosis of UTUC. They suggested that preoperative hydronephrosis was significantly associated with poor survival. Similarly, the latest two-center Japan study (26) depicted that preoperative hydronephrosis was an independent predictor of shorter recurrent-free survival. To the best of our knowledge, the present study is the largest one investigating the relationship between preoperative hydronephrosis and oncological outcomes. With adjustment of potential confounding factors, it was independently associated with OS, CSS, and DFS. One possible mechanism to shed light on our finding is that the presence of preoperative hydronephrosis may mostly be attributed to luminal obstruction caused by ureteral tumors. In the present study, more than 90% of patients presenting with preoperative hydronephrosis had ureteral tumors. Although the prognostic role of primary tumor location remains contentious, Yu et al. (9) pointed out that ureteral UC was a significantly adverse predicting factor for OS, CSS, DFS, and IVRFS, in comparison with renal pelvic UC. Moreover, a thin-walled structure of the ureter with an extensive anastomosing network of arterial supply and venous and lymphatic drainage may be one of the mechanisms which promote cancer spreading and poorer prognosis. Another explanation is that some renal pelvic tumors may block the ureteropelvic junction and increase intrarenal pressure that impede flow of lymphatics and vasculature, which might induce increased cancer seeding (27).

A systematic review of European Association of Urology (28) suggested that the oncological outcomes of open RNU may be better than those of laparoscopic RNU as bladder cuff was excised laparoscopically and in locally advanced high-risk UTUC. Despite better perioperative outcomes utilizing the laparoscopic approach, its oncological safety continues to be debatable. Even though some propensity-score matching analyses were presented, no consistent conclusion can be drawn (29, 30). In the most recent meta-analysis comparing laparoscopic versus open RNU, Piszczek et al. (3) found comparable oncological outcomes in UTUC patients, even in locally advanced disease. Intriguingly, our multivariate analysis showed better OS, CSS, and DFS for the laparoscopic surgical approach. It partly can be explained by the high incidence of UTUC in Taiwan, which contribute to high surgical volume in Taiwanese regional hospitals and medical centers. Notwithstanding there was no census regarding the number of RNU per year recognized as high surgical volume, regional variations were clearly described in the reviewed literature. In the States, from the National Cancer Database, Sui et al. (31) defined high-volume hospitals as more than 6 RNU performed each year. The results of their multivariate analyses accorded with our assumption, which indicated that performance of RNU at high-volume hospitals was associated with better long-term survival. In Japan, Sugihara et al. (32) depicted less than 20

TABLE 2 | Comparative univariate and multivariate Cox regression analyses of overall survival (OS) and cancer-specific survival (CSS) in patients with UTUC.

	OS				CSS			
	Univariate		Multivariate		Univariate		Multivariate	
	HR (95% CI)	*p*	HR (95% CI)	*p*	HR (95% CI)	*p*	HR (95% CI)	*p*
Gender								
Female	0.90 (0.77–1.06)	0.226			0.93 (0.74–1.16)	0.500		
Age ≥70	2.13 (1.80–2.51)	<0.001**	2.16 (1.81–2.56)	<0.001**	1.63 (1.30–2.05)	<0.001**	1.59 (1.25–2.01)	<0.001**
Carcinoma *in situ*	1.11 (0.90–1.38)	0.323			0.987 (0.73–1.33)	0.930		
Tumor size								
Reference: <1 cm								
≥1 and <2 cm	0.94 (0.65–1.35)	0.726	0.84 (0.57–1.22)	0.358	0.91 (0.50–1.65)	0.750	0.63 (0.34–1.18)	0.148
≥2 and <3 cm	1.12 (0.79–1.59)	0.542	0.90 (0.62–1.31)	0.586	1.41 (0.81–2.46)	0.230	0.87 (0.48–1.56)	0.632
≥3 cm	1.69 (1.23–2.33)	0.001**	1.05 (0.74–1.50)	0.776	2.67 (1.601–4.45)	<0.001**	1.11 (0.64–1.94)	0.707
Tumor location								
Renal pelvis	0.98 (0.82–1.16)	0.808			1.02 (0.80–1.30)	0.865		
Proximal ureter	1.18 (0.98–1.43)	0.077			1.24 (0.96–1.60)	0.099		
Middle ureter	1.16 (0.93–1.45)	0.198			1.37 (1.03–1.83)	0.032*	1.08 (0.79–1.49)	0.626
Distal ureter	1.27 (1.04–1.54)	0.019*	1.14 (0.93–1.40)	0.219	1.45 (1.12–1.88)	0.005**	1.22 (0.92–1.63)	0.168
Bladder cuff	2.15 (1.47–3.14)	<0.001**	0.87 (0.57–1.32)	0.513	2.65 (1.65–4.27)	<0.001**	0.91 (0.53–1.54)	0.718
Multifocality	1.44 (1.22–1.70)	<0.001**	1.12 (0.94–1.33)	0.223	1.71 (1.37–2.14)	<0.001**	1.15 (0.90–1.48)	0.265
Preoperative hydronephrosis	1.56 (1.31–1.87)	<0.001**	1.43 (1.19–1.72)	<0.001**	1.70 (1.32–2.17)	<0.001**	1.52 (1.16–1.98)	0.002**
Lymphovascular invasion	2.50 (2.10–2.97)	<0.001**	1.38 (1.14–1.68)	0.001**	3.49 (2.79, 4.38)	<0.001**	1.36 (1.06–1.75)	0.016*
Positive surgical margin	4.35 (3.26–5.79)	<0.001**	1.93 (1.38–2.70)	<0.001**	6.03 (4.33, 8.41)	<0.001**	2.12 (1.42–3.16)	<0.001**
Tumor necrosis	1.62 (1.33–1.98)	<0.001**	1.10 (0.89–1.36)	0.392	1.92 (1.48, 2.49)	<0.001**	1.08 (0.82–1.43)	0.592
Tumor grading								
Low grade	1		1		1		1	
High grade	1.64 (1.29–2.10)	<0.001**	1.07 (0.82–1.40)	0.599	3.68 (2.26–6.01)	<0.001**	1.68 (1.00–2.81)	0.049*
Cell type								
Reference: urothelial carcinoma (UC)								
UC with variants	1.97 (1.55–2.51)	<0.001**	1.32 (1.01–1.71)	0.041*	2.60 (1.94–3.49)	<0.001**	1.37 (1.00–1.90)	0.054
Bladder UC								
Previous	1.18 (0.85–1.63)	0.314	1.37 (0.98–1.91)	0.065	1.05 (0.66–1.68)	0.842	1.34 (0.83–2.17)	0.238
Synchronous	1.55 (1.26–1.91)	<0.001**	1.50 (1.20–1.87)	<0.001**	1.69 (1.28–2.21)	<0.001**	1.52 (1.12–2.04)	0.007**
Pathological T stage								
Reference: Ta/Tis								
T1	1.16 (0.86–1.58)	0.328	1.16 (0.84–1.61)	0.359	1.35 (0.74–2.49)	0.330	1.20 (0.64–2.28)	0.570
T2	1.66 (1.23–2.24)	0.001**	1.40 (1.00–1.95)	0.048*	3.07 (1.75–5.40)	<0.001**	2.07 (1.12–3.79)	0.019*
T3	2.89 (2.21, 3.78)	<0.001**	2.20 (1.59–3.05)	<0.001**	7.94 (4.75–13.27)	<0.001**	4.70 (2.62–8.41)	<0.001**
T4	8.59 (6.04–12.22)	<0.001**	4.84 (3.15–7.45)	<0.001**	23.64 (13.29–42.04)	<0.001**	8.77 (4.47–17.20)	<0.001**
Pathological N stage								
Reference: N0								
N1	3.67 (2.27–5.93)	<0.001**	2.54 (1.55–4.17)	<0.001**	5.50 (3.27–9.25)	<0.001**	3.54 (2.05–6.13)	<0.001**
N2	3.05 (2.03–4.61)	<0.001**	1.87 (1.22–2.87)	0.004**	3.99 (2.42–6.57)	<0.001**	1.91 (1.13–3.23)	0.016*
N*x*	1.03 (0.83–1.27)	0.804	1.10 (0.88–1.37)	0.391	0.99 (0.74–1.33)	0.942	1.16 (0.86–1.56)	0.344
RNU techniques								
Reference: open								
Hand-assisted laparoscopic	0.79 (0.65–0.96)	0.017*	0.81 (0.66–0.99)	0.036*	0.71 (0.54–0.92)	0.009**	0.82 (0.62–1.09)	0.168
Robot-assisted	0.44 (0.28–0.70)	0.001**	0.48 (0.30–0.77)	0.002**	0.50 (0.29–0.85)	0.010*	0.60 (0.35–1.04)	0.067
Laparoscopic	0.62 (0.48–0.79)	<0.001**	0.67 (0.52–0.87)	0.002**	0.46 (0.33–0.65)	<0.001**	0.55 (0.39–0.79)	0.001**
LESS	0.24 (0.03–1.74)	0.160	0.15 (0.02–1.12)	0.064	0.48 (0.07–3.43)	0.462	0.21 (0.03–1.58)	0.128

** means "p < 0.05"; ** dictates "p < 0.01.*

procedures per year as low-volume institutes. They found that minimally invasive RNU was more likely to be offered at high-volume hospitals. In our series, with a cutoff level of 20 minimally invasive RNU each year, higher hospital volume (≧20) was significantly associated with better OS. All these results corroborate our explanation that surgical volume may be a pivotal predicting factor in survival following RNU.

Of note, a high proportion (72.7%) of minimally invasive approaches was evident in our contemporary cohort. Whereas one theory attributed recurrence to carbon dioxide insufflation and pneumoperitoneum, neither port site metastasis nor peritoneal dissemination was registered in the present study. Another possible mechanism explaining better survival following laparoscopic RNU is delicate manipulation of the upper tract with meticulous prevention of urine spillage. Early ureteral clipping to reduce drop metastasis and prompt urine drainage to avoid cancer seeding are of paramount importance in our surgical training and routine practice of RNU. Additionally, when observing the trend of different RNU approaches within decades, the numbers of minimally invasive RNU have been increasing since 2000. Between 2006 and 2015, the most common approach was hand-assisted laparoscopic RNU in Taiwan.

TABLE 3 | Comparative univariate and multivariate analyses of disease-free survival (DFS) and intravesical recurrence-free survival (IVRFS) in patients with UTUC.

	DFS				IVRFS			
	Univariate		Multivariate		Univariate		Multivariate	
	HR (95% CI)	*p*	HR (95% CI)	*p*	HR (95% CI)	*p*	HR (95% CI)	*p*
Gender								
Female	0.91 (0.76–1.10)	0.314			0.55 (0.46–0.66)	<0.001**	0.60 (0.50–0.72)	<0.001**
Age ≥70	1.36 (1.13–1.64)	0.001**	1.27 (1.05–1.54)	0.014*	1.04 (0.87–1.24)	0.689		
CIS	1.06 (0.83–1.36)	0.645			1.22 (0.97–1.53)	0.092		
Tumor size								
Reference: <1 cm								
≥1 and <2 cm	0.94 (0.58–1.53)	0.816	0.74 (0.45–1.21)	0.225	0.95 (0.67–1.34)	0.751		
≥2 and <3 cm	1.40 (0.89–2.19)	0.145	0.99 (0.62–1.58)	0.956	0.88 (0.62–1.24)	0.452		
≥3 cm	2.63 (1.75–3.97)	<0.001**	1.35 (0.87–2.10)	0.184	0.99 (0.73–1.36)	0.972		
Tumor location								
Renal pelvis	1.12 (0.92–1.37)	0.274			0.90 (0.75–1.09)	0.269		
Proximal ureter	1.23 (1.00–1.52)	0.053			1.17 (0.95–1.44)	0.133		
Middle ureter	1.26 (0.98–1.62)	0.071			1.28 (1.00–1.63)	0.046*	1.11 (0.86–1.43)	0.416
Distal ureter	1.33 (1.07–1.65)	0.011*	1.23 (0.97–1.57)	0.084	1.70 (1.39–2.09)	<0.001**	1.49 (1.20– 1.85)	<0.001**
Bladder cuff	2.41 (1.58–3.67)	<0.001**	0.78 (0.49–1.25)	0.295	1.63 (1.02–2.61)	0.042*	1.07 (0.65– 1.76)	0.781
Multifocality	1.75 (1.45–2.11)	<0.001**	1.27 (1.03–1.55)	0.024*	1.57 (1.31–1.88)	<0.001**	1.30 (1.07–1.58)	0.010*
Preoperative hydronephrosis	1.37 (1.13–1.67)	0.002**	1.29 (1.04–1.59)	0.019*	1.29 (1.07–1.55)	0.008**	1.20 (0.99–1.46)	0.062
Lymphovascular invasion	3.26 (2.70–3.94)	<0.001**	1.37 (1.10–1.69)	0.004**	1.07 (0.86–1.34)	0.545		
Positive surgical margin	4.28 (3.14–5.83)	<0.001**	1.84 (1.29–2.64)	0.001**	0.88 (0.50–1.57)	0.668		
Tumor necrosis	1.85 (1.48–2.30)	<0.001**	1.04 (0.82–1.32)	0.754	0.96 (0.75–1.24)	0.767		
Tumor grading								
Low grade								
High grade	3.84 (2.56–5.74)	<0.001**	1.93 (1.26–2.94)	0.002**	0.80 (0.64–0.997)	0.047*	0.81 (0.63–1.03)	0.084
Cell type								
Reference: urothelial carcinoma (UC)								
UC with variants	2.14 (1.65–2.76)	<0.001**	1.24 (0.94–1.64)	0.128	0.65 (0.44–0.95)	0.027*	0.69 (0.47–1.02)	0.065
Bladder UC								
Previous	1.08 (0.74–1.58)	0.684	1.30 (0.88–1.93)	0.183	2.02 (1.50–2.71)	<0.001**	1.65 (1.22–2.23)	0.001**
Synchronous	1.76 (1.41–2.20)	<0.001**	1.62 (1.27–2.07)	<0.001**	1.68 (1.34–2.10)	<0.001**	1.33 (1.04–1.70)	0.022*
Pathological T stage								
Reference: Ta/Tis								
T1	1.37 (0.87–2.16)	0.176	1.16 (0.72–1.86)	0.551	1.06 (0.82–1.39)	0.647	1.17 (0.89–1.53)	0.269
T2	3.06 (2.01–4.67)	<0.001**	1.99 (1.27–3.14)	0.003**	1.13 (0.86–1.50)	0.378	1.18 (0.87–1.59)	0.291
T3	6.32 (4.29–9.30)	<0.001**	3.52 (2.27–5.46)	<0.001**	1.12 (0.87–1.45)	0.378	1.27 (0.96–1.69)	0.096
T4	16.77 (10.63– 26.45)	<0.001**	6.22 (3.65–10.60)	<0.001**	0.28 (0.10–0.77)	0.013*	0.34 (0.12–0.93)	0.035*
Pathological N stage								
Reference: N0								
N1	4.85 (3.03–7.76)	<0.001**	3.57 (2.19–5.83)	<0.001**	1.12 (0.55–2.30)	0.759		
N2	5.17 (3.50–7.65)	<0.001**	2.71 (1.79–4.09)	<0.001**	0.74 (0.36–1.52)	0.416		
N*x*	1.04 (0.82–1.32)	0.759	1.23 (0.96–1.58)	0.110	0.97 (0.78–1.21)	0.802		
RNU techniques								
Reference: open								
Hand-assisted laparoscopic	0.76 (0.61–0.96)	0.020*	0.98 (0.77–1.25)	0.875	1.15 (0.90–1.48)	0.258		
Robot-assisted	0.80 (0.55–1.17)	0.249	1.01 (0.68–1.50)	0.953	1.11 (0.75–1.64)	0.611		
Laparoscopic	0.59 (0.45–0.78)	<0.001**	0.73 (0.55–0.96)	0.027*	1.17 (0.89–1.54)	0.250		
LESS	0.34 (0.05–2.46)	0.286	0.20 (0.03–1.46)	0.111	0.83 (0.21–3.39)	0.800		

** means "p < 0.05"; ** dictates "p < 0.01.*

It can be alluded that the hand-assisted laparoscopic procedure might accelerate the transition of open to laparoscopic RNU. Not only could it preserve the conventional open method of bladder cuff excision, but also it assisted in the development of laparoscopic ureteric, perihilar, and perirenal dissection. After such transitional period, the proportion of laparoscopic RNU became the largest between 2016 and 2021. Simultaneously, the number of robotic RNU has been increasing since 2011. Undoubtfully, selection bias favoring the laparoscopic approach was commonly observed in a myriad of studies (28). In our series, with reference to T4 tumors, 36 (9.4%) patients were in the open RNU group and 15 (3.0%) in the laparoscopic group. Regarding T3 tumors, the numbers of patients were similar in both open (126, 33%) and laparoscopic (165, 33.4%) approaches. Undeniably, as UTUC invaded adjacent organs, surgeons still preferred open surgery for T4 tumors. Nevertheless, our registry data revealed that minimally invasive operations were yet undertaken in patients with locally advanced or even nodal diseases. With accumulated surgical experience of RNU, regardless of open or minimally invasive access, Taiwanese urologists became accustomed to various pathological circumstances and delivered better quality of surgical oncology

practice, thereby explaining better survival outcomes for the laparoscopic approach.

Several limitations of the present study merit discussion. Firstly, the data were retrospectively recruited and analyzed. On account of multi-institutional collaborations, these operations were performed by various surgeons at each institution and the surgical approach, especially pertaining to the management of the distal ureteral cuff, was decided at individual's discretion. Nevertheless, potential confounding factors were adjusted by multivariate Cox regression analyses to identify independently significant predictors. Furthermore, the multi-institutional study included a wider range of population groups, increasing the generalizability of the results. Secondly, lymph node yields and precise nodal status were lacking. Given there was no substantial evidence of therapeutic effect and standardized template of regional lymphadenectomy, it was merely provided in UTUC patients with suspiciously nodal disease. Thirdly, centralized pathological and radiological reviews were not conducted. To mitigate the influence of intra- and interobserver variability, we utilized a standardized format that was based on the principles of pathology management for urothelial cancer in the NCCN guidelines and the AJCC TNM staging system, to ensure accordance of interpretation. Additionally, neoadjuvant or adjuvant systemic therapy was not depicted in the present study. The patients receiving systemic therapy accounted for a fairly small portion of our database. Even though these patients were excluded from the present cohort, our outcomes remained unchanged.

Another limitation needs to be addressed: the pathological staging of synchronous bladder UC was not registered in our database. With regard to the bladder disease, complexity would be expected and more sophisticated variables were required, such as tumor location (trigone, ureteral orifices or other parts of the urinary bladder), intravesical chemotherapy or Bacillus Calmette-Guérin induction or maintenance, subsequent treatment modalities (systemic chemotherapy, chemoradiation or radical cystectomy), and recurrent disease status. Owing to limited human resources, after discussion within our consensus conferences, details of synchronous bladder UC were reduced to the presence or not of the disease. Nevertheless, in our experiences, most of them were nonmuscle invasive UC of the urinary bladder, because merely 33 patients in our cohort received systemic chemotherapy for bladder cancer. Only 2 of them underwent neoadjuvant chemotherapy and hence it might be speculated that the number of simultaneous radical cystectomy was extremely low in our database. It is plausible that most patients with synchronous bladder UC were treated by transurethral endoscopic resection.

Undoubtedly, the retrospective nature of the multi-institutional study introduced hospital variations and selection bias. However, a single-institution experience could hardly represent the clinical behavior of UTUC in Taiwan. Notwithstanding the rarity of this disease around the world, the long-term observations from our multicenter effort may contribute to improved prognostic prediction and surgical treatment advances. Following statistical control of confounding factors, several significantly beneficial and adverse predictors were identified. Further prospective well-designed researches are warranted to validate our findings and elucidate the underlying mechanism. In light of the real-world context, we believe this multi-institutional collaboration may be a considerable help in medical progress of treating UTUC.

CONCLUSION

This multi-institutional collaborative study in Taiwan recognized synchronous UC in the urinary bladder as a harbinger of poor prognosis for patients with UTUC. In addition, the presence of preoperative hydronephrosis was corroborated as an adverse prognostic factor for UTUC. Interestingly, our multivariate analysis suggested laparoscopic RNU might provide better oncological control. Further randomized controlled trials are warranted to validate our finding.

DATA AVAILABILITY STATEMENT

The raw data supporting the conclusions of this article will be made available by the authors, without undue reservation.

ETHICS STATEMENT

The studies involving human participants were reviewed and approved by Kaohsiung Veterans General Hospital (IRB No.: VGHKS14-CT3-06). Written informed consent for participation was not required for this study in accordance with the national legislation and the institutional requirements.

AUTHOR CONTRIBUTIONS

C-HCha, C-PH, W-JW, and C-CL contributed to conception and design of the study. C-HChe and C-YH organized the database. CC-L, C-ChiY, and C-YT performed the statistical analysis. I-HC wrote the first draft of the manuscript. W-CW, J-ST, W-RL, Y-HJ, Y-KL, Y-CJ, I-SC, TH, AC, Y-TC, J-SC, B-JC, Y-CT, WL, C-CW, J-TL, and C-CheY wrote sections of the manuscript. All authors contributed to manuscript revision and read and approved the submitted version.

ACKNOWLEDGMENTS

All members of the Taiwan Upper Tract Urothelial Carcinoma Collaboration group: AC, B-JC, C-HCha, C-YH, Cheng-Huang Shen, Cheng-Kuang Yang, Cheng-Ling Lee, Chen-Hsun Ho, Che-Wei Chang, C-CW, Chieh-Chun Liao, Chien-Hui Ou, Chih-Chen Hsu, C-ChiY, Chih-Hung Lin, Chih-Ming Lu, Chih-Yin Yeh, C-CL, C-PH, Chi-Rei Yang, C-WL, Chuan-Shu

Chen, C-HChe, C-YT, C-YL, Chun-Hou Liao, Chun-Kai Hsu, Fang-Yu Ku, Hann-Chorng Kuo, Han-Yu Weng, Hao-Han Chang, Hong-Chiang Chang, Hsiao-Jen Chung, Hsin-Chih Yeh, Hsu-Che Huang, I-SC, I-HC, Jen-Kai Fang, J-ST, J-TL, Jian-Hua Hong, J-SC, Jungle Chi-Hsiang Wu, Kai-Jie Yu, Keng-Kok Tan, Kuan-Hsun Huang, Kun-Lin Hsieh, Lian-Ching Yu, Lun-Hsiang Yuan, Hao-Lun Luo, Marcelo Chen, Min-Hsin Yang, Pai-Yu Cheng, Po-Hung Lin, Richard Chen-Yu Wu, See-Tong Pang, Shin-Hong Chen, Shin-Mei Wong, Shiu-Dong Chung, Shi-Wei Huang, Shuo-Meng Wang, Shu-Yu Wu, Steven Kuan-Hua Huang, Ta-Yao Tai, TH, Ting-En Tai, Victor Chia-Hsiang Lin, Wei-Chieh Chen, Wei-Ming Li, W-YL, Wen-Hsin Tseng, W-JW, W-RL, Y-CT, Yen-Chuan Ou, Y-CJ, Yeong-Shiau Pu, Yi-Chia Lin, Yi-Hsuan Wu, Yi-Huei Chang, Yi-Sheng Lin, Yi-Sheng Tai, Y-KL, Y-HJ, Yu-Che Hsieh, Yu-Chi Chen, Yu-Ching Wen, Y-TC, Zhe-Rui Yang.

REFERENCES

1. Soria F, Shariat SF, Lerner SP, Fritsche HM, Rink M, Kassouf W, et al. Epidemiology, Diagnosis, Preoperative Evaluation and Prognostic Assessment of Upper-Tract Urothelial Carcinoma (UTUC). *World J Urol* (2017) 35(3):379–87. doi: 10.1007/s00345-016-1928-x
2. Yeh HC, Margulis V, Singla N, Hernandez E, Panwar V, Woldu SL, et al. PTRF Independently Predicts Progression and Survival in Multiracial Upper Tract Urothelial Carcinoma Following Radical Nephroureterectomy. *Urol Oncol* (2020) 38(5):496–505. doi: 10.1016/j.urolonc.2019.11.010
3. Piszczek R, Nowak L, Krajewski W, Chorbinska J, Poletajew S, Moschini M, et al. Oncological Outcomes of Laparoscopic Versus Open Nephroureterectomy for the Treatment of Upper Tract Urothelial Carcinoma: An Updated Meta-Analysis. *World J Surg Oncol* (2021) 19 (1):129. doi: 10.1186/s12957-021-02236-z
4. Shao IH, Chang YH, Pang ST. Recent Advances in Upper Tract Urothelial Carcinomas: From Bench to Clinics. *Int J Urol* (2019) 26(2):148–59. doi: 10.1111/iju.13826
5. Wu YT, Luo HL, Wang HJ, Chen YT, Cheng YT, Chiang PH. Gender Effect on the Oncologic Outcomes of Upper Urinary Tract Urothelial Carcinoma in Taiwan. *Int Urol Nephrol* (2020) 52(6):1043–8. doi: 10.1007/s11255-020-02396-z
6. Jan HC, Hu CY, Yang WH, Ou CH. Combination of Platelet-Lymphocyte Ratio and Monocyte-Lymphocyte Ratio as a New Promising Prognostic Factor in Upper Tract Urothelial Carcinoma With Large Tumor Sizes > 3 Cm. *Clin Genitourin Cancer* (2020) 18(4):e484–500. doi: 10.1016/j.clgc.2019.12.008
7. Yeh HC, Chien TM, Wu WJ, Li CC, Li WM, Ke HL, et al. Is Preoperative Anemia a Risk Factor for Upper Tract Urothelial Carcinoma Following Radical Nephroureterectomy? *Urol Oncol* (2016) 34(8):337.e331–339. doi: 10.1016/j.urolonc.2016.03.018
8. Li CC, Chang TH, Wu WJ, Ke HL, Huang SP, Tsai PC, et al. Significant Predictive Factors for Prognosis of Primary Upper Urinary Tract Cancer After Radical Nephroureterectomy in Taiwanese Patients. *Eur Urol* (2008) 54 (5):1127–34. doi: 10.1016/j.eururo.2008.01.054
9. Yu LC, Chang CH, Huang CP, Huang CY, Hong JH, Tai TY, et al. Prognostic Significance of Primary Tumor Location in Upper Tract Urothelial Carcinoma Treated With Nephroureterectomy: A Retrospective, Multi-Center Cohort Study in Taiwan. *J Clin Med* (2020) 9(12):3866. doi: 10.3390/jcm9123866
10. Huang CC, Su YL, Luo HL, Chen YT, Sio TT, Hsu HC, et al. Gender Is a Significant Prognostic Factor for Upper Tract Urothelial Carcinoma: A Large Hospital-Based Cancer Registry Study in an Endemic Area. *Front Oncol* (2019) 9:157. doi: 10.3389/fonc.2019.00157
11. Lughezzani G, Sun M, Perrotte P, Shariat SF, Jeldres C, Budaus L, et al. Gender-Related Differences in Patients With Stage I to III Upper Tract Urothelial Carcinoma: Results From the Surveillance, Epidemiology, and End Results Database. *Urology* (2010) 75(2):321–7. doi: 10.1016/j.urology.2009.09.048
12. Shariat SF, Favaretto RL, Gupta A, Fritsche HM, Matsumoto K, Kassouf W, et al. Gender Differences in Radical Nephroureterectomy for Upper Tract Urothelial Carcinoma. *World J Urol* (2011) 29(4):481–6. doi: 10.1007/s00345-010-0594-7
13. Tanaka N, Kikuchi E, Kanao K, Matsumoto K, Shirotake S, Kobayashi H, et al. The Predictive Value of Positive Urine Cytology for Outcomes Following Radical Nephroureterectomy in Patients With Primary Upper Tract Urothelial Carcinoma: A Multi-Institutional Study. *Urol Oncol* (2014) 32 (1):48.e19–26. doi: 10.1016/j.urolonc.2013.07.003
14. Kang M, Kim HS, Jeong CW, Kwak C, Kim HH, Ku JH. Conditional Survival and Associated Prognostic Factors in Patients With Upper Tract Urothelial Carcinoma After Radical Nephroureterectomy: A Retrospective Study at a Single Institution. *Cancer Res Treat* (2016) 48(2):621–31. doi: 10.4143/crt.2015.220
15. Hurel S, Roupret M, Seisen T, Comperat E, Phe V, Droupy S, et al. Influence of Preoperative Factors on the Oncologic Outcome for Upper Urinary Tract Urothelial Carcinoma After Radical Nephroureterectomy. *World J Urol* (2015) 33(3):335–41. doi: 10.1007/s00345-014-1311-8
16. Chou YH, Chang WC, Wu WJ, Li CC, Yeh HC, Hou MF, et al. The Association Between Gender and Outcome of Patients With Upper Tract Urothelial Cancer. *Kaohsiung J Med Sci* (2013) 29(1):37–42. doi: 10.1016/j.kjms.2012.08.006
17. Pignot G, Colin P, Zerbib M, Audenet F, Soulie M, Hurel S, et al. Influence of Previous or Synchronous Bladder Cancer on Oncologic Outcomes After Radical Nephroureterectomy for Upper Urinary Tract Urothelial Carcinoma. *Urol Oncol* (2014) 32(1):23.e21–28. doi: 10.1016/j.urolonc.2012.08.010
18. Mullerad M, Russo P, Golijanin D, Chen HN, Tsai HH, Donat SM, et al. Bladder Cancer as a Prognostic Factor for Upper Tract Transitional Cell Carcinoma. *J Urol* (2004) 172(6 Pt 1):2177–81. doi: 10.1097/01.ju.0000144505.40915.98
19. Sfakianos JP, Cha EK, Iyer G, Scott SN, Zabor EC, Shah RH, et al. Genomic Characterization of Upper Tract Urothelial Carcinoma. *Eur Urol* (2015) 68 (6):970–7. doi: 10.1016/j.eururo.2015.07.039
20. Audenet F, Isharwal S, Cha EK, Donoghue MTA, Drill EN, Ostrovnaya I, et al. Clonal Relatedness and Mutational Differences Between Upper Tract and Bladder Urothelial Carcinoma. *Clin Cancer Res* (2019) 25(3):967–76. doi: 10.1158/1078-0432.CCR-18-2039
21. van Doeveren T, van de Werken HJG, van Riet J, Aben KKH, van Leeuwen PJ, Zwarthoff EC, et al. Synchronous and Metachronous Urothelial Carcinoma of the Upper Urinary Tract and the Bladder: Are They Clonally Related? A Systematic Review. *Urol Oncol* (2020) 38(6):590–8. doi: 10.1016/j.urolonc.2020.01.008
22. van Doeveren T, Nakauma-Gonzalez JA, Mason AS, van Leenders G, Zuiverloon TCM, Zwarthoff EC, et al. The Clonal Relation of Primary Upper Urinary Tract Urothelial Carcinoma and Paired Urothelial Carcinoma of the Bladder. *Int J Cancer* (2021) 148(4):981–7. doi: 10.1002/ijc.33327
23. Petros FG, Choi W, Qi Y, Moss T, Li R, Su X, et al. Expression Analysis of Same-Patient Metachronous and Synchronous Upper Tract and Bladder Urothelial Carcinoma. *J Urol* (2021) 206(3):548–57. doi: 10.1097/JU.0000000000001788
24. Sikic D, Keck B, Wach S, Taubert H, Wullich B, Goebell PJ, et al. Immunohistochemiocal Subtyping Using CK20 and CK5 can Identify Urothelial Carcinomas of the Upper Urinary Tract With a Poor Prognosis. *PLoS One* (2017) 12(6):e0179602. doi: 10.1371/journal.pone.0179602
25. Tian Y, Gong Y, Pang Y, Wang Z, Hong M. Clinical and Prognostic Value of Preoperative Hydronephrosis in Upper Tract Urothelial Carcinoma: A Systematic Review and Meta-Analysis. *PeerJ* (2016) 4:e2144. doi: 10.7717/peerj.2144
26. Fukui T, Kanno T, Kobori G, Moroi S, Yamada H. Preoperative Hydronephrosis as a Predictor of Postnephroureterectomy Survival in Patients With Upper Tract Urothelial Carcinoma: A Two-Center Study in Japan. *Int J Clin Oncol* (2020) 25(3):456–63. doi: 10.1007/s10147-019-01535-6
27. Chung PH, Krabbe LM, Darwish OM, Westerman ME, Bagrodia A, Gayed BA, et al. Degree of Hydronephrosis Predicts Adverse Pathological Features

and Worse Oncologic Outcomes in Patients With High-Grade Urothelial Carcinoma of the Upper Urinary Tract. *Urol Oncol* (2014) 32(7):981–8. doi: 10.1016/j.urolonc.2014.02.018

28. Peyronnet B, Seisen T, Dominguez-Escrig JL, Bruins HM, Yuan CY, Lam T, et al. Oncological Outcomes of Laparoscopic Nephroureterectomy Versus Open Radical Nephroureterectomy for Upper Tract Urothelial Carcinoma: An European Association of Urology Guidelines Systematic Review. *Eur Urol Focus* (2019) 5(2):205–23. doi: 10.1016/j.euf.2017.10.003
29. Kim SH, Song MK, Kim JK, Hong B, Kang SH, Ku JH, et al. Laparoscopy Versus Open Nephroureterectomy in Prognostic Outcome of Patients With Advanced Upper Tract Urothelial Cancer: A Retrospective, Multicenter, Propensity-Score Matching Analysis. *Cancer Res Treat* (2019) 51(3):963–72. doi: 10.4143/crt.2018.465
30. Moschini M, Zamboni S, Afferi L, Pradere B, Abufaraj M, Soria F, et al. Comparing Oncological Outcomes of Laparoscopic vs Open Radical Nephroureterectomy for the Treatment of Upper Tract Urothelial Carcinoma: A Propensity Score-Matched Analysis. *Arab J Urol* (2020) 19 (1):31–6. doi: 10.1080/2090598X.2020.1817720
31. Sui W, Wallis CJD, Luckenbaugh AN, Barocas DA, Chang SS, Penson DF, et al. The Impact of Hospital Volume on Short-Term and Long-Term Outcomes for Patients Undergoing Radical Nephroureterectomy for Upper Tract Urothelial Carcinoma. *Urology* (2021) 147:135–42. doi: 10.1016/j.urology.2020.07.062
32. Sugihara T, Yasunaga H, Horiguchi H, Fujimura T, Nishimatsu H, Tsuru N, et al. Regional, Institutional and Individual Factors Affecting Selection of Minimally Invasive Nephroureterectomy in Japan: A National Database Analysis. *Int J Urol* (2013) 20(7):695–700. doi: 10.1111/iju.12031

Conflict of Interest: The authors declare that the research was conducted in the absence of any commercial or financial relationships that could be construed as a potential conflict of interest.

Publisher's Note: All claims expressed in this article are solely those of the authors and do not necessarily represent those of their affiliated organizations, or those of the publisher, the editors and the reviewers. Any product that may be evaluated in this article, or claim that may be made by its manufacturer, is not guaranteed or endorsed by the publisher.

frontiers in Oncology

REVIEW
published: 09 March 2022
doi: 10.3389/fonc.2022.759153

Impact of Circadian Rhythms on the Development and Clinical Management of Genitourinary Cancers

Priya Kaur[1], *Nihal E. Mohamed*[1], *Maddison Archer*[1], *Mariana G. Figueiro*[2,3]* *and Natasha Kyprianou*[1,3,4]*

[1] Department of Urology, Icahn School of Medicine at Mount Sinai, New York, NY, United States, [2] Light and Health Research Center, Department of Population Health Science and Policy, Icahn School of Medicine at Mount Sinai, New York, NY, United States, [3] Tisch Cancer Institute, Mount Sinai Health, New York, NY, United States, [4] Department of Oncological Sciences, Icahn School of Medicine at Mount Sinai, New York, NY, United States

OPEN ACCESS

Edited by:
Alexandre Zlotta,
University of Toronto, Canada

Reviewed by:
Jianbo Li,
Case Western Reserve University, United States
Edyta Reszka,
Nofer Institute of Occupational Medicine, Poland
Armiya Sultan,
Jamia Millia Islamia, India

***Correspondence:**
Natasha Kyprianou
Natasha.Kyprianou@mountsinai.org
Mariana G. Figueiro
Mariana.Figueiro@mountsinai.org

Specialty section:
This article was submitted to Genitourinary Oncology, a section of the journal Frontiers in Oncology

Received: 16 August 2021
Accepted: 24 January 2022
Published: 09 March 2022

Citation:
Kaur P, Mohamed NE, Archer M, Figueiro MG and Kyprianou N (2022) Impact of Circadian Rhythms on the Development and Clinical Management of Genitourinary Cancers. Front. Oncol. 12:759153. doi: 10.3389/fonc.2022.759153

The circadian system is an innate clock mechanism that governs biological processes on a near 24-hour cycle. Circadian rhythm disruption (i.e., misalignment of circadian rhythms), which results from the lack of synchrony between the master circadian clock located in the suprachiasmatic nuclei (SCN) and the environment (i.e., exposure to day light) or the master clock and the peripheral clocks, has been associated with increased risk of and unfavorable cancer outcomes. Growing evidence supports the link between circadian disruption and increased prevalence and mortality of genitourinary cancers (GU) including prostate, bladder, and renal cancer. The circadian system also plays an essential role on the timely implementation of chronopharmacological treatments, such as melatonin and chronotherapy, to reduce tumor progression, improve therapeutic response and reduce negative therapy side effects. The potential benefits of the manipulating circadian rhythms in the clinical setting of GU cancer detection and treatment remain to be exploited. In this review, we discuss the current evidence on the influence of circadian rhythms on (disease) cancer development and hope to elucidate the unmet clinical need of defining the extensive involvement of the circadian system in predicting risk for GU cancer development and alleviating the burden of implementing anti-cancer therapies.

Keywords: prostate cancer, kidney cancer, bladder cancer, genitourinary cancers, melatonin, chronotherapy, circadian rhythm, CLOCK proteins

INTRODUCTION

In 2017, three investigators were jointly awarded the Nobel Prize in Physiology or Medicine for their work on molecular mechanisms controlling the circadian system. The circadian system is an innate clock mechanism that governs biological processes on a near 24-hour cycle (1, 2). The evolutionary-conserved process regulates the sleep-wake cycle as well as molecular and cellular operations. The master clock is located in the suprachiasmatic nuclei (SCN) of the hypothalamus (3). The clock

responds to environmental cues, such as light-dark patterns, to allow an individual to maintain synchrony with the external environment (4). In other words, through light-dark signals from the environment, the SCN is synchronized to the local position on Earth (3). In addition, clock genes in the SCN use neural signals to synchronize peripheral clocks located in the body to the external solar day (3). The circadian clock intrinsically drives transcriptional and translational feedback loops (TTFL) that regulate bodily activities (2, 5). The near 24-h cycles of gene expression are promoted by two activator clock proteins, Brain and Muscle ARNT-Like 1 (BMAL1) and Circadian Locomotor Output Cycles Kaput (CLOCK), and two repressor proteins, Period (PER) and Cryptochrome (CRY) (5). Disruption and mutation of the four integral clock proteins can misalign circadian rhythms (CRs, endogenous rhythms that are generated and regulated by then master circadian clock and repeat themselves roughly every 24 hour) such as core body temperature, hormone secretion, and sleep-wake activity (6).

Circadian rhythms disruption (CRDs; which result in misalignment of circadian rhythms, such as hormone production and the sleep-wake cycle have been shown to correlate with increased prevalence and mortality of GU cancers (7). Non-pharmacological interventions including chronotherapy and melatonin have been implicated in the treatment of CRDs. The four integral clock proteins, PER, CRY, BMAL1, and CLOCK, all have complex molecular roles that can improve our understanding of cancer risk and biologically/clinically relevant outcomes (1, 6). Yet, non-pharmacological treatments of chronotherapy and melatonin (e.g., light therapy, behavioral interventions) have diminished the toxicity of chemotherapeutic and immunotherapeutic drugs, while increasing their overall efficacy against aggressive disease (7). In this review we discuss the current evidence recognizing the significant role CRs play in GU cancer risk, development, and treatment outcomes.

EFFECT OF ENVIRONMENTAL CUES ON CRs

The daily light-dark pattern reaching the retina is the primary input to synchronize the biological clock to the 24-h solar day (6). If humans are not exposed to a sufficient amount of light from the right spectrum for an adequate amount of time, and with the right timing, the biological clock becomes desynchronized with the solar day, resulting in CRDs (8). CRDs are primarily caused by alterations in the circadian clock (i.e., the timekeeping system) or by a misalignment between the endogenous CR (e.g., sleep-wake cycle and hormone production) and the external factors that affect the timing, quality, or duration of sleep (e.g., sleep hygiene, environment, behavior, and social factors) (6, 8). CRDs can profoundly impact physical and daily functioning and have been linked to increased risk of insomnia, heart attacks, immune system imbalance, inflammation, diabetes, and obesity in healthy and chronic disease populations (9–11).

Recent studies confirmed associations between CRDs, increased cancer risk, and worse cancer outcomes (3, 12). Additionally, several environmental and behavioral conditions that may increase CRDs could also be independently associated with increased cancer risks (e.g., jet lag, shift work, and exposure to light at night) (12). Interestingly, a few studies showed that blind individuals with no light perception are less at risk of developing cancer (13, 14). Understanding the molecular mechanisms of the master clock in relation to its role in cell proliferation, DNA damage response, and apoptosis may provide insight into combating cancer incidence and prevalence (15).

CRDs AND INCREASED RISK OF GENITOURINARY CANCER

Evidence suggests that CRDs have a role in an increased risk of cancer progression, leading to unresponsive disease, especially in endocrine-based cancers (16). In the majority of patients treated for genitourinary cancer (GU), including prostate, kidney, and bladder cancer, there is an emergence of tumor recurrence due to therapeutic resistance (17). Prostate cancer (PCa) patients are especially at risk of developing castration-resistant prostate cancer (CRPC) after initially promising therapy with androgen deprivation (ADT) (18). The androgen receptor (AR) remains a prominent driver of therapeutic resistance in PCa (19). AR variants, amplification, and mutations all serve as mechanisms of CRPC progression (19). Despite the implementation of ADT, cells can develop sensitivity to low levels of androgens and lead to treatment-resistance and recurrent fatal disease (19).

In patients with renal cell carcinoma (RCC), there is a progression to chemotherapy-resistant disease that fails to respond to tyrosine kinase inhibitors, although there is burgeoning hope with new small molecule inhibitors (20). The mechanisms of resistance to therapy in RCC are still not fully defined. However, it is hypothesized that angiogenic escape is a possible mechanism that can occur from chronic vascular endothelial growth factor (VEGF) suppression (21). Angiogenic escape involves restoring blood follow in the tumor-associated vasculature, increasing the chances of therapeutic resistance (21).

Abbreviations: ADT, androgen deprivation therapy; Akt, protein kinase B; MAPKs –mitogen-activated protein kinase; AR, androgen receptor; BMAL1, Brain and Muscle ARNT-Like; CCGs, clock-controlled genes; CRDs, circadian rhythms disruption; CR, circadian rhythms; CLOCK, Circadian Locomotor Output Cycles Kaput; CRPC, castration-resistant prostate cancer; CRY, cryptochrome; EGF, epidermal growth factor; EMT, epithelial-to-mesenchymal transition; ET-1, endothelial-1; GSK-3β, glycogen synthase kinase-3β; GU, genitourinary; HIF-1α, hypoxia-inducible factor 1 alpha; IL-2, interleukin-2; MAPK, mitogen-activated protein kinase; MET, mesenchymal-to-epithelial transition; MIBC, muscle-invasive bladder cancer; MLT, melatonin; MMP, matrix metalloprotease; NMIBC, non-muscle-invasive bladder cancer; PBT, proton beam therapy; PCa, prostate cancer; PER, period; RCC, renal cell carcinoma; REV-ERBα (NR1D1), nuclear receptor subfamily 1 group D member 1; RORα, retinoid-related orphan receptor alpha; RORE, retinoid-related orphan receptors response elements; SCN, suprachiasmatic nuclei; TTFL, transcriptional and translational feedback loop; UBC, urinary bladder cancer; VEGF, vascular endothelial growth factor.

Metastatic urothelial cancer of the bladder has also been shown to be resistant to immunotherapy and chemotherapy (22). Cisplatin is a key component of chemotherapies treating bladder cancer and is the target of therapeutic resistance (23). There are many ways resistance can arise in bladder cancer, including reduced intracellular accumulation of cisplatin and increased sequestration (23). These factors all enable the cancer cells to elude the therapeutic potential of cisplatin.

CHRONO-PHARMACOLOGICAL TREATMENTS OF CRDs

Chronotherapy and melatonin are the two most promising non-pharmacological options to improve current anti-cancer drugs. Chronotherapy refers to the optimal dosing time of drugs where high efficacy and low toxicity are achieved (24). Time-dependent dosing relies on the oscillations of genes involved in drug absorption, distribution, metabolism, and excretion (24). Melatonin is a pineal gland hormone and is concurrently released during the hours of sleep (25, 26). However, it also possesses anti-tumorigenic abilities through an unknown mechanism of action (25, 26). Nocturnal melatonin secretion can persists in constant darkness, but exposure to light during the nighttime can suppress the release of the hormone into the bloodstream (25). The endogenous activity of the central clock results in melatonin production, so suppression of melatonin can lead to stimulation of cancer development (27). The possibility of chronotherapy and melatonin supplementation can be applied as a new platform to enhance the efficacy of chemotherapy drugs through precise time-dependent administration (28). A review by Bermu´ dez-Guzma´ and colleagues showed that melatonin, used as adjunct treatment concurrent with chemotherapy or radiotherapy, significantly improved tumor remission and 1-year survival (28). Co-administering melatonin and cancer treatments could also result in the patient having fewer adverse effects and improved outcomes (29).

CRITICAL EFFECTORS OF THE CIRCADIAN CLOCK

The regulation of the CRs occurs at the transcriptional level. There are four key circadian clock proteins: BMAL1, PER (1–3), CLOCK, and CRY (1-2) (**Figure 1**) (30). Brain and Muscle Arnt-like protein, also known as BMAL1, is an integral transcription factor (31). It is a known activator of the master clock and is present in the transcriptional feedback loop (32). REV-ERBα (NR1D1) and RORα are two major nuclear receptors involved in the regulatory loop for BMAL1 (**Figure 1**) (33, 34). The heterodimer of BMAL1 and CLOCK binds to the E-box motif and activates the transcription of REV-ERBα, RORα, two repressor proteins, PER and CRY, as well as other clock-controlled genes (CCGs) (**Figure 1**) (32). CRY is known to be the primary driver of the circadian oscillator through repressing

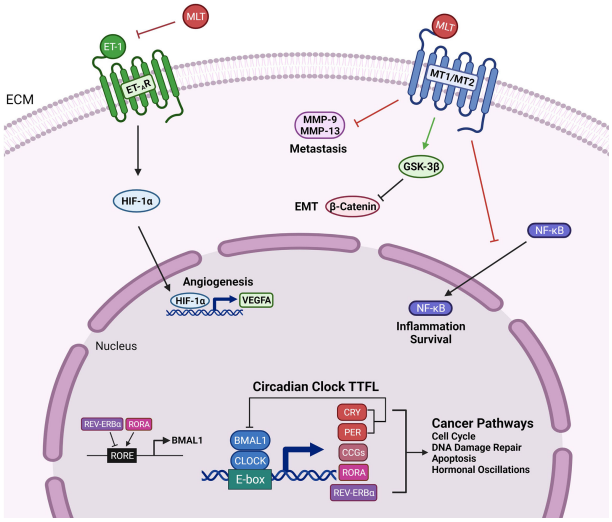

FIGURE 1 | Genetic Outcomes of the Circadian Clock Proteins and Clinical Management Techniques. Circadian clock transcription-translation feedback loop (TTFL) is controlled by two activator proteins Brain and Muscle ARNT-Like 1 (BMAL1) and Circadian Locomotor Output Cycles Kaput (CLOCK), and two repressor proteins, Period (PER) and Cryptochrome (CRY). BMAL1 and CLOCK heterodimerize and bind to the E-box motif to activate the transcription of CRY (1-2), PER (1-3), clock-controlled genes (CCGs), RORα, REV-ERBα. CRY and PER establish the primary negative feedback loop by inhibiting the BMAL1 and CLOCK heterodimer. In the secondary feedback loop, RORα activates, and REV-ERBα inhibits the transcription of BMAL1. Circadian clock proteins mediate several cancer pathways such as cell cycle regulation, DNA damage repair, apoptosis, and hormonal changes. Melatonin binds to the MT1 and MT2 receptors and targets inflammation and survival pathways by preventing the translocation of NF-κB to the nucleus. Melatonin interferes with EMT and metastasis by downregulating β-catenin through activation of GSK-3β and inhibiting the expression of matrix metalloproteinases-9 and -13. The inhibition of endothelin-1 (ET-1) by melatonin leads to reduced activity of angiogenic factors HIF-1α and VEGFA.

the CLOCK : BMAL1 heterodimer (**Figure 1**) (35). PER2 is the sole protein that interacts with CLOCK, whereas both PER and CRY proteins interact with BMAL1 (36). Future research on the binding and repression of the CLOCK : BMAL1 transcriptional activity will clarify the other regulatory roles of the proteins in the CRs (36).

Disruption of gene expression may lead to diseases since the clock proteins are involved in several transcriptional pathways. For instance, it was found that if the *PER2* gene is downregulated, there is an increased risk for breast cancer (37). In contrast, if the *PER2* gene is overexpressed, it may confer tumor-suppressive properties (38). In colorectal cancer, increased levels of BMAL1 have been related to decreased survival, and similarly, reduced levels of PER2 and PER3 have led to more inadequate tumor differentiation (39). Other studies have found that the clock gene expressions were reduced to 60% in melanoma and naevus tumors, highlighting their role in transcription regulation and tumorigenesis (40). With increasing evidence, research suggests that the clock proteins are also involved in genotoxic stress and aging, which are two factors that can also lead to carcinogenesis (41). Thus, disturbances of the circadian clock gene expression

leading to interesting downstream effects can play a role in the carcinogenesis of various cancers.

Other factors, such as exposure to light at the wrong circadian time (e.g., exposure to ambient electric light during night shifts) or not enough light exposure at the right circadian time (e.g., not enough exposure to daylight), can alter the timing of the biological clock in humans (42). In particular, melatonin, a pineal gland hormone, can be affected by the amount and distribution of light signals picked up by the retina (43). With increased exposure to light at night, blood melatonin levels may be suppressed, leading to CRDs (43). Melatonin influences CRY1 expression, and melatonin suppression resulting from increased exposure to light at night, can compromise CRY1's function in regulating CRs (44). Thus, electric light at night in the environment can disrupt pineal function and thus be linked to a higher incidence of hormone-related cancers such as PCa and breast cancer (43). The indirect light-induced stimulation of tumor development may be associated with the inhibitory clock proteins PER1 and PER2 (44). Specifically, disrupting PER2, CRY2, or BMAL1 in various tissues can increase the likelihood of cancer development (44). A light-induced signaling pathway is also involved in regulating the cell division cycle (44, 45). AP-1 is a transcription factor involved in maintaining biological processes, such as cell proliferation and apoptosis (45), and was found to have light-dependent activation in the SCN, adding to evidence that light plays a vital role in cancer development and circadian rhythm regulation (45).

CRDs AND GU CANCERS

Prostate Cancer

Prostate cancer (PCa) is the second most frequent cancer diagnosis made in men with 1,276,106 new cases of reported worldwide in 2018 (46). In the United States, an estimated 248,530 new cases and 34,130 deaths are estimated in 2021 (47). Although differences in PCa incidence rates worldwide reflect differences in the use of diagnostic testing and PCa screening guidelines, both incidence and mortality rates are strongly related to age with the highest incidence being seen in elderly men (> 65 years of age) (46). In the United States, PCa screening is highly recommended at age 40 for men with familial history and men of African ancestry (48).

For early stage PCa patients survival is 99% for the first five years after localized treatment (49). However, eventually, many PCa patients develop therapeutic resistance to ADT, otherwise known as castration-resistant prostate cancer (CRPC) (50). This leads to an incurable disease in which 19.5% of patients died from metastatic-CRPC in 2020 (51). There has been a recent shift to using taxane-based chemotherapy to treat CRPC patients (52). Taxanes are an excellent option for resistant PCa as they stimulate apoptosis by disrupting the G2/M-phase of the cell cycle (53). Despite the benefits of taxanes, 1st and 2nd line taxane chemotherapy (Docetaxel and Cabazitaxel, respectively) in patients with advanced metastatic disease, ultimately, emergence of therapeutically resistant tumors leads to lethality.

Significantly enough, disruption of CRDs have been implicated in PCa risk and progression (54). Compelling evidence suggests a significant correlation between light exposure at night and increased PCa incidence (54). Additional studies from independent investigators have exploited melatonin suppression and shift work and their positive correlations with PCa risk (55, 56). Increased risk of PCa among night male shift workers is attributed to changes in amplitude of melatonin and associated changes in sex hormone secretion that contribute to Epithelial-to-mesenchymal transition (EMT) typically involved in PCa development (55, 56). Two pathways may result in reduced amplitude of melatonin among male night shift workers; a) the acute melatonin suppression through exposure to electric light after dusk (57); and b) the decreased melatonin levels through CRDs (58), that consequentially results in desynchronization of the peripheral clocks, promoting cell growth and tumor development (58). Melatonin may suppress PCa growth by down regulating transcription, secretion, or activity of growth factors; it may stimulate the immune system through increased production of interleukin-2 and interleukin-4 by T-helper cells; lastly, it may protect DNA against oxidative damage by scavenging free radicals (58). It is thus apparent that disruption of the CRs can lead to increased PCa risk (**Table 1**). Moreover, growing evidence supports an intricate relationship between PCa, and the effector proteins functionally associated with the circadian clock. These proteins regulate cancer mechanisms such as apoptosis or proliferative cancers (58, 59). A study found that PER2 and CLOCK protein levels were downregulated, and in contrast, BMAL1 was upregulated in PCa tissue (60). Another circadian repressor protein, CRY1, is a known regulator of cell proliferation and DNA repair (61).

TABLE 1 | Genetic Involvement of the circadian system in GU cancers and clinical management options.

GU Cancers (Tumor Type)	Mechanisms of Disruption of Circadian Rhythms	Effects of Melatonin	Therapeutic Targets with Chronotherapy
Prostate Cancer	Downregulated PER2 and CLOCK (60)↓ Upregulated BMAL1 and CRY1 (60, 61),↑	Downregulates MMP-13 (109)	PBT (123) Docetaxel (115)
Kidney Cancer	Downregulated CLOCK, CRY1, CRY2, and BMAL1 (80)↓	Suppresses the Akt/MAPKs pathway (113) Downregulates MMP-9 (113)	Interferon-alpha (122) IL-2 (122)
Bladder Cancer	Downregulated BMAL1↓ Upregulated CLOCK and CRY1 (89)↑	Prevents the nuclear translocation of NF-κB (110) Induces apoptosis (110, 112)	Doxorubicin-cisplatin (122)

The role of the four clock proteins, BMAL1, CLOCK, PER, and CRY, were evaluated in relation to three GU cancers. The genetic effects of melatonin supplementation were explored as well as the primary therapeutic targets of chronotherapy to manage GU cancers.

CRY1 was upregulated in PCa and thus indicated a poor outcome for metastatic-CRPC (61). Like many clock proteins, CRY1 has transcriptional control aside from its role in regulating the circadian clock (61). Clock proteins are crucial for the proper functioning of the cell, especially in the case of cell growth/death, homeostasis, metabolism, and hormone release (60). When protein expression is disturbed, the CRs are also disrupted, which can amount to several disease states such as PCa (61). The mechanistic underpinnings of these proteins are still being studied and could provide profound insight into designing molecular therapies to treat cancers (62, 63).

The tumor microenvironment is a critical biological dynamic entity that merits exploitation in functional exchange with the external environment (light, temperature, specifically impacted by the circadian clock). EMT in solid tumors (including PCa) has been defined to play a significant role in cancer and a major contributor to metastasis (64). EMT is characterized by the loss of cell-cell adhesion, increased cell motility, and reduced E-cadherin expression, a structural adhesion molecule (65). E-cadherin, a calcium-dependent protein involved in cell-cell adhesion, is crucial for preventing PCa cells from migrating to bones to facilitate metastatic disease (66). Some several molecular mechanisms and pathways influence EMT, such as epidermal growth factor (EGF) and mitogen-activated protein kinase (MAPK) (67). Changes in signaling pathways ultimately alter the expression of transcription factors such as Snail and Zeb-1 (67). As a result of activation of these transcriptional repressors, E-cadherin expression levels are repressed, ultimately leading to enhanced mesenchymal and migratory markers in mesenchymal cells (68). Thus, EMT is functionally linked to promoting PCa metastatic progression, leading to stemness, therapeutic resistance, and ultimately lethal disease (68). Work from our group demonstrated that interconversion of EMT to mesenchymal-to-epithelial transition (MET) is observed in advanced PCa pre-clinical models in response to treatment with the second line taxane chemotherapy, cabazitaxel (52). This dynamically transient EMT-MET cycling allows cabazitaxel to prime the cells to retain a non-migratory phenotype, reducing the chances of metastasis (52). There is an ongoing effort to identify a temporal therapeutic window that can enable cells to overcome resistance by anti-androgen action (52).

Similar to phenotypic EMT navigating PCa, chronic CRs has been demonstrated to lead to the metastatic spread of breast cancer (65). CRs have a role in hormone expression and promote an immunosuppressive phenotype in endocrine-related cancers (69). Circadian-regulated transcription factors, such as PER2 and BMAL1, can regulate EMT through influencing EMT signaling effectors responsible for stemness and cell migration (69). Downregulated PER2 was associated with a higher likelihood of EMT in breast tissue, while downregulated BMAL1 decreased the invasion of mesenchymal cells in colorectal cancer (69). Melatonin was also found to regulate EMT and molecular pathways underlying the phenotypic conversion and cell invasiveness (65). MLT can activate GSK3β, an enzyme involved in cell proliferation, which reduces β-catenin levels, and subsequently leads to restoration of E-cadherin in human breast cancer cells (**Figure 1**) (65).

Kidney Cancer

Kidney cancer accounted for nearly 431,300 cases worldwide in 2020 and has been increasing in recent years (70, 71). The median age of diagnosis is 65 years (72) (**Table 1**). Many tumors comprise kidney cancer, with 90% being RCC cases (73). Within the various molecular subtypes of RCC, clear cell RCC leads to the most deaths (73). The mortality rate of 30-40% for RCC is significantly greater than prostate and bladder cancers (74). Kidney cancer tends to be resistant to chemotherapy and radiation therapy, making immunotherapy the best option (75). With increased attention on potential mechanisms of progression such as angiogenesis and altered hypoxia signals, CRs research could explore ways to reduce the disease burden (76). Circadian pathways help maintain physiological fluctuations, such as water transport and essential renal function (77). Almost 43% of all protein-coding genes throughout the body showed CRs in transcription, many of them being in the kidney (77, 78). These gene expressions peak right before dawn and dusk (78). In a study linking the dysregulation of the circadian clock and RCC, clock genes were transcriptionally different in diseased versus healthy tissue (79). For example, CLOCK, CRY1, and CRY2 levels were downregulated in kidney cancer tissue (80). Patients that retained high levels of CLOCK had a better prognosis than those without (80). Like PCa, the clock proteins significantly predict the risk and progression of kidney cancer through intricate molecular mechanisms.

The clock proteins are crucial for regulating CRs and immune system function (81). The immune checkpoint pathway is suppressed when the clock protein BMAL1 is downregulated, causing sepsis (81). Sepsis and cancer share many immunological properties, so immunomodulatory agents could successfully treat both diseases (81). Increased expression of PD-1 and its ligand, PD-L1, help stimulate tumor-directed cytotoxic T cell function in both sepsis and cancer (81). The loss of the clock gene, BMAL1, showed increased PD-L1 expression in macrophages, which is associated with poorer sepsis survival (81).

Bladder Cancer

Bladder cancer is ranked in the top ten most common cancers worldwide (82). Around 2.1% of cancer deaths are caused by urinary bladder cancer (UBC) each year, resulting in a high mortality rate (47). In Europe, the five-year survival rate for UBC was 68% (83). Unlike PCa, UBC has poorer outcomes within five years of being diagnosed. However, it has a higher survival rate than kidney cancer in Europe, which is 60% (83). UBC follows a similar prevalence trend of other GU cancer. It is less common in sub-Saharan Africa, India, and Mongolia and more common in Western Europe and Australia (84). The geographic distribution may be partly explained by exposure to tobacco, environmental pollutants, and occupational carcinogens, which are invariably linked to UBC incidence (85).

UBC can develop into either muscle-invasive bladder cancer (MIBC) or non-muscle-invasive bladder cancer (NMIBC) (86). For NMIBC, the course-of-treatment usually involves

maintenance immunotherapy, whereas MIBC often requires chemotherapy (86). Combination chemotherapy provides good outcomes initially in impairing tumor growth, but it ultimately fails as cancer cells develop therapeutic resistance (87). Cisplatin is a first-line chemotherapy treatment that directly interacts with the circadian clock proteins and enhances the body's natural response to cancerous cells (88). It upregulates CLOCK and BMAL1, resulting in increased proliferation and increased apoptosis, respectively (88). In bladder cancer tissue from human specimens, BMAL1 was downregulated, and CLOCK was upregulated, so cisplatin acts differently on both proteins through unclear mechanisms (89). Cisplatin has multiple opposing effects on tumor growth, resulting in stimulating pro-cancer effects (88). Thus our current understanding begs the question of interrogating the impact of disruption of circadian clock proteins on the molecular mechanisms underlying cell proliferation and apoptosis. In the context of contributing to therapeutic resistance, another clock protein, CRY1, was found to inhibit paclitaxel-induced senescence in bladder cancer cells (90). Typically, in urothelial tumors, CRY1 has been detected to be downregulated (89). While senescence causes cells to halt dividing, it also provides a way for cancer cells to become resistant to treatment (91). When the second-line therapy of paclitaxel is used, it prevents cell arrest and promotes the degradation of p53 (90). Healthy adults continually degrade p53, which is a tumor suppressor to stimulate p53 turnover (92). CRY1 is crucial in preventing the senescence induced by paclitaxel and delaying drug resistance (90).

THE CIRCADIAN CLOCK AS THE NEW FRONTIER TO OVERCOME THERAPEUTIC RESISTANCE

Melatonin Treatment

Melatonin (MLT) is a pineal gland hormone that can phase shift the SCN and provide timing information to the body (93). The pineal gland is crucial in regulating tumor growth and could become a target for therapeutics development (94). Melatonin levels naturally increase during dusk and taper off at dawn (95). Interestingly, subjects in perpetual darkness, such as visually impaired individuals, still display a 24.2-h cycle of melatonin and can have typical endogenous CRs (96).

The molecular mechanisms *via* which melatonin influences tumor cell proliferation and cancer metabolism are not clearly defined. Growing evidence suggests that melatonin may decrease the activity of endothelin-1 (ET-1), leading to downstream effects of downregulating hypoxia-inducible factor 1 alpha (HIF-1α) and VEGF, which both contribute to promoting angiogenesis (**Figure 1**) (97, 98). Preventing angiogenesis remains a critical goal to impair metastasis of kidney cancer (21). Significantly, it can also regulate breast cancer growth through two membrane melatonin receptors, MT1 and MT2, which are expressed in breast tissue, and impact survival signaling pathways (97). An overall decrease in melatonin levels has been associated with a higher risk of cancer, neurological disorders, and sleeping disorders (99). Thus, melatonin proves to be an effective and attractive therapy to improve the efficacy to toxicity ratio of anti-cancer drugs (100).

One of the most well-known hypotheses is that MLT is an epigenetic regulator that can prevent tumor growth by inhibiting telomerase activity and regulating linoleic acid uptake and metabolism, both crucial to proliferation (101). Circadian-dependent administration of MLT may confer tumor-suppressive properties (102). Melatonin has also been a potent, safe, and low-cost therapeutic in cancer research (103). A randomized controlled trial of solid tumors found that MLT reduces death by nearly a year (103). MLT also stimulates a robust chemotherapy response in palliative cancer care compared to receiving only supportive care (104). The patient's quality of life is improved by reducing the side effects such as asthenia and thrombocytopenia (104). Thus, melatonin may enhance the therapeutic efficacy of patients with resistant GU cancers.

Despite the uncertainty that surrounds melatonin's impact on cancer as a clinical disease, its protective benefits in human PCa are becoming increasingly evident. Men with high levels of urinary melatonin were less likely to develop advanced PCa (105). Advanced PCa is characterized by metastasis which involves tumor migration and invasion and ultimately lethal disease (106). Approximately 80% of patients with advanced PCa develop bone metastasis, a process that is linked with the expression of matrix metalloproteases (MMP) (107). Matrix metalloproteases are proteolytic enzymes responsible for breaking down connective tissue and allowing tumors to invade other tissues (108). MLT downregulates MMP-13 expression, which may suppress the metastasis of PCa (**Figure 1**) (109). MMP-13 is another excellent target for future therapeutic studies of PCa. It is of major significance to understand the molecular mechanisms driving the anti-tumor and anti-invasion properties of this agent.

MLT inhibits bladder and kidney cancer growth and metastasis (109). MLT prevents the nuclear translocation of NF-κB and decreases the expression of pro-inflammatory intermediates (**Figure 1**) (110). Recent studies have shown that MLT treatment resulted in increased apoptosis through NF-κB regulation in human gastric (111) and bladder cancer cells (110, 112). Moreover, MLT suppresses the Akt/MAPKs pathway and downregulates MMP-9, crucial for RCC progression (113). Through binding to the active site of MMP-9, MLT can arrest associated inflammatory signals that contribute to tumor growth (**Figure 1**) (114). Given the rapidly growing evidence at the mechanistic level, one could propose that MLT confers considerable transcriptional and post-translational control that are still not well understood.

Chronotherapy

Chronotherapy involves orchestrating the timing of treatment administration to match the body's endogenous CRs (115). This method has shown unequivocal success in tumor outcome and improved management of the disease (116). In addition, circadian dosing is crucial in limiting the toxicity of anti-cancer drugs and maximizing their efficacy (115). A

characteristic example of an optimized (time-dependent response) is the first-line taxane chemotherapy, docetaxel, which is shown to have the best clinical outcome if administered in PCa patients between 6 and 9 am (115).

One must also consider that many cancer patients in late stages report having increased CRD with irregular sleep schedules (117). In breast cancer specifically almost 72% of advanced cancer patients display moderate-to-severe sleep disturbances (118). Chronotherapy could reduce the side effects of chemotherapy while also promoting a strong therapeutic response. In a retrospective study, patients undergoing high-dose radiotherapy for PCa in the evening had more GI complications than those in the morning (119). The toxicity of the drug is also decreased when administering the treatment in alignment with circadian oscillations. Lower toxicity levels could significantly relieve patients who have PCa, especially since GU cancer patients are older on average (119). There should also be a shift to similarly evaluating circadian-based dosing in therapy-resistant cancer patients. A circadian-modified infusion schedule can also allow clinicians to administer higher drug doses to induce a powerful response without the lethal toxicity. For example, patients with RCC could receive higher doses of floxuridine on a circadian-modified infusion schedule than on a continuous infusion schedule (120). This provides unique opportunities for a rigorous and impactful treatment of GU cancers while in their non-resistant phases for a better outcome. Chronotherapeutic schedules can also increase long-term survival and overall quality of life while on chemotherapies, such as oxaliplatin for metastatic colorectal cancer (121). In patients with metastatic UBC, treatment with doxorubicin-cisplatin resulted in a 57% objective response rate when coupled with chronotherapy (122). Other therapeutic options such as interferon-alpha and IL-2 (Interleukin-2) are promising agents to slow metastatic RCC, but they come at the risk of significant toxicity (122). By optimizing drug administration when toxicity would be minimized, clinicians can better use readily available compounds to treat GU cancers (122). Chronotherapy is not limited to only chemotherapy and immunotherapy in enhancing their treatment response outcomes. It can also be applied to radiation techniques, such as proton beam therapy (PBT), which directs smaller radiation doses at localized PCa (123). PBT was observed to have less severe lower urinary tract symptoms when given in the morning than in the afternoon (123).

Personalized medicine approaches can pave treatment strategies towards increasing patient survival and improving the quality of life for cancer patients. One may also consider that specializing current treatment methods according to a person's chronotype, defined as a person's preference for timing of sleep and activity, may lead to improved clinical outcomes. While chronotherapy has provided encouraging results in rendering cancer therapies more tolerable, more clinical studies are warranted. A significant issue is that much of the current research on chronotherapy in anti-cancer drugs do not have a strict time interval. Without a specific period, it is difficult for clinicians to administer treatment at the optimal time for maximum efficacy. Thus, there is an unmet need to functionally define the role of the CRs in cancer research.

Environmental and Behavioral Interactions

Prior work in chronic disease patient populations suggests significant effects of environmental and behavioral interventions on reducing CRDs, including light therapies, physical activities, and diet modification which could, in turn, improve cancer patient outcomes (124, 125). Light is the strongest synchronizer of CRs, and exposure to ambient light at the right time could reduce CRDs and, thus, improve cancer patient physical and functional outcomes (126–130). Endocrine disruption due to exposure light during the circadian night has been implicated as carcinogenic, both in animal studies and in epidemiological studies in humans (131).

Evidence also suggests that physical activity could affect CRs (132–134). It has been shown that 1–3 hours of intense exercise can induce significant circadian phase shifts depending on the duration, intensity, and frequency of physical activities (132–134). Studies showed that early morning physical activities are associated with phase delays in the circadian clock (134, 135). However, early morning exercise offered protective effects for breast and PCa patients with an evening chronotype (136). Other studies showed that physical activities later at night induced phase delays in melatonin secretion (137). Individuals placed on prolonged periods of bed rest without exercise also show a circadian phase delay (125). Circadian misalignment is also observed when individuals participate in restrictive movement of one limb but not the other (125). This selective exercise leads to changes in the regulation of the clock genes, which are implicated in cancer pathways (**Figure 1**) (125). Additional assessment of the optimal time to exercise that can mitigate increased cancer risk and CRDs (124). One must note here that, while some studies show that exercise can alter circadian phase, its impact on the circadian clock is significantly less than the impact of light-dark patterns reaching the retina.

Lifestyle patterns in feeding/meal consumption (e.g., late-night meals) and diet programs (e.g., high fat diet) have been found to also influence circadian patterns in humans, although behavioral and sociocultural factors often control this (124). These circadian eating patterns are mirrored by both the gastrointestinal system, leading to rhythms in digestive secretions, gut motility, absorption of digested food, and blood nutrient concentrations (124). Feedback loops exist between the hormones controlling the circadian clock and those directing appetite and satiety, such as leptin, orexin, and ghrelin (124). Considering the roles of clock-related hormones, a food-entrainable circadian clock in humans may be present (124, 138, 139). Food-based entrainment enhances the synchronization of the peripheral and master clock, which can positively impact cancer regulation (124). Thus, in addition to understanding the impact of light exposure patterns, a further investigation into the interactive impact of exercise, diet, and nutrition on the risk, development, and clinical outcomes of GU cancers is likely to be impactful.

CONCLUSION

A systematic review and meta-analysis of the previous studies in breast cancer female patients revealed a positive relationship between indicators of CRDs (e.g., nightshift work) and breast cancer risk (58). Changes in hormone secretion, caused by CRDs, was proposed as a contributing factor to the observed increase in breast cancer risk (58). Although breast cancer occurs predominantly in women, the biology and epidemiology of breast cancer share some similar features of GU cancer specially PCa (57, 58). For example, tumor progression in both breast cancer and PCa is strongly affected by sex hormones, which are, to a larger extent, influenced by CRDs and reduced amplitude of nighttime hormone melatonin.

The role of the CRs extends past currently known molecular regulations in transcription and translation. Given the extensive part of the four clock proteins (CRY, PER, BMAL1, and CLOCK), the circadian clock may regulate many cancer mechanisms such as apoptosis and therapeutic resistance (140, 141). Advanced GU cancers have poor outcomes and high mortality rates, making the development of therapeutic targets a time-sensitive task (142). A pioneering research study of circulating tumor cells, which are biomarkers of metastasis, has shown to follow specific circadian rhythmicity in animal models of PCa (143). By targeting PCa treatment to coincide when circulating tumor cells are at their highest concentration in the bloodstream, clinicians may be able to produce robust patient responses to treatment (143). Chronotherapy and MLT supplementation have also both proven to increase the efficacy of various chemotherapies and immunotherapies (121, 144). These are underused and beneficial tools that can diminish disease burden and progression.

Moving forward, the focus is the pursuit of CRs as defense mechanisms the body can engage to optimize therapeutic responses in patients diagnosed and treated for GU cancers. Circadian-based treatments can modulate the pharmacological ability of anti-cancer drugs towards improving therapeutic outcomes and be potentially incorporated into clinical trials for treatment optimization and improved patient survival. One may argue that the simple method of syncing drug administration with the body's endogenous circadian clock can maximize the efficacy of clinically approved treatment strategies in managing advanced GU cancers. Moreover, the circadian clock provides an informative new platform about the optimal timing and dosing of the drug, compared to traditional pharmacokinetics and pharmacodynamics. Given the impact of the circadian clock on cancer progression and treatment response, the promise of enabling a viable defense against the GU tumors emerges. Driven by advanced technology, ongoing efforts from different centers focus on defining the roles of the clock proteins and their downstream effects in progression and clinical management of GU cancers to advanced disease. Thus whole-genome approaches, genomics, and proteomics would enable the detection of protein expression patterns and temporal networks of the clock proteins. Moreover, clinical studies implementing chronotherapy and melatonin supplementation are currently lacking in large patient cohorts ranked by their circadian profiles. The circadian-rhythms-navigated therapies pave the way for more effective implementation of current treatment modalities, their optimization towards overcoming therapeutic resistance and improving the quality of life in patients with GU malignancies.

AUTHOR CONTRIBUTIONS

Conceptualization: NM, PK, NK, MF. Resources: NM, MF, NK. Writing: PK, NM, MA, MF, MK. Figure preparation: MA, PK. Review and Editing: MF, NK. All authors contributed to the article and approved the final submitted version.

FUNDING

This work was supported by the following funding: Grant # R01 CA232574/National Institutes of Health/NCI (NK); Grant #R01OH01668/NIH/NIOSH (MF); Department of Defense W81XWH-17-1-0590 #PC160194 and the National Institute of Nursing Research (1R21 NR0165)18-01A1 (NM).

ACKNOWLEDGMENTS

The authors recognize the Icahn School of Medicine at Mount Sinai Summer Undergraduate Research Program (for supporting PK). **Figure 1** was produced using BioRender.com.

REFERENCES

1. Sulli G, Lam MTY, Panda S. Interplay Between Circadian Clock and Cancer: New Frontiers for Cancer Treatment. *Trends Cancer* (2019) 5(8):475–94. doi: 10.1016/j.trecan.2019.07.002
2. Sahar S, Sassone-Corsi P. Metabolism and Cancer: The Circadian Clock Connection. *Nat Rev Cancer* (2009) 9(12):886–96. doi: 10.1038/nrc2747
3. Shafi AA, Knudsen KE. Cancer and the Circadian Clock. *Cancer Res* (2019) 79(15):3806–14. doi: 10.1158/0008-5472.CAN-19-0566
4. Partch CL, Green CB, Takahashi JS. Molecular Architecture of the Mammalian Circadian Clock. *Trends Cell Biol* (2014) 24(2):90–9. doi: 10.1016/j.tcb.2013.07.002
5. Chiou YY, Yang Y, Rashid N, Ye R, Selby CP, Sancar A. Mammalian Period Represses and De-Represses Transcription by Displacing CLOCK-BMAL1 From Promoters in a Cryptochrome-Dependent Manner. *Proc Natl Acad Sci USA* (2016) 113(41):E6072–e9. doi: 10.1073/pnas.1612917113
6. Koch BC, Nagtegaal JE, Kerkhof GA, ter Wee PM. Circadian Sleep-Wake Rhythm Disturbances in End-Stage Renal Disease. *Nat Rev Nephrol* (2009) 5(7):407–16. doi: 10.1038/nrneph.2009.88
7. Altman BJ. Cancer Clocks Out for Lunch: Disruption of Circadian Rhythm and Metabolic Oscillation in Cancer. *Front Cell Dev Biol* (2016) 4:62. doi: 10.3389/fcell.2016.00062
8. Figueiro MG. Disruption of Circadian Rhythms by Light During Day and Night. *Curr Sleep Med Rep* (2017) 3(2):76–84. doi: 10.1007/s40675-017-0069-0

9. Mormont MC, Waterhouse J, Bleuzen P, Giacchetti S, Jami A, Bogdan A, et al. Marked 24-H Rest/Activity Rhythms Are Associated With Better Quality of Life, Better Response, and Longer Survival in Patients With Metastatic Colorectal Cancer and Good Performance Status. *Clin Cancer Res Off J Am Assoc Cancer Res* (2000) 6(8):3038–45.
10. Levin RD, Daehler MA, Grutsch JF, Quiton J, Lis CG, Peterson C, et al. Circadian Function in Patients With Advanced Non-Small-Cell Lung Cancer. *Br J Cancer* (2005) 93(11):1202–8. doi: 10.1038/sj.bjc.6602859
11. Walker WH, Walton JC, DeVries AC, Nelson RJ. Circadian Rhythm Disruption and Mental Health. *Trans Psychiatry* (2020) 10(1):28. doi: 10.1038/s41398-020-0694-0
12. Erren TC, Pape HG, Reiter RJ, Piekarski C. Chronodisruption and Cancer. *Die Naturwissenschaften* (2008) 95(5):367–82. doi: 10.1007/s00114-007-0335-y
13. Flynn-Evans EE, Stevens RG, Tabandeh H, Schernhammer ES, Lockley SW. Total Visual Blindness Is Protective Against Breast Cancer. *Cancer Causes Control CCC* (2009) 20(9):1753–6. doi: 10.1007/s10552-009-9405-0
14. Lockley SW, Arendt J, Skene DJ. Visual Impairment and Circadian Rhythm Disorders. *Dialogues Clin Neurosci* (2007) 9(3):301–14. doi: 10.31887/DCNS.2007.9.3/slockley
15. Wood PA, Yang X, Hrushesky WJ. Clock Genes and Cancer. *Integr Cancer therapies* (2009) 8(4):303–8. doi: 10.1177/1534735409355292
16. Russart KLG, Nelson RJ. Light at Night as an Environmental Endocrine Disruptor. *Physiol Behav* (2018) 190:82–9. doi: 10.1016/j.physbeh.2017.08.029
17. Zarrabi K, Paroya A, Wu S. Emerging Therapeutic Agents for Genitourinary Cancers. *J Hematol Oncol* (2019) 12(1):89. doi: 10.1186/s13045-019-0780-z
18. Begemann D, Wang Y, Yang W, Kyprianou N. Androgens Modify Therapeutic Response to Cabazitaxel in Models of Advanced Prostate Cancer. *Prostate* (2020) 80(12):926–37. doi: 10.1002/pros.24015
19. Chandrasekar T, Yang JC, Gao AC, Evans CP. Mechanisms of Resistance in Castration-Resistant Prostate Cancer (CRPC). *Trans Andrology Urol* (2015) 4(3):365–80. doi: 10.3978/j.issn.2223-4683.2015.05.02
20. Siska PJ, Beckermann KE, Rathmell WK, Haake SM. Strategies to Overcome Therapeutic Resistance in Renal Cell Carcinoma. *Urologic Oncol* (2017) 35(3):102–10. doi: 10.1016/j.urolonc.2016.12.002
21. Rini BI. New Strategies in Kidney Cancer: Therapeutic Advances Through Understanding the Molecular Basis of Response and Resistance. *Clin Cancer Res an Off J Am Assoc Cancer Res* (2010) 16(5):1348–54. doi: 10.1158/1078-0432.CCR-09-2273
22. Wołącewicz M, Hrynkiewicz R, Grywalska E, Suchojad T, Leksowski T, Roliński J, et al. Immunotherapy in Bladder Cancer: Current Methods and Future Perspectives. *Cancers* (2020) 12(5):1181. doi: 10.3390/cancers12051181
23. Galluzzi L, Senovilla L, Vitale I, Michels J, Martins I, Kepp O, et al. Molecular Mechanisms of Cisplatin Resistance. *Oncogene* (2012) 31(15):1869–83. doi: 10.1038/onc.2011.384
24. Dong D, Yang D, Lin L, Wang S, Wu B. Circadian Rhythm in Pharmacokinetics and its Relevance to Chronotherapy. *Biochem Pharmacol* (2020) 178:114045. doi: 10.1016/j.bcp.2020.114045
25. Zhdanova IV, Lynch HJ, Wurtman RJ. Melatonin: A Sleep-Promoting Hormone. *Sleep* (1997) 20(10):899–907. doi: 10.1093/sleep/20.10.899
26. Menéndez-Menéndez J, Martínez-Campa C. Melatonin: An Anti-Tumor Agent in Hormone-Dependent Cancers. *Int J Endocrinol* (2018) 2018:3271948. doi: 10.1155/2018/3271948
27. Blask DE. Melatonin, Sleep Disturbance and Cancer Risk. *Sleep Med Rev* (2009) 13(4):257–64. doi: 10.1016/j.smrv.2008.07.007
28. Bermúdez-Guzmán L, Blanco-Saborío A, Ramírez-Zamora J, Lovo E. The Time for Chronotherapy in Radiation Oncology. *Front Oncol* (2021) 11:687672. doi: 10.3389/fonc.2021.687672
29. Talib WH, Alsayed AR, Abuawad A, Daoud S, Mahmod AI. Melatonin in Cancer Treatment: Current Knowledge and Future Opportunities. *Molecules* (2021) 26(9):2506. doi: 10.3390/molecules26092506
30. Ye R, Selby CP, Chiou YY, Ozkan-Dagliyan I, Gaddameedhi S, Sancar A. Dual Modes of CLOCK:BMAL1 Inhibition Mediated by Cryptochrome and Period Proteins in the Mammalian Circadian Clock. *Genes Dev* (2014) 28(18):1989–98. doi: 10.1101/gad.249417.114
31. Kiyohara YB, Tagao S, Tamanini F, Morita A, Sugisawa Y, Yasuda M, et al. The BMAL1 C Terminus Regulates the Circadian Transcription Feedback Loop. *Proc Natl Acad Sci USA* (2006) 103(26):10074–9. doi: 10.1073/pnas.0601416103
32. Menet JS, Pescatore S, Rosbash M. CLOCK:BMAL1 is a Pioneer-Like Transcription Factor. *Genes Dev* (2014) 28(1):8–13. doi: 10.1101/gad.228536.113
33. Solt LA, Kojetin DJ, Burris TP. The REV-ERBs and RORs: Molecular Links Between Circadian Rhythms and Lipid Homeostasis. *Future medicinal Chem* (2011) 3(5):623–38. doi: 10.4155/fmc.11.9
34. Duez H, Staels B. Rev-Erb-Alpha: An Integrator of Circadian Rhythms and Metabolism. *J Appl Physiol (Bethesda Md 1985)* (2009) 107(6):1972–80. doi: 10.1152/japplphysiol.00570.2009
35. Ishikawa T, Hirayama J, Kobayashi Y, Todo T. Zebrafish CRY Represses Transcription Mediated by CLOCK-BMAL Heterodimer Without Inhibiting its Binding to DNA. *Genes to Cells devoted to Mol Cell Mech* (2002) 7(10):1073–86. doi: 10.1046/j.1365-2443.2002.00579.x
36. Langmesser S, Tallone T, Bordon A, Rusconi S, Albrecht U. Interaction of Circadian Clock Proteins PER2 and CRY With BMAL1 and CLOCK. *BMC Mol Biol* (2008) 9:41. doi: 10.1186/1471-2199-9-41
37. Chen ST, Choo KB, Hou MF, Yeh KT, Kuo SJ, Chang JG. Deregulated Expression of the PER1, PER2 and PER3 Genes in Breast Cancers. *Carcinogenesis* (2005) 26(7):1241–6. doi: 10.1093/carcin/bgi075
38. Miyazaki K, Wakabayashi M, Hara Y, Ishida N. Tumor Growth Suppression *In Vivo* by Overexpression of the Circadian Component, PER2. *Genes to Cells Devoted to Mol Cell Mech* (2010) 15(4):351–8. doi: 10.1111/j.1365-2443.2010.01384.x
39. Karantanos T, Theodoropoulos G, Pektasides D, Gazouli M. Clock Genes: Their Role in Colorectal Cancer. *World J Gastroenterol* (2014) 20(8):1986–92. doi: 10.3748/wjg.v20.i8.1986
40. Lengyel Z, Lovig C, Kommedal S, Keszthelyi R, Szekeres G, Battyáni Z, et al. Altered Expression Patterns of Clock Gene mRNAs and Clock Proteins in Human Skin Tumors. *Tumour Biol J Int Soc Oncodevelopmental Biol Med* (2013) 34(2):811–9. doi: 10.1007/s13277-012-0611-0
41. Kondratov RV, Antoch MP. The Clock Proteins, Aging, and Tumorigenesis. *Cold Spring Harbor Symp quantitative Biol* (2007) 72:477–82. doi: 10.1101/sqb.2007.72.050
42. Farhud D, Aryan Z. Circadian Rhythm, Lifestyle and Health: A Narrative Review. *Iranian J Public Health* (2018) 47(8):1068–76.
43. Stevens RG, Rea MS. Light in the Built Environment: Potential Role of Circadian Disruption in Endocrine Disruption and Breast Cancer. *Cancer causes control CCC* (2001) 12(3):279–87. doi: 10.1023/A:1011237000609
44. Lahti T, Merikanto I, Partonen T. Circadian Clock Disruptions and the Risk of Cancer. *Ann Med* (2012) 44(8):847–53. doi: 10.3109/07853890.2012.727018
45. Uchida Y, Hirayama J, Nishina H. A Common Origin: Signaling Similarities in the Regulation of the Circadian Clock and DNA Damage Responses. *Biol Pharm Bull* (2010) 33(4):535–44. doi: 10.1248/bpb.33.535
46. Rawla P. Epidemiology of Prostate Cancer. *World J Oncol* (2019) 10(2):63–89. doi: 10.14740/wjon1191
47. Siegel RL, Miller KD, Fuchs HE, Jemal A. Cancer Statistics, 2021. *CA: Cancer J Clin* (2021) 71(1):7–33. doi: 10.3322/caac.21654
48. Carter HB, Albertsen PC, Barry MJ, Etzioni R, Freedland SJ, Greene KL, et al. Early Detection of Prostate Cancer: AUA Guideline. *J Urol* (2013) 190:(2):419–26. doi: 10.1016/j.juro.2013.04.119
49. Harris KS, Kerr BA. Prostate Cancer Stem Cell Markers Drive Progression, Therapeutic Resistance, and Bone Metastasis. *Stem Cells Int* (2017) 2017:8629234. doi: 10.1155/2017/8629234
50. Polotti CF, Kim CJ, Chuchvara N, Polotti AB, Singer EA, Elsamra S. Androgen Deprivation Therapy for the Treatment of Prostate Cancer: A Focus on Pharmacokinetics. *Expert Opin Drug Metab Toxicol* (2017) 13(12):1265–73. doi: 10.1080/17425255.2017.1405934
51. Wade CA, Kyprianou N. Profiling Prostate Cancer Therapeutic Resistance. *Int J Mol Sci* (2018) 19(3):904. doi: 10.3390/ijms19030904
52. Martin SK, Pu H, Penticuff JC, Cao Z, Horbinski C, Kyprianou N. Multinucleation and Mesenchymal-To-Epithelial Transition Alleviate Resistance to Combined Cabazitaxel and Antiandrogen Therapy in

Advanced Prostate Cancer. *Cancer Res* (2016) 76(4):912–26. doi: 10.1158/0008-5472.CAN-15-2078
53. Bumbaca B, Li W. Taxane Resistance in Castration-Resistant Prostate Cancer: Mechanisms and Therapeutic Strategies. *Acta Pharm Sin B* (2018) 8(4):518–29. doi: 10.1016/j.apsb.2018.04.007
54. Sigurdardottir LG, Valdimarsdottir UA, Fall K, Rider JR, Lockley SW, Schernhammer E, et al. Circadian Disruption, Sleep Loss, and Prostate Cancer Risk: A Systematic Review of Epidemiologic Studies. *Cancer epidemiology Biomarkers Prev Publ Am Assoc Cancer Research cosponsored by Am Soc Prev Oncol* (2012) 21(7):1002–11. doi: 10.1158/1055-9965.EPI-12-0116
55. Bartsch C, Bartsch H, Schmidt A, Ilg S, Bichler KH, Flüchter SH. Melatonin and 6-Sulfatoxymelatonin Circadian Rhythms in Serum and Urine of Primary Prostate Cancer Patients: Evidence for Reduced Pineal Activity and Relevance of Urinary Determinations. *Clinica chimica acta; Int J Clin Chem* (1992) 209(3):153–67. doi: 10.1016/0009-8981(92)90164-L
56. Kubo T, Ozasa K, Mikami K, Wakai K, Fujino Y, Watanabe Y, et al. Prospective Cohort Study of the Risk of Prostate Cancer Among Rotating-Shift Workers: Findings From the Japan Collaborative Cohort Study. *Am J Epidemiol* (2006) 164(6):549–55. doi: 10.1093/aje/kwj232
57. Stevens RG, Blask DE, Brainard GC, Hansen J, Lockley SW, Provencio I, et al. Meeting Report: The Role of Environmental Lighting and Circadian Disruption in Cancer and Other Diseases. *Environ Health Perspect* (2007) 115(9):1357–62. doi: 10.1289/ehp.10200
58. Fu L, Pelicano H, Liu J, Huang P, Lee C. The Circadian Gene Period2 Plays an Important Role in Tumor Suppression and DNA Damage Response *In Vivo*. *Cell* (2002) 111(1):41–50. doi: 10.1016/S0092-8674(02)00961-3
59. Hua H, Wang Y, Wan C, Liu Y, Zhu B, Yang C, et al. Circadian Gene Mper2 Overexpression Induces Cancer Cell Apoptosis. *Cancer Sci* (2006) 97 (7):589–96. doi: 10.1111/j.1349-7006.2006.00225.x
60. Jung-Hynes B, Huang W, Reiter RJ, Ahmad N. Melatonin Resynchronizes Dysregulated Circadian Rhythm Circuitry in Human Prostate Cancer Cells. *J pineal Res* (2010) 49(1):60–8. doi: 10.1111/j.1600-079X.2010.00767.x
61. Li HX. The Role of Circadian Clock Genes in Tumors. *OncoTargets Ther* (2019) 12:3645–60. doi: 10.2147/OTT.S203144
62. Momma T, Okayama H, Saitou M, Sugeno H, Yoshimoto N, Takebayashi Y, et al. Expression of Circadian Clock Genes in Human Colorectal Adenoma and Carcinoma. *Oncol Lett* (2017) 14(5):5319–25. doi: 10.3892/ol.2017.6876
63. Benna C, Helfrich-Förster C, Rajendran S, Monticelli H, Pilati P, Nitti D, et al. Genetic Variation of Clock Genes and Cancer Risk: A Field Synopsis and Meta-Analysis. *Oncotarget* (2017) 8(14):23978–95. doi: 10.18632/oncotarget.15074
64. Harner-Foreman N, Vadakekolathu J, Laversin SA, Mathieu MG, Reeder S, Pockley AG, et al. A Novel Spontaneous Model of Epithelial-Mesenchymal Transition (EMT) Using a Primary Prostate Cancer Derived Cell Line Demonstrating Distinct Stem-Like Characteristics. *Sci Rep* (2017) 7:40633. doi: 10.1038/srep40633
65. Mao L, Dauchy RT, Blask DE, Slakey LM, Xiang S, Yuan L, et al. Circadian Gating of Epithelial-to-Mesenchymal Transition in Breast Cancer Cells *via* Melatonin-Regulation of GSK3β. *Mol Endocrinol (Baltimore Md)* (2012) 26 (11):1808–20. doi: 10.1210/me.2012-1071
66. Putzke AP, Ventura AP, Bailey AM, Akture C, Opoku-Ansah J, Celiktaş M, et al. Metastatic Progression of Prostate Cancer and E-Cadherin Regulation by Zeb1 and SRC Family Kinases. *Am J Pathol* (2011) 179(1):400–10. doi: 10.1016/j.ajpath.2011.03.028
67. Odero-Marah V, Hawsawi O, Henderson V, Sweeney J. Epithelial-Mesenchymal Transition (EMT) and Prostate Cancer. *Adv Exp Med Biol* (2018) 1095:101–10. doi: 10.1007/978-3-319-95693-0_6
68. Montanari M, Rossetti S, Cavaliere C, D'Aniello C, Malzone MG, Vanacore D, et al. Epithelial-Mesenchymal Transition in Prostate Cancer: An Overview. *Oncotarget* (2017) 8(21):35376–89. doi: 10.18632/oncotarget.15686
69. Hadadi E, Acloque H. Role of Circadian Rhythm Disorders on EMT and Tumour-Immune Interactions in Endocrine-Related Cancers. *Endocrine-related Cancer* (2021) 28(2):R67–r80. doi: 10.1530/ERC-20-0390
70. Xu W, Atkins MB, McDermott DF. Checkpoint Inhibitor Immunotherapy in Kidney Cancer. *Nat Rev Urol* (2020) 17(3):137–50. doi: 10.1038/s41585-020-0282-3
71. Ferlay J, Colombet M, Soerjomataram I, Parkin DM, Piñeros M, Znaor A, et al. Cancer Statistics for the Year 2020: An Overview. *Int J Cancer* (2021) 149:778–89. doi: 10.1002/ijc.33588
72. Motzer RJ, Agarwal N, Beard C, Bolger GB, Boston B, Carducci MA, et al. NCCN Clinical Practice Guidelines in Oncology: Kidney Cancer. *J Natl Compr Cancer Network JNCCN* (2009) 7(6):618–30. doi: 10.6004/jnccn.2009.0043
73. Hsieh JJ, Purdue MP, Signoretti S, Swanton C, Albiges L, Schmidinger M, et al. Renal Cell Carcinoma. *Nat Rev Dis Primers* (2017) 3:17009. doi: 10.1038/nrdp.2017.9
74. Bhatt JR, Finelli A. Landmarks in the Diagnosis and Treatment of Renal Cell Carcinoma. *Nat Rev Urol* (2014) 11(9):517–25. doi: 10.1038/nrurol.2014.194
75. George CM, Stadler WM. The Role of Systemic Chemotherapy in the Treatment of Kidney Cancer. *Cancer Treat Res* (2003) 116:173–82. doi: 10.1007/978-1-4615-0451-1_10
76. Chappell JC, Payne LB, Rathmell WK. Hypoxia, Angiogenesis, and Metabolism in the Hereditary Kidney Cancers. *J Clin Invest* (2019) 129 (2):442–51. doi: 10.1172/JCI120855
77. Solocinski K, Gumz ML. The Circadian Clock in the Regulation of Renal Rhythms. *J Biol Rhythms* (2015) 30(6):470–86. doi: 10.1177/0748730415610879
78. Zhang R, Lahens NF, Ballance HI, Hughes ME, Hogenesch JB. A Circadian Gene Expression Atlas in Mammals: Implications for Biology and Medicine. *Proc Natl Acad Sci USA* (2014) 111(45):16219–24. doi: 10.1073/pnas.1408886111
79. Mazzoccoli G, De Cata A, Piepoli A, Vinciguerra M. The Circadian Clock and the Hypoxic Response Pathway in Kidney Cancer. *Tumour Biol J Int Soc Oncodevelopmental Biol Med* (2014) 35(1):1–7. doi: 10.1007/s13277-013-1076-5
80. Zhou L, Luo Z, Li Z, Huang Q. Circadian Clock is Associated With Tumor Microenvironment in Kidney Renal Clear Cell Carcinoma. *Aging* (2020) 12 (14):14620–32. doi: 10.18632/aging.103509
81. Deng W, Zhu S, Zeng L, Liu J, Kang R, Yang M, et al. The Circadian Clock Controls Immune Checkpoint Pathway in Sepsis. *Cell Rep* (2018) 24(2):366–78. doi: 10.1016/j.celrep.2018.06.026
82. Antoni S, Ferlay J, Soerjomataram I, Znaor A, Jemal A, Bray F. Bladder Cancer Incidence and Mortality: A Global Overview and Recent Trends. *Eur Urol* (2017) 71(1):96–108. doi: 10.1016/j.eururo.2016.06.010
83. Marcos-Gragera R, Mallone S, Kiemeney LA, Vilardell L, Malats N, Allory Y, et al. Urinary Tract Cancer Survival in Europe 1999-2007: Results of the Population-Based Study EUROCARE-5. *Eur J Cancer (Oxford Engl 1990)* (2015) 51(15):2217–30. doi: 10.1016/j.ejca.2015.07.028
84. Richters A, Aben KKH, Kiemeney L. The Global Burden of Urinary Bladder Cancer: An Update. *World J Urol* (2020) 38(8):1895–904. doi: 10.1007/s00345-019-02984-4
85. Sanli O, Dobruch J, Knowles MA, Burger M, Alemozaffar M, Nielsen ME, et al. Bladder Cancer. *Nat Rev Dis Primers* (2017) 3:17022. doi: 10.1038/nrdp.2017.22
86. Kamat AM, Hahn NM, Efstathiou JA, Lerner SP, Malmström PU, Choi W, et al. Bladder Cancer. *Lancet (London England)* (2016) 388(10061):2796–810. doi: 10.1016/S0140-6736(16)30512-8
87. Massari F, Santoni M, Ciccarese C, Brunelli M, Conti A, Santini D, et al. Emerging Concepts on Drug Resistance in Bladder Cancer: Implications for Future Strategies. *Crit Rev oncology/hematology* (2015) 96(1):81–90. doi: 10.1016/j.critrevonc.2015.05.005
88. Sadiq Z, Varghese E, Büsselberg D. Cisplatin's Dual-Effect on the Circadian Clock Triggers Proliferation and Apoptosis. *Neurobiol Sleep Circadian Rhythms* (2020) 9:100054. doi: 10.1016/j.nbscr.2020.100054
89. Litlekalsoy J, Rostad K, Kalland KH, Hostmark JG, Laerum OD. Expression of Circadian Clock Genes and Proteins in Urothelial Cancer Is Related to Cancer-Associated Genes. *BMC Cancer* (2016) 16:549. doi: 10.1186/s12885-016-2580-y
90. Jia M, Su B, Mo L, Qiu W, Ying J, Lin P, et al. Circadian Clock Protein CRY1 Prevents Paclitaxel–Induced Senescence of Bladder Cancer Cells by Promoting P53 Degradation. *Oncol Rep* (2021) 45(3):1033–43. doi: 10.3892/or.2020.7914
91. Gordon RR, Nelson PS. Cellular Senescence and Cancer Chemotherapy Resistance. *Drug resistance updates Rev commentaries antimicrobial*

Anticancer chemotherapy (2012) 15(1-2):123–31. doi: 10.1016/j.drup.2012.01.002
92. Ashcroft M, Kubbutat MH, Vousden KH. Regulation of P53 Function and Stability by Phosphorylation. *Mol Cell Biol* (1999) 19(3):1751–8. doi: 10.1128/MCB.19.3.1751
93. Liu C, Weaver DR, Jin X, Shearman LP, Pieschl RL, Gribkoff VK, et al. Molecular Dissection of Two Distinct Actions of Melatonin on the Suprachiasmatic Circadian Clock. *Neuron* (1997) 19(1):91–102. doi: 10.1016/S0896-6273(00)80350-5
94. Lissoni P, Viviani S, Bajetta E, Buzzoni R, Barreca A, Mauri R, et al. A Clinical Study of the Pineal Gland Activity in Oncologic Patients. *Cancer* (1986) 57(4):837–42. doi: 10.1002/1097-0142(19860215)57:4<837::AID-CNCR2820570425>3.0.CO;2-O
95. Hill SM, Belancio VP, Dauchy RT, Xiang S, Brimer S, Mao L, et al. Melatonin: An Inhibitor of Breast Cancer. *Endocrine-Related Cancer* (2015) 22(3):R183–204. doi: 10.1530/ERC-15-0030
96. Brzezinski A. Melatonin in Humans. *New Engl J Med* (1997) 336(3):186–95. doi: 10.1056/NEJM199701163360306
97. Reiter RJ, Rosales-Corral SA, Tan DX, Acuna-Castroviejo D, Qin L, Yang SF, et al. Melatonin, a Full Service Anti-Cancer Agent: Inhibition of Initiation, Progression and Metastasis. *Int J Mol Sci* (2017) 18(4):843. doi: 10.3390/ijms18040843
98. Dai M, Cui P, Yu M, Han J, Li H, Xiu R. Melatonin Modulates the Expression of VEGF and HIF-1 Alpha Induced by CoCl2 in Cultured Cancer Cells. *J pineal Res* (2008) 44(2):121–6. doi: 10.1111/j.1600-079X.2007.00498.x
99. Hardeland R. Melatonin in Aging and Disease -Multiple Consequences of Reduced Secretion, Options and Limits of Treatment. *Aging Dis* (2012) 3 (2):194–225.
100. Reiter RJ, Tan DX, Sainz RM, Mayo JC, Lopez-Burillo S. Melatonin: Reducing the Toxicity and Increasing the Efficacy of Drugs. *J Pharm Pharmacol* (2002) 54(10):1299–321. doi: 10.1211/002235702760345374
101. Korkmaz A, Reiter RJ. Epigenetic Regulation: A New Research Area for Melatonin? *J pineal Res* (2008) 44(1):41–4. doi: 10.1111/j.1600-079X.2007.00509.x
102. Bondy SC, Campbell A. Mechanisms Underlying Tumor Suppressive Properties of Melatonin. *Int J Mol Sci* (2018) 19(8):2205. doi: 10.3390/ijms19082205
103. Mills E, Wu P, Seely D, Guyatt G. Melatonin in the Treatment of Cancer: A Systematic Review of Randomized Controlled Trials and Meta-Analysis. *J Pineal Res* (2005) 39(4):360–6. doi: 10.1111/j.1600-079X.2005.00258.x
104. Lissoni P. Is There a Role for Melatonin in Supportive Care? *Supportive Care Cancer Off J Multinational Assoc Supportive Care Cancer* (2002) 10(2):110–6. doi: 10.1007/s005200100281
105. Tai S-Y, Huang S-P, Bao B-Y, Wu M-T. Urinary Melatonin-Sulfate/Cortisol Ratio and the Presence of Prostate Cancer: A Case-Control Study. *Sci Rep* (2016) 6(1):29606. doi: 10.1038/srep29606
106. Pienta KJ, Loberg R. The "Emigration, Migration, and Immigration" of Prostate Cancer. *Clin Prostate Cancer* (2005) 4(1):24–30. doi: 10.3816/CGC.2005.n.008
107. Chen PC, Tang CH, Lin LW, Tsai CH, Chu CY, Lin TH, et al. Thrombospondin-2 Promotes Prostate Cancer Bone Metastasis by the Up-Regulation of Matrix Metalloproteinase-2 Through Down-Regulating miR-376c Expression. *J Hematol Oncol* (2017) 10(1):33. doi: 10.1186/s13045-017-0390-6
108. Gong Y, Chippada-Venkata UD, Oh WK. Roles of Matrix Metalloproteinases and Their Natural Inhibitors in Prostate Cancer Progression. *Cancers* (2014) 6(3):1298–327. doi: 10.3390/cancers6031298
109. Wang SW, Tai HC, Tang CH, Lin LW, Lin TH, Chang AC, et al. Melatonin Impedes Prostate Cancer Metastasis by Suppressing MMP-13 Expression. *J Cell Physiol* (2021) 236(5):3979–90. doi: 10.1002/jcp.30150
110. Pourhanifeh MH, Hosseinzadeh A, Juybari KB, Mehrzadi S. Melatonin and Urological Cancers: A New Therapeutic Approach. *Cancer Cell Int* (2020) 20 (1):444. doi: 10.1186/s12935-020-01531-1
111. Li W, Wang Z, Chen Y, Wang K, Lu T, Ying F, et al. Melatonin Treatment Induces Apoptosis Through Regulating the Nuclear Factor-κb and Mitogen-Activated Protein Kinase Signaling Pathways in Human Gastric Cancer SGC7901 Cells. *Oncol Lett* (2017) 13(4):2737–44. doi: 10.3892/ol.2017.5785
112. Nopparat C, Chantadul V, Permpoonputtana K, Govitrapong P. The Anti-Inflammatory Effect of Melatonin in SH-SY5Y Neuroblastoma Cells Exposed to Sublethal Dose of Hydrogen Peroxide. *Mech Ageing Dev* (2017) 164:49–60. doi: 10.1016/j.mad.2017.04.001
113. Lin YW, Lee LM, Lee WJ, Chu CY, Tan P, Yang YC, et al. Melatonin Inhibits MMP-9 Transactivation and Renal Cell Carcinoma Metastasis by Suppressing Akt-MAPKs Pathway and NF-κb DNA-Binding Activity. *J Pineal Res* (2016) 60(3):277–90. doi: 10.1111/jpi.12308
114. Rudra DS, Pal U, Maiti NC, Reiter RJ, Swarnakar S. Melatonin Inhibits Matrix Metalloproteinase-9 Activity by Binding to its Active Site. *J pineal Res* (2013) 54(4):398–405. doi: 10.1111/jpi.12034
115. Mormont M-C, Levi F. Cancer Chronotherapy: Principles, Applications, and Perspectives. *Cancer* (2003) 97: (1):155–69. doi: 10.1002/cncr.11040
116. Lévi F, Okyar A. Circadian Clocks and Drug Delivery Systems: Impact and Opportunities in Chronotherapeutics. *Expert Opin Drug Delivery* (2011) 8 (12):1535–41. doi: 10.1517/17425247.2011.618184
117. Payne JK. Altered Circadian Rhythms and Cancer-Related Fatigue Outcomes. *Integr Cancer therapies* (2011) 10(3):221–33. doi: 10.1177/1534735410392581
118. Fiorentino L, Ancoli-Israel S. Sleep Dysfunction in Patients With Cancer. *Curr Treat Options Neurol* (2007) 9(5):337–46. doi: 10.1007/s11940-007-0019-0
119. Hsu FM, Hou WH, Huang CY, Wang CC, Tsai CL, Tsai YC, et al. Differences in Toxicity and Outcome Associated With Circadian Variations Between Patients Undergoing Daytime and Evening Radiotherapy for Prostate Adenocarcinoma. *Chronobiology Int* (2016) 33(2):210–9. doi: 10.3109/07420528.2015.1130049
120. Hrushesky WJ, von Roemeling R, Lanning RM, Rabatin JT. Circadian-Shaped Infusions of Floxuridine for Progressive Metastatic Renal Cell Carcinoma. *J Clin Oncol Off J Am Soc Clin Oncol* (1990) 8(9):1504–13. doi: 10.1200/JCO.1990.8.9.1504
121. Lévi F. Circadian Chronotherapy for Human Cancers. *Lancet Oncol* (2001) 2 (5):307–15. doi: 10.1016/S1470-2045(00)00326-0
122. Kobayashi M, Wood PA, Hrushesky WJ. Circadian Chemotherapy for Gynecological and Genitourinary Cancers. *Chronobiology Int* (2002) 19 (1):237–51. doi: 10.1081/CBI-120002600
123. Negoro H, Iizumi T, Mori Y, Matsumoto Y, Chihara I, Hoshi A, et al. Chronoradiation Therapy for Prostate Cancer: Morning Proton Beam Therapy Ameliorates Worsening Lower Urinary Tract Symptoms. *J Clin Med* (2020) 9(7):2263. doi: 10.3390/jcm9072263
124. Forbes-Robertson S, Dudley E, Vadgama P, Cook C, Drawer S, Kilduff L. Circadian Disruption and Remedial Interventions: Effects and Interventions for Jet Lag for Athletic Peak Performance. *Sports Med (Auckland NZ)* (2012) 42(3):185–208. doi: 10.2165/11596850-000000000-00000
125. Mendt S, Gunga H-C, Felsenberg D, Belavy DL, Steinach M, Stahn AC. Regular Exercise Counteracts Circadian Shifts in Core Body Temperature During Long-Duration Bed Rest. *NPJ Microgravity* (2021) 7(1):1. doi: 10.1038/s41526-020-00129-1
126. Duffy JF, Czeisler CA. Effect of Light on Human Circadian Physiology. *Sleep Med Clinics* (2009) 4(2):165–77. doi: 10.1016/j.jsmc.2009.01.004
127. Jewett ME, Rimmer DW, Duffy JF, Klerman EB, Kronauer RE, Czeisler CA. Human Circadian Pacemaker is Sensitive to Light Throughout Subjective Day Without Evidence of Transients. *Am J Physiol* (1997) 273(5 Pt 2): R1800–9. doi: 10.1152/ajpregu.1997.273.5.R1800
128. Figueiro MG. Individually Tailored Light Intervention Through Closed Eyelids to Promote Circadian Alignment and Sleep Health. *Sleep Health* (2015) 1(1):75–82. doi: 10.1016/j.sleh.2014.12.009
129. Figueiro M, Saldo E, Rea M, Kubarek K, Cunningham J, Rea M. Developing Architectural Lighting Designs to Improve Sleep in Older Adults. *Open Sleep J* (2008) 1:40–51. doi: 10.2174/1874620900801010040
130. Figueiro MG, Bierman A, Plitnick B, Rea MS. Preliminary Evidence That Both Blue and Red Light can Induce Alertness at Night. *BMC Neurosci* (2009) 10(1):105. doi: 10.1186/1471-2202-10-105
131. Erren TC, Lewis P, Morfeld P. The Riddle of Shiftwork and Disturbed Chronobiology: A Case Study of Landmark Smoking Data Demonstrates Fallacies of Not Considering the Ubiquity of an Exposure. *J Occup Med Toxicol (London England)* (2020) 15:10. doi: 10.1186/s12995-020-00263-2

132. Atkinson G, Fullick S, Grindey C, Maclaren D. Exercise, Energy Balance and the Shift Worker. *Sports Med (Auckland NZ)* (2008) 38(8):671–85. doi: 10.2165/00007256-200838080-00005
133. Atkinson G, Edwards B, Reilly T, Waterhouse J. Exercise as a Synchroniser of Human Circadian Rhythms: An Update and Discussion of the Methodological Problems. *Eur J Appl Physiol* (2007) 99(4):331–41. doi: 10.1007/s00421-006-0361-z
134. Baehr EK, Eastman CI, Revelle W, Olson SH, Wolfe LF, Zee PC. Circadian Phase-Shifting Effects of Nocturnal Exercise in Older Compared With Young Adults. *Am J Physiol Regulatory Integr Comp Physiol* (2003) 284(6):R1542–50. doi: 10.1152/ajpregu.00761.2002
135. Youngstedt SD, Kripke DF, Elliott JA. Circadian Phase-Delaying Effects of Bright Light Alone and Combined With Exercise in Humans. *Am J Physiol Regulatory Integr Comp Physiol* (2002) 282(1):R259–66. doi: 10.1152/ajpregu.00473.2001
136. Weitzer J, Castaño-Vinyals G, Aragonés N, Gómez-Acebo I, Guevara M, Amiano P, et al. Effect of Time of Day of Recreational and Household Physical Activity on Prostate and Breast Cancer Risk (MCC-Spain Study). *Int J Cancer* (2021) 148(6):1360–71. doi: 10.1002/ijc.33310
137. Atkinson G, Drust B, Reilly T, Waterhouse J. The Relevance of Melatonin to Sports Medicine and Science. *Sports Med (Auckland NZ)* (2003) 33(11):809–31. doi: 10.2165/00007256-200333110-00003
138. Fuller PM, Lu J, Saper CB. Differential Rescue of Light- and Food-Entrainable Circadian Rhythms. *Sci (New York NY)* (2008) 320 (5879):1074–7. doi: 10.1126/science.1153277
139. Saper CB, Fuller PM. Inducible Clocks: Living in an Unpredictable World. *Cold Spring Harbor Symp quantitative Biol* (2007) 72:543–50. doi: 10.1101/sqb.2007.72.008
140. Fu L, Kettner NM. The Circadian Clock in Cancer Development and Therapy. *Prog Mol Biol Trans Sci* (2013) 119:221–82. doi: 10.1016/B978-0-12-396971-2.00009-9
141. Battaglin F, Chan P, Pan Y, Soni S, Qu M, Spiller ER, et al. Clocking Cancer: The Circadian Clock as a Target in Cancer Therapy. *Oncogene* (2021) 40 (18):3187–200. doi: 10.1038/s41388-021-01778-6
142. Penticuff JC, Woolbright BL, Sielecki TM, Weir SJ, Taylor JA 3rd. MIF Family Proteins in Genitourinary Cancer: Tumorigenic Roles and Therapeutic Potential. *Nat Rev Urol* (2019) 16(5):318–28. doi: 10.1038/s41585-019-0171-9
143. Zhu X, Suo Y, Fu Y, Zhang F, Ding N, Pang K, et al. *In Vivo* Flow Cytometry Reveals a Circadian Rhythm of Circulating Tumor Cells. *Light: Sci Appl* (2021) 10(1):110. doi: 10.1038/s41377-021-00542-5
144. Srinivasan V, Spence DW, Pandi-Perumal SR, Trakht I, Cardinali DP. Therapeutic Actions of Melatonin in Cancer: Possible Mechanisms. *Integr Cancer Therapies* (2008) 7(3):189–203. doi: 10.1177/1534735408322846

Conflict of Interest: The authors declare that the research was conducted in the absence of any commercial or financial relationships that could be construed as a potential conflict of interest.

frontiers in Oncology

MINI REVIEW
published: 10 March 2022
doi: 10.3389/fonc.2022.865350

Anti-Androgen Receptor Therapies in Prostate Cancer: A Brief Update and Perspective

Jian Huang[1], *Biyun Lin*[1] *and Benyi Li*[2*]

[1] Pathological Diagnosis and Research Center, The Affiliated Hospital of Guangdong Medical University, Zhanjiang, China,
[2] Department of Urology, The University of Kansas Medical Center, Kansas City, KS, United States

Prostate cancer is a major health issue in western countries and is the second leading cause of cancer death in American men. Prostate cancer depends on the androgen receptor (AR), a transcriptional factor critical for prostate cancer growth and progression. Castration by surgery or medical treatment reduces androgen levels, resulting in prostatic atrophy and prostate cancer regression. Thus, metastatic prostate cancers are initially managed with androgen deprivation therapy. Unfortunately, prostate cancers rapidly relapse after castration therapy and progress to a disease stage called castration-resistant prostate cancer (CRPC). Currently, clinical treatment for CRPCs is focused on suppressing AR activity with antagonists like Enzalutamide or by reducing androgen production with Abiraterone. In clinical practice, these treatments fail to yield a curative benefit in CRPC patients in part due to AR gene mutations or splicing variations, resulting in AR reactivation. It is conceivable that eliminating the AR protein in prostate cancer cells is a promising solution to provide a potential curative outcome. Multiple strategies have emerged, and several potent agents that reduce AR protein levels were reported to eliminate xenograft tumor growth in preclinical models *via* distinct mechanisms, including proteasome-mediated degradation, heat-shock protein inhibition, AR splicing suppression, blockage of AR nuclear localization, AR N-terminal suppression. A few small chemical compounds are undergoing clinical trials combined with existing AR antagonists. AR protein elimination by enhanced protein or mRNA degradation is a realistic solution for avoiding AR reactivation during androgen deprivation therapy in prostate cancers.

Keywords: androgen receptor, prostate cancer, small interfering RNA, protein degradation, PROTAC

OPEN ACCESS

Edited by:
Olivier Cuvillier, UPR8241 Laboratoire de Chimie de Coordination (LCC), France

Reviewed by:
Elahe A. Mostaghel, Fred Hutchinson Cancer Research Center, United States
Antimo Migliaccio, University of Campania Luigi Vanvitelli, Italy

***Correspondence:**
Benyi Li
bli@kumc.edu

Specialty section:
This article was submitted to Genitourinary Oncology, a section of the journal Frontiers in Oncology

Received: *29 January 2022*
Accepted: *17 February 2022*
Published: *10 March 2022*

Citation:
Huang J, Lin B and Li B (2022) Anti-Androgen Receptor Therapies in Prostate Cancer: A Brief Update and Perspective. Front. Oncol. 12:865350. doi: 10.3389/fonc.2022.865350

INTRODUCTION

Prostate cancer is the second most common type of cancer diagnosed in men worldwide and the second leading cause of male cancer-related deaths in the U.S. (1). The American Cancer Society estimates about 268,490 new cases of prostate cancer and about 34,500 deaths from prostate cancer in the U.S. this year (1). According to the American Cancer Society data (cancer.org), patients with local or regional stage prostate cancer have nearly a 100% 5-year survival rate; however, the survival rate is only 30% for men diagnosed with distal metastasis.

Currently, localized prostate cancer is primarily treated with surgical removal of the gland or radiation therapy if a patient's condition is not permissive for surgery. Distal metastasis occurs in high-risk patients, including locally advanced (positive surgical margin) or high-grade (Gleason sum score ≥ 8) tumors, which is the sole cause of death from prostate cancer (2). This short review work will discuss the current treatment options and recent development of anti-androgen receptor (AR) therapeutic approaches for metastatic prostate cancer (**Table 1** and **Figure 1**).

ANDROGEN DEPRIVATION AND ANTI-ANDROGEN THERAPIES IN THE CLINIC

Metastatic prostate cancers are initially treated with androgen deprivation therapy (ADT) because prostate tissue (benign or malignant) expresses androgen receptor (AR) protein that is critical for prostate cancer development and progression (3, 4). Castration by surgery or medical treatment reduces androgen hormones, resulting in prostatic atrophy and cancer regression (5). This approach was developed eighty years ago in 1941 (3, 4). Since then, prostate cancer treatment has been mainly focused on reducing androgen levels and blocking androgen-induced AR activation (5). However, prostate cancers often relapse and progress to a stage termed as castration-resistant prostate cancers (CRPC) (67, 68), and the majority of these CRPCs still depend on the AR signaling for growth and progression (the AR addictiveness) (69, 70).

The mechanisms for CRPC progression include AR gene mutation, amplification, transcriptional splicing, and crosstalks with cellular signal pathways, plus *de novo* androgen synthesis by the malignant prostate cells (5). Therefore, clinical therapies use anti-androgens (Flutamide, Bicalutamide, Enzalutamide, Apalutamide, and Darolutamide) to competitively suppress androgen-induced AR activation or CYP17A1 inhibitor (Abiraterone) to reduce androgen production in prostate cancer tissues (5). So far in the clinic, these therapies provided certain clinical benefits of survival extension in CRPC patients (71). However, with the widespread use of Enzalutamide and Abiraterone, a subset of CRPC patients developed neuroendocrine progression, termed as anti-AR treatment-induced NEPC (t-NEPC) (72, 73), accounting for more than 25-30% mortality of CRPC fatality (74). There were multiple

TABLE 1 | Summary of AR-targeted therapeutic agents for prostate cancers.

Therapeutic Target	Agent Or Approach	Mechasnism Of Action	Current Stage	Reference
Testicular androgens	surgical castration	testis removal	in clinic use	(3)
	GnRH antagonist	reducing testersterone production	in clinic use	(4)
	GnRH agonist	reducing testersterone production	in clinic use	(4)
Adrenal or cancer androgens all androgens	Abiraterone	CYP17A1 inhibition	in clinic use	(5)
	Flutamide	blocking androgen-AR binding	in clinic use	(5)
	Bicalutamide	blocking androgen-AR binding	in clinic use	(5)
	Enzalutamide	blocking androgen-AR binding	in clinic use	(5)
	Apalutamide	blocking androgen-AR binding	in clinic use	(5)
	Darolutamide	blocking androgen-AR binding	in clinic use	(5)
AR mRNA	antisense oligonucleotides	mRNA-based protein translation and mRNA stability	pre-clinical	(6–14)
	small interfering RNA	mRNA silencing	pre-clinical	(15–23)
Full length AR protein	ARCC-4/ARV-110	PROTAC-mediated AR degradation	phase-1 clinical trial	NCT03888612
	ARD series	PROTAC-mediated AR degradation	pre-clinical	(24–31)
	TD-802	PROTAC-mediated AR degradation	pre-clinical	(32)
	A031	PROTAC-mediated AR degradation	pre-clinical	(33)
	MTX-23	PROTAC-mediated AR degradation	pre-clinical	(34)
	A9/A16	PROTAC-mediated AR degradation	cell culture model	(35, 36)
	SNIPER-51	PROTAC-mediated AR degradation	cell culture model	(37)
Full-length/variant AR protein	UT-34	AR NTD binding and degradation	pre-clinical	(38)
	Ailanthone	co-chaperone p23 binding and AR degradation	pre-clinical	(39)
	HG122	proteasome-based AR degradation	pre-clinical	(40)
	CUDC-101	AR degradation due to unknown mechanism	pre-clinical	(41)
	ASC-J9	AR degradation due to unknown mechanism	pre-clinical	(42–47)
AR splicing variants	Niclosamide	AR-V7 degradation	phase-1 clinical trial	NCT03123978
	Niclosamide	AR-V7 degradation	phase-1 clinical trial	NCT02807805
	Thailanstatins	suppressing splicing event for AR-V7	pre-clinical	(48–50)
	Rutaecarpine	AR-v7 degradation via GPR78/SIAH2 pathway	pre-clinical	(51)
	Indisulam	Suppressing AR-V7 splicing factor RBM39	pre-clinical	(52)
	Nobiletin	AR-V7 degradation via blocking USP14/USP22	pre-clinical	(53)
AR NTD inhibitor	EPI series/EPI-7386	suppressing AR NTD TAU-5 activity	phase-1/2 clinical trial	NCT05075577
	EPI series/EPI-7387	suppressing AR NTD TAU-5 activity	phase-1 clinical trial	NCT04421222
	QW07	suppressing AR NTD activity	pre-clinical	(54)
AR nuclear translocation	EPPI/CPPI	blocking AR nuclear translocation	pre-clinical	(55–57)
	IMPPE	blocking AR translocation and inducing AR degradation	pre-clinical	(58)
	JJ-450	blocking AR translocation and transactivation	pre-clinical	(59–62)
AR DND-hinge antagonist	VPC-14228/14449	blocking AR dimerization and DNA binding	pre-clinical	(63–66)

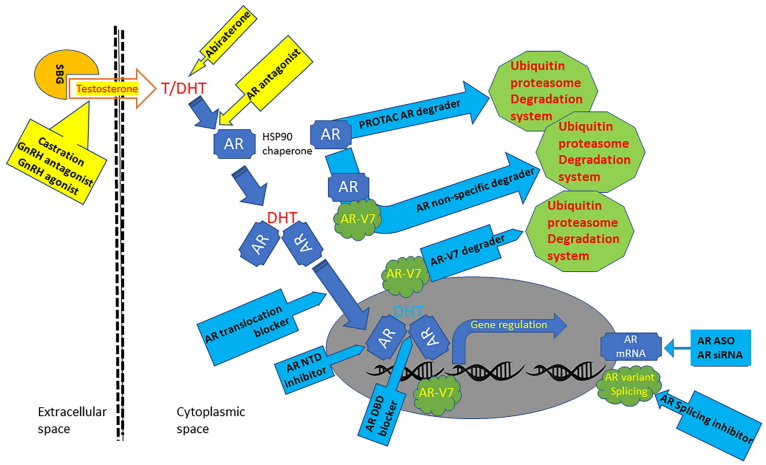

FIGURE 1 | Graphic scheme of AR-targeted agents. Androgens are bonded with steroid-binding globulins (SBG) in the bloodstream for systemic circulation. Androgen testosterone (T) is converted to potent form dihydrotestosterone (DHT) in the cytoplasm by 5a-reductase. The AR protein bonds with HSP90 chaperones and resides in the cytoplasmic compartment before androgen binding. Androgen binding alters AR conformation and promotes its translocation into the nuclear compartment, where it interacts with chromatin DNA to regulate gene expression. AR gene mRNA is aberrantly spliced in advanced prostate cancers to generate variant proteins like AR-V7, which is constantly active without androgen binding. Current clinical therapies for metastatic prostate cancers (yellow background box) include castration, GnRH agonist and antagonist, Abiraterone, and AR antagonists. Several AR-targeted treatments under development (blue background box) include AR PROTAC and non-specific degraders, AR-V7 degraders, AR-NTD inhibitor, AR-DBD blocker, AR nuclear translocation blockers, AR splicing inhibitors.

mechanisms involved in NEPC progression, including attenuated control of transcriptional factors, metabolic alterations, aberrant activation of cellular kinases, long noncoding RNAs, transcriptional splicing, and epigenetic modifications (75–87). It is postulated that extensive stress of AR inhibition under the long-term ADT condition forced an epigenetic reprogramming of CRPC cells into neuroendocrinal trans-differentiation (88–93). Treatment option for NEPC patients is limited in the clinic and the salvage platinum-based chemotherapy only provided very little survival benefit (75).

AR PROTEIN ELIMINATION APPROACHES IN PRECLINICAL DEVELOPMENT PHASE

The AR protein is a nuclear receptor expressed in benign and malignant prostate tissues, critical for prostate physiological functionality and prostate cancer progression (94, 95). As a transcriptional factor, the AR protein modulates gene expression after being activated by androgens *via* binding on its C-terminal ligand-binding domain (95). Given that hormone therapy, including ADT and anti-androgens for the last eighty years, has been failed to be a curable approach for metastatic prostate cancers, eliminating the AR protein in prostate cancer cells recently emerged as a realistic solution for a potentially curable result.

Antisense Oligonucleotide Technology

Antisense oligonucleotides (ASOs) are synthetic complementary single-stranded deoxyribonucleotides used to target messenger RNA (mRNA) of targeted genes, resulting in RNase H endonuclease-dependent mRNA cleavage or blockage of protein translation (6). Dr. Klocker's group reported the first study using the ASO technology against the AR gene in 2000, which showed a suppressive effect on prostate cancer LNCaP cell growth (7). A follow-up study by the same group showed the *in vivo* effectiveness of suppressing LNCaP-derived xenograft tumors in nude mice (8). These initial results were supported by the studies from other groups (9, 10). Possibly due to the suppressive nature of ASOs on target gene expression, the AR protein was not eliminated from cancer cells. Also, the results only showed a moderate suppressive effect on tumor growth because of the difficulty in tissue delivery of the ASO molecules. However, these AR-targeted ASOs showed an enhanced effect when combined with other gene targets (EZH2 or Clusterin) for Enzalutamide-resistant CRPC models (11–14). A recent report achieved a successful *in vivo* delivery of AR-specific ASO using lipid-based nanotechnology. A profound suppressive effect was achieved in the prostate cancer xenograft model, together with a significant reduction of the AR protein levels in xenograft tumor tissues (96).

Small Interfering RNA Technology

Since the introduction of small interfering RNA (siRNA) technology in 2001 (97, 98), knocking down gene expression in living organisms became possible. To overcome the clinical obstacle of anti-AR treatment resistance, we hypothesized that eliminating AR protein from prostate cancer cells might completely shut down AR signaling, leading to cell death or growth arrest. Knocking down AR gene expression in prostate cancer cells resulted in profound apoptotic cell death in multiple prostate cancer cell lines, androgen-responsive or castration-resistant (15). Nanoparticle-based prostate cancer-specific delivery approach and adenoviral approach to systemically deliver the AR siRNA expression particles documented a rapid

xenograft tumor regression and eradication owing to robust cell death *in vivo* (16, 17). These findings were overwhelmingly supported by reports from other groups using divergent approaches to knock down AR gene expression (18–23). These results confirmed that eliminating AR protein (full length or truncated) will overcome treatment resistance in advanced prostate cancers.

PROTAC Technology

PROTAC stands for proteolysis targeting chimera. It uses a small bifunctional molecule with two binding moieties connected by a linker to bring together a targeted protein and cellular proteolytic machinery, ubiquitin E3 ligase-mediated proteasome degradation system (99, 100). This technology selectively removes specific proteins like the AR protein for a therapeutic purpose (101, 102). Several descent review articles summarized the technique description and the usage of various E3 ligases (103–106). We will only discuss the PROTAC molecules designed for the AR protein.

The first AR-targeted PROTAC approach was reported in 2004, which used a synthetic peptide targeting the E3 ligase fused to either an artificial FKBP12 ligand or dihydrotestosterone (DHT) (24). After several optimizations, a potent AR-specific PROTAC molecule ARCC-4 was developed with a nanomole concentration efficiency (25). Its further modified version, ARV-110, is being tested in clinical trials in metastatic prostate cancer patients (26). The first trial is a phase-1b open-label clinical trial (NCT05177042) to assess the combination of ARV-110 and Abiraterone in patients with metastatic prostate cancer with PSA progression after Abiraterone treatment. It is estimated to finish at the end of April of 2023. The second one is a phase-1/2 open-label single-agent dose escalation and cohort expansion trial to assess the safety and tolerability of ARV-110 (NCT03888612). It will be finished at the end of February 2023.

The AR degrader (ARD) series of PROTAC molecules (ARD-61, -69, -266, -2128, -2585) were reported from Dr. Wang's group at the University of Michigan (27–31). Their latest molecule, ARD-2585, is a potent (DC_{50} < 0.1 nM) oral agent and has at least 10-fold more potent than ARV-110 (27). These molecules differ in distinct E3 ligase binding domains, AR antagonists, and variable lengths of the linkers. Unfortunately, both ARV-110 and ARD-2585 molecules depend on binding with the AR LBD. Therefore, it is not effective on the AR splicing variants like AR-V7.

Other AR-targeted PROTAC molecules with animal testing data include TD-802 (DC_{50} = 12.5 nM) (32) and A031 (IC_{50} < 0.25 μM) (33) that promote degradation of the full-length AR protein. MTX-23 was shown to promote protein degradation of both the full-length and AR-V7 variant AR protein (DC_{50} = 0.37-2 μM) (34). In addition, three PROTAC molecules, A9/A16 (35, 36) and AR SNIPER-51 compounds (37), were only tested in cell culture models.

Other Unique Molecules for AR Degradation

UT-34 is a small molecule that exerts potent AR degradation activity *in vitro* (1-10 μM) and *in vivo via* ubiquitin-proteaseom pathway (38). It was optimized from its two previous versions, UT-69 and UT-155 (107). UT-34 binds with the AR N-terminal AF-1 domain and thus targets both the full-length and splicing variant proteins. UT-34 has a good pharmacological profile of oral bioavailability and suppressed xenograft tumor growth derived from Enzalutamide-resistant prostate cancer cells at a dose of 60 mg/kg/day (38).

Ailanthone was initially identified as an inhibitor of AR transactivation *via* a high throughput screening assay and was later found to induce protein degradation of both full-length and splicing variant AR proteins *via* targeting an HSP90 co-chaperon protein p23 (39). Ailanthone exhibited a strong anti-cancer effect in both *in vitro* cell culture models (0.2-0.4 μM) and *in vivo* xenograft models (2 mg/kg/day) of prostate cancer (39). It also showed excellent drug-like properties as tested in preclinical models (108, 109).

HG122 was identified as an inhibitor of AR activity *via* an MMTV-luciferase assay-based high throughput screening (40). HG122 suppressed AR-positive prostate cancer cell growth with an IC_{50} of 7-9 μM, compared to AR-negative cells at 20 μM. HG122 suppressed AR transcriptional activity and promoted AR degradation *via* the proteasome pathway. In animal experiments, HG122 suppressed 22RV1 cell-derived xenograft tumor growth by 82% at a dose of 10 mg/kg/day, compared to a 60% reduction by Enzalutamide at the exact dosing (40). However, it is unclear how HG122 promoted AR degradation by the proteasome machinery.

AR Splicing Variant V7-Specific Degraders and Inhibitors

The full-length AR protein has four distinct domains, N-terminal (NTD), DNA-binding (DBD), hinge region, and C-terminal ligand-binding (LBD). In prostate cancers, the transcriptional splicing variants of the AR gene have been linked to castration-resistance of prostate cancer after ADT and anti-AR therapy with Enzalutamide and Abiraterone (110–112). Because these AR variant proteins lack the AR C-terminal LBD region due to gene splicing truncated or deleted, they are not responding to current anti-AR drugs that target the LBD. Therefore, those PROTAC molecules using the LBD ligands are not working on these splicing variant AR proteins (113–115). These variant proteins represent a massive obstacle to clinical management in advanced prostate cancers.

Niclosamide is an FDA-approved oral anti-helminthic drug used to treat parasitic infections. In an AR-V7-driven luciferase-based high-throughput screening assay, Niclosamide was identified as an effective inhibitor of AR-V7 activity. A mechanistic study showed that it enhanced the AR-V7 protein degradation *via* the ubiquitin-proteasome pathway in prostate cancer cells at 0.5-1.0 μM without affecting the full-length AR protein (116). Combinational treatment with Enzalutamide and Niclosamide suppressed CRPC xenograft tumor growth in mice at a dose of 25 mg/kg/day (117). Although the first clinical trial (NCT02532114) with a single dose of Niclosamide was failed in reaching the effective serum concentration (118), a recent phase-Ib trial with reformulated Niclosamide plus Abiraterone achieved the proposed clinical benefit (119),

representing a new hope for AR-V7 positive CRPC patients (NCT03123978/NCT02807805).

CUDC-101 is a small molecule of inhibitor for multiple targets, including histone deacetylase (HDAC), epidermal growth factor receptor (EGFR) and HER2/Neu. It was recently found to inhibit the transcriptional activities of the full-length AR and AR-v7 protein (0.3 μM for 24 h) *via* a HDAC-related mechanism in prostate cancer 22RV1 cells (41). It also suppressed 22RV1 cell-derived xenograft tumor growth in nude mice at a dose of 50 mg/kg/day for 14 days (41). However, severe side effects will be expected in a clinical test due to its action on multiple targets.

ASC-J9 is a curcumin analog (dimethyl-curcumin) with multiple protein targets (120–125), including the AR proteins (42–44). ASC-J9 induced protein degradation of the full-length AR and AR-V7 proteins *via* the ubiquitin-proteasome pathway in prostate cancer cells (44) and suppressed xenograft tumor growth derived from CRPC cells (42, 45). It overcame Enzalutamide resistance in preclinical CRPC xenograft models (46) and sensitized prostate cancers to radiation therapy in animal models (47). However, ASC-J9 was only tested in clinical trials for skin acne care (NCT01289574 and NCT00525499).

Thailanstatins are bacteria-derived natural products with potent inhibitory activity toward pre-mRNA splicing events (48). Since AR-V7 is mainly generated by pre-mRNA splicing (49), Thailanstatin D (TST-D) was tested in AR-V7 positive prostate cancer cells for cytotoxicity. TST-D was shown to reduce AR-V7 mRNA and protein levels (at 5 nM concentration) by disrupting the U2AF65/SAP155 splicing complex that is critical for the AR-V7 pre-mRNA expression and suppressed CRPC cell-derived xenograft tumor growth (50% inhibition at 0.3 mg/kg/day after four days) (50). It is postulated that combinational treatment of TST-D with Enzalutamide or Abiraterone might achieve a more profound anti-tumor effect in CRPC models.

Rutaecarpine is a cardiovascular protective alkaloid extracted from the Chinese medicine *Evodia rutaecarpa* (126). It was identified as a potent AR-V7 inhibitor in an AR-V7-driven luciferase screening assay (51). A mechanistic study revealed that Rutaecarpine promoted AR-V7 degradation by enhancing AR-V7 interaction with GPR78 and ubiquitin E3 ligase SIAH2. Its DC_{50} for AR-V7 degradation was about 20 μM and completely blocked 22RV1 cell-derived xenograft tumor growth in nude mice at 40 mg/kg/2day (51). Since it also did not affect the full-length AR protein, it is needed to test its synergistic effect with AR antagonists like Enzalutamide and Abiraterone *in vivo*.

Indisulam belongs to a new class of compound sulfonamide with potential antineoplastic activity (127) *via* selectively degrading oncogenic proteins like pre-mRNA splicing factor RBM39 (52). Because pre-mRNA splicing is critical for AR-V7 expression, Indisulam was shown to suppress AR-V7 expression *via* RBM39-dependent mechanism. Indisulam treatment blocked Enzalutamide-induced AR-V7 expression in VCaP cells (10 μM concentration) and suppressed VCaP cell-derived xenograft tumor growth in nude mice at a dose of 25 mk/kg/day (52).

Nobiletin is a plant flavonoid extracted from *citrus peels* and possesses broad anti-cancer activity (128, 129). A recent study showed that Nobiletin moderately reduced AR-V7 protein level in 22RV-1 cells at 20 μM concentration and synergistically suppressed (at 40 mg/kg/2day) 22RV1 cell-derived xenograft tumor growth with Enzalutamide (20 mg/kg/2day) (53). The mechanistic study revealed that Nobiletin disrupted AR-V7 interaction with two deubiquitinases, USP14 and USP22, leading to proteasome-based AR-V7 degradation (53).

AR N-TERMINAL SPECIFIC INHIBITORS

In contrast to the CTD, the AR NTD has very few mutations without truncation (130). For example, the cBioportal database showed only 9 (0.145%) point-mutations identified from the NTD regions in 6334 prostate cancer specimens. There are two transactivation unit (TAU-1, aa100-370) and TAU-5 (aa360-485) motifs within the AR NTD (131). The TAU-1 motif is critical for the full-length AR activation after ligand binding, while the TAU-5 motif functions as a constitutive active motif for truncated AR protein (e.g., AR-V7) (132, 133). Especially, the TAU-1/TAU-5 motifs are rarely mutated or deleted in prostate cancer patients, making them a feasible target for prostate cancer therapy (130).

EPI series compounds are the first class of AR NTD inhibitors. The first compound EPI-001 was identified by screening a library of marine sponge extracts to inhibit AR NTD transactivation activity (134). EPI-001 binds to the TAU-5 motif and inhibits AR NTD activity at a relatively high dose (>25 μM in cell culture models) (135, 136). EPI compounds also suppressed tumor growth in VCaP and LNCaP95 cell-derived xenograft models at 100-200 mg/kg/day doses (135, 137). Although the older EPI compounds did not affect AR protein levels (the full length and AV variants), the new analog EPI-7170 suppressed AR-V7 expression in CRPC cells (138). EPI-002 (commercial name Ralaniten) is one of the four EPI-001 stereoisomers, and its pro-drug EPI-506 (Ralaniten acetate) was failed in a phase-I clinical trial due to excessive pill burden and poor oral bioavailability (139, 140). The newest analog, EPI-7386, showed 20-fold higher anti-androgenic potency than Ralaniten (141), and it is being tested in clinical trials in combination with Enzalutamide (NCT05075577/NCT04421222).

QW07 is a small synthetic molecule identified as an AR NTD-specific inhibitor *via* an AR-NTD-driven luciferase high-throughput screening (54). QW07 suppressed the activity of AR full-length and splicing variants at 5-8 μM in prostate cancer cells, which is more potent than EPI-001 (54). QW07 binds with the AR NTD directly and suppresses AR recruitment onto the target gene promoter. In animal xenograft experiments, QW07 inhibited tumor growth derived from prostate cancer 22RV1 and VCaP cells at a dose of 40 mg/kg/day, similar to EPI-001. However, QW07 did not affect AR protein expression (the full length or splicing variants).

AR NUCLEAR TRANSLOCATION BLOCKERS

As a transcription factor, the AR proteins translocate into the nuclear compartment after being activated by the androgens (5).

In the nuclear, AR protein interacts with the androgen response elements in the gene promoter region to modulate gene expression. The AR protein has one nuclear localization sequence or signal (NLS) in each domain, the NTD region (aa294-556), the DBD-hinge region (aa617-633), and the LBD region (aa666-919) (142–144). In the absence of androgens, the AR protein is exported from the nuclear compartment *via* its nuclear export signal (NES, aa743-817) within the LBD region (145). In CRPC tissue or cells that androgen levels are deficient due to androgen deprivation therapy, the NLS in the NTD region is responsible for AR nuclear localization (143). Blocking AR nuclear translocation with a potent NLS inhibitor is feasible to suppress prostate cancer development and progression by shutting down AR-modulated gene expression.

EPPI and CPPI are small molecules identified as inhibitors of AR nuclear translocation in Dr. Z Wang's lab using a 2GFP-AR fusing protein-based high-throughput screening approach (55). Both EPPI and CPPI at 25 μM inhibited AR nuclear localization in prostate cancer cells, which was reversed when the androgen level (R1881) was over 1.0 nM level, a physiological androgen concentration (56). Also, CPPI at a 50 mg/kg/day dose suppressed tumor growth in LNCaP but not PC-3 cell-derived xenograft models with or without castration, indicating an AR-specific effect (56). Further analysis revealed that CPPI blocked AR nuclear import and promoted AR degradation in the nuclear compartment through MDM2-dependent proteasome mechanism in CRPC cells (C4-2 and LNCaP95) and xenograft tumor models, leading to sharp retardation of tumor growth (57). No effect was observed for CPPI or EPPI on the AR variant proteins (57).

IMPPE (SID3712502) was another small molecule identified from the 2GFP-AR fusing protein screening assay with a robust inhibitory effect at 2.0 μM concentration on AR nuclear translocation and its downstream target PSA gene expression, plus downregulation of AR gene expression at a higher concentration of 10 μM (55). Further study found that IMPPE inhibited both full-length and LBD-lacking AR activity at a relatively high dose (>10 μM) and suppressed 22RV1 but not PC-3 cell-derived xenograft tumor growth at a dose of 25 mg/kg/day in castrated nude mice (58).

JJ-450 is an IMPPE scaffold analog with higher potency and better physicochemical properties (59). JJ-450 at 10 μM concentration inhibited both the transcriptional activities of the full-length and splicing variant AR proteins in CRPC cells by blocking AR binding to its target gene promoter without affecting AR protein levels (59). In CRPC xenograft models derived from 22RV1 and VCaP cells, JJ-450 at 10 mg/kg/day dose suppressed xenograft tumor growth by 60%, slightly better than Enzalutamide (59). Especially, JJ-450 was found to block the nuclear translocation and activity of the AR F876L mutant protein identified from Enzalutamide-resistant CRPC patients and LNCaP cells after long-term exposure to Enzalutamide (60–62).

AR DBDH ANTAGONISTS

The AR DBD-Hinge region has P-box and D-box motifs responsible for dimerization and DNA binding after androgen stimulation (146). Using a virtual *in-silico* drug design approach (63–65), a surface-exposed region (aa579-610) on the AR DBDH domain was discovered as a potential target site by small-molecule compounds, including VPC-14228 and VPC-14449 (66). These two compounds at 10 μM concentration selectively suppressed AR (full-length and splicing variant proteins) but not ER or GR activity by blocking AR interaction with the target gene promoters without affecting AR nuclear translocation and protein stability (66). In LNCaP cell-derived xenograft experiments, VPC-1449 at 100 mg/kg/day dose suppressed tumor growth at a similar extent as Enzalutamide (10 mg/kg/day) (66).

CONCLUSION AND PERSPECTIVES

The AR protein is critical for prostate cancer progression by transcriptionally modulating gene expression after activation by androgens *via* binding on its LBD. Metastatic prostate cancers are initially treated with androgen deprivation or castration therapies (surgical or medical) based on the findings reported about 80-years ago. However, this androgen removal approach is not curative for prostate cancers, and the diseases often relapse and progress to the CRPC stage. Since most of these CRPCs are still AR addictive, current clinical therapies mainly focus on blocking androgen to bind with the AR LBD (AR antagonists) or reducing androgen production (CYP17a1 inhibitors) in non-testis tissues, including prostate cancer tissues. However, treatment resistance eventually develops in part due to AR gene mutation and mRNA splicing events (e.g., AR-V7) in virtually all CRPC patients. Furthermore, after long-term treatment with AR antagonists, up to 20% of CRPC patients will develop an even more aggressive subtype, neuroendocrinal prostate cancer (NEPC). Therefore, the androgen removal and blockage approach are non-curative and leads to a more aggressive disease.

To overcome this obstacle of treatment resistance, research has shifted from androgens to the AR protein in the last 20 years (**Figure 1**). The initial approach was the antisense oligonucleotides (ASO) targeting the AR mRNA to reduce AR protein production in prostate cancer cells. Due to the inhibitory nature of the ASO approach on protein production, tumor growth was only suppressed but not eradicated in xenograft models. In contrast, our group used the siRNA approach that efficiently eliminated the AR protein from prostate cancer cells. Nanoparticle-loaded AR siRNA resulted in xenograft tumor regression and eradication owing to robust cell death after AR protein removal in prostate cancer cells. Unfortunately, this AR siRNA project was stalled due to a failure in the patent application.

Targeting AR protein stability has emerged in recent years as the hotspot in developing new therapeutics for advanced prostate cancers, and several small molecules were reported to reduce AR protein stability. The curcumin analog ASC-J9, Ailanthone, HG122, and CUDC-101 induced AR protein degradation in prostate cancer cells. However, the AR or prostate cancer tissue specificity is not established with these small molecules.

The PROTAC technique for AR-specific degradation showed a promising result. The AR PROTAC ARV-110 is tested as a combinational treatment with Abiraterone in a clinical trial. However, these AR CTD-targeting PROTACs utilized AR LBD ligands, and therefore, they are inactive on AR CTD splicing variants, a critical mechanism for treatment resistance in CRPC patients. Interestingly, some other agents specifically targeted the AR-V7 variant for degradation, including Niclosamide, CUDC-101, Thailanstatins, Rutaecarpine, Indisulam, and Nobiletin. Combining AR antagonists, PROTAC molecules, and AR-V7 inhibitors might provide synergistic effects in the clinic.

Targeting AR NTD is another approach to bypass AR CTD splicing defects. The first generation of AR NTD inhibitor EPI compounds was failed in clinical trials due to excessive bill burden. The second generation of EPI compound with 20-fold higher potency is being tested as a combinational treatment with Enzalutamide in a clinical trial. UT-34 targets the AR NTD and is also waiting for a clinical test.

AR nuclear translocation is an important event for its activity as a transcription factor. Two novel compounds, IMPPE and JJ-450, were recently developed to block AR nuclear translocation. These two compounds showed a very permissive result in animal models. In addition, an AR DBD blocking agent VPC-14449 was reported to suppress AR interaction with its target gene promoter in the nuclear compartment and was found to suppress tumor growth in mice. These compounds are all needed for clinical testing.

AR activity is only temporally suppressed during prostate cancer treatment by androgen deprivation and AR antagonists. Due to these treatment stresses, prostate cancer cells used other cellular signal pathways and/or splicing variants for AR reactivation, resulting in treatment resistance. Therefore, complete removal of the AR protein from prostate cancer cells will eliminate all events of AR reactivation after ADT and anti-AR therapy. Especially in the early phase of treatment, most prostate cancer cells are still AR-dependent. Simultaneously removal of the AR protein and androgens will result in robust cell death, leading to a possible curative result or long-term disease-free survival. In addition, early reduction of the AR protein in the androgen-responsive phase of prostate cancer will reduce the likelihood of transcriptional reprogramming (88, 93, 147). Also, tissue-specific delivery of the AR protein degradation agents will restrict potential side effects.

AUTHOR CONTRIBUTIONS

All authors participated in drafting the manuscript. All authors contributed to the article and approved the submitted version.

FUNDING

This work was partially supported by a grant from KUMC Lied pilot program and DoD PCRP PC190026 to Benyi Li, MD/PhD.

ACKNOWLEDGMENTS

We are grateful for all the talented investors who developed those elegant AR-targeted agents. We are also sorry for not citing all the reports in the field due to the limited space in this mini-review article.

REFERENCES

1. Siegel RL, Miller KD, Fuchs HE, Jemal A. Cancer Statistics, 2022. *CA Cancer J Clin* (2022) 72(1):7–33. doi: 10.3322/caac.21708
2. Pagliuca M, Buonerba C, Fizazi K, Di Lorenzo G. The Evolving Systemic Treatment Landscape for Patients With Advanced Prostate Cancer. *Drugs* (2019) 79(4):381–400. doi: 10.1007/s40265-019-1060-5
3. Huggins C. Prostatic Cancer Treated by Orchiectomy; the Five Year Results. *J Am Med Assoc* (1946) 131:576–81. doi: 10.1001/jama.1946.02870240008003
4. Van Poppel H, Abrahamsson PA. Considerations for the Use of Gonadotropin-Releasing Hormone Agonists and Antagonists in Patients With Prostate Cancer. *Int J Urol* (2020) 27(10):830–37. doi: 10.1111/iju.14303
5. Estebanez-Perpina E, Bevan CL, McEwan IJ. Eighty Years of Targeting Androgen Receptor Activity in Prostate Cancer: The Fight Goes on. *Cancers (Basel)* (2021) 13(3):509–27. doi: 10.3390/cancers13030509
6. Di Fusco D, Dinallo V, Marafini I, Figliuzzi MM, Romano B, Monteleone G. Antisense Oligonucleotide: Basic Concepts and Therapeutic Application in Inflammatory Bowel Disease. *Front Pharmacol* (2019) 10:305. doi: 10.3389/fphar.2019.00305
7. Eder IE, Culig Z, Ramoner R, Thurnher M, Putz T, Nessler-Menardi C, et al. Inhibition of LncaP Prostate Cancer Cells by Means of Androgen Receptor Antisense Oligonucleotides. *Cancer Gene Ther* (2000) 7(7):997–1007. doi: 10.1038/sj.cgt.7700202
8. Eder IE, Hoffmann J, Rogatsch H, Schafer G, Zopf D, Bartsch G, et al. Inhibition of LNCaP Prostate Tumor Growth *In Vivo* by an Antisense Oligonucleotide Directed Against the Human Androgen Receptor. *Cancer Gene Ther* (2002) 9(2):117–25. doi: 10.1038/sj.cgt.7700416
9. Ko YJ, Devi GR, London CA, Kayas A, Reddy MT, Iversen PL, et al. Androgen Receptor Down-Regulation in Prostate Cancer With Phosphorodiamidate Morpholino Antisense Oligomers. *J Urol* (2004) 172(3):1140–4. doi: 10.1097/01.ju.0000134698.87862.e6
10. Hamy F, Brondani V, Spoerri R, Rigo S, Stamm C, Klimkait T. Specific Block of Androgen Receptor Activity by Antisense Oligonucleotides. *Prostate Cancer Prostat Dis* (2003) 6(1):27–33. doi: 10.1038/sj.pcan.4500603
11. Yamamoto Y, Lin PJ, Beraldi E, Zhang F, Kawai Y, Leong J, et al. siRNA Lipid Nanoparticle Potently Silences Clusterin and Delays Progression When Combined With Androgen Receptor Cotargeting in Enzalutamide-Resistant Prostate Cancer. *Clin Cancer Res* (2015) 21(21):4845–55. doi: 10.1158/1078-0432.CCR-15-0866
12. Yamamoto Y, Loriot Y, Beraldi E, Zhang F, Wyatt AW, Al Nakouzi N, et al. Generation 2.5 Antisense Oligonucleotides Targeting the Androgen Receptor and Its Splice Variants Suppress Enzalutamide-Resistant Prostate Cancer Cell Growth. *Clin Cancer Res* (2015) 21(7):1675–87. doi: 10.1158/1078-0432.CCR-14-1108
13. Xiao L, Tien JC, Vo J, Tan M, Parolia A, Zhang Y, et al. Epigenetic Reprogramming With Antisense Oligonucleotides Enhances the Effectiveness of Androgen Receptor Inhibition in Castration-Resistant Prostate Cancer. *Cancer Res* (2018) 78(20):5731–40. doi: 10.1158/0008-5472.CAN-18-0941
14. De Velasco MA, Kura Y, Sakai K, Hatanaka Y, Davies BR, Campbell H, et al. Targeting Castration-Resistant Prostate Cancer With Androgen Receptor Antisense Oligonucleotide Therapy. *JCI Insight* (2019) 4(17):e122688–711. doi: 10.1172/jci.insight.122688
15. Liao X, Tang S, Thrasher JB, Griebling TL, Li B. Small-Interfering RNA-Induced Androgen Receptor Silencing Leads to Apoptotic Cell Death in

Prostate Cancer. *Mol Cancer Ther* (2005) 4(4):505–15. doi: 10.1158/1535-7163.MCT-04-0313
16. Yang J, Xie SX, Huang Y, Ling M, Liu J, Ran Y, et al. Prostate-Targeted Biodegradable Nanoparticles Loaded With Androgen Receptor Silencing Constructs Eradicate Xenograft Tumors in Mice. *Nanomed (Lond)* (2012) 7 (9):1297–309. doi: 10.2217/nnm.12.14
17. Sun A, Tang J, Terranova PF, Zhang X, Thrasher JB, Li B. Adeno-Associated Virus-Delivered Short Hairpin-Structured RNA for Androgen Receptor Gene Silencing Induces Tumor Eradication of Prostate Cancer Xenografts in Nude Mice: A Preclinical Study. *Int J Cancer* (2010) 126(3):764–74. doi: 10.1002/ijc.24778
18. Luna Velez MV, Verhaegh GW, Smit F, Sedelaar JPM, Schalken JA. Suppression of Prostate Tumor Cell Survival by Antisense Oligonucleotide-Mediated Inhibition of AR-V7 mRNA Synthesis. *Oncogene* (2019) 38(19):3696–709. doi: 10.1038/s41388-019-0696-7
19. Lee JB, Zhang K, Tam YY, Tam YK, Belliveau NM, Sung VY, et al. Lipid Nanoparticle siRNA Systems for Silencing the Androgen Receptor in Human Prostate Cancer In Vivo. *Int J Cancer* (2012) 131(5):E781–90. doi: 10.1002/ijc.27361
20. Snoek R, Cheng H, Margiotti K, Wafa LA, Wong CA, Wong EC, et al. *In Vivo* Knockdown of the Androgen Receptor Results in Growth Inhibition and Regression of Well-Established, Castration-Resistant Prostate Tumors. *Clin Cancer Res* (2009) 15(1):39–47. doi: 10.1158/1078-0432.CCR-08-1726
21. Cheng H, Snoek R, Ghaidi F, Cox ME, Rennie PS. Short Hairpin RNA Knockdown of the Androgen Receptor Attenuates Ligand-Independent Activation and Delays Tumor Progression. *Cancer Res* (2006) 66 (21):10613–20. doi: 10.1158/0008-5472.CAN-06-0028
22. Haag P, Bektic J, Bartsch G, Klocker H, Eder IE. Androgen Receptor Down Regulation by Small Interference RNA Induces Cell Growth Inhibition in Androgen Sensitive as Well as in Androgen Independent Prostate Cancer Cells. *J Steroid Biochem Mol Biol* (2005) 96(3-4):251–8. doi: 10.1016/j.jsbmb.2005.04.029
23. Compagno D, Merle C, Morin A, Gilbert C, Mathieu JR, Bozec A, et al. SIRNA-Directed *In Vivo* Silencing of Androgen Receptor Inhibits the Growth of Castration-Resistant Prostate Carcinomas. *PloS One* (2007) 2 (10):e1006. doi: 10.1371/journal.pone.0001006
24. Schneekloth JS Jr, Fonseca FN, Koldobskiy M, Mandal A, Deshaies R, Sakamoto K, et al. Chemical Genetic Control of Protein Levels: Selective *In Vivo* Targeted Degradation. *J Am Chem Soc* (2004) 126(12):3748–54. doi: 10.1021/ja039025z
25. Salami J, Alabi S, Willard RR, Vitale NJ, Wang J, Dong H, et al. Androgen Receptor Degradation by the Proteolysis-Targeting Chimera ARCC-4 Outperforms Enzalutamide in Cellular Models of Prostate Cancer Drug Resistance. *Commun Biol* (2018) 1:100. doi: 10.1038/s42003-018-0105-8
26. Snyder LB, Neklesa TK, Chen X, Dong H, Ferraro C, Gordon DA, et al. Discovery of ARV-110, a First in Class Androgen Receptor Degrading PROTAC for the Treatment of Men With Metastatic Castration Resistant Prostate Cancer. *Cancer Res* (2021) 81(13_Supplement):43. doi: 10.1158/1538-7445.AM2021-43
27. Xiang W, Zhao L, Han X, Qin C, Miao B, McEachern D, et al. Discovery of ARD-2585 as an Exceptionally Potent and Orally Active PROTAC Degrader of Androgen Receptor for the Treatment of Advanced Prostate Cancer. *J Med Chem* (2021) 64(18):13487–509. doi: 10.1021/acs.jmedchem.1c00900
28. Han X, Wang C, Qin C, Xiang W, Fernandez-Salas E, Yang CY, et al. Discovery of ARD-69 as a Highly Potent Proteolysis Targeting Chimera (PROTAC) Degrader of Androgen Receptor (AR) for the Treatment of Prostate Cancer. *J Med Chem* (2019) 62(2):941–64. doi: 10.1021/acs.jmedchem.8b01631
29. Han X, Zhao L, Xiang W, Qin C, Miao B, McEachern D, et al. Strategies Toward Discovery of Potent and Orally Bioavailable Proteolysis Targeting Chimera Degraders of Androgen Receptor for the Treatment of Prostate Cancer. *J Med Chem* (2021) 64(17):12831–54. doi: 10.1021/acs.jmedchem.1c00882
30. Zhao L, Han X, Lu J, McEachern D, Wang S. A Highly Potent PROTAC Androgen Receptor (AR) Degrader ARD-61 Effectively Inhibits AR-Positive Breast Cancer Cell Growth *In Vitro* and Tumor Growth In Vivo. *Neoplasia* (2020) 22(10):522–32. doi: 10.1016/j.neo.2020.07.002
31. Han X, Zhao L, Xiang W, Qin C, Miao B, Xu T, et al. Discovery of Highly Potent and Efficient PROTAC Degraders of Androgen Receptor (AR) by Employing Weak Binding Affinity VHL E3 Ligase Ligands. *J Med Chem* (2019) 62(24):11218–31. doi: 10.1021/acs.jmedchem.9b01393
32. Takwale AD, Jo SH, Jeon YU, Kim HS, Shin CH, Lee HK, et al. Design and Characterization of Cereblon-Mediated Androgen Receptor Proteolysis-Targeting Chimeras. *Eur J Med Chem* (2020) 208:112769. doi: 10.1016/j.ejmech.2020.112769
33. Chen L, Han L, Mao S, Xu P, Xu X, Zhao R, et al. Discovery of A031 as Effective Proteolysis Targeting Chimera (PROTAC) Androgen Receptor (AR) Degrader for the Treatment of Prostate Cancer. *Eur J Med Chem* (2021) 216:113307. doi: 10.1016/j.ejmech.2021.113307
34. Lee GT, Nagaya N, Desantis J, Madura K, Sabaawy HE, Kim WJ, et al. Effects of MTX-23, a Novel PROTAC of Androgen Receptor Splice Variant-7 and Androgen Receptor, on CRPC Resistant to Second-Line Antiandrogen Therapy. *Mol Cancer Ther* (2021) 20(3):490–9. doi: 10.1158/1535-7163.MCT-20-0417
35. Xie H, Liang JJ, Wang YL, Hu TX, Wang JY, Yang RH, et al. The Design, Synthesis and Anti-Tumor Mechanism Study of New Androgen Receptor Degrader. *Eur J Med Chem* (2020) 204:112512. doi: 10.1016/j.ejmech.2020.112512
36. Liang JJ, Xie H, Yang RH, Wang N, Zheng ZJ, Zhou C, et al. Designed, Synthesized and Biological Evaluation of Proteolysis Targeting Chimeras (PROTACs) as AR Degraders for Prostate Cancer Treatment. *Bioorg Med Chem* (2021) 45:116331. doi: 10.1016/j.bmc.2021.116331
37. Shibata N, Nagai K, Morita Y, Ujikawa O, Ohoka N, Hattori T, et al. Development of Protein Degradation Inducers of Androgen Receptor by Conjugation of Androgen Receptor Ligands and Inhibitor of Apoptosis Protein Ligands. *J Med Chem* (2018) 61(2):543–75. doi: 10.1021/acs.jmedchem.7b00168
38. Ponnusamy S, He Y, Hwang DJ, Thiyagarajan T, Houtman R, Bocharova V, et al. Orally Bioavailable Androgen Receptor Degrader, Potential Next-Generation Therapeutic for Enzalutamide-Resistant Prostate Cancer. *Clin Cancer Res* (2019) 25(22):6764–80. doi: 10.1158/1078-0432.CCR-19-1458
39. He Y, Peng S, Wang J, Chen H, Cong X, Chen A, et al. Ailanthone Targets P23 to Overcome MDV3100 Resistance in Castration-Resistant Prostate Cancer. *Nat Commun* (2016) 7:13122–35. doi: 10.1038/ncomms13122
40. Cong X, He Y, Wu H, Wang D, Liu Y, Shao T, et al. Regression of Castration-Resistant Prostate Cancer by a Novel Compound Hg122. *Front Oncol* (2021) 11:650919. doi: 10.3389/fonc.2021.650919
41. Sun H, Mediwala SN, Szafran AT, Mancini MA, Marcelli M. CUDC-101, a Novel Inhibitor of Full-Length Androgen Receptor (flAR) and Androgen Receptor Variant 7 (AR-V7) Activity: Mechanism of Action and *In Vivo* Efficacy. *Horm Cancer* (2016) 7(3):196–210. doi: 10.1007/s12672-016-0257-2
42. Yamashita S, Lai KP, Chuang KL, Xu D, Miyamoto H, Tochigi T, et al. ASC-J9 Suppresses Castration-Resistant Prostate Cancer Growth Through Degradation of Full-Length and Splice Variant Androgen Receptors. *Neoplasia* (2012) 14(1):74–83. doi: 10.1593/neo.111436
43. Wang R, Lin W, Lin C, Li L, Sun Y, Chang C. ASC-J9((R)) Suppresses Castration Resistant Prostate Cancer Progression *via* Degrading the Enzalutamide-Induced Androgen Receptor Mutant AR-F876L. *Cancer Lett* (2016) 379(1):154–60. doi: 10.1016/j.canlet.2016.05.018
44. Lai KP, Huang CK, Chang YJ, Chung CY, Yamashita S, Li L, et al. New Therapeutic Approach to Suppress Castration-Resistant Prostate Cancer Using ASC-J9 *via* Targeting Androgen Receptor in Selective Prostate Cells. *Am J Pathol* (2013) 182(2):460–73. doi: 10.1016/j.ajpath.2012.10.029
45. Cheng MA, Chou FJ, Wang K, Yang R, Ding J, Zhang Q, et al. Androgen Receptor (AR) Degradation Enhancer ASC-J9((R)) in an FDA-Approved Formulated Solution Suppresses Castration Resistant Prostate Cancer Cell Growth. *Cancer Lett* (2018) 417:182–91. doi: 10.1016/j.canlet.2017.11.038
46. Wang R, Sun Y, Li L, Niu Y, Lin W, Lin C, et al. Preclinical Study Using Malat1 Small Interfering RNA or Androgen Receptor Splicing Variant 7 Degradation Enhancer ASC-J9((R)) to Suppress Enzalutamide-Resistant Prostate Cancer Progression. *Eur Urol* (2017) 72(5):835–44. doi: 10.1016/j.eururo.2017.04.005
47. Chou FJ, Chen Y, Chen D, Niu Y, Li G, Keng P, et al. Preclinical Study Using Androgen Receptor (AR) Degradation Enhancer to Increase Radiotherapy Efficacy *via* Targeting Radiation-Increased AR to Better Suppress Prostate Cancer Progression. *EBioMedicine* (2019) 40:504–16. doi: 10.1016/j.ebiom.2018.12.050

48. Liu X, Biswas S, Berg MG, Antapli CM, Xie F, Wang Q, et al. Genomics-Guided Discovery of Thailanstatins A, B, and C As pre-mRNA Splicing Inhibitors and Antiproliferative Agents From Burkholderia Thailandensis Msmb43. *J Nat Prod* (2013) 76(4):685–93. doi: 10.1021/np300913h
49. Dehm SM, Tindall DJ. Alternatively Spliced Androgen Receptor Variants. *Endocr Relat Cancer* (2011) 18(5):R183–96. doi: 10.1530/ERC-11-0141
50. Wang B, Lo UG, Wu K, Kapur P, Liu X, Huang J, et al. Developing New Targeting Strategy for Androgen Receptor Variants in Castration Resistant Prostate Cancer. *Int J Cancer* (2017) 141(10):2121–30. doi: 10.1002/ijc.30893
51. Liao Y, Liu Y, Xia X, Shao Z, Huang C, He J, et al. Targeting GRP78-Dependent AR-V7 Protein Degradation Overcomes Castration-Resistance in Prostate Cancer Therapy. *Theranostics* (2020) 10(8):3366–81. doi: 10.7150/thno.41849
52. Melnyk JE, Steri V, Nguyen HG, Hann B, Feng FY, Shokat KM. The Splicing Modulator Sulfonamide Indisulam Reduces AR-V7 in Prostate Cancer Cells. *Bioorg Med Chem* (2020) 28(20):115712. doi: 10.1016/j.bmc.2020.115712
53. Liu Y, Yu C, Shao Z, Xia X, Hu T, Kong W, et al. Selective Degradation of AR-V7 to Overcome Castration Resistance of Prostate Cancer. *Cell Death Dis* (2021) 12(10):857. doi: 10.1038/s41419-021-04162-0
54. Peng S, Wang J, Chen H, Hu P, He XL, He Y, et al. Regression of Castration-Resistant Prostate Cancer by a Novel Compound QW07 Targeting Androgen Receptor N-Terminal Domain. *Cell Biol Toxicol* (2020) 36 (5):399–416. doi: 10.1007/s10565-020-09511-x
55. Johnston PA, Nguyen MM, Dar JA, Ai J, Wang Y, Masoodi KZ, et al. Development and Implementation of a High-Throughput High-Content Screening Assay to Identify Inhibitors of Androgen Receptor Nuclear Localization in Castration-Resistant Prostate Cancer Cells. *Assay Drug Dev Technol* (2016) 14(4):226–39. doi: 10.1089/adt.2016.716
56. Masoodi KZ, Xu Y, Dar JA, Eisermann K, Pascal LE, Parrinello E, et al. Inhibition of Androgen Receptor Nuclear Localization and Castration-Resistant Prostate Tumor Growth by Pyrroloimidazole-Based Small Molecules. *Mol Cancer Ther* (2017) 16(10):2120–9. doi: 10.1158/1535-7163.MCT-17-0176
57. Lv S, Song Q, Chen G, Cheng E, Chen W, Cole R, et al. Regulation and Targeting of Androgen Receptor Nuclear Localization in Castration-Resistant Prostate Cancer. *J Clin Invest* (2021) 131(4):e141335–50. doi: 10.1172/JCI141335
58. Masoodi KZ, Eisermann K, Yang Z, Dar JA, Pascal LE, Nguyen M, et al. Inhibition of Androgen Receptor Function and Level in Castration-Resistant Prostate Cancer Cells by 2-[(Isoxazol-4-Ylmethyl)Thio]-1-(4-Phenylpiperazin-1-Yl)Ethanone. *Endocrinology* (2017) 158(10):3152–61. doi: 10.1210/en.2017-00408
59. Yang Z, Wang D, Johnson JK, Pascal LE, Takubo K, Avula R, et al. A Novel Small Molecule Targets Androgen Receptor and Its Splice Variants in Castration-Resistant Prostate Cancer. *Mol Cancer Ther* (2020) 19(1):75–88. doi: 10.1158/1535-7163.MCT-19-0489
60. Wu Z, Wang K, Yang Z, Pascal LE, Nelson JB, Takubo K, et al. A Novel Androgen Receptor Antagonist JJ-450 Inhibits Enzalutamide-Resistant Mutant AR(F876L) Nuclear Import and Function. *Prostate* (2020) 80 (4):319–28. doi: 10.1002/pros.23945
61. Joseph JD, Lu N, Qian J, Sensintaffar J, Shao G, Brigham D, et al. A Clinically Relevant Androgen Receptor Mutation Confers Resistance to Second-Generation Antiandrogens Enzalutamide and ARN-509. *Cancer Discov* (2013) 3(9):1020–9. doi: 10.1158/2159-8290.CD-13-0226
62. Azad AA, Volik SV, Wyatt AW, Haegert A, Le Bihan S, Bell RH, et al. Androgen Receptor Gene Aberrations in Circulating Cell-Free DNA: Biomarkers of Therapeutic Resistance in Castration-Resistant Prostate Cancer. *Clin Cancer Res* (2015) 21(10):2315–24. doi: 10.1158/1078-0432.CCR-14-2666
63. Lack NA, Axerio-Cilies P, Tavassoli P, Han FQ, Chan KH, Feau C, et al. Targeting the Binding Function 3 (BF3) Site of the Human Androgen Receptor Through Virtual Screening. *J Med Chem* (2011) 54(24):8563–73. doi: 10.1021/jm201098n
64. Munuganti RS, Leblanc E, Axerio-Cilies P, Labriere C, Frewin K, Singh K, et al. Targeting the Binding Function 3 (BF3) Site of the Androgen Receptor Through Virtual Screening. 2. Development of 2-((2-Phenoxyethyl) Thio)-1h-Benzimidazole Derivatives. *J Med Chem* (2013) 56(3):1136–48. doi: 10.1021/jm3015712
65. Li H, Ren X, Leblanc E, Frewin K, Rennie PS, Cherkasov A. Identification of Novel Androgen Receptor Antagonists Using Structure- and Ligand-Based Methods. *J Chem Inf Model* (2013) 53(1):123–30. doi: 10.1021/ci300514v
66. Dalal K, Roshan-Moniri M, Sharma A, Li H, Ban F, Hassona MD, et al. Selectively Targeting the DNA-Binding Domain of the Androgen Receptor as a Prospective Therapy for Prostate Cancer. *J Biol Chem* (2017) 292 (10):4359. doi: 10.1074/jbc.A117.553818
67. Xu J, Qiu Y. Current Opinion and Mechanistic Interpretation of Combination Therapy for Castration-Resistant Prostate Cancer. *Asian J Androl* (2019) 21(3):270–8. doi: 10.4103/aja.aja_10_19
68. Scher HI, Sawyers CL. Biology of Progressive, Castration-Resistant Prostate Cancer: Directed Therapies Targeting the Androgen-Receptor Signaling Axis. *J Clin Oncol* (2005) 23(32):8253–61. doi: 10.1200/JCO.2005.03.4777
69. Dai C, Heemers H, Sharifi N. Androgen Signaling in Prostate Cancer. *Cold Spring Harb Perspect Med* (2017) 7(9):a030452–5469. doi: 10.1101/cshperspect.a030452
70. Feng Q, He B. Androgen Receptor Signaling in the Development of Castration-Resistant Prostate Cancer. *Front Oncol* (2019) 9:858. doi: 10.3389/fonc.2019.00858
71. Crawford ED, Schellhammer PF, McLeod DG, Moul JW, Higano CS, Shore N, et al. Androgen Receptor Targeted Treatments of Prostate Cancer: 35 Years of Progress With Antiandrogens. *J Urol* (2018) 200(5):956–66. doi: 10.1016/j.juro.2018.04.083
72. Puca L, Vlachostergios PJ, Beltran H. Neuroendocrine Differentiation in Prostate Cancer: Emerging Biology, Models, and Therapies. *Cold Spring Harb Perspect Med* (2019) 9(2):a030593–612. doi: 10.1101/cshperspect.a030593
73. Niu Y, Guo C, Wen S, Tian J, Luo J, Wang K, et al. ADT With Antiandrogens in Prostate Cancer Induces Adverse Effect of Increasing Resistance, Neuroendocrine Differentiation and Tumor Metastasis. *Cancer Lett* (2018) 439:47–55. doi: 10.1016/j.canlet.2018.09.020
74. Huang YH, Zhang YQ, Huang JT. Neuroendocrine Cells of Prostate Cancer: Biologic Functions and Molecular Mechanisms. *Asian J Androl* (2019) 21 (3):291–5. doi: 10.4103/aja.aja_128_18
75. Wang Y, Wang Y, Ci X, Choi SYC, Crea F, Lin D, et al. Molecular Events in Neuroendocrine Prostate Cancer Development. *Nat Rev Urol* (2021) 18 (10):581–96. doi: 10.1038/s41585-021-00490-0
76. Zhang Y, Zheng D, Zhou T, Song H, Hulsurkar M, Su N, et al. Androgen Deprivation Promotes Neuroendocrine Differentiation and Angiogenesis Through CREB-EZH2-TSP1 Pathway in Prostate Cancers. *Nat Commun* (2018) 9(1):4080. doi: 10.1038/s41467-018-06177-2
77. Reina-Campos M, Linares JF, Duran A, Cordes T, L'Hermitte A, Badur MG, et al. Increased Serine and One-Carbon Pathway Metabolism by PKClambda/iota Deficiency Promotes Neuroendocrine Prostate Cancer. *Cancer Cell* (2019) 35(3):385–400.e9. doi: 10.1016/j.ccell.2019.01.018
78. Singh N, Ramnarine VR, Song JH, Pandey R, Padi SKR, Nouri M, et al. The Long Noncoding RNA H19 Regulates Tumor Plasticity in Neuroendocrine Prostate Cancer. *Nat Commun* (2021) 12(1):7349. doi: 10.1038/s41467-021-26901-9
79. Lee AR, Gan Y, Xie N, Ramnarine VR, Lovnicki JM, Dong X. Alternative RNA Splicing of the GIT1 Gene is Associated With Neuroendocrine Prostate Cancer. *Cancer Sci* (2019) 110(1):245–55. doi: 10.1111/cas.13869
80. VanDeusen HR, Ramroop JR, Morel KL, Bae SY, Sheahan AV, Sychev Z, et al. Targeting RET Kinase in Neuroendocrine Prostate Cancer. *Mol Cancer Res* (2020) 18(8):1176–88. doi: 10.1158/1541-7786.MCR-19-1245
81. Hu CY, Wu KY, Lin TY, Chen CC. The Crosstalk of Long Non-Coding RNA and MicroRNA in Castration-Resistant and Neuroendocrine Prostate Cancer: Their Interaction and Clinical Importance. *Int J Mol Sci* (2021) 23 (1):392–408. doi: 10.3390/ijms23010392
82. Enriquez C, Cancila V, Ferri R, Sulsenti R, Fischetti I, Milani M, et al. Castration-Induced Downregulation of SPARC in Stromal Cells Drives Neuroendocrine Differentiation of Prostate Cancer. *Cancer Res* (2021) 81 (16):4257–74. doi: 10.1158/0008-5472.CAN-21-0163
83. Baca SC, Takeda DY, Seo JH, Hwang J, Ku SY, Arafeh R, et al. Reprogramming of the FOXA1 Cistrome in Treatment-Emergent Neuroendocrine Prostate Cancer. *Nat Commun* (2021) 12(1):1979. doi: 10.1038/s41467-021-22139-7

84. Kim DH, Sun D, Storck WK, Welker Leng K, Jenkins C, Coleman DJ, et al. BET Bromodomain Inhibition Blocks an AR-Repressed, E2F1-Activated Treatment-Emergent Neuroendocrine Prostate Cancer Lineage Plasticity Program. *Clin Cancer Res* (2021) 27(17):4923–36. doi: 10.1158/1078-0432.CCR-20-4968
85. Li Y, Xie N, Chen R, Lee AR, Lovnicki J, Morrison EA, et al. RNA Splicing of the BHC80 Gene Contributes to Neuroendocrine Prostate Cancer Progression. *Eur Urol* (2019) 76(2):157–66. doi: 10.1016/j.eururo.2019.03.011
86. Guo H, Ci X, Ahmed M, Hua JT, Soares F, Lin D, et al. ONECUT2 is a Driver of Neuroendocrine Prostate Cancer. *Nat Commun* (2019) 10(1):278. doi: 10.1038/s41467-018-08133-6
87. Lee AR, Gan Y, Tang Y, Dong X. A Novel Mechanism of SRRM4 in Promoting Neuroendocrine Prostate Cancer Development *via* a Pluripotency Gene Network. *EBioMedicine* (2018) 35:167–77. doi: 10.1016/j.ebiom.2018.08.011
88. Gritsina G, Gao WQ, Yu J. Transcriptional Repression by Androgen Receptor: Roles in Castration-Resistant Prostate Cancer. *Asian J Androl* (2019) 21(3):215–23. doi: 10.4103/aja.aja_19_19
89. Cejas P, Xie Y, Font-Tello A, Lim K, Syamala S, Qiu X, et al. Subtype Heterogeneity and Epigenetic Convergence in Neuroendocrine Prostate Cancer. *Nat Commun* (2021) 12(1):5775. doi: 10.1038/s41467-021-26042-z
90. Liu Q, Pang J, Wang LA, Huang Z, Xu J, Yang X, et al. Histone Demethylase PHF8 Drives Neuroendocrine Prostate Cancer Progression by Epigenetically Upregulating Foxa2. *J Pathol* (2021) 253(1):106–18. doi: 10.1002/path.5557
91. Ge R, Wang Z, Montironi R, Jiang Z, Cheng M, Santoni M, et al. Epigenetic Modulations and Lineage Plasticity in Advanced Prostate Cancer. *Ann Oncol* (2020) 31(4):470–9. doi: 10.1016/j.annonc.2020.02.002
92. Davies A, Zoubeidi A, Selth LA. The Epigenetic and Transcriptional Landscape of Neuroendocrine Prostate Cancer. *Endocr Relat Cancer* (2020) 27(2):R35–50. doi: 10.1530/ERC-19-0420
93. Berger A, Brady NJ, Bareja R, Robinson B, Conteduca V, Augello MA, et al. N-Myc-Mediated Epigenetic Reprogramming Drives Lineage Plasticity in Advanced Prostate Cancer. *J Clin Invest* (2019) 129(9):3924–40. doi: 10.1172/JCI127961
94. Vickman RE, Franco OE, Moline DC, Vander Griend DJ, Thumbikat P, Hayward SW. The Role of the Androgen Receptor in Prostate Development and Benign Prostatic Hyperplasia: A Review. *Asian J Urol* (2020) 7(3):191–202. doi: 10.1016/j.ajur.2019.10.003
95. Liu S, Kumari S, Hu Q, Senapati D, Venkadakrishnan VB, Wang D, et al. A Comprehensive Analysis of Coregulator Recruitment, Androgen Receptor Function and Gene Expression in Prostate Cancer. *Elife* (2017) 6:e28482–513. doi: 10.7554/eLife.28482
96. Guan J, Guo H, Tang T, Wang Y, Wei Y, Seth P, et al. iRGD-Liposomes Enhance Tumor Delivery and Therapeutic Efficacy of Antisense Oligonucleotide Drugs Against Primary Prostate Cancer and Bone Metastasis. *Adv Funct Mater* (2021) 31(24):2100478–89. doi: 10.1002/adfm.202100478
97. Bernstein E, Caudy AA, Hammond SM, Hannon GJ. Role for a Bidentate Ribonuclease in the Initiation Step of RNA Interference. *Nature* (2001) 409 (6818):363–6. doi: 10.1038/35053110
98. Elbashir SM, Harborth J, Lendeckel W, Yalcin A, Weber K, Tuschl T. Duplexes of 21-Nucleotide RNAs Mediate RNA Interference in Cultured Mammalian Cells. *Nature* (2001) 411(6836):494–8. doi: 10.1038/35078107
99. Sakamoto KM, Kim KB, Kumagai A, Mercurio F, Crews CM, Deshaies RJ. Protacs: Chimeric Molecules That Target Proteins to the Skp1-Cullin-F Box Complex for Ubiquitination and Degradation. *Proc Natl Acad Sci USA* (2001) 98(15):8554–9. doi: 10.1073/pnas.141230798
100. Burslem GM, Crews CM. Proteolysis-Targeting Chimeras as Therapeutics and Tools for Biological Discovery. *Cell* (2020) 181(1):102–14. doi: 10.1016/j.cell.2019.11.031
101. Bekes M, Langley DR, Crews CM. PROTAC Targeted Protein Degraders: The Past Is Prologue. *Nat Rev Drug Discov* (2022) 2022:1–20. doi: 10.1038/s41573-021-00371-6
102. Qi SM, Dong J, Xu ZY, Cheng XD, Zhang WD, Qin JJ. PROTAC: An Effective Targeted Protein Degradation Strategy for Cancer Therapy. *Front Pharmacol* (2021) 12:692574. doi: 10.3389/fphar.2021.692574
103. Chen X, Shen H, Shao Y, Ma Q, Niu Y, Shang Z. A Narrative Review of Proteolytic Targeting Chimeras (PROTACs): Future Perspective for Prostate Cancer Therapy. *Transl Androl Urol* (2021) 10(2):954–62. doi: 10.21037/tau-20-1357
104. Mohler ML, Sikdar A, Ponnusamy S, Hwang DJ, He Y, Miller DD, et al. An Overview of Next-Generation Androgen Receptor-Targeted Therapeutics in Development for the Treatment of Prostate Cancer. *Int J Mol Sci* (2021) 22 (4):2124–43. doi: 10.3390/ijms22042124
105. Zeng S, Huang W, Zheng X, Liyan C, Zhang Z, Wang J, et al. Proteolysis Targeting Chimera (PROTAC) in Drug Discovery Paradigm: Recent Progress and Future Challenges. *Eur J Med Chem* (2021) 210:112981. doi: 10.1016/j.ejmech.2020.112981
106. Wang Y, Jiang X, Feng F, Liu W, Sun H. Degradation of Proteins by PROTACs and Other Strategies. *Acta Pharm Sin B* (2020) 10(2):207–38. doi: 10.1016/j.apsb.2019.08.001
107. Ponnusamy S, Coss CC, Thiyagarajan T, Watts K, Hwang DJ, He Y, et al. Novel Selective Agents for the Degradation of Androgen Receptor Variants to Treat Castration-Resistant Prostate Cancer. *Cancer Res* (2017) 77 (22):6282–98. doi: 10.1158/0008-5472.CAN-17-0976
108. Hu P, Guo D, Xie J, Chen H, Hu S, Bian A, et al. Determining the Drug-Like Properties of Ailanthone, a Novel Chinese Medicine Monomer With Anti-CRPC Activity. *Planta Med* (2020) 86(7):482–8. doi: 10.1055/a-1125-0385
109. Tang S, Ma X, Lu J, Zhang Y, Liu M, Wang X. Preclinical Toxicology and Toxicokinetic Evaluation of Ailanthone, a Natural Product Against Castration-Resistant Prostate Cancer, in Mice. *Fitoterapia* (2019) 136:104161. doi: 10.1016/j.fitote.2019.04.016
110. Kanayama M, Lu C, Luo J, Antonarakis ES. AR Splicing Variants and Resistance to AR Targeting Agents. *Cancers (Basel)* (2021) 13(11):2563–78. doi: 10.3390/cancers13112563
111. Moll JM, Hofland J, Teubel WJ, de Ridder CMA, Taylor AE, Graeser R, et al. Abiraterone Switches Castration-Resistant Prostate Cancer Dependency From Adrenal Androgens Towards Androgen Receptor Variants and Glucocorticoid Receptor Signalling. *Prostate* (2022) 82(5):505–16. doi: 10.1002/pros.24297
112. Sun F, Chen HG, Li W, Yang X, Wang X, Jiang R, et al. Androgen Receptor Splice Variant AR3 Promotes Prostate Cancer *via* Modulating Expression of Autocrine/Paracrine Factors. *J Biol Chem* (2014) 289(3):1529–39. doi: 10.1074/jbc.M113.492140
113. Hu R, Dunn TA, Wei S, Isharwal S, Veltri RW, Humphreys E, et al. Ligand-Independent Androgen Receptor Variants Derived From Splicing of Cryptic Exons Signify Hormone-Refractory Prostate Cancer. *Cancer Res* (2009) 69 (1):16–22. doi: 10.1158/0008-5472.CAN-08-2764
114. Kallio HML, Hieta R, Latonen L, Brofeldt A, Annala M, Kivinummi K, et al. Constitutively Active Androgen Receptor Splice Variants AR-V3, AR-V7 and AR-V9 are Co-Expressed in Castration-Resistant Prostate Cancer Metastases. *Br J Cancer* (2018) 119(3):347–56. doi: 10.1038/s41416-018-0172-0
115. Kohli M, Ho Y, Hillman DW, Van Etten JL, Henzler C, Yang R, et al. Androgen Receptor Variant AR-V9 Is Coexpressed With AR-V7 in Prostate Cancer Metastases and Predicts Abiraterone Resistance. *Clin Cancer Res* (2017) 23(16):4704–15. doi: 10.1158/1078-0432.CCR-17-0017
116. Liu C, Lou W, Zhu Y, Nadiminty N, Schwartz CT, Evans CP, et al. Niclosamide Inhibits Androgen Receptor Variants Expression and Overcomes Enzalutamide Resistance in Castration-Resistant Prostate Cancer. *Clin Cancer Res* (2014) 20(12):3198–210. doi: 10.1158/1078-0432.CCR-13-3296
117. Liu C, Armstrong CM, Lou W, Lombard AP, Cucchiara V, Gu X, et al. Niclosamide and Bicalutamide Combination Treatment Overcomes Enzalutamide- and Bicalutamide-Resistant Prostate Cancer. *Mol Cancer Ther* (2017) 16(8):1521–30. doi: 10.1158/1535-7163.MCT-16-0912
118. Schweizer MT, Haugk K, McKiernan JS, Gulati R, Cheng HH, Maes JL, et al. A Phase I Study of Niclosamide in Combination With Enzalutamide in Men With Castration-Resistant Prostate Cancer. *PloS One* (2018) 13(6):e0198389. doi: 10.1371/journal.pone.0198389
119. Parikh M, Liu C, Wu CY, Evans CP, Dall'Era M, Robles D, et al. Phase Ib Trial of Reformulated Niclosamide With Abiraterone/Prednisone in Men With Castration-Resistant Prostate Cancer. *Sci Rep* (2021) 11(1):6377. doi: 10.1038/s41598-021-85969-x
120. Hu H, Zhou H, Xu D. A Review of the Effects and Molecular Mechanisms of Dimethylcurcumin (ASC-J9) on Androgen Receptor-Related Diseases. *Chem Biol Drug Des* (2021) 97(4):821–35. doi: 10.1111/cbdd.13811

121. Tian H, Chou FJ, Tian J, Zhang Y, You B, Huang CP, et al. ASC-J9(R) Suppresses Prostate Cancer Cell Proliferation and Invasion *via* Altering the ATF3-PTK2 Signaling. *J Exp Clin Cancer Res* (2021) 40(1):3. doi: 10.1186/s13046-020-01760-2
122. Huang CP, Chen J, Chen CC, Liu G, Zhang Y, Messing E, et al. ASC-J9(R) Increases the Bladder Cancer Chemotherapy Efficacy *via* Altering the Androgen Receptor (AR) and NF-kappaB Survival Signals. *J Exp Clin Cancer Res* (2019) 38(1):275. doi: 10.1186/s13046-019-1258-0
123. Lin W, Luo J, Sun Y, Lin C, Li G, Niu Y, et al. ASC-J9((R)) Suppresses Prostate Cancer Cell Invasion *via* Altering the Sumoylation-Phosphorylation of STAT3. *Cancer Lett* (2018) 425:21–30. doi: 10.1016/j.canlet.2018.02.007
124. Wen S, Tian J, Niu Y, Li L, Yeh S, Chang C. ASC-J9((R)), and Not Casodex or Enzalutamide, Suppresses Prostate Cancer Stem/Progenitor Cell Invasion *via* Altering the EZH2-STAT3 Signals. *Cancer Lett* (2016) 376(2):377–86. doi: 10.1016/j.canlet.2016.01.057
125. Wen S, Niu Y, Lee SO, Yeh S, Shang Z, Gao H, et al. Targeting Fatty Acid Synthase With ASC-J9 Suppresses Proliferation and Invasion of Prostate Cancer Cells. *Mol Carcinog* (2016) 55(12):2278–90. doi: 10.1002/mc.22468
126. Tian KM, Li JJ, Xu SW. Rutaecarpine: A Promising Cardiovascular Protective Alkaloid From Evodia Rutaecarpa (Wu Zhu Yu). *Pharmacol Res* (2019) 141:541–50. doi: 10.1016/j.phrs.2018.12.019
127. Supuran CT. Indisulam: An Anticancer Sulfonamide in Clinical Development. *Expert Opin Investig Drugs* (2003) 12(2):283–7. doi: 10.1517/13543784.12.2.283
128. Goh JXH, Tan LT, Goh JK, Chan KG, Pusparajah P, Lee LH, et al. Nobiletin and Derivatives: Functional Compounds From Citrus Fruit Peel for Colon Cancer Chemoprevention. *Cancers (Basel)* (2019) 11(6):867–900. doi: 10.3390/cancers11060867
129. Ashrafizadeh M, Zarrabi A, Saberifar S, Hashemi F, Hushmandi K, Hashemi F, et al. Nobiletin in Cancer Therapy: How This Plant Derived-Natural Compound Targets Various Oncogene and Onco-Suppressor Pathways. *Biomedicines* (2020) 8(5):110–40. doi: 10.3390/biomedicines8050110
130. Sadar MD. Discovery of Drugs That Directly Target the Intrinsically Disordered Region of the Androgen Receptor. *Expert Opin Drug Discov* (2020) 15(5):551–60. doi: 10.1080/17460441.2020.1732920
131. Jenster G, van der Korput HA, Trapman J, Brinkmann AO. Identification of Two Transcription Activation Units in the N-Terminal Domain of the Human Androgen Receptor. *J Biol Chem* (1995) 270(13):7341–6. doi: 10.1074/jbc.270.13.7341
132. Berrevoets CA, Doesburg P, Steketee K, Trapman J, Brinkmann AO. Functional Interactions of the AF-2 Activation Domain Core Region of the Human Androgen Receptor With the Amino-Terminal Domain and With the Transcriptional Coactivator TIF2 (Transcriptional Intermediary Factor2). *Mol Endocrinol* (1998) 12(8):1172–83. doi: 10.1210/mend.12.8.0153
133. Metzger E, Muller JM, Ferrari S, Buettner R, Schule R. A Novel Inducible Transactivation Domain in the Androgen Receptor: Implications for PRK in Prostate Cancer. *EMBO J* (2003) 22(2):270–80. doi: 10.1093/emboj/cdg023
134. Andersen RJ, Mawji NR, Wang J, Wang G, Haile S, Myung JK, et al. Regression of Castrate-Recurrent Prostate Cancer by a Small-Molecule Inhibitor of the Amino-Terminus Domain of the Androgen Receptor. *Cancer Cell* (2010) 17(6):535–46. doi: 10.1016/j.ccr.2010.04.027
135. Myung JK, Banuelos CA, Fernandez JG, Mawji NR, Wang J, Tien AH, et al. An Androgen Receptor N-Terminal Domain Antagonist for Treating Prostate Cancer. *J Clin Invest* (2013) 123(7):2948–60. doi: 10.1172/JCI66398
136. De Mol E, Fenwick RB, Phang CT, Buzon V, Szulc E, de la Fuente A, et al. EPI-001, A Compound Active Against Castration-Resistant Prostate Cancer, Targets Transactivation Unit 5 of the Androgen Receptor. *ACS Chem Biol* (2016) 11(9):2499–505. doi: 10.1021/acschembio.6b00182
137. Yang YC, Banuelos CA, Mawji NR, Wang J, Kato M, Haile S, et al. Targeting Androgen Receptor Activation Function-1 With EPI to Overcome Resistance Mechanisms in Castration-Resistant Prostate Cancer. *Clin Cancer Res* (2016) 22(17):4466–77. doi: 10.1158/1078-0432.CCR-15-2901
138. Hirayama Y, Tam T, Jian K, Andersen RJ, Sadar MD. Combination Therapy With Androgen Receptor N-Terminal Domain Antagonist EPI-7170 and Enzalutamide Yields Synergistic Activity in AR-V7-Positive Prostate Cancer. *Mol Oncol* (2020) 14(10):2455–70. doi: 10.1002/1878-0261.12770
139. Maurice-Dror C, Le Moigne R, Vaishampayan U, Montgomery RB, Gordon MS, Hong NH, et al. A Phase 1 Study to Assess the Safety, Pharmacokinetics, and Anti-Tumor Activity of the Androgen Receptor N-Terminal Domain Inhibitor Epi-506 in Patients With Metastatic Castration-Resistant Prostate Cancer. *Invest New Drugs* (2021). doi: 10.1007/s10637-021-01202-6
140. Le Moigne R, Zhou HJ, Obst JK, Banuelos CA, Jian KZ, Williams D, et al. Lessons Learned From the Metastatic Castration Resistant Prostate Cancer Phase I Trial of EPI-506, a First-Generation Androgen Receptor N-Terminal Domain Inhibitor. *J Clin Oncol* (2019) 37(7_Supplement):257. doi: 10.1200/JCO.2019.37.7_suppl.257
141. Le Moigne R, Pearson P, Lauriault V, Hong NH, Virsik P, Zhou HJ, et al. Preclinical and Clinical Pharmacology of EPI-7386, an Androgen Receptor N-Terminal Domain Inhibitor for Castration-Resistant Prostate Cancer. *J Clin Oncol* (2021) 39(6_Supplement):119. doi: 10.1200/JCO.2021.39.6_suppl.119
142. Kaku N, Matsuda K, Tsujimura A, Kawata M. Characterization of Nuclear Import of the Domain-Specific Androgen Receptor in Association With the Importin Alpha/Beta and Ran-Guanosine 5'-Triphosphate Systems. *Endocrinology* (2008) 149(8):3960–9. doi: 10.1210/en.2008-0137
143. Dar JA, Masoodi KZ, Eisermann K, Isharwal S, Ai J, Pascal LE, et al. The N-Terminal Domain of the Androgen Receptor Drives its Nuclear Localization in Castration-Resistant Prostate Cancer Cells. *J Steroid Biochem Mol Biol* (2014) 143:473–80. doi: 10.1016/j.jsbmb.2014.03.004
144. Zhou ZX, Sar M, Simental JA, Lane MV, Wilson EM. A Ligand-Dependent Bipartite Nuclear Targeting Signal in the Human Androgen Receptor. Requirement for the DNA-Binding Domain and Modulation by NH2-Terminal and Carboxyl-Terminal Sequences. *J Biol Chem* (1994) 269(18):13115–23. doi: 10.1016/S0021-9258(17)36806-0
145. Saporita AJ, Zhang Q, Navai N, Dincer Z, Hahn J, Cai X, et al. Identification and Characterization of a Ligand-Regulated Nuclear Export Signal in Androgen Receptor. *J Biol Chem* (2003) 278(43):41998–2005. doi: 10.1074/jbc.M302460200
146. Shaffer PL, Jivan A, Dollins DE, Claessens F, Gewirth DT. Structural Basis of Androgen Receptor Binding to Selective Androgen Response Elements. *Proc Natl Acad Sci USA* (2004) 101(14):4758–63. doi: 10.1073/pnas.0401123101
147. Labrecque MP, Alumkal JJ, Coleman IM, Nelson PS, Morrissey C. The Heterogeneity of Prostate Cancers Lacking AR Activity Will Require Diverse Treatment Approaches. *Endocr Relat Cancer* (2021) 28(8):T51–66. doi: 10.1530/ERC-21-0002

Conflict of Interest: The authors declare that the research was conducted in the absence of any commercial or financial relationships that could be construed as a potential conflict of interest.

frontiers | Frontiers in Oncology

ORIGINAL RESEARCH
published: 14 July 2022
doi: 10.3389/fonc.2022.858813

High Carbohydrate Antigen 19-9 Levels Indicate Poor Prognosis of Upper Tract Urothelial Carcinoma

Seung-hwan Jeong[1], *Jang Hee Han*[1], *Chang Wook Jeong*[1,2], *Hyeon Hoe Kim*[1,2], *Cheol Kwak*[1,2], *Hyeong Dong Yuk*[1,2*] *and Ja Hyeon Ku*[1,2*]

[1] Department of Urology, Seoul National University Hospital, Seoul, South Korea, [2] Department of Urology, Seoul National University College of Medicine, Seoul, South Korea

Upper tract urothelial carcinoma (UTUC) occurs in urothelial cells from the kidney and the ureters. Carbohydrate antigen 19-9 (CA 19-9) is a tumor marker for pancreatic and gastrointestinal cancers, and its high levels are associated with poor prognosis in bladder cancer. In this study, prospective patients enrolled in the registry of Seoul National University were retrospectively examined to determine the clinical significance of CA 19-9 in UTUC. In 227 patients, high serum CA 19-9 levels reflected a high tumor burden represented by high T and N stages, leading to adverse prognosis in metastasis-free or overall survival. Subsequently, propensity score matching analysis showed that the CA 19-9 level is an independent prognostic factor of UTUC.

Keywords: CA 19-9, UTUC, prognosis, survival, metastasis

OPEN ACCESS

Edited by:
Ronald M. Bukowski,
Cleveland Clinic, United States

Reviewed by:
Daanesh Huned,
Tan Tock Seng Hospital, Singapore
Bao Guan,
Peking University, China

***Correspondence:**
Hyeong Dong Yuk
hinayuk@naver.com
Ja Hyeon Ku
kuuro70@snu.ac.kr

Specialty section:
This article was submitted to Genitourinary Oncology, a section of the journal Frontiers in Oncology

Received: *20 January 2022*
Accepted: *13 June 2022*
Published: *14 July 2022*

Citation:
Jeong S-h, Han JH, Jeong CW, Kim HH, Kwak C, Yuk HD and Ku JH (2022) High Carbohydrate Antigen 19-9 Levels Indicate Poor Prognosis of Upper Tract Urothelial Carcinoma. Front. Oncol. 12:858813. doi: 10.3389/fonc.2022.858813

INTRODUCTION

Urothelial carcinoma arises from epithelial cells lining the urinary system. Most urothelial carcinomas occur in the urinary bladder, whereas upper tract urothelial carcinoma (UTUC), involving the renal calyx, pelvis, and ureter, accounts for 5%–10% of urothelial carcinomas (1, 2). The prognosis of UTUC depends on the T stage, which shows a 5-year survival rate from 90.2% to 18.5% through stages T1 to T4 (3). Risk classification stratifies UTUC as low- or high-risk, with low-risk cases allowing kidney-sparing surgeries, such as segmental ureterectomy and endoscopic ablation (4). In contrast, definitive treatment with nephroureterectomy is required for high-risk patients with adverse features. In addition, perioperative chemotherapy provides benefits in overall survival (OS) and cancer-specific survival with much concrete evidence in an adjuvant setting (5). The clinical staging of UTUC is restricted because of the pitfalls of computed tomography (CT) urography in discriminating between the T stages of carcinoma *in situ* and T2 (6). Thus, appropriate tools are required to evaluate the disease burden and to stratify risk classification.

Carbohydrate antigen 19-9 (CA 19-9) is a sialylated Lewis antigen. It is a tumor marker that predicts tumor stage, disease burden, and recurrence in pancreatic and gastrointestinal cancers (7–9). Although CA 19-9 is not a diagnostic marker in urothelial carcinoma, it is reportedly associated with the disease burden and aggressive features of bladder cancer, implying poor prognosis (10–12). In the present study, serum CA 19-9 levels in patients with UTUC were evaluated to reveal its clinical relevance implicating tumor burdens and clinical outcomes.

MATERIALS AND METHODS

Study Subjects

The analyzed clinical data were of patients with UTUC enrolled in the Seoul National University Prospective Enrolled Registry for urothelial cancer from March 2016 to December 2020 with institutional review board approval (IRB No. 2201-032-1289) (13). From 420 patients, 227 patients whose preoperative serum CA 19-9 levels were measured were selected and stratified into low- (≤ 37 U/ml) and high-CA 19-9 (> 37 U/ml) level groups as normal value of CA 19-9 is considered to be lower than 37 U/ml (14). Preoperative and postoperative data, including the underlying disease, clinical and pathologic stage, and findings, were queried and compared.

Statistical Analysis

Two-tailed t-tests were performed on parametric values, such as age, body mass index (BMI), and CA 19-9 level. The chi-square test was performed for categorical variables, including sex, underlying disease status, clinical and pathologic stage, hydronephrosis, perioperative chemotherapy, and tumor grade. Metastasis-free survival and OS were analyzed using Kaplan–Meier survival analysis, with the log-rank test for significance evaluation. To alleviate confounding effects derived from tumor burdens correlated with CA 19-9 levels, propensity score matching (PSM) was conducted to match pathologic T and N stages with a 1:4 ratio in both patient groups. Statistical analysis was performed using XLSTAT (version 2021.5-life sciences). Statistical significance was set at $p < 0.05$.

RESULTS

CA 19-9 Is Related to High Tumor Burden

In a total of 227 patients, 199 and 28 patients were classified into low- and high-CA 19-9-level groups, respectively. The two groups were similar in terms of demographic findings, such as sex (male proportion of 71% vs. 57.1%, p = 0.126), age (70.4 vs. 71.8 years, p = 0.485), and BMI (24.7 vs. 24.1%, p = 0.388) (**Table 1**). Underlying diseases, including hypertension, diabetes mellitus,

TABLE 1 | Characteristics of patients with low or high CA19-9 level.

	CA19-9 Low (n = 199)	CA19-9 High (n = 28)	*P* value
Sex	142 (71.4%)	16 (57.1%)	0.126
Man	57 (28.6%)	12 (42.9%)	
Woman			
Age	70.4	71.8	0.485
BMI	24.7	24.1	0.388
HTN	121 (60.8%)	15 (53.6%)	0.465
DM	66 (33.2%)	9 (32.1%)	0.914
Liver disease	18 (9.05%)	1 (3.57%)	0.327
Dyslipidemia	60 (30.2%)	9 (32.1%)	0.830
Clinical T stage	15 (7.54%)	0	0.016
Ta	64 (32.2%)	5 (17.9%)	
T1	78 (39.2%)	14 (50%)	
T2	42 (21.1%)	8 (28.6%)	
T3	0	1 (3.6%)	
T4			
Hydronephrosis	96 (48.2%)	18 (64.3%)	0.112
Neoadjuvant CTx	6 (3.02%)	1 (3.57%)	0.873
Operation	82 (41.2%)	14 (50%)	0.665
Open	28 (14.1%)	3 (10.7%)	
Laparoscopic	89 (44.7%)	11 (38.3%)	
Robotic			
Pathologic T stage	45 (22.6%)	3 (10.7%)	0.037
Ta	6 (3.0%)	0	
CIS	52 (26.1%)	4 (14.3%)	
T1	23 (11.6%)	2 (7.1%)	
T2	72 (36.2%)	18 (64.3%)	
T3	1 (0.5%)	1 (3.6%)	
T4			
Pathologic N stage	164 (82.4%)	16 (57.1%)	0.002
Nx	27 (13.6%)	6 (21.4%)	
N0	1 (0.5%)	1 (3.6%)	
N1	7 (3.5%)	5 (17.9%)	
N2			
Histologic Grade	166 (83.4%)	24 (85.7%)	0.758
Low grade	33 (16.6%)	4 (14.3%)	
High grade			
Adjuvant CTx	45 (22.6%)	8 (28.6%)	0.485
CA 19-9 (U/mL)	7.73	255.96	< 0.0001

liver disease, and dyslipidemia, were also similar between the two groups. Cisplatin-based neoadjuvant chemotherapy was administered to 3.02% and 3.57% patients in the low- and high-CA 19-9-level groups, respectively (p = 0.873). All patients underwent nephroureterectomy *via* open, laparoscopic, or robotic procedures in similar proportions (p = 0.665). The clinical stage was significantly higher in the high-CA 19-9-level group, represented by 32.6% of the T3 or T4 stage population, compared with 21.1% in the low-CA 19-9-level group (p = 0.016). Accordingly, hydronephrosis was more prevalent in the high-CA 19-9-level group, without statistical significance. The pathologic T stage was higher in those with high CA 19-9 levels, with 69.9% of them having stage T3 or T4 tumors, compared to 36.7% of those with low CA 19-9 levels (p = 0.037). Furthermore, pathologic N1 or N2 stage was diagnosed in 21.5% of the patients in the high-CA 19-9 level group, which was higher than 4.0% in the low-CA 19-9 level group (p = 0.002). Cisplatin-based adjuvant chemotherapy was administered to similar proportion of patients in the two groups (22.6% vs. 28.6%, p = 0.485). Both the 2-year metastasis-free survival (77.0% vs. 22.5%, p = 0.003) and OS (96.4% vs. 79.8%, p = 0.007) rates were significantly higher in the low-CA 19-9-level group (**Figure 1**). COX regression analysis was performed to reveal factors associated with metastasis. Among the included variables, high CA19-9 level, high T stage and N stage were significantly associated with the risk of metastasis (**Table 2**).

PSM Revealed CA 19-9 as an Independent Factor for Tumor Burden and Prognosis

In the high-CA 19-9-level group, the tumor burden was higher, leading to poor prognosis. To identify CA 19-9 as an independent prognostic factor, PSM analysis was performed for pathological T and N stages. In the PSM cases, demographic findings and underlying diseases remained relatively different between the two groups (**Table 3**). Clinical stage did not differ between the two groups (p = 0.123), which was reflected in the incidence of hydronephrosis (p = 0.269). Neoadjuvant or adjuvant chemotherapy was administered to similar proportion of patients in both groups. The pathologic T stage was matched in similar proportions between the two groups, represented by 64.3% and 67.9% of patients with T3 or higher stage in the low- and high-CA 19-9-level groups, respectively (p = 0.904). The pathologic N stage tended to be higher in the high-CA 19-9 level group, without statistical significance (p = 0.13). Interestingly, in the PSM analysis, the two-year metastasis free survival (71.2% vs. 22.5%, p = 0.031) and OS (95.4% vs. 79.8%, p = 0.029) rates were significantly higher in the low-CA 19-9-level group (**Figure 2**).

DISCUSSION

In bladder cancer, CA 19-9 is associated with adverse pathologic stages, characterized by muscular layer invasion and metastasis, thereby leading to poorer survival rates in bladder cancer patients with high CA 19-9 levels (12, 15). Furthermore, accumulating data suggest that urothelial cancers might produce CA19-9 to reflect tumor aggressiveness and tumor burdens (10, 12, 16).

However, there have been no reports evaluating the prognostic value of CA 19-9 for UTUC. In the present study, CA 19-9 was associated with a high tumor burden represented by higher T and N stages, and led to worse outcomes in metastasis-free survival and OS. CA 19-9 is highly expressed in the serum of patients with pancreatic or colon cancer (17). In pancreatic cancer, CA 19-9 is a useful diagnostic and prognostic marker for evaluating the tumor stage, treatment response, and OS. Similar to the study on UTUC, preoperative CA 19-9 levels are associated with tumor resectability and pancreatic cancer stage. A decrease in CA 19-9 levels after surgery reflects favorable survival outcomes, and elevated CA 19-9 levels imply worse survival outcomes (18). In addition, the CA 19-9 level is useful for evaluating disease progression or remission in response to treatment (19, 20). This study investigated only preoperative CA 19-9 levels, but serial measurements following treatment would be valuable in predicting prognostic outcomes. The diagnostic value of CA 19-9 is disappointing because of high false-positive rates in normal conditions and other diseases, such as liver

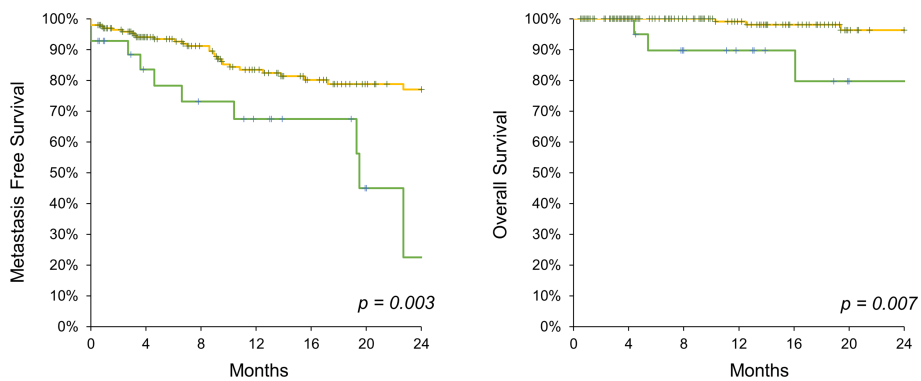

FIGURE 1 | Kaplan-Meier analysis on metastasis free survival (left) and overall survival (right) comparing CA 19-9 high (green line) and low (yellow line) UTUC patients.

TABLE 2 | COX regression analysis for metastasis.

	HR (95% CI)	*P* value
Age	1.02 (0.981 - 1.057)	0.337
CA 19-9 (U/ml)	1.001 (1.000 – 1.003)	0.036
Hydronephrosis	1.36 (0.709 – 2.601)	0.357
Histologic grade	Reference	Reference
Low grade	0.232 (0.063 – 1.96)	0.232
High grade		
Pathologic T stage	Reference	Reference
Ta	1.87E-7 (0.000 – 0.000)	0.995
CIS	6.89 (0.87 – 54.679)	0.068
T1, T2	30.36 (3.661 – 251.81)	0.002
T3, T4		
Pathologic N stage	Reference	Reference
N0	0.752 (0.328 – 1.725)	0.501
Nx	0.67 (0.081 – 5.684)	0.719
N1	4.63 (1.529 – 14.016)	0.007
N2		

cirrhosis, pancreatitis, and benign gastrointestinal diseases (21). However, in discriminating between benign and malignant pancreatic nodules, it is valuable, with a specificity of 90%.

In this study, PSM analysis was conducted to mitigate adverse features, such as T and N stages, reflecting tumor burden, which is associated with poor outcomes. PSM corrected the imbalance between low- and high-CA 19-9 level groups regarding T and N stages, reflecting tumor burden. Interestingly, after PSM analysis, high CA 19-9 levels indicated worse prognosis, thereby affirming CA 19-9 as an independent prognostic marker, not only based on tumor burden but also its aggressiveness. Similar findings have been reported in pancreatic cancer, providing worse prognosis in

TABLE 3 | Characteristics of propensity score matched patients.

	CA19-9 Low (n = 112)	CA19-9 High (n = 28)	*P* value
Sex	81 (72.3%)	16 (57.1%)	0.119
Man	31 (27.7%)	12 (42.9%)	
Woman			
Age	70.9	71.8	0.667
BMI	24.6	24.1	0.458
HTN	63 (56.3%)	15 (53.6%)	0.799
DM	39 (34.8%)	9 (32.1%)	0.789
Liver disease	12 (10.7%)	1 (3.6%)	0.244
Dyslipidemia	28 (25%)	9 (32.1%)	0.443
Clinical stage	9 (8%)	0	0.123
Ta	27 (24.1%)	5 (17.9%)	
T1	44 (39.3%)	14 (50%)	
T2	32 (28.6%)	8 (28.6%)	
T3	0	1 (3.6%)	
T4			
Hydronephrosis	59 (52.7%)	18 (64.3%)	0.269
Neoadjuvant CTx	4 (3.57%)	1 (3.57%)	1.0
Operation	63 (56.3%)	14 (50%)	0.835
Open	10 (8.9%)	3 (10.7%)	
Laparoscopic	38 (34.8%)	11 (38.3%)	
Robotic			
Pathologic T stage	11 (9.8%)	3 (10.7%)	0.904
Ta	1 (0.9%)	0	
CIS	17 (15.2%)	4 (14.3%)	
T1	11 (9.8%)	2 (7.1%)	
T2	71 (63.4%)	18 (64.3%)	
T3	1 (0.9%)	1 (3.6%)	
T4			
Pathologic N stage	83 (74.1%)	16 (57.1%)	0.130
Nx	21 (18.8%)	6 (21.4%)	
N0	1 (0.9%)	1 (3.6%)	
N1	7 (6.3%)	5 (17.9%)	
N2			

(Continued)

TABLE 3 | Continued

	CA19-9 Low (n = 112)	CA19-9 High (n = 28)	*P* value
Histologic Grade	104 (92.9%)	24 (85.7%)	0.227
Low grade	8 (7.1%)	4 (14.3%)	
High grade			
Adjuvant CTx	43 (38.4%)	8 (28.6%)	0.334
CA19-9 (U/mL)	7.37	255.96	< 0.0001

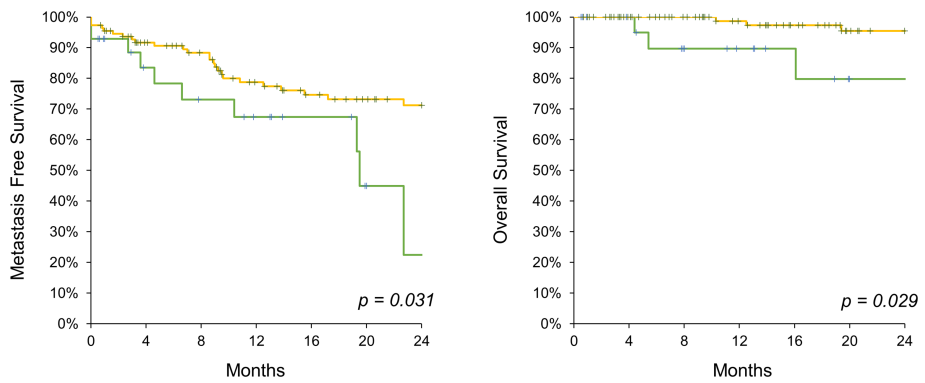

FIGURE 2 | Kaplan-Meier analysis on metastasis free survival (left) and overall survival (right) comparing CA 19-9 high (green line) and low (yellow line) UTUC patients following propensity score matching.

multivariate analysis of CA 19-9 level, tumor grade, and tumor size (22). Furthermore, in colorectal cancer, high CA 19-9 levels are related to poor oncologic outcomes, including OS and disease-free survival on PSM analysis (23).

This study is limited by the fact that it had a relatively small sample size and a retrospective study design. However, this report is valuable, considering the low incidence of UTUC with concomitant measurement of CA 19-9 and data queries from a prospective patient enrollment system. Moreover, monitoring CA 19-9 levels may provide preoperative risk classification and facilitate strategic follow-up and adjuvant treatment. Thus, further studies are required to include a larger number of patients and serial follow-up of CA 19-9 in the treatment course.

DATA AVAILABILITY STATEMENT

The raw data supporting the conclusions of this article will be made available by the authors, without undue reservation.

ETHICS STATEMENT

The studies involving human participants were reviewed and approved by Institutional review board of Seoul National University Hospital. Written informed consent for participation was not required for this study in accordance with the national legislation and the institutional requirements.

AUTHOR CONTRIBUTIONS

Conceptualization: S-HJ. Data collection: S-HJ, JH, HY, CJ, HK, JK, CK. Data analysis: S-HJ, HY, JK. Data visualization: S-HJ. Data interpretation: S-HJ, JH, HY, CJ, HK, CK, JK. Manuscript writing: S-HJ. Supervision: S-HJ, HY, JK. All authors contributed to the article and approved the submitted version.

FUNDING

This research was supported by a Basic Science Research Program through National Research Foundation of Korea (NRF), funded by the Ministry of Education (NRF-2018R1D1A1B07041191) and by Seoul National University Hospital (0320202190).

ACKNOWLEDGMENTS

We would like to thank Editage (www.editage.co.kr) for editing and reviewing this manuscript for English language.

REFERENCES

1. Soualhi A, Rammant E, George G, Russell B, Enting D, Nair R, et al. The Incidence and Prevalence of Upper Tract Urothelial Carcinoma: A Systematic Review. *BMC Urol* (2021) 21:1–11. doi: 10.1186/s12894-021-00876-7
2. Lughezzani G, Sun M, Perrotte P, Shariat SF, Jeldres C, Budäus L, et al. Gender-Related Differences in Patients With Stage I to III Upper Tract Urothelial Carcinoma: Results From the Surveillance, Epidemiology, and End Results Database. *Urology* (2010) 75:321–7. doi: 10.1016/j.urology.2009.09.048
3. Wang Q, Zhang T, Wu J, Wen J, Tao D, Wan T, et al. Prognosis and Risk Factors of Patients With Upper Urinary Tract Urothelial Carcinoma and Postoperative Recurrence of Bladder Cancer in Central China. *BMC Urol* (2019) 19:1–8. doi: 10.1186/s12894-019-0457-5
4. Seisen T, Peyronnet B, Dominguez-Escrig JL, Bruins HM, Yuan CY, Babjuk M, et al. Oncologic Outcomes of Kidney-Sparing Surgery Versus Radical Nephroureterectomy for Upper Tract Urothelial Carcinoma: A Systematic Review by the EAU Non-Muscle Invasive Bladder Cancer Guidelines Panel. *Eur Urol* (2016) 70:1052–68. doi: 10.1016/j.eururo.2016.07.014
5. Leow JJ, Chong YL, Chang SL, Valderrama BP, Powles T, Bellmunt J. Neoadjuvant and Adjuvant Chemotherapy for Upper Tract Urothelial Carcinoma: A 2020 Systematic Review and Meta-Analysis, and Future Perspectives on Systemic Therapy. *Eur Urol* (2021) 79:635–54. doi: 10.1016/j.eururo.2020.07.003
6. Honda Y, Nakamura Y, Teishima J, Goto K, Higaki T, Narita K, et al. Clinical Staging of Upper Urinary Tract Urothelial Carcinoma for T Staging: Review and Pictorial Essay. *Int J Urol* (2019) 26:1024–32. doi: 10.1111/iju.14068
7. Gao Y, Wang J, Zhou Y, Sheng S, Qian SY, Huo X. Evaluation of Serum CEA, CA19-9, CA72-4, CA125 and Ferritin as Diagnostic Markers and Factors of Clinical Parameters for Colorectal Cancer. *Sci Rep* (2018) 8:1–9. doi: 10.1038/s41598-018-21048-y
8. Luo G, Jin K, Deng S, Cheng H, Fan Z, Gong Y, et al. Roles of CA19-9 in Pancreatic Cancer: Biomarker, Predictor and Promoter. *Biochim Biophys Acta - Rev Cancer* (2021) 1875:188409. doi: 10.1016/j.bbcan.2020.188409
9. Tsai S, George B, Wittmann D, Ritch PS, Krepline AN, Aldakkak M, et al. Importance of Normalization of CA19-9 Levels Following Neoadjuvant Therapy in Patients With Localized Pancreatic Cancer. *Ann Surg* (2020) 271:740–7. doi: 10.1097/SLA.0000000000003049
10. Pall M, Iqbal J, Singh SK, Rana SV. CA 19-9 as a Serum Marker in Urothelial Carcinoma. *Urol Ann* (2012) 4:98–101. doi: 10.4103/0974-7796.95555
11. Washino S, Hirai M, Matsuzaki A, Kobayashi Y. Clinical Usefulness of CEA, CA19-9, and CYFRA 21-1 as Tumor Markers for Urothelial Bladder Carcinoma. *Urol Int* (2011) 87:420–8. doi: 10.1159/000327517
12. Hegele A, Mecklenburg V, Varga Z, Olbert P, Hofmann R, Barth P. CA19.9 and CEA in Transitional Cell Carcinoma of the Bladder: Serological and Immunohistochemical Findings. *Anticancer Res* (2010) 30:5195–200.
13. Jeong CW, Suh J, Yuk HD, Tae BS, Kim M, Keam B, et al. Establishment of the Seoul National University Prospectively Enrolled Registry for Genitourinary Cancer (SUPER-GUC): A Prospective, Multidisciplinary, Bio-Bank Linked Cohort and Research Platform. *Investig Clin Urol* (2019) 60:235–43. doi: 10.4111/icu.2019.60.4.235
14. Marrelli D, Caruso S, Pedrazzani C, Neri A, Fernandes E, Marini M, et al. CA19-9 Serum Levels in Obstructive Jaundice: Clinical Value in Benign and Malignant Conditions. *Am J Surg* (2009) 198:333–9. doi: 10.1016/j.amjsurg.2008.12.031
15. Wang QH, Ji ZG, Chen ZG, Li HZ, Fan H, Fan XR, et al. Serum CA 19-9 as a Good Prognostic Biomarker in Patients With Bladder Cancer. *Int J Surg* (2015) 15:113–6. doi: 10.1016/j.ijsu.2015.01.031
16. Sashide K, Isobe H, Wakumoto Y, Hanazawa K, Fujita K, Fujime M. CA19-9 as a Serum Marker for Poor Prognosis in Urothelial Carcinoma. *Urol Int* (2004) 72:112–7. doi: 10.1159/000075963
17. Koprowski H, Herlyn M, Steplewski Z, Sears HF. Specific Antigen in Serum of Patients With Colon Carcinoma. *Sci (80-)* (1981) 212:53–5. doi: 10.1126/science.6163212
18. Poruk KE, Gay DZ, Brown K, Mulvihill JD, Boucher KM, Scaife CL, et al. The Clinical Utility of CA 19-9 in Pancreatic Adenocarcinoma: Diagnostic and Prognostic Updates. *Curr Mol Med* (2013) 13:340–51. doi: 10.2174/156652413805076876
19. Lohrmann C, O'Reilly EM, O'Donoghue JA, Pandit-Taskar N, Carrasquillo JA, Lyashchenko SK, et al. Retooling a Blood-Based Biomarker: Phase I Assessment of the High-Affinity CA19-9 Antibody HuMAB-5B1 for Immuno-PET Imaging of Pancreatic Cancer. *Clin Cancer Res* (2019) 25:7014–23. doi: 10.1158/1078-0432.CCR-18-3667
20. Azizian A, Rühlmann F, Krause T, Bernhardt M, Jo P, König A, et al. CA19-9 for Detecting Recurrence of Pancreatic Cancer. *Sci Rep* (2020) 10:1–10. doi: 10.1038/s41598-020-57930-x
21. Kim S, Park BK, Seo JH, Choi J, Choi JW, Lee CK, et al. Carbohydrate Antigen 19-9 Elevation Without Evidence of Malignant or Pancreatobiliary Diseases. *Sci Rep* (2020) 10:1–9. doi: 10.1038/s41598-020-65720-8
22. Mattiucci GC, Morganti AG, Cellini F, Buwenge M, Casadei R, Farioli A, et al. Prognostic Impact of Presurgical CA19-9 Level in Pancreatic Adenocarcinoma: A Pooled Analysis. *Transl Oncol* (2019) 12:1–7. doi: 10.1016/j.tranon.2018.08.017
23. Shin JK, Kim HC, Lee WY, Yun SH, Cho YB, Huh JW, et al. High Preoperative Serum CA 19-9 Levels Can Predict Poor Oncologic Outcomes in Colorectal Cancer Patients on Propensity Score Analysis. *Ann Surg Treat Res* (2019) 96:107–15. doi: 10.4174/astr.2019.96.3.107

Conflict of Interest: The authors declare that the research was conducted in the absence of any commercial or financial relationships that could be construed as a potential conflict of interest.

Advantages of publishing in Frontiers

OPEN ACCESS
Articles are free to read for greatest visibility and readership

FAST PUBLICATION
Around 90 days from submission to decision

HIGH QUALITY PEER-REVIEW
Rigorous, collaborative, and constructive peer-review

TRANSPARENT PEER-REVIEW
Editors and reviewers acknowledged by name on published articles

Frontiers
Avenue du Tribunal-Fédéral 34
1005 Lausanne | Switzerland

Visit us: www.frontiersin.org
Contact us: frontiersin.org/about/contact

REPRODUCIBILITY OF RESEARCH
Support open data and methods to enhance research reproducibility

DIGITAL PUBLISHING
Articles designed for optimal readership across devices

FOLLOW US
@frontiersin

IMPACT METRICS
Advanced article metrics track visibility across digital media

EXTENSIVE PROMOTION
Marketing and promotion of impactful research

LOOP RESEARCH NETWORK
Our network increases your article's readership